



US Army Corps
of Engineers

AD-A227 913



**DREDGING OPERATIONS TECHNICAL
SUPPORT PROGRAM**

MISCELLANEOUS PAPER D-90-4

FILE COPY

2

**ENGINEERING DESIGN AND ENVIRONMENTAL
ASSESSMENT OF DREDGED MATERIAL
OVERFLOW FROM HYDRAULICALLY FILLED
HOPPER BARGES IN MOBILE BAY, ALABAMA**

by

Douglas G. Clarke, Jurij Homziak, Robert L. Lazor, Michael R. Palermo

Environmental Laboratory

Glynn E. Banks, Howard A. Benson, Billy H. Johnson, Tamsen Smith-Dozier

Hydraulics Laboratory

DEPARTMENT OF THE ARMY

Waterways Experiment Station, Corps of Engineers
3909 Halls Ferry Road, Vicksburg, Mississippi 39180-6199

Gene Revelas

Science Applications International Corporation
Newport, Rhode Island 02840

Michael R. Dardeau

Dauphin Island Sea Lab
Dauphin Island, Alabama 36528



September 1990

Final Report

DTIC
ELECTE
OCT 31 1990
S B D

Approved for Public Release; Distribution Unlimited

Prepared for DEPARTMENT OF THE ARMY
US Army Corps of Engineers
Washington, DC 20314-1000

and US Army Engineer District, Mobile
Mobile, Alabama 36628-0001

Destroy this report when no longer needed. Do not return
it to the originator.

The findings in this report are not to be construed as an official
Department of the Army position unless so designated
by other authorized documents.

The contents of this report are not to be used for
advertising, publication, or promotional purposes.
Citation of trade names does not constitute an
official endorsement or approval of the use of
such commercial products.

The D-series of reports includes publications of the
Environmental Effects of Dredging Programs:
Dredging Operations Technical Support
Long-Term Effects of Dredging Operations
Interagency Field Verification of Methodologies for
Evaluating Dredged Material Disposal Alternatives
(Field Verification Program)

Unclassified

SECURITY CLASSIFICATION OF THIS PAGE

REPORT DOCUMENTATION PAGE				Form Approved OMB No. 0704-0188	
1a. REPORT SECURITY CLASSIFICATION Unclassified			1b. RESTRICTIVE MARKINGS		
2a. SECURITY CLASSIFICATION AUTHORITY			3 DISTRIBUTION/AVAILABILITY OF REPORT Approved for public release, distribution unlimited.		
2b. DECLASSIFICATION/DOWNGRADING SCHEDULE					
4. PERFORMING ORGANIZATION REPORT NUMBER(S) Miscellaneous Paper D-90-4			5 MONITORING ORGANIZATION REPORT NUMBER(S)		
6a. NAME OF PERFORMING ORGANIZATION See reverse.		6b. OFFICE SYMBOL (If applicable)	7a. NAME OF MONITORING ORGANIZATION		
6c. ADDRESS (City, State, and ZIP Code) See reverse.			7b. ADDRESS (City, State, and ZIP Code)		
8a. NAME OF FUNDING/SPONSORING ORGANIZATION US Army Corps of Engineers; USAED, Mobile		8b. OFFICE SYMBOL (If applicable)	9. PROCUREMENT INSTRUMENT IDENTIFICATION NUMBER		
8c. ADDRESS (City, State, and ZIP Code) Washington, DC 20314-1000; Mobile, AL 36628-0001			10. SOURCE OF FUNDING NUMBERS		
			PROGRAM ELEMENT NO.	PROJECT NO.	TASK NO.
					WORK UNIT ACCESSION NO.
11. TITLE (Include Security Classification) Engineering Design and Environmental Assessment of Dredged Material Overflow from Hydraulically Filled Hopper Barges in Mobile Bay, Alabama					
12. PERSONAL AUTHOR(S) See reverse.					
13a. TYPE OF REPORT Final report		13b. TIME COVERED FROM _____ TO _____	14. DATE OF REPORT (Year, Month, Day) September 1990		15. PAGE COUNT 352
16. SUPPLEMENTARY NOTATION Available from National Technical Information Service, 5285 Port Royal Road, Springfield, VA 22161.					
17. COSATI CODES			18. SUBJECT TERMS (Continue on reverse if necessary and identify by block number)		
FIELD	GROUP	SUB-GROUP	See reverse.		
19. ABSTRACT (Continue on reverse if necessary and identify by block number)					
<p>Barge overflow was investigated as a cost-effective option for future dredging needs in Mobile Bay, Alabama. Tests of hopper barge loading characteristics with overflow operations were conducted in Mobile Bay. In theory, overflow would allow denser materials to settle within the barge while less dense materials were shunted overboard. Increased density of barge-held materials would then translate to cost savings via a reduced requirement for transport to a distant approved disposal site. Thus, one major objective of the study was an engineering evaluation of equipment performance during the tests. A second major objective was to obtain field data for an assessment of the environmental consequences of overflow. In support of both objectives, modeling studies were performed to simulate overflows that would be associated with routine dredging operations.</p> <p style="text-align: right;">→ JVE 2</p> <p style="text-align: right;">(Continued)</p>					
20. DISTRIBUTION/AVAILABILITY OF ABSTRACT <input checked="" type="checkbox"/> UNCLASSIFIED/UNLIMITED <input type="checkbox"/> SAME AS RPT <input type="checkbox"/> DTIC USERS			21. ABSTRACT SECURITY CLASSIFICATION Unclassified		
22a. NAME OF RESPONSIBLE INDIVIDUAL			22b. TELEPHONE (Include Area Code)		22c. OFFICE SYMBOL

Unclassified

SECURITY CLASSIFICATION OF THIS PAGE

6. NAME AND ADDRESS OF PERFORMING ORGANIZATION (Continued).

USAEWES, Environmental and Hydraulics Laboratories, 3909 Halls Ferry Road, Vicksburg, MS 39180-6199; Science Applications International Corporation, Newport, RI 02840; Dauphin Island Sea Lab, Dauphin Island, AL 36528.

12. PERSONAL AUTHOR(S) (Continued).

Clarke, Douglas G.; Homziak, Jurij; Lazor, Robert L.; Palermo, Michael R.; Banks, Glynn E.; Benson, Howard A.; Johnson, Billy H.; Smith-Dozier, Tamsen; Revelas, Gene; Dardeau, Michael R.

18. SUBJECT TERMS (Continued).

Deposited sediments
Dredging
Engineering design
Environmental impacts
Hopper barges
Overflow
Suspended sediments

19. ABSTRACT (Continued).

Eight separate tests were conducted. Three tests occurred at a site in lower Mobile Bay, and five tests at an upper bay site. Three tests (one lower bay, two upper bay) involved dredging in maintenance materials, and five tests (two lower bay, three upper bay) involved new work or deepening materials. (JES) ←

Measured increases in loading obtained by overflow of hydraulically filled hopper barges with the equipment and techniques used were too small to justify their routine application on strictly an economic basis. However, engineering solutions such as incorporation of y-valves to divert low-density flows from the barges could conceivably improve observed loading characteristics. Addition modifications to dredging techniques, such as allowance for wider sweeps of the cutterhead or shortening the length of pipeline between the dredge and the hopper barge, could contribute to overall improvements in performance. Overflow operations involving mechanically rather than hydraulically filled barges may provide another means of achieving economic benefits.

With respect to environmental concerns, overflow operations in which the point of discharge lies close to the channel represent a relatively safe dredging alternative. Evidence from both field and modeling studies indicates that acute impacts due to suspension of sediments in the water column or accumulation of overflow sediments on the bottom would be restricted to the side slopes of the navigation channel and small patches of adjacent shallow, flat habitat. Given the current state of knowledge regarding the adaptations and tolerances of organisms in the Mobile Bay system, these small areal-scale impacts would be short-term in nature and would not have significant impacts on biological communities in Mobile Bay.

Unclassified

SECURITY CLASSIFICATION OF THIS PAGE

SUMMARY

Overflow Test Objectives

Barge overflow was investigated as a cost-effective option for future dredging needs in Mobile Bay, Alabama. Tests of hopper barge loading characteristics with overflow operations were conducted in Mobile Bay during December 1987. In theory, overflow would allow denser materials to settle within the barge while less dense materials were shunted overboard. Increased density of barge-held materials would then translate to cost savings via a reduced requirement for transport to a distant approved disposal site. Thus, one major objective of the study was an engineering evaluation of equipment performance during the tests. A second major objective was to obtain field data for an assessment of the environmental consequences of overflow. In support of both objectives, modeling studies were performed to simulate overflows that would be associated with routine dredging operations.

Eight separate tests were conducted. Three tests occurred at a site in lower Mobile Bay, and five tests at an upper bay site. Three tests (one lower bay, two upper bay) involved dredging in maintenance materials, and five tests (two lower bay, three upper bay) involved new work or deepening materials.

Engineering Considerations



Equipment configuration

A hydraulic cutterhead dredge (26-in. (66-cm) suction pipe) was used to pump navigation channel sediments to a spider barge assembly that distributed slurries through six outlets into a split-hull hopper barge (4,020-cu yd (3,074-cu m) capacity). Loading was measured as a function of displacement of the barge during filling and overflow. Barge displacement was monitored by pressure gages mounted in stilling wells at opposite corners of the bow and stern of the hopper barge. Plots of barge displacement versus time for each test were used to estimate loading.

Loading characteristics

Solids concentrations of barge inflow samples taken from the pipeline were higher than calculated values based on barge displacement and pipeline density instrumentation. This difference indicates that the apparatus for obtaining pipeline samples may not have yielded representative samples.

For	
<input checked="checked" type="checkbox"/>	<input type="checkbox"/>
<input type="checkbox"/>	<input type="checkbox"/>
on	
on/	
Availability Codes	
Dist	Avail and/or Special
A-1	

However, comparisons of inflow solids concentrations, as calculated by barge displacement and pipeline instrumentation, and overflow concentrations indicate minimal retention of solids for maintenance tests at both lower and upper bay sites and new work tests at the lower bay sites.

Results of load monitoring efforts indicated that increases in load were marginal for all tests. Gains in loading ranged from approximately 4 to 8 percent with maximum loading occurring during new work tests at the upper bay site. Increased loading at the upper bay site for new work materials can be accounted for by the presence of comparatively coarser sediments at that site.

Environmental Considerations

Suspended sediment plumes

Plume tracking efforts were impaired by severe weather conditions on several dates. However, results of suspended sediment samples taken at predetermined fixed points and from mobile units responding to tidal influences indicate that most of the volume of overflow material descended quickly through the water column in the immediate area of the hopper barge. Surface plumes were restricted to thin veneers that were difficult to discern from background concentrations. Aerial photography conducted during a number of tests did not detect the presence of extensive suspended sediment plumes.

Numerical modeling

Existing models were adapted to predict spatial, temporal, and concentration attributes of suspended sediment plumes generated by overflow from either maintenance or new work dredging operations. Assumptions of overflow rates and overflow sediment concentration were based on best available information. Model runs were performed for discharges on either side of the navigation channel under various conditions of tidal velocities, wind velocities, and freshwater inflows to the estuary. In the case of both maintenance and new work dredging, suspended sediment concentrations were found to decay rapidly due to diffusion and settling. Results of the plume tracking efforts, which were designed to verify the modeling approach, support these findings.

Model predictions of sediment deposition resulting from overflow events were also generated. The fundamental conclusion of the sediment deposition modeling efforts was that the vast majority of overflow material was redeposited in the channel. Results were similar for both maintenance and new

work dredging scenarios, and were consistent with the findings of the sediment profiling camera surveys.

Sediment profiling imagery

Sediment profiling camera stations were occupied on a preoverflow and postoverflow basis at both test sites. Deposition appeared to be restricted to within 100 to 200 m of the point of overflow. All observed depositional layers were thin (less than 2 cm thick). Evidence of overflow-induced deposition was somewhat more widespread at the lower bay site than at the upper bay site.

Analyses of the sediment profile images indicated that surface sediments were disturbed by natural processes throughout the study areas. No obvious differences were seen between kinetic regimes of the near-channel stations and outlying areas. Gradients in chemical and biological parameters such as depth of the Redox Potential Discontinuity and infaunal successional stage were noted extending laterally east and west from the test sites, and along the north-south bay axis. The observed gradients reflected large-scale (baywide, patterns of water circulation and organic enrichment.

Impact assessment

A review of the technical literature with regard to suspended and deposited sediment effects on estuarine living resources was conducted. A predominance of information supports a general conclusion that organisms adapted to naturally turbid estuarine habitats such as Mobile Bay are very tolerant of moderately high concentrations of suspended sediments and thin layers of sediment deposition. Acute impacts to nonmobile benthos would be restricted to small patches of bottom habitat immediately adjacent to the navigation channel. There is very little probability that measurable population responses to overflow operations would occur beyond 200 m of the channel.

Cumulative effects of deposition as a dredging operation moved northward along the channel were examined. Individual deposition "footprints" from the numerical modeling exercises were superimposed using information on dredge rates of advance and barge-filling cycles. Substantial amounts of sediment were noted to settle into some model cells representing bottom habitat adjacent to the channel; the absolute amount of bottom area receiving significant sedimentation was small.

Conclusions

Measured increases in loading obtained by overflow of hydraulically filled hopper barges with the equipment and techniques used were too small to justify their routine application on strictly an economic basis. However, engineering solutions such as incorporation of y-valves to divert low-density flows from the barges could conceivably improve observed loading characteristics. Additional modifications to dredging techniques, such as allowance for wider sweeps of the cutterhead or shortening the length of pipeline between the dredge and the hopper barge, could contribute to overall improvements in performance. Overflow operations involving mechanically rather than hydraulically filled barges may provide another means of achieving economic benefits.

With respect to environmental concerns, overflow operations in which the point of discharge lies close to the channel represent a relatively safe dredging alternative. Evidence from both field and modeling studies indicates that acute impacts due to suspension of sediments in the water column or accumulation of overflow sediments on the bottom would be restricted to the side slopes of the navigation channel and small patches of adjacent shallow, flat habitat. Given the current state of knowledge regarding the adaptations and tolerances of organisms in the Mobile Bay system, these small areal-scale impacts would be short-term in nature and would not have significant impacts on biological communities in Mobile Bay.

PREFACE

This report discusses work performed by the Environmental Laboratory (EL) and the Hydraulics Laboratory (HL) of the US Army Engineer Waterways Experiment Station (WES) in response to a request by the US Army Engineer District (USAED), Mobile, Mobile, AL. The study was sponsored by the USAED, Mobile. Partial support for publication of the report was provided by the Headquarters, US Army Corps of Engineers (HQUSACE), under the Dredging Operations Technical Support (DOTS) Program. DOTS is managed through the Environmental Effects of Dredging Programs (EEDP) of the EL. Dr. Robert M. Engler was Manager of the EEDP; Mr. Thomas R. Patin was Manager of the DOTS Program. Technical Monitor was Mr. Joseph Wilson, HQUSACE.

The report was prepared by personnel of the Environmental Resources Division (ERD) and Environmental Engineering Division (EED), EL, and the Estuaries and Waterways Divisions, HL. Study participants included Dr. Douglas G. Clarke, Dr. Jurij Homziak, and Mr. Robert L. Lazor, ERD; Dr. Michael R. Palermo, EED; Dr. Billy H. Johnson, Waterways Division, HL; Mr. Howard A. Benson, Ms. Tamsen Smith-Dozier, and Mr. Glynn E. Banks, Estuaries Division, HL; Mr. Gene Revelas, Science Applications International, Inc.; and Mr. Michael R. Dardeau, Dauphin Island Sea Lab, Dauphin Island, Alabama.

The WES gratefully acknowledges the direction of Messrs. Dewayne Imsand, Project Manager, and Paul Bradley, Field Operations Coordinator for the USAED, Mobile. The provision of dredging logs for the overflow tests by Mr. Thomas Turner, a consultant to the Mobile District, greatly assisted the evaluation of equipment performance. Access to meteorological data records at the Dauphin Island Sea Lab was kindly given by Dr. William Schroeder. The assistance of the US Fish and Wildlife Service in support of aerial photography overflights is also gratefully acknowledged.

The report was prepared under the direct supervision of Mr. Edward J. Pullen, Chief, Coastal Ecology Group, ERD, and under the general supervision of Dr. C. J. Kirby, Chief, ERD, EL; Dr. Raymond L. Montgomery, Chief, EED, EL; Mr. W. H. McAnally, Jr., Chief, Estuaries Division, HL; Mr. George M. Fisackerly, Chief, Estuarine Processes Branch; and Mr. M. B. Boyd, Chief, Waterways Division, HL. Dr. John Harrison was Chief of EL, and Mr. Frank A. Herrmann was Chief of HL.

Commander and Director of WES was COL Larry B. Fulton, EN. Technical Director was Dr. Robert W. Whalin.

This report should be cited as follows:

Environmental and Hydraulics Laboratories. 1990. "Engineering Design and Environmental Assessment of Dredged Material Overflow from Hydraulically Filled Hopper Barges in Mobile Bay, Alabama," Miscellaneous Paper D-90-4, US Army Engineer Waterways Experiment Station, Vicksburg, MS.

CONTENTS

	<u>Page</u>
SUMMARY.....	1
PREFACE.....	5
CONVERSION FACTORS, NON-SI TO SI (METRIC) UNITS OF MEASUREMENT.....	9
PART I: INTRODUCTION.....	10
Objectives and Scope.....	10
Report Organization.....	11
PART II: BACKGROUND INFORMATION.....	14
Geomorphology and Hydrology.....	14
Meteorological Conditions.....	14
Mobile Bay Sediments.....	15
References.....	16
PART III: DREDGING EQUIPMENT AND OPERATIONAL TECHNIQUES.....	20
Dredging Equipment.....	20
Dredging Techniques.....	21
Daily Log of Test Operations.....	22
Evaluation of Dredging Operations.....	26
Site Bathymetry.....	29
PART IV: HOPPER BARGE, LOADING EQUIPMENT, AND OPERATIONS.....	43
Hopper Barge Description.....	43
Loading Equipment Description.....	43
Hopper Barge Draft Instrumentation.....	44
Visual Draft Measurements.....	44
Loading Characteristics.....	45
PART V: DREDGED MATERIAL AND OVERFLOW CHARACTERISTICS.....	54
In Situ Sediment Characteristics.....	54
Inflow Characteristics.....	55
Characteristics of Material in Loaded Barges.....	58
Overflow Characteristics.....	60
PART VI: SUSPENDED SEDIMENT PLUME TRACKING.....	85
Background.....	85
Methods.....	85
Test Procedures.....	88
Results of Plume Tracking Tests....	90
PART VII: NUMERICAL MODELING OF DREDGED MATERIAL OVERFLOW PLUMES IN MOBILE BAY.....	143
Theoretical Aspects of Plume Model.....	143
Input Data.....	147
Application Using Field Data from Overflow Tests.....	147
Application to Maintenance Dredging.....	149
Application to New Work Dredging.....	150
References.....	151

	<u>Page</u>
PART VIII: SEDIMENT-PROFILING SURVEY.....	197
Methodology.....	197
Results of Sediment-Profiling Surveys.....	205
Summary and Conclusions.....	213
References.....	214
PART IX: ENVIRONMENTAL ASSESSMENT OF BARGE OVERFLOW IN MOBILE BAY, ALABAMA.....	244
Characterization of Mobile Bay Benthic Communities.....	245
Environmental Concerns Associated with Disposal.....	249
References.....	262
APPENDIX A: HOPPER BARGE OPERATIONS DATA.....	A1
APPENDIX B: REPRESENTATIVE MONTHLY BOUNDARY CONDITIONS.....	B1
APPENDIX C: OVERFLOW TEST OPERATIONS.....	C1

CONVERSION FACTORS, NON-SI TO SI (METRIC)
UNITS OF MEASUREMENT

Non-SI units of measurement used in this report can be converted to SI (metric) units as follows:

<u>Multiply</u>	<u>By</u>	<u>To Obtain</u>
cubic feet	0.02831685	cubic meters
cubic yards	0.7645549	cubic meters
degrees (angle)	0.01745329	radians
Fahrenheit degrees	5/9	Celsius degrees or kelvins*
feet	0.3048	meters
gallons (US liquid)	3.785412	cubic decimeters
horsepower (550 foot-pounds (force) per second)	745.6999	watts
inches	2.54	centimeters
knots (international)	0.5144444	meters per second
ounces (mass)	28.34952	grams
pounds (mass)	0.4535924	kilograms
tons (long, 2,240 pounds, mass)	1,016.047	kilograms
tons (2,000 pounds, mass)	907.1847	kilograms
yards	0.9144	meters

* To obtain Celsius (C) temperature readings from Fahrenheit (F) readings, use the following formula: $C = (5/9)(F - 32)$. To obtain Kelvin (K) readings, use: $K = (5/9)(F - 32) + 273.15$.

ENGINEERING DESIGN AND ENVIRONMENTAL ASSESSMENT
OF DREDGED MATERIAL OVERFLOW FROM HYDRAULICALLY
FILLED HOPPER BARGES IN MOBILE BAY, ALABAMA

PART I: INTRODUCTION*

Objectives and Scope

Deepening of the existing main Mobile Bay navigation channel from the entrance channel in Gulf of Mexico waters through the bay to the Port of Mobile, Alabama, has been authorized by Congress. The US Army Engineer District, Mobile, has direct responsibility for dredging and dredged material disposal operations necessary to accomplish this mission. Under the presently legislated mandate, the Mobile District must dispose of all deepening dredged material and future maintenance material at an approved offshore disposal site in the Gulf of Mexico. Based upon the capability of a typical hydraulic dredge to pump 25 to 30 percent solids from the sediments characteristic of Mobile Bay, hopper barges would be required to transport disposal loads with a high water content to the offshore disposal site. Because of the transportation distances and attendant high per-cubic-yard cost of this mode of disposal, a need was perceived by the Mobile District to explore environmentally safe and cost-effective alternatives.

One option not identified in the original feasibility study for the deepening project was barge overflow. The operational objective of overflow would be to achieve increased density of sediments retained within the barges, thereby reducing the total number of barge transits to and from the disposal site. The Mobile District and the US Army Engineer Waterways Experiment Station (WES), in cooperation with the US Environmental Protection Agency (USEPA), and in consultation with other Federal and state agencies, developed a study plan to investigate the barge overflow alternative. The test was designed with two major objectives: to quantitatively determine the amount of overflow required to obtain improved economic loading of the hopper barges and to evaluate the environmental impacts associated with elevated

* Written by Douglas Clarke and Robert Lazor, Environmental Laboratory, WES.

concentrations of suspended sediments and increased sedimentation rates that would result from overflow operations in Mobile Bay.

In brief, the study plan consisted of a multidisciplinary approach involving (a) an engineering solution to a dredge and barge configuration that would enhance the probability of obtaining economic loading, (b) characterization of sediments in situ prior to dredging, in the hydraulic pipeline, in the hopper barge during various stages of loading, and in the actual overflow, (c) numerical modeling of the spatial extent and concentrations or thicknesses of suspended and deposited sediments produced by the overflow, (d) field sampling of suspended sediment plumes to verify the modeling efforts, (e) sediment profiling imagery to provide ground truth for model predictions of sedimentation and to assess acute impacts to the benthos, and (f) an overall environmental assessment based on the above efforts and historical information on Mobile Bay faunal assemblages. The Mobile District contracted a dredge plant solely for the purposes of the field test, so that the tests could be performed under controlled conditions, but simulating as closely as possible a "typical" dredging scenario. Separate tests were run on both maintenance materials and new work deepening materials.

Overflow tests were conducted during the period 2-9 December 1987. The actual dates, times, and tidal conditions under which each test was performed are summarized in Table 1. Three of the eight tests were conducted at a lower bay site, and the remaining five tests took place at an upper bay site. Pertinent data on durations and volumes of overflow and material type are also given in Table 1.

Report Organization

The report is organized into nine parts. The order of presentation is designed to allow the reader to follow a logical sequence of topics covering engineering and environmental aspects of the overall study. Part I defines the objectives of the study. Part II provides brief descriptions of the geographical setting for the study as well as prevailing weather conditions and sedimentary regimes. Part III lists the specifications of the dredge plant and associated equipment used during the overflow tests and describes operational procedures on a test-by-test basis. A description of the specialized equipment used to place dredged material into hopper barges and a characterization of the hopper barge loading process are given in Part IV.

Part V compares sediment characteristics for samples taken in situ, in the pipeline, in the loaded hopper barge, and in the overflow. In Part VI, the methodology for and results of suspended sediment plume tracking efforts are given. Predictions of suspended sediment spatial distribution and concentration, and the short-term sedimentation pattern of overflow sediments for the test cases and hypothetical channel dredging operations, are presented in Part VII. In Part VIII, preoverflow and postoverflow operation comparisons of physical and biological benthic conditions, based on sediment profiling imagery, are depicted. All of the above contributing sources of information, in addition to a summary of the state of knowledge of benthic communities in Mobile Bay, are incorporated into an environmental assessment of the potential consequences of routine overflow disposal operations presented as Part IX.

Interest in barge overflow alternatives for disposal of dredged material is not confined to the Mobile District. The potential economic gains of overflow are substantial. Although overflow operations will involve somewhat different engineering and environmental considerations on a case-by-case basis (e.g., in shallow- versus deep-water systems, in open bodies of water versus restricted waterways), the results reported herein should have relevance to proposed overflow applications elsewhere. It is hoped that these studies will contribute to engineering solutions for environmentally acceptable disposal options adapted to regional conditions.

Table 1
Summary of Barge Overflow Test Conditions

<u>Test Number</u>	<u>Bay Site</u>	<u>Date</u>	<u>Material Type*</u>	<u>Tidal Condition</u>	<u>Overflow Start Time, hr</u>	<u>Overflow Stop Time, hr</u>	<u>Overflow Volume (gal)**</u>
1	Lower	12/3/87	M	Flood	1119	1137	293,824
2	Lower	12/4/87	NW	Ebb	0857	0913	269,330
3	Lower	12/4/87	NW	Flood	1247	1305	362,206
4	Upper	12/6/87	M	Ebb	0943	1021	718,208
5	Upper	12/6/87	M	Flood	1346	1422	673,320
6	Upper	12/7/87	NW	Ebb	0915	0942	696,550
7	Upper	12/8/87	NW	Ebb	0957	1028	837,928
8	Upper	12/9/87	NW	Flood	1459	1556	1,381,445

* M = maintenance dredging material; NW = new work dredging material.

** To convert gallons (US liquid) to cubic decimeters, multiply by 3.785412.

PART II: BACKGROUND INFORMATION*

A basic understanding of the estuarine system as a whole is essential to an environmental assessment as embodied in this report. Biological resources cannot be isolated from the geological, physical, and chemical settings in which they live. A detailed review of nonbiological aspects of the Mobile Bay ecosystem is beyond the scope of this report. The reader is referred to several recent symposia that provide detailed overviews of the current state of knowledge of natural resources of the Mobile Bay estuary (Loyacano and Smith 1979, Lowery 1987). This section is intended to form a framework of information on physical factors important to later discussions of biological topics.

Geomorphology and Hydrology

Mobile Bay is located in southwest Alabama (Figure 1). The major source of freshwater inflow to the bay is derived from the Mobile River system, which is comprised of the Alabama and Tombigbee Rivers. The Mobile River system receives flow from the sixth largest drainage basin in the United States. According to Schroeder (1979), average annual discharge into the bay is approximately 1,750 cu m/sec. In terms of volume, this freshwater discharge ranks fourth among river systems in the United States. Outflow from the bay occurs via Main Pass between Dauphin Island and Fort Morgan Peninsula, and Mississippi Sound between Dauphin Island and Cedar Point. Estimates of annual suspended sediment load entering Mobile Bay range from 2.1 to 8.3 million tons,** with a mean of approximately 4.7 million tons per year (Ryan 1969). Mobile Bay is a relatively shallow estuary, as the majority of the water body is between 1.8 and 3.0 m deep (Figure 2).

Meteorological Conditions

The overall shallowness of the water body in conjunction with relatively long fetches in the directions of prevailing winds are contributing factors to

* Written by Douglas Clarke, Environmental Laboratory, WES.

** A table of factors for converting non-SI units of measurement to SI (metric) units is presented on page 9.

a characterization of Mobile Bay as a "wind-driven" system. This is an important consideration in any attempt to put suspended and deposited sediment effects on biotic components into perspective. Organisms inhabiting the Mobile Bay estuary are exposed to resuspension events brought on by natural phenomena (gales and hurricanes) as well as by anthropogenic activities such as navigation channel dredging, prop wash and bow wave action from vessel traffic, and commercial and recreational shrimp trawling. In addition to sediment load inputs from riverflows entering the bay, prevailing wind/wave-generated turbulent forces are an important determinant of ambient suspended sediment concentrations. These factors are addressed in more detail in Part IX.

Wind conditions for the Mobile Bay system have been described by Chermock (1974) and more recently by Schroeder and Wiseman (1985). The directions of prevailing winds in the Mobile Bay area are highly variable, although seasonal patterns emerge. The following summary is taken from Schroeder and Wiseman (1985). In early spring (March), winds shift largely between southeasterly, northerly, southerly, and easterly components. Southeasterly winds clearly dominate during the months of April and May, with southerly winds also contributing during May. During summer (June and July) prevailing winds shift to southerly and southwesterly components, then return to easterly, southeasterly, and southerly winds in August. With the advent of fall, beginning in September, the winds shift again to northerly and northeasterly components. In October and November a consistent pattern of northerly wind predominance occurs, with some additional influence of northeasterly and easterly components. The winter months are clearly dominated by northerly winds. With respect to velocities, highest mean wind speeds occur in January, December, October, March, November, February, and April (between 8.1 and 7.4 knots in descending order). July and August are characterized by lowest mean wind velocities (5.2 and 5.3 knots, respectively), whereas intermediate mean velocities (6.0 to 6.8 knots) are seen during May, June, and September.

Mobile Bay Sediments

Two major studies have documented the sedimentary environment of Mobile Bay. The first was a description of sediment types and distribution reported by Ryan (1969). Based on 190 grab samples, Ryan produced a map that characterized the upper several inches of sediment throughout the bay. In 1980,

Isphording and Lamb prepared a similar map of sediment types and distribution based on 237 sediment samples. Figure 3 illustrates the basic pattern of the Mobile Bay surficial sediment regime as described by Isphording and Lamb (1980).

Sands are found near the periphery of the bay in waters generally shallower than 4 ft. Central portions of the bay are characterized by finer sediments. The sandy margins grade rapidly into clay components with increasing distance from the shorelines. The southern, lower basin of the bay contains wide expanses of clay and silty clay bottoms. The deeper portions of the upper bay show a more complex sediment distribution, reflecting the dynamic influence of the multiple outlets of the Mobile, Tensaw, Blakeley, and Apalachee Rivers. Likewise, the area adjacent to the main pass to the Gulf of Mexico is influenced by strong tidal currents.

The upper and lower bay overflow test sites are located in variable mixed sediment and predominantly silty clay areas, respectively. The differences in sediment characteristics at each site will be referred to in later sections of this report.

References

- Chermock, R. L. 1974. The environment of offshore and estuarine Alabama. Information Series 51. Geological Survey of Alabama, University, AL.
- Isphording, W. C., and Lamb, G. M. 1980. The sediments of Mobile Bay: A report for the Alabama Coastal Area Board. Dauphin Island Sea Lab Technical Report 80-002. Dauphin Island, AL.
- Loyacano, H. A., and Smith, J. P., eds. 1979. Symposium on the natural resources of the Mobile Estuary, Alabama. Alabama Coastal Area Board, Mississippi-Alabama Sea Grant Consortium, US Fish and Wildlife Service. Published by US Army Engineer District, Mobile, Mobile, AL.
- Lowery, T. A., ed. 1987. Symposium on the natural resources of the Mobile Bay estuary. Alabama Sea Grant Extension Service, Mobile, AL.
- Ryan, J. J. 1969. A sedimentological study of Mobile Bay, Alabama. Contribution 30. Florida State University Sedimentological Research Laboratory, Tallahassee.
- Schroeder, W. W. 1979. Dispersion and impact of Mobile River system waters in Mobile Bay, Alabama. Water Resources Research Institute Bulletin 37. Auburn University, Auburn, AL.
- Schroeder, W. W., and Wiseman, W. J. 1985. An analysis of the winds (1974-1984) and sea level elevations (1973-1983) in coastal Alabama. Mississippi-Alabama Sea Grant Consortium Publication No. MASGP-84-024, Ocean Springs, MS.

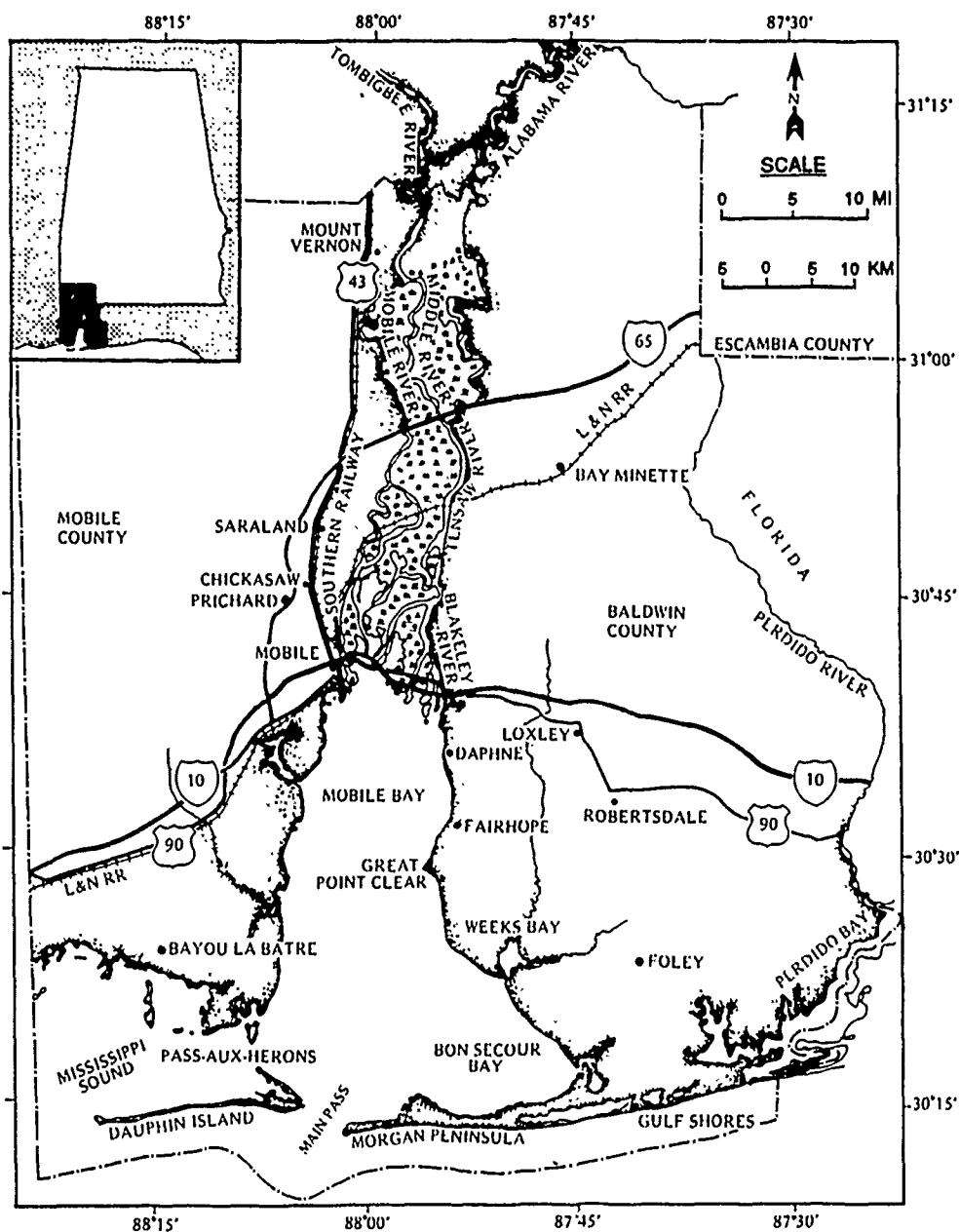


Figure 1. Location and landmarks of the Mobile Bay estuary

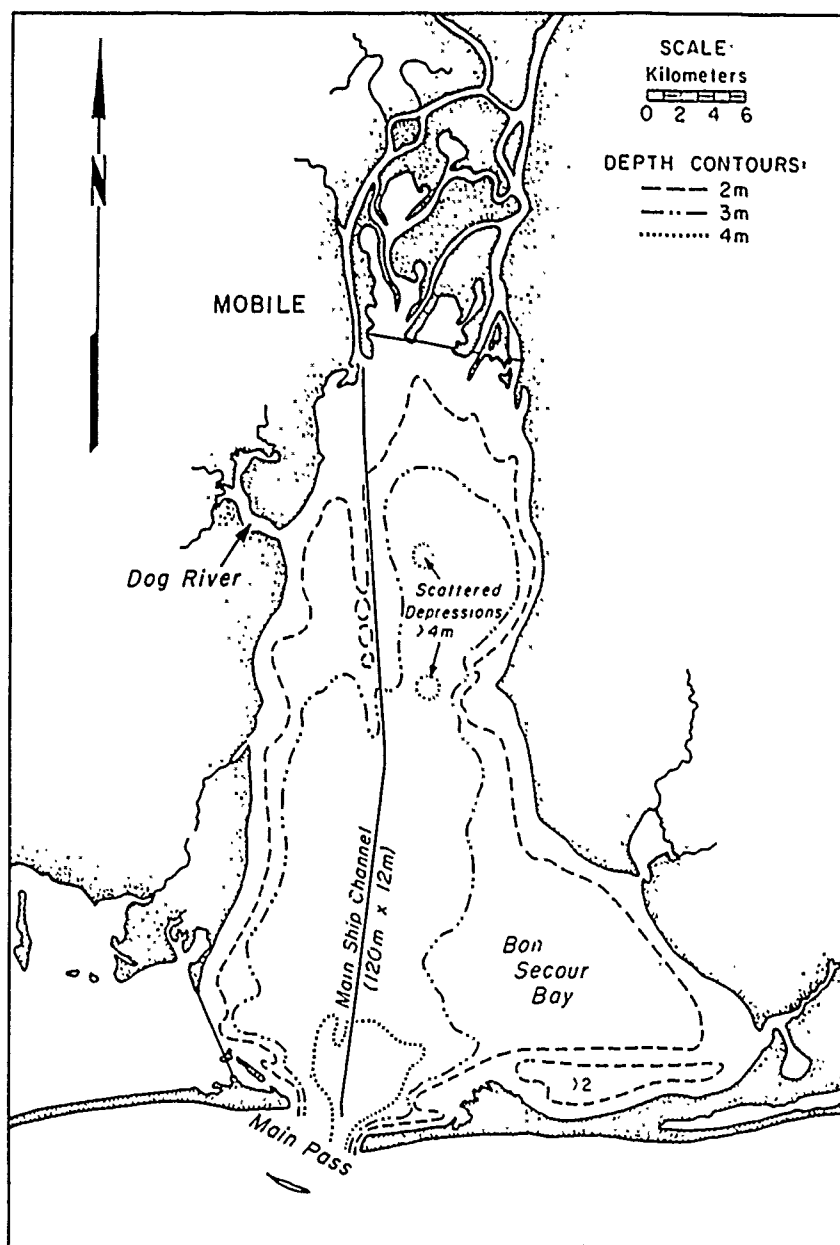


Figure 2. Bathymetry of Mobile Bay (from Schroeder 1979)

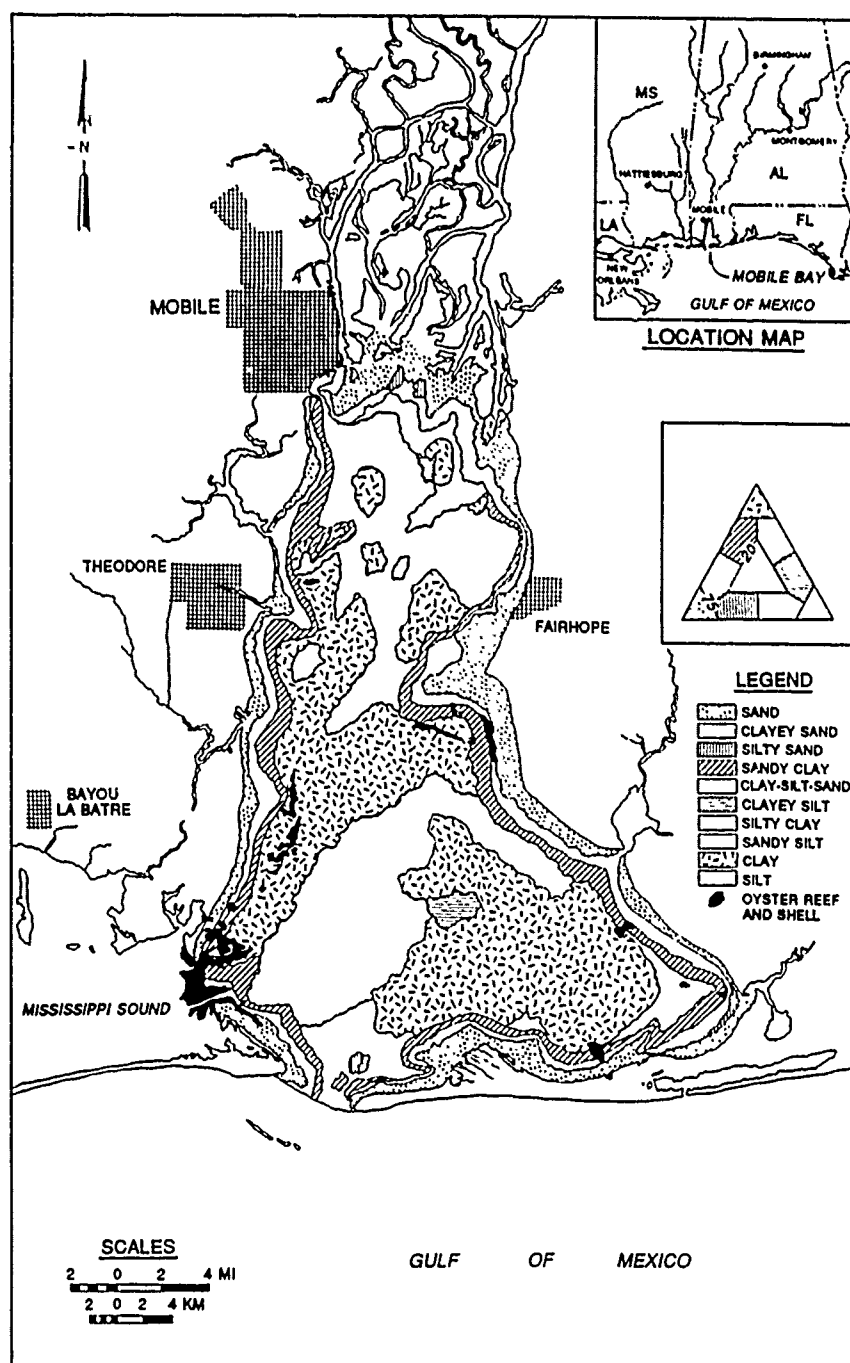


Figure 3. Distribution of sediment types in Mobile Bay (from Isphording and Lamb 1980)

PART III: DREDGING EQUIPMENT AND OPERATIONAL TECHNIQUES*

Dredging Equipment

Although the dredging conducted in this study was performed in an "experimental" mode, the dredging equipment and technique used were typical of those commonly used in maintenance and new work dredging operations for the Mobile Bay ship channel. Engineering modifications were confined to the barge loading and monitoring equipment as described elsewhere in this report. The employment of typical dredging equipment was intentional in order that the results of the study would be applicable to future dredging operations. A primary objective of the operational dredging phase of the study was to maximize the efficiency of the dredge in pumping the highest practical density of solids. Individual tests were devoted to either maintenance or new work materials using optimal techniques for each.

Contracting the required dredging equipment was planned in consideration of the study objectives. Contract specifications included equipment performance criteria to maximize specific gravities of the slurry being pumped, to minimize excessive pumping of low solids concentrations of slurry, and to discharge slurry into the hopper barges at the slowest possible velocity to enhance settling of materials within the barges.

The successful bidder for the dredging tests was T. L. James and Company, Inc., of New Orleans, LA. In addition to cost and availability considerations, the cutterhead dredge *George D. Williams* (Figure 4), was selected to perform these tests because it represented a type of dredge most likely to be used in projected Mobile Bay dredging operations. The pertinent specifications of the *George D. Williams* are as follows:

- Overall hull length - 165 ft
- Ladder length - 69.5 ft
- Hull width - 36 ft
- Average draft - 8 ft
- Hull depth - 10.5 ft
- Main pump power - 4,000 hp variable speed
- Ladder pump power - 600 hp constant speed
- Suction pipe size - 26 in. inside diameter (I.D.)
- Discharge pipe size - 24 in. I.D.
- Cutter configuration - 5 blades, 5 ft long, 7-ft diameter, nonserrated basketcutter

* Written by Glynn Banks, Hydraulics Laboratory, WES.

Cutter power - 500 hp constant speed (25.6 rpm)
Spud configuration - conventional (nonsliding) with 17-ft spacing
Effective swing configuration - for a swing angle of 40 deg to
each side of center line, the dredge has an effective length of
221.5 ft at a 40-ft digging depth, thus sweeping a channel
width of 285 ft

Three dredging consultants were tasked with analyzing the equipment provided by the successful bidder in order to recommend the most efficient operational configuration of the pumping system. These expert consultants were Messrs. Thomas Turner, Charles Woodberry, and Carl Hackenjos. Their consultation was used throughout the field tests to develop the most efficient yet practical modes of both maintenance and new work dredging. T. L. James and Company officials and staff cooperated fully with the consultants and District personnel in all aspects of the project.

A conventional flat-deck barge (35 × 195 × 8 ft) was customized by T. L. James and Company to provide a loading and distribution arrangement to discharge the dredged slurry into 4,000-cu yd split-hull hopper barges. Approximately 1,300 ft of steel pontoon line utilizing typical ball joints was attached to the 24-in. discharge line at the stern of the dredge. The pontoon line terminated at the customized discharge barge nicknamed the "spider barge." A manifold arrangement using three 15.375-in. I.D. branch pipes was attached to the tapering discharge line (Figure 5). Internal diverter plates were installed into the tapered discharge line to equalize distribution of solids into the three branch pipes. Each 15.375-in. I.D. branch pipe was further divided into two 12-in. I.D. downcomers of flexible reinforced vinyl hose (Figure 6). The flexible hose allowed the discharge points to be submerged during most of the filling cycle in order to minimize turbulence within the barge. The "spider barge" arrangement is shown in Figure 7.

Dredging Techniques

Both maintenance materials (predominantly fine, silty muds) and new work materials (soft clays and sandy clays) were dredged in this study. It was anticipated that maintenance materials could be transported satisfactorily at pipeline velocities of approximately 12 fps whereas new work materials would require approximately 18 fps. The latter velocity is an estimate for most cutterhead dredges of this size when operating with relatively short pipeline lengths. A dye injection system was used at the start of operations on

December 3, 1987, to calibrate the pipeline velocity meter. Dye was injected into the suction pipe of the dredge immediately on the inflow side of the main dredge pump. The velocity was calculated by dividing the length (1,442 ft) of the pipeline from the pump to a sampling valve on the spider barge by the time required for the dye to traverse this length. A Polysonics velocity gage was calibrated based on the dye test velocity of 12.53 fps as a reference for flow measurements during all ensuing tests.

From historical records of soundings made after routine maintenance dredging operations (Figures 8 and 9), it was concluded that most sediments down to -47 mllw elevation were of a maintenance type. (MLLW refers to Mean Low Low Water Datum, which is equivalent to the National Geodetic Vertical Datum (NGVD) plus 0.47 ft.) These records were also used to determine the areas where the depth of cut was equal to or greater than the cutterhead depth. For maximum efficiency, the suction pipe located within the cutterhead was buried in the bottom sediments. These materials are generally silty muds that are easy to dredge and transport hydraulically. Maintenance dredging tests were conducted by dredging 200- to 285-ft channel widths to an elevation of -47 mllw. With the exception of Test 8, digging depths for new work material tests were set at -52 mllw in the same reaches that had been previously dredged at -47 mllw for the maintenance dredging tests. Digging depth for Test 8 was -57 ft mllw. All tests were scheduled to avoid, when possible, the passage of large ships while the dredge was in operation. Test times were predetermined to coincide with predicted flood and ebb tidal conditions at both sites.

Daily Log of Test Operations

Test 1 - December 3, 1987

Maintenance material - Lower bay site (east side of channel adjacent to navigation Beacon 44)
Digging width, 200 ft; digging depth, -47 mllw

Test operations began at 10:32 a.m. by priming the pump with clear water. At 10:35 a.m. dredging operations were under way and maintenance materials were being delivered to the 4,000-cu yd hopper barge. The barge was filled to the point of overflow at 11:19 a.m. Digging operations continued until 11:33 a.m., and at 11:35 a.m. the dredge pump was shut down, allowing 5 min for flushing the pipeline with clear water. A 2- to 3-min pipeline

flushing cycle was also used on all subsequent tests. The barge filling time of 48-min confirmed that a 12-fps average velocity had been achieved for transport of maintenance materials. Pump speed for this test was set at 425 rpm.

The dredged area covered in this test consisted of 13 advances of the digging sweep for a theoretical 78 ft of forward progress of the dredge. The digging spud did not reach hard bottom on each "set" and slipped an average of 3.1 ft backward on each of the 13 advances. This pattern of slippage was observed on all subsequent tests due to the soft nature of the sediments that surrounded the pivot point of the spuds. The positions in the swing cycle at which the spuds were dropped to advance the dredge were adjusted to compensate for this pattern of slippage. A full cutterhead "bite" was achieved on Tests 2 through 8.

Test 2 - December 4, 1987

New work material - Lower bay site
Digging width, 200 ft; digging depth, -52 mllw

Test operations began at 8:27 a.m. with a pump speed of 600 rpm, which corresponded to a pipeline velocity of 16 fps. Dredging operations were conducted in the same area of the channel that had been previously swept of maintenance sediments during the preceding dredging test.

Overflow of the hopper barge occurred at 8:57 a.m. The barge loading chart for this test indicated a definite leveling off in displacement of the barge, slightly more abrupt than in the previous maintenance test.

The advance of the dredge in this test as denser new work materials were encountered was 40 ft.

Test 3 - December 4, 1987

New work material - Lower bay site
Digging width, 200 ft; digging depth, -52 mllw

Test operations were conducted in the same portion of the channel that had been cleared of maintenance sediments the previous day. Pumping operations began at 12:18 p.m. with a pipeline velocity of approximately 16 fps. Overflow of the dump scow was reported at 12:47 p.m. Negligible increase in barge displacement was recorded after overflow.

Although dredging operations were not affected by large swells and high winds, suspended sediment sampling was not conducted due to hazardous working conditions on the survey vessels.

Test 4 - December 6, 1987

Maintenance material - Upper bay site (east side of channel adjacent to navigation Beacon 66)

Digging width, 285 ft; digging depth, -48 mllw

Based on sediment coring logs, it was anticipated that maintenance sediments at this site would have more sands than the sediments dredged at the lower bay test site. Pumping operations began at 9:07 a.m. with a pump speed of 425 rpm, the same speed that was used for maintenance materials at the lower site. Due to the higher percentage of sands in the sediments here, the pump speed had to be increased to 500 rpm to reduce the possibility of plugging the discharge line. The specific gravity of the slurry varied greatly during this test, thus influencing the pipeline velocity. The average maintenance sediment target velocity of 12 fps could not be maintained throughout the test.

Overflow of the hopper barge began at 9:43 a.m., and the loading curve depicting the scow displacement leveled off rapidly as in the previous tests. Total advance of the dredge for this test was 46 ft.

Test 5 - December 6, 1987

Maintenance material - Upper bay site

Digging width, 285 ft; digging depth, -48 mllw

This test was a continuation of the same track line that had been used in the previous test. This test was initiated prior to the predetermined flood tide condition due to impending ship traffic arrivals and departures.

Due to the problems encountered in maintaining a steady specific gravity of the slurry in the previous test, the pump speed was increased from 500 to 525 rpm. Dredging operations began at 1:13 p.m., followed by barge overflow at 1:46 p.m. After a total advance of 68.3 ft, dredging operations ceased at 2:16 p.m. with only a slight detectable increase in barge load after overflow.

Test 6 - December 7, 1987

New work material - Upper bay site

Digging width, 240 ft; digging depth, -53 mllw

This test was conducted in the area of the channel that had been previously cleared of maintenance sediments the previous day. The width of the dredge swing was reduced from 285 to 240 ft to ensure that only new work materials would be encountered.

A pump speed of 600 rpm was initially used in this test because that speed corresponded to the 16-fps pipeline velocity that had been used in the

new work material dredge test at the lower site on December 4, 1987. As dredging operations began at 8:46 a.m., it became apparent that the pipeline velocity was too slow to safely convey these denser sediments. When the pump speed was increased to 625 rpm, a steady pipeline velocity was achieved while pumping a rather consistent slurry of 1.5 specific gravity. A slurry of this high density is not usually maintained in normal dredging operations due to the chance of plugging the discharge lines.

Overflow of the hopper barge began at 9:15 a.m., and pumping was stopped at 9:40 a.m. after a total dredge advance of 29.5 ft.

The barge load curve depicted a larger total displacement than in some of the previous tests due to the higher density of the new work materials and greater average specific gravity of the slurry being pumped. The load curve leveled off rapidly as in the preceding tests.

Test 7 - December 8, 1987

New work material - Upper bay site
Digging width, 240 ft; digging depth, -53 mllw

Weather and sea conditions were extremely severe on this date. No sediment plume sampling boats could be used, and the offshore crewboat could not dock beside the dump scow due to extreme swells. Since winds were gusting to greater than 35 knots, the ladder pump on the dredge was used to pump water prior to test operations to provide stability to the floating discharge pipeline.

At 9:30 a.m. the barge dumped excess water that had been pumped for pipeline stability reasons, and dredging operations began immediately. Using the same 625-rpm pump speed as in the previous new work material test, the dredge filled the hopper barge to overflow capacity by 9:57 a.m. Dredging operations ceased at 10:25 a.m. after a total advance of 39 ft. Sea conditions were sufficiently rough during the barge-loading cycle that, once overflow occurred, periodic surface waves within the barge were set in motion by large swells rocking the spider barge and tethered hopper barge. This caused the overflow to occur in pulses rather than in a steady, even flow.

Test 8 - December 9, 1987

New work material - Upper bay site
Digging width - 240 ft; digging depth, -57 mllw

A decision was reached to extend the period of overflow during this test in order to determine if longer overflow times would show any improvement in loading characteristics and to generate a larger suspended sediment plume.

The dredge was positioned in the channel in the area that had been previously cleared of maintenance sediments on December 6, 1987. Pumping operations began at 2:28 p.m. Higher cutterhead-motor amperages than in all previous tests confirmed that the new work material at this deeper depth of 57 ft was of a denser nature than all other materials encountered. Overflow of the hopper barge began at 2:59 p.m., and pumping was continued until 3:52 p.m. The total dredge advance was 61.7 ft, which occurred in 10 forward advances of the digging spud.

Loading curve data for the hopper barge depicted minor fluctuations in barge displacement during the overflow operation, but no strikingly significant increase in barge load was recorded by allowing overflow for approximately 1 hr as compared to previous overflows of 15 to 30 min.

Evaluation of Dredging Operations

Pumping times, average pipeline flow rates based on time to fill the 4,000-cu yd hopper barges, and average pipeline velocities based on these associated flow rates for the 24-in.-outside diameter discharge line are summarized in Table 2. This table also provides an estimate of the total overflow volume based on the average flow rate prior to overflow and the total time of pumping after overflow started. These calculations of overflow volumes do not take into account any slight leakage that occurred in the hinged joint seals on the barge above the deck level of the barge. If such leakage had occurred, the amount was in all probability insignificant.

Procedures that would have allowed the dredge to cut at least a 275-ft-wide channel could potentially reduce the overall time of stepping-ahead based on the 17-ft distance between the spuds, the 5-ft length of the cutter, and the overall effective length of the dredge when digging. By reducing the amount of time spent in pumping low concentrations of slurry and by ensuring that the suction pipe intake is always buried in material, increases in the overall average specific gravity of slurry pumped for a dredging cycle will occur. All tests were conducted with this in mind given the available data characterizing the channel cross-sectional distribution of maintenance versus new work materials. A clean-up sweep or extra swing of the suction-pipe was not necessary when dredging maintenance materials due to the ease and efficiency of suction intake of the soft marine deposits.

Maintenance operations were conducted in a "swing and step" fashion with a theoretical forward advance step of 6 ft, thus providing a full length of the cutterhead to be exposed in the material to be dredged. A typical swing cycle for maintenance dredging consisted of starting at 10 deg on the port side of the channel center line and commencing the swing using the starboard spud. For this particular dredge, the starboard spud served as the walking spud. When the dredge's gyrocompass reached a heading of 10 deg to the starboard side of the center line as the dredge swung in the starboard direction, the port spud (working spud) was dropped and the walking spud raised. The dredge would then continue to swing toward the starboard direction to the edge of the cut. Upon reaching the starboard corner of the cut, the leverman would reverse the swinging process and swing the dredge in the port direction to the port corner of the cut, at which time he would reverse swing direction again. While swinging in the starboard direction, the leverman would stop the swing when the dredge gyrocompass reached 10 deg to the port side of the channel center line. At this point, the starboard spud was dropped and the port spud raised, thus advancing the dredge the desired 6 ft.

The same cycle was employed for new work materials, except that the advance angle was generally reduced to 7 deg to produce an actual forward advance of 4.5 ft. The forward advance of the dredge for the new work material operations was set at 4.5 ft to allow for some collapse of the vertical face of the dredged cut. The swing speed was adjusted as required throughout each test to optimize the specific gravity with the constraint of avoidance of an overload in the available power to the electric cutterhead drive motor, or the electric-drive swing winches.

Examination of production meter data for each of the tests (Figures 10 and 11) indicates that an inverse relationship between the instantaneous specific gravity of the slurry and the instantaneous pipeline velocity was present during all tests. This pattern was more consistent among new work tests due to the denser, more cohesive nature of the new work material. A less consistent relationship was observed for the maintenance tests. Large spikes in velocity records during all tests are indicative of low concentrations being conveyed during the stepping process of advancing the dredge.

When the predredge survey records and the corresponding production meter readings for each test condition are considered, it becomes evident that extremely low sediment concentrations were pumped during a substantial portion of the dredging swing cycle. For operations in maintenance material, slightly

lower concentrations were observed when the cutterhead was in the center of the channel, where less material was available. Thicker deposits of maintenance materials were observed near the toe of the side slopes of the channel. Deposit thickness was not a factor for new work tests. The density profiles also depict a period of low sediment concentration flow during the stepping-ahead process of the dredge. These periods of low production efficiency typically approximate 50 percent, but may vary between 15 and 75 percent.* The dredge efficiency is generally lowest when dredging maintenance material that consists of fluid sediments.

Based on these observations, the total amount of time involved in pumping low-sediment concentration waters could potentially be reduced by modification of the dredge's spud arrangement and hoisting machinery. An alternative to major dredge design modifications, suggested by the Mobile District, would be the installation of an automatic low-density discharge system to exclude low-sediment density slurry from entering the barge. This system would incorporate a "Y" or similar type valve arrangement to shunt waters with a low sediment concentration overboard and direct only high-sediment content waters to the barge. In principle, this system would employ continuous monitoring of the flow concentration to the barge by means of a nuclear density transmission gage. The gage would be located near the end of the pipeline to detect changes in flow density immediately before release to the barge. When a decrease in flow density is detected, the Y valve would automatically be triggered to open and direct the low-sediment content waters overboard. When the flow density increases to a specified threshold, the Y valve would close and allow flow to the barge to resume.

To derive estimates of the potential improvement in barge loading that could be obtained if an adequate low-density water shunting system could be designed, production records for the eight individual tests were examined. Based on the information collected on barge filling times, barge capacity, and approximations of the time that water with virtually no suspended solids was being pumped, the volume of low-density water placed in each barge load was estimated. The estimates of percent of hopper barge capacity lost to low-density waters are given in Table 3. Although these values are based on rough approximations, they give some indication of the improvement in loading that

* T. M. Turner. 1984. Fundamentals of hydraulics dredging. Cornell Maritime Press, Centreville, MD.

could be realized if the water with no suspended solids, i.e., a specific gravity of 1.0 g/cm^3 , had been excluded from the barges. The calculated percentages of barge volume available for higher density waters with an operating shunt system for the three maintenance tests are 48, 28, and 17 percent with an average of 31 percent. Values for the new work material tests are 30, 24, 21, 26, and 10 percent with an average of 22 percent.

Among the three maintenance material tests, the first test, as shown in Table 3, is atypical in that 21 of the 44 min from test start to the point of overflow was spent pumping low-density slurry. This resulted in the singularly high value of 48 percent of barge capacity lost to low-density flow. If the high value of 48 percent is discounted, the maintenance material test average value would be 23 percent. Likewise, if the low value of 10 percent is ignored in the calculation of lost barge capacity for the new work material tests, the value becomes 25 percent. The low value of 10 percent was also atypical due to the greater depth of cutterhead placement in this particular test. During this test the collapse of material in front of the cutterhead essentially buried the suction aperture, thereby excluding excessive water intake.

These indirect estimates of potential loading improvements result from exclusion of low-density flows (i.e., specific gravity less than 1.1 g/cm^3) from discharge into the barges. If overboard discharges of slurries of density higher than 1.0 g/cm^3 were allowed, even better loading characteristics would be obtainable (see Part IX, which analyzes impacts due to overboard discharges of slurries). Improved loading would incrementally increase as higher density slurries were shunted from the barges. The Y-valve discharge system merits further investigation due to the potentially significant savings it may afford. Additional engineering and dredging modifications to the equipment and techniques employed in these tests, in combination with the Y-valve apparatus, could maximize the probability of improved loading. For example, provision of wider cutterhead sweeps of the channel cross section and a decrease in the length of pipeline between the dredge and the barge could contribute to improved loading.

Site Bathymetry

A detailed hydrographic survey was conducted prior to and at the completion of each overflow test at both the upper and lower bay sites. Vertical

control (survey reference elevation) for the lower bay site was provided by a fixed gage (BN 310) located at the mouth of East Fowl River, Alabama, for both the predredging and postdredging surveys. Vertical control for the upper bay site was provided by a recording tide gage located on the navigation Beacon 66 pile cluster for both surveys.

The surveys were taken using an automated gyrographic surveying system, with range/range positioning conducted by Pyburn and Odom, Inc. The soundings were obtained by a digital depth sounder (ECHOTRAC, Model DF 3200) with a single-frequency, 24-kHz transducer. This frequency is used by Corps Districts to survey channels where low-density suspensions known as fluff or fluid mud are found. Although the Fathometer was calibrated each day of the survey by using a speed-of-sound meter, the plotted elevations may vary slightly due to bottom density changes and localized siltation of the water column in the immediate vicinity of the dredging operation.

Horizontal control for these surveys was referenced to the Alabama State Plane Coordinate system (West Zone). The baseline for the lower bay site surveys was computed to the alignment between the Front and Rear Range Lights of Mobile Middle Bay Light (Figures 12 and 13). The plotted stations are referenced to the Front Range Light of the Mobile Middle Bay Light, as determined by Pyburn and Odom, Inc. Station numbers increase in the southerly direction from 0+00 at the Front Range Light.

The baseline for the upper bay test site surveys was measured along the designated center line of the main Mobile Bay ship channel (Figures 14-15). The stations shown are referenced to the Front Range Light in upper Mobile Bay with the same type of numbering system as was used at the lower bay site.

Plots of the predredging and postdredging surveys for both test sites are shown in Figures 12-15. Cross line data (survey lines perpendicular to the channel center line) were taken at 100-ft intervals across the test areas. Profile lines (survey lines parallel to the channel center line) were run as required to supplement the cross line data due to limited dredge advance distances for each test operation. Cross line data from historical and predredge surveys were plotted to determine the type of material (maintenance versus new work) to be encountered during a given test. This direct comparison allowed an estimate to be made of the lowest elevation of maintenance sediments. Previous maintenance dredging operations had incidentally removed small deposits of new work material in some channel sections, thus creating the somewhat variable maintenance elevations noted during the overflow tests.

Table 2
Summary of Operating Times, Flow Rates, and Volumes for Hopper
Barge Overflow Tests Conducted in Mobile Bay, Alabama

Date	Test No.	Material Type*	Test Site**	Dredging Start Time	Overflow Start Time	Dredging Stop Time	Pumping Stop Time	Overflow Stop Time	Average Flow Rate gal/min	Average Velocity fps	Total Slurry gal	Total Overflow Volume gal
12/3/87	1	M	L	1035	1119	1133	1135	1137	18,364	13.0	1,101,840	293,824
12/4/87	2	NW	L	0827	0857	0905	0907	0913	26,933	19.1	1,077,320	269,330
12/4/87	3	NW	L	1218	1247	1258	1300	1305	27,862	19.8	1,170,204	362,206
12/6/87	4	M	U	0907	0943	1013	1015	1021	22,444	15.9	1,526,192	718,208
12/6/87	5	M	U	1310	1346	1414	1416	1422	22,444	15.9	1,481,304	673,320
12/7/87	6	NW	U	0846	0915	0937	0940	0942	27,862	19.8	1,505,548	696,550
12/8/87	7	NW	U	0930	0957	1022	1025	1028	29,926	21.2	1,645,930	837,928
12/8/87	8	NW	U	1428	1459	1550	1552	1556	26,065	18.5	2,189,460	1,381,445

* M = maintenance material; NW = new work material.

** L = lower bay site; U = Upper Bay site.

Table 3

Evaluation of Mobile Bay Hopper Barge Overflow Tests - Diversion of
Low-Density Pipeline Slurries

Test No.	Material*	Site**	Time to Overflow min	Approximate Low-Density		Average Flow Rate gal/min	Approximate Low-Density Pumped Volume cu yd	Estimated Loss of Barge Capacity to Low- Density Inflows	
				Pumping Time min				Density Inflows percent	
1	M	L	44	21		18,364	1,910		48
2	NW	L	30	9		26,933	1,200		30
3	NW	L	29	7		27,862	966		24
4	M	U	36	10		22,444	1,111		28
5	M	U	36	6		22,444	667		17
6	NW	U	29	6		27,862	828		21
7	NW	U	27	7		29,926	1,037		26
8	NW	U	31	3		26,065	387		10

Note: Low-density inflows defined herein as equal to or less than a specific gravity of 1.0 g/cm³. Time to overflow values were measured during each test. Low-density pumping time values were estimated from production charts for each test. Average flow rates were calculated as the barge capacity divided by the time required to fill the barge to the point of overflow for each test. Low-density pumped volume was estimated as the product of the low-density pumping time and the average flow rate, converted to cubic yards. The estimated loss of barge capacity was then calculated as the low-density pumped volume divided by the actual barge capacity (4,020 cu yd), expressed as a percentage.

* M = maintenance material; NW = new work material.

** L = lower bay site; U = upper bay site.

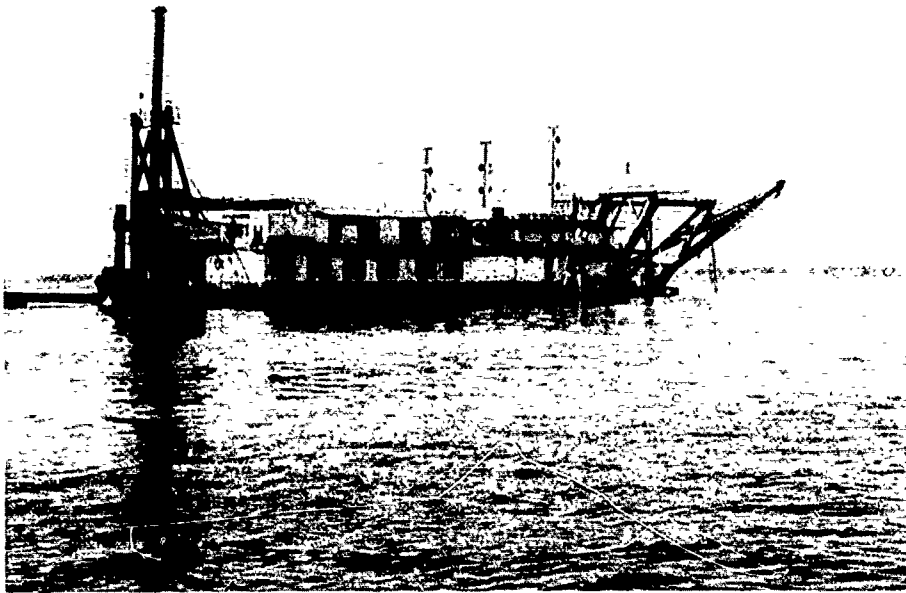


Figure 4. Cutterhead dredge, *George D. Williams*

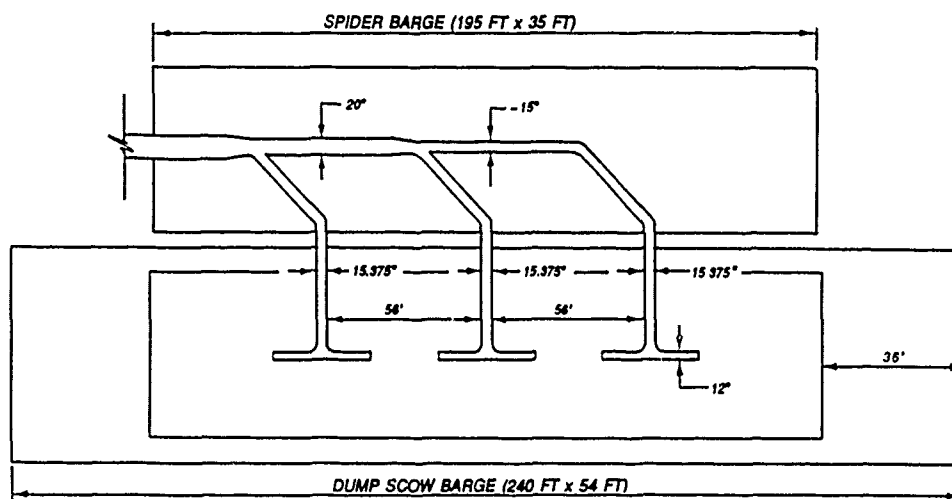
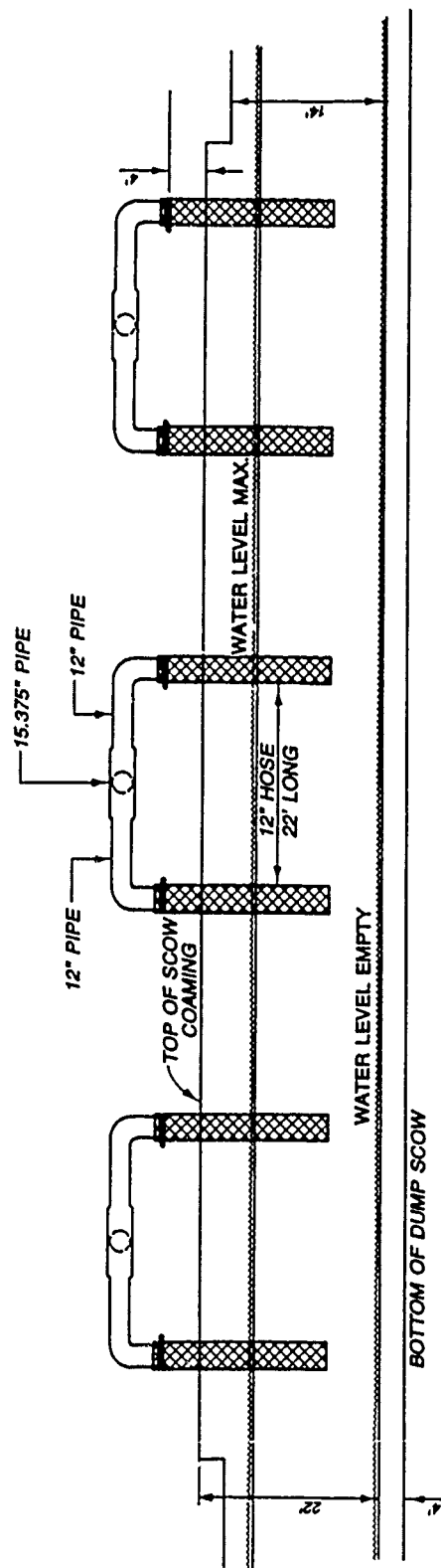


Figure 5. Manifold arrangement on the spider barge



ELEVATION VIEW

Figure 6. Flexible hose dispersion system

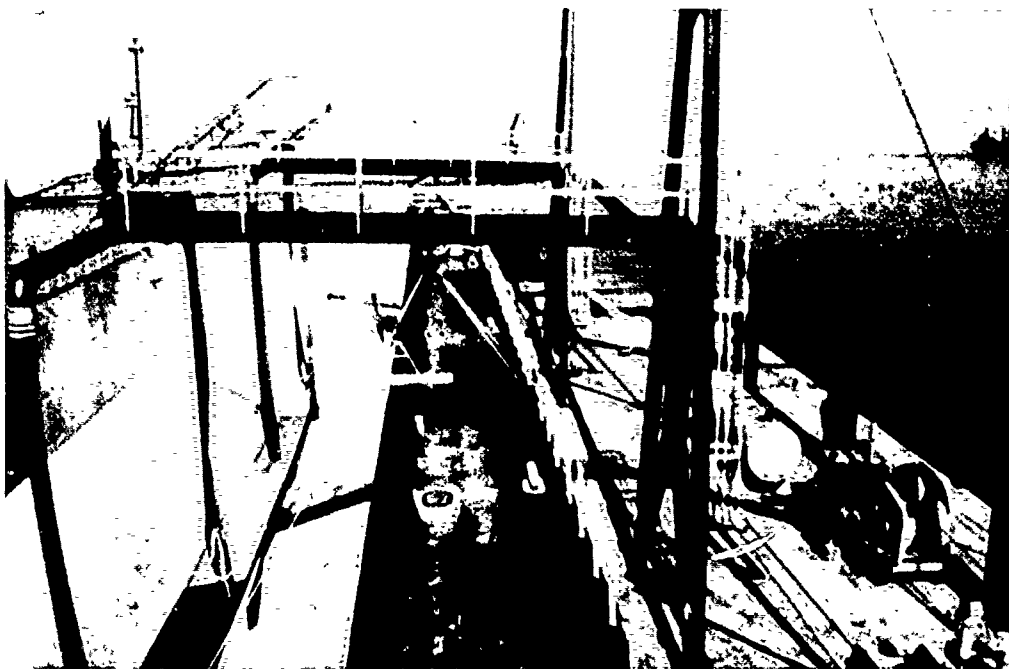


Figure 7. Dump scow and spider barge

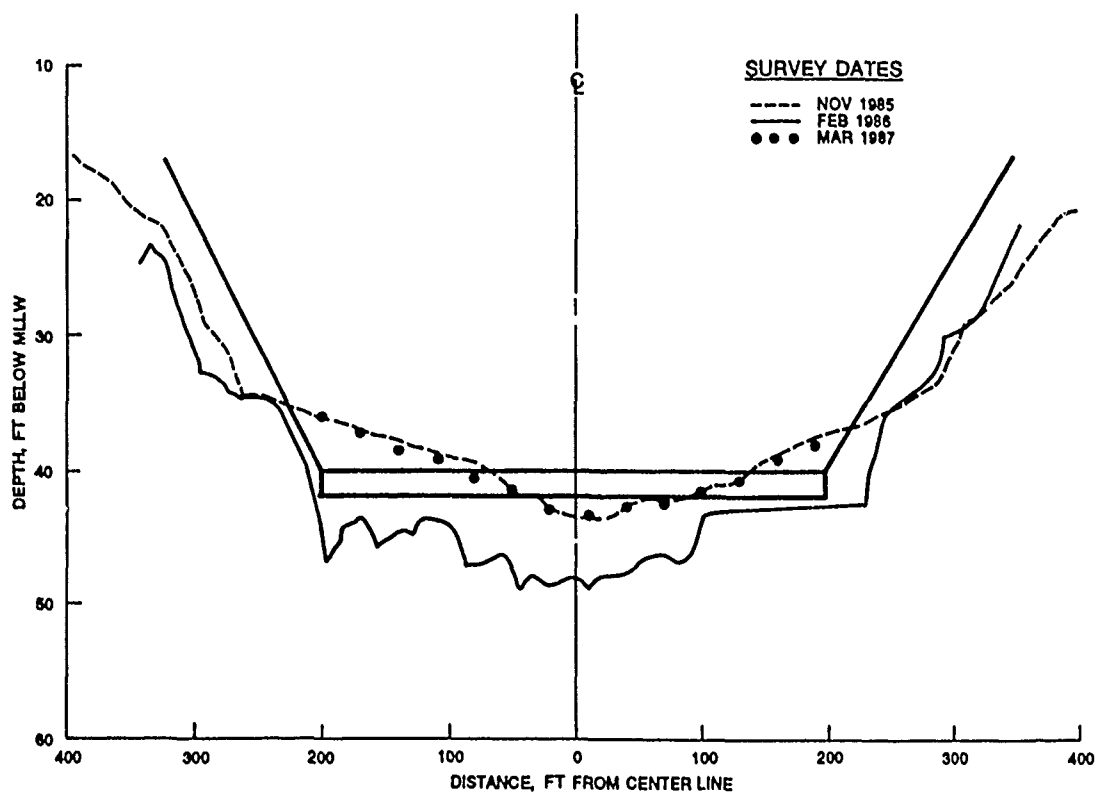


Figure 8. Historical after-dredging surveys - Sta 1027+50

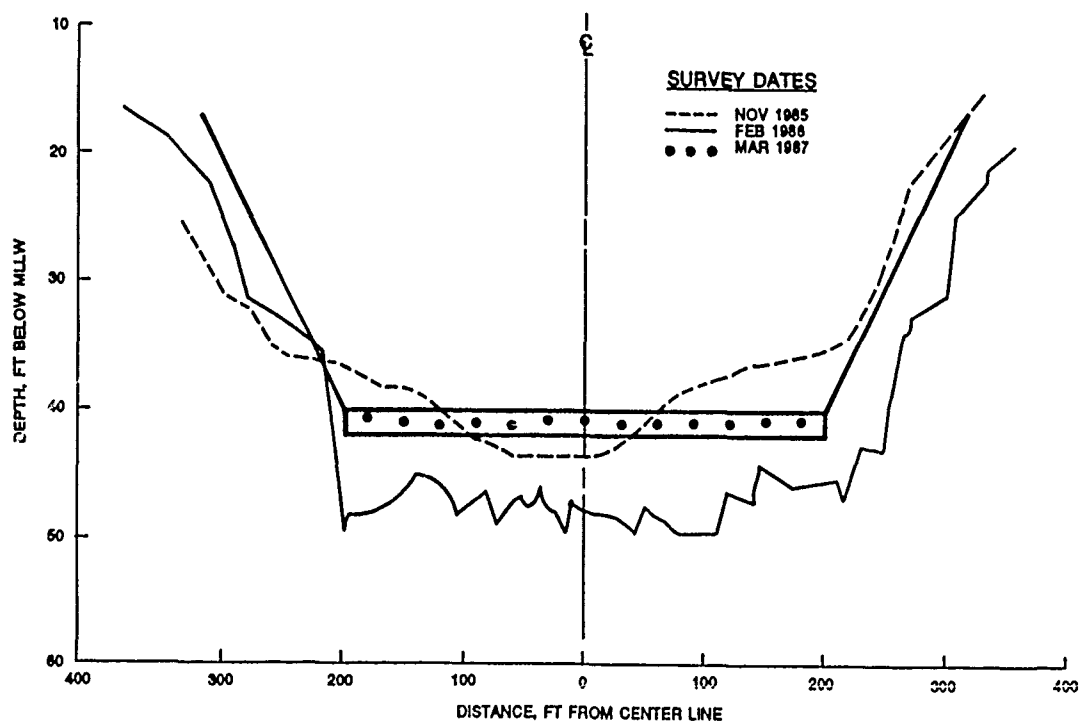


Figure 9. Historical after-dredging surveys - Sta 495+00, upper site near Beacon 66

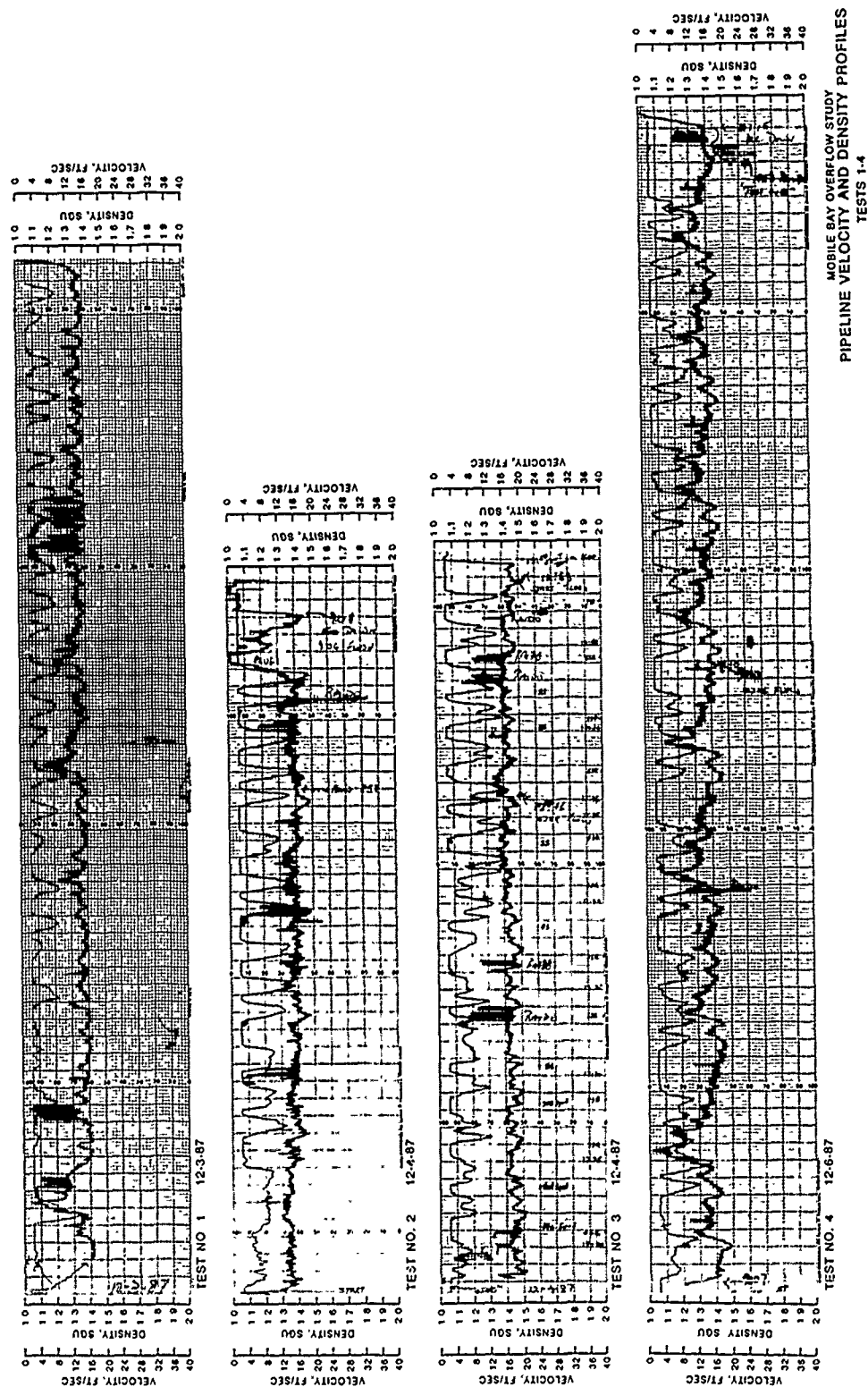


Figure 10. Pipeline velocity (fps) and density (specific gravity units) profiles, Tests 1-4

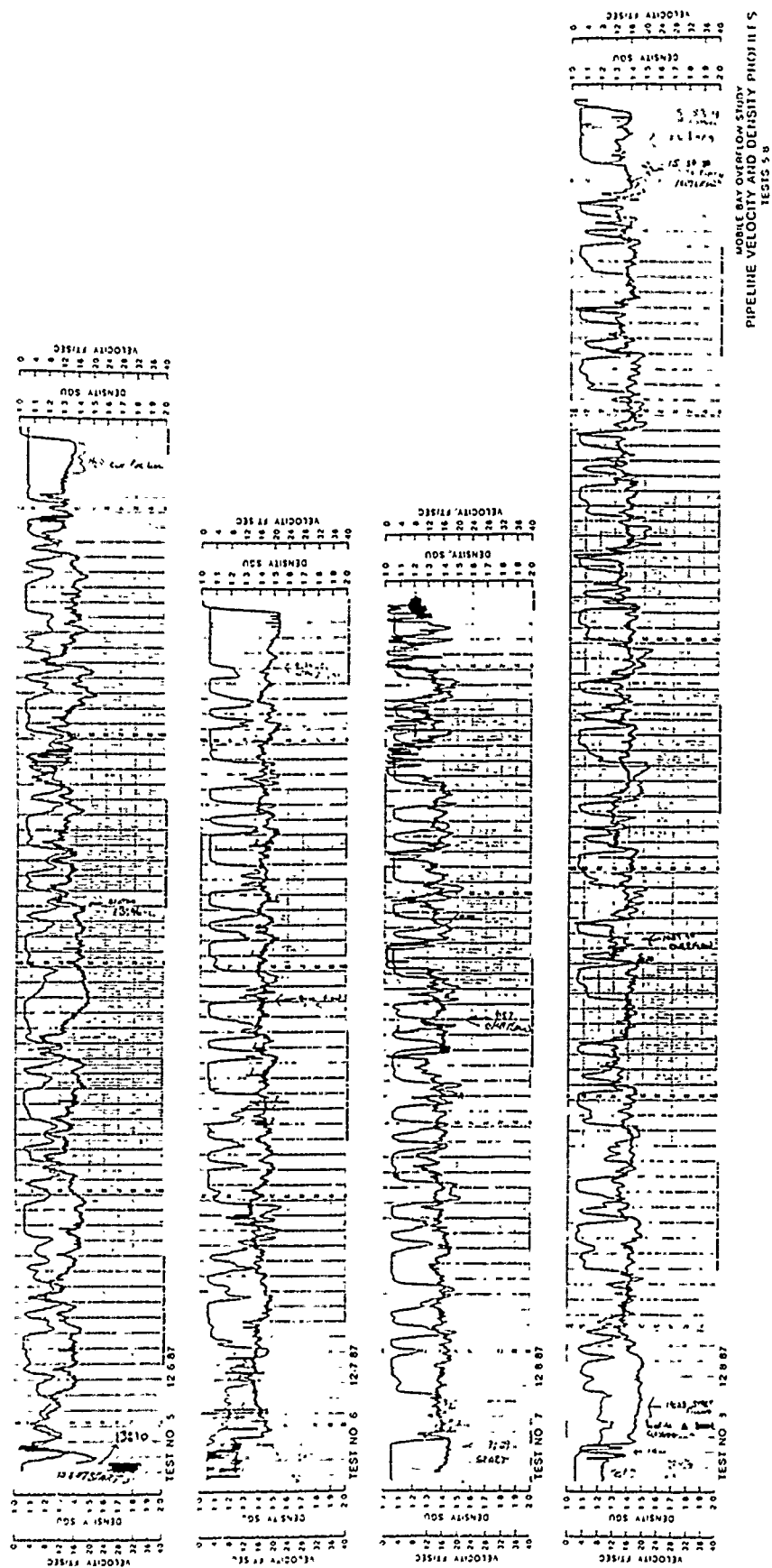


Figure 11. Pipeline velocity (fps) and density profiles, Tests 5-8

88+00	89+00	90+00	91+00	92+00	93+00	94+00	95+00	96+00	97+00	98+00	99+00
-13.1	-12.4	-13.3	-12.6	-12.7	-12.2	-12.6	-12.2	-12.9	-12.4	-12.3	-12.3
-13.0	-12.5	-13.0	-12.8	-12.6	-12.6	-12.6	-12.5	-12.6	-12.4	-12.7	-12.7
-12.9	-11.8	-13.6	-12.8	-12.8	-12.8	-12.9	-12.5	-12.7	-12.7	-12.6	-12.9
-13.2	-12.4	-13.5	-13.0	-13.0	-13.1	-13.3	-13.3	-12.9	-13.1	-12.8	-12.6
-13.2	-13.5	-13.6	-13.4	-13.0	-13.2	-13.6	-12.6	-13.0	-14.4	-12.9	-13.1
-13.3	-13.3	-13.6	-13.4	-14.2	-13.4	-13.4	-13.2	-13.2	-13.6	-13.0	-13.8
-13.8	-28.7	-13.8	-13.2	-12.9	-13.2	-13.4	-13.7	-13.4	-14.9	-13.1	-14.0
-14.0	-13.9	-13.8	-13.8	-13.7	-13.0	-13.3	-13.3	-13.3	-13.4	-14.1	-13.5
-14.5	-14.0	-14.0	-14.3	-14.4	-13.7	-14.5	-13.7	-13.5	-14.1	-13.5	-13.6
-14.6	-14.1	-15.1	-14.3	-14.7	-14.2	-14.7	-14.2	-13.5	-14.0	-13.7	-14.1
-15.1	-14.4	-14.8	-14.0	-14.8	-14.2	-14.7	-14.2	-14.1	-14.2	-13.9	-14.4
-15.2	-14.8	-15.5	-15.2	-14.7	-14.7	-15.1	-14.6	-14.5	-14.4	-14.3	-14.8
-15.4	-15.3	-15.3	-15.0	-15.4	-15.2	-14.9	-15.0	-14.5	-14.3	-14.6	-14.6
-15.7	-15.7	-15.8	-15.6	-15.4	-15.4	-15.5	-15.4	-14.9	-15.4	-14.7	-15.1
-17.6	-16.0	-16.2	-15.8	-16.0	-16.2	-15.3	-15.8	-15.4	-15.6	-15.1	-15.4
-17.1	-16.4	-16.7	-16.3	-16.6	-16.5	-16.6	-15.8	-15.9	-15.2	-16.0	-16.4
-17.3	-16.8	-17.3	-16.8	-17.2	-16.7	-17.0	-17.0	-15.4	-16.4	-16.3	-16.3
-18.1	-16.9	-17.5	-17.4	-18.0	-17.4	-21.4	-17.1	-16.9	-17.7	-17.0	-17.0
-18.5	-18.8	-18.6	-18.7	-18.0	-18.4	-22.5	-18.0	-17.5	-17.5	-17.1	-17.7
-19.5	-18.5	-18.9	-18.9	-19.0	-18.8	-19.3	-18.8	-18.0	-18.7	-17.7	-19.3
-19.8	-20.4	-20.5	-20.0	-20.6	-19.0	-20.1	-19.8	-19.2	-20.5	-19.4	-21.0
-20.9	-20.1	-21.0	-20.0	-21.2	-22.3	-22.1	-22.6	-21.0	-23.1	-22.2	-24.2
-22.3	-22.0	-23.3	-22.0	-22.6	-22.1	-23.0	-24.4	-24.5	-26.0	-27.2	-29.0
-25.4	-23.0	-24.9	-24.2	-26.0	-26.6	-25.3	-27.2	-26.7	-30.0	-28.1	-29.4
-29.4	-28.4	-31.4	-26.8	-30.0	-28.2	-29.7	-31.5	-30.3	-31.8	-30.4	-31.0
-33.7	-32.0	-34.6	-35.9	-33.6	-35.6	-33.2	-34.4	-34.0	-33.9	-32.2	-33.4
-37.3	-36.4	-37.3	-35.5	-35.8	-35.8	-36.0	-36.3	-36.2	-35.4	-39.0	-36.3
-37.8	-37.6	-37.5	-37.8	-37.4	-36.9	-37.4	-38.2	-36.7	-37.9	-36.1	-36.8
-39.0	-43.6	-38.0	-38.1	-39.3	-36.1	-39.0	-38.2	-37.8	-37.6	-37.1	-37.6
-39.7	-40.7	-38.7	-39.1	-36.4	-39.2	-38.5	-38.9	-40.4	-38.2	-38.6	-39.0
-41.3	-41.2	-41.6	-36.5	-38.8	-36.1	-40.0	-41.5	-39.7	-39.2	-38.0	-40.4
-40.2	-40.9	-40.4	-39.3	-39.6	-39.4	-39.9	-39.0	-41.6	-40.3	-37.8	-43.1
-44.9	-42.1	-41.5	-41.2	-37.6	-41.6	-43.4	-40.2	-39.3	-40.6	-39.6	-39.2
-40.8	-42.4	-41.4	-42.5	-38.4	-40.6	-41.0	-43.8	-41.1	-40.2	-40.2	-42.9
-42.1	-44.1	-41.6	-43.5	-38.4	-41.0	-41.4	-40.8	-42.8	-43.1	-42.5	-43.9
-43.7	-45.7	-42.0	-44.5	-39.4	-43.8	-42.2	-42.1	-42.9	-43.8	-42.3	-44.4
-42.2	-44.8	-43.4	-43.4	-43.6	-44.0	-44.2	-44.6	-42.2	-43.4	-42.2	-42.7
-44.8	-44.3	-43.3	-44.6	-44.7	-44.8	-44.5	-44.8	-43.7	-44.2	-43.0	-44.0
-44.6	-44.5	-44.0	-45.2	-45.1	-45.0	-45.0	-44.6	-44.2	-44.7	-44.8	-42.8
-44.6	-44.8	-43.4	-45.1	-45.7	-45.6	-44.7	-45.1	-43.1	-43.1	-43.9	-46.0
-43.4	-43.6	-44.9	-41.9	-41.8	-42.4	-42.3	-44.2	-40.6	-41.5	-43.2	-43.6
-41.7	-43.6	-41.5	-44.2	-41.9	-42.7	-43.1	-41.1	-41.4	-39.5	-41.1	-41.4
-41.9	-41.8	-42.7	-44.2	-42.5	-42.7	-40.2	-42.2	-40.5	-40.4	-42.7	-44.4
-40.6	-39.6	-42.5	-42.7	-42.0	-42.4	-40.9	-42.8	-40.3	-41.6	-40.2	-42.3
-39.8	-40.1	-43.8	-40.1	-39.0	-41.9	-40.3	-39.0	-38.7	-39.0	-39.5	-42.2
-40.2	-39.3	-38.8	-41.1	-38.8	-38.8	-38.6	-40.7	-36.7	-38.6	-38.6	-38.7
-42.2	-38.7	-38.6	-38.3	-38.3	-39.2	-36.9	-39.3	-39.1	-38.4	-36.6	-38.4
-38.5	-43.2	-38.1	-39.7	-37.8	-38.8	-39.0	-37.4	-36.7	-37.1	-37.9	-38.2
-42.0	-39.3	-40.7	-41.1	-37.4	-37.5	-38.8	-37.7	-36.3	-36.2	-37.3	-37.1
-39.7	-36.6	-37.0	-38.3	-37.2	-38.8	-37.5	-36.8	-37.2	-37.4	-37.8	-36.0
-36.0	-36.7	-36.4	-36.5	-36.0	-36.8	-36.5	-35.7	-36.4	-37.2	-36.2	-35.0
-35.2	-34.8	-34.7	-35.9	-35.5	-35.6	-34.6	-34.4	-34.8	-34.8	-35.1	-33.6
-33.8	-33.6	-33.1	-33.7	-31.4	-35.4	-32.1	-32.0	-33.9	-32.2	-30.8	-31.5
-29.3	-30.8	-33.0	-29.5	-28.3	-29.7	-29.5	-28.9	-33.7	-28.2	-30.5	-27.5
-24.6	-27.5	-24.6	-28.2	-26.3	-26.7	-24.6	-24.2	-25.2	-24.5	-27.7	-23.9
-20.8	-22.4	-21.5	-22.8	-22.1	-24.0	-22.1	-20.6	-21.4	-21.3	-22.8	-20.6
-18.9	-20.3	-18.6	-20.2	-19.0	-19.6	-19.0	-18.6	-20.1	-19.2	-20.0	-18.2
-17.4	-18.2	-17.6	-17.9	-17.2	-18.0	-17.2	-17.2	-17.6	-17.0	-18.3	-16.7
-16.4	-16.5	-16.2	-17.0	-16.2	-16.2	-16.5	-16.1	-16.2	-15.9	-16.1	-15.8
-14.6	-15.7	-15.5	-15.6	-14.4	-15.8	-15.5	-15.0	-15.5	-15.5	-15.4	-14.8
-14.7	-14.9	-14.6	-14.9	-14.7	-15.4	-15.1	-14.4	-14.4	-13.9	-14.8	-13.9
-13.9	-14.1	-14.1	-14.0	-13.7	-14.3	-13.6	-14.0	-13.9	-13.9	-14.0	-13.6
-13.4	-13.5	-13.4	-13.8	-13.4	-13.9	-13.3	-13.1	-13.8	-13.5	-13.4	-13.0
-13.3	-13.5	-12.5	-13.3	-13.3	-13.2	-12.8	-12.8	-12.9	-12.8	-13.8	-12.6
-11.5	-13.2	-12.8	-13.2	-13.4	-12.8	-12.7	-12.1	-12.7	-12.5	-12.7	-12.3
-12.8	-13.1	-12.4	-12.7	-12.0	-12.5	-12.3	-12.1	-12.1	-12.1	-12.7	-12.1
-12.4	-12.7	-12.2	-12.3	-11.9	-12.3	-12.1	-11.8	-12.1	-11.9	-11.8	-11.5
-11.0	-12.2	-12.4	-12.2	-11.8	-12.2	-11.8	-11.9	-11.6	-11.6	-11.6	-11.1
-12.1	-12.6	-11.7	-11.5	-11.4	-11.3	-11.6	-11.8	-11.8	-11.2	-11.2	-11.0
-12.2	-10.5	-11.8	-10.7	-11.4	-11.8	-11.4	-11.4	-11.2	-11.0	-11.9	-10.5
-11.7	-11.3	-11.7	-11.2	-11.4	-11.8	-11.0	-10.9	-11.1	-10.8	-11.0	-10.8
-11.4	-11.3	-11.3	-11.5	-11.4	-11.1	-11.1	-11.3	-10.9	-10.7	-10.8	-10.5
-11.4	-10.9	-10.8	-11.1	-10.9	-10.9	-11.1	-10.9	-10.8	-10.7	-10.7	-10.6
-11.0	-11.2	-10.5	-10.8	-10.6	-11.3	-10.8	-10.5	-10.9	-10.9	-10.5	-10.4
-11.0	-11.2	-10.9	-10.8	-10.8	-10.7	-10.6	-10.7	-10.7	-10.1	-10.7	-10.4
-11.1	-10.3	-12.5	-10.8	-10.5	-10.5	-10.6	-10.1	-10.5	-10.9	-10.3	-10.3
-10.8		-10.9	-10.7	-10.4	-10.5	-10.5	-10.1	-10.3	-10.6	-10.4	-10.2
			-10.6	-10.4	-10.4	-10.4					
				-10.4	-10.3	-10.0					
						-10.3					

C/L STA 100+00

Figure 12. Lower test site, December 2, 1987, predredge survey

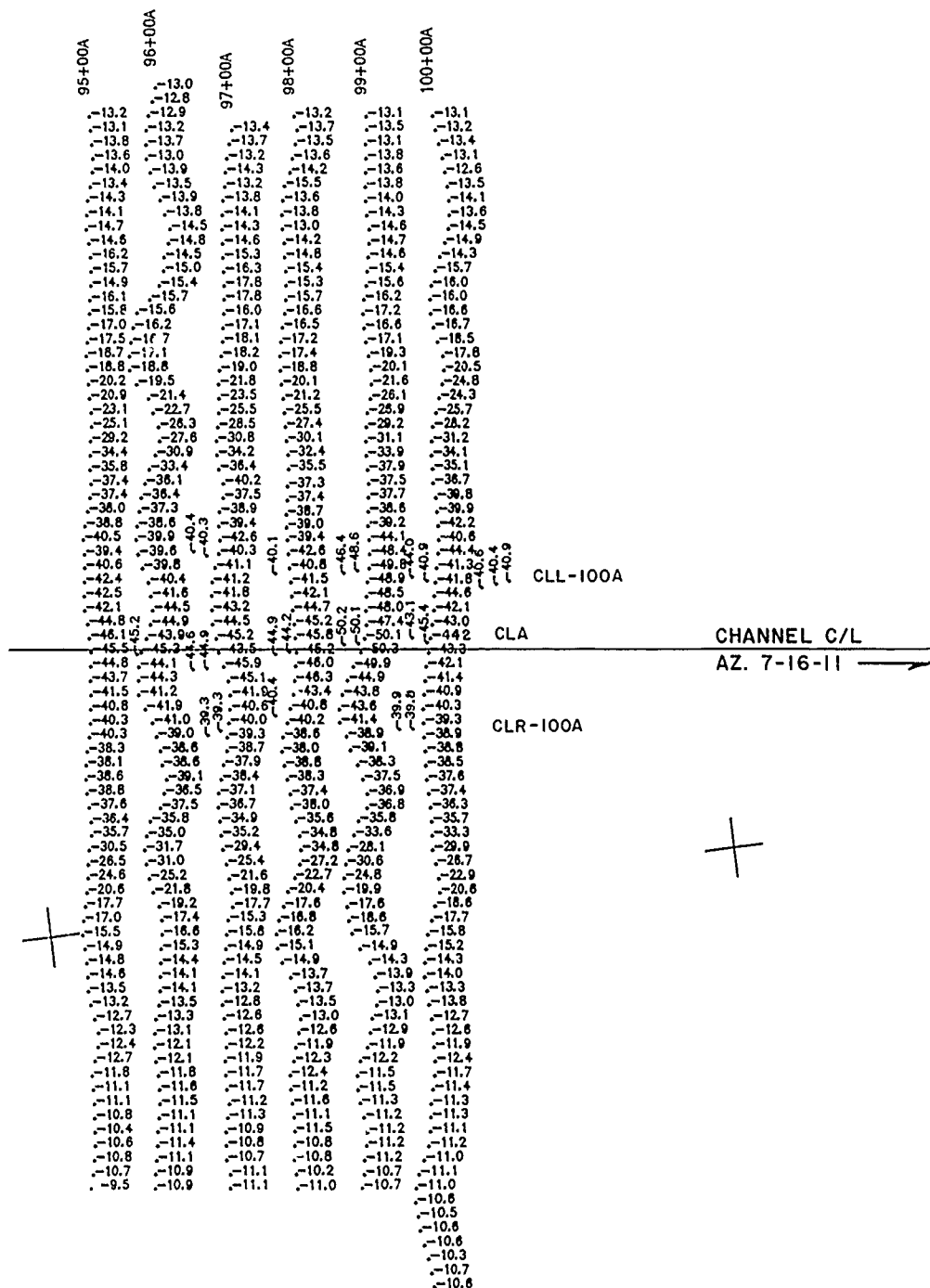


Figure 13. Lower test site, December 5, 1987, postdredge survey

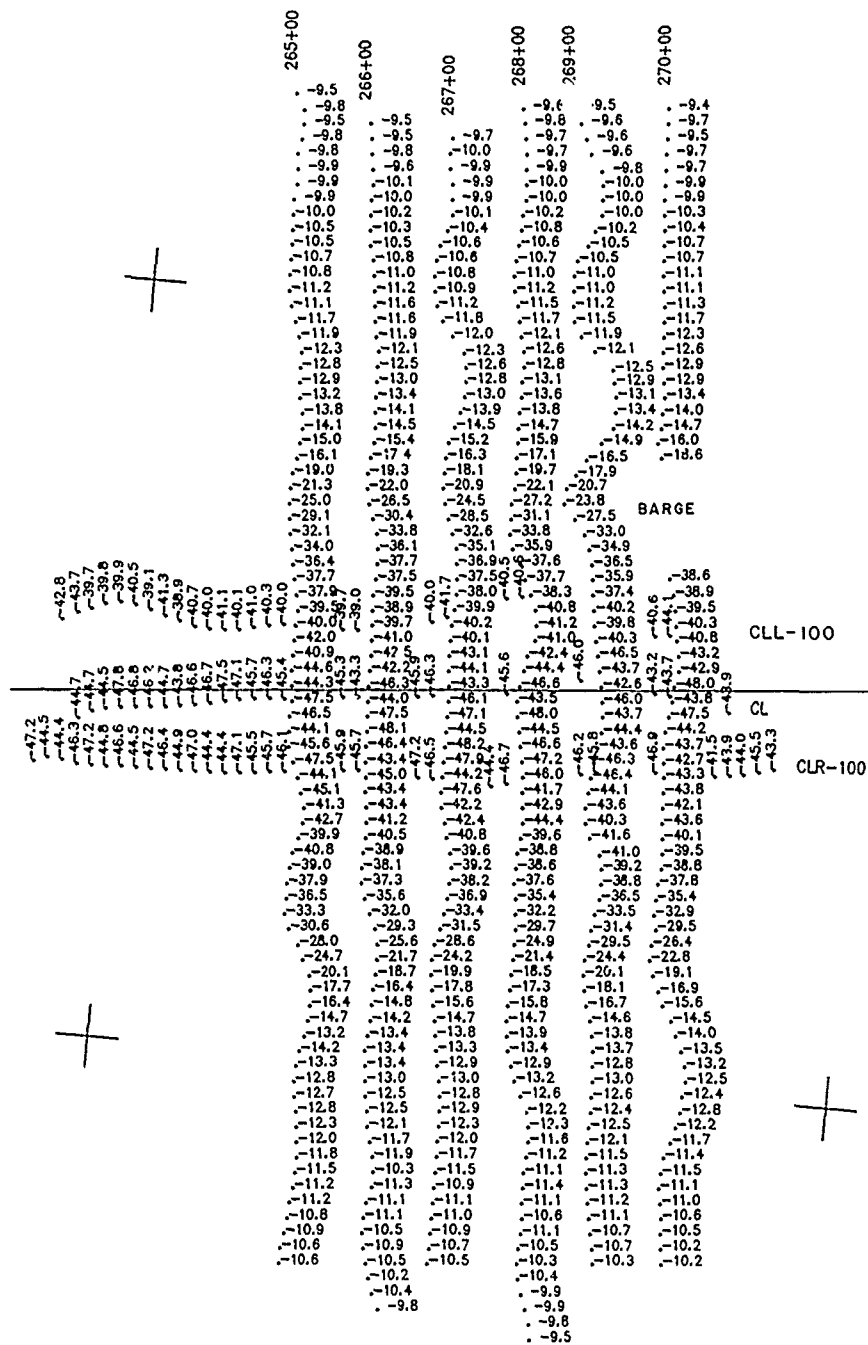


Figure 14 Upper test site, December 5, 1987, predredge survey

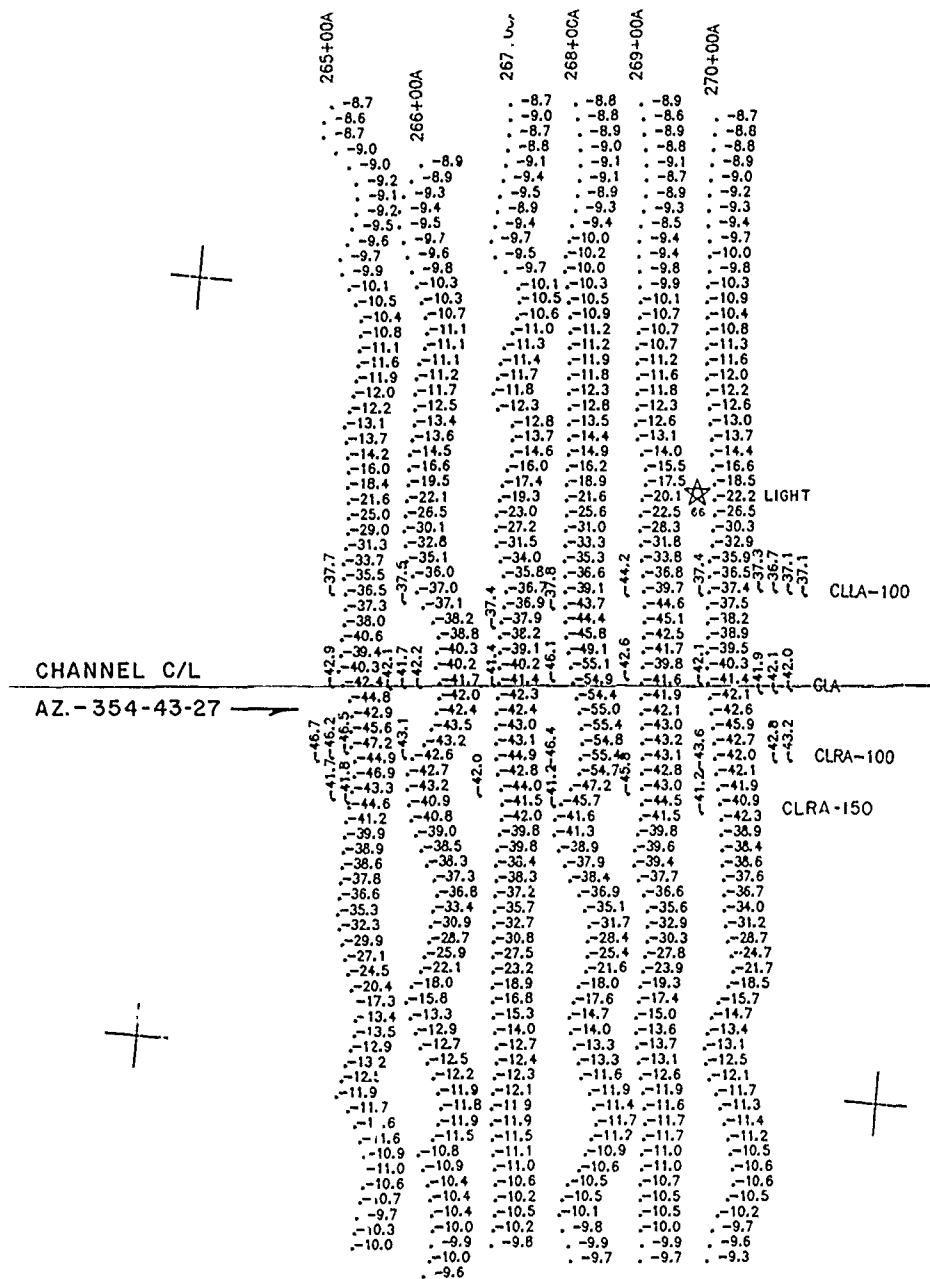


Figure 15. Upper test site, December 10, 1987, postdredge survey

PART IV: HOPPER BARGE, LOADING EQUIPMENT, AND OPERATIONS*

Hopper Barge Description

Two identical hopper barges, each with a nominal capacity of 4,000 cu yd, were used for the study. These barges were constructed just prior to the study and had never been in service. The barges were of the split-hull type, with overall dimensions of 240 by 54 by 22 ft. The barges were designed to squat several inches at the stern when fully loaded, which tended to confine the overflow to the stern end of the barge. The design of the hopper barge is illustrated in Figure 16. A photograph of one of the hopper barges is shown as Figure 17. The barges had a maximum draft of approximately 20 ft and a filled volume of 4,020 cu yd when fully loaded to the top of the coaming. The relationship between load in long tons and draft is shown in Figure 18.

Loading Equipment Description

A specially designed barge with a manifold slurry discharge system was used for loading the hopper barges. This barge was termed the "spider" barge. The manifold system was necessary to evenly distribute inflow within the barge, reduce the velocity of inflow, and thereby reduce turbulence. This would allow for the most efficient retention of solids possible. The manifold consisted of a three-pipe system each with a "T" section. The main dredge pipe was reduced in inside diameter size along the manifold, from 24 to 20 in. and from 20 to 15 in. I.D. Each of the three discharge pipes was 15 in. I.D. with two flexible 12-in. I.D. downcomers, resulting in six equally spaced discharge points along the length of the barge.

Each of the downcomers was 22 ft long and was extended to near the bottom of the hopper barge when filling commenced. The flexible downcomers allowed the hopper barges to be placed alongside the spider barge without raising and lowering the manifold. Layout of the spider barge is illustrated in Figure 19. Photographs of the spider barge and downcomers are shown in Figures 20 and 21.

* Written by Tamsen Smith-Dozier, Hydraulics Laboratory, and Michael R. Palermo, Environmental Laboratory, WES.

Hopper Barge Draft Instrumentation

To quickly determine those test conditions (e.g., pump speed, material density, duration of overflow, etc.) which resulted in optimum economic loading, a means for continuous monitoring of barge load was required for the study. Pressure transducers with telemetry provided the capability of accurately monitoring the change in hopper barge draft in a real-time mode. An ENDECO 1150 Digital Telemetry Water Level Reporting system was used. Stilling wells, shown in Figures 22 and 23, were mounted at opposite corners of the bow and stern of each hopper barge. Prior to each test, a strain gage pressure sensor was placed in each stilling well. This sensor was attached to a deck unit that housed the electronics and a radio transceiver for telemetry. The sensor had an accuracy of 0.05 ft and resolution of 0.012 ft. Pressure was measured for 49 sec of every minute to filter out wave action or other noise. Changes in barometric pressure were automatically compensated for by a vented cable from the sensor attached to the deck unit. A thermistor bead was used to compensate for temperature effects on the strain gage. Figure 24 shows the topside unit (in a wooden box that was later mounted on a nearby steel brace) and the transceiver. The pressure sensor was attached to an aluminum pole for deployment and retrieval from the stilling well (top visible in Figure 24).

An ENDECO 1142 base station was located aboard the dredge. This station consisted of an IBM computer and transceiver which, upon command, queried the water level indicators on the hopper barges for the most recent measurements. Water level readings were updated at each unit every 2 min.

Prior to each test, upon installation of the pressure sensors, a reading was obtained from each instrument corresponding to the empty hopper barge. Once loading began, this reading was subtracted from the subsequent data so that the change in draft at each end of the barge was calculated and recorded. Stern and bow measurements were averaged, and these data were plotted as loading progressed.

Visual Draft Measurements

During Test 3, the electronic water level data acquisition system was inoperative, and changes in draft were obtained manually by measurements of the distance between levels of the water surface and the deck of the barge. These measurements were made less frequently and, due to wave action, were

less accurate than those made electronically. During Tests 6-8, the telemetry capability of the system became inoperative, and visual observations were made for immediate updates of draft changes. However, electronic recording of barge draft by the deck units remained operative, and these data were reduced as soon as possible after the conclusion of each test. The data presented in this section for those tests are electronically recorded values.

Loading Characteristics

Figures A1-A8 (see Appendix A) are plots of the change in draft of the hopper barge during the filling and overflow cycles for each of the eight tests. Tables A1-A8 (Appendix A) list the sequence of measured draft values. At the lower bay site for both maintenance and new work material (Tests 1-3), there was not a significant increase in draft after overflow began. The average increase in draft during overflow was 0.2 to 0.3 ft, and this occurred during the first few minutes after overflow began. This represented a change in load of approximately 4 percent calculated using the barge draft versus load relationship. A contributing factor to the observed slight increase in draft was the hydraulic head of water standing above the rim of the hopper as spill progressed. No further measurable increase was obtained by overflowing for more than a few minutes. At the upper site the same loading characteristics were observed for the maintenance material (Tests 4 and 5). However, for the new work material at the upper site (Tests 6-8), an increase in draft up to 0.7 to 0.8 ft was gradually obtained by allowing overflow for approximately 20 min. An increase in draft of 0.87 ft was realized during Test 8 when overflow occurred for 50 min. This represented an increase in load of approximately 7 percent calculated using the hopper barge draft versus load relationship.

A comparison of bulk density and corresponding solids concentration of the material in loaded barges at the point of overflow as determined using three methods is presented in Part V (see Table 4). First, values were determined by laboratory testing of inflow samples as described in Part V. Second, values were calculated from the barge displacement at the time of overflow. And third, values were determined by averaging the pipeline density as measured by instrumentation described in Part III. The values from barge displacement and pipeline density were generally in close agreement, while values determined by inflow samples were consistently higher.

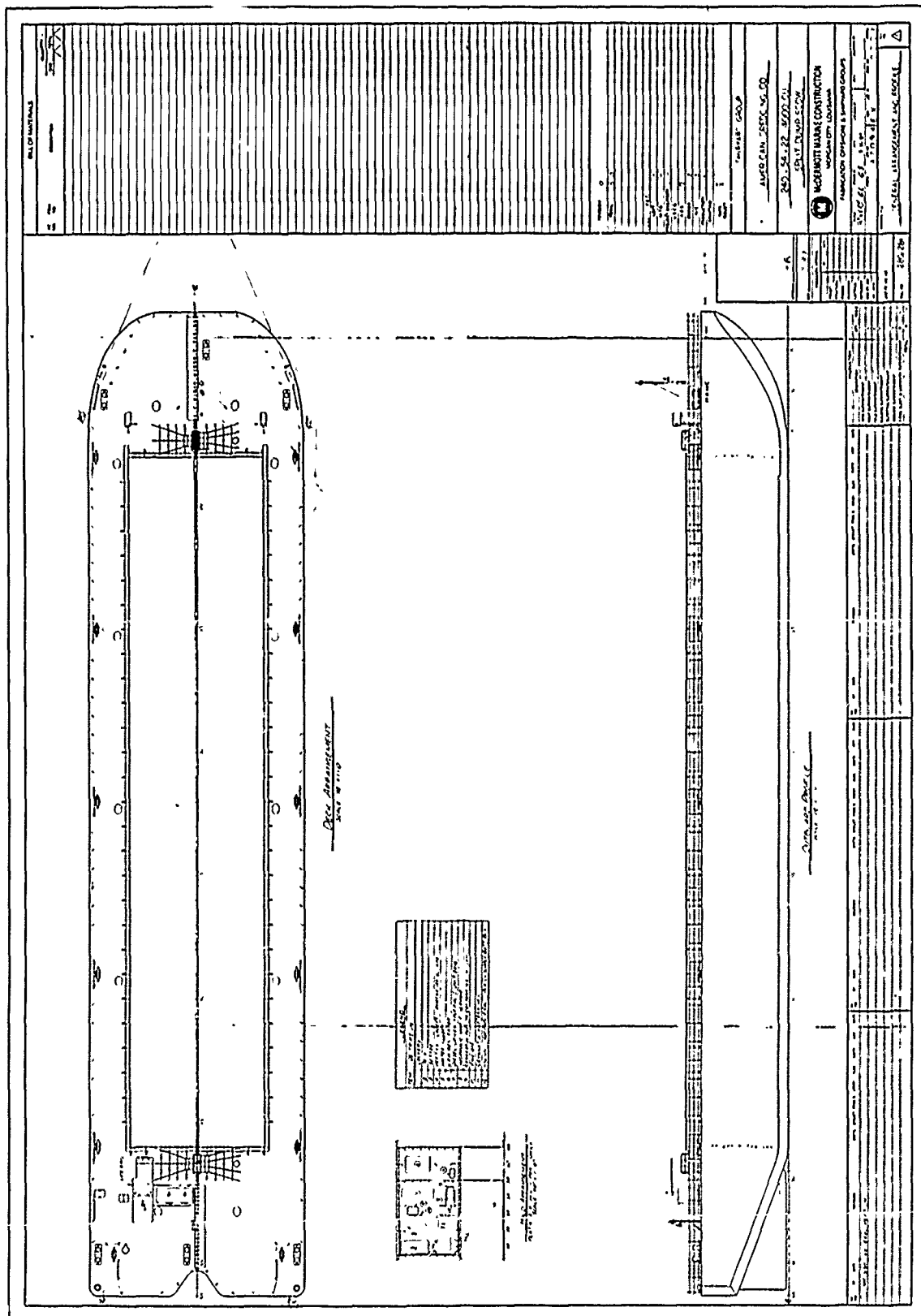


Figure 16. Configuration of hopper barges



Figure 17. Hopper barge

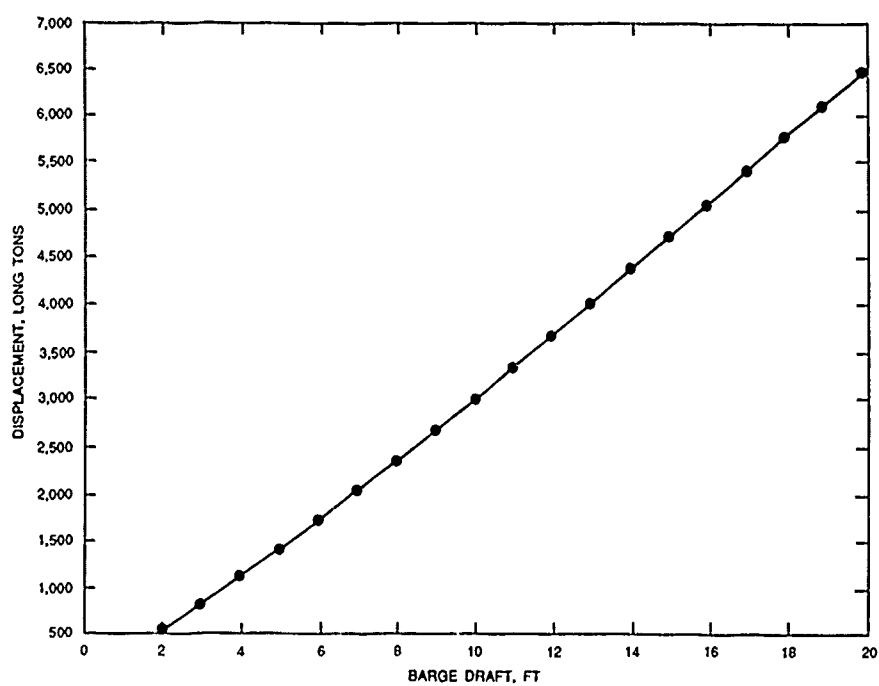


Figure 18. Relationship between load and draft for hopper barge

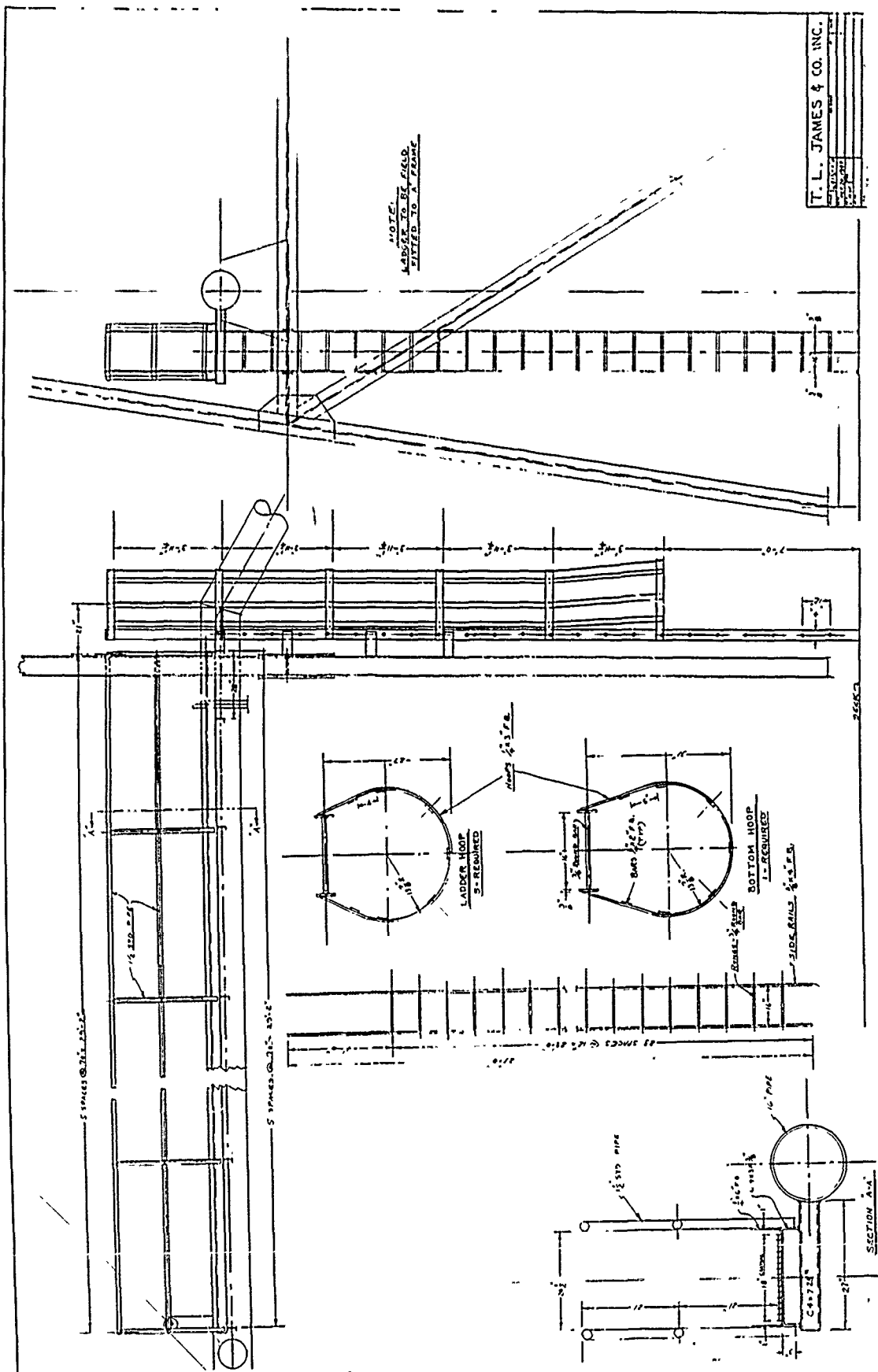
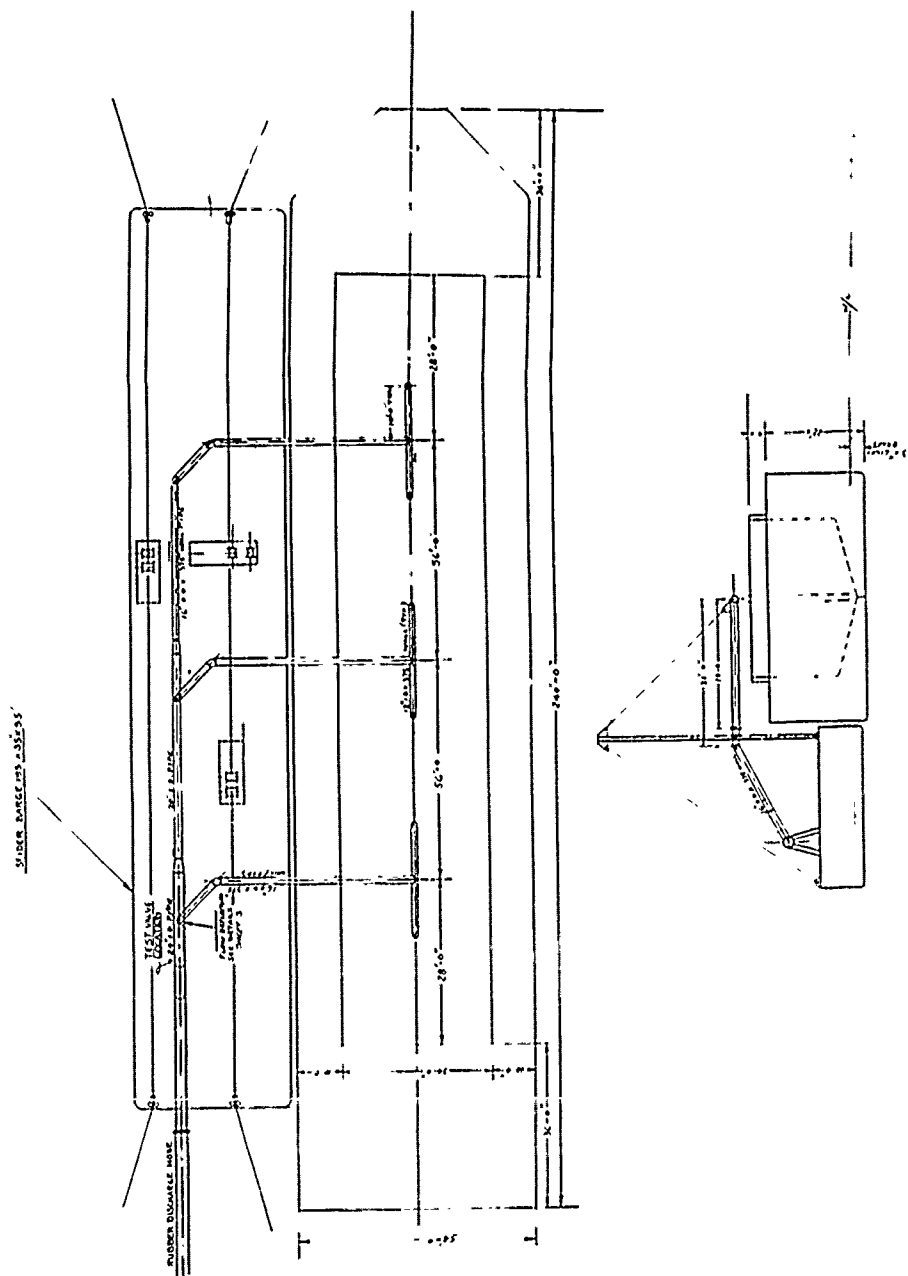




Figure 19. (Sheet 2 of 3)



SHEET 1 OF 3 SHEETS

T. L. JAMES & CO. INC.	
DATE	12-13-43
BY	
CHECKED	
APPROVED	
PROJECT	
DESCRIPTION	
SCALE	

Figure 19. (Sheet 3 of 3)

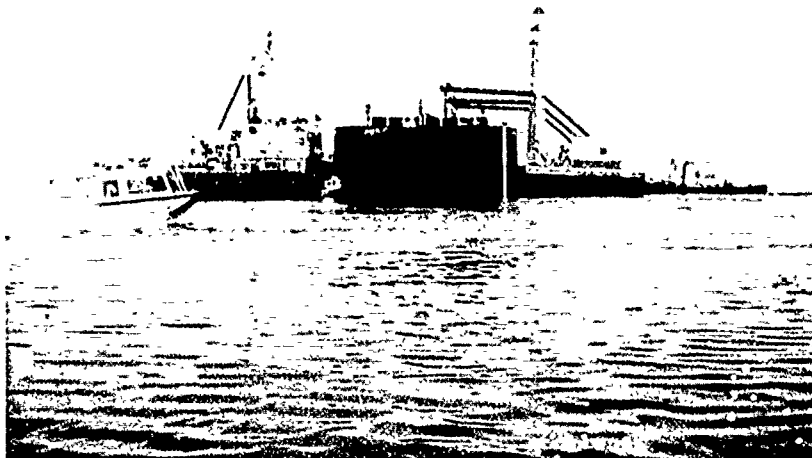


Figure 20. Spider barge



Figure 21. Downcomers



Figure 23. Stilling well mounted to scow

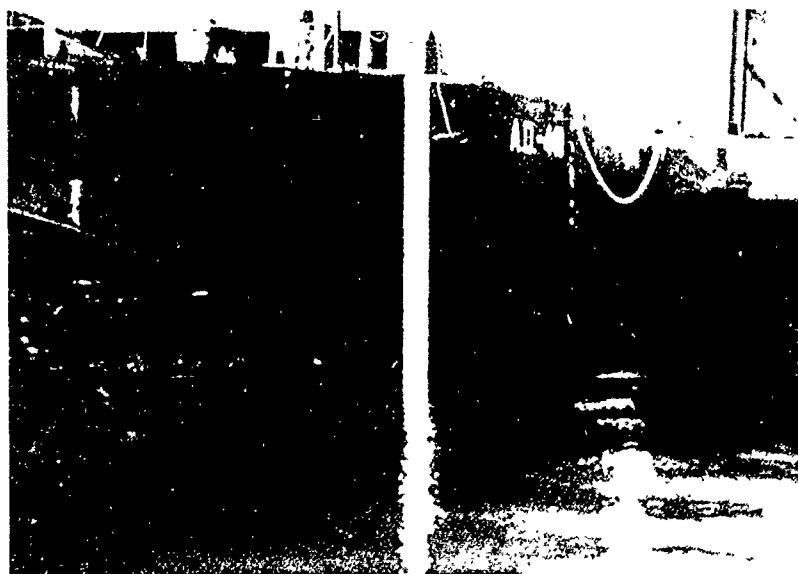


Figure 24. Water level indicator with telemetry used to monitor scow draft

PART V: DREDGED MATERIAL AND OVERFLOW CHARACTERISTICS*

This part of the report describes the characteristics of the in situ sediment, the inflow to the barges, the material retained in the barges, and the barge overflow. The characteristics are based on visual observations made during the loading and overflow process and sampling and laboratory testing. Data describing solids concentrations, grain size distributions, plasticity indexes, and classification under the Unified Soil Classification System (USCS) are presented.

In Situ Sediment Characteristics

The in situ sediment characteristics of Mobile Bay were briefly described in Part II. Generalized sediment profiles of two test areas within the channel, as determined by vibracore borings, are presented in Figures 25 and 26. In general, the channel sediments north of Gaillard Island are a mixture of sands, silty sands, clayey sands, and sandy clays. The material becomes progressively finer from north to south. South of Gaillard Island, the channel sediments are almost entirely soft marine clays.

The borings were taken at stations near the two test sites (see Figures 8 and 9, Part III). The depths of dredging for the new work and maintenance tests are indicated. The material at both test locations was visually classified as a soft marine clay (CH). The two sites differ with respect to in situ water content of the sediment. At the lower site, the water content ranges from 60 to 98 percent, while at the upper site the water content ranges from 29 to 67 percent. Only one sample, at -46.5 NGVD at the lower site, was analyzed for Atterberg limits; it had a liquid limit of 77 percent and a plastic limit of 22 percent. The liquid and plastic limits are the water contents at which a given soil sample exhibits the lower limits of liquid or plastic behavior.

* Written by Michael R. Palermo, Environmental Laboratory, WES.

Inflow Characteristics

Visual observations

Because the flexible downcomers from the spider barge extended to near the bottom of the barge, the visual observation of inflow to the barges was limited to the initial period of filling. Beyond that point only the rising surface of the material accumulating in the barges could be seen. For most tests, the slurry entering the barges from the downcomers was visibly fine-grained and uniform in appearance. For Tests 6 through 8, however, sand was visibly apparent during the initial filling stages. Samples taken from the dredge pipe (see paragraphs below) could be examined at close hand. Clay balls were not visually observed in the inflow for any of the eight tests. The consistency of the inflow was very plastic for Tests 1 through 5, in some cases having the consistency of toothpaste. For Tests 6 through 8, fine sand was seen in the inflow. A photograph of the inflow from the downcomers during the initial stages of filling for Test 1 is shown as Figure 27.

Sampling and testing

The spider barge was equipped with a test valve attached to the main dredge pipe. The purpose of the test valve was to allow direct sampling of the dredged material inflow pumped into the hopper barges. The test valve consisted of a 4-in. U-shaped pipe joined at a tee section with a butterfly valve. The ends of the U-shaped pipe were attached to the main dredge pipe in a 45-deg orientation. This arrangement was chosen to allow for representative sampling of the lighter suspended material in the upper portion of the flow and the heavier material near the bottom of the flow. A diagram of the test valve is shown as Figure 28.

Samples of the inflow were taken by opening the test valve, allowing the flow to clear the test valve piping of residual material from previous samplings, and directly filling sample containers. Excess material was allowed to flow into a 55-gal drum with a bottom-mounted drain pipe that discharged the excess material over the side of the spider barge. The barrel prevented material from spilling over a large area of the deck during the sampling process. The process took less than 10 sec per sample. Samples of the inflow were taken using the test valve at approximately 5-min intervals throughout filling and overflow for each test. A photograph of the inflow sampling operation is shown as Figure 29.

The water content and grain size distribution of all inflow samples were determined. All water contents were also converted to values of solids concentration in grams per liter. In addition, a composite of all inflow samples for each respective test was used to determine the Atterberg limits of inflow material.

Solids concentration

Suspended solids concentrations of inflow and overflow samples are plotted in Figures 30-37. Significant variations in the inflow suspended solids concentrations are apparent, reflecting the typical methods of operation of a swinging cutterhead dredge. Generally, higher concentrations were noted for a full-width cut of the dredge and lower concentrations during dredge advancement periods (see Figures 12-15 in Part III for typical cyclic dredging pattern). The mean inflow concentrations for each test (Table 4) ranged from 218 to 633 g/l. These concentrations are high as compared with data from previous studies for measured pipeline concentration for operating conditions involving longer pipeline lengths and typical fine-grained maintenance sediments.*,**

For Tests 1 through 5, involving maintenance and new work material at the lower bay site and maintenance material at the upper bay site, the inflow concentrations of the samples were 339 g/l or less. However, for Tests 6 through 8, involving new work material at the upper bay site, the concentrations were much higher, from 506 to 633 g/l.

These results indicated consistently higher concentrations than calculated concentrations for the loaded barges. Mean concentrations and corresponding bulk densities measured by the inflow samples, calculated by barge draft, and calculated from pipeline density instrumentation are compared in Table 5. The higher values from the inflow samples could be due to a higher fraction of the heavier material within the bottom portion of the pipeline being taken by the U-shaped pipe sampling apparatus.

* R. L. Montgomery. 1978. Methodology for design of fine-grained dredged material containment areas for solids retention. Technical Report D-78-56. US Army Engineer Waterways Experiment Station, Vicksburg, MS.

** M. R. Palermo, R. L. Montgomery, and M. Poindexter. 1978. Guidelines for designing, operating, and managing dredged material containment areas. Technical Report DS-78-10, US Army Engineer Waterways Experiment Station, Vicksburg, MS.

Grain size distribution

The grain size distributions for the inflow and overflow samples are plotted in Figures 38-45. The figures show the bounds within which all inflow and overflow distributions fall. The mean of the D50 values (the grain size for which 50 percent of the particles by weight are finer) for each test are shown in Table 4, and the percent coarse sand (passing the No. 40 sieve) and percent fines (passing the No. 200 sieve) are shown in Table 6. Fifty percent of the particles on a dry weight basis are smaller than the D50 grain size, while 50 percent are larger. The D50 grain size can therefore be considered average grain size on a dry weight basis. The D50 values for the tests followed trends similar to the suspended solids concentrations. The mean of the D50 inflow values for Tests 1 through 5 were all below 0.003 mm (silt or clay), while values for Tests 6 through 8 ranged from 0.076 to 0.100 mm (fine sand). The percent fines are also correspondingly higher for Tests 1 to 5 as compared with Tests 6 to 8.

Atterberg limits

Atterberg limit results for the composite samples of inflow for each test are given in Table 6 and plotted on the plasticity chart in Figure 46. These results are quite consistent with the grain size distributions. Only the fraction passing the No. 40 sieve size (0.042 mm), consisting of fine sands, silts, and clays, is used to determine the limits. This material fraction is plotted as a high plasticity clay (CH) for Tests 1 through 5 and as low plasticity clay for Tests 6 through 8, with a clear distinction between the two sample groupings.

The tendency of material to form clay balls was of interest, because clay balls would tend to be easily retained in the barges during overflow, resulting in a potentially larger increase in load. Sorenson* presented information on the relative tendency of material to form clay balls as a function of Atterberg limits, in situ density, and shear strength. He stated that formation of clay balls is likely when liquid limits are between 35 to 50 percent and 80 to 120 percent, plastic limits are higher than 20 to 30 percent, density is higher than 1.5 to 1.7, and shear strength exceeds 25 kPa. These very broad guidelines regarding Atterberg limits were generally

* A. H. Sorenson. 1984. Soil analysis and dredging. Proceedings of the Specialty Conference Dredging '84. American Society of Civil Engineers, Clearwater, FL.

satisfied by all the material dredged in this study. The guideline on in situ density was marginally satisfied for maintenance material at the lower site, which had in situ density of 1.47. In situ density of material at the upper site approaches 1.9, indicating that clay balls would have a much greater tendency to form. Since clay lumps were observed in the barge samples at the lower site, and more consistent clay balls were observed at the upper site, the guidance of Sorenson seems to be qualitatively verified for the Mobile Bay sediments.

USCS classification

The Unified Soil Classification System was used to classify the composite inflow samples based on the grain size distributions and Atterberg limits. Inflow materials from Tests 1 through 5 were classified as a highly plastic clay (CH), whereas materials from Tests 6 through 8 were classified as a clayey sand (SC).

Characteristics of Material in Loaded Barges

Visual observations

As the barge filled to near overflow, the nature of the near-surface portion of the slurry layer was determined. A surface layer of slurry with water-like consistency a few inches thick was evident. Below this, the layer was viscous to the feel. When overflow began, the thin surficial slurry layer overflowed first, followed by the more viscous slurry. Barge sampling described below showed that some clay balls had accumulated at the bottom of the barges. For Tests 1 through 5, the balls were soft lumps of material. For Tests 6 through 8, a smaller proportion of stiffer balls was present within a fine sand matrix. However, the depth of accumulation of the clay lumps could not be determined. Photographs of the surface and bottom materials from the barge are presented as Figures 47 and 48.

Sampling and testing

Immediately following the end of overflow for each test barge, samples were taken of the material in the barges. The purpose of these samples was to supplement the density measurements for the loaded barges and to detect any layering and distribution of material density within the barges. A summary of the barge samples is given in Table 7. For some tests, samples were taken both prior to overflow and following the end of overflow. For one test, the material was sampled at near surface and middepth using a sampler consisting

simply of a 1-ft section of 4-in.-diam PVC pipe with end-stoppers attached to a pole. The sampler was lowered to the desired sampling depth and opened to retrieve a sample. However, due to the thick consistency of the material, difficulties were encountered in obtaining a representative sample at the desired depths. Consequently, this sampling method was abandoned. The majority of samples were taken at the bottom depth of the barge using a Petersen dredge grab sampler. The sampler was mounted at the center point of the bow coaming using a portable winch and boom. A photograph of the sampling apparatus is shown in Figure 49. The sampler had an empty weight of approximately 90 lb, and no difficulty was encountered in penetrating to the bottom of the filled barge. All barge samples were analyzed for water content and grain size.

Solids concentration

Solids concentrations of the barge samples are summarized in Table 6. The solids concentrations of material at bottom depth in the barges were substantially higher than mean inflow concentrations. For Tests 1 through 5, involving maintenance and new work material at the lower site and maintenance material at the upper site, the barge concentrations ranged from 151 to 579 g/ℓ. However, for Tests 6 through 8, involving new work material at the upper site, the concentrations were much higher, ranging from 1,211 to 1,478 g/ℓ. The higher concentrations of samples at bottom depth in the barges indicate an accumulation of clay balls and coarse material and a layering effect within the barges.

Grain size distribution

The percent sand and fines and the D50 grain size values from the barge samples are shown in Tables 6 and 7. Grain size distribution of material at the bottom of the barge was generally coarser than that of both the inflow and overflow materials. This indicated that retention of coarser sand particles within the barges occurred. Material entered the barges through downcomers extending to near the bottom of the barges. It is possible that only finer particle fractions were displaced upward to form more fluid upper layers of material.

Overflow Characteristics

Visual observations

At the initial point of overflow, a thin surficial foamy slurry overflowed first. This surficial layer was completely overflowed within the first minute or less. As overflow continued, a more viscous slurry was evident in the overflow for Tests 1 through 5. For Tests 6 through 8, the overflow was a slurry with fine sand, and material was observed to accumulate in a compacted mound on the deck of the barge. No clay balls could be seen spilling over the coaming for any of the tests, indicating that no clay balls were present in the upper portion of the barge material subject to overflow. As overflow progressed, the concentration of the slurry remained essentially constant for all tests.

Sampling and testing

Samples of the overflow were taken by directly filling 250-ml sample containers at timed intervals during the overflow event. The sample containers were filled with a composite sample of the overflow along the entire length of barge coaming involved with the overflow. This was accomplished by filling the sample container while walking along the coaming. The filling procedure was accomplished such that the volume of composite overflow sample taken from various points along the coaming was in proportion to the relative flow rate of the overflow at those points. This provided the most representative sample possible. Samples of overflow were taken at approximately 2-min intervals. The overflow samples were analyzed for solids concentration and grain size. A photograph of the overflow sampling operation is shown as Figure 50.

Solids concentration

The solids concentrations of the overflow samples are shown in Figures 30-37. These figures clearly show that the solids concentration of overflow remained essentially constant during the period of overflow for all tests. This indicates that the barges had an attenuating effect, reducing the variability of overflow concentrations as compared to the highly variable inflow concentration.

The mean overflow concentrations for each test are shown in Table 4 and ranged from 102 to 212 g/l. For Tests 1 through 5, involving maintenance and new work material at the lower site and maintenance material at the upper site, the inflow concentrations averaged 153 g/l. For Tests 6 through 8,

involving new work material at the upper site, the concentrations were somewhat higher, averaging 196 g/l. The higher concentrations for Tests 6 through 8 could be due to the higher inflow concentrations for these tests.

Grain size distribution

The grain size distributions for the overflow samples are plotted in Figures 38-45. The percent sands and fines are shown in Table 6. The mean D50 values for each test are shown in Table 4. Unlike the D50 values for inflow, which showed a wide difference between Tests 1 through 5 as compared to Tests 6 through 8, the overflow D50 values were similar for all tests, ranging from 0.001 to 0.04 mm.

Table 4
Inflow and Overflow Characteristics

Test No.	Inflow					Overflow	
	Mean Solids Concentrations As Determined From			Average Solids Concentration g/l	Mean D50* mm	Mean Solids Concentration g/l	Mean D50* mm
	Inflow Samples g/l	Barge Displacement g/l	Pipeline Density g/l				
1	218	70	60	116	0.002	102	0.001
2	344	110	150	201	0.002	156	0.002
3	342	300	140	260	0.001	155	0.002
4	339	105	105	183	0.003	163	0.003
5	339	100	140	193	0.001	192	0.001
6	633	220	200	351	0.076	212	0.004
7	615	260	220	365	0.089	207	0.004
8	506	300	280	362	0.100	170	0.040

* The mean value of the D50 grain size for all samples. The D50 is flat grain size for which 50 percent of the particles by weight are finer.

Table 5
Densities and Average Concentrations of
Material in Pipeline, Inflow Samples,
and Barges

Test No.	Pipeline Samples		Inflow Samples		Barge Samples	
	Solids		Solids		Solids	
	Specific Gravity	Concentration g/l	Specific Gravity	Concentration g/l	Specific Gravity	Concentration g/l
1	1.03	60.00	1.14	218.00	1.04	70.00
2	1.10	150.00	1.22	344.00	1.07	110.00
3	1.09	140.00	1.22	342.00	1.19	300.00
4	1.07	105.00	1.22	339.00	1.07	105.00
5	1.09	140.00	1.22	339.00	1.06	100.00
6	1.13	200.00	1.40	633.00	1.14	220.00
7	1.14	220.00	1.39	615.00	1.16	260.00
8	1.18	280.00	1.32	506.00	1.19	300.00

Table 6
Characteristics of Inflow, Barge, and Overflow Samples

Test No.	Percent Coarse Sand	Percent Fine Sand	Percent Silt and Clay	Atterberg Limits		USCS Classification
				Liquid Limit percent	Plastics Limit percent	
Inflow Samples						
1	0-6	0-8	86-100	138	34	CH
2	0-5	0-3	92-100	118	28	CH
3	0-5	0-4	91-100	111	28	CH
4	0-6	0-10	84-100	119	29	CH
5	0-1	0-9	90-100	127	32	CH
6	0-7	14-53	40-86	45	15	CL/SC
7	0-15	43-50	35-57	45	15	CL/SC
8	0-16	14-60	24-86	34	14	CL/SC

<u>Test No.</u>	<u>Percent Coarse Sand</u>	<u>Percent Fine Sand</u>	<u>Percent Silt and Clay</u>	<u>Percent Coarse Sand</u>	<u>Percent Fine Sand</u>	<u>Percent Silt and Clay</u>
<u>Barge Samples (Bottom of Barge)</u>				<u>Overflow Samples</u>		
1	no sample			0-6	0-4	90-100
2	0	3	97	0-5	0	95-100
3	0	4	96	0-9	0-4	87-100
4	0	4	96	0-4	0-5	91-100
5	0	3	97	0-1	0-9	90-100
6	32	53	17	0-6	10-34	60-90
7	20	62	18	0-8	3-26	66-97
8	21	65	14	0	2-52	48-98

Table 7
Solids Concentrations and D50 Values
for Barge Samples

<u>Test No.</u>	<u>Sample Description</u>	<u>Solids Concentration g/l</u>	<u>D50 mm</u>
1	Preoverflow, bottom	376	No sample
1	Postoverflow, bottom	382	0.045
2	Postoverflow, bottom	368	0.001
3	Postoverflow, bottom	574	0.001
4	Postoverflow, upper	151	No sample
4	Postoverflow, middle	163	No sample
4	Postoverflow, bottom	170	0.035
5	Postoverflow, bottom	386	0.015
6	Postoverflow, bottom	1,478	0.300
7	Postoverflow, bottom	1,211	0.250
8	Postoverflow, bottom	1,353	0.330

PROJECT. MOBILE HARBOR CHANNEL DEEPENING					
LOCATION. BETWEEN BN 43 & 44, C/L CHANNEL					
N. 150,100 E. 337,800					
TOTAL DEPTH OF HOLE 30.0' (EL. - 72.0)			DATE HOLE STARTED. AUG. 1984		
ELEVATION TOP OF HOLE - 42.0			DATUM. MLLW ± .3 FT		
ELEV	DEP	LEG	CLASSIFICATION OF MATERIALS (DESCRIPTION)	W.C	REMARKS
	0		(CH) BLACK FAT CLAY, VERY SOFT FLUFF		
	2			98	1
	4		LIGHT GRAY, SOFT		DEPTH 4.5'- 5.0'
	6				
	8			93	2
	10				DEPTH 11.5'-12.0'
	12				
	14			60	3
	16				DEPTH 19.5' - 20.0'
	18				
	20				
	22				
	24		(CH) LIGHT GRAY FAT CLAY, SOFT		
	26				
	28		LIGHT GRAY, HIGHLY ORGANIC WITH WOOD FRAGMENTS		
	30		BOTTOM OF HOLE		
				LAB DATA SAMCLASS LL PL PI #	
				1 CH 77 22 55	

Figure 25. Boring log for Station 1027+50, located near the lower Mobile Bay barge overflow test site

PROJECT: MOBILE HARBOR CHANNEL DEEPENING								
LOCATION: BETWEEN BN C/L CHANNEL								
N 202,600 E 334,427								
TOTAL DEPTH OF HOLE: 30.0' (EL. - 72.0)				DATE HOLE STARTED: AUG. 1984				
ELEVATION TOP OF HOLE: - 42.0				DATUM: MLLW ± .3 FT				
ELEV	DEP	LEG	CLASSIFICATION OF MATERIALS (DESCRIPTION)	W.C	SAMP NO.1	REMARKS		
-43.0	0		(CH) GRAY FAT CLAY, SOFT, WITH SOME SAND			DEPTH 2.5' - 3.0'		
	2							
	4							
	6							
	8			29	1			
	10						DEPTH 7.5' - 8.0'	
	12							
	14							
	16							
	18							
	20				32	2		
	22		DARK GRAY TO GRAY, SOFT, WITH ORGANIC MATERIAL OF WOOD, ROOTS & LEAVES				DEPTH 14.5' - 15.0'	
	24							
	26							
	28							
	30							
	32						DEPTH 19.5' - 20.0'	
	34							
	36							
	38							
	40							
	42						DEPTH 19.5' - 20.0'	
	44							
	46							
	48							
	50							
	52						DEPTH 19.5' - 20.0'	
	54							
	56							
	58							
	60							
	62					DEPTH 19.5' - 20.0'		
	64							
	66							
	68							
	70							
	72					DEPTH 19.5' - 20.0'		
	74							
	76							
	78							
	80							
	82					DEPTH 19.5' - 20.0'		
	84							
	86							
	88							
	90							
	92					DEPTH 19.5' - 20.0'		
	94							
	96							
	98							
	100							
	102					DEPTH 19.5' - 20.0'		
	104							
	106							
	108							
	110							
	112					DEPTH 19.5' - 20.0'		
	114							
	116							
	118							
	120							
	122					DEPTH 19.5' - 20.0'		
	124							
	126							
	128							
	130							
	132					DEPTH 19.5' - 20.0'		
	134							
	136							
	138							
	140							
	142					DEPTH 19.5' - 20.0'		
	144							
	146							
	148							
	150							
	152					DEPTH 19.5' - 20.0'		
	154							
	156							
	158							
	160							
	162					DEPTH 19.5' - 20.0'		
	164							
	166							
	168							
	170							
	172					DEPTH 19.5' - 20.0'		
	174							
	176							
	178							
	180							
	182					DEPTH 19.5' - 20.0'		
	184							
	186							
	188							
	190							
	192					DEPTH 19.5' - 20.0'		
	194							
	196							
	198							
	200							
	202					DEPTH 19.5' - 20.0'		
	204							
	206							
	208							
	210							
	212					DEPTH 19.5' - 20.0'		
	214							
	216							
	218							
	220							
	222					DEPTH 19.5' - 20.0'		
	224							
	226							
	228							
	230							
	232					DEPTH 19.5' - 20.0'		
	234							
	236							
	238							
	240							
	242					DEPTH 19.5' - 20.0'		
	244							
	246							
	248							
	250							
	252					DEPTH 19.5' - 20.0'		
	254							
	256							
	258							
	260							
	262					DEPTH 19.5' - 20.0'		
	264							
	266							
	268							
	270							
	272					DEPTH 19.5' - 20.0'		
	274							
	276							
	278							
	280							
	282					DEPTH 19.5' - 20.0'		
	284							
	286							
	288							
	290							
	292					DEPTH 19.5' - 20.0'		
	294							
	296							
	298							
	300							
	302					DEPTH 19.5' - 20.0'		
	304							
	306							
	308							
	310							
	312					DEPTH 19.5' - 20.0'		
	314							
	316							
	318							
	320							
	322					DEPTH 19.5' - 20.0'		
	324							
	326							
	328							
	330							
	332					DEPTH 19.5' - 20.0'		
	334							
	336							
	338							
	340							
	342					DEPTH 19.5' - 20.0'		
	344							
	346							
	348							
	350							
	352					DEPTH 19.5' - 20.0'		
	354							
	356							
	358							
	360							
	362					DEPTH 19.5' - 20.0'		
	364							
	366							
	368							
	370							
	372					DEPTH 19.5' - 20.0'		
	374							
	376							
	378							
	380							
	382					DEPTH 19.5' - 20.0'		
	384							
	386							
	388							
	390							
	392					DEPTH 19.5' - 20.0'		
	394							
	396							
	398							
	400							
	402					DEPTH 19.5' - 20.0'		
	404							
	406							
	408							
	410							
	412					DEPTH 19.5' - 20.0'		
	414							
	416							
	418							
	420							
	422					DEPTH 19.5' - 20.0'		
	424							
	426							
	428							
	430							
	432					DEPTH 19.5' - 20.0'		
	434							
	436							
	438							
	440							
	442					DEPTH 19.5' - 20.0'		
	444							
	446							
	448							
	450							
	452					DEPTH 19.5' - 20.0'		
	454							
	456							
	458							
	460							
	462					DEPTH 19.5' - 20.0'		
	464							
	466							
	468							
	470							
	472					DEPTH 19.5' - 20.0'		
	474							
	476							
	478							
	480							
	482					DEPTH 19.5' - 20.0'		
	484							
	486							
	488							
	490							
	492					DEPTH 19.5' - 20.0'		
	494							
	496							
	498							
	500							
	502					DEPTH 19.5' - 20.0'		
	504							
	506							
	508							
	510							
	512					DEPTH 19.5' - 20.0'		
	514							
	516							
	518							
	520							
	522					DEPTH 19.5' - 20.0'		
	524							
	526							
	528							
	530							
	532					DEPTH 19.5' - 20.0'		
	534							
	536							
	538							
	540							
	542					DEPTH 19.5' - 20.0'		
	544							
	546							
	548							
	550							
	552					DEPTH 19.5' - 20.0'		
	554							
	556							
	558							
	560							
	562					DEPTH 19.5' - 20.0'		
	564							
	566							
	568							
	570							
	572					DEPTH 19.5' - 20.0'		
	574							
	576							
	578							
	580							
	582					DEPTH 19.5' - 20.0'		
	584							
	586							
	588							
	590							
	592					DEPTH 19.5' - 20.0'		
	594							
	596							
	598							
	600							
	602					DEPTH 19.5' - 20.0'		
	604							
	606							
	608							
	610							
	612					DEPTH 19.5' - 20.0'		
	614							
	616							
	618							
	620							
	622					DEPTH 19.5' - 20.0'		
	624							
	626							
	628							
	630							
	632					DEPTH 19.5' - 20.0'		
	634							
	636							
	638							
	640							
	642					DEPTH 19.5' - 20.0'		
	644							
	646							
	648							
	650							
	652					DEPTH 19.5' - 20.0'		
	654							
	656							
	658							
	660							
	662					DEPTH 19.5' - 20.0'		
	664							
	666							

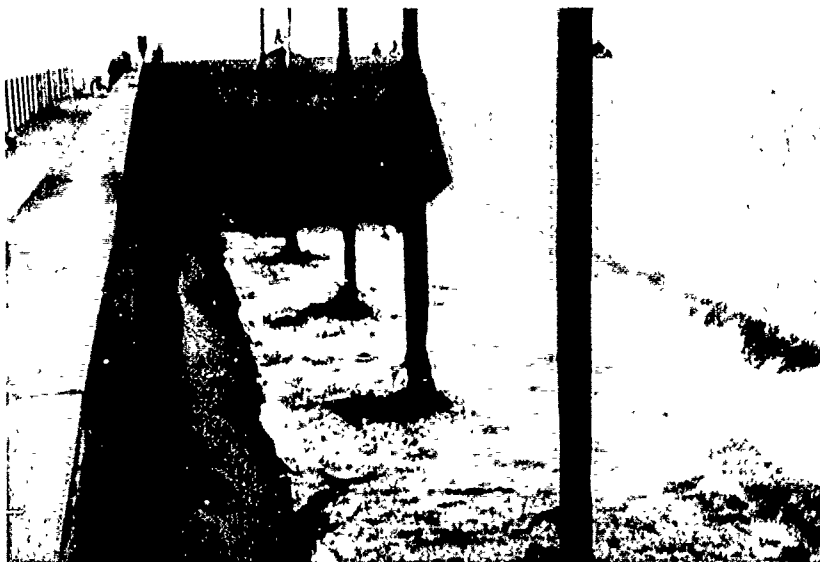


Figure 27. Inflow from downcomers during initial stages of filling

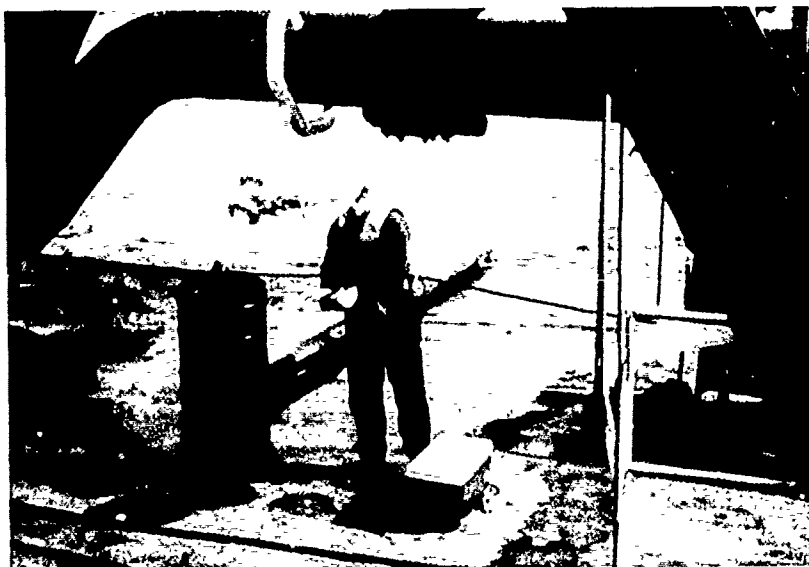


Figure 29. Inflow sampling valve

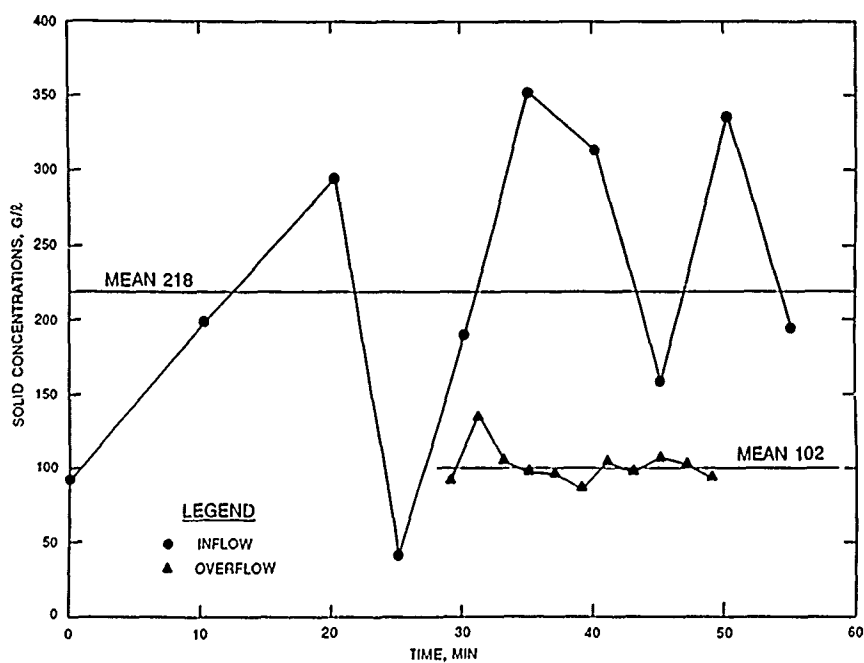


Figure 30. Inflow and overflow suspended solids concentrations for Test 1

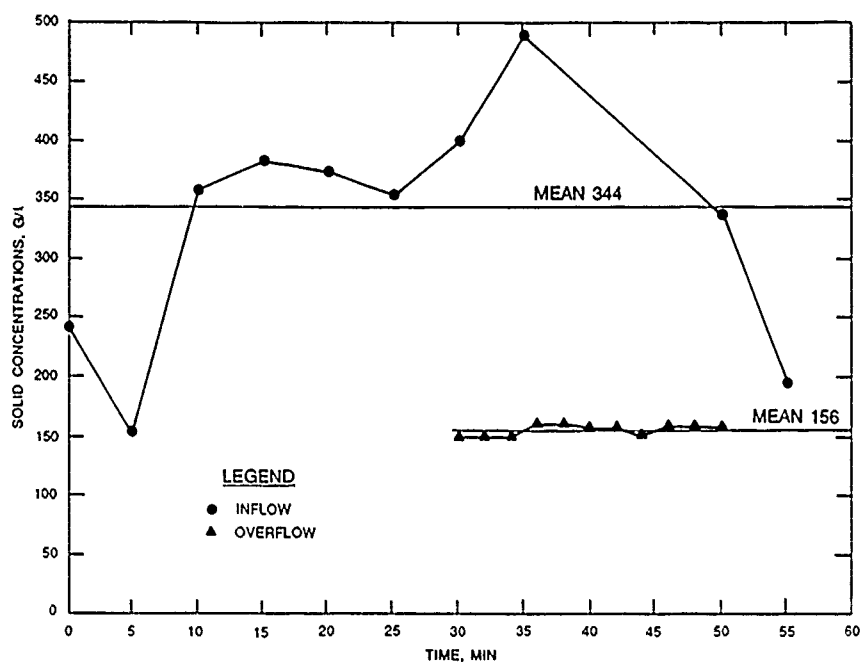


Figure 31. Inflow and overflow suspended solids concentrations for Test 2

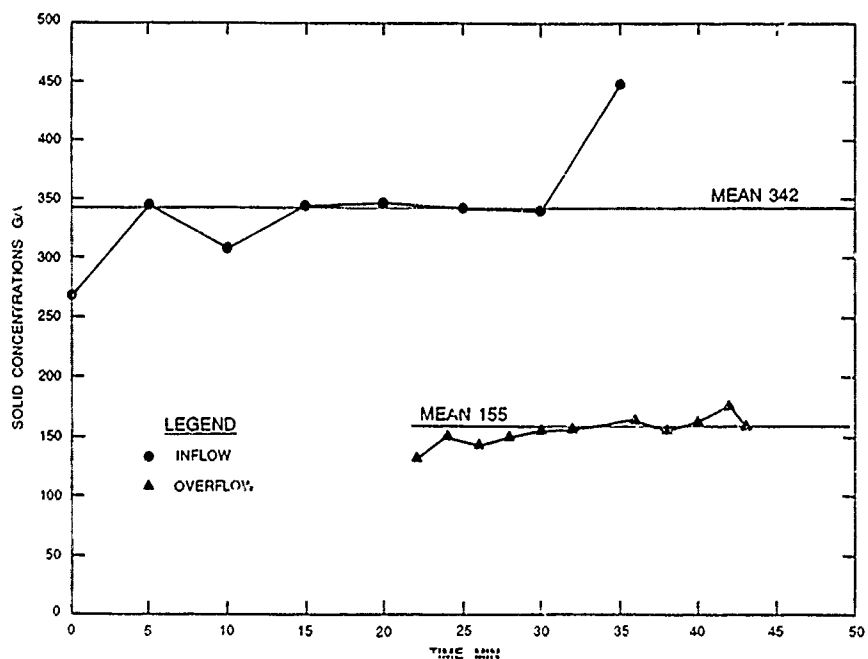


Figure 32. Inflow and overflow suspended solids concentrations for Test 3

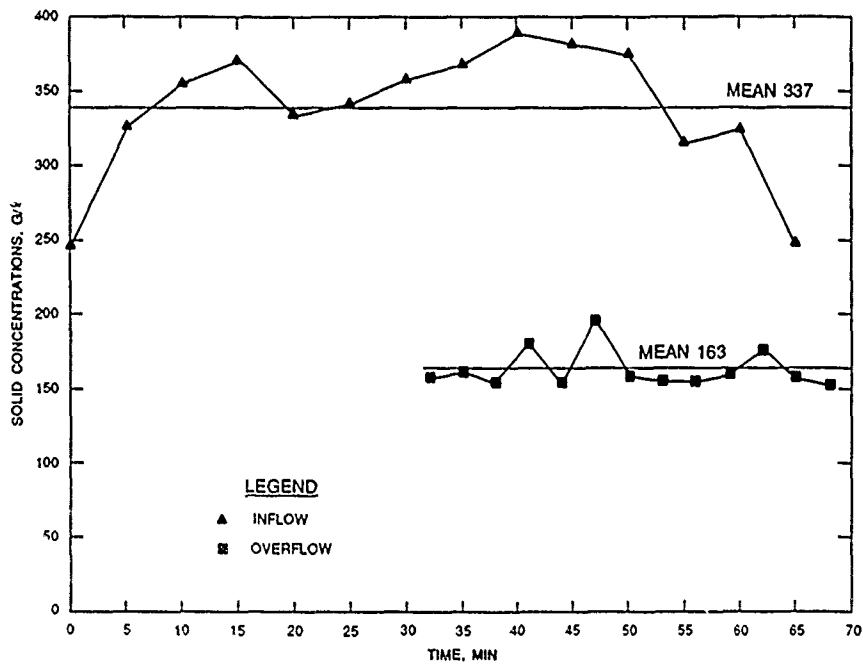


Figure 33. Inflow and overflow suspended solids concentrations for Test 4

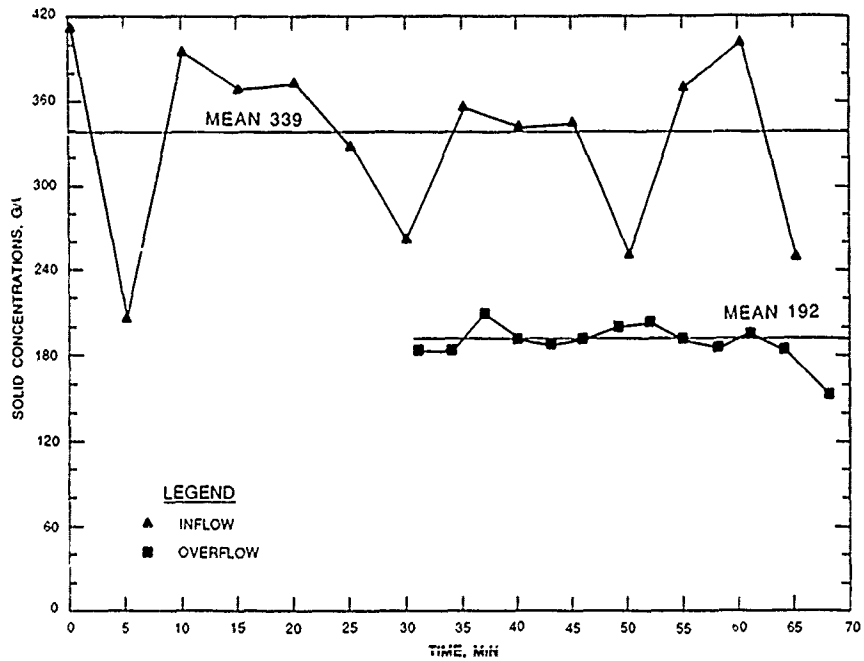


Figure 34. Inflow and overflow suspended solids concentrations for Test 5

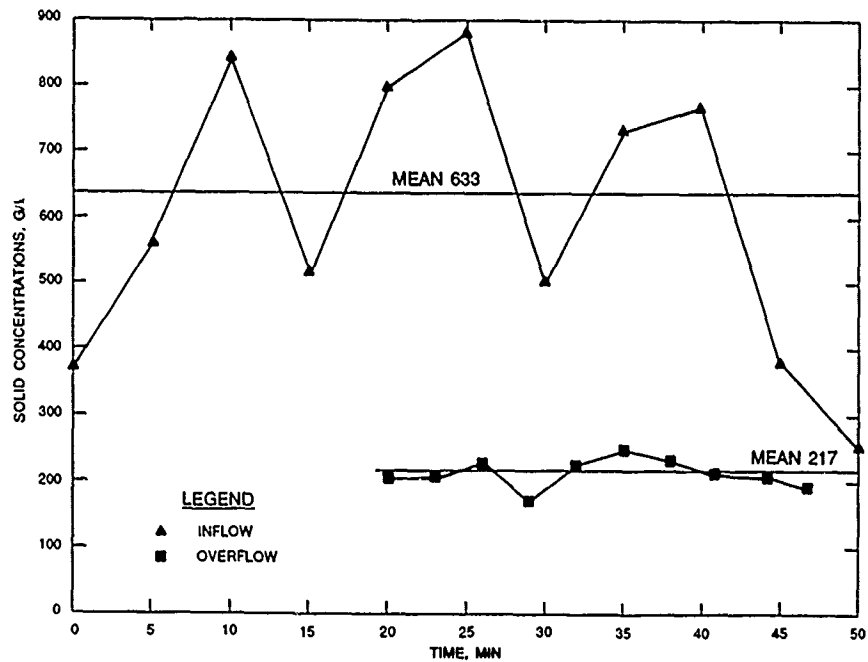


Figure 35. Inflow and overflow suspended solids concentrations for Test 6

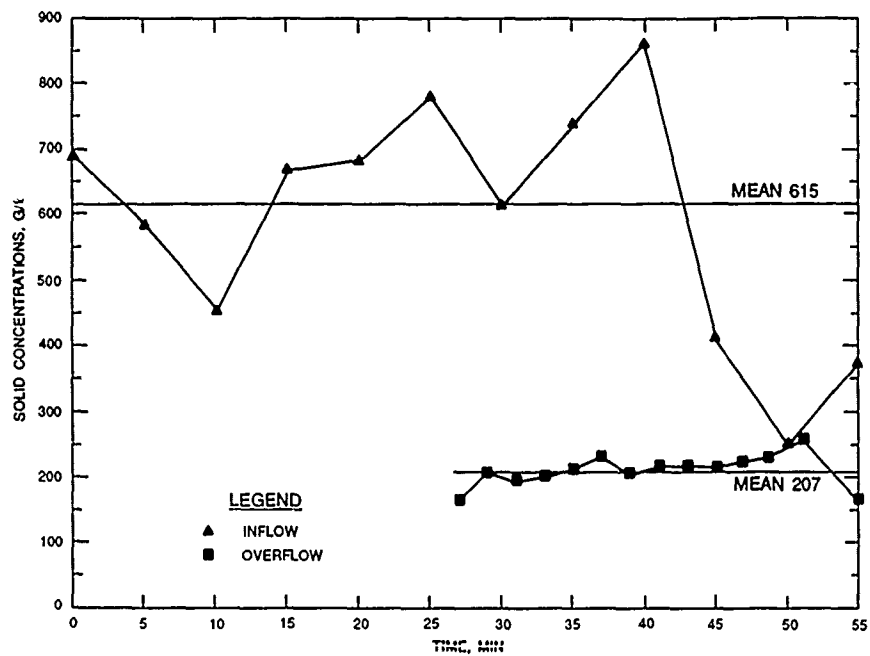


Figure 36. Inflow and overflow suspended solids concentrations for Test 7

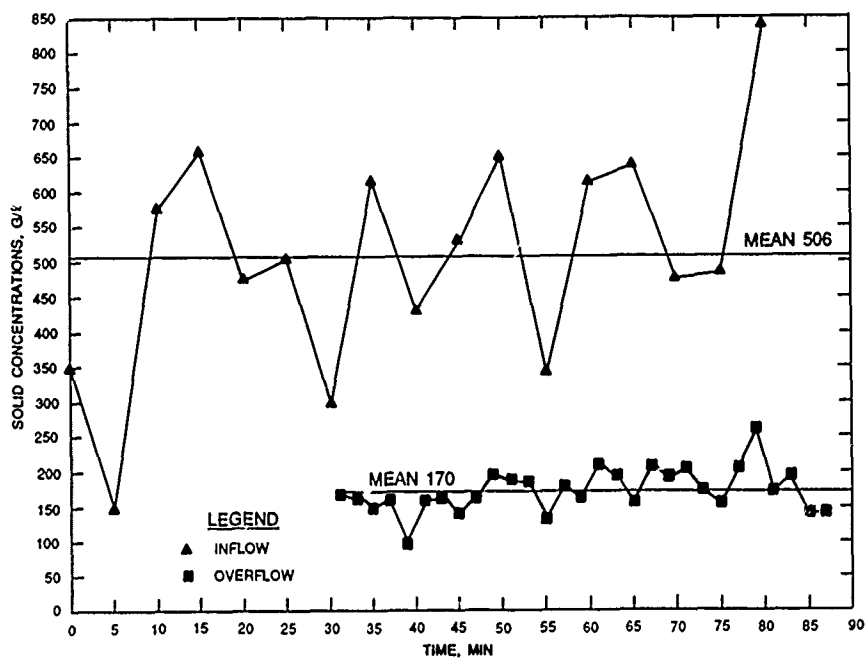


Figure 37. Inflow and overflow suspended solids concentrations for Test 8

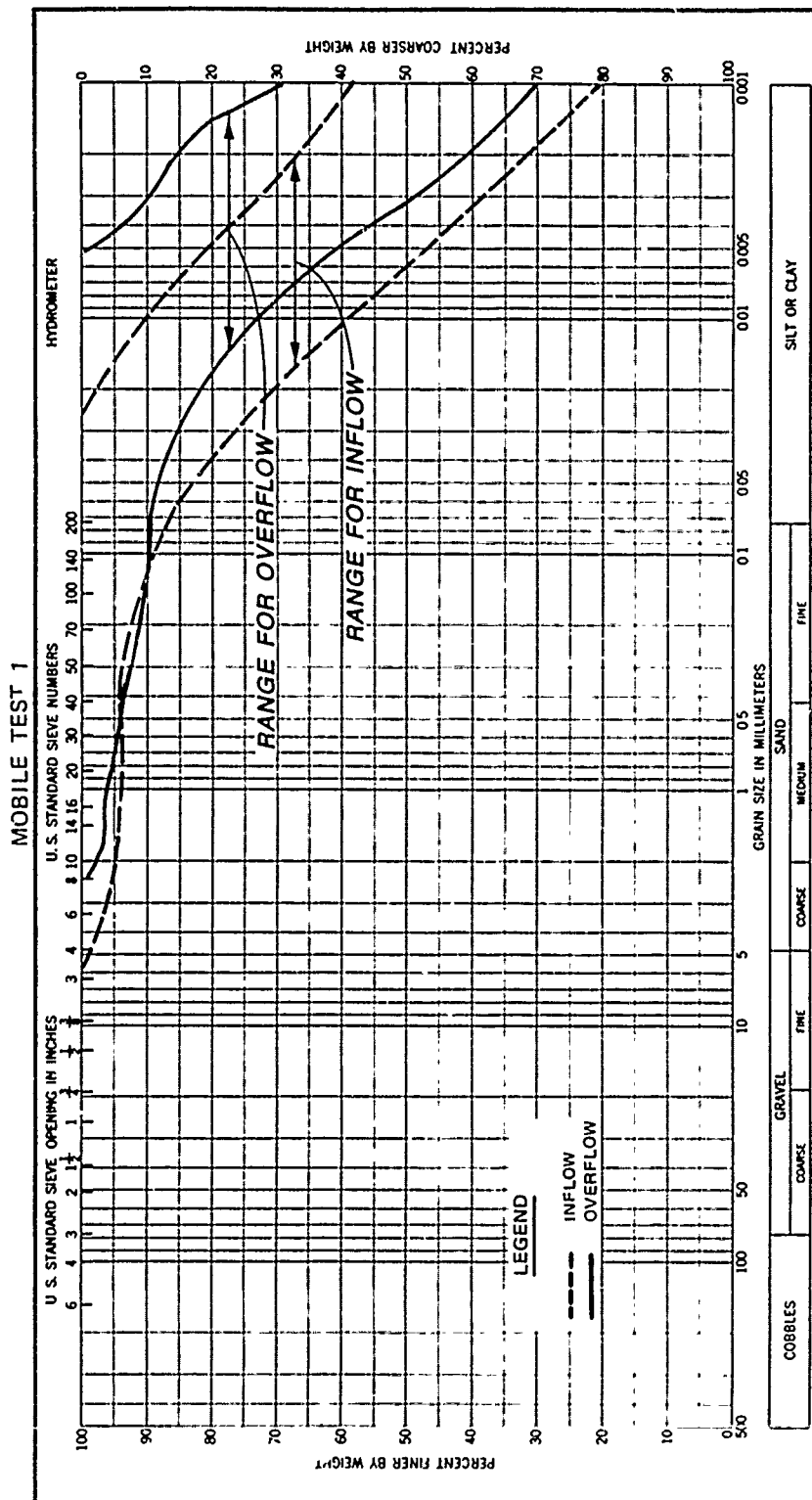


Figure 38. Grain size distribution, Test 1

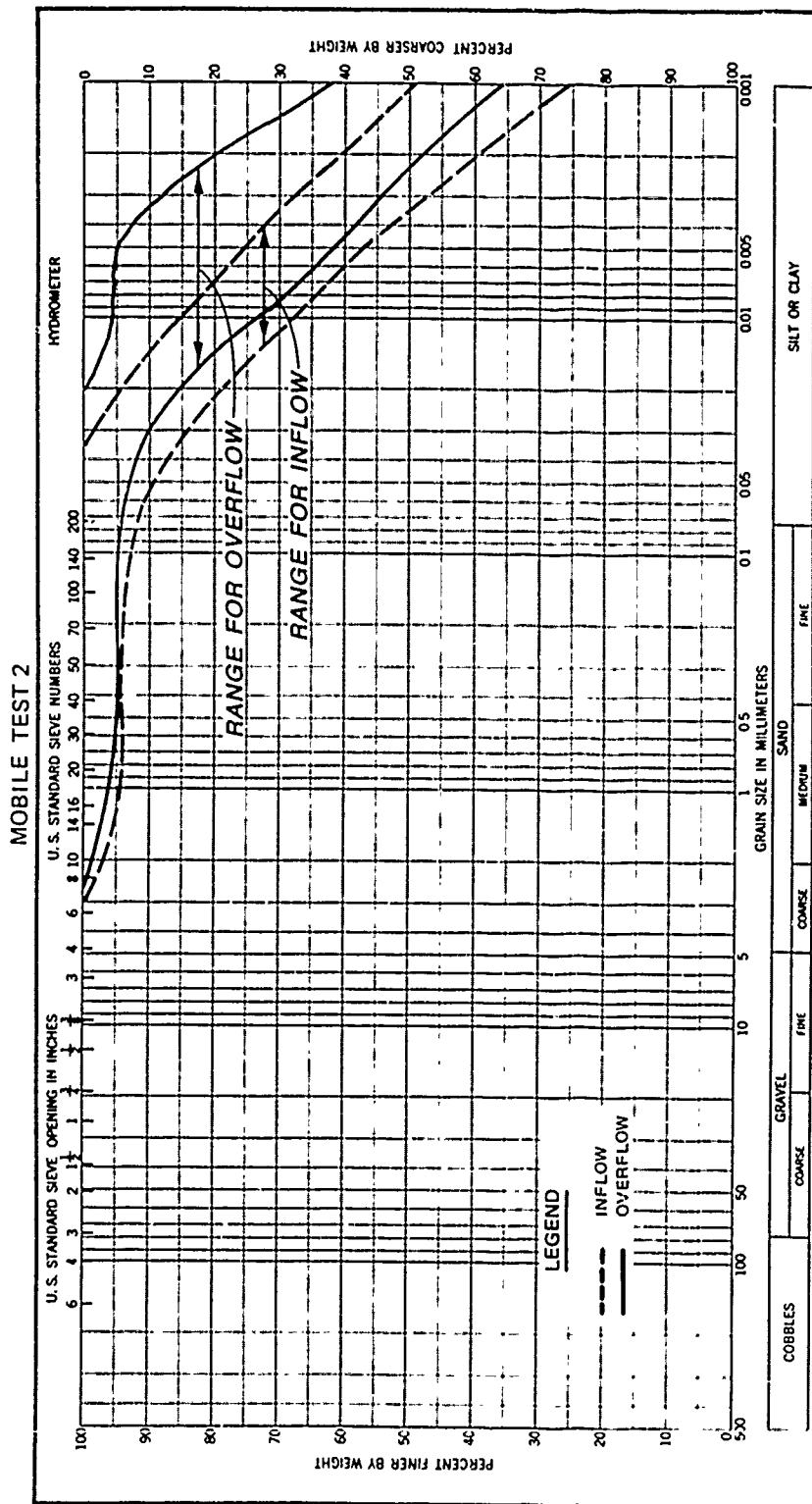


Figure 39. Grain size distribution, Test 2

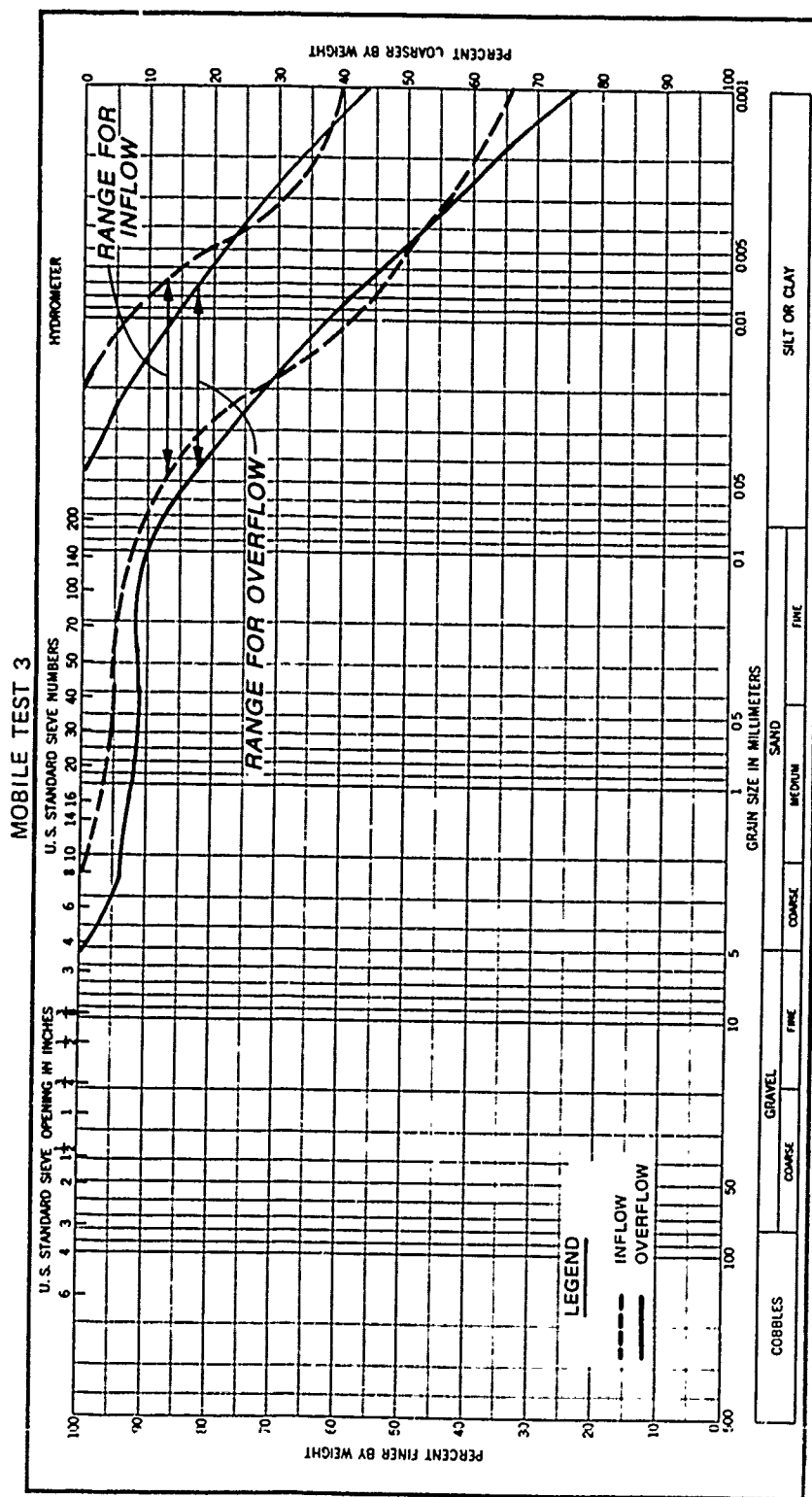


Figure 40. Grain size distribution, Test 3

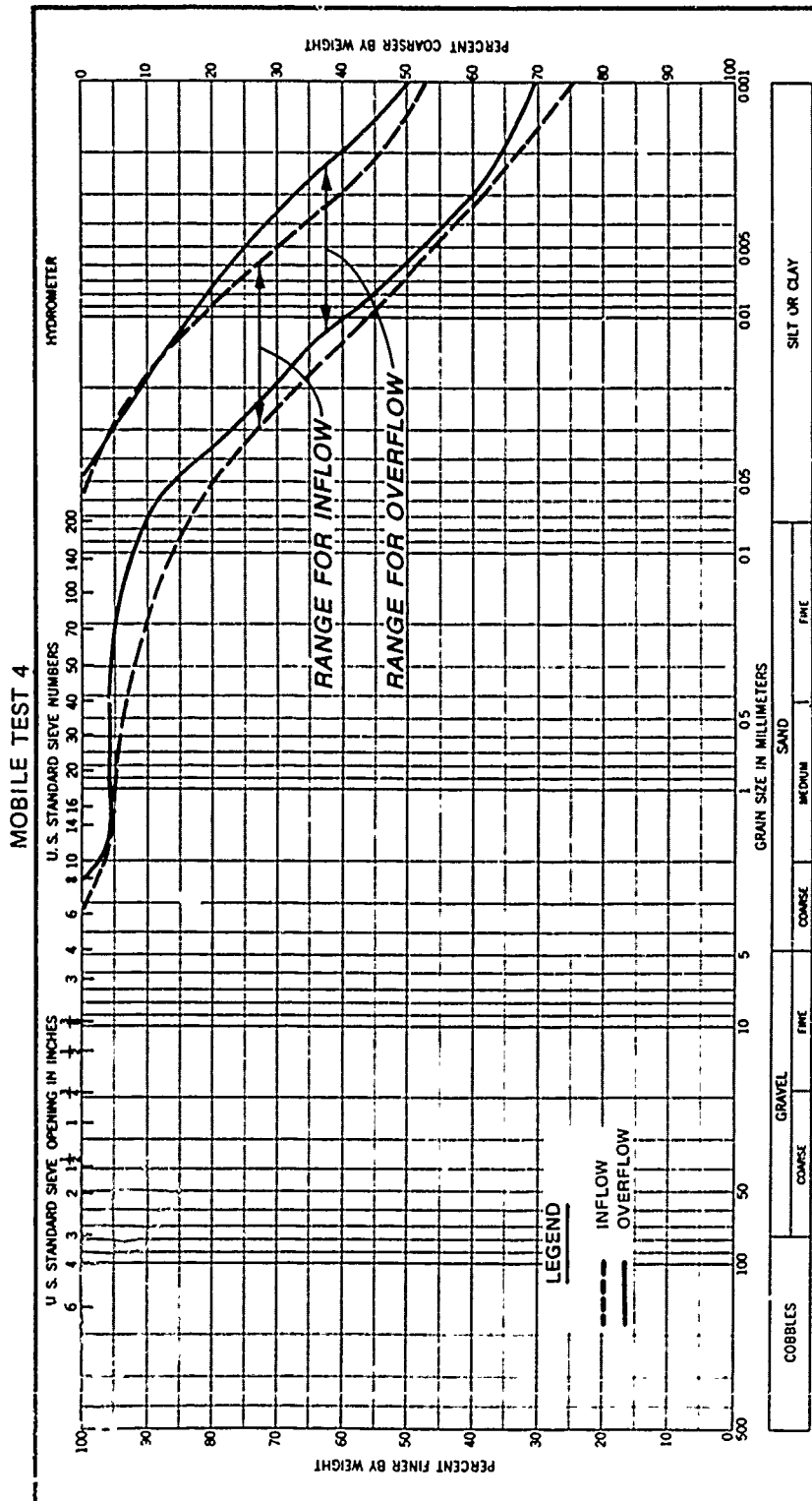


Figure 41. Grain size distribution, Test 4

MOBILE TEST 5

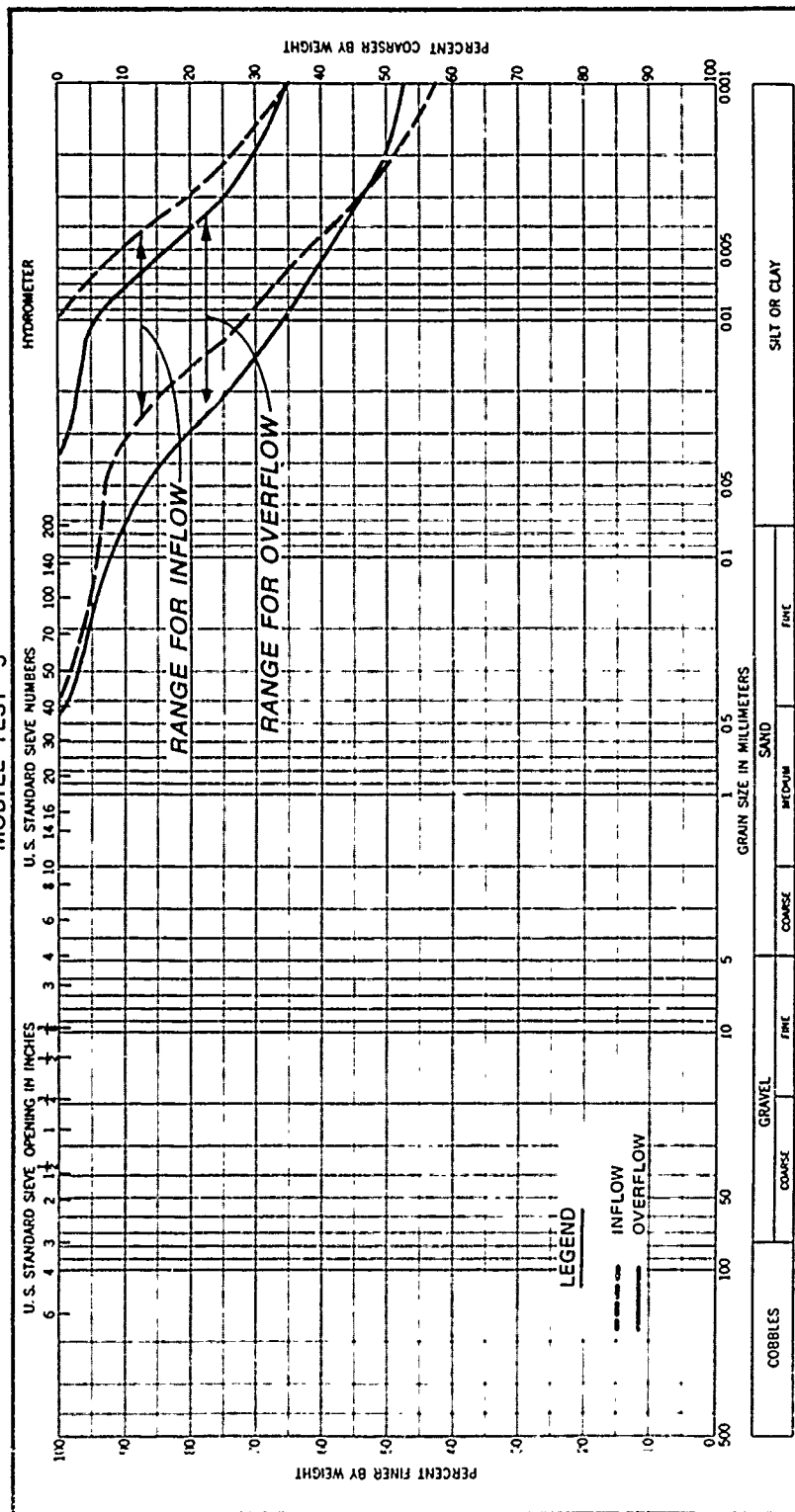


Figure 42. Grain size distribution, Test 5

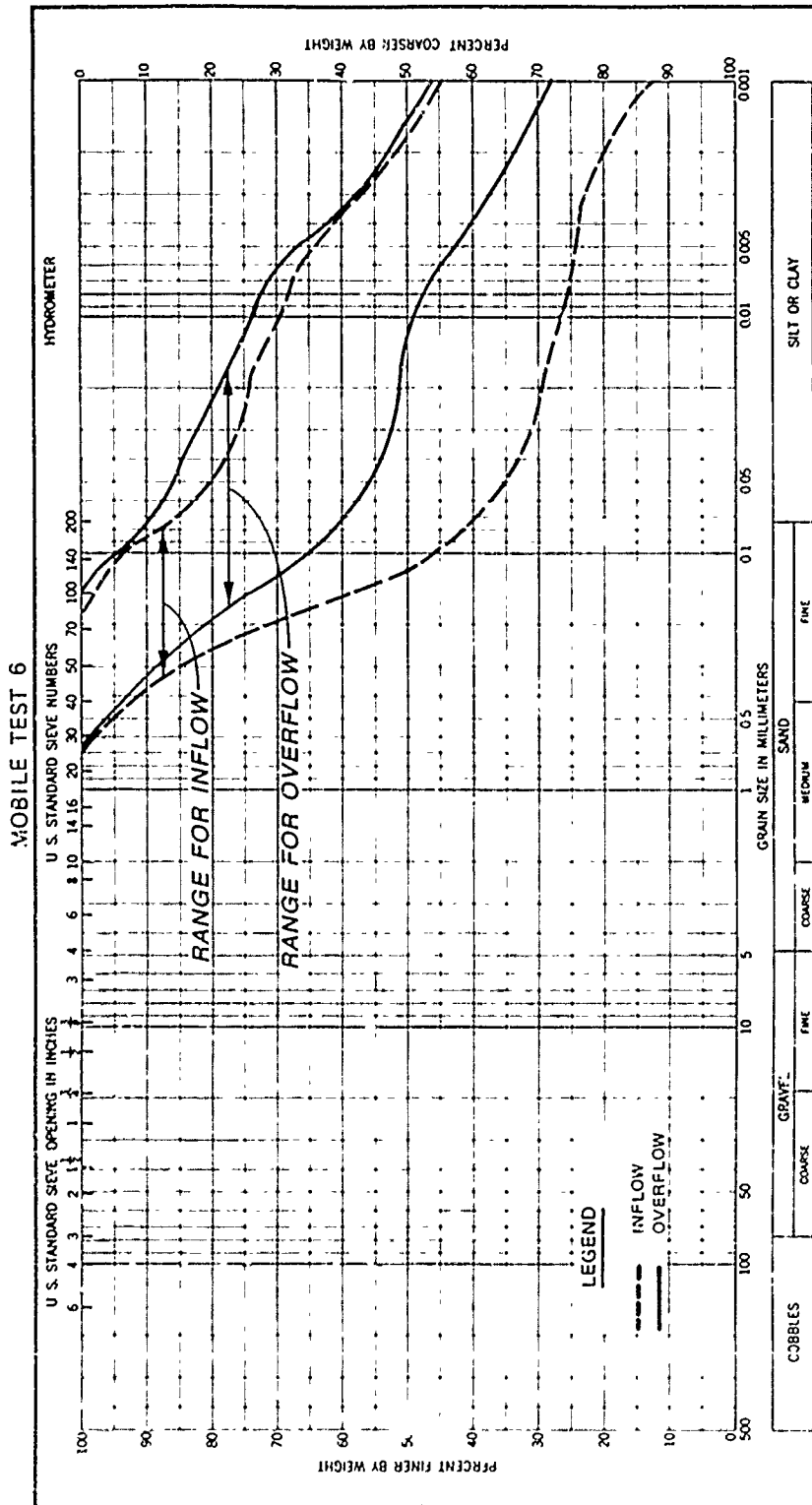


Figure 43. Grain size distribution, Test 6

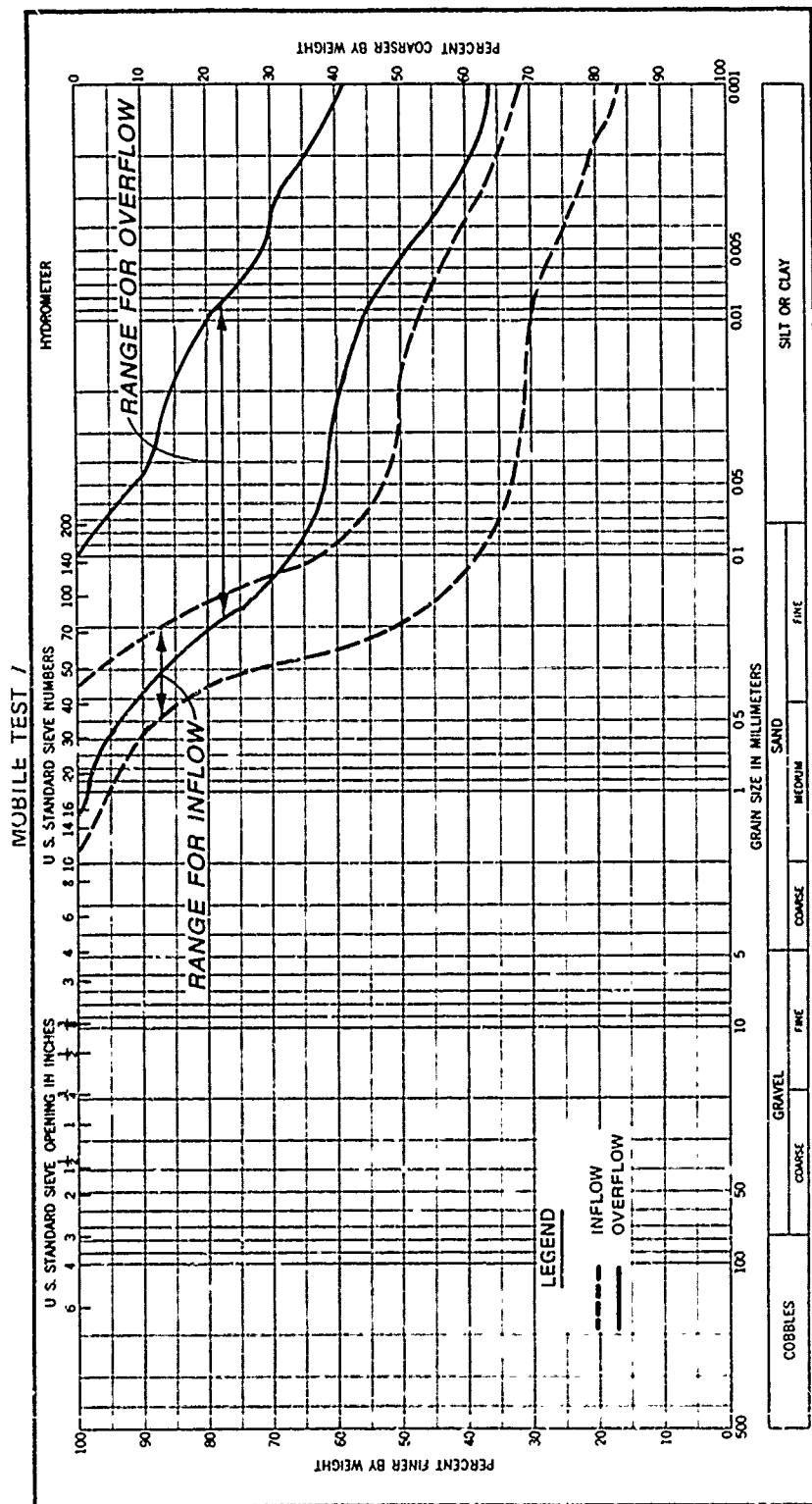


Figure 44. Grain size distribution, Test 7

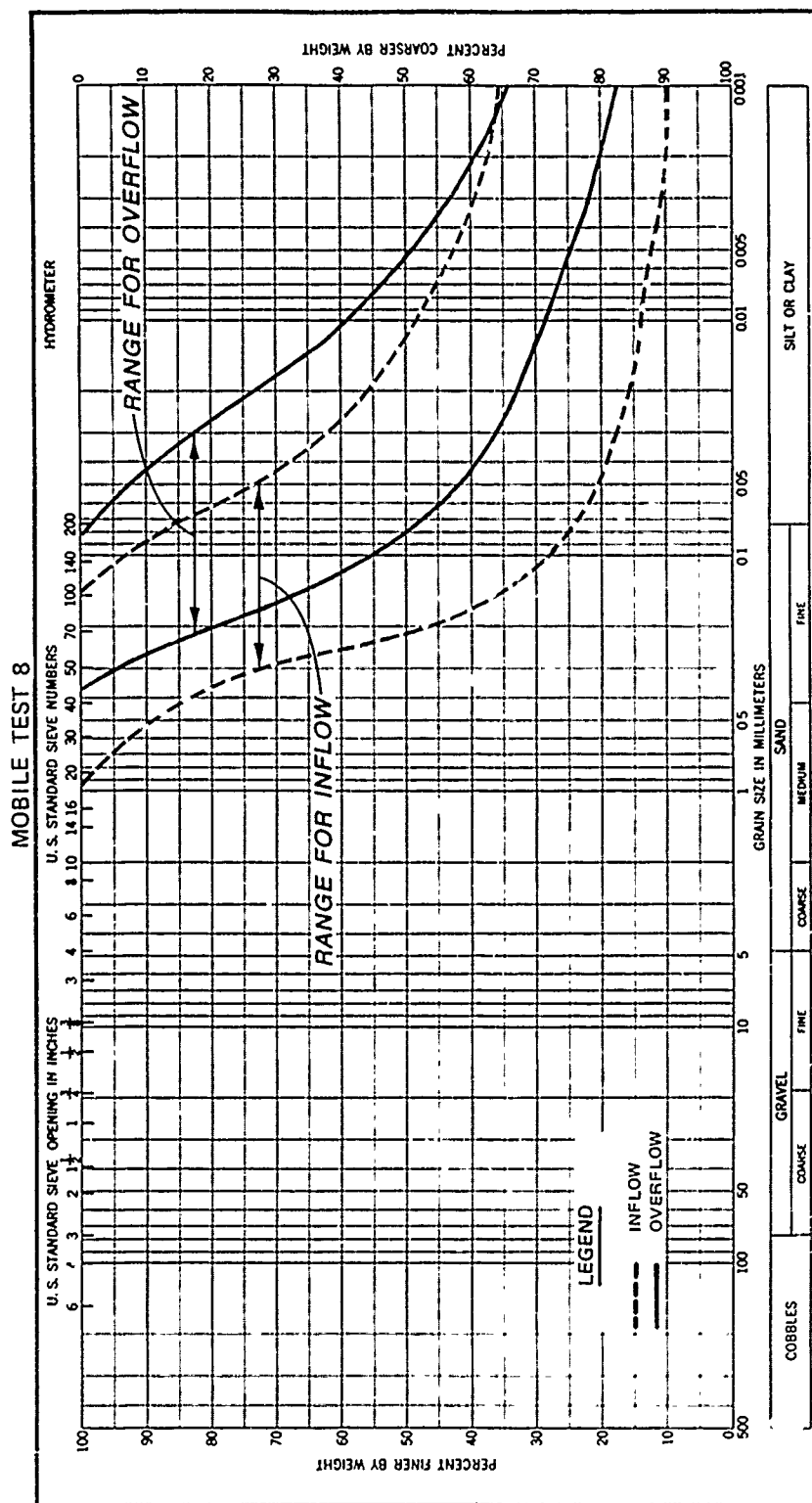


Figure 45. Grain size distribution, Test 8

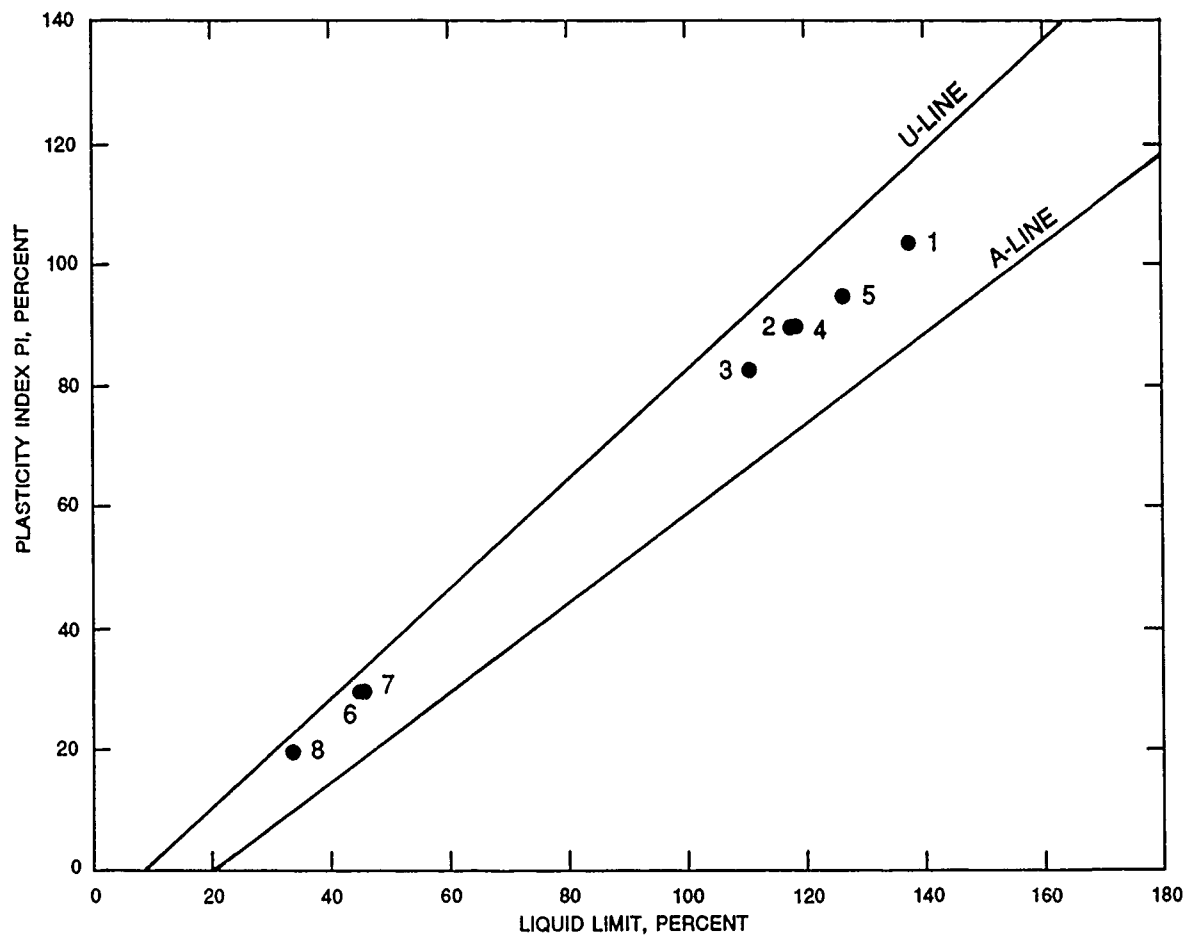


Figure 46. Plasticity chart



Figure 47. Near-surface material in hopper barge



Figure 48. Bottom material in hopper barge

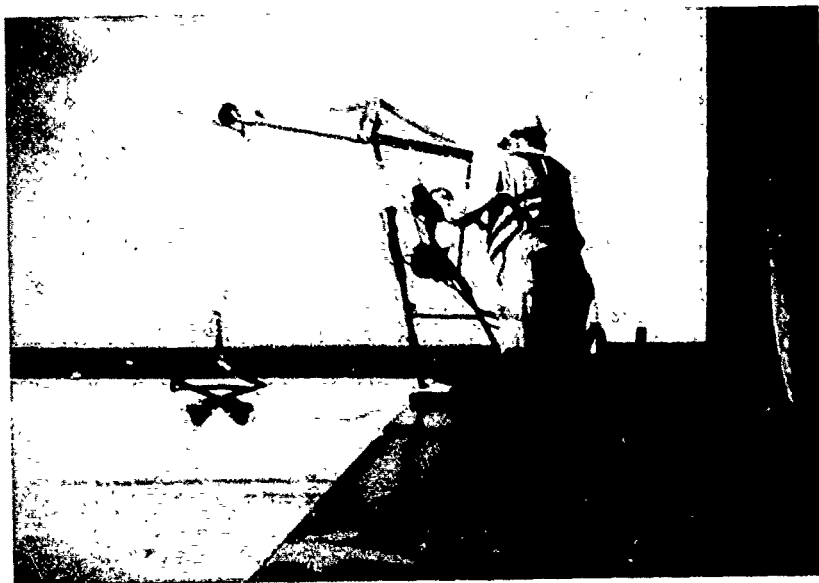


Figure 49. Petersen dredge sampler

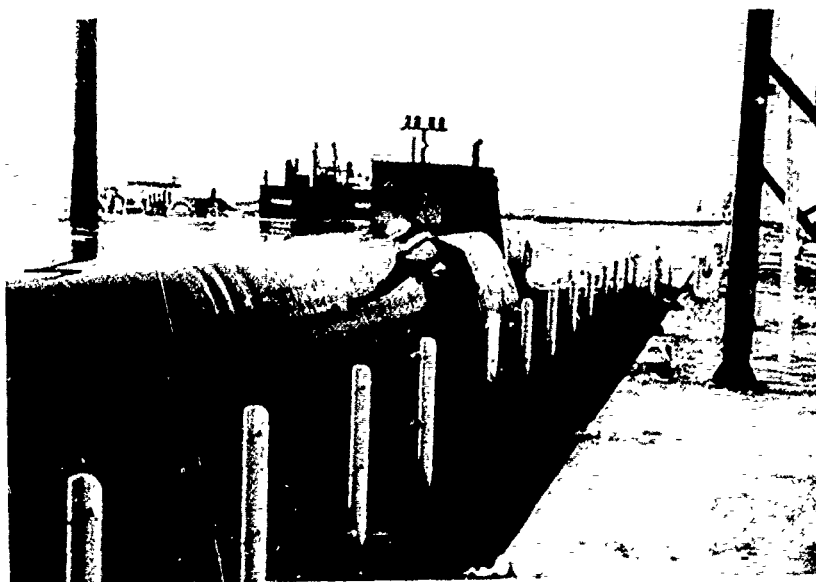


Figure 50. Overflow sampling operation

PART VI: SUSPENDED SEDIMENT PLUME TRACKING*

Background

Suspended sediment plume tracking efforts were conducted in association with four overflow events. These tests included a flood tide condition on December 3, 1987, and an ebb tide condition on December 4, 1987, at the lower bay site adjacent to Beacon 44. In addition, plumes generated during a mixed flood and ebb tide condition on December 6, 1987, as well as a flood tide condition on December 9, 1987, at the upper bay site adjacent to Beacon 66 were investigated. Several other overflow and loading tests occurred, but due to severely inclement weather causing safety hazards, plume tracking efforts were aborted. The data gathered also include tide data at two locations in Mobile Bay (Beacon 66 and near Beacon 50); current velocities at two locations just upstream of the dredge (one station in the channel and one on the shallow flats in the bay proper); and suspended sediment concentrations determined from samples taken manually from small boats and automatically by buoyed remote water samplers.

All waters of Mobile Bay and the Mobile River, as well as all or portions of their tributaries, are influenced by tidal fluctuations. The estuary is diurnal, with one tide daily, and the tidal cycle is approximately 25 hr in duration. Tidal fluctuations typically vary from less than 1 ft during neap tides to 2.5 ft during spring tides. Normal tidal cycles are greatly affected by winds. Prevailing winds of several hours duration can be more responsible for water-surface elevations and circulation patterns within the bay than the tides. These conditions were considered in the design of the suspended sediment plume tracking efforts.

Methods

Tidal elevation measurements

Tidal elevations were measured by a system consisting of a stilling well and float that was connected by a wire rope to a recording device. The tide gages were Fischer and Porter Company Type 1550 punched tape level recorders

* Written by Howard A. Benson, Hydraulics Laboratory, WES.

(Figure 51). The gages recorded elevations to the nearest 0.01 ft and had a range of 100 ft. The units were powered by a 7.5-v battery. A timer activated the recording mechanism every 15 min, and the float elevation was punched on 16-channel, foil-backed paper tapes. The float was a 3-in.-diam aluminum cylinder, and the stilling well was a 4-in.-diam plastic pipe. Water in the stilling well responded to water levels outside the well by flow through a 15-ft-long, 3/8-in.-diam copper tube. The tube's outer end was protected against clogging by a cylindrical copper filter.

Vertical control for the tide gage assemblies was arbitrary. The 15-ft-long tube used as the stilling well port was designed to minimize short-period oscillations and to cause the well to respond linearly to fluctuations in the outside water level. Response characteristics of the tide wells have been determined by testing.* Figure 52 shows the derived amplitude and phase response characteristics of the tide wells. It can be seen that amplitude decreases sharply for periods less than 50 min and is less than 10 percent for periods under 1 min. The half-amplitude period is 9 min. The amplitude response is essentially unity, and phase lag approaches zero at tidal periods.

Initial synchronization of the tide recorder timer is within ± 5 sec of the National Bureau of Standards (NBS) time standard. Bench tests of the timers have shown them to exhibit negligible error in time for individual readings over a 1-hr period. Gage time is typically accurate to ± 2 min per month. In practice, gage and NBS times are recorded when tapes are removed so that timing errors can be identified. Relative accuracy is affected by temperature of the water, float, and wire, plus salinity changes of the water inside the well. Relative accuracy is considered to be within 0.1 ft.

Water current measurements

The equipment used to obtain water current velocity and direction data from a boat consisted of a current meter, direction indicator, and weight (fish), all suspended by a wire rope, plus remote readout devices and a support frame (Figure 53). The current meter is a vertical-axis, cup-type meter (Gurley Model 665) with a remote, direct-reading speed indicator. The direction indicator consists of a remote-reading magnesyn compass mounted just above the current meter in a waterproof cylindrical housing. Suspended below the meter is a finned, streamlined weight (fish) that holds the sensors in a

* W. H. McAnally, Jr. 1979. Water level measuring by Estuaries Division, Hydraulics Laboratory. Memorandum for Record. US Army Engineer Waterways Experiment Station, Vicksburg, MS.

vertical attitude facing into the flow. The sensor assembly is supported by a 1/8-in. wire rope from a portable support frame that is equipped with a winch to raise and lower the assembly. An indicator on the winch shows the sensor's depth below the water's surface.

The Gurley current meters have been found to have a threshold speed of less than 0.2 fps and at 75° F to give the correct current speed to within +3 to -5 percent for speeds of 1 to 7 fps, and ± 0.1 fps for speeds less than 1 fps.* Error due to temperature change is approximately 0.05 percent per degree deviation from 75° F. At flow speeds greater than 3 fps, readings near the surface tend to be somewhat low due to sensor inclination. Accuracy of the direction indicator is within 10 deg at speeds greater than 0.5 fps, but strong wave action moving the boat can cause temporary errors greater than this.

Water samplers

Discrete water samples were taken at predetermined depths in the water column by pumping through a 3/8-in. plastic tube with an incoming tip mounted just below the current meter and pointed into the flow. A small pump onboard each survey boat delivered the water to sample bottles.

The equipment used to obtain the automatic, remote water samples was the Isco Company Model 2700 sampler (Figure 54). This sampler is a portable, programmable device designed to collect up to 24 sequential samples or a single composite sample. Samples may be collected at equal time intervals from 1 to 9999 min. Sample volumes up to 1,000 ml may be selected.

Sample analysis

Water samples to be used for salinity and suspended sediment measurements were placed in 8-oz plastic bottles. The salinity of discrete water samples was measured in the laboratory, using a Beckman Model RA5 salinometer with automatic temperature compensation. The salinometer was calibrated with Standard Sea Water and was accurate to within ± 0.2 ppt. Total suspended solids (TSS) was determined by filtration of samples. Nuclepore polycarbonate filters with 0.40- μ pore size were used. The filters were desiccated and preweighed; then a vacuum system (8-lb vacuum maximum) was used to draw the sample through the filter. The filters and holders were then washed with distilled water. The filters were dried at 105° C for 1 hr and then

* Ibid.

reweighed. The TSS was then calculated based on the filter and the volume of the filtered sample.

Test Procedures

The disposal scow overflow tests in Mobile Bay were conducted during the period December 3-9, 1987. Eight tests were conducted at two locations: an upper bay site at channel Beacon 66, and a lower bay site at channel Beacon 44. The tests were conducted for both ebb and flood tide conditions, and for maintenance and new work material at each site.

Two recording tide gages (Figure 55) were installed during the first week of November 1987 and remained in operation throughout the test period. The gages were checked and serviced periodically during the test period. Tidal measurements for the two sites in Mobile Bay during the study period are presented in Figures 56-59. Recording tide gages were installed on November 2, 1987, at channel Beacon 66 (tide gage 1) and on the first range marker just north of channel Beacon 50 (TG2). The gages were retrieved on December 10, 1987, at the conclusion of the tests. Figure 56 depicts a condensed tidal curve for TG1. Figure 57 displays the tidal curves in 5-day plots for TG1. Figure 58 represents a condensed tidal curve for TG2, and Figure 59 shows the tidal curves in 5-day plots for TG2. The gages were not "shot" in order to establish a reference datum; therefore, the vertical datum set at each gage is arbitrary. The vertical datum was chosen so as not to be confused with mlw or NGVD.

Sampling boat ranges were established based on the distance that the overflow plume was expected to travel in 1 hr. As the plume approached each range, sampling was initiated as soon as an indication of an increase in ambient turbidity was noted. Water samples were collected at surface, middepth, and bottom. The sampling boats proceeded across their ranges collecting samples at intervals of approximately 15 min until the turbidity decreased to the preestablished background level. Turbidity was monitored by use of an optical backscatter instrument. Spacing between ranges and stations varied daily depending on field conditions. Normally, each sampling boat would deploy four anchored buoys at uniform distances across the given range. The location of the first buoy would be designated as Station 2, whereas the location of the second buoy would be designated as Station 4. Station 1 would be located approximately 50 ft to the west of the first buoy. Station 3 would

then be located equidistant between Stations 2 and 4. This deployment of working buoys continued along the range to a terminus at Station 8, 9, or 10.

Automatic water samplers were set up and deployed at strategic locations to provide additional spatial coverage. The portable samplers were deployed in an anchored inflatable boat. Start time was preset based on the anticipated time of overflow for a particular test, and sequential samples were obtained at preprogrammed intervals thereafter. The locations of the sampling ranges and automatic water samplers are shown in Figures 60-63. These figures show the position of the hopper barge in relation to the sampling ranges, the point at which overflow occurred, the channel center line, station locations, and the area dredged.

During each overflow event, a boat was alternately moved between two stations located just upstream of the dredge collecting current velocity and direction measurements at half-hourly intervals. A "channel" station was established approximately 300 yd upstream of the dredge, and a "bay" station in the shallow flats approximately 300 yd to the east of the channel station. At the bay station, data were collected at two to three separate depths; at the channel station, data were collected at five depths.

Before each test, drogues were released near the hopper barge overflow location and tracked to determine general flow patterns. The range/range positioning system described previously (see Part III) was used for these tracking activities. A small flag attached to the top may have slightly influenced the drift pattern of a given drogue due to wind forces. However, a large cloth rudder attached 3 to 6 ft below the drogue's surface buoy ensured that the predominant direction of drift was determined by water currents. Plume tracking drogues were deployed near the port and starboard corners of the stern of the hopper barge (overflow always occurred at the stern) at the start and end of actual overflow. These data are presented in Figures 60-63. (Tabular listings of the times and computed average velocities of each drogue's movements between positioning fixes are given as Tables 30-34.) The plotted drogue positions for each test represent the anticipated flow pattern of surface plume movement. The computed surface velocities based on time and position calculations agreed in general with the velocities measured by remote current meters at each site.

The test procedures varied somewhat on a day-to-day basis depending on the field conditions encountered. The weather, specifically very strong winds (20 to 25 knots) made conditions in the smaller sampling boats unsafe on

several days. Decisions were made at these times to cancel plume monitoring because of the potential safety hazards.

After several tests had been completed, it became apparent that the major portion of overflow material was rapidly sinking to the bottom and not forming a substantial surface turbidity plume. This process made detection of elevated turbidity levels along the ranges difficult, although adjustments to range locations and spacing were made daily.

During several of the tests, the hopper barge was placed next to the spider barge in such a manner that overflow occurred at the upcurrent end. Consequently, the overflow material passed under the hopper barge or between the hopper barge and the spider barge. This made optimal placement of sampling boats and devices difficult on several occasions. Ship traffic, dredging contractor's workboats, and obstructions caused by the dredge pipeline also created many problems for the sampling boats.

Results of Plume Tracking Tests

Data collected during the hopper barge overflow tests include tidal measurements; water current direction and velocity measurements; suspended sediment concentrations at various times and depths from survey boat samples; and suspended sediment concentrations from samples taken automatically.

Overflow Test 1

Figure 60 shows the locations of the sampling stations in relation to the hopper barge and the dredged area for the flood tide condition test on December 3, 1987. Table 8 lists the coordinates of the dredge, the hopper barge, and the data collection buoys. The table shows the station number along the survey baseline and the offset distance in feet from the baseline to the buoys. Table 9 lists the data collected by the sampling boats. The tables list the range and station number, the offset distance from the baseline, the time the sample was collected, the depth at which the sample was taken, and the sediment concentration of the sample.

Overflow Test 2

Due to unsafe working conditions caused by the weather, the decision was made to cancel plume monitoring of this test.

Overflow Test 3

Figure 61 shows the locations of the sampling stations in relation to the hopper barge and the dredged area for the ebb tidal condition test on

December 4, 1987. Table 10 lists the coordinates of the hopper barge and the data collection buoys. Table 11 lists the data collected by the sampling boats. The tables list the range and station number, the offset distance from the baseline, the time and depth at which the sample was collected, and the sediment concentration of the sample.

Overflow Test 4

Figure 62 shows the locations of the hopper barge, the automatic samplers, and the sampling stations for the ebb tidal condition test on December 6, 1987. Table 12 lists the coordinates of the hopper barge, the automatic samplers, the data collection buoys, and the location of the velocity stations. Table 13 presents the data collected by the sampling boats for this test. Listed are the range and station numbers, the offset distance from the baseline, the time and depth at which the sample was collected, and the suspended sediment concentration of the sample. Tables 14 and 15 present the data collected from the north and south automatic samplers for this test. The tables present the location of the samplers, the overall depth of the water, the depth at which the sample was taken, the time the sample was taken, and the suspended sediment concentration of the sample.

Overflow Test 5

Figure 63 shows the locations of the hopper barge, the dredged area, the south automatic sampler, and the sampling stations for the flood tidal condition test on December 6, 1987. Table 16 lists the coordinates of the hopper barge, the coordinates of the south automatic sampler, and the locations of the data collection buoys. Table 17 presents the data collected by the sampling boats, including the range and station number, the distance offset from the baseline, the time and depth at which the sample was collected, and the suspended sediment concentration of the samples. Table 18 presents the data from the south automatic sampler for this test. The table shows the location of the sampler, the overall water depth, the depth at which the samples were collected, the time they were collected, and the suspended sediment concentrations.

Water current velocity data were collected at two locations. One station was north of the dredge in the channel (V1), and the other station was approximately 200 yd to the east of the channel in the shallow flats (V2). Data were collected at half-hourly intervals at five depths for V1 and at two depths for V2. The data are presented in Figures 64-68 for the five depths at V1 and in Figures 69 and 70 for the two depths at V2. The figures present the

velocity in feet per second versus time (CST) in hours. The velocity data are also presented in Tables 19-23 for Station V1 and in Tables 24 and 25 for Station V2. The tables list the appropriate test date, time, depth, velocity, and direction.

Overflow Tests 6 and 7

Due to unsafe working conditions, caused by the weather, the decision was made to cancel plume monitoring for these tests.

Overflow Test 8

Figure 71 shows the location of the hopper barge, the dredged area, the automatic sampler, and the sampling stations for the flood tidal condition test on December 9, 1987. Table 26 lists the coordinates of the hopper barge, the automatic samplers, the data collection buoys, and the location of the velocity station. Table 27 presents the data collected by the sampling boats. The table lists the range and station number, the distance offset from the baseline, the time the samples were taken, the depth of the samples, and the suspended sediment concentrations of the samples. Table 28 presents the suspended sediment concentrations from the automatic samplers. The table lists the location, the overall water depth, the depths at which the samples were taken, and the times for this test.

Table 29 presents a salinity profile taken in the channel at Station 66 on December 10, 1987. The table lists the depth in feet and the salinity in parts per thousand. Salinity ranged from 12.01 ppt at the surface to 33.08 ppt at a depth of 45 ft.

Table 8
Location of Data Collection Buoys
Test 1

<u>Buoy No.</u>	<u>Station</u> <u>ft</u>	<u>Offset</u> <u>ft</u>	<u>Coordinates</u>	
			<u>X</u>	<u>Y</u>
1-2	114+72	83	337,226	148,930
1-4	114+93	199	337,338	148,895
1-6	114+83	296	337,433	148,902
1-8	114+78	395	337,535	148,891
2-2	103+01	104	337,395	150,089
2-4	103+15	209	337,497	150,062
2-6	103+08	291	337,579	150,060
2-8	103+21	389	337,676	150,038
3-2	100+50	100	337,423	150,341
3-4	100+50	200	337,522	150,329
3-6	100+50	308	337,629	150,318
3-8	100+49	389	337,711	150,310
3-10	100+59	511	337,831	150,291
4-2	97+37	90	337,452	150,650
4-4	97+54	215	337,574	150,620
4-6	97+51	309	337,669	150,613
4-8	97+51	396	337,755	150,606

Note. Dredge head location on 12/03/87 at 0825:
X = 337,383 Y = 150,538
Station 98+55 - Offset = 35 ft

Northwest corner of overflow barge:
X = 337,504 Y = 149,554
Station 108+20 - Offset = 280 ft

Table 9
Sampling Data, Test 1

<u>Range</u>	<u>Station</u>	<u>Offset ft</u>	<u>Time CST</u>	<u>Depth ft</u>	<u>Concentration g/l</u>
1	1	25	1100 1058	3.0 10.0	0.006 * 0.010
1	1	25	1139 1137 1135	3.0 23.5 45.0	0.004 0.015 1.052
1	2 (1A)	83	1145 1144 1143	3.0 20.3 39.5	0.003 0.013 0.415
1	3	141	1153 1152 1151	3.0 21.3 40.5	0.007 0.044 6.292
1	4 (1B)	199	1159 1158 1157	3.0 19.5 37.5	0.002 0.014 0.319
1	5	247	1205 1204 1203	3.0 18.7 35.5	0.002 0.012 0.168
1	6 (1C)	296	1211 1210 1208	3.0 13.7 25.5	0.003 0.036 0.534
1	7	346	1217 1216 1214	3.0 12.4 22.8	0.003 0.013 0.295
1	8 (1D)	395	1222 1221 1220	3.0 10.3 18.6	0.002 0.005 0.240
1	9	446	1228 1227 1225	3.0 8.5 14.9	0.004 0.005 0.023

(Continued)

* Background.

(Sheet 1 of 3)

Table 9 (Continued)

<u>Range</u>	<u>Station</u>	<u>Offset ft</u>	<u>Time GST</u>	<u>Depth ft</u>	<u>Concentration g/l</u>
2	1	49	1100	3.0	0.010 *
			1058	10.0	0.014
2	1	49	1153	3.0	N/A
			1151	21.0	N/A
			1150	41.0	N/A
2	2 (2A)	104	1204	3.0	0.013
			1202	21.5	0.018
			1159	41.0	0.816
2	3	159	1210	3.0	0.004
			1209	18.0	0.021
			1208	37.0	0.217
2	4 (2B)	209	1217	3.0	0.002
			1216	18.0	0.011
			1215	37.0	0.213
2	5	250	1223	3.0	0.003
			1222	15.5	0.045
			1220	29.0	0.760
2	6 (2C)	291	1228	3.0	0.002
			1227	12.0	0.034
			1226	23.0	0.165
2	8 (2D)	389	1234	3.0	0.005
			1232	9.0	0.006
			1231	16.0	0.046
2	9	438	1238	3.0	0.004
			1237	8.5	0.012
			1236	15.0	0.036
2	10	487	1242	3.0	0.004
			1241	8.0	0.007
			1240	14.0	0.046
3	1	50	1205	3.0	0.007
			1204	21.5	0.481
			1204	42.0	0.863

(Continued)

* Background.

(Sheet 2 of 3)

Table 9 (Concluded)

<u>Range</u>	<u>Station</u>	<u>Offset ft</u>	<u>Time GST</u>	<u>Depth ft</u>	<u>Concentration g/l</u>
3	2	100	1214	3.0	0.005
			1213	21.0	0.013
			1210	40.0	0.193
3	3	150	1221	3.0	0.043
			1220	21.5	0.222
			1217	41.0	1.622
3	4	200	1228	3.0	0.019
			1226	19.0	0.181
			1225	36.0	0.227
3	5	254	1234	3.0	0.016
			1233	18.0	0.342
			1232	34.0	0.367
3	6	308	1239	3.0	0.049
			1238	16.0	0.255
			1237	30.0	0.171
3	7	348	1244	3.0	0.018
			1243	11.9	0.161
			1242	21.8	0.179
3	8	389	1248	3.0	0.017
			1247	9.8	0.055
			1246	17.9	0.053
3	9	429	1253	3.0	0.004
			1252	8.9	0.029
			1251	15.5	0.045

(Sheet 3 of 3)

Table 10
Location of Data Collection Buoys
Test 2

<u>Buoy No.</u>	<u>Station</u>	<u>Offset</u>	<u>Coordinates</u>	
	<u>ft</u>	<u>ft</u>	<u>X</u>	<u>Y</u>
1-2	114+80	280	337,420	148,899
1-4	114+50	409	337,552	148,917
1-6	113+78	504	337,656	148,978
1-8	113+42	658	337,815	148,005
2-3	116+47	473	337,591	148,717
2-4	116+34	508	337,628	148,726
2-6	115+39	724	337,856	148,804
3-2	120+24	302	337,463	148,348
3-4	120+11	544	337,616	148,348
3-6	120+14	664	337,735	148,336
3-8	120+24	862	337,932	148,314
4-2	136+05	630	337,500	146,760
4-4	138+58	934	337,781	146,487

Note: North auto sampler:
X = 337,611 Y = 148,954
Station 114+07 - Offset = 462 ft

South auto sampler:
X = 337,816 Y = 148,404
Station 119+42 - Offset = 735 ft

Northwest corner of overflow barge:
X = 337,544 Y = 149,406
Station 109+64 - Offset = 338 ft

Table 11
Sampling Data, Test 2

<u>Range</u>	<u>Station</u>	<u>Offset ft</u>	<u>Time CST</u>	<u>Depth ft</u>	<u>Concentration g/l</u>
1	1	216	0911	3.0	0.041
			0910	20.0	0.018
			0909	38.0	0.044
1	2 (1A)	280	0919	3.0	0.010
			0918	15.0	0.014
			0916	28.0	0.018
1	3	344	0924	3.0	0.024
			0924	10.5	0.010
			0922	19.0	0.012
1	4 (1B)	409	0933	3.0	0.050
			0933	9.6	0.049
			0933	17.2	0.267
1	5	456	0934	3.0	0.049
			0934	9.6	0.070
			0934	17.2	0.066
1	6 (1C)	504	0937	3.0	0.018
			0936	9.5	0.068
			0935	17.0	0.057
1	7	581	0948	3.0	0.009
			0947	8.1	0.019
			0946	17.0	0.061
1	8 (1D)	658	0953	3.0	0.008
			0952	8.1	0.062
			0951	13.5	0.047
1	9	735	0957	3.0	0.011
			0956	8.1	0.036
			0955	12.5	0.027
2	1	256	0900	3.0	0.011*
			0858	34.0	0.001

(Continued)

* Background.

(Sheet 1 of 3)

Table 11 (Continued)

<u>Range</u>	<u>Station</u>	<u>Offset ft</u>	<u>Time CST</u>	<u>Depth ft</u>	<u>Concentration g/l</u>
2	1	256	0924	3.0	0.014
			0923	18.0	0.021
			0922	34.0	0.016
2	2	403	0928	3.0	0.018
			0927	10.0	0.098
			0926	18.0	1.556
2	3 (2A)	473	0938	3.0	0.057
			0938	10.0	0.072
			0936	16.0	0.036
2	4 (2B)	508	0944	3.0	0.032
			0942	9.0	0.030
			0941	16.0	0.039
2	5	616	0955	3.0	0.035
			0949	8.0	0.032
			0941	14.0	0.037
2	6 (2C)	724	1002	3.0	0.023
			1000	8.0	0.035
			0958	14.0	0.084
2	7	780	1006	3.0	0.022
			1006	7.0	0.017
			1005	12.0	0.031
2	8	840	1012	3.0	0.013
			1011	7.0	0.022
			1010	12.0	0.039
2	9	900	1017	3.0	0.017
			1016	6.5	0.012
			1015	11.0	0.033
3	1	316	0946	3.0	0.012
			0945	12.6	0.011
			0944	23.5	0.016

(Continued)

(Sheet 2 of 3)

Table 11 (Concluded)

<u>Range</u>	<u>Station</u>	<u>Offset ft</u>	<u>Time GST</u>	<u>Depth ft</u>	<u>Concentration g/l</u>
3	2 (3A)	392	0951	3.0	0.020
			0950	9.4	0.015
			0945	16.8	0.026
3	3	468	0955	3.0	0.027
			0954	8.7	0.020
			0953	15.4	0.029
3	4 (3B)	544	1000	3.0	0.019
			0959	8.0	0.018
			0958	14.0	0.022
3	6 (3C)	664	1016	3.0	0.020
			1014	7.7	0.021
			1013	12.6	0.033
3	8 (3D)	862	1020	3.0	0.016
			1019	7.0	0.024
			1018	12.0	0.047
4	1	478	1013	3.0	0.018
			1011	7.0	0.014
			1010	10.0	0.015
4	2 (4A)	630	1020	3.0	0.020
			1019	6.5	0.020
			1018	11.0	0.025
4	3	782	1026	3.0	0.035
			1025	6.3	0.042
			1024	10.0	0.143
4	4 (4B)	934	1031	3.0	0.038
			1030	5.5	0.041
			1029	9.0	0.039

(Sheet 3 of 3)

Table 12
Location of Data Collection Buoys
Test 4

<u>Buoy No.</u>	<u>Station</u> <u>ft</u>	<u>Offset</u> <u>ft</u>	<u>Coordinates</u>	
			<u>X</u>	<u>Y</u>
1-1	283+50	-127	334,528	200,923
1-3	284+00	230	334,887	200,912
1-5	284+40	387	335,048	200,879
2-1	287+40	-196	334,495	200,530
2-3	287+40	- 24	334,666	200,551
2-5	286+60	217	334,902	200,621
2-7	287+20	359	335,046	200,601
3-1	281+80	-270	334,461	200,088
3-5	290+30	181	334,898	200,274
3-7	290+80	314	335,033	200,247
4-2	296+00	-235	334,536	199,659
4-4	296+20	- 72	334,700	199,652
4-6	296+00	266	335,035	199,716

Note: North auto sampler:
X = 334,798 Y = 200,882
Station 284+20 - Offset = 138 ft

South auto sampler:
X = 334,696 Y = 200,207
Station 290+80 - Offset = -26 ft

Northwest corner of overflow barge:
X = 334,793 Y = 201,405
Station 282+00 - Offset = 181 ft

Table 13
Sampling Data, Test 4

<u>Range</u>	<u>Station</u>	<u>Offset ft</u>	<u>Time CST</u>	<u>Depth ft</u>	<u>Concentration g/l</u>
1	1 (1A)	-127	0952	3.0	0.017 *
			0951	20.5	0.032
			0950	36.0	0.050
1	1 (1A)	-127	1003	3.0	0.010
			1002	20.5	0.032
			1001	37.0	0.067
1	2	5	1013	3.0	0.012
			1012	15.5	0.030
			1011	30.0	0.078
1	3 (1B)	138	1018	3.0	0.005
			1017	19.5	0.030
			1016	34.0	0.275
1	4	184	1022	3.0	0.006
			1021	14.0	0.039
			1020	22.0	0.190
1	5 (1C)	230	1027	3.0	0.009
			1026	16.0	0.032
			1025	27.0	0.036
1	6	308	1031	3.0	0.015
			1030	9.5	0.018
			1029	16.0	0.050
1	7 (1D)	387	1036	3.0	0.004
			1035	18.0	0.042
			1034	31.0	0.062
1	8	437	1041	3.0	0.011
			1040	11.0	0.020
			1039	17.0	0.048
1	1 (1A)	-127	1049	3.0	0.008
			1048	21.0	0.036
			1047	37.0	1.060

(Continued)

* Background.

(Sheet 1 of 5)

Table 13 (Continued)

<u>Range</u>	<u>Station</u>	<u>Offset ft</u>	<u>Time CST</u>	<u>Depth ft</u>	<u>Concentration g/l</u>
1	3 (1B)	-127	1055	3.0	0.008
			1054	20.0	0.041
			1053	35.0	0.130
1	5 (1C)	230	1059	3.0	0.010
			1057	15.5	0.029
			1056	26.0	0.051
1	7 (1D)	387	1104	3.0	0.005
			1103	12.0	0.016
			1102	21.0	0.057
2	2 (2A)	-196	0949	3.0	0.014 *
			0948	20.5	0.029
			0947	39.0	0.101
2	1 (2A)	-196	1010	3.0	0.011
			1009	20.0	0.050
			1008	38.0	0.574
2	2	-110	1016	3.0	0.017
			1015	22.0	0.068
			1014	42.0	5.980
2	3 (2B)	-24	1022	3.0	0.031
			1021	21.5	0.032
			1020	41.0	4.090
2	4	97	1026	3.0	0.022
			1025	20.0	0.179
			1024	38.0	0.194
2	5 (2C)	217	1031	3.0	0.020
			1029	20.0	0.031
			1028	38.0	0.062
2	6	288	1036	3.0	0.026
			1035	18.0	0.033
			1034	34.0	0.028

(Continued)

* Background.

(Sheet 2 of 5)

Table 13 (Continued)

<u>Range</u>	<u>Station</u>	<u>Offset</u> <u>ft</u>	<u>Time</u> <u>CST</u>	<u>Depth</u> <u>ft</u>	<u>Concentration</u> <u>g/l</u>
2	7 (2D)	359	1040	3.0	0.021
			1040	18.5	0.032
			1039	35.0	0.033
2	8	409	1045	3.0	0.032
			1044	20.0	0.046
			1043	38.0	0.141
2	1 (2A)	-196	1054	3.0	0.016
			1053	20.0	0.031
			1052	38.0	0.398
2	3 (2B)	-24	1059	3.0	0.053
			1058	22.5	0.104
			1057	43.0	2.171
2	5 (2C)	217	1105	3.0	0.027
			1104	22.0	0.037
			1103	42.0	0.259
2	7 (2D)	359	1109	3.0	0.019
			1108	21.5	0.026
			1107	41.0	0.051
3	1 (3A)	-270	0956	3.0	0.024
			0955	10.3	0.055
			0954	18.5	0.089
3	2	-148	1010	3.0	0.031
			1010	19.0	0.542
			1009	36.0	0.694
3	3	-26	1016	3.0	0.012
			1015	14.3	0.588
			1014	26.5	0.109
3	4	78	1021	3.0	0.023
			1020	19.3	0.276
			1019	36.5	0.183

(Continued)

(Sheet 3 of 5)

Table 13 (Continued)

<u>Range</u>	<u>Station</u>	<u>Offset ft</u>	<u>Time CST</u>	<u>Depth ft</u>	<u>Concentration g/l</u>
3	5 (3B)	181	1025	3.0	0.035
			1024	16.0	0.051
			1023	30.0	0.041
3	6	248	1029	3.0	0.042
			1028	19.3	0.045
			1028	36.5	0.057
3	7 (3C)	314	1034	3.0	0.010
			1032	19.3	0.031
			1031	36.5	0.033
3	8	364	1038	3.0	0.015
			1037	21.0	0.040
			1037	40.0	0.059
3	1 (3a)	-270	1047	3.0	0.030
			1046	13.0	0.056
			1044	24.0	0.460
3	3	-26	1052	3.0	0.037
			1051	15.5	0.079
			1050	29.0	0.170
3	5 (3B)	181	1057	3.0	0.014
			1056	17.3	0.259
			1055	32.5	0.040
3	7	314	1103	3.0	0.035
			1102	18.0	0.052
			1100	37.0	0.105
4	1	-315	1000	3.0	0.010
			0959	6.6	0.046
			0958	11.3	0.035
4	2 (4A)	-235	1008	3.0	0.015
			1007	7.2	0.043
			1006	12.5	0.036

(Continued)

(Sheet 4 of 5)

Table 13 (Concluded)

<u>Range</u>	<u>Station</u>	<u>Offset ft</u>	<u>Time CST</u>	<u>Depth ft</u>	<u>Concentration g/l</u>
4	3	-153	1014	3.0	0.011
			1013	8.8	0.036
			1011	13.2	0.043
4	4 (4B)	-72	1019	3.0	0.012
			1018	8.8	0.036
			1017	15.7	0.041
4	5	14	1024	3.0	0.006
			1023	8.7	0.023
			1022	15.4	0.042
4	6	98	1028	3.0	0.008
			1028	11.8	0.023
			1027	21.7	0.047
4	7	181	1038	3.0	0.004
			1035	12.0	0.018
			1035	22.5	0.050
4	8 (4C)	266	1044	3.0	0.008
			1043	18.6	0.031
			1042	35.2	0.033
4	1	-315	1051	3.0	0.006
			1050	6.9	0.010
			1049	11.8	0.030
4	2 (4A)	-235	1058	3.0	0.003
			1057	7.3	0.026
			1056	12.6	0.044
4	4 (4B)	-72	1105	3.0	0.003
			1104	8.4	0.026
			1103	14.8	0.029
4	8 (4C)	266	1113	3.0	0.005
			1112	13.7	0.017
			1111	25.5	0.030

(Sheet 5 of 5)

Table 14
Automatic Sampler Data.
North Samplers, Test 4

Time CST	Concentration at 15 ft	Concentration at 30 ft
	<u>g/l</u>	<u>g/l</u>
0950	0.023	0.182
0955	0.018	0.431
1000	0.025	0.119
1005	0.028	0.154
1010	0.028	0.097
1015	0.028	0.286
1020	0.030	0.776
1025	0.025	0.536
1030	0.021	0.739
1035	0.025	1.914
1040	0.028	0.738
1045	0.050	0.183
1050	0.032	0.119
1055	0.029	0.080
1100	0.030	0.058
1105	0.034	0.037
1110	0.033	0.041
1115	0.041	0.036
1120	0.045	0.040
1125	0.015	0.039

Note: Station 284+20; Offset = 138 ft; Overall depth, 39 ft.

Table 15
Automatic Sampler Data,
South Samplers, Test 4

Time CST	Concentration at 15 ft	Concentration at 30 ft
	<u>g/l</u>	<u>g/l</u>
0950	0.024	0.039
0955	0.025	0.041
1000	0.016	0.041
1005	0.022	0.042
1010	0.026	0.037
1015	0.015	0.039
1020	0.021	0.035
1025	0.021	0.037
1030	0.022	0.037
1035	0.023	0.044
1040	0.021	0.050
1045	0.024	0.056
1050	0.025	0.050
1055	0.022	0.053
1100	0.022	0.048
1105	0.022	0.049
1110	0.021	0.040
1115	N/A	0.043

Note: Station 290+80; Offset = -26 ft; Overall Depth, 39 ft.

Table 16
Location of Data Collection Buoys
Test 5

<u>Buoy No.</u>	<u>Station</u> <u>ft</u>	<u>Offset</u> <u>ft</u>	<u>Coordinates</u>	
			<u>X</u>	<u>Y</u>
1-2	278+40	-94	334,512	201,448
1-4	277+40	178	334,776	201,553
1-6	277+70	289	334,891	201,515
1-8	277+70	382	334,982	201,538
2-2	275+50	9	334,590	201,724
2-4	276+30	336	334,924	201,670
2-6	276+00	400	334,982	201,728
2-8	275+50	554	335,133	201,779
3-2	274+00	163	334,731	201,878
3-4	273+30	300	334,859	201,983
3-6	273+70	386	334,948	201,953
3-8	272+70	552	335,105	202,063
4-2	270+20	195	334,729	202,253
4-4	270+50	274	334,808	202,252
4-6	270+70	387	334,922	202,245
4-8	271+00	454	334,992	202,210

Note: North auto sampler:
X = 334,768 Y = 202,036
Station 272+60 - Offset = 215 ft

South auto sampler:
X = 334,743 Y = 201,600
Station 277+00 - Offset = 150 ft

Northwest corner of overflow barge:
X = 334,786 Y = 201,378
Station 279+00 - Offset = 172 ft

Table 17
Sampling Data, Test 5

<u>Range</u>	<u>Station</u>	<u>Offset ft</u>	<u>Time CST</u>	<u>Depth ft</u>	<u>Concentration g/l</u>
1	1	-145	1355	3.0	0.008
			1354	6.0	0.005
			1353	10.0	0.012
1	2 (1A)	-94	1359	3.0	0.016
			1358	8.0	0.018
			1357	14.0	0.017
2	1	-99	1403	3.0	0.007
			1402	5.5	0.010
			1401	9.0	0.189
2	2 (2A)	9	1408	3.0	0.019
			1406	6.5	0.014
			1406	11.0	0.014
3	2 (3A)	162	1410	3.0	0.012
			1409	19.0	0.030
			1408	35.0	0.486
3	3	231	1414	3.0	0.008
			1413	14.0	0.017
			1412	25.0	0.200
3	4 (3B)	300	1418	3.0	0.011
			1417	9.5	0.013
			1417	17.0	0.050
3	5	343	1422	3.0	0.011
			1421	7.5	0.010
			1420	12.0	0.014
3	6 (3C)	386	1428	3.0	0.005
			1427	5.0	0.012
			1423	10.0	0.012
3	7	469	1435	3.0	0.007
			1434	5.5	0.011
			1432	8.0	0.012

(Continued)

Table 17 (Concluded)

<u>Range</u>	<u>Station</u>	<u>Offset ft</u>	<u>Time CST</u>	<u>Depth ft</u>	<u>Concentration g/l</u>
3	9	635	1440	3.0	0.007
			1440	5.5	0.007
			1439	9.0	0.014
1	1 (1A)	-145	1416	3.0	0.006
			1415	5.5	0.015
			1414	9.0	0.010
1	2	-94	1420	3.0	0.011
			1419	7.0	0.019
			1418	12.0	0.018
2	1	-99	1424	3.0	0.004
			1423	4.0	0.006
			1422	6.0	0.008
2	2 (2A)	9	1428	3.0	0.008
			1427	6.0	0.016
			1426	10.0	0.025
1	1 (1A)	-145	1432	3.0	0.008
			1431	6.5	0.014
			1430	11.0	0.018
1	2	-94	1436	3.0	0.007
			1435	5.0	0.007
			1434	8.0	0.011
2	1	-99	1440	3.0	0.004
			1439	5.0	0.013
			1438	8.0	0.011
2	2 (2A)	9	1443	3.0	0.003
			1442	6.0	0.013
			1441	10.0	0.012
4	1	97	1335	3.0	0.008 *
			1334	19.6	0.016
			1332	37.3	0.053

* Background.

Table 18
Automatic Sampler Data,
South Samplers, Test 5

<u>Time</u> <u>CST</u>	<u>Concentration at 15 ft</u> <u>g/l</u>	<u>Concentration at 30 ft</u> <u>g/l</u>
1350	0.015	0.029
1355	0.014	0.029
1400	0.013	0.050
1405	0.014	0.086
1410	0.020	0.027
1415	0.024	0.036
1420	0.020	0.073
1425	0.017	0.191
1430	0.018	0.067
1435	0.047	0.041
1440	0.040	0.039
1445	0.027	0.032
1450	0.030	0.032
1455	N/A	0.033

Note: Station 277+00; Offset = 150 ft; Overall Depth, 39 ft.

Table 19
Field Survey Data, Tests 4 and 5, Station V1, Surface - December 6, 1987

<u>Time</u> <u>CST</u>	<u>Depth</u> <u>ft</u>	<u>Velocity</u> <u>fps</u>	<u>Direction</u> <u>deg mag</u>
0713	3.0	1.1	8
0749		1.1	6
0828		1.0	356
0913		1.3	356
0953		1.2	4
1031		1.2	358
1135		1.1	350
1204		1.0	349
1244		1.0	354
1308		0.6	7
1339		0.4	38
1358		0.3	346
1443		0.3	23

Table 20
Field Survey Data, Tests 4 and 5, Station V1.
Quarter Depth - December 6, 1987

<u>Time</u> <u>CST</u>	<u>Depth</u> <u>ft</u>	<u>Velocity</u> <u>fps</u>	<u>Direction</u> <u>deg mag</u>
0711	10.1	1.1	355
0745	9.7	1.1	352
0825	10.3	0.9	353
0911	10.0	1.2	348
0952	9.7	1.2	351
1029	9.5	1.0	352
1118	9.5	0.7	339
1203	9.5	1.0	356
1243	9.5	0.7	351
1307	10.3	0.5	350
1338	10.0	0.4	337
1357	10.0	0.3	350
1441	10.1	0.4	4

Table 21
Field Survey Data, Tests 4 and 5, Station V1.
Middepth - December 6, 1987

<u>Time</u> <u>CST</u>	<u>Depth</u> <u>ft</u>	<u>Velocity</u> <u>fps</u>	<u>Direction</u> <u>deg mag</u>
0708	20.2	1.0	338
0742	19.3	1.0	352
0821	20.5	1.0	348
0907	20.0	1.2	349
0949	19.5	1.3	340
1027	19.0	1.0	340
1115	19.0	0.9	4
1202	19.0	0.8	320
1242	19.0	0.4	334
1306	20.5	0.4	130
1336	20.0	0.4	174
1356	20.0	0.5	141
1438	20.2	0.8	186

Table 22

Field Survey Data, Tests 4 and 5, Station V1.Three-quarter Depth - December 6, 1987

<u>Time</u> <u>CST</u>	<u>Depth</u> <u>ft</u>	<u>Velocity</u> <u>fps</u>	<u>Direction</u> <u>deg mag</u>
0705	30.3	1.2	334
0740	29.7	1.1	350
0817	30.8	1.0	350
0905	30.0	1.3	352
0946	29.2	1.1	344
1025	28.5	1.0	342
1113	28.5	0.8	26
1201	28.5	1.1	308
1241	28.5	0.8	244
1305	30.8	0.7	154
1334	30.0	0.9	166
1355	30.0	0.8	150
1436	30.3	0.9	153

Table 23

Field Survey Data, Tests 4 and 5, Station V1.Bottom Depth - December 6, 1987

<u>Time</u> <u>CST</u>	<u>Depth</u> <u>ft</u>	<u>Velocity</u> <u>fps</u>	<u>Direction</u> <u>deg mag</u>
0703	37.5	0.9	346
0738	36.5	1.0	348
0814	37.0	0.9	348
0902	36.0	1.1	344
0944	35.0	0.8	343
1023	34.0	0.8	342
1111	34.0	0.8	42
1200	34.0	0.8	168
1240	34.0	1.0	218
1304	37.0	0.8	146
1332	36.0	0.9	138
1354	36.0	0.9	130
1433	36.4	1.0	174

Table 24
Field Survey Data, Tests 4 and 5, Station V2.
Surface - December 6, 1987

<u>Time</u> <u>CST</u>	<u>Depth</u> <u>ft</u>	<u>Velocity</u> <u>fps</u>	<u>Direction</u> <u>deg mag</u>
0721	3.0	1.1	6
0759		1.0	8
0849		1.0	4
0928		1.4	356
1007		1.3	344
1049		1.3	352
1141		1.1	346
1216		1.0	4
1254		1.1	359
1320		0.8	358
1346		0.7	358
1421		0.7	358
1458		0.6	330

Table 25
Field Survey Data, Tests 4 and 5, Station V2.
Bottom Depth - December 6, 1987

<u>Time</u> <u>CST</u>	<u>Depth</u> <u>ft</u>	<u>Velocity</u> <u>fps</u>	<u>Direction</u> <u>deg mag</u>
0719	5.0	1.1	348
0757	5.0	0.8	342
0847	5.0	1.2	356
0926	5.0	1.3	343
1005	5.0	1.3	342
1047	5.0	1.1	356
1139	4.1	1.1	345
1215	4.0	1.1	342
1253	4.5	1.2	354
1319	5.0	0.8	358
1345	5.5	0.9	356
1420	6.0	0.8	352
1457	5.0	0.6	341

Table 26
Location of Data Collection Buoys
Test 8

<u>Buoy No.</u>	<u>Station</u> <u>ft</u>	<u>Offset</u> <u>ft</u>	<u>Coordinates</u>	
			<u>X</u>	<u>Y</u>
1-2	278+00	-173	334,431	201,473
1-4	278+00	-44	334,558	201,502
1-6	278+00	51	334,655	201,486
1-8	278+00	242	334,844	201,515
1-10	278+00	372	334,977	201,480
2-2	276+25	-56	334,531	201,655
2-4	276+25	128	334,715	201,670
2-6	276+40	260	334,848	201,666
2-8	276+25	376	334,962	201,694
2-10	276+25	533	335,119	201,707

Note: Auto sampler:

X = 334,729 Y = 201,627

Station 276+60 - Offset = 138 ft

East velocity station:

X = 334,982 Y = 202,982

Station 263+40 - Offset = 520 ft

West velocity station:

X = 261+20 Y = 203,156

Station 261+40 - Offset = 30 ft

Northwest corner of overflow barge:

X = 334,827 Y = 201,403

Station 279+00 - Offset = 215 ft

Table 27
Sampling Data, Test 8

<u>Range</u>	<u>Station</u>	<u>Offset ft</u>	<u>Time CST</u>	<u>Depth ft</u>	<u>Concentration g/l</u>
1	2 (1A)	-173	1506	3.0	0.018
			1505	21.0	0.034
			1504	38.0	2.435
1	2 (1A)	-173	1513	3.0	0.017
			1512	21.0	0.034
			1511	38.0	3.482
1	4 (1B)	-44	1522	3.0	0.042
			1521	23.0	0.052
			1520	42.0	1.125
1	6 (1C)	51	1527	3.0	0.031
			1526	21.0	0.031
			1525	38.0	1.336
1	7	146	1530	3.0	0.010
			1529	19.5	0.033
			1528	35.0	1.428
1	8 (1D)	242	1536	3.0	0.005
			1535	15.5	1.318
			1534	27.0	1.007
2	2 (2A)	-56	1540	3.0	0.038
			1539	23.0	0.036
			1538	42.0	2.777
2	3	36	1545	3.0	0.022
			1545	21.0	0.026
			1544	38.0	1.452
2	4 (2B)	128	1548	3.0	0.012
			1548	19.5	0.034
			1547	35.0	1.451
2	5	194	1553	3.0	0.024
			1552	18.5	0.738
			1551	33.0	0.620

(Continued)

(Sheet 1 of 4)

Table 27 (Continued)

<u>Range</u>	<u>Station</u>	<u>Offset ft</u>	<u>Time GST</u>	<u>Depth ft</u>	<u>Concentration g/l</u>
1	4 (1B)	-44	1557	3.0	0.009
			1556	22.5	0.024
			1555	41.0	0.591
1	6 (1C)	51	1601	3.0	0.007
			1600	21.0	0.042
			1559	38.0	1.735
1	8 (1D)	242	1605	3.0	0.060
			1604	14.5	3.063
			1603	25.0	2.109
2	2 (2A)	-56	1609	3.0	0.006
			1608	22.5	0.007
			1607	41.0	0.434
2	3	36	1613	3.0	0.006
			1613	21.0	0.014
			1612	38.0	0.037
2	4 (2B)	128	1617	3.0	0.011
			1616	19.5	0.018
			1615	35.0	0.125
1	8 (1D)	242	1439	3.0	0.007
			1437	7.9	0.011
			1435	13.8	0.043
1	7	146	1505	3.0	0.012
			1504	7.8	0.022
			1503	13.6	0.078
1	8 (1D)	242	1510	3.0	0.009
			1509	7.6	0.022
			1507	13.3	0.112
1	9	307	1517	3.0	0.012
			1515	7.6	0.034
			1514	13.2	0.090

(Continued)

(Sheet 2 of 4)

Table 27 (Continued)

<u>Range</u>	<u>Station</u>	<u>Offset ft</u>	<u>Time CST</u>	<u>Depth ft</u>	<u>Concentration g/l</u>
2	6 (2C)	260	1524	3.0	0.011
			1523	11.1	0.037
			1521	20.2	0.092
2	7	318	1529	3.0	0.010
			1527	8.8	0.022
			1526	15.7	0.061
2	8 (2D)	376	1534	3.0	0.020
			1533	7.6	0.016
			1532	13.2	0.037
2	9	454	1539	3.0	0.006
			1538	6.8	0.009
			1537	11.6	0.034
2	10 (2E)	533	1545	3.0	0.005
			1544	5.8	0.009
			1543	9.6	0.011
2	11	611	1551	3.0	0.004
			1550	5.7	0.010
			1549	9.4	0.012
1	7	146	1557	3.0	0.015
			1555	7.9	0.017
			1554	13.8	3.077
1	8 (1D)	242	1602	3.0	0.031
			1601	7.6	0.046
			1600	13.3	0.097
1	9	307	1607	3.0	0.009
			1605	7.0	0.010
			1604	12.0	0.016
2	6 (2C)	260	1613	3.0	0.009
			1612	10.7	0.212
			1611	19.4	2.388

(Continued)

(Sheet 3 of 4)

Table 27 (Concluded)

<u>Range</u>	<u>Station</u>	<u>Offset ft</u>	<u>Time CST</u>	<u>Depth ft</u>	<u>Concentration g/l</u>
2	7	318	1619	3.0	0.032
			1618	7.7	0.018
			1617	13.4	0.048
2	8 (2D)	376	1625	3.0	0.007
			1624	7.6	0.009
			1622	13.2	0.043
2	9	454	1631	3.0	0.009
			1629	6.9	0.022
			1628	11.9	0.033
2	10 (2E)	533	1638	3.0	0.010
			1636	6.1	0.012
			1634	10.2	0.032
2	11	611	1645	3.0	0.008
			1643	5.9	0.009
			1641	9.8	0.020

Table 28
Automatic Samplers Data, Test 8

<u>Time</u> <u>CST</u>	<u>Concentration</u> <u>at 5 ft, g/l</u>	<u>Concentration</u> <u>at 18 ft, g/l</u>	<u>Concentration</u> <u>at 33 ft, g/l</u>
1440	0.008	0.020	0.414
1445	0.007	0.117	1.136
1450	0.006	0.024	0.320
1455	0.006	0.020	0.028
1500	0.006	0.022	0.172
1505	0.006	0.019	0.047
1510	0.008	0.016	0.200
1515	0.006	0.030	0.884
1520	0.006	0.019	0.608
1525	0.005	0.028	0.994
1530	0.004	0.804	1.230
1535	0.006	0.718	0.314
1540	0.007	0.304	1.050
1545	0.007	0.412	0.570
1550	0.007	0.380	0.594
1555	0.006	0.690	0.858
1600	0.008	0.364	0.098
1605	0.008	1.858	0.120
1610	0.008	0.646	0.132
1615	0.010	0.039	0.135
1620	0.008	0.030	0.082
1625	0.008	0.018	0.079
1630	0.008	0.016	0.141
1635	0.007	0.029	0.157

Note: Station 276+60 - Offset = 138 ft; Overall depth, 38 ft.

Table 29
Salinity Profile, Channel Marker 66
December 10, 1987

<u>Depth</u> <u>ft</u>	<u>Salinity</u> <u>ppt</u>
2 (Surface)	12.01
5	17.87
10	20.41
15	22.84
20	25.89
25	30.06
30	30.09
35	32.26
40	33.00
45 (Bottom)	33.08

Table 30
Drogue Velocity Data
Test 1

<u>Fix No.</u>	<u>Station ft</u>	<u>Offset ft</u>	<u>Time CST</u>	<u>Azimuth deg mag</u>	<u>Velocity fps</u>	<u>Coordinates</u>	
						<u>X</u>	<u>Y</u>
<u>Current Flow Test, Drop 1</u>							
1	108+14	409	1127			337,634	159,548
				209	0.44		
2	105+58	515	1138			337,772	149,795
				204	0.84		
3	99+99	688	1149			338,015	150,336
				200	0.96		
4	92+85	854	1202			338,272	151,042
<u>Current Flow Test, Drop 3</u>							
1	108+20	428	1136			337,652	149,540
				197	0.66		
2	94+88	667	1211			338,059	150,846

Table 31
Drogue Velocity Data
Test 2

<u>Fix No.</u>	<u>Station ft</u>	<u>Offset ft</u>	<u>Time CST</u>	<u>Azimuth deg mag</u>	<u>Velocity fps</u>	<u>Coordinates</u>	
						<u>X</u>	<u>Y</u>
<u>Current Flow Test, Drop 1</u>							
1	122+14	614	0900			337,788	149,145
				0	1.13		
2	117+72	686	0908			337,788	148,575
				4	1.05		
3	125+23	731	0920			338,738	147,827
<u>Current Flow Test, Drop 2</u>							
1	109+64	274	0901			337,479	149,412
				7	0.99		
2	117+58	281	0914			337,386	148,623
				359	0.81		
3	143+86	676	1008			337,446	145,980

Table 32
Drogue Velocity Data
Test 4

Fix No.	Station ft	Offset ft	Time CST	Azimuth deg mag	Velocity fps	Coordinates X Y	
Current Flow Test, Drop 1							
1	279+25	51	0945			334,666	201,363
				359	0.64		
2	284+78	8	1000			334,674	200,808
				344	0.55		
3	291+60	132	1021			334,861	200,141
				52	0.34		
4	295+25	-430	1053			334,335	199,723
Current Flow Test, Drop 2							
1	280+50	449	0948			335,074	201,279
				345	0.62		
2	292+98	663	1022			335,402	200,048
				16	0.39		
3	299+25	419	1050			335,217	199,402
Current Flow Test, Drop 3							
1	279+30	54	1017			334,670	201,360
				16	0.45		
2	286+58	-227	1042			334,451	200,606
				28	0.48		
3	292+64	-622	1106			334,119	199,967
Current Flow Test, Drop 4							
1	279+50	440	1019			335,057	201,363
				350	0.82		
2	292+15	535	1104			335,267	200,122
				358	0.36		
3	296+43	513	1104			335,285	199,689

Table 33
Drogue Velocity Data
Test 5

<u>Fix No.</u>	<u>Station ft</u>	<u>Offset ft</u>	<u>Time CST</u>	<u>Azimuth deg mag</u>	<u>Velocity fps</u>	<u>Coordinates</u>	
						<u>X</u>	<u>Y</u>
<u>Current Flow Test, Drop 1</u>							
1	279+80	425	1348			335,043	201,343
				348	0.30		
2	284+35	478	1413			335,139	200,892
				54	0.17		
3	286+58	116	1453			334,798	200,641
<u>Current Flow Test, Drop 2</u>							
1	279+25	117	1349			334,792	201,378
				22	0.24		
2	282+18	27	1412			334,669	201,070

Table 34
Drogue Velocity Data
Test 8

<u>Fix No.</u>	<u>Station ft</u>	<u>Offset ft</u>	<u>Time CST</u>	<u>Azimuth deg mag</u>	<u>Velocity fps</u>	<u>Coordinates</u>	
						<u>X</u>	<u>Y</u>
<u>Current Flow Test, Drop 1</u>							
1	279+25	145	1501			334,760	201,370
				358	0.29		
2	282+00	131	1517			334,771	201,095
				337	0.17		
3	283+00	162	1527			334,811	201,000
				1	0.24		
4	286+05	131	1548			334,808	200,692
				350	0.26		
5	288+80	155	1606			334,858	200,416
<u>Current Flow Test, Drop 2</u>							
1	279+60	409	1508			335,022	201,361
				4	0.56		
2	282+25	361	1516			335,002	201,094
				352	0.38		
3	284+95	371	1528			335,038	200,822
				344	0.31		
4	288+80	445	1549			335,147	200,444
				328	0.24		
5	291+10	562	1607			335,285	200,221

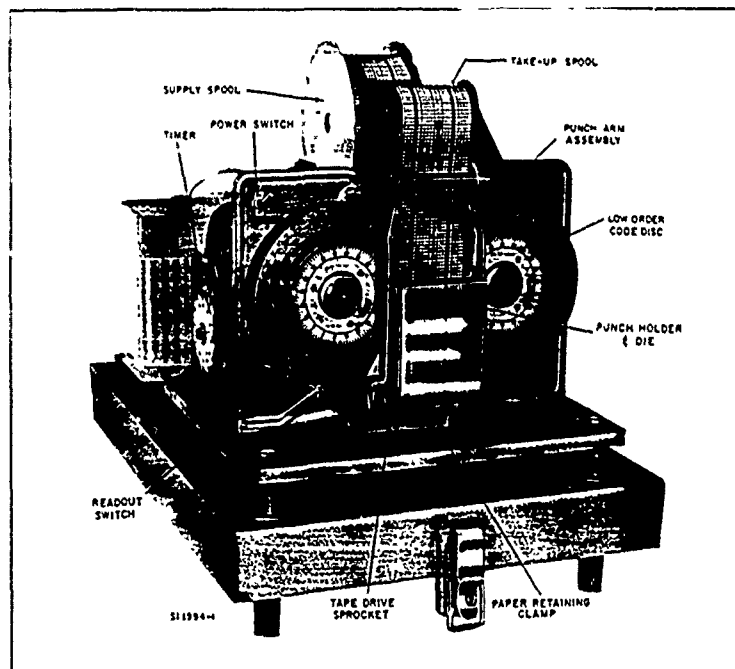


Figure 51. Water level recorder (1550)

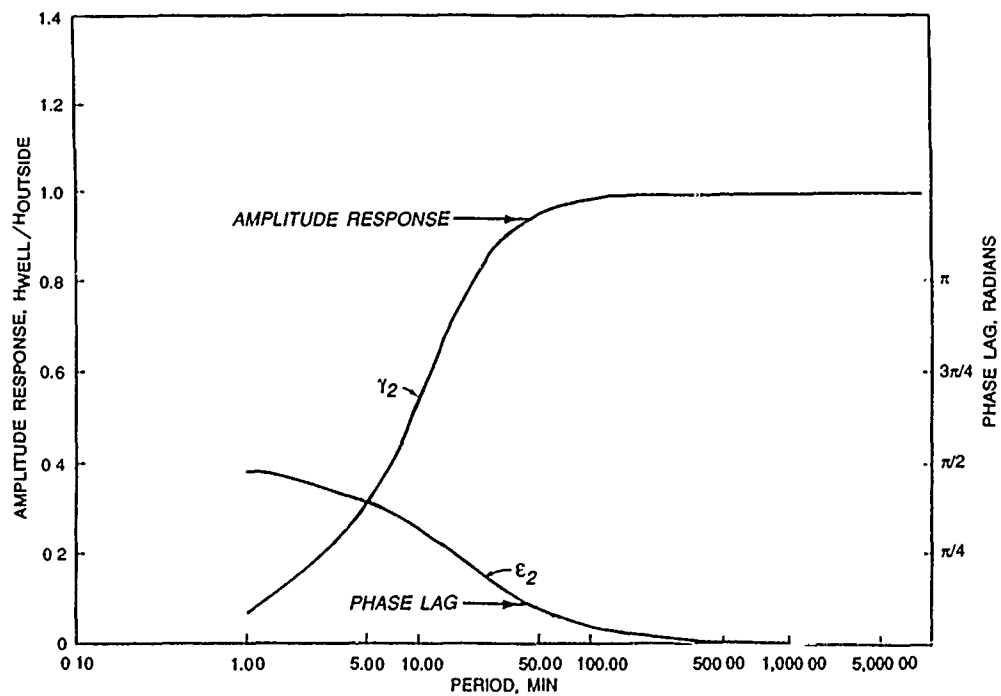


Figure 52. Response characteristics of standard tide well port used by WES

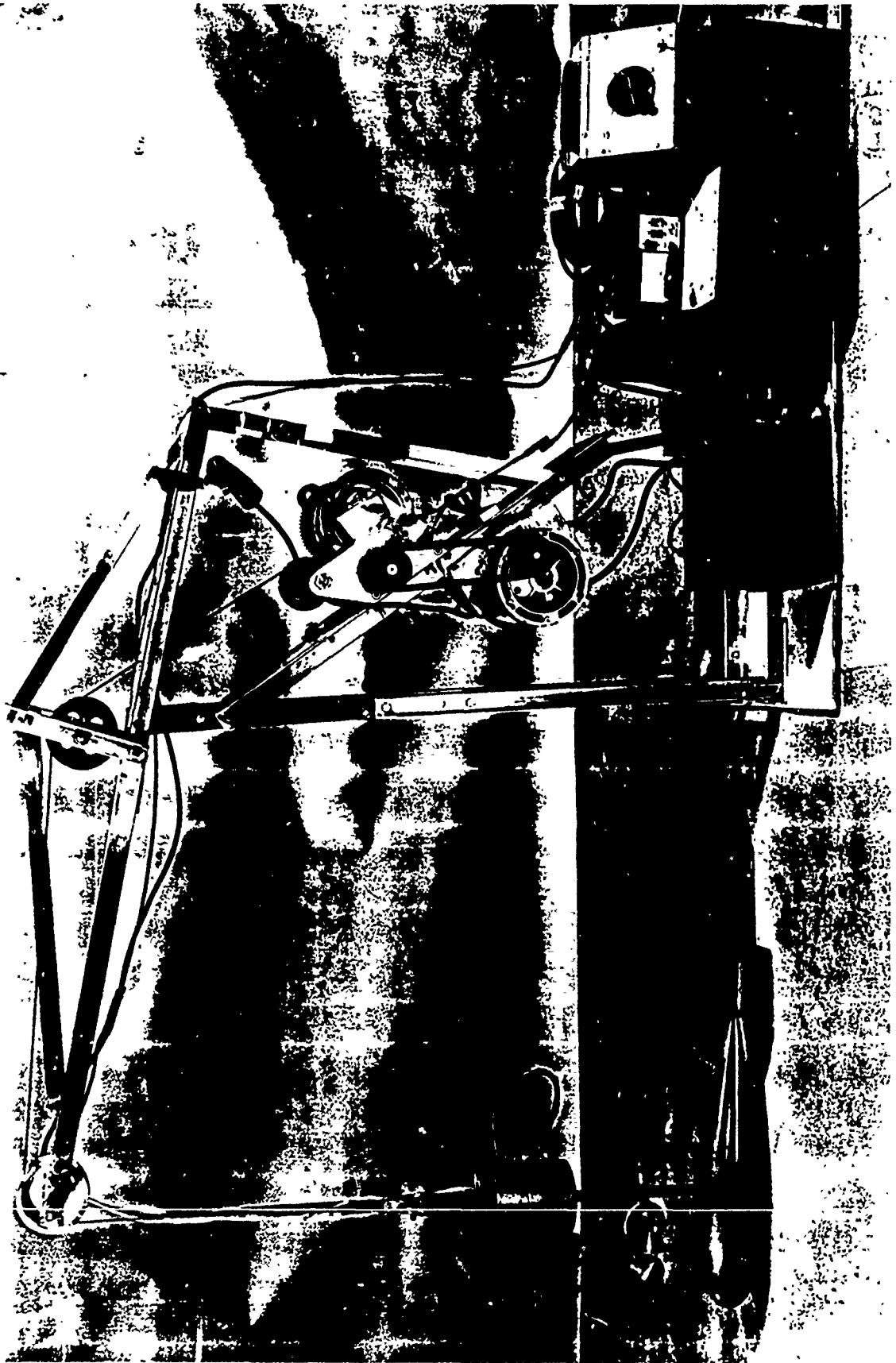
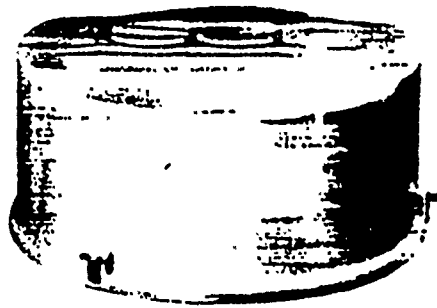
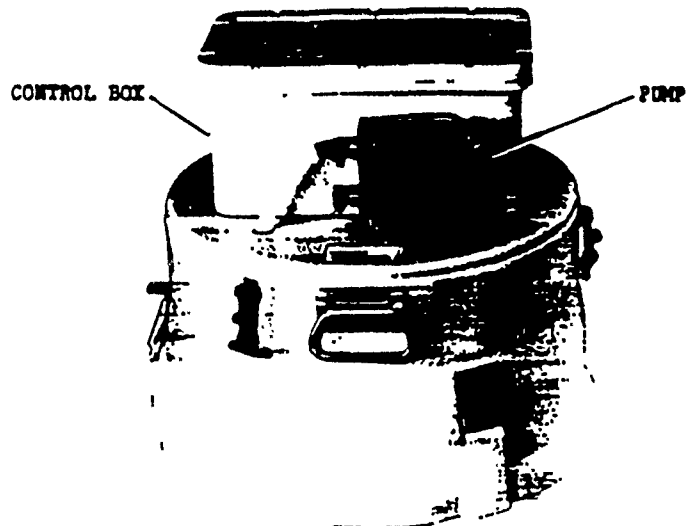


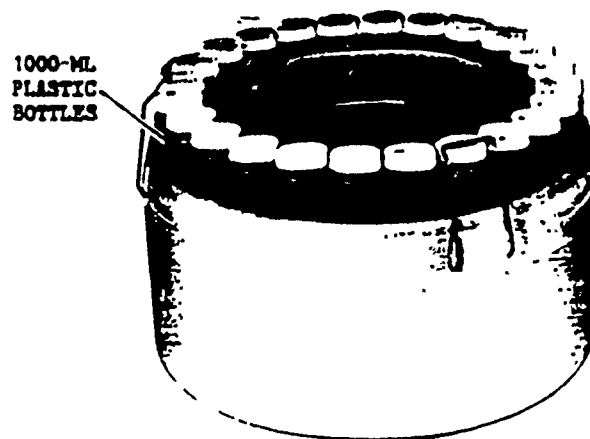
Figure 53. Over-the-side assembly



a. Cover



b. Center section



c. Sample bottle tub

Figure 54. Model 2700 sampler

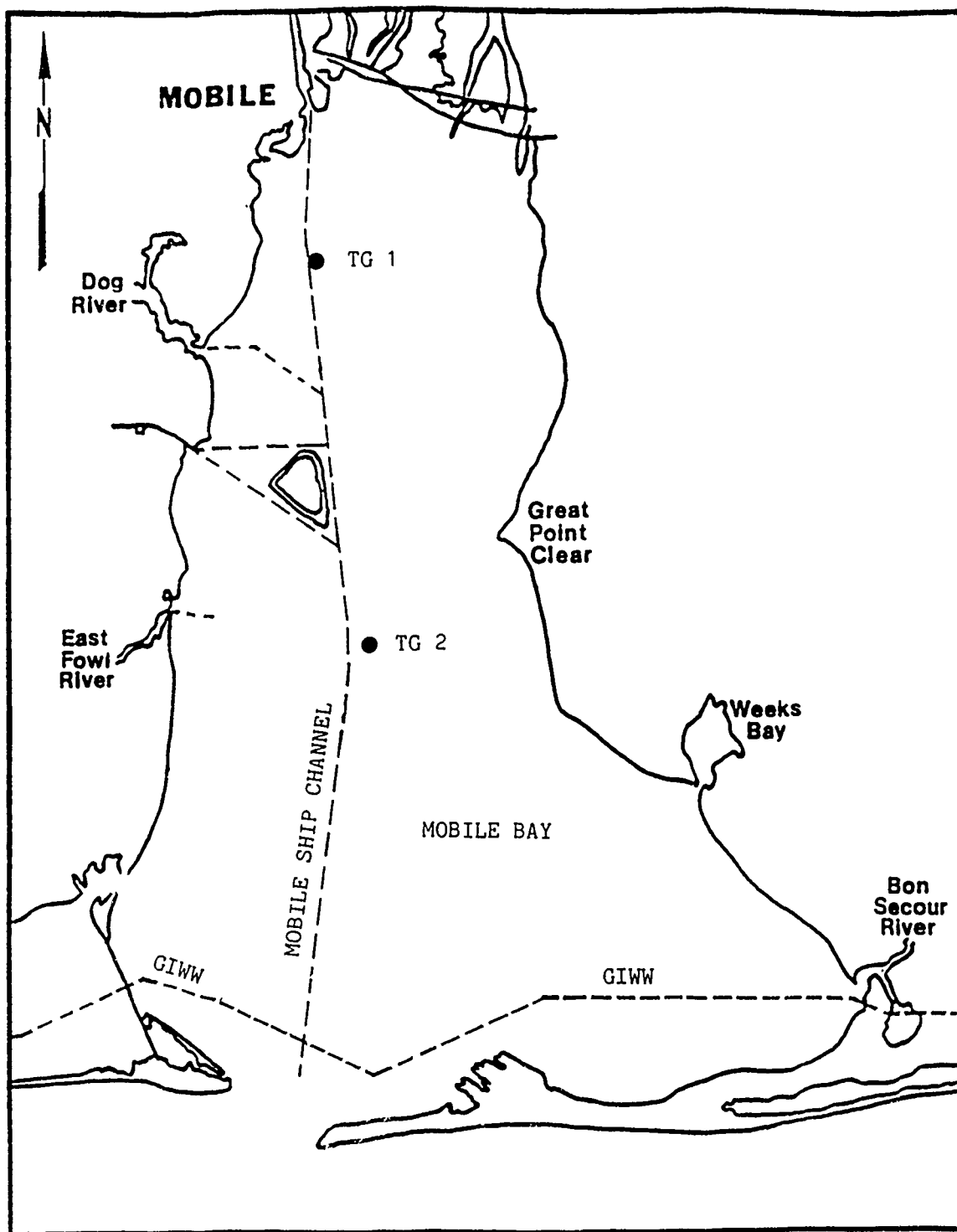


Figure 55. Tide gage locations

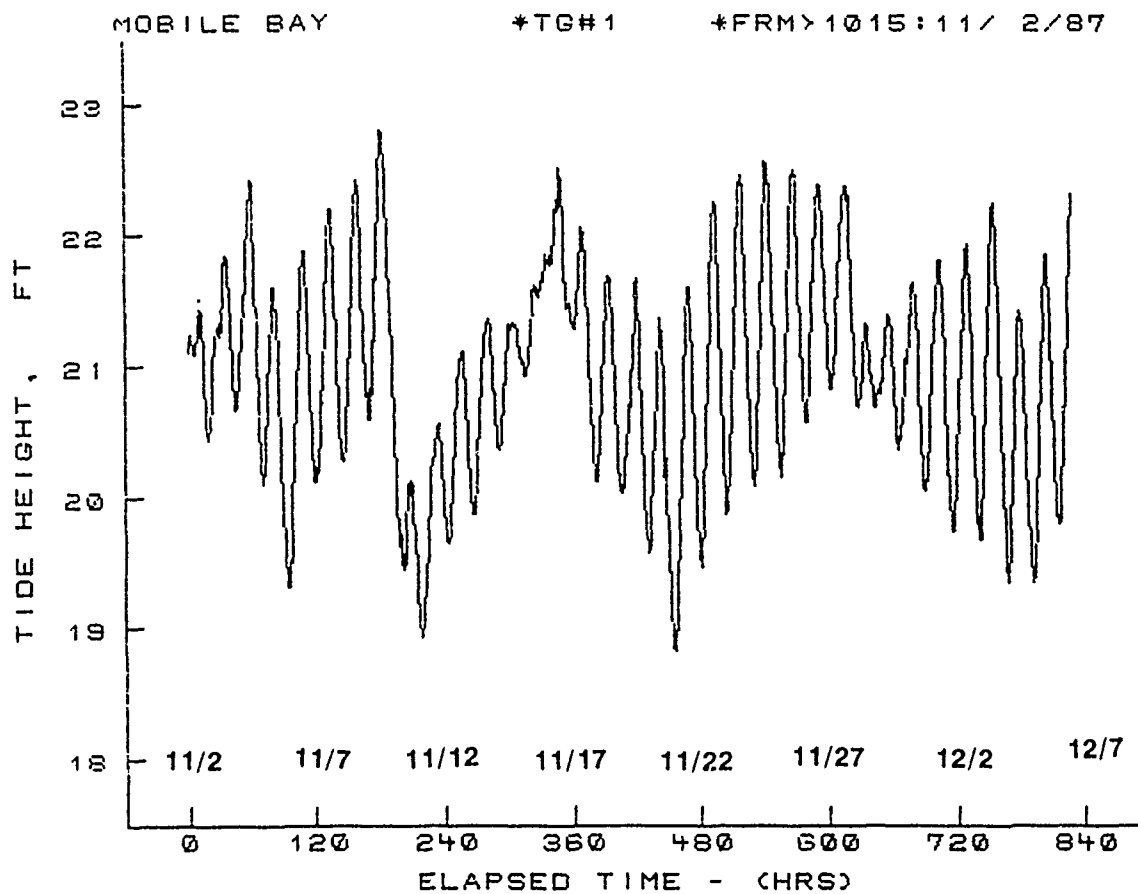


Figure 56. Water-surface elevations (arbitrary datum), tide gage 1
(condensed record)

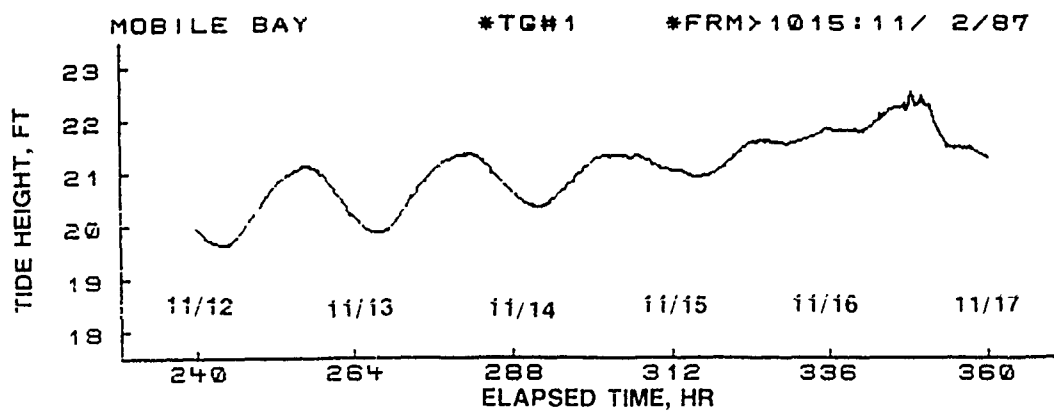
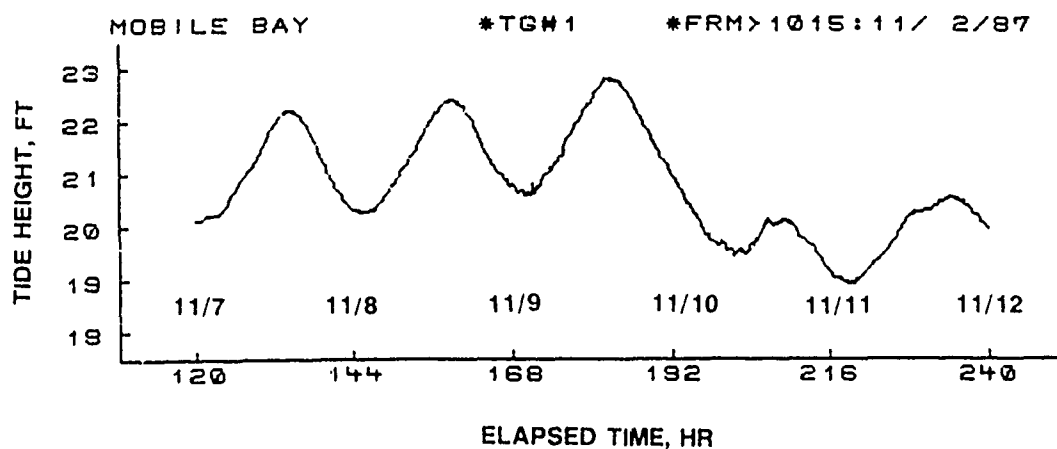
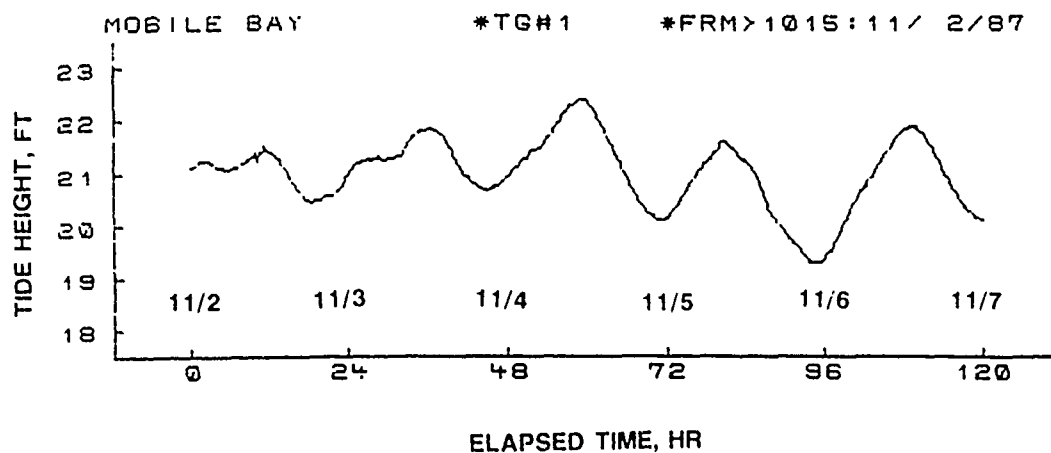


Figure 57. Water-surface elevations (arbitrary datum), tide gage 1
(Sheet 1 of 3)

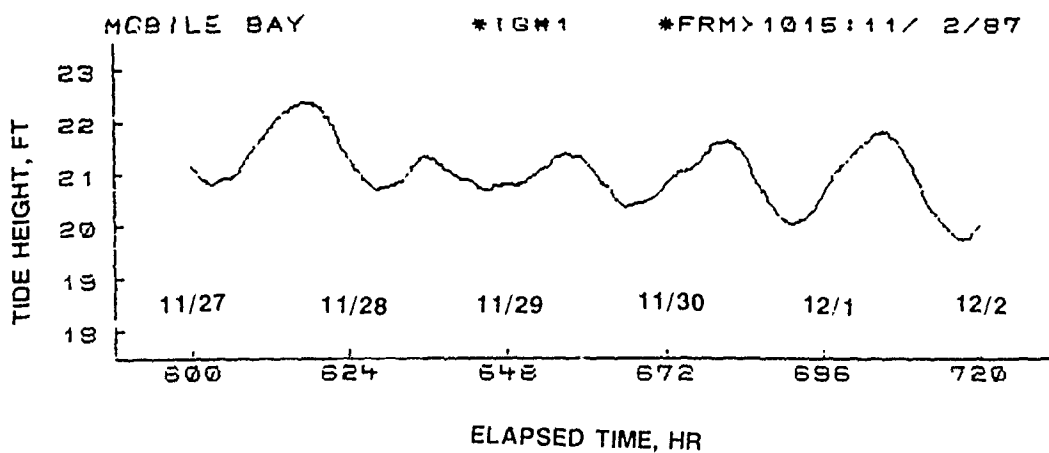
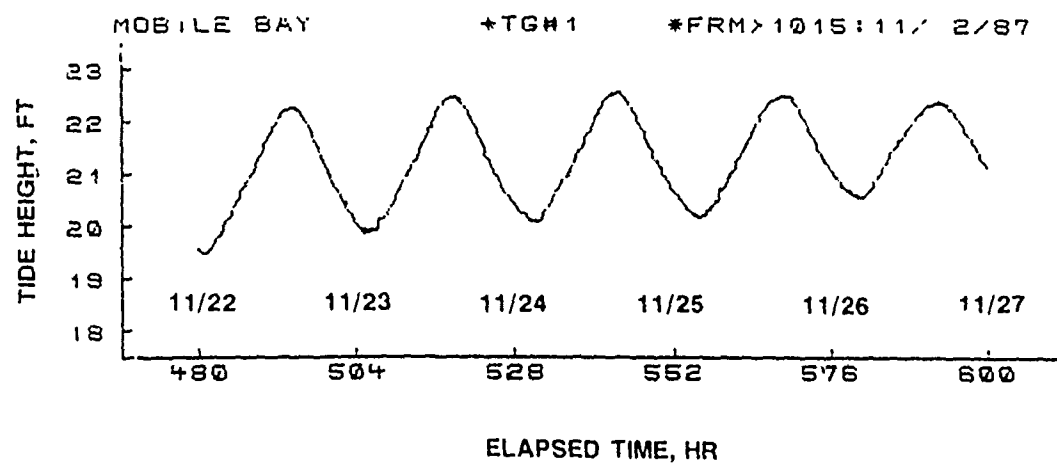
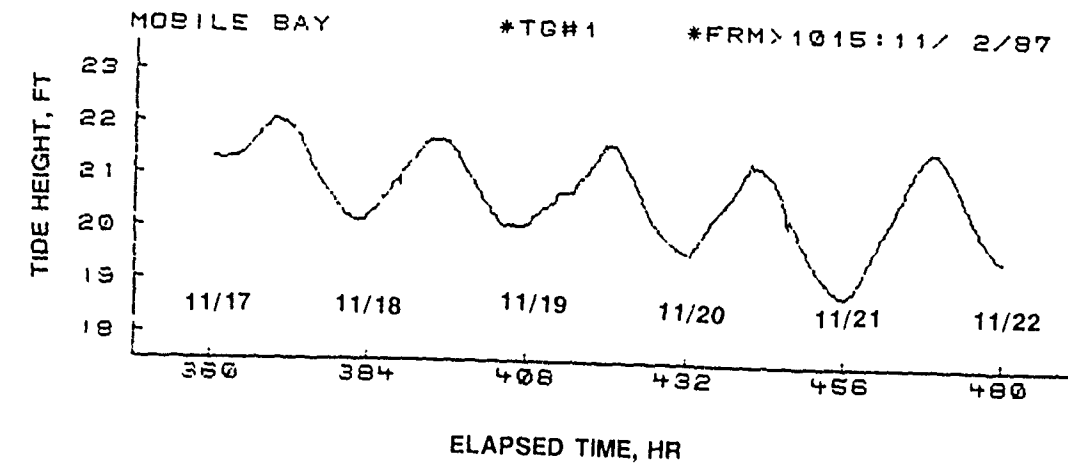


Figure 57. (Sheet 2 of 3)

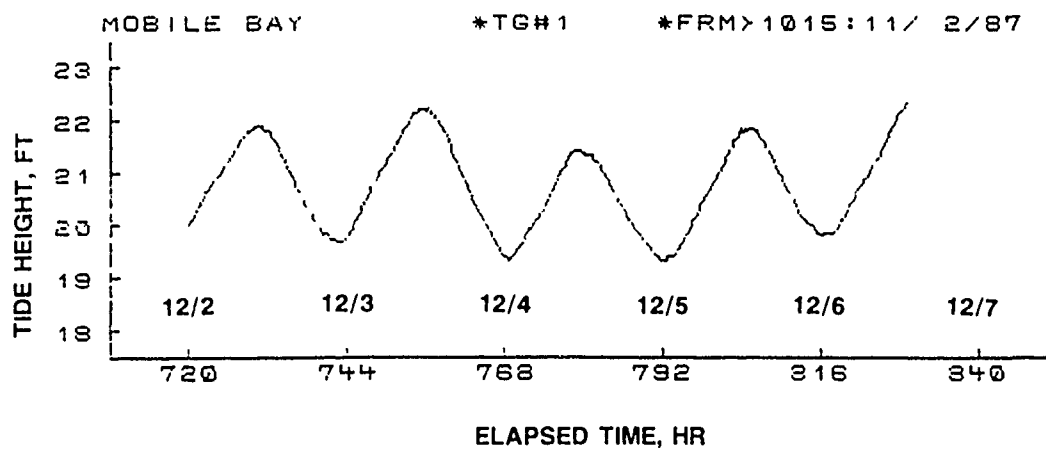


Figure 57. (Sheet 3 of 3)

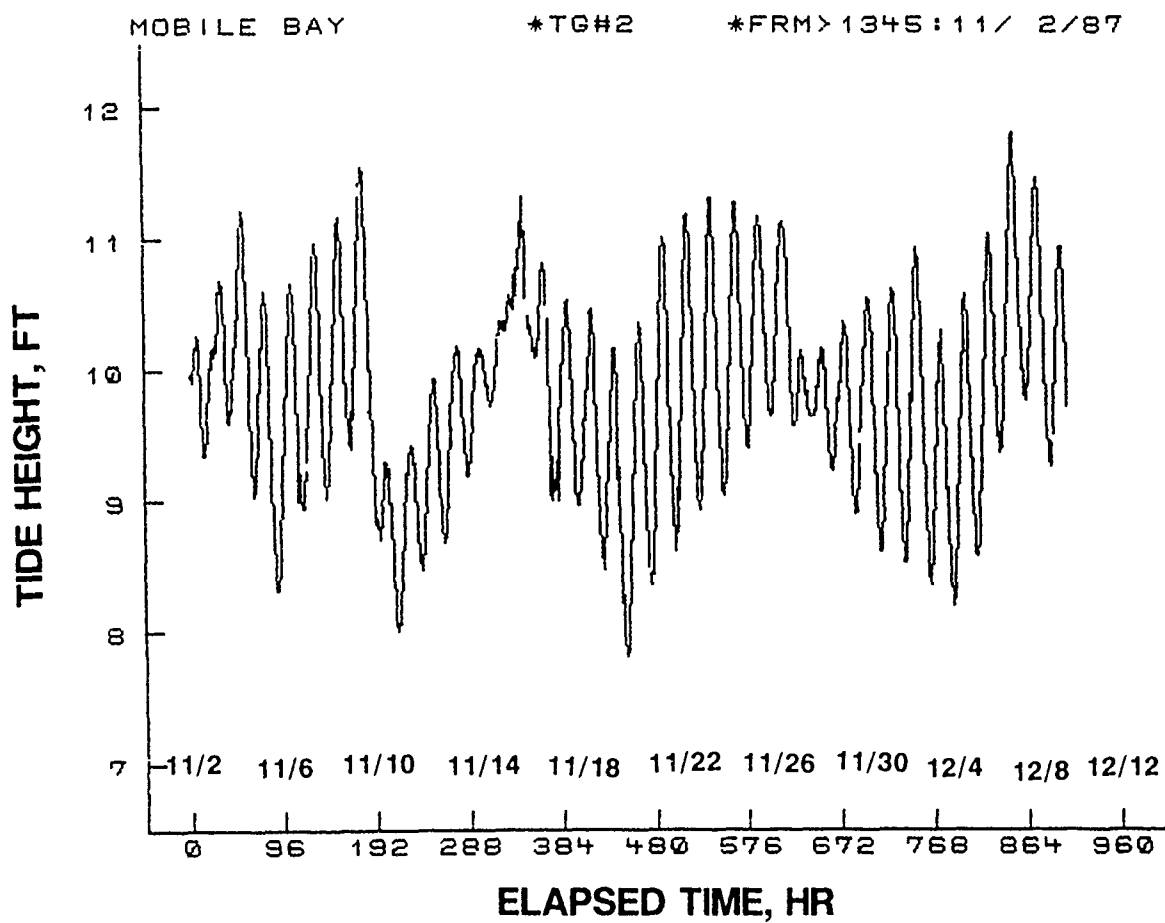


Figure 58. Water-surface elevations (arbitrary datum), tide gage 2
(condensed record)

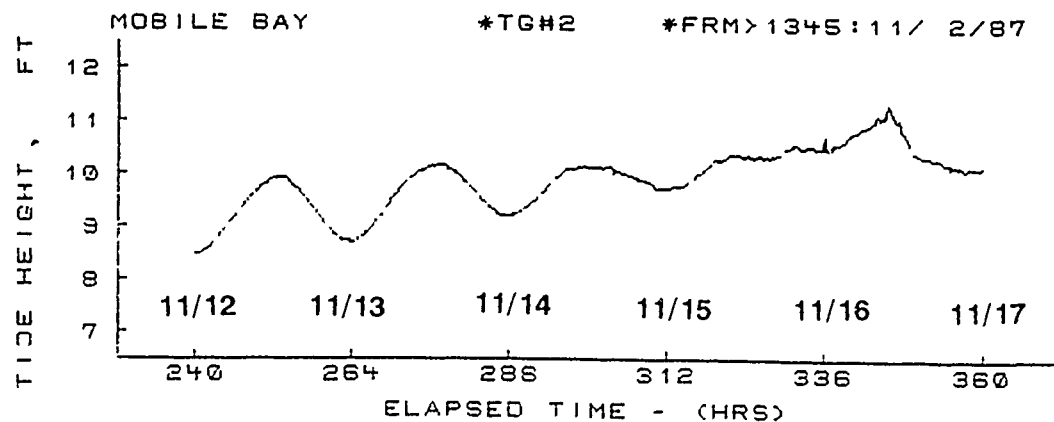
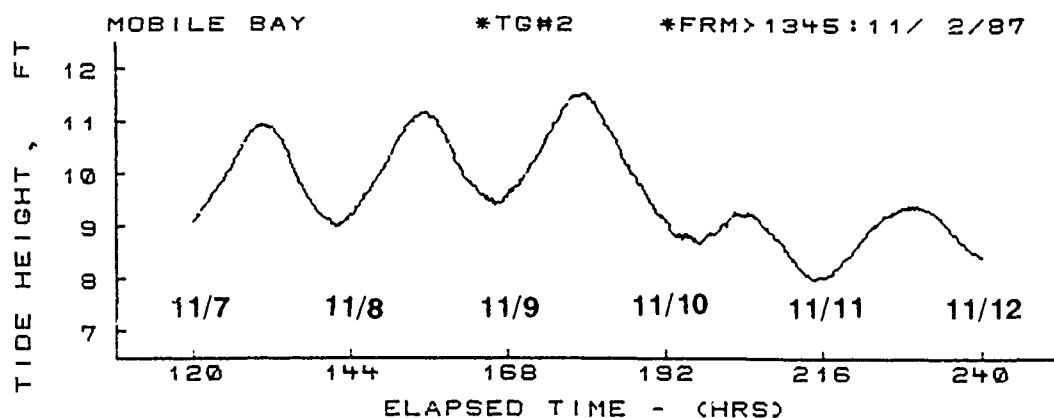
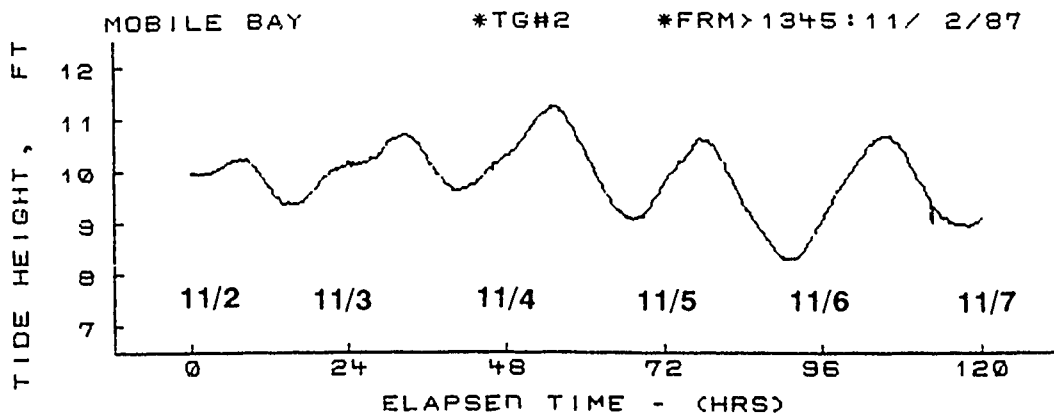


Figure 59. Water-surface elevations (arbitrary datum), tide gage 2
(Sheet 1 of 3)

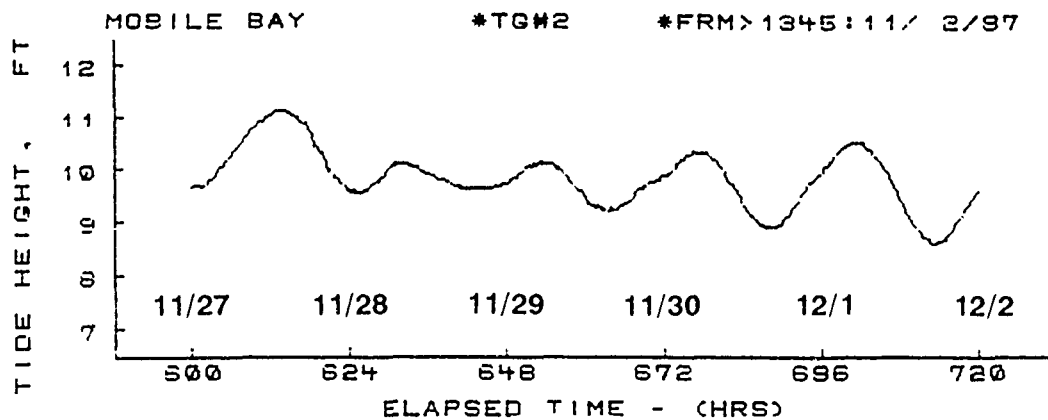
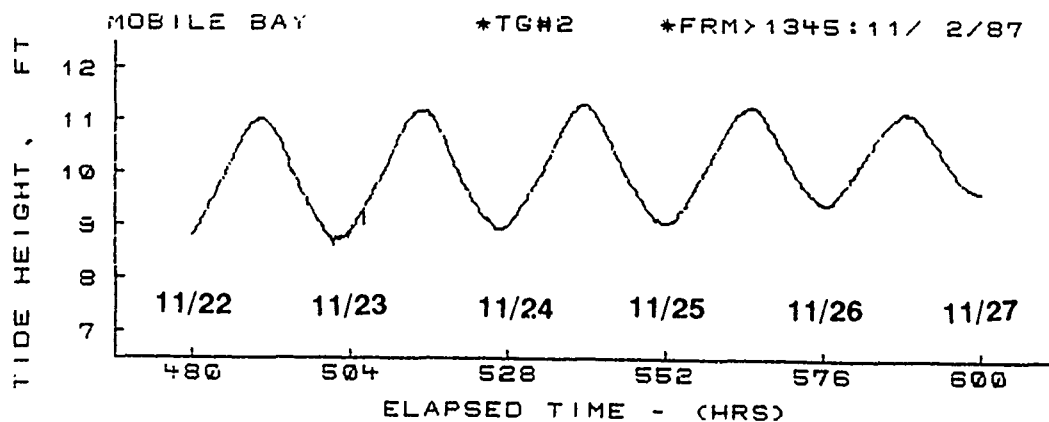
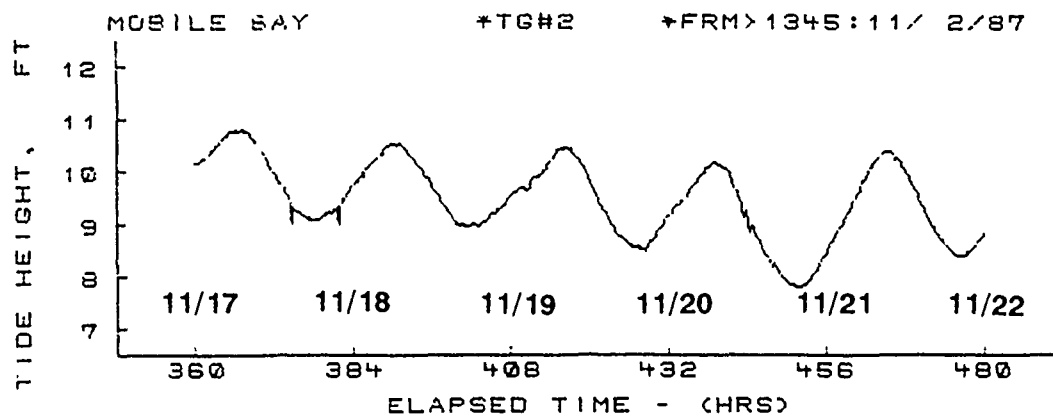


Figure 59. (Sheet 2 of 3)

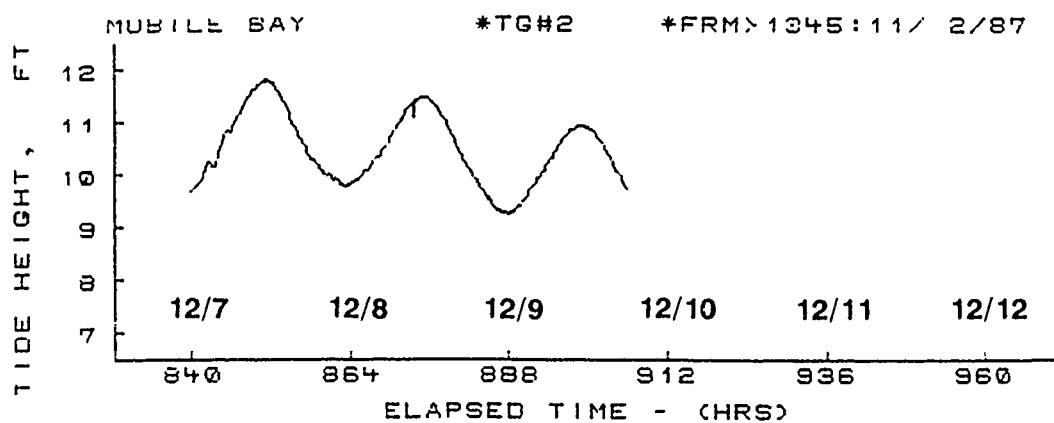
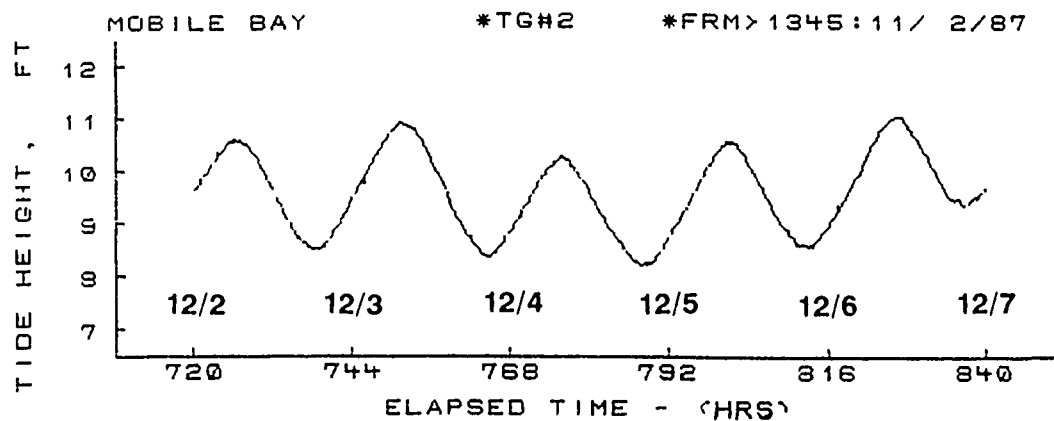


Figure 59. (Sheet 3 of 3)

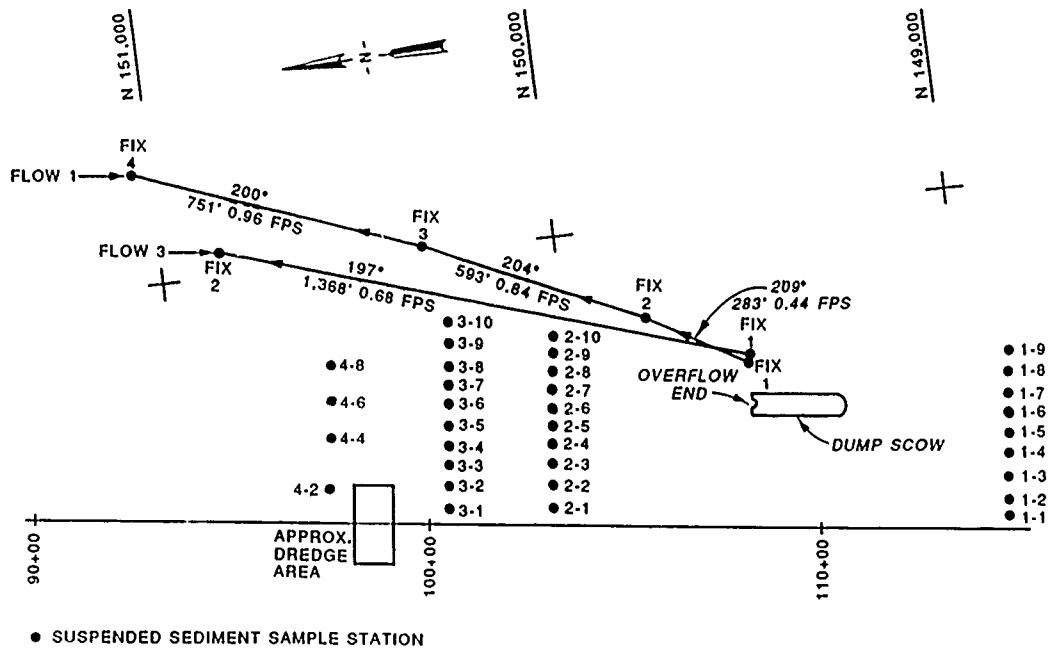


Figure 60. Location of sampling stations, lower bay, Test 1 (not to scale)

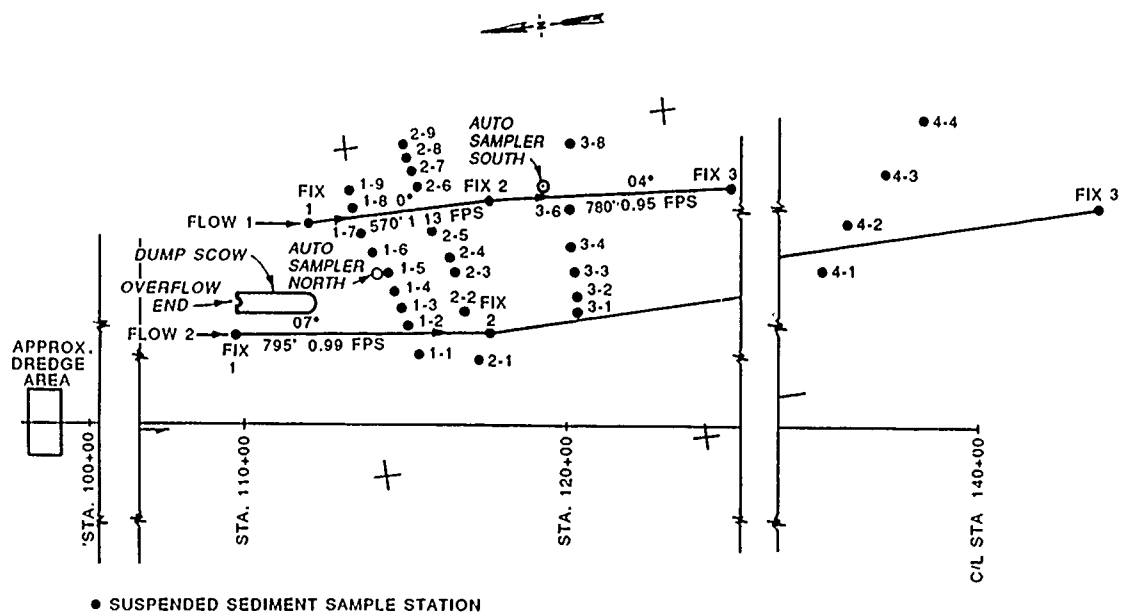


Figure 61. Location of sampling stations, lower bay, Test 2 (not to scale)

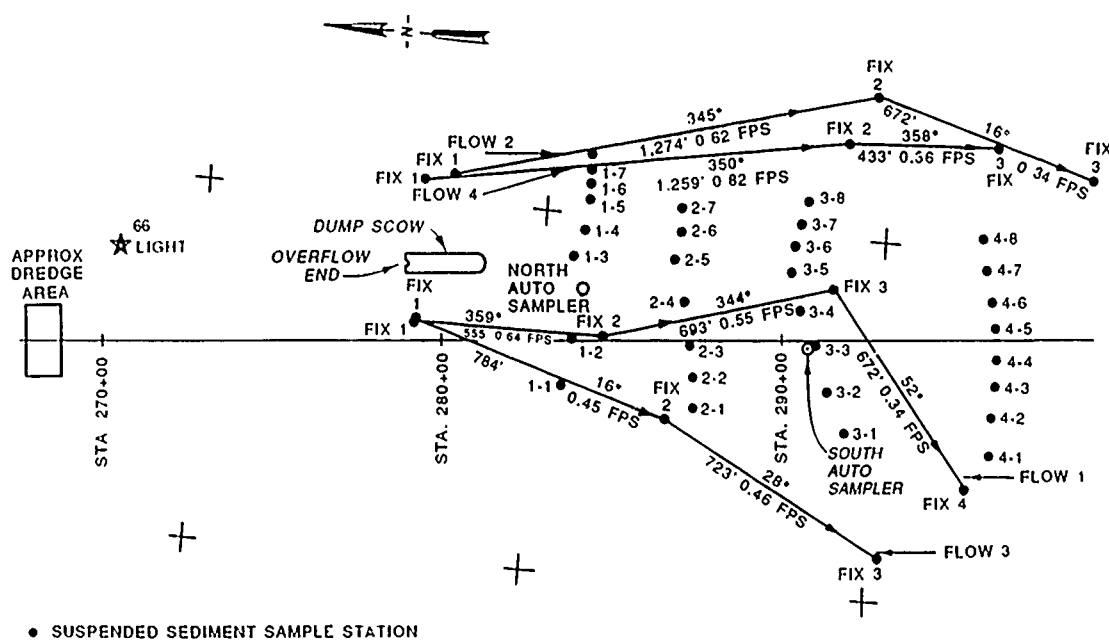


Figure 62. Location of sampling stations, upper bay, Test 4 (not to scale)

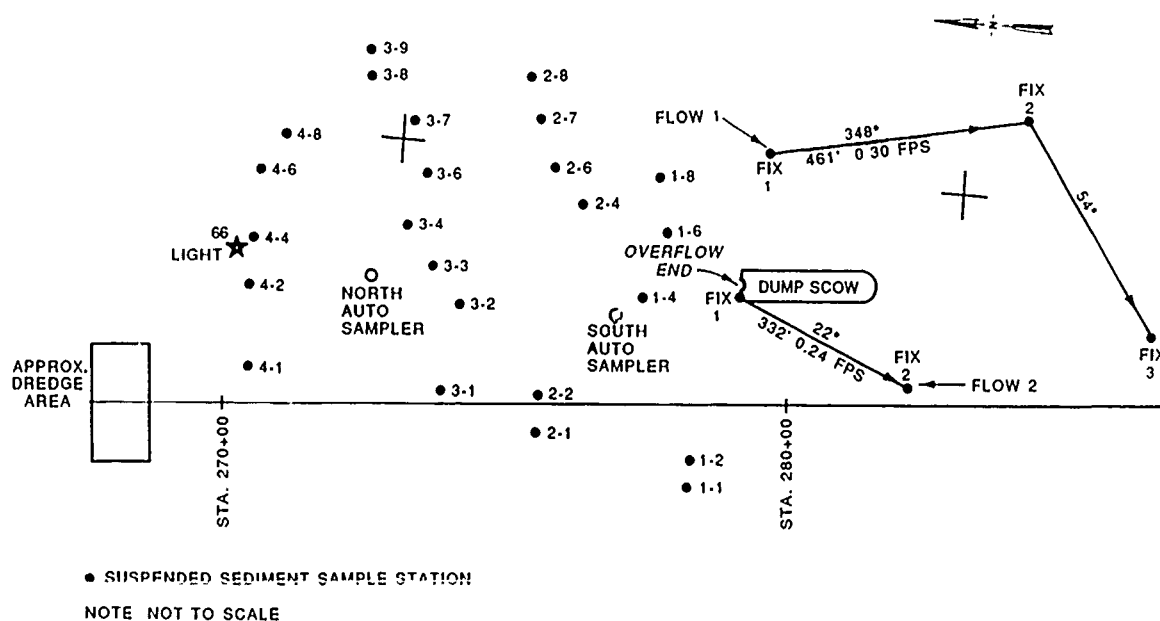


Figure 63. Location of sampling stations, upper bay, Test 5 (not to scale)

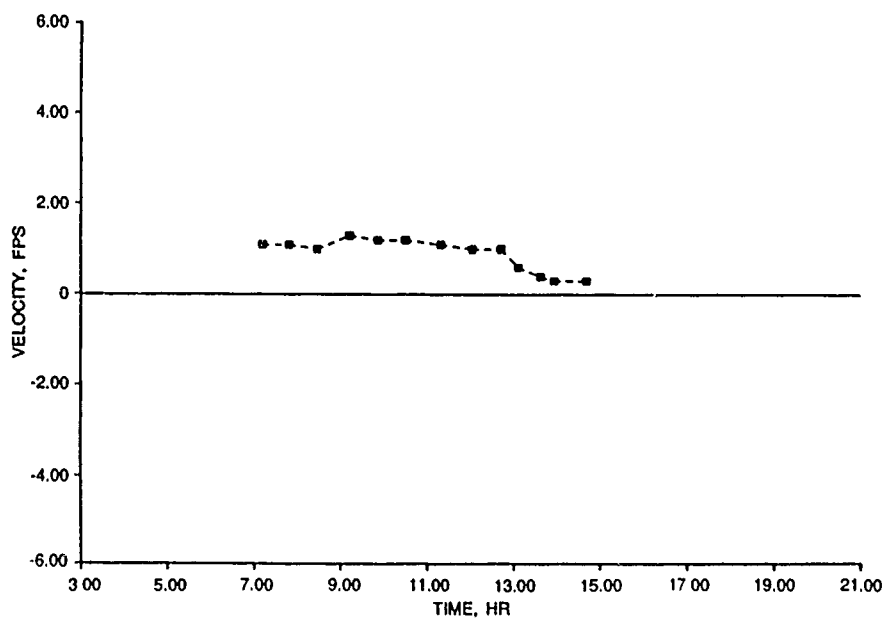


Figure 64. Velocity profile in channel north of dredge, Tests 4 and 5, sta V1, surface

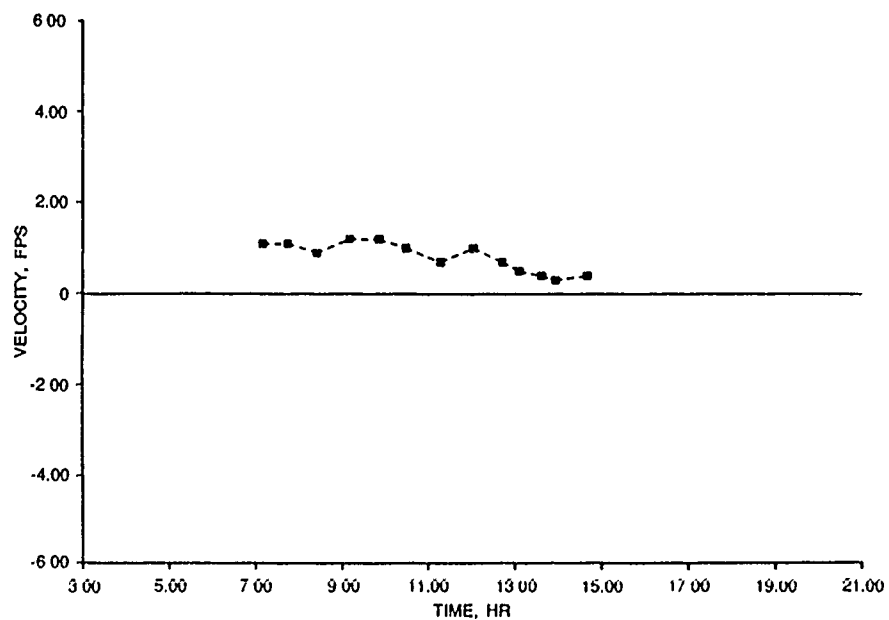


Figure 65. Velocity profile in channel north of dredge, Tests 4 and 5, sta V1, quarter depth

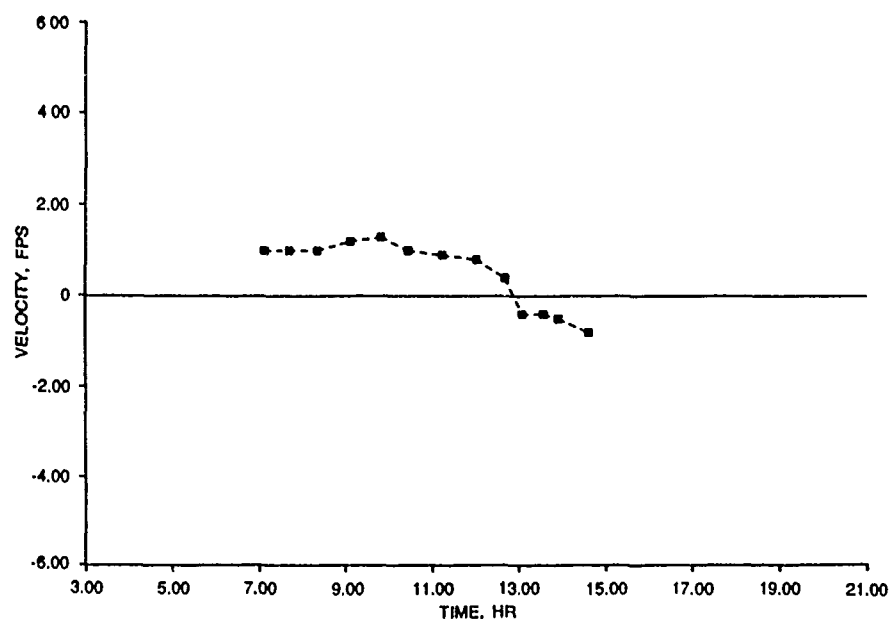


Figure 66. Velocity profile in channel north of dredge, Tests 4 and 5, sta V1, middepth

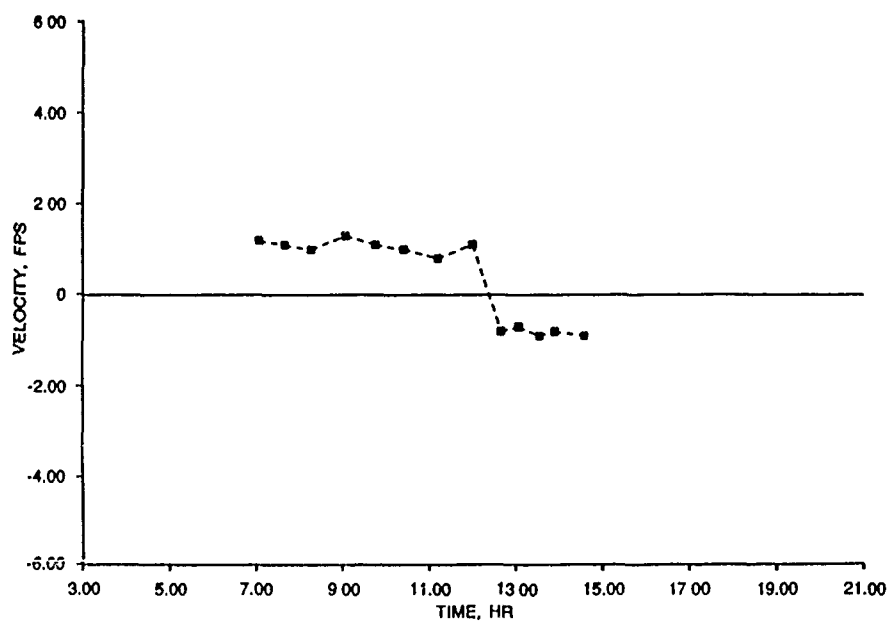


Figure 67. Velocity profile in channel north of dredge, Tests 4 and 5, sta V1, three-quarter depth

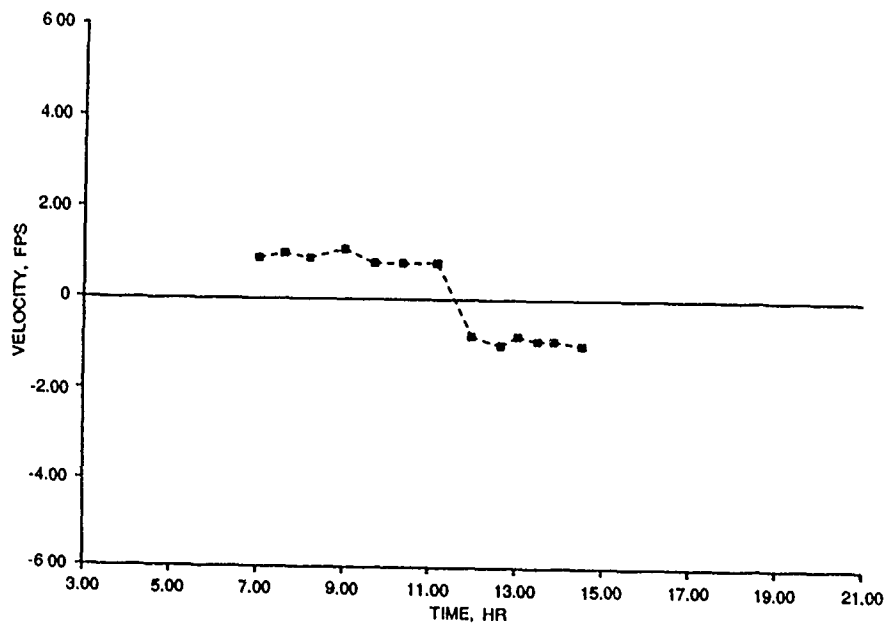


Figure 68. Velocity profile in channel north of dredge, Tests 4 and 5, sta V1, bottom

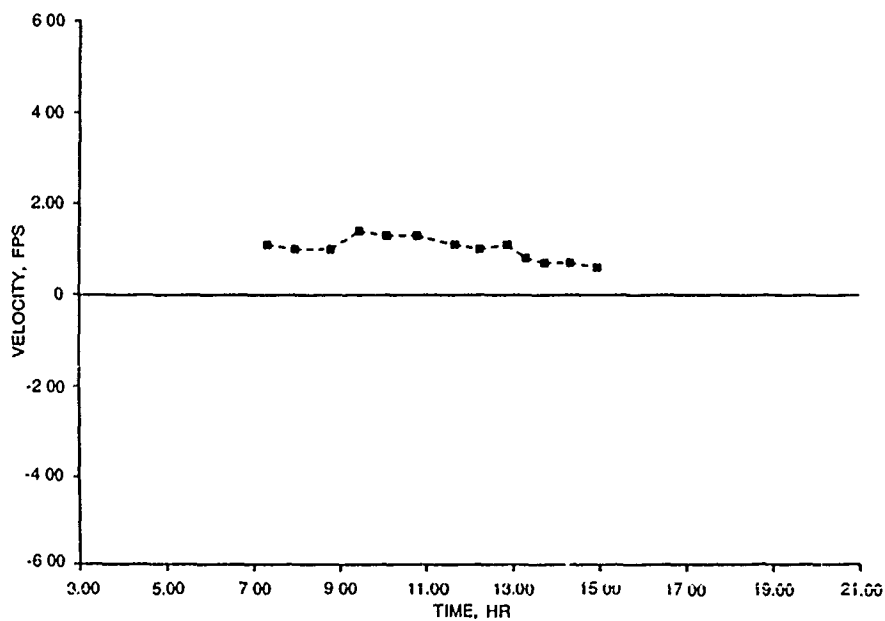


Figure 69. Velocity profile in shallows east of channel, Tests 4 and 5, Sta V2, surface

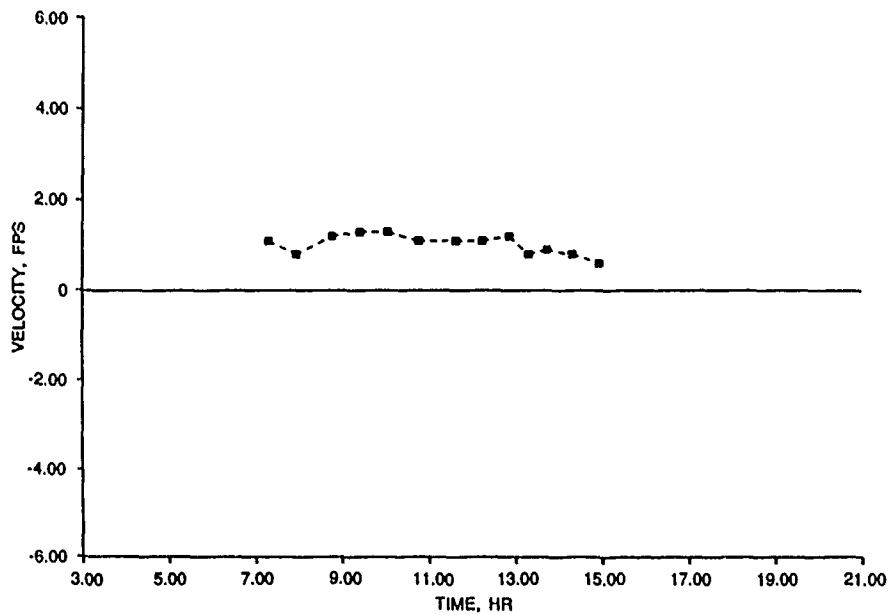


Figure 70. Velocity profile in shallows east of channel, Tests 4 and 5, sta V2, bottom

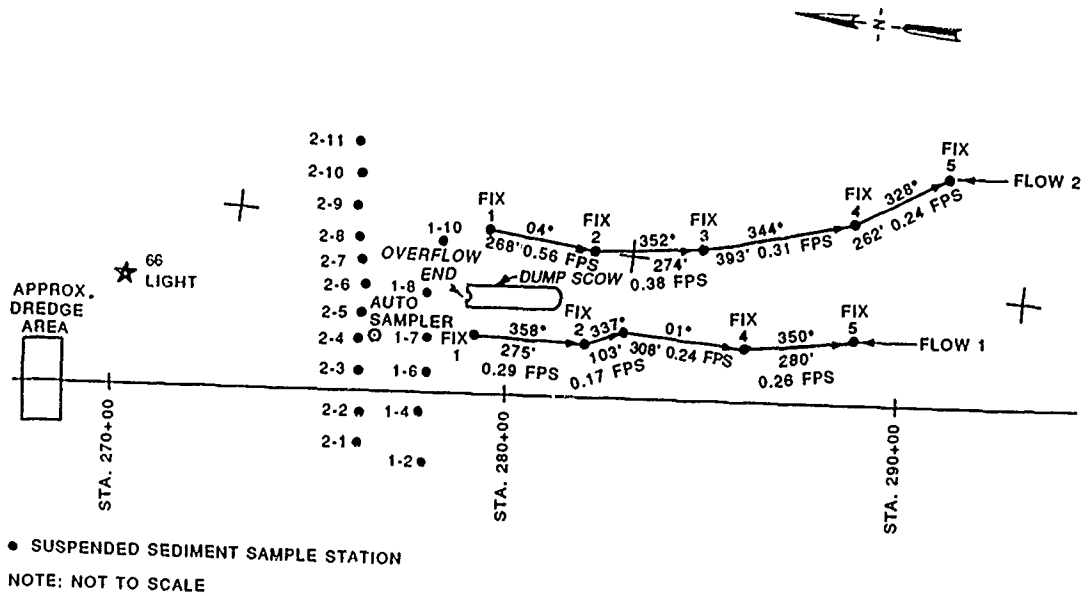


Figure 71. Location of sampling stations, upper bay, Test 8 (not to scale)

PART VII: NUMERICAL MODELING OF DREDGED MATERIAL OVERFLOW PLUMES IN MOBILE BAY*

To address the question of the environmental impact of dredged material overflow from disposal barges, a prediction of the physical fate of the material released into the water column is required. Under the Dredged Material Research Program, numerical disposal models for instantaneous disposal from bottom dumping barges and continuous disposal from pipelines were developed by Brandsma and Divoky (1976). Each computes dynamic descent and collapse phases before placing the suspended sediment in a passive transport-diffusion phase. Since the overflow from disposal barges contains very low concentrations of sediment, dynamic phases due to density effects are considered negligible. Thus, the controlling processes are advection, diffusion, and settling of the suspended sediment.

The historical approach for making suspended sediment computations is to numerically solve a three-dimensional (3D) time-varying transport-diffusion equation. However, with such an approach, computations can become costly on large 3D grids, and numerical problems (e.g., numerical diffusion) must be addressed. An alternative is a combined analytical-numerical approach proposed by Brandsma and Sauer (1983) that employs the concept of small Gaussian sediment "clouds." This approach assumes a Gaussian distribution of suspended sediment within each small cloud and places no restriction on the bottom topography, ambient currents, or the effect of water column stratification on vertical turbulence.

Theoretical Aspects of Plume Model

As illustrated in Figure 72, during an overflow operation sediment is stored in small clouds. These clouds are created at a specified time interval, Δt_c , and are characterized by a lateral dimension (L), thickness, sediment mass, and centroid location (x_o, y_o). At the end of each computational time step, all existing clouds are diffused, transported, and settled.

* Written by Billy H. Johnson, Hydraulics Laboratory, WES.

Assuming a Gaussian distribution, the concentration of suspended sediment of a particular type (e.g., sand, silt, or clay) in an individual cloud is given by

$$C = \frac{m}{(2\pi)^{3/2} \sigma_x \sigma_y \sigma_z} \exp \left\{ -\frac{1}{2} \left[\frac{(x - x_o)^2}{\sigma_x^2} + \frac{(y - y_o)^2}{\sigma_y^2} + \frac{(z - z_o)^2}{\sigma_z^2} \right] \right\} \quad (1)$$

where

m = total mass of sediment contained in the cloud

$\sigma_x, \sigma_y, \sigma_z$ = standard deviations

x_o, y_o, z_o = coordinates of cloud centroid

x, y, z = spatial coordinates

At the end of each time step, each cloud is advected horizontally by the input velocity field. Thus, the new position of the cloud centroid is determined from

$$x_{o_new} = x_{o_old} + u\Delta t \quad (2)$$

$$z_{o_new} = z_{o_old} + w\Delta t$$

where

u, w = local ambient horizontal components of the velocity

Δt = long-term time step

In addition to the advection or transport of a cloud, the cloud grows both horizontally and vertically as a result of turbulent diffusion. The horizontal diffusion is based upon a 4/3 power law. Therefore, the diffusion coefficient is given as

$$K_{x,z} = A_L L^{4/3} \quad (3)$$

where A_L is a dissipation parameter and L is the horizontal dimension of the cloud that is assumed to represent four standard deviations. An expression for the horizontal growth of a small cloud can then be derived as

$$\sigma_{x,z_{\text{new}}} = \sigma_{x,z_{\text{old}}} \left(1 + 4^{4/3} \frac{2}{3} \frac{A_L \Delta t}{\sigma_{x,z_{\text{old}}}^{2/3}} \right)^{3/2} \quad (4)$$

where the subscript "new" represents values at the present computational time and "old" represents values at the previous time step.

Vertical growth is similarly achieved by employing the Fickian expression

$$\sigma_y = (2K_y t)^{1/2} \quad (5)$$

where

K_y = vertical diffusion coefficient
 t = time since formation of the cloud

From Equation 5,

$$\frac{d\sigma_y}{dt} = K_y (2K_y t)^{-1/2} \quad (6)$$

and thus,

$$\sigma_{y_{\text{new}}} = \sigma_{y_{\text{old}}} + \frac{K_y}{\sigma_{y_{\text{old}}}} \Delta t \quad (7)$$

The vertical diffusivity is a monotonically nonincreasing function of the gradient Richardson number R_i , which is defined as

$$R_i = \frac{g/\rho \frac{\partial \rho}{\partial y}}{\frac{\partial |\vec{v}|^2}{\partial y}} \quad (8)$$

where

g = gravitational acceleration

ρ = water density

$|\vec{v}|$ = absolute value of the ambient current

Since there is little vertical mixing when the stability of the ambient water is greater than that corresponding to $R_i = 4$, as discussed by Okubo (1962), the diffusion coefficient can be related to the water column stratification by

$$K_y = K_{y_0} (1 - 0.25R_i) \quad 0 \leq R_i \leq 4 \quad (9)$$

where K_{y_0} is the value for a well-mixed water column. Kent and Pritchard (1959) showed that K_{y_0} in well-mixed estuaries can be related to the mean flow and the water depth by

$$K_{y_0} = 8.6 \times 10^{-3} \frac{Uz^2(H-z)^2}{H^3} \quad (10)$$

where U is the mean horizontal velocity, z is the depth of the point of interest, and H is the total depth, all expressed in non-SI units.

The discussion above pertains to computations that are made on individual clouds. When output is desired at the end of a particular time step, the concentration C_T of each solid type at a vertical location y is given at each point of a horizontal grid by summing the contributions from individual clouds to yield

$$C_T = (2\pi)^{-3/2} \sum_{i=1}^N \frac{m_i}{\sigma_{x_i} \sigma_{y_i} \sigma_{z_i}} \exp \left\{ -\frac{1}{2} \left[\frac{(x - x_{o_i})^2}{\sigma_{x_i}^2} + \frac{(y - y_{o_i})^2}{\sigma_{y_i}^2} + \frac{(z - z_{o_i})^2}{\sigma_{z_i}^2} \right] \right\} \quad (11)$$

where N is the number of small clouds of particular solid type.

In addition to the horizontal advection and diffusion of material, settling of the suspended solids occurs. Suspended sediment concentrations and the amount and spatial distribution of solid material deposited on the

bottom are determined as functions of time. The model does not calculate movement of material after its initial deposition.

Input Data

The overflow material is broken into sediment fractions, with a settling velocity prescribed for each fraction. If a sediment fraction is specified as being cohesive, its settling velocity is computed as a function of the suspended sediment concentration of that solid type. The following algorithm is used

$$V_S \begin{cases} = 0.0017 & \text{if } C \leq 25 \text{ mg/l} \\ = 2.34 \times 10^{-5} C^{4/3} & \text{if } 25 \leq C \leq 300 \text{ mg/l} \\ = 0.047 & \text{if } C > 300 \text{ mg/l} \end{cases} \quad (12)$$

where

V_S = settling velocity, ft/sec

C = suspended sediment concentration, mg/l

In addition to sediment characteristics and discharge rate of the overflow, the ambient current, water density, and bottom topography must be prescribed. Either of the two options shown in Figure 73 for the ambient current is currently allowed in the code, with the simplest case being time-invariant profiles for a constant water depth. The ambient density profile is entered as a function of water depth at the deepest point in the disposal site.

Application Using Field Data from Overflow Tests

As shown in Figure 74, overflow operations at two locations (upper site and lower site) in Mobile Bay were monitored during December 1987. Details of plume tracking efforts during the field tests can be found in Part VI. Several disposal plumes covering a range of flow conditions and material characteristics were monitored for the purpose of providing data to verify the numerical plume model. Characteristics of overflow Tests 1-6 are given in Table 35. The ambient current was applied as vertically averaged.

As can be seen from an inspection of the recorded plume data presented in Part VI, essentially no elevated sediment concentrations were detected along the projected path of the plumes. Wind conditions during most tests were quite high, which resulted in generally high ambient suspended sediment concentrations in Mobile Bay and made the detection of artificially created plumes difficult. The obvious conclusion from the plume data is that most of the overflow material is deposited rather quickly within a short distance from the point of overflow. Aerial photographs are presented as Photos C1-C12 (Appendix C).

Since the settling velocity is computed for cohesive sediments and the vertical diffusion coefficient is computed from Equation 10, the only free parameter to be specified in the numerical model is the dissipation coefficient A_L in Equation 3 for the horizontal diffusion coefficient. As can be seen in Figure 75, the value for this parameter ranges from near zero to 0.005, with the larger values being more appropriate in estuarine environments. The value selected here was 0.003. The impact on suspended sediment concentrations varying A_L from 0.001 to 0.005 is shown in Figure 76.

Eight disposal tests were monitored. However, since few plume data were collected, only the first six tests have been modeled. Modeling Tests 7 and 8 would not have provided any additional insight. Depositional results computed by the model for the first six tests are summarized in Table 36. Virtually all of the solids contained in the overflow in Tests 1-3 were computed to be deposited within 10 to 15 min after overflow ceased. Conditions for Tests 4-6 were such that a slightly longer time was required. Contour plots of the thickness of deposition after virtually all material is deposited are presented as Figures 77-82. As can be seen, deposition occurs primarily in or along the edge of the channel and normally occurs over a longitudinal extent of less than 1,000 ft with a lateral extent of less than 400 ft. In all computations, overflow was assumed to occur near the side of the channel in a water depth of 22 ft. A cross section of the bottom topography used in the model is presented as Figure 83. Contour plots of suspended sediment concentrations at depths of 3 and 10 ft below the water surface at 10 min after termination of overflow are presented as Figures 84-95. Maximum computed concentrations above background along the plume center line at various times after the overflow was terminated are presented in Table 37. As can be seen, suspended sediment concentrations are quickly reduced to near-background levels within 15 to 20 min for all tests.

There is no claim that the results presented constitute a quantitative verification of the plume model. However, it is believed that in a qualitative sense, model results agree with the conclusion drawn from the field plume data, i.e., that the majority of the overflow material deposits rather quickly near the overflow source. It should be noted that, by placing the overflow material at the sea surface rather than allowing for some plunging into the water column, model results are conservative with respect to the time required for a given percent of material to be deposited.

Application to Maintenance Dredging

The numerical plume model was next applied to predict overflow plumes generated during two assumed maintenance dredging schedules. Based upon historical dredging records, the Mobile District suggested that model runs be made assuming in one case that maintenance dredging would begin in March and end in July, and in the second case that dredging would begin in October and end in February. The dredging was assumed to begin at the lower end of the navigation channel and proceed at a uniform rate to the upper end.

Model runs were made assuming an average of the conditions in Table 35 for the overflow tests on maintenance material. Therefore, the material was assumed to be all silty-clay with a sediment concentration of $0.055 \text{ ft}^3/\text{ft}^3$. The overflow discharge was assumed to be 40 cfs and had a duration of 30 min. Results for overflow on both sides of the channel for both maximum flood and ebb velocities were computed for each of the five months of the two dredging schedules.

A numerical hydrodynamic model of Mobile Bay developed by Raney and Youngblood (1982) was used to provide the maximum flood and ebb velocities for each month at the location along the navigation channel where dredging would occur during that month, based upon a uniform rate of movement of the dredge up the channel. The hydrodynamic model was run for this study with tides, freshwater inflow, and wind conditions considered typical for each month of the year. These were determined jointly by Raney and the Mobile District and are discussed in Appendix B. The numerical grid used in the hydrodynamic model is presented as Figure 96.

Results of the plume modeling in the form of depositional thickness in centimeters are presented in Figures 96-106 for overflow plumes computed for each of the 10 months involved in the two maintenance dredging periods,

namely, March-July and October-February. In addition to the thickness of deposition, the maximum suspended sediment concentrations (at depths of 3 and 10 ft at the moment overflow stops and 10 min later) are presented in Table 38 along with the vertically averaged ambient velocity used in the simulation. Variable V_c is the velocity component along the channel, and V_{ac} is the velocity component across the channel. The obvious conclusions concerning the physical fate of overflow materials that can be drawn from these results are that the vast majority of the material will be redeposited in the channel and that suspended sediment concentrations are rapidly reduced due to diffusion and settling. Estimates of the environmental impact of such conditions are given in Part IX.

Application to New Work Dredging

Work on deepening the navigation channel is ongoing, with the work having been initiated in October 1987. Current plans call for the completion of the deepening project in May 1990.

In consultation with the Mobile District, it was agreed to represent new work material south of Gaillard Island as all silty-clay, and new work material north of the island as 30 percent sand and 70 percent silty-clay. The overflow rate at locations south of Theodore Island was taken to be 40 cfs with a duration of 17 min, whereas the rate used for north of the island was 60 cfs with a duration of 30 min. These conditions represent approximate averages of the conditions in the field tests for the overflow of new work material at the lower and upper bay sites, respectively.

The dredging schedule for the deepening project is shown in Table 39. Maximum flood and ebb velocities for each of the months at a particular location, based upon the dredging schedule, were again taken from the hydrodynamic model results provided by Raney. Depositional patterns for overflow from both the right and left sides of the channel during maximum flood and ebb conditions for each of the months listed in Table 39 are given in Figures 107-133. Maximum suspended sediment concentrations at depths of 3 and 10 ft resulting from overflow during both maximum flood and ebb conditions are presented in Table 40 when overflow stops and 10 min later. The vertically averaged flow velocity specified is also given. As was observed in the computations for the case of overflow of maintenance material, the vast majority of the new work material will be redeposited in the channel. The

environmental impact associated with these overflow plumes is discussed in Part IX.

References

- Brandsma, M. G., and Divoky, D. J. 1976 (May). Development of models for prediction of short-term fate of dredged material discharged in the estuarine environment. Contract Report D-76-5. US Army Engineer Waterways Experiment Station, Vicksburg, MS.
- Brandsma, M. G., and Sauer, T. C. 1983. Mud discharge model - report and user's guide. Exxon Production Research Company, Houston, TX.
- Kent, R. E., and Pritchard, D. W. 1959. A test of mixing length theories in a coastal plain estuary, Journal of Marine Research, Vol 18, pp 62-72.
- Lawing, R. J., Boland, R. A., and Bobb, W. H. 1975. Effects of proposed Theodore ship channel and disposal areas on tides, currents, salinities, and dye dispersion. Mobile Bay Model Study Report 1, Technical Report H-75-13. US Army Engineer Waterways Experiment Station, Vicksburg, MS.
- Okubo, A. 1962. A review of theoretical models for turbulence diffusion in the sea. Journal of the Oceanographic Society of Japan, 20th Anniversary Volume, pp 286-320.
- Psinakis, W. L. 1987. Availability and compilation of selected streamflow data for the Mobile River and the lower Tombigbee River. US Geological Survey Open-File Report 87-201. Montgomery, AL.
- Raney, D. C., and Youngblood, J. N. 1982. Hydrodynamics of Mobile Bay and Mississippi Sound - Net cross channel flows in Mobile Bay. BER Report No. 285-112. University of Alabama, Tuscaloosa, AL.
- Schroeder, W. W., and Wiseman, W. J., Jr. 1985. An analysis of the winds (1974-1984) and sea level elevations (1973-1983) in coastal Alabama. Mississippi-Alabama Sea Grant Consortium Publication No. MASGP-84-024. Ocean Springs, MS.
- US Army Engineer District, Mobile. 1985. Improvement of navigation on the lower Black Warrior-Tombigbee River System. General Design Memorandum COESAM/ENYD-85/001. Mobile, AL.

Table 35
Characteristics of Overflow Tests

Test	Date	Tide*	Site**	Velocity, fps		Overflow Duration min	Overflow Density ρ_{av} , mg/ ℓ	Material Type	Sediment Type	Overflow Rate, cfs
				V_c †	V_{ac} ††					
1	12/3/87	F	L	0.799	0.260	18	1.07	Maintenance	100% silt-clay	36.37
2	12/4/87	E	L	-0.985	0.174	16	1.10	New work	100% silt-clay	37.50
3	12/4/87	F	L	0.799	0.260	18	1.10	New work	100% silt-clay	44.84
4	12/6/87	E	U	-0.808	0.142	38	1.10	Maintenance	95% silt-clay 5% fine sand	42.11
5	12/6/87	F	U	0.297	0.042	36	1.12	Maintenance	95% silt-clay 5% fine sand	41.67
6	12/7/87	E	U	-0.808	0.142	28	1.13	New work	75% silt-clay 25% fine sand	55.43

* F = flood, E = ebb.

** L = lower site, U = upper site.

† Along the channel.

†† Across the channel and positive to the east.

Table 36
Computed Deposition from Overflow Tests

Test	Percent Deposited			
	10 min*	20 min	30 min	50 min
1	13.9	66.9	98.8	--
2	10.9	68.5	98.8	--
3	14.0	67.0	98.8	--
4	2.7	21.7	47.0	73.3
5	2.9	21.6	46.8	73.8
6 (clay fraction)	3.8	29.8	64.1	92.4
6 (sand fraction)	10.6	44.8	80.5	99.4

* Time from initiation of overflow.

Table 37
Maximum Computed Concentrations Above Background
from Overflow Tests

Test	Time min*	Depth - 3 ft		Depth - 10 ft	
		Maximum Concentration mg/l	Distance from Overflow, ft	Maximum Concentration mg/l	Distance from Overflow, ft
1	0	3,960	100	11,400	100
	5	495	300	3,170	300
	10	52	500	407	500
	15	1	800	21	800
2	0	4,500	100	9,220	200
	5	718	300	4,740	300
	10	119	600	947	600
	15	9	900	94	900
3	0	6,490	100	20,600	100
	5	849	300	5,440	300
	10	90	500	697	500
	15	2	800	38	800
4	0	5,470	100	20,700	100
	5	646	300	3,430	300
	10	176	500	1,190	600
	15	56	800	454	800
	20	15	1,000	119	1,100
5	0	2,290	100	12,800	100
	5	1,690	100	9,160	100
	10	376	200	2,240	200
	15	106	300	653	300
	20	32	400	209	400
6 (silt-clay fraction)	0	6,640	100	28,500	100
	5	840	300	4,460	300
	10	229	500	1,500	600
	15	74	800	590	800
	20	19	1,000	160	1,100
6 (sand fraction)	0	481	100	3,170	100
	5	15	300	439	300
	10	0	-	29	500

* Time after overflow stops.

Table 38
Suspended Sediment Concentrations from
Overflow of Maintenance Material

Month	Tide*	Side of Channel**	Silty-Clay Maximum Concentration, mg/l				Velocity, fps	
			0 min†		10 min		V _c ‡	V _{ac} ‡‡
			3 ft††	10 ft	3 ft	10 ft		
March	F	R	Results		239	1,960	0.246	0.066
	E	R	not printed		184	590	-0.819	-0.295
	F	L			284	1,720	0.281	0.017
	E	L	5,810	17,300	72	557	-0.821	-0.241
April	F	R	Results		224	1,940	0.262	0.009
	E	R	not printed		181	1,090	-0.640	0.033
	F	L			257	1,570	0.230	0.019
	E	L			149	1,240	-0.743	-0.041
May	F	R	813	6,540	264	2,290	-0.139	0.010
	E	R	4,310	18,000	168	1,010	-0.730	-0.032
	F	L	303	1,800	205	1,260	-0.048	0.020
	E	L	5,450	16,500	123	1,050	-0.887	-0.032
June	F	R	695	4,060	327	1,990	-0.115	-0.007
	E	R	3,330	18,300	180	1,410	-0.540	0.106
	F	L	372	2,960	208	1,700	-0.023	0.068
	E	L	1,840	13,400	229	1,970	-0.268	0.015
July	F	R	841	4,890	336	2,040	-0.135	-0.005
	E	R	5,490	18,200	157	1,250	-0.783	0.081
	F	L	175	1,500	115	1,030	-0.034	0.001
	E	L	3,160	16,500	194	1,160	-0.615	0.028
October	F	R	3,640	17,000	196	1,510	0.581	0.138
	E	R	4,380	18,100	212	674	-0.688	-0.265
	F	L	4,960	17,600	144	865	0.876	0.082
	E	L	3,960	17,600	177	142	-0.614	-0.164
November	F	R	4,340	17,500	136	1,110	0.679	0.059
	E	R	2,460	15,000	204	1,230	-0.486	-0.037
	F	L	3,620	17,000	159	950	0.663	0.078
	E	L	2,300	14,000	235	1,410	-0.441	-0.004
December	F	R	4,070	17,600	163	984	0.709	-0.003
	E	R	3,430	18,100	166	1,420	-0.580	0.017
	F	L	4,960	17,900	145	1,230	0.737	-0.030
	E	L	2,930	16,300	198	1,190	-0.581	0.055
January	F	R	2,400	14,700	219	1,320	0.466	-0.067
	E	R	4,730	10,900	146	1,090	-0.965	0.151
	F	L	1,060	8,400	243	2,110	0.170	0.006
	E	L	2,610	17,200	188	1,630	-0.412	-0.045
February	F	R	1,780	10,100	284	1,700	0.273	-0.092
	E	R	5,470	17,000	54	440	-2.484	0.240
	F	L	1,020	7,820	274	2,270	0.148	-0.057
	E	L	8,130	10,200	85	693	-2.154	-0.045

* F - flood, E - ebb.

** R - right side, L - left side.

† Time after overflow was terminated.

†† Depth.

‡ Velocity component along channel - positive is to the north.

‡‡ Velocity component across channel - positive is to the east.

Table 39
Mobile Ship Channel Deepening.
Schedule of New Work Dredging

<u>Date</u>	<u>Percent of Completion*</u>
October 1987 (begin)	0.2
Nov	1.4
Dec	1.4**
Jan 1988	1.4**
Feb	1.4**
Mar	1.4**
Apr	2.8
May	5.6
Jun	8.4
Jul	11.2
Aug	14.0
Sep	21.1
Oct	28.2
Nov	35.3
Dec	38.1
Jan 1989	40.9
Feb	43.7
Mar	46.5
Apr	49.3
May	52.1
Jun	54.9
Jul	57.7
Aug	64.8
Sep	71.9
Oct	79.0
Nov	81.8
Dec	84.6
Jan 1990	87.4
Feb	90.2
Mar	93.0
Apr	95.8
May	98.6
May 15 (end)	100.00

* Percent of channel completed during month shown.

** No production.

Table 40
Maximum Computed Concentrations for Overflow of
New Work Material

Month	Tide*	Side of Channel**	Silty-Clay				Sand				Velocity, fps	
			Maximum Concentration, mg/ℓ				Maximum Concentration, mg/ℓ				V _c	V _{ac}
			0 min†	10 ft	10 min	3 ft	0 min	10 ft	10 min	3 ft		
Nov 87	F	R	6,300	6,400	9	93					2.478	0.887
	E	R	48,300	13,900	64	509					-1.73	0.223
	F	L	3,370	13,000	12	71				N/A†	2.59	0.547
	E	L	43,000	9,520	95	564					-1.841	0.016
Apr 88	F	R	3,520	18,400	177	1,460					0.578	0.049
	E	R	42,700	9,330	105	336					-1.760	-0.549
	F	L	3,740	17,300	157	938				N/A	0.668	0.078
	E	L	45,600	11,800	61	466					-1.782	-0.247
May 88	F	R	42,500	9,320	107	640					1.481	-0.150
	E	R	54,300	18,400	115	367					-1.596	0.420
	F	L	6,340	12,300	124	1,020				N/A	1.113	-0.181
	E	L	51,100	16,400	102	789					-1.609	-0.111
June 88	F	R	48,700	13,600	110	349					1.536	-0.188
	E	R	40,700	8,270	128	410					-1.431	-0.350
	F	L	10,300	9,170	52	373				N/A	1.171	-0.285
	E	L	38,700	7,680	102	835					-1.469	-0.051

(Continued)

* F = flood, E = ebb.

** R = right, L = left.

† Time after overflow was terminated.

†† Depth.

‡ New work material south of Gaillard did not contain a sand fraction.

(Sheet 1 of 5)

Table 40 (Continued)

Month	Tide	Side of Channel	Silty-Clay				Sand				Velocity, fps	
			Maximum Concentration, mg/ℓ				Maximum Concentration, mg/ℓ				V _c	V _{ac}
			0 min	3 ft	10 ft	10 min	0 min	3 ft	10 ft	10 min		
July 88	F	R	11,000	8,510	107	866					1.214	0.059
	E	R	5,280	10,800	161	503					-1.066	-0.227
	F	L	52,220	17,300	74	577				N/A	1.651	-0.214
	E	L	5,300	12,400	117	987					-1.092	-0.014
Aug 88	F	R	4,800	10,500	96	746					0.961	0.214
	E	R	149	860	0	11					-0.812	-0.150
	F	L	8,030	9,920	121	663				N/A	1.151	0.160
	E	L	5,320	14,700	151	1,170					-0.914	-0.134
Sept 88	F	R	5,900	17,100	60	424					0.823	0.281
	E	R	3,680	17,300	200	642					-0.622	-0.241
	F	L	5,130	18,900	168	532				N/A	0.822	0.206
	E	L	4,380	17,800	162	1,220					-0.658	-0.138
Oct 88	F	R	5,780	17,200	112	914					0.854	0.167
	E	R	2,480	15,100	221	1,160					-0.457	-0.144
	F	L	3,640	17,200	167	943				N/A	0.647	0.146
	E	L	2,930	18,100	226	1,770					-0.423	-0.131
Nov 88	F	R	5,800	18,400	160	1,250					0.793	0.164
	E	R	2,240	13,500	238	1,440					-0.412	-0.015
	F	L	3,150	16,800	199	1,190				N/A	0.597	0.113
	E	L	2,670	17,500	197	1,670					-0.409	-0.027
Dec 88	F	R	4,630	17,900	142	1,180					0.699	0.048
	E	R	2,210	13,100	233	1,420					-0.400	-0.019
	F	L	2,310	14,000	240	1,450				N/A	0.428	0.063
	E	L	2,980	16,600	201	1,210					-0.582	0.032

(Continued)

Table 40 (Continued)

Month	Tide	Side of Channel	Silty-Clay				Sand				Velocity	
			Maximum Concentration, mg/ℓ				Maximum Concentration, mg/ℓ				V _c	V _{ac}
			0 min	3 ft	10 ft	10 min	0 min	3 ft	10 ft	10 min		
Jan 89	F	R	4,460	17,800	138	1,140					0.685	-0.047
	E	R	2,250	13,500	239	1,440					-0.415	-0.011
	F	L	3,820	17,400	157	952				N/A	0.675	0.083
	E	L	2,650	17,400	191	1,650					-0.408	-0.010
Feb 89	F	R	3,510	18,400	166	1,440					0.586	0.002
	E	R	2,520	15,400	205	1,230					-0.490	-0.003
	F	L	3,320	18,500	157	1,370				N/A	0.553	-0.001
	E	L	3,010	18,400	184	1,550					-0.483	-0.030
Mar 89	F	R	252	1,490	204	1,230					-0.051	-0.001
	E	R	4,610	14,000	150	895					-0.946	-0.020
	F	L	173	1,020	157	947				N/A	-0.029	0.013
	E	L	4,660	10,500	120	1,010					-0.988	-0.019
Apr 89	F	R	907	7,170	268	2,300					0.150	0.016
	E	R	4,620	14,200	150	897					-0.943	-0.051
	F	L	171	1,010	156	942				N/A	0.016	0.027
	E	L	7,230	11,700	113	939					-1.150	-0.027
May 89	F	R	865	4,990	340	2,050					0.141	0.015
	E	R	4,390	18,300	171	1,030					-0.730	-0.032
	F	L	267	1,580	212	1,280				N/A	0.050	0.021
	E	L	5,550	16,800	126	1,070					-0.887	-0.014
June 89	F	R	2,020	14,200	257	2,080					0.269	0.074
	E	R	2,910	18,100	221	1,760					-0.440	0.089
	F	L	1,270	7,190	265	1,590				N/A	0.176	0.080
	E	L	3,990	17,900	167	1,370					-0.639	-0.051

(Continued)

Table 40 (Continued)

Month	Tide	Side of Channel	Silty-Clay				Sand				Velocity, fps	
			Maximum Concentration, mg/l				Maximum Concentration, mg/l				V _c	V _{ac}
			3 ft	10 ft	3 ft	10 min	3 ft	10 ft	3 ft	10 min		
July 89	F	R	2,250	15,400	243	1,950					0.306	0.077
	E	R	2,250	13,500	239	1,440					-0.408	-0.078
	F	L	2,070	12,000	209	1,200					0.340	0.106
	E	L	3,700	18,200	185	1,490					-0.600	-0.075
Aug 89	F	R	2,550	17,000	179	1,550					0.386	0.010
	E	R	1,920	10,900	269	1,630					0.313	-0.010
	F	L	1,280	9,920	209	1,820					0.195	-0.003
	E	L	1,690	9,510	287	1,740					-0.255	0.060
Sep 89	F	R	1,210	6,700	459	2,460	10	397	0	24	0.083	-0.118
	E	R	2,640	14,900	273	1,640	143	2,580	0	22	-0.337	-0.097
	F	L	4,670	23,700	232	1,880	393	7,800	0	0	0.616	0.061
	E	L	1,470	11,200	353	2,880	4.6	545	0	0	0.156	-0.065
Oct 89	F	R	1,330	7,670	422	2,560	14	496	0	24	0.153	-0.043
	E	R	3,840	23,500	241	1,990	229	5,950	0	0	-0.484	0.042
	F	L	3,850	23,500	245	2,010	230	5,950	0	0	0.482	0.051
	E	L	1,790	13,700	249	2,150	8.6	838	0	0	-0.205	-0.011
Nov 89	F	R	2,330	12,600	457	1,480	82	1,780	3.3	62	0.195	-0.236
	E	R	5,940	24,800	199	1,620	553	9,880	0	0	-0.726	0.063
	F	L	6,350	25,000	111	875	623	10,300	0	0	0.701	-0.251
	E	L	5,610	24,400	178	1,520	508	9,390	0	0	-0.707	-0.013
Dec 89	F	R	4,290	22,600	222	1,330	409	6,740	0	21	0.646	-0.115
	E	R	5,710	21,300	59	474	567	9,380	0	0	-2.408	0.236
	F	L	4,000	23,700	217	1,740	267	6,370	0	0	0.505	-0.074
	E	L	12,600	7,230	99	587	1,250	1,550	0	12	-2.093	0.043

(Continued)

Table 40 (Concluded)

Month	Tide*	Side of Channel**	Silty-Clay						Sand						Velocity, fps	
			Maximum Concentration, mg/l			Maximum Concentration, mg/l			Maximum Concentration, mg/l			Maximum Concentration, mg/l			V _c	V _{ac}
			0 min	10 ft	10 min	0 min	10 ft	10 min	0 min	10 ft	10 min	0 min	10 ft	10 min		
Jan 90	F	R	2,080	11,600	357	2,170	54	1,330	0	16	0.239	0.239	-0.060			
	E	R	3,850	17,700	107	636	362	6,400	0	14	-2.631	-2.631	-0.036			
	F	L	2,810	19,400	316	2,590	50	2,670	0	0	0.300	0.300	-0.059			
	E	L	9,610	11,300	109	876	1,070	3,070	0	0	-2.129	-2.129	-0.167			
Feb 90	F	R	1,970	11,100	339	2,060	45	1,170	0	16	0.231	0.231	-0.019			
	E	R	10,300	9,200	99	589	1,020	1,970	0	13	-2.877	-2.877	-0.024			
	F	L	2,100	15,800	266	2,320	15	1,240	0	0	0.236	0.236	-0.003			
	E	L	21,500	6,320	109	917	2,410	1,810	0	0	-1.999	-1.999	-0.013			
Mar 90	F	R	1,110	6,410	441	2,670	8.4	344	0	23	0.127	0.127	-0.047			
	E	R	22,300	4,350	118	489	2,210	1,850	1	19	-3.097	-3.097	-0.177			
	F	L	695	5,700	314	2,730	0	112	0	0	-0.101	-0.101	-0.008			
	E	L	11,500	9,320	95	783	1,280	2,510	-	0	-2.104	-2.104	-0.036			
Apr 90	F	R	1,700	9,650	324	1,960	28	830	0	21	0.186	0.186	-0.070			
	E	R	3,840	17,700	119	380	361	6,370	3	33	-2.566	-2.566	-0.586			
	F	L	225	1,890	151	1,310	0	16	0	0	-0.023	-0.023	-0.021			
	E	L	51,200	25,300	113	671	5,070	9,140	0	14	-1.692	-1.692	0.130			
May 90	F	R	6,560	25,900	195	1,620	619	1,080	0	0	0.785	0.785	0.036			
	E	R	51,200	25,300	126	405	5,070	9,130	3	35	-1.575	-1.575	-0.633			
	F	L	2,790	16,100	293	1,780	180	3,050	0	15	0.389	0.389	0.003			
	E	L	46,900	20,000	121	950	5,250	8,660	0	0	-1.565	-1.565	-0.090			

(Sheet 5 of 5)

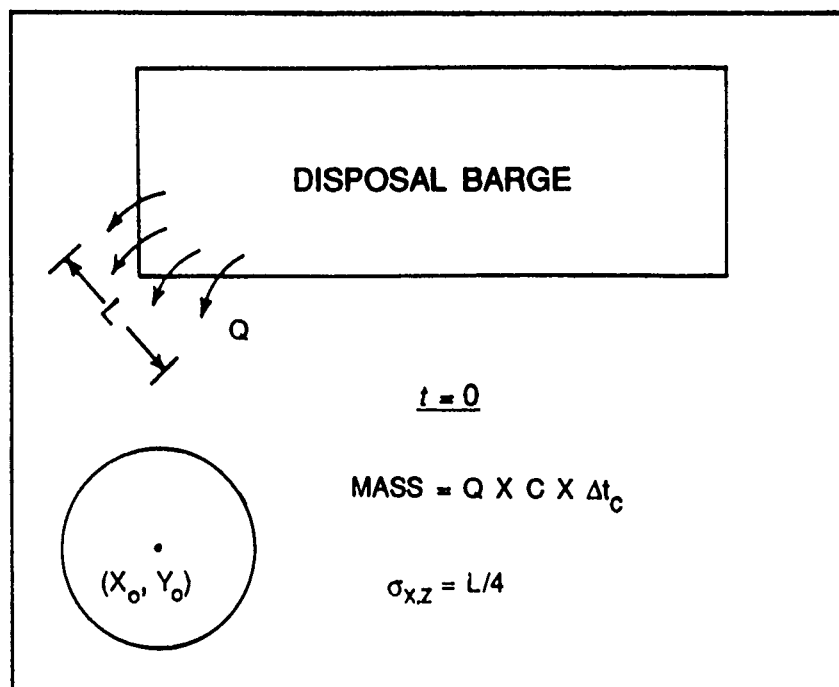
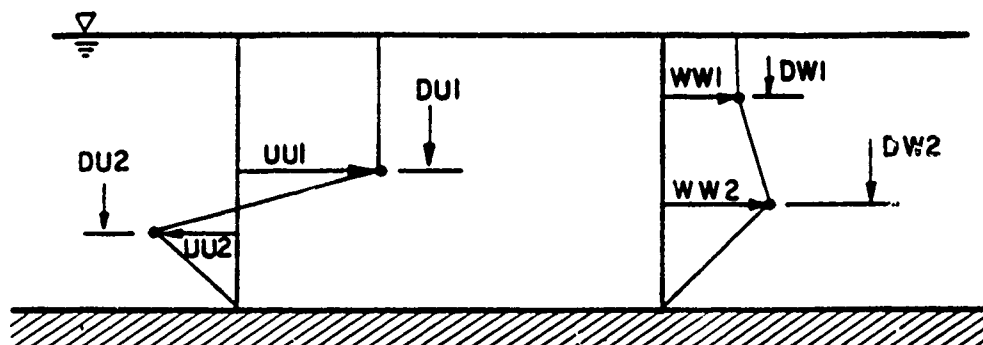
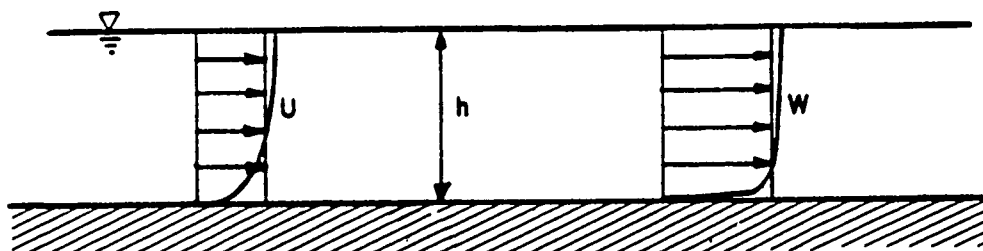


Figure 72. Creation of small clouds



a. Simple orthogonal velocity profiles for constant depth.
Applied everywhere in field



b. Vertically averaged velocity profiles for variable depths
with equivalent logarithmic profiles superimposed

Figure 73. Velocity options

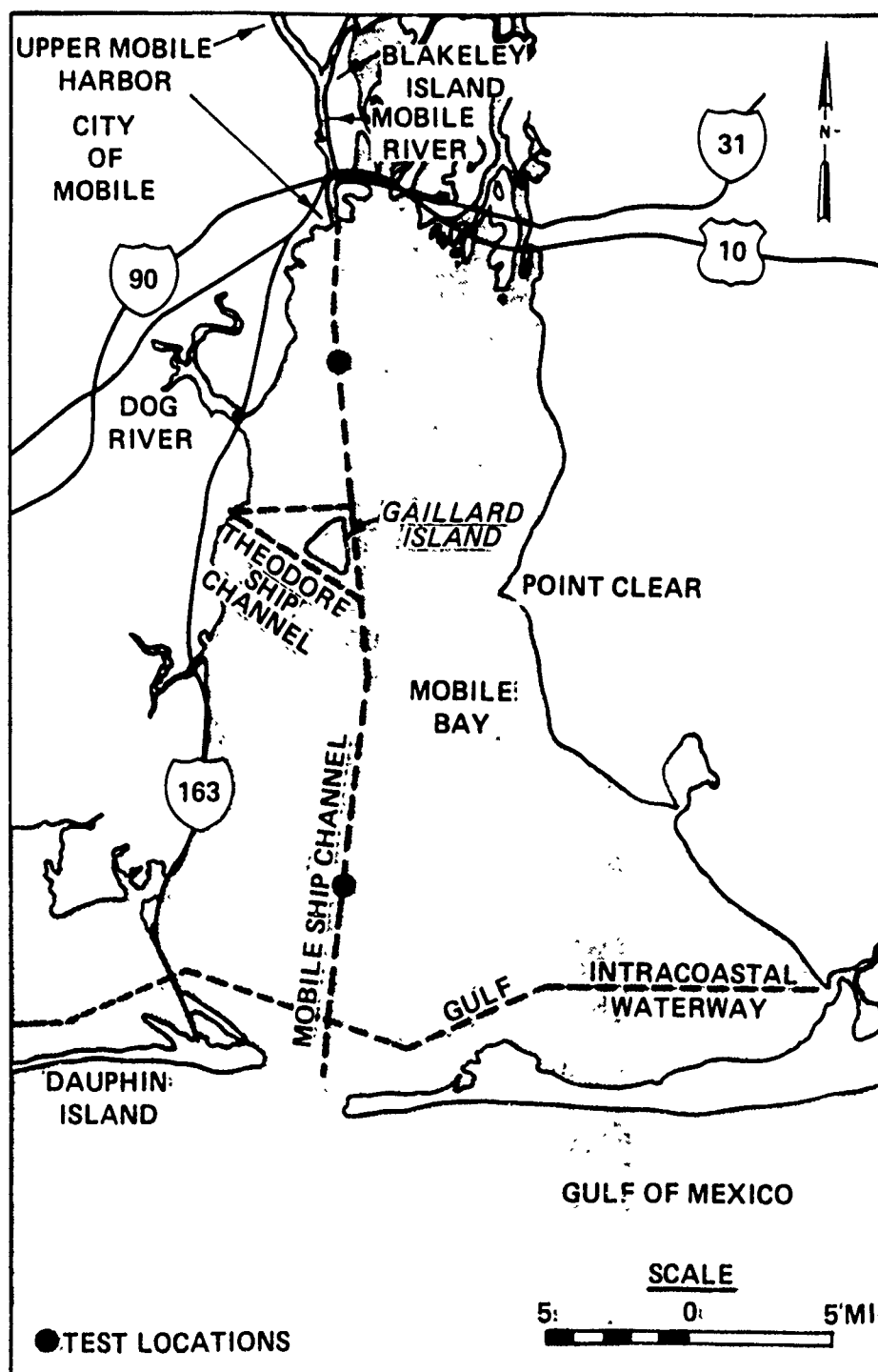


Figure 74. Mobile Bay

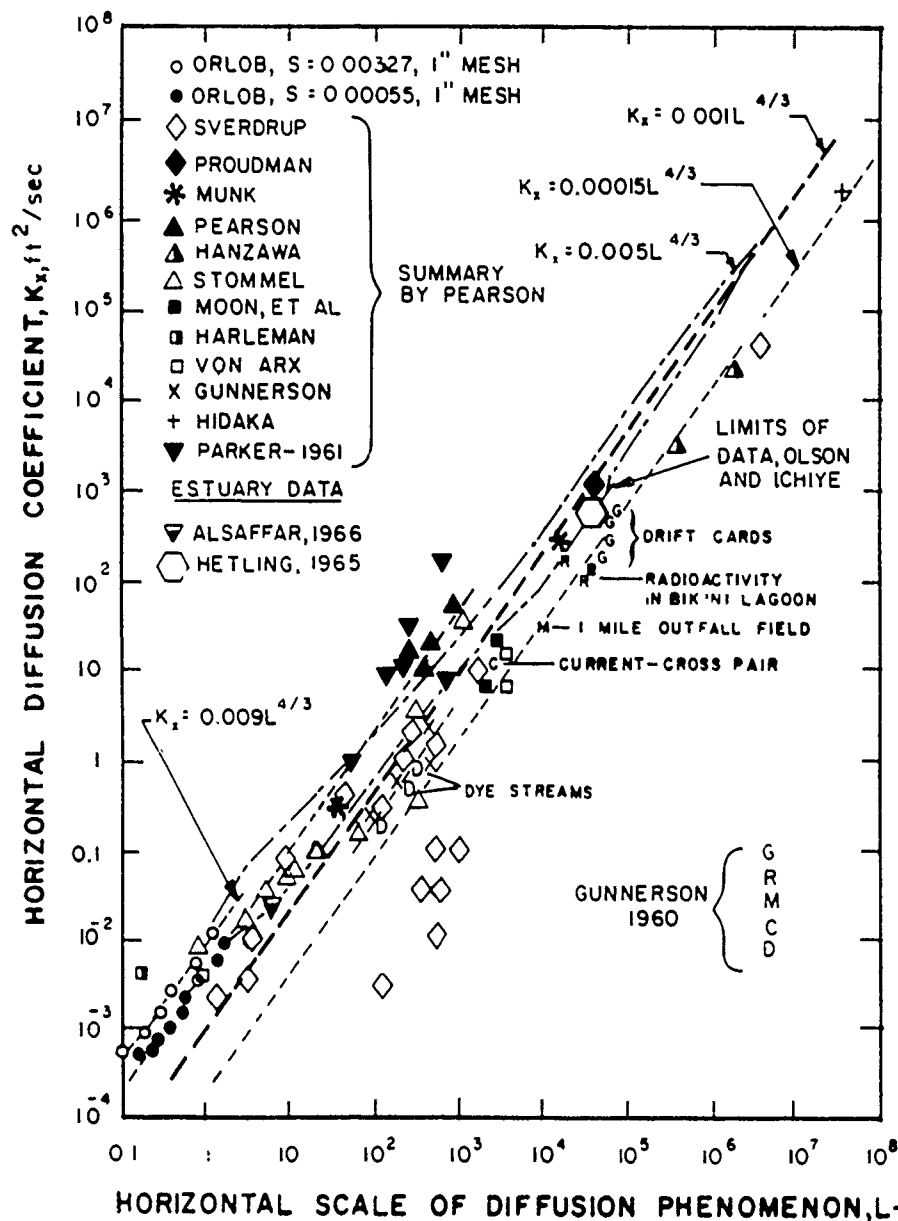


Figure 75. Field data on horizontal diffusion (from Brandsma and Divoky 1976)

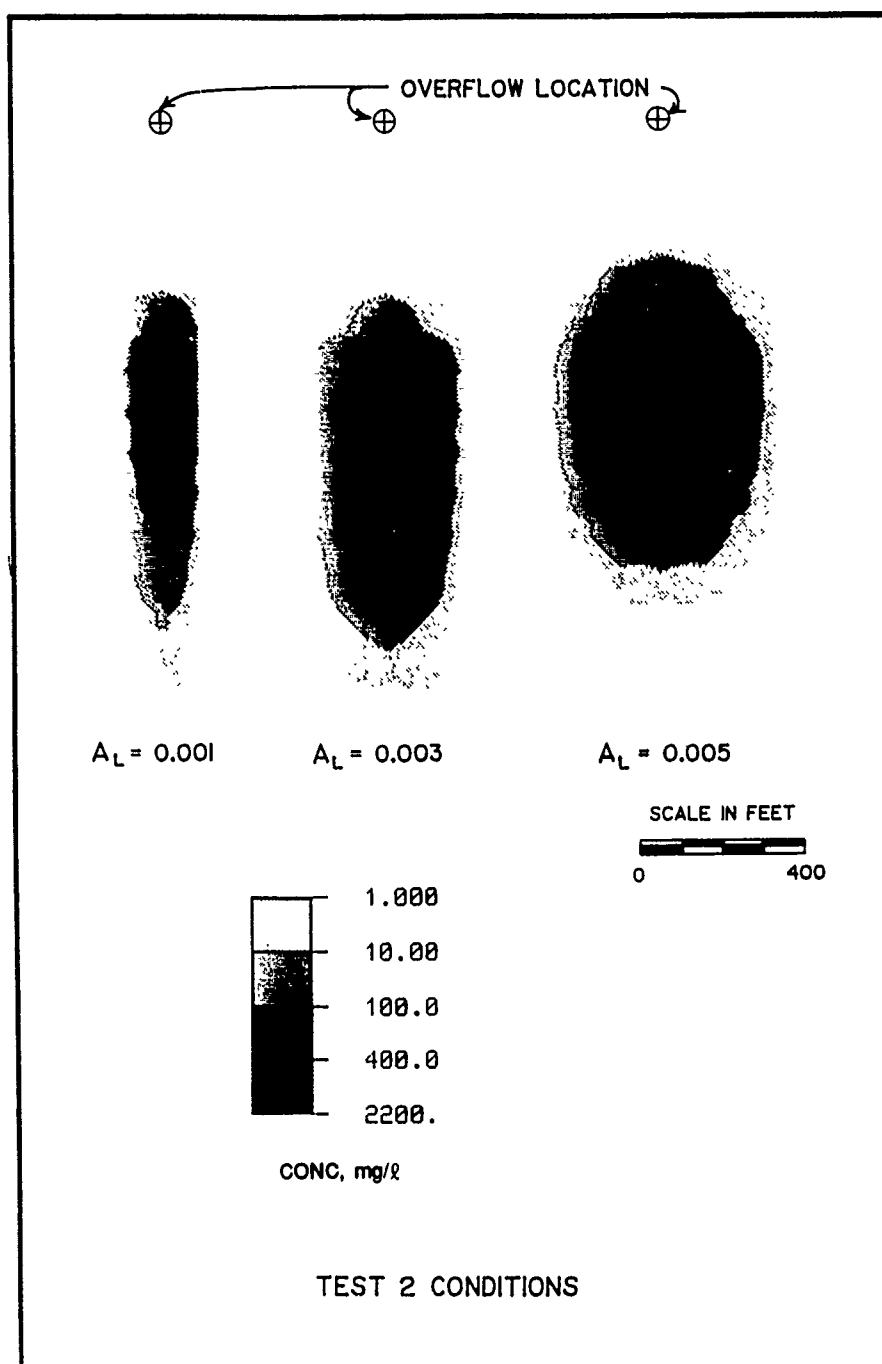


Figure 76. Influence of A_L on suspended sediment concentrations at 10 ft below the water surface 10 min after stopping overflow

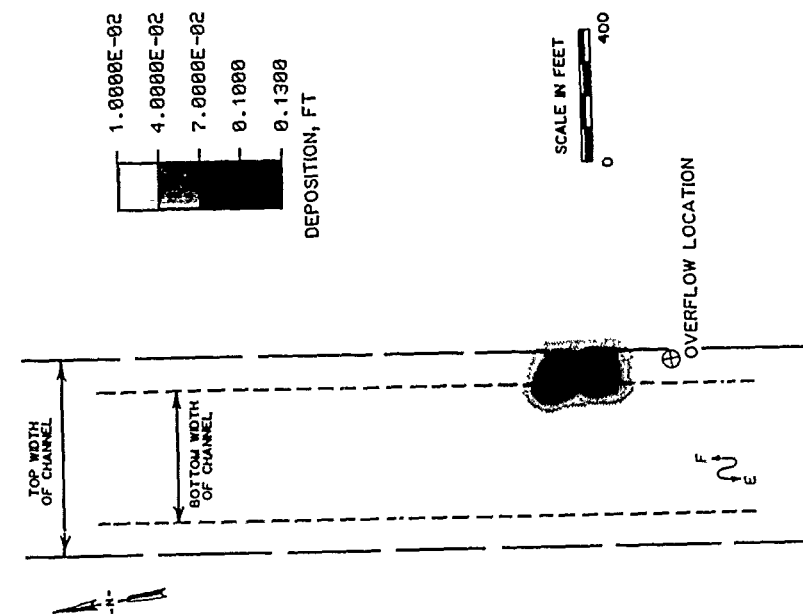


Figure 77. Computed bottom deposition of material in Test 1

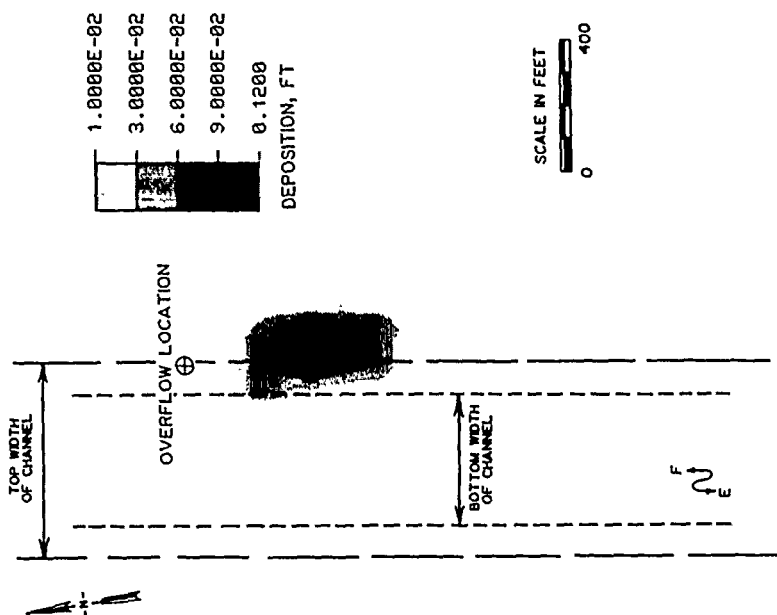


Figure 78. Computed bottom deposition of material in Test 2

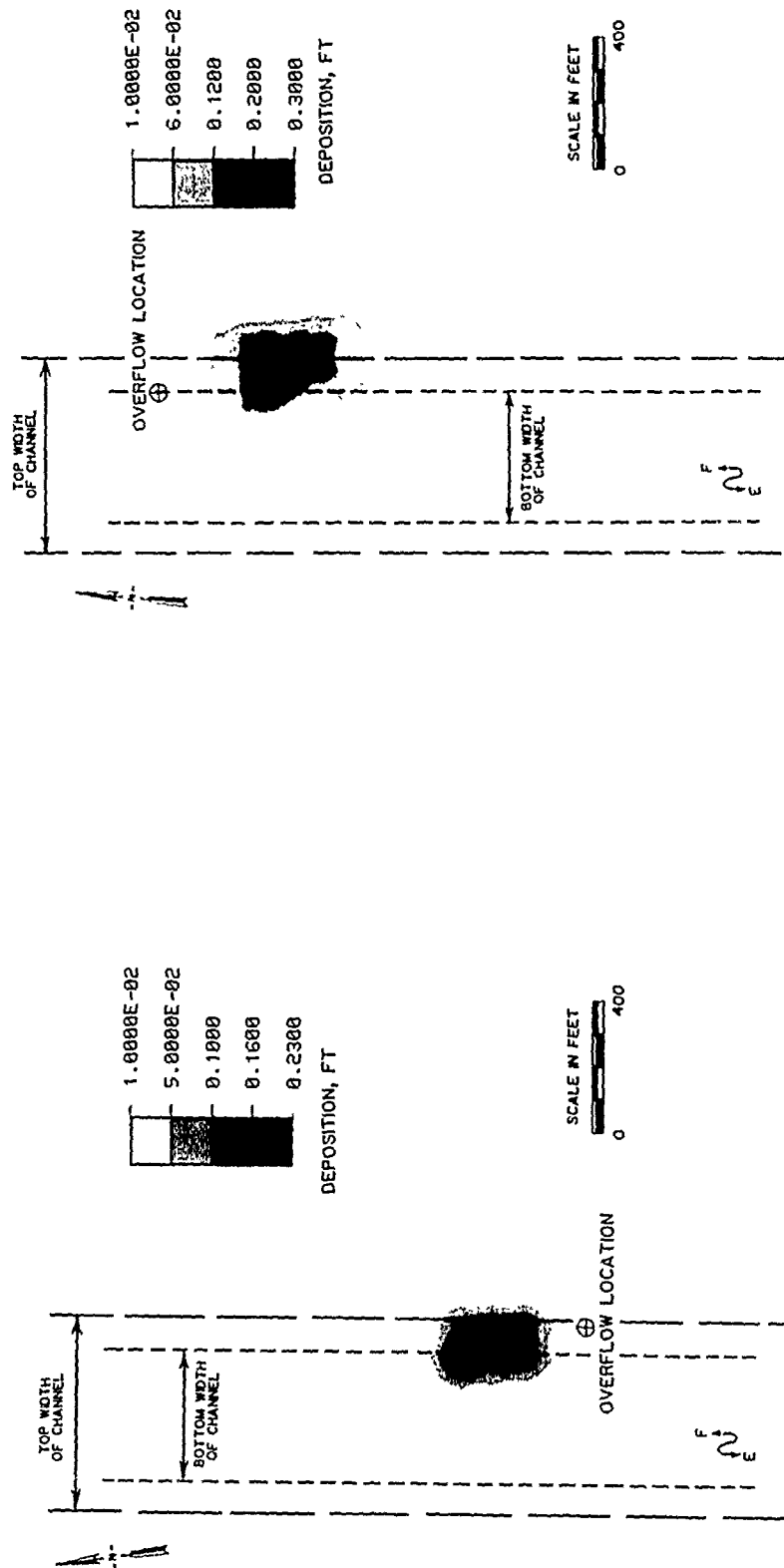


Figure 79. Computed bottom deposition of material in Test 3

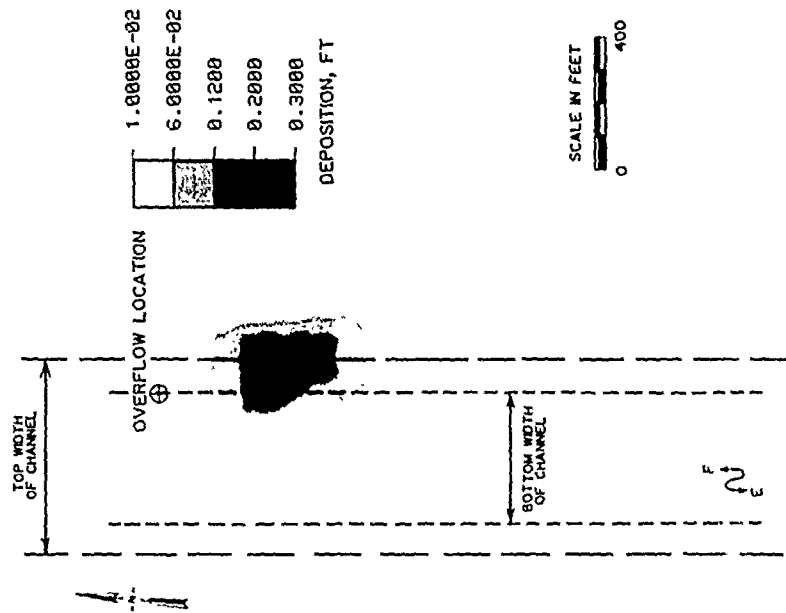


Figure 80. Computed bottom deposition of material in Test 4



Figure 81. Computed bottom deposition of material in Test 5

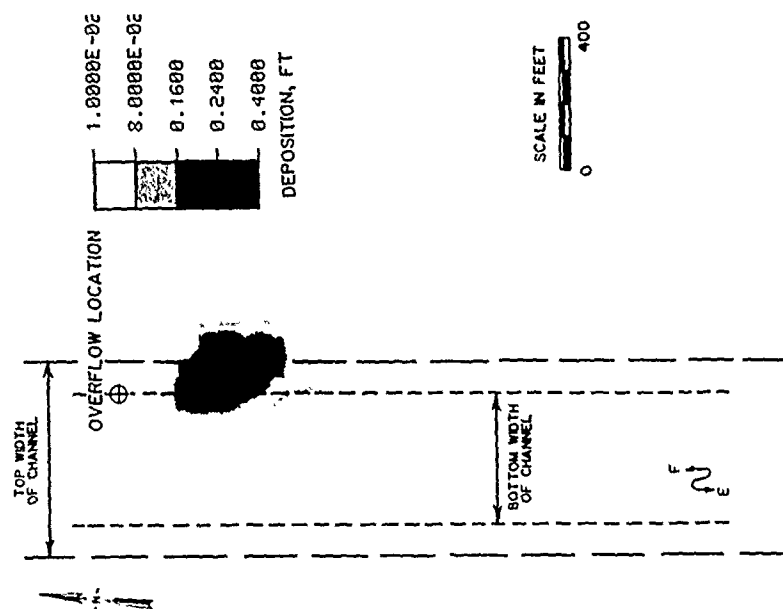


Figure 82. Computed bottom deposition of material in Test 6

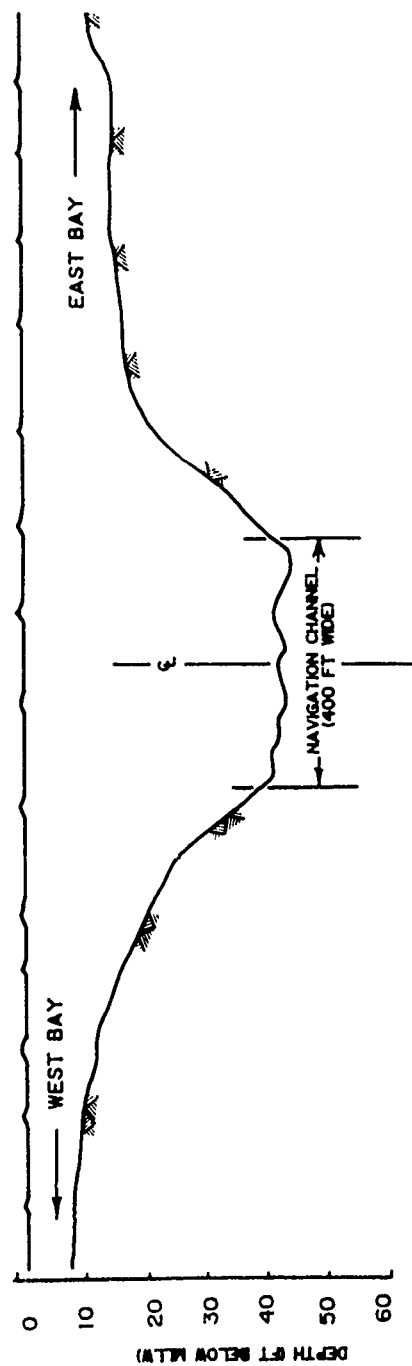


Figure 83. Cross section of bottom topography used in model

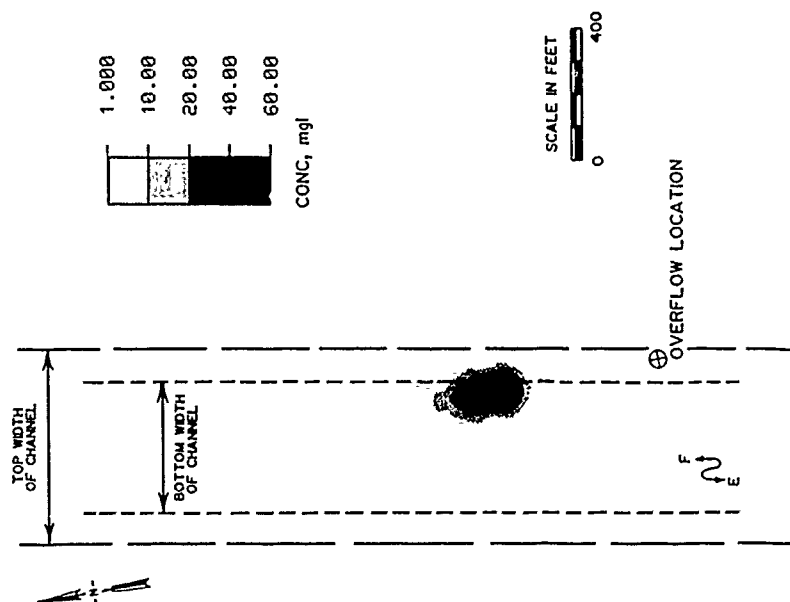


Figure 84. Computed suspended sediment concentrations in Test 1 at 3 ft below the water surface 10 min after stopping overflow

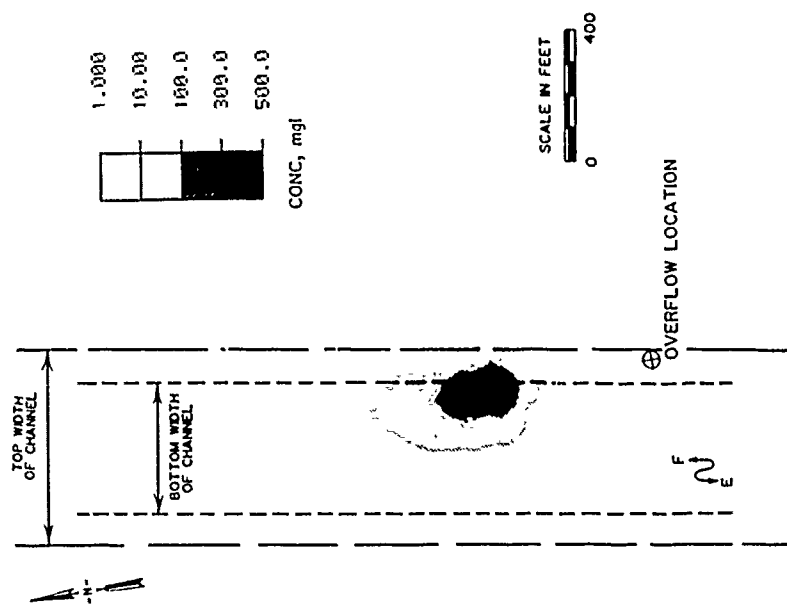


Figure 85. Computed suspended sediment concentrations in Test 1 at 10 ft below the water surface 10 min after stopping overflow

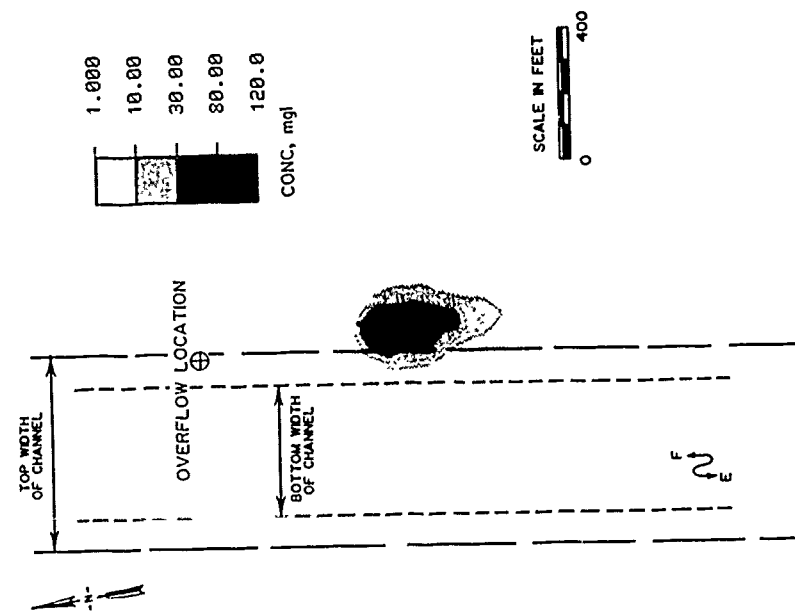


Figure 86. Computed suspended sediment concentrations in Test 2 at 3 ft below the water surface 10 min after stopping the overflow

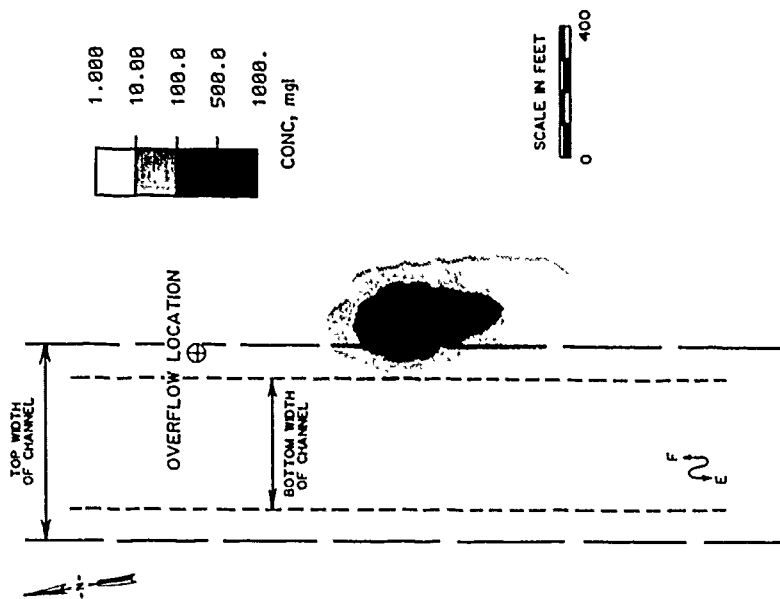


Figure 87. Computed suspended sediment concentrations in Test 2 at 10 ft below the water surface 10 min after stopping the overflow

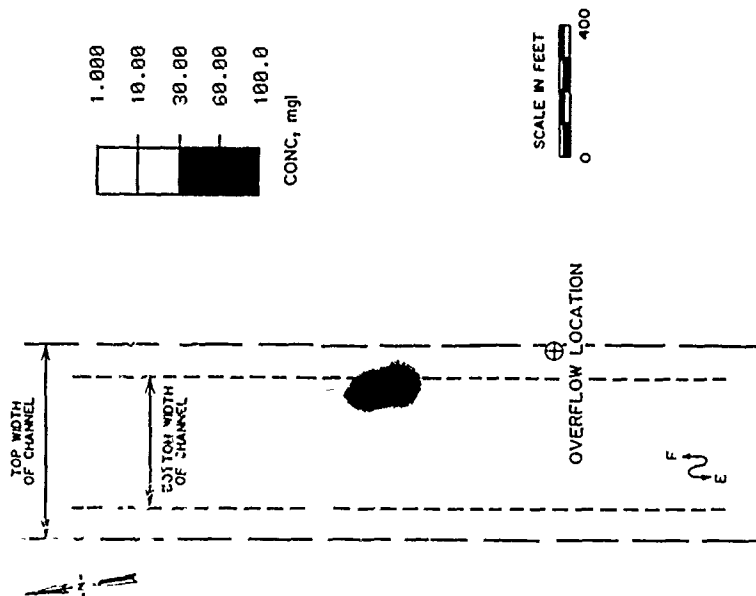


Figure 88. Computed suspended sediment concentrations in Test 3 at 3 ft below the water surface 10 min after stopping overflow



Figure 89. Computed suspended sediment concentrations in Test 3 at 10 ft below the water surface 10 min after stopping overflow



Figure 90. Computed suspended sediment concentrations in Test 4 at 3 ft below the water surface 10 min after stopping overflow

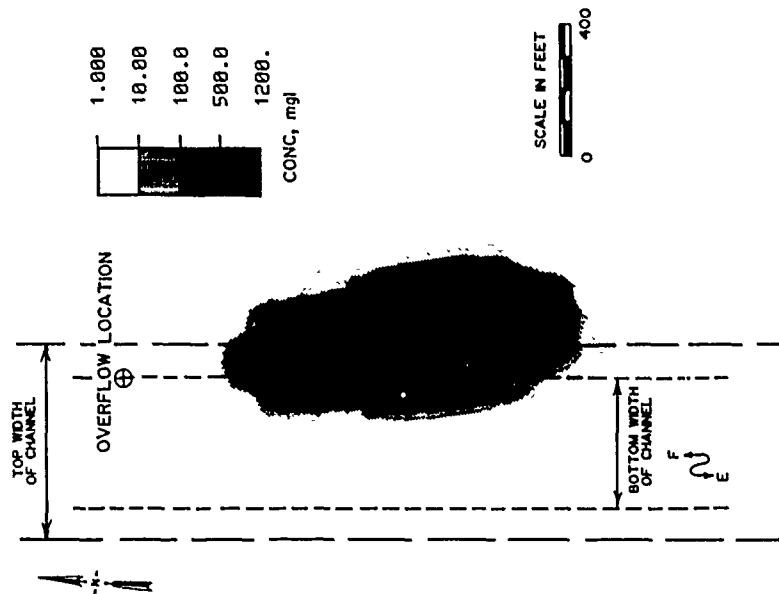


Figure 91. Computed suspended sediment concentrations in Test 4 at 10 ft below the water surface 10 min after stopping overflow

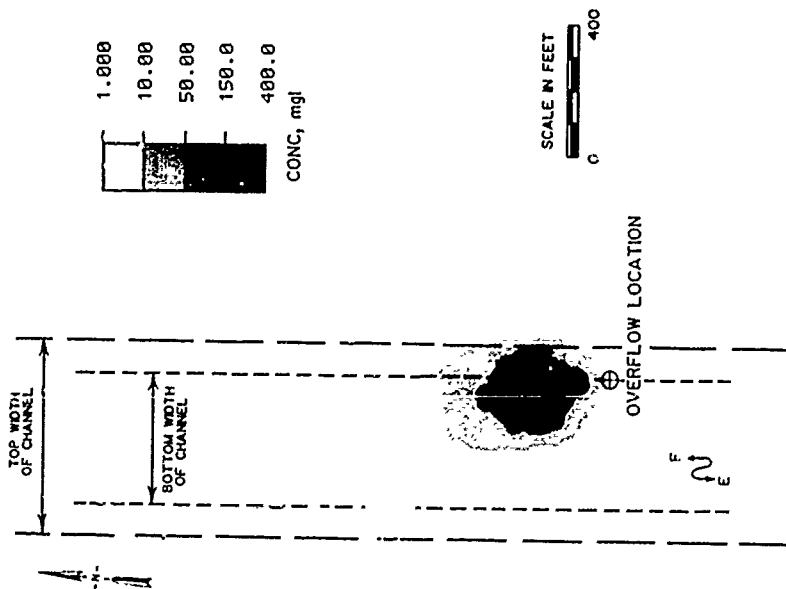


Figure 92. Computed suspended sediment concentrations in Test 5 at 3 ft below the water surface 10 min after stopping overflow

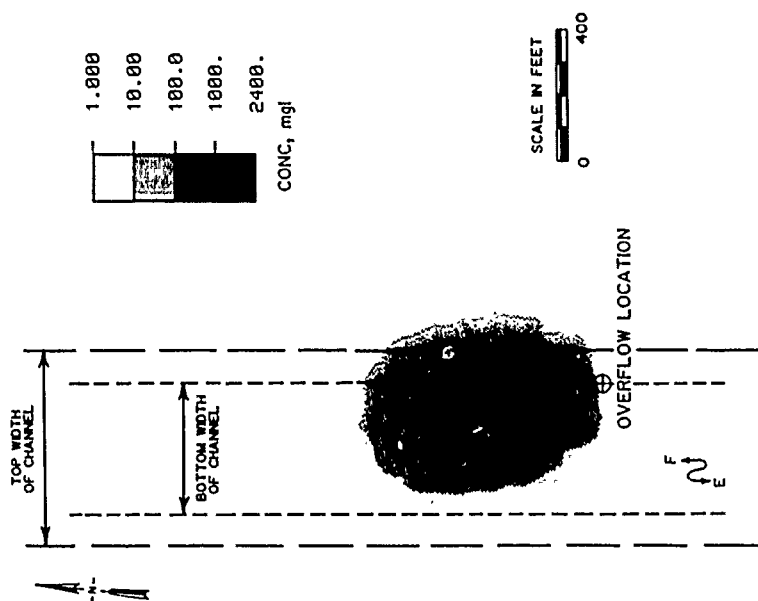


Figure 93. Computed suspended sediment concentrations in Test 5 at 10 ft below the water surface 10 min after stopping overflow

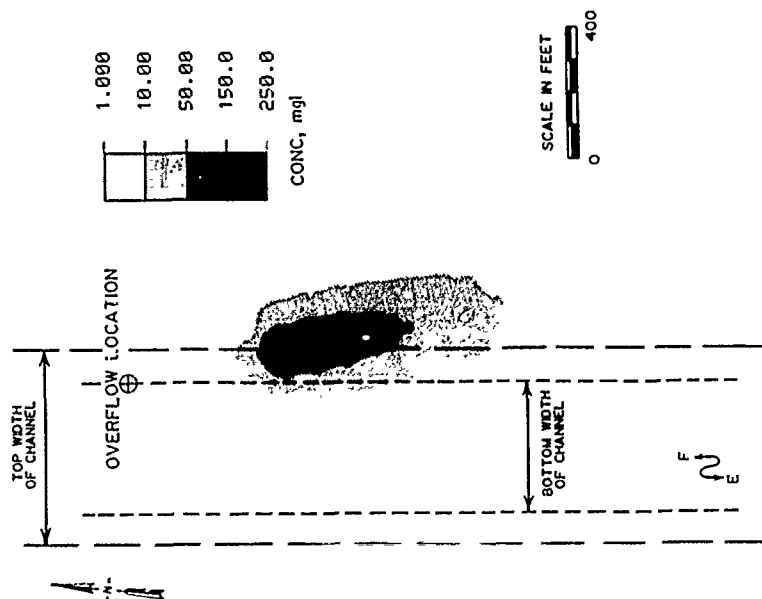


Figure 94. Computed suspended sediment concentrations in Test 6 at 3 ft below the water surface 10 min after stopping overflow

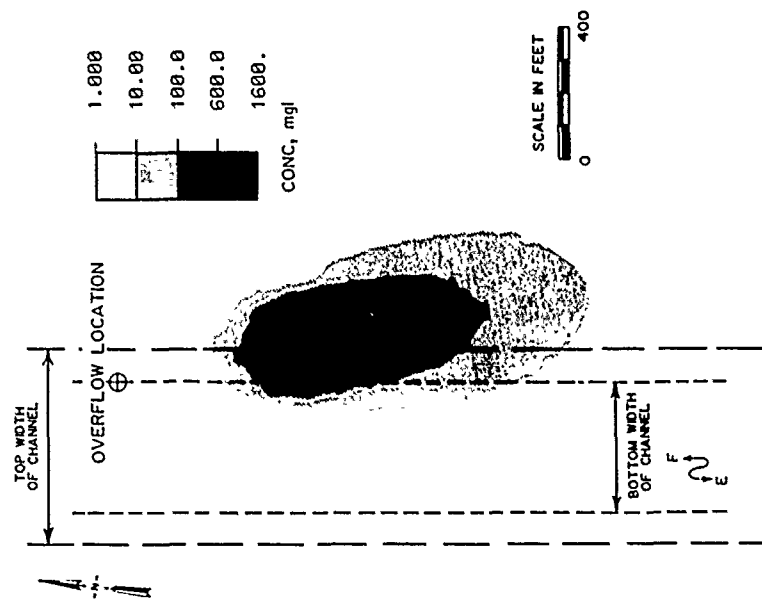


Figure 95. Computed suspended sediment concentrations in Test 6 at 10 ft below the water surface 10 min after stopping overflow

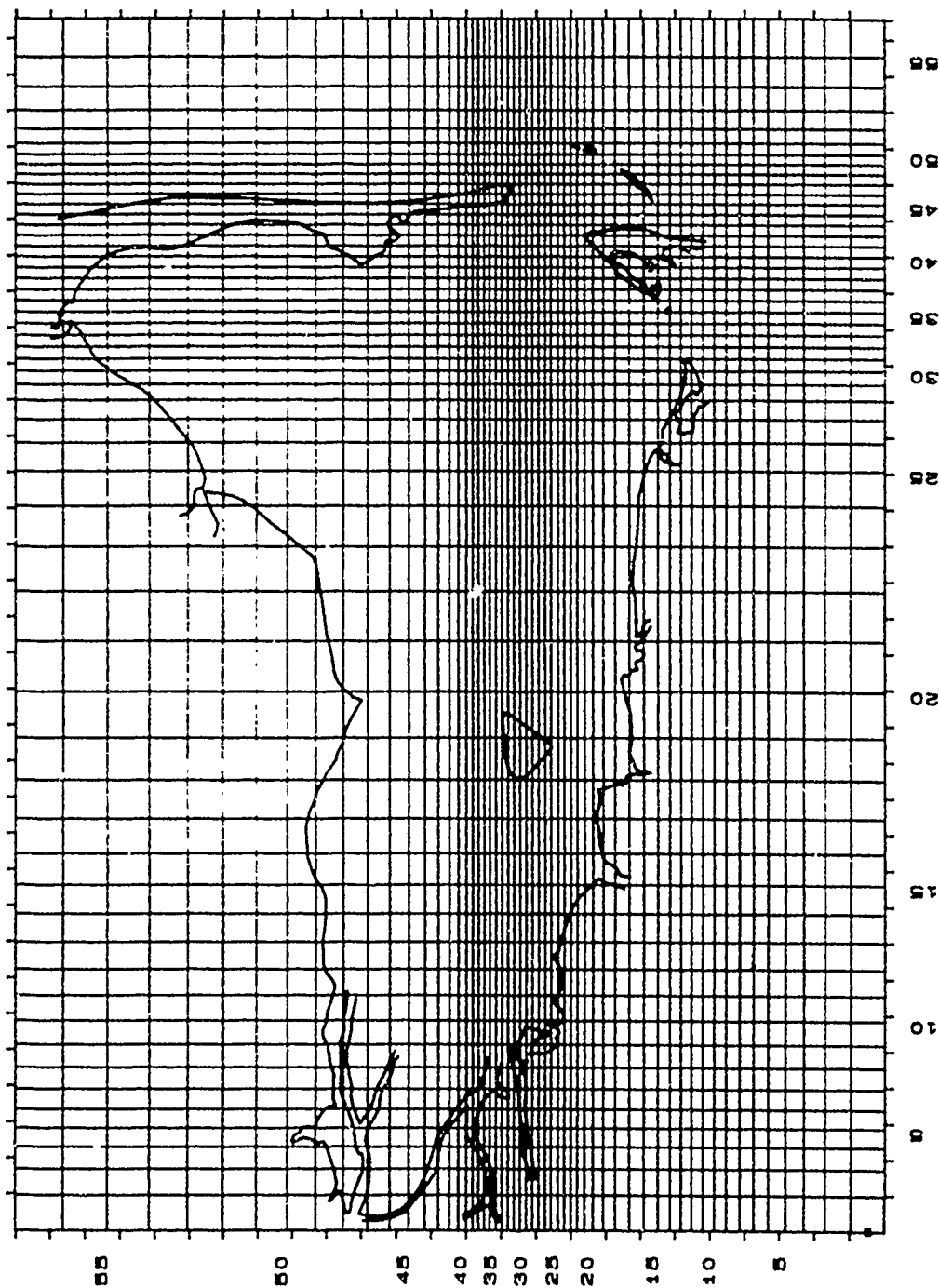
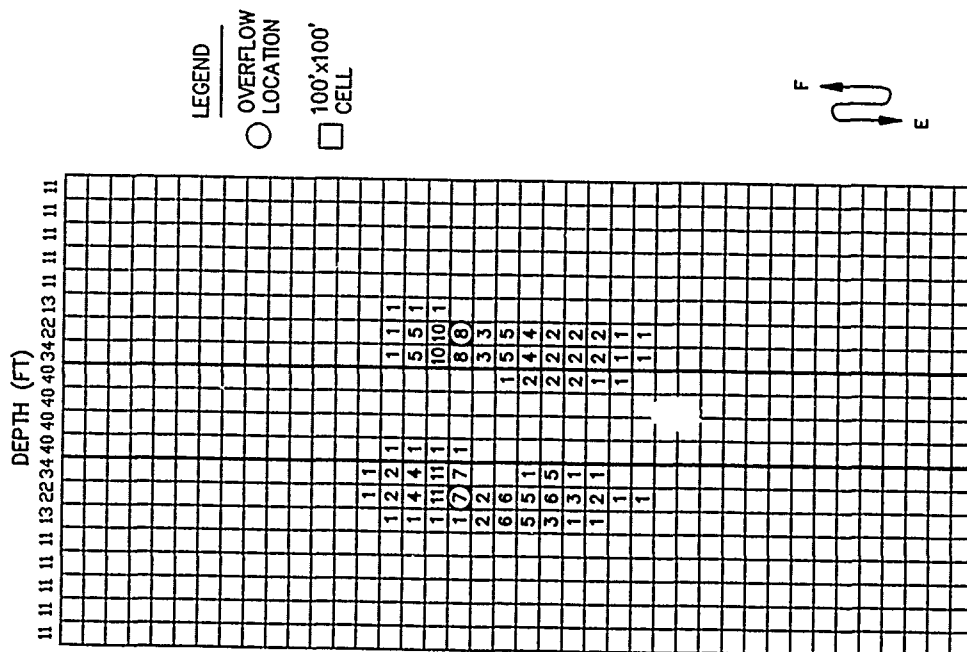
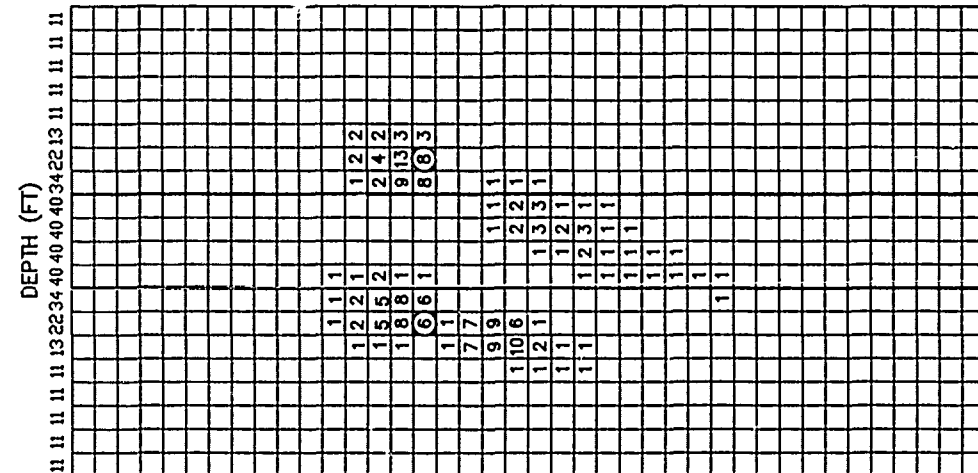


Figure 96. Finite difference grid used in Mobile Bay hydrodynamic model



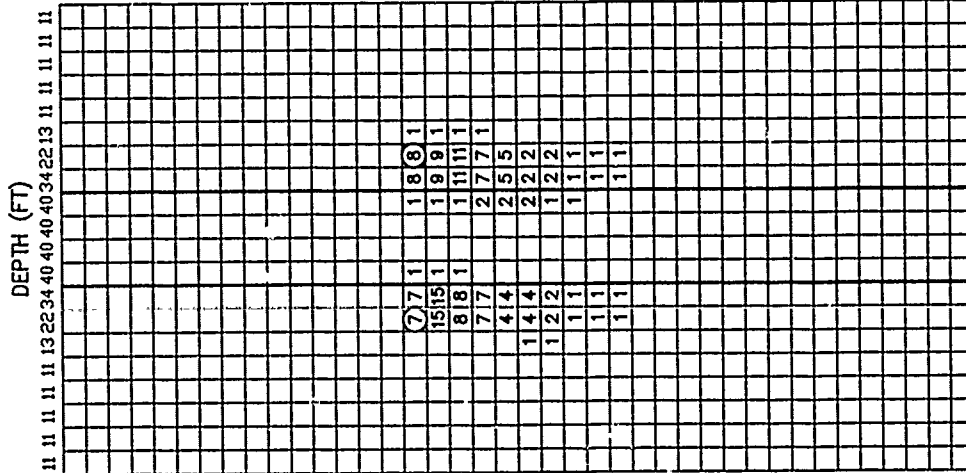


Figure 99. Computed depositional thickness (in centimeters) for overflow of maintenance material dredged in May

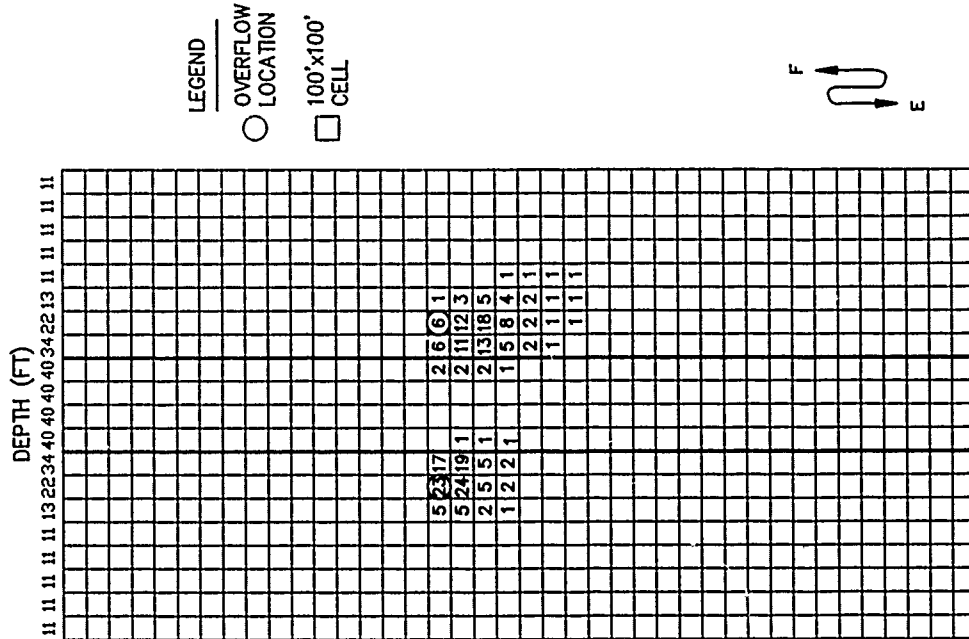


Figure 100. Computed depositional thickness (in centimeters) for overflow of maintenance material dredged in June

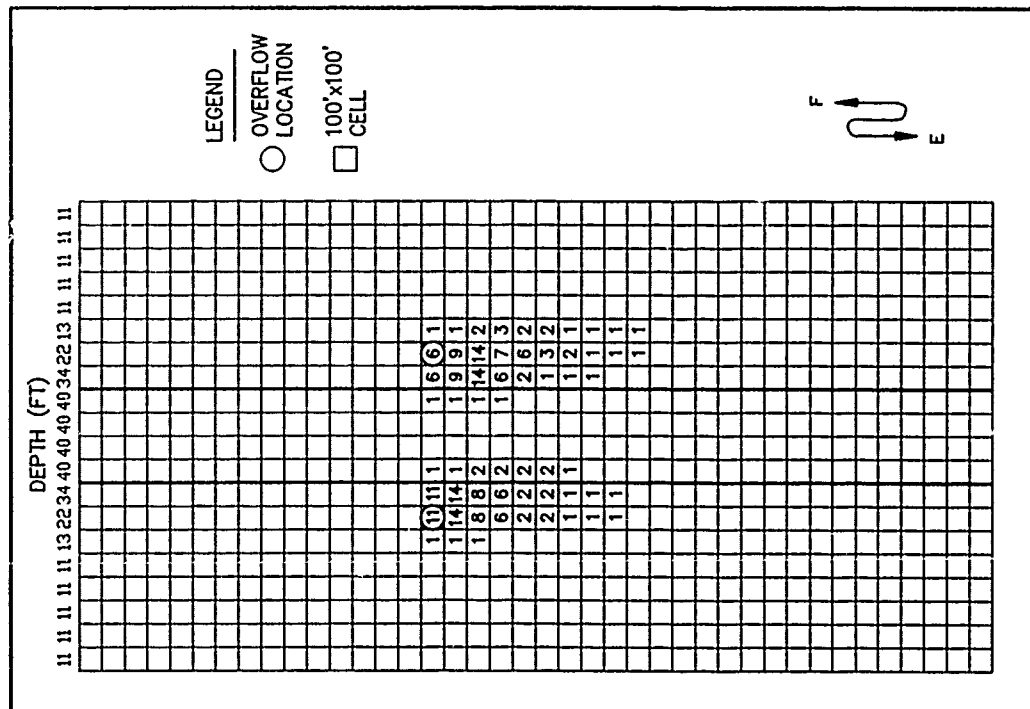


Figure 101. Computed depositional thickness (in centimeters) for overflow of maintenance material dredged in July

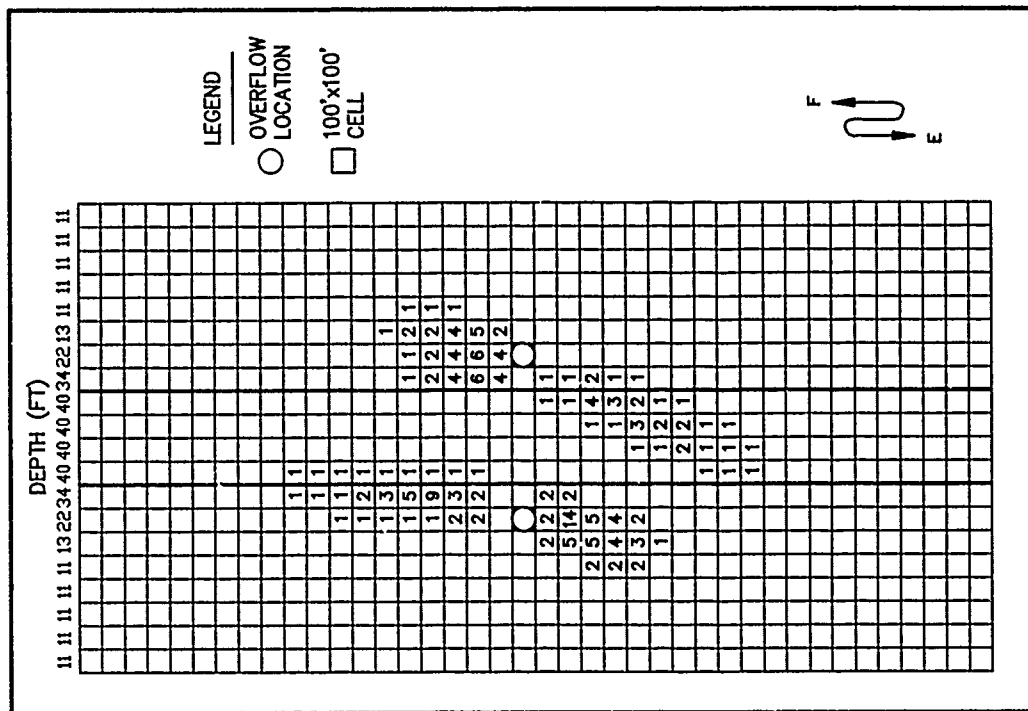


Figure 102. Computed depositional thickness (in centimeters) for overflow of maintenance material dredged in October

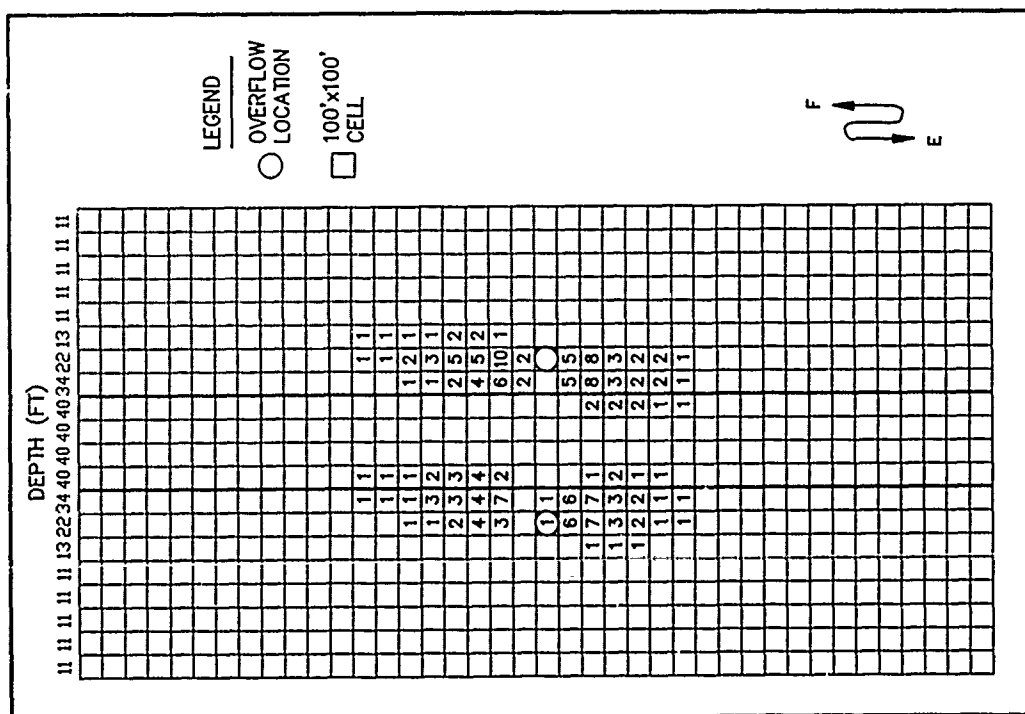


Figure 103. Computed depositional thickness (in centimeters) for overflow of maintenance material dredged in November

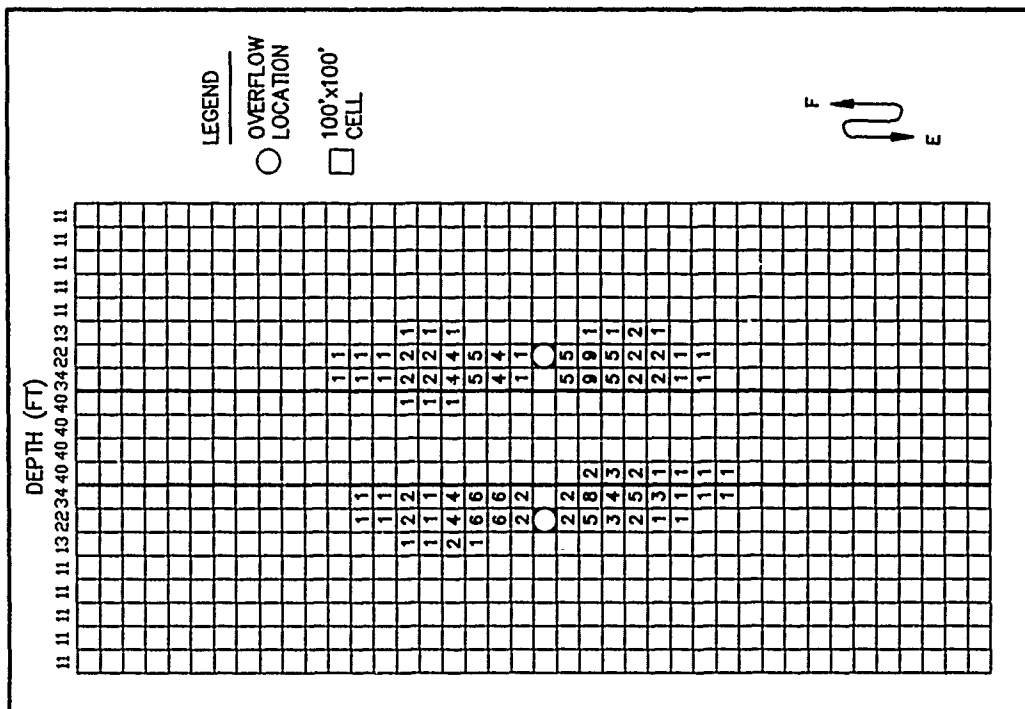


Figure 104. Computed depositional thickness (in centimeters) for overflow of maintenance material dredged in December

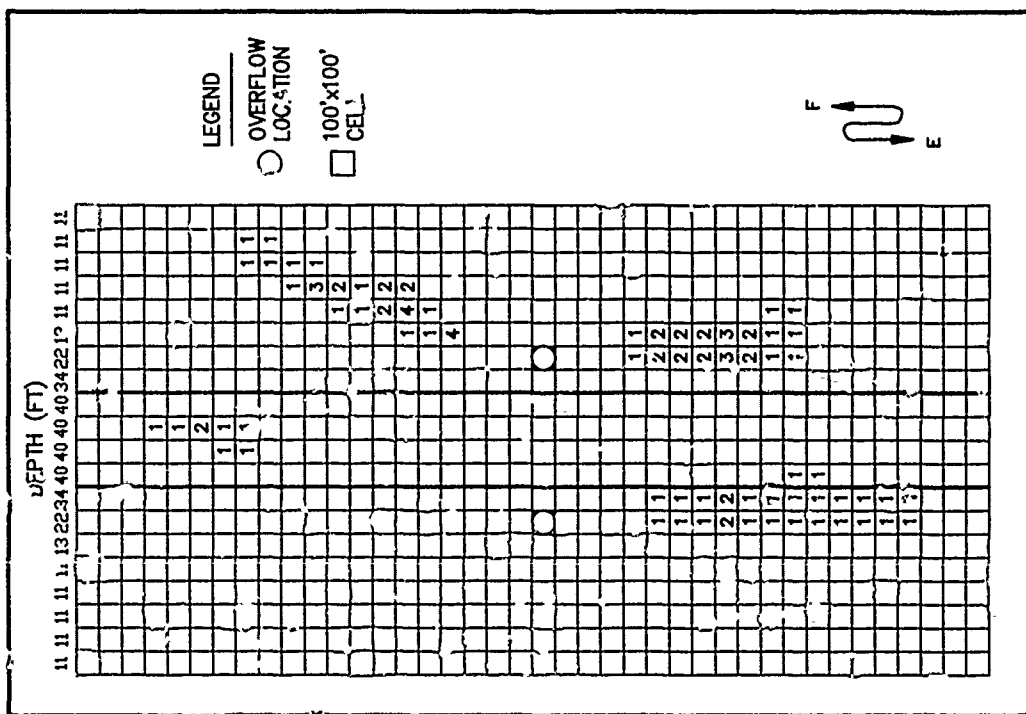


Figure 107. Computed depositional thickness (in centimeters) for overflow of new work material dredged in November 1987

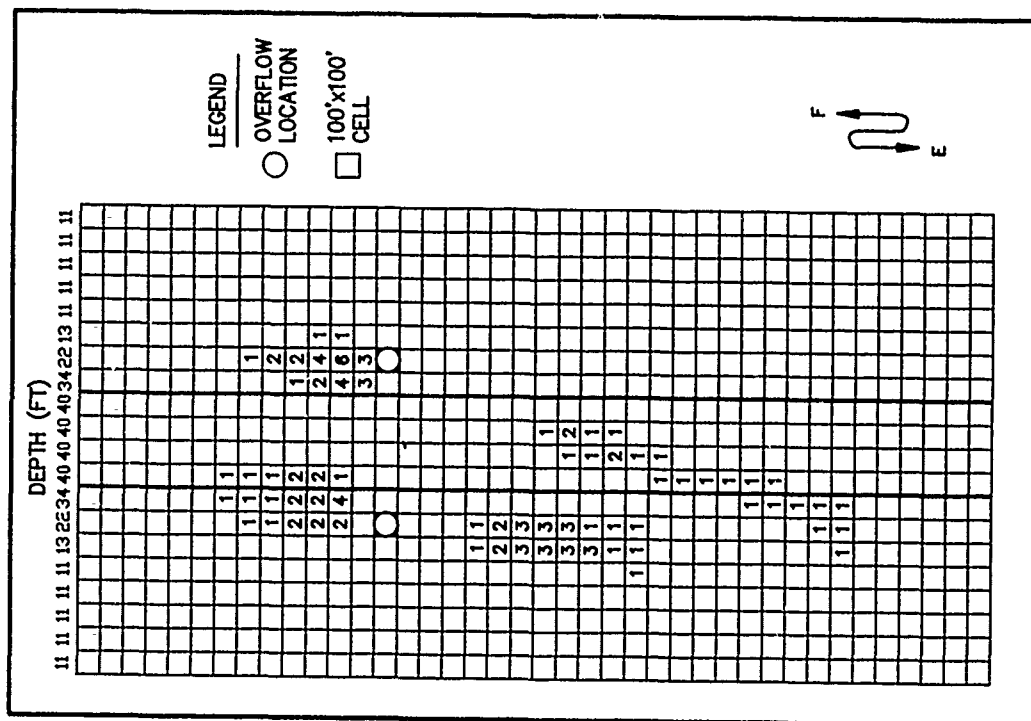


Figure 108. Computed depositional thickness (in centimeters) for overflow of new work material dredged in April 1988

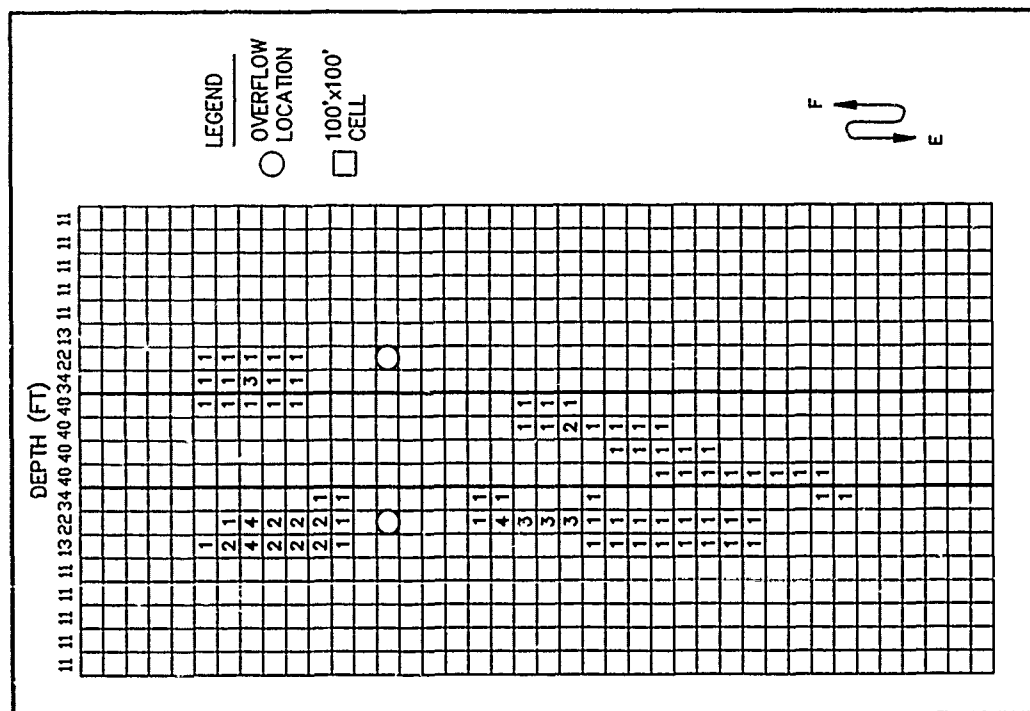


Figure 109. Computed depositional thickness (in centimeters) for overflow of new work material dredged in May 1988

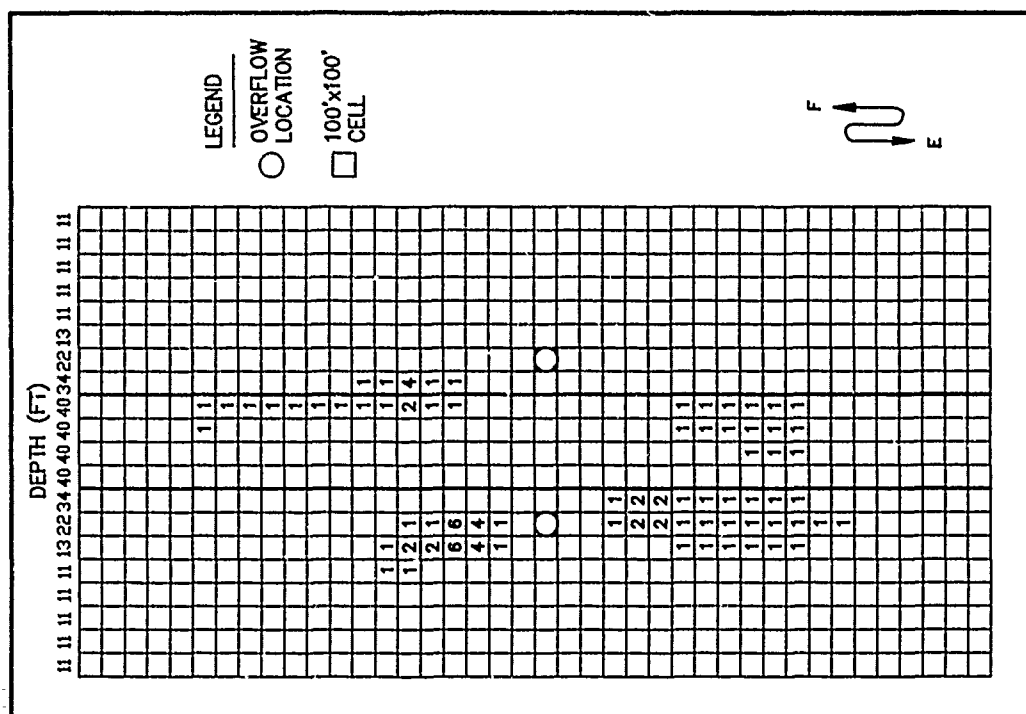


Figure 110. Computed depositional thickness (in centimeters) for overflow of new work material dredged in June 1988

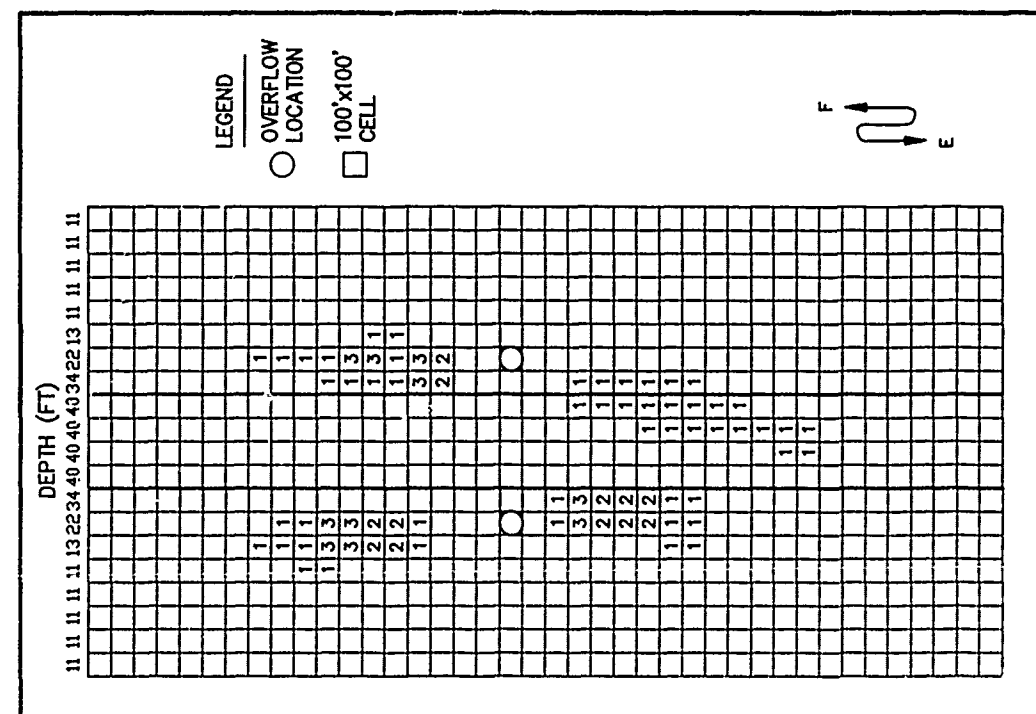


Figure 111. Computed depositional thickness (in centimeters) for overflow of new work material dredged in July 1988

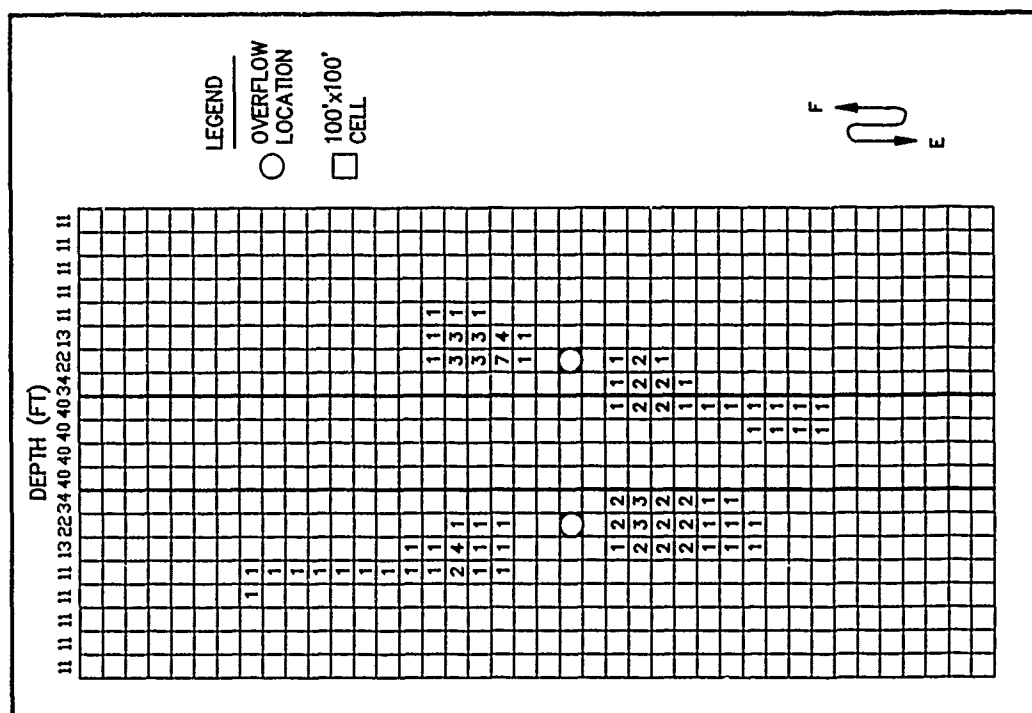
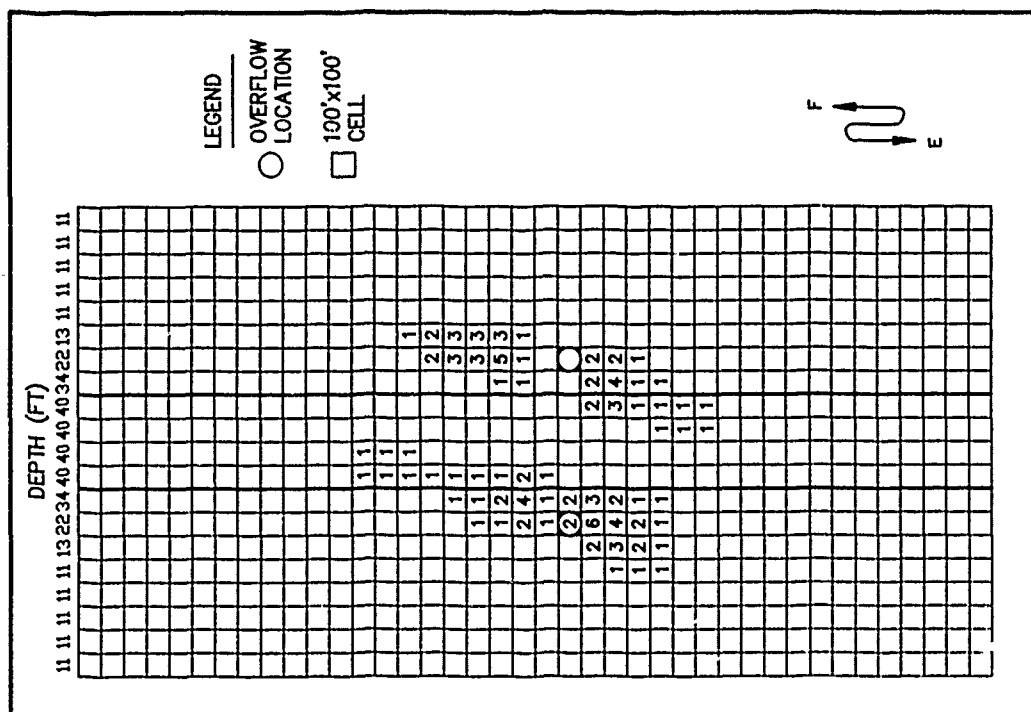
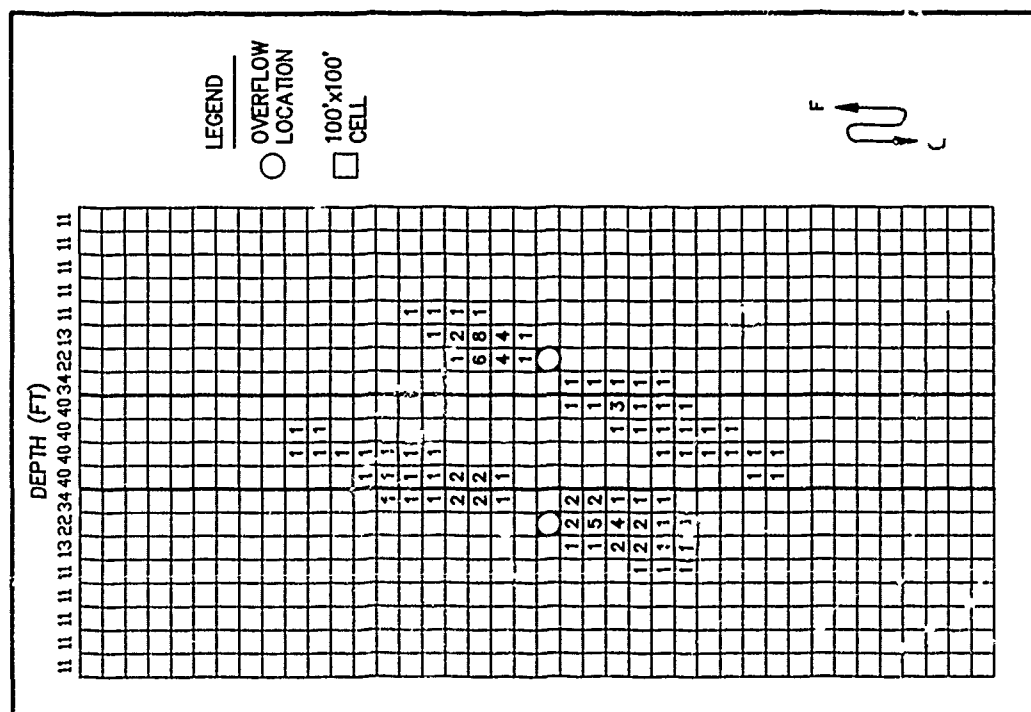


Figure 112. Computed depositional thickness (in centimeters) for overflow of new work material dredged in August 1988



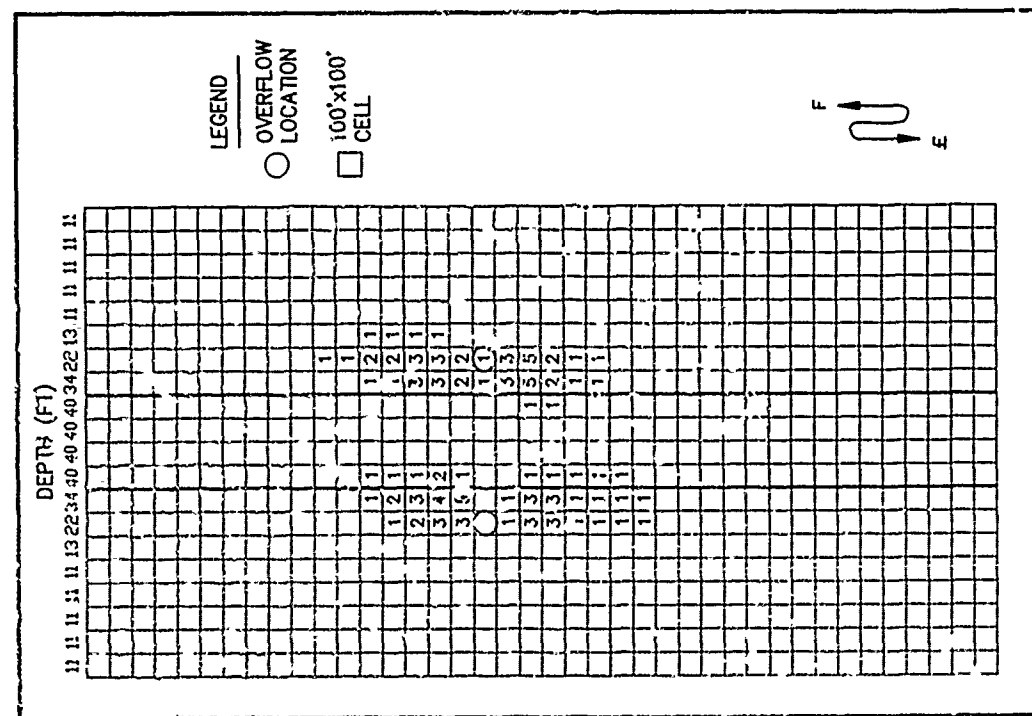


Figure 115. Computed depositional thickness (in centimeters) for overflow of new work material dredged in November 1988

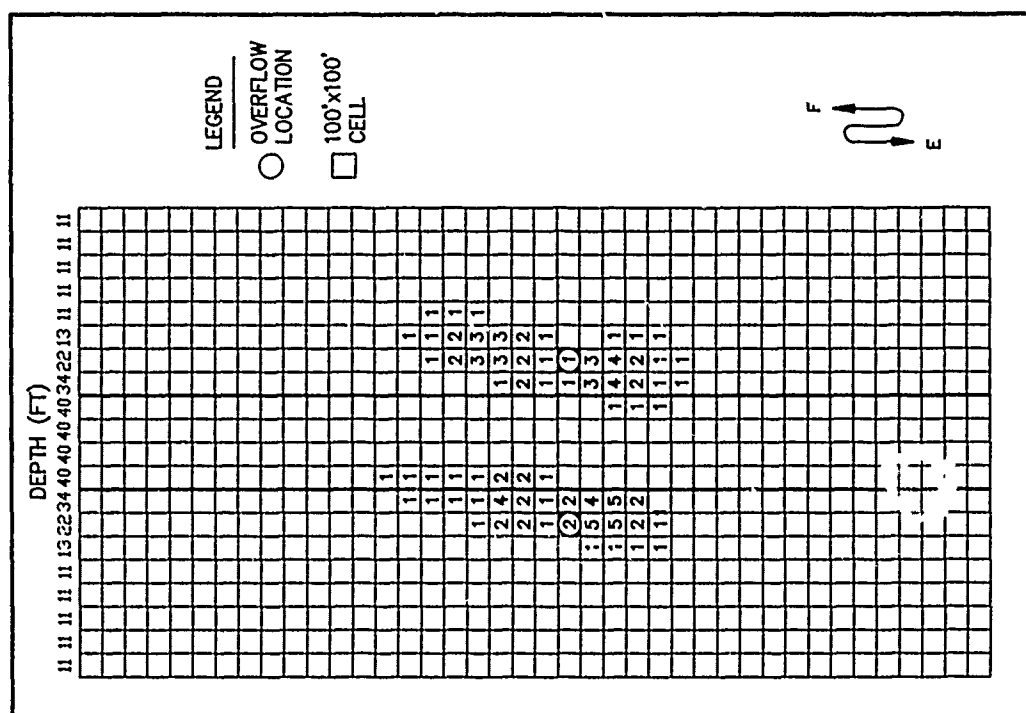
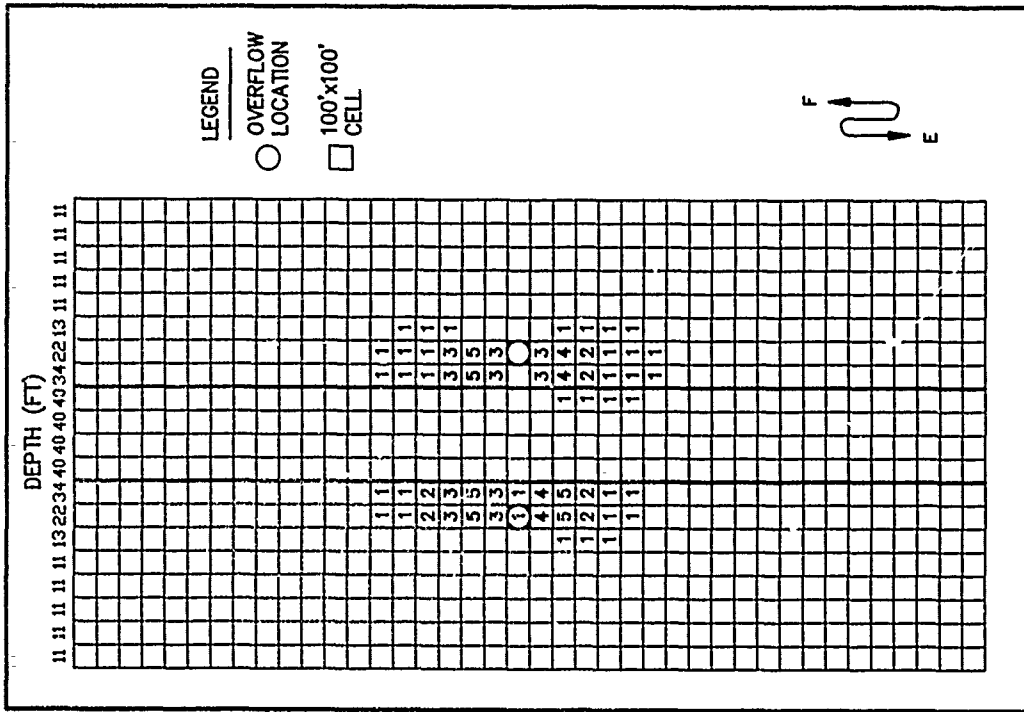
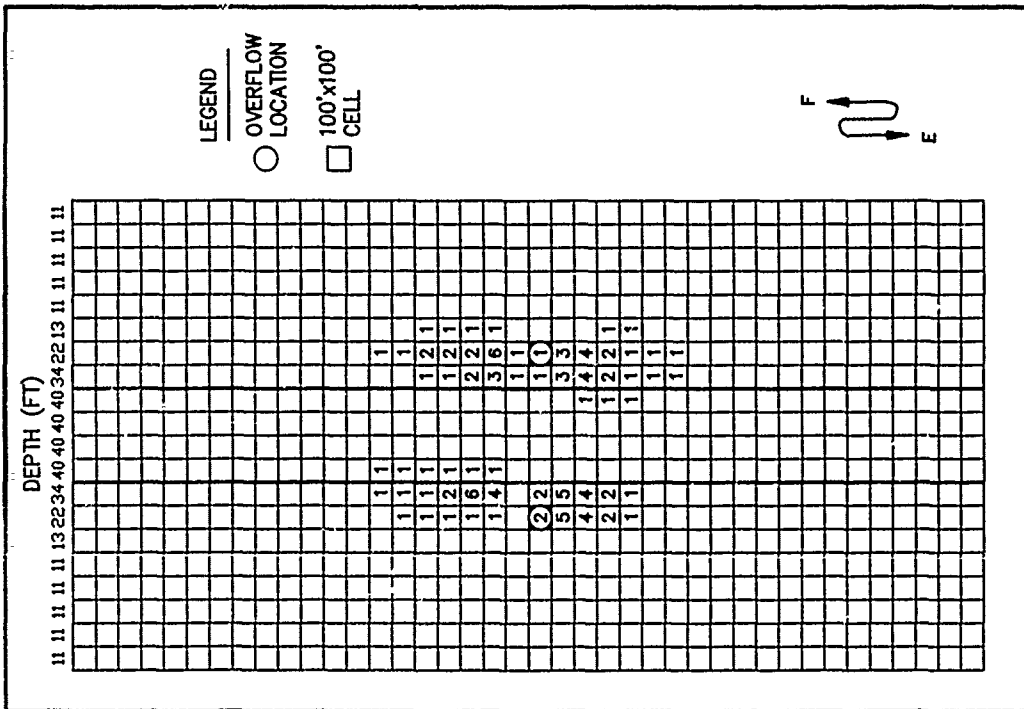


Figure 116. Computed depositional thickness (in centimeters) for overflow of new work material dredged in December 1988



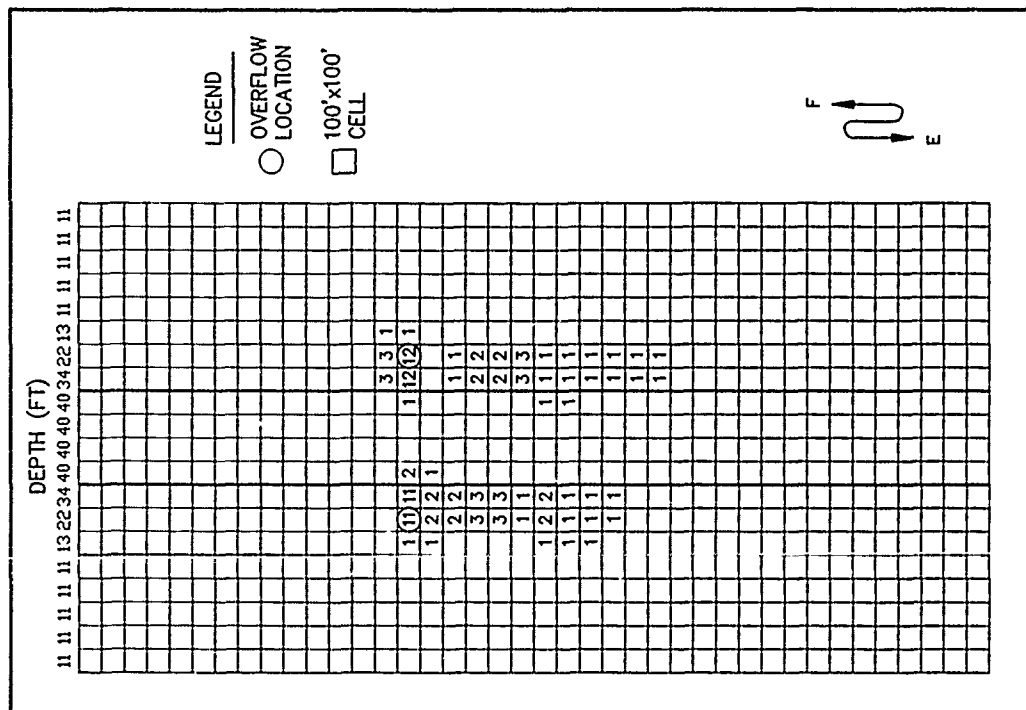


Figure 119. Computed depositional thickness (in centimeters) for overflow of new work material dredged in March 1989

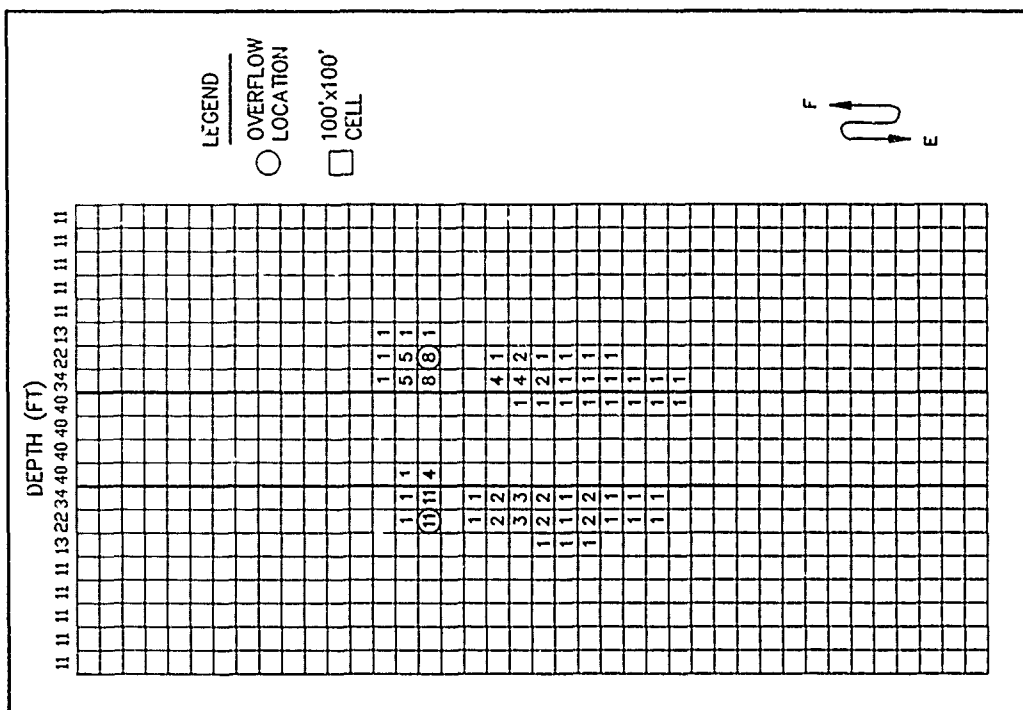
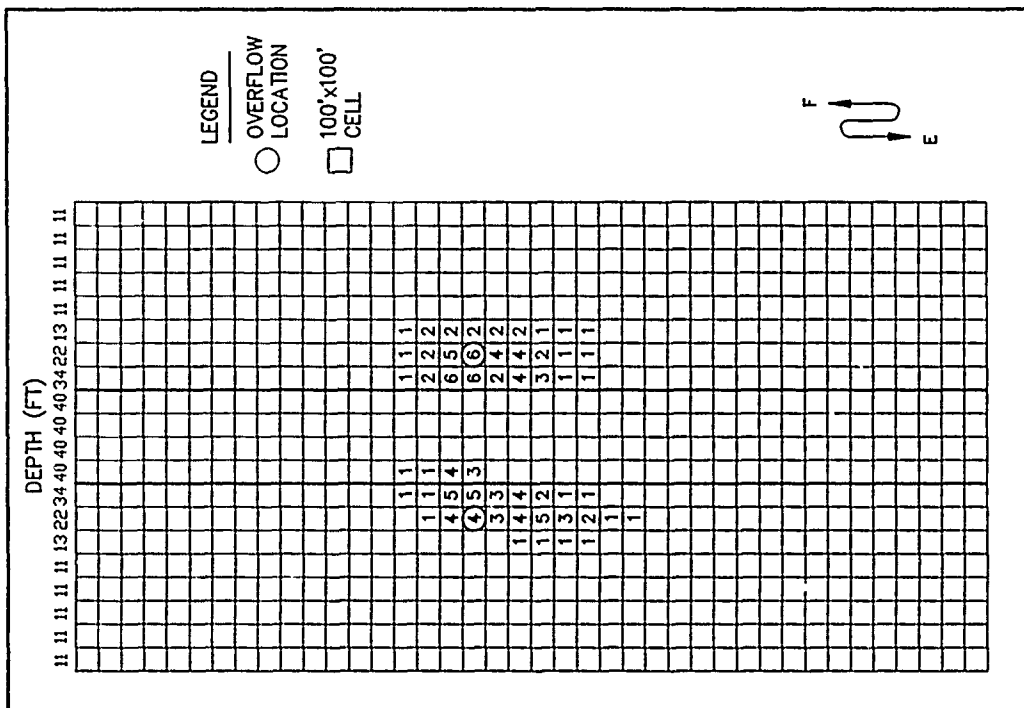
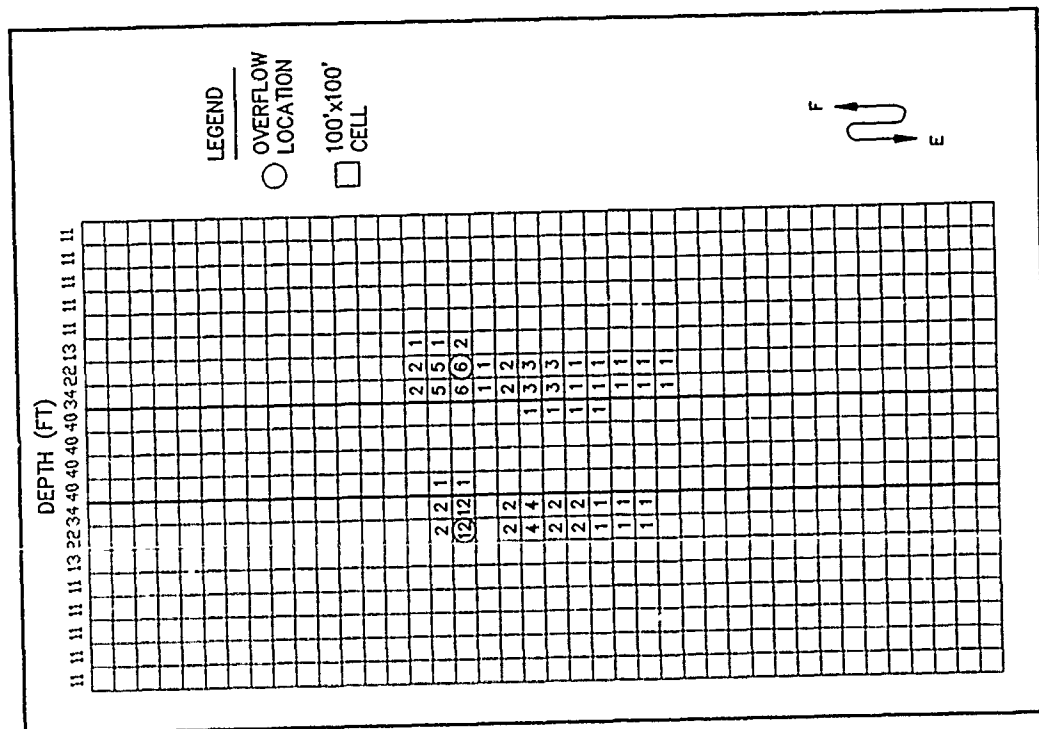


Figure 120. Computed depositional thickness (in centimeters) for overflow of new work material dredged in April 1989



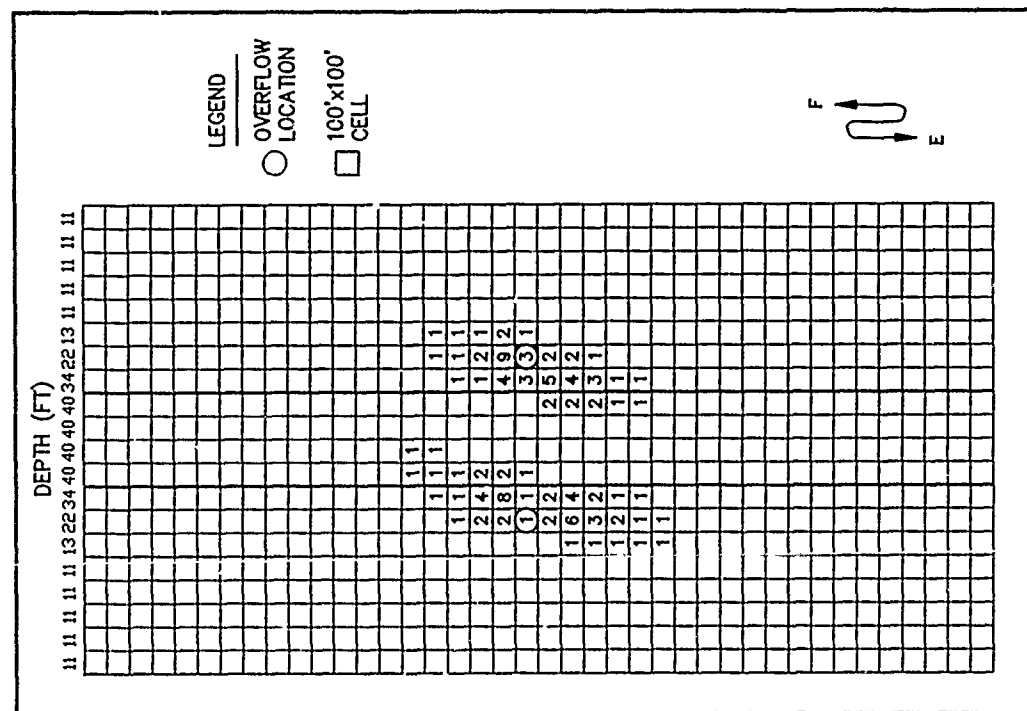


Figure 123. Computed depositional thickness (in centimeters) for overflow of new work material dredged in July 1989

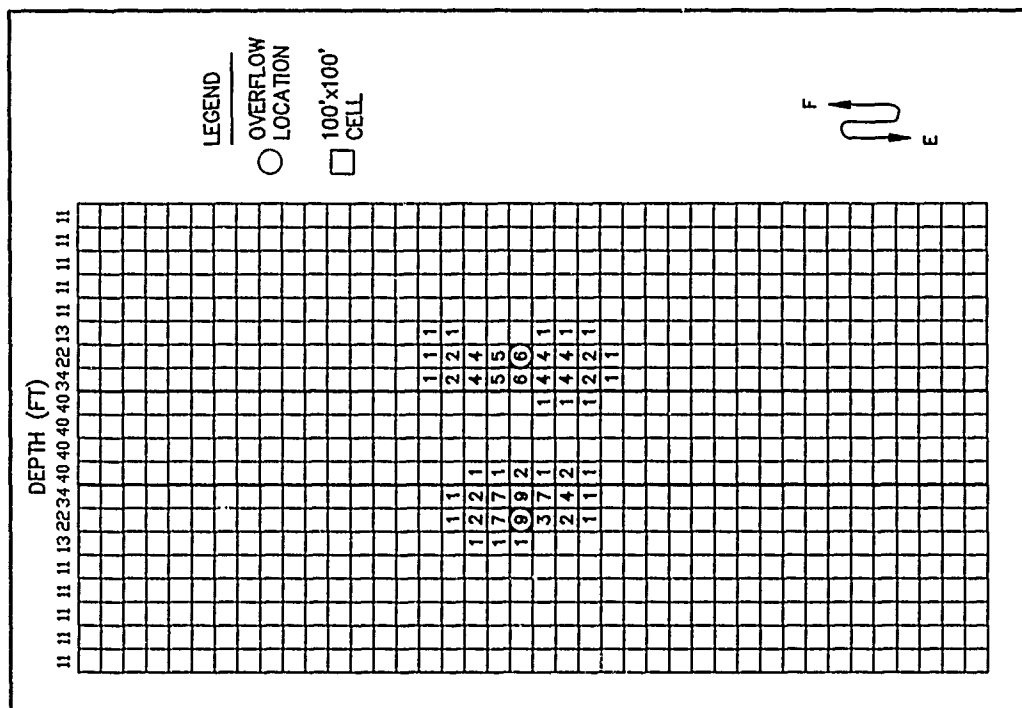
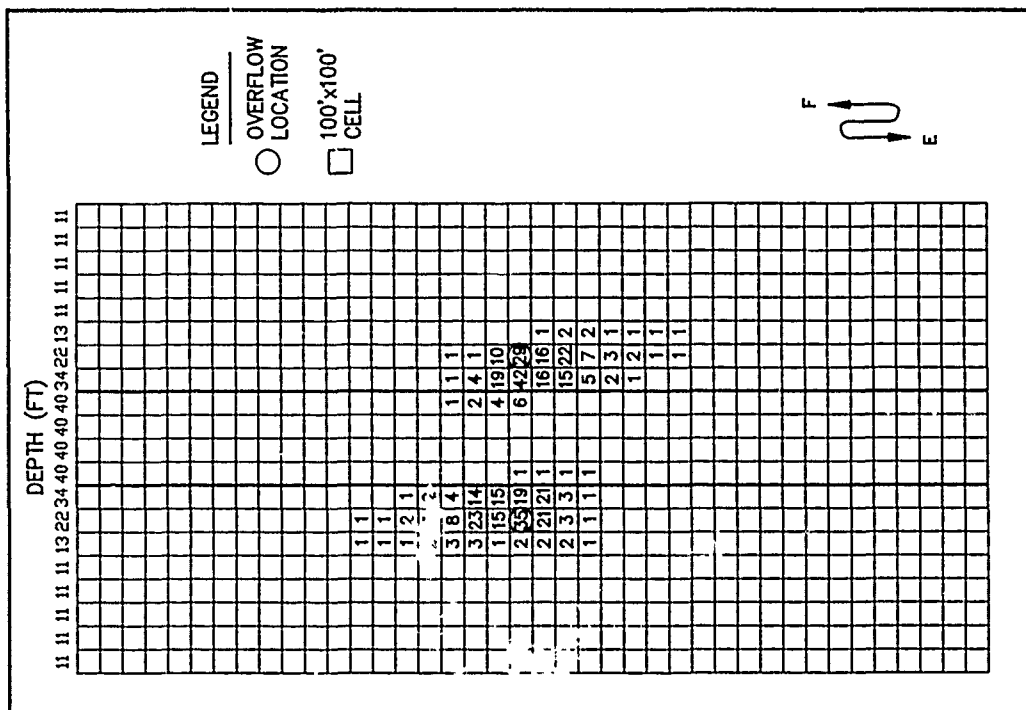
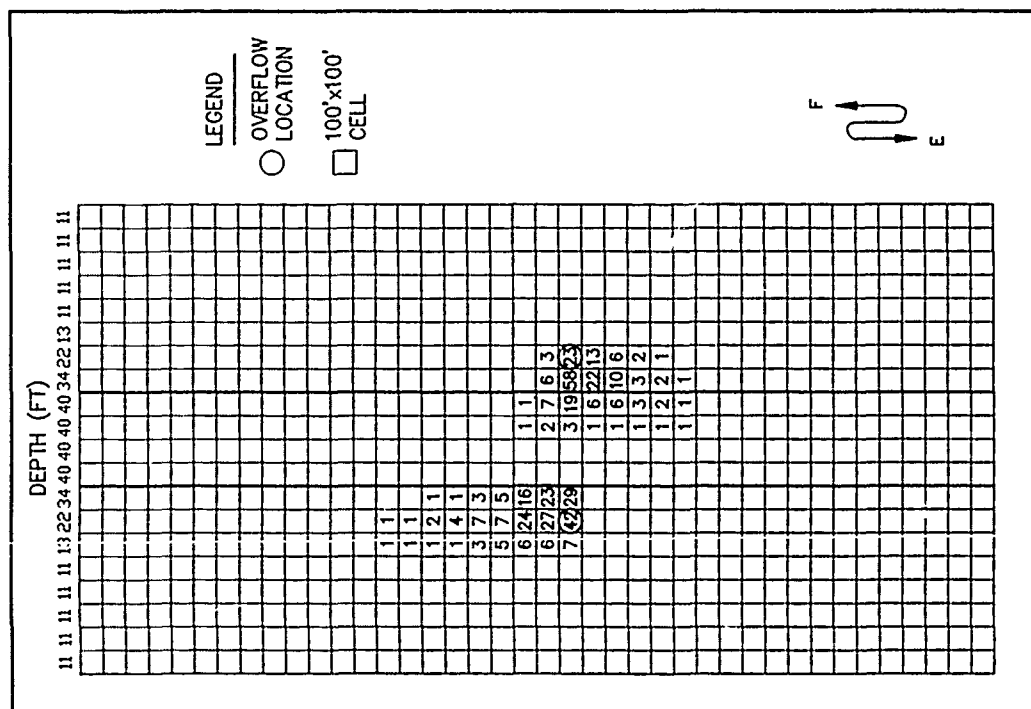
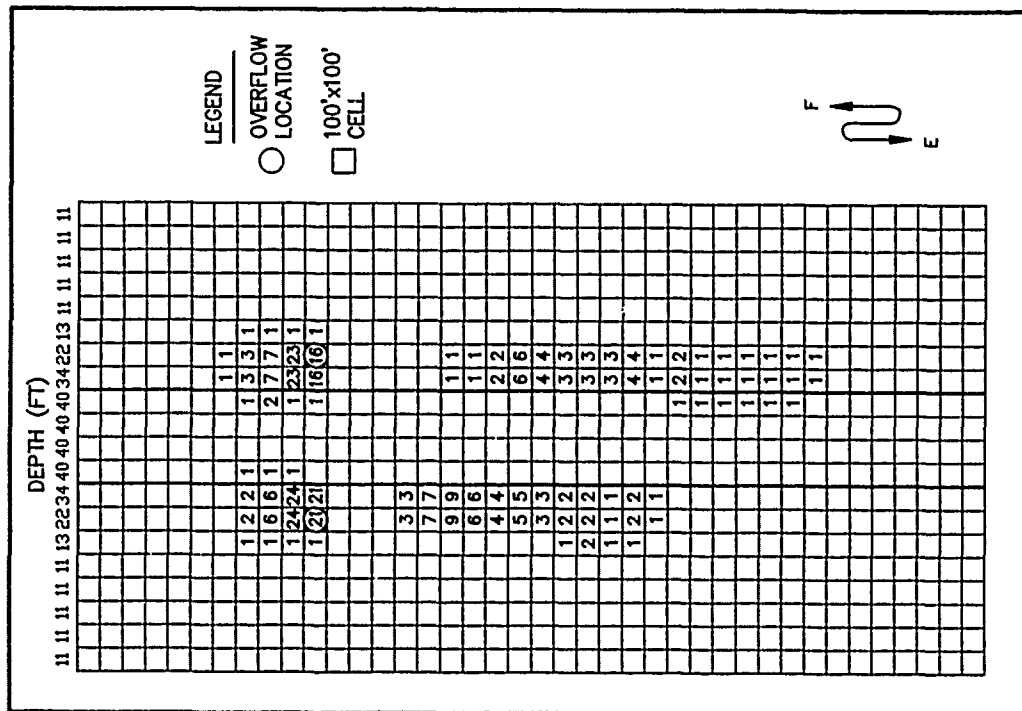
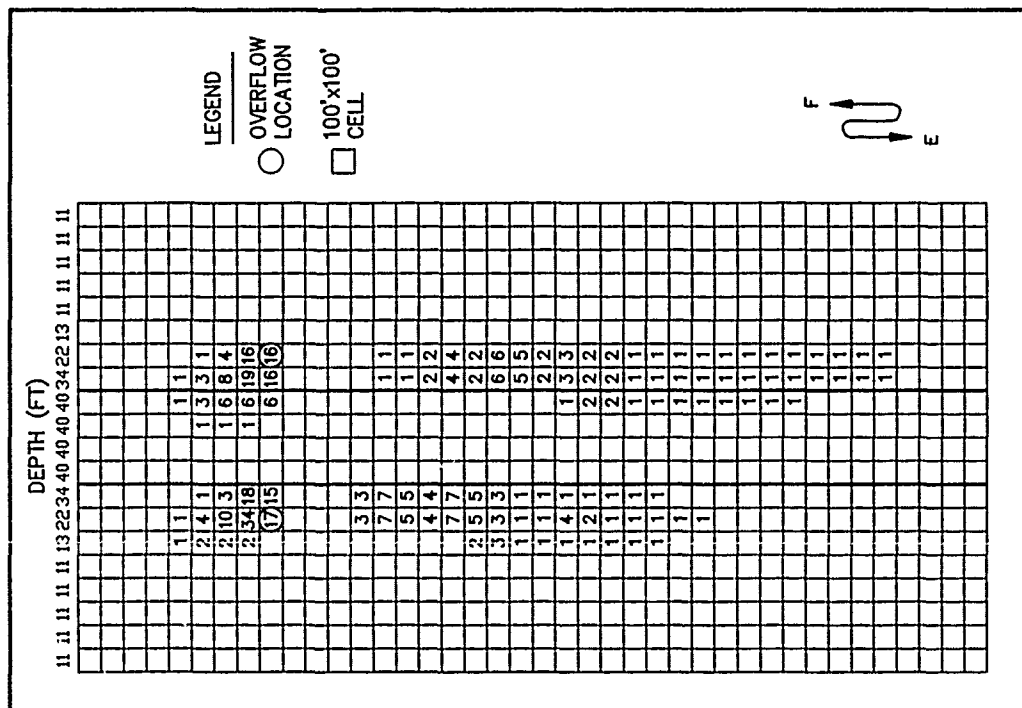


Figure 124. Computed depositional thickness (in centimeters) for overflow of new work material dredged in August 1989





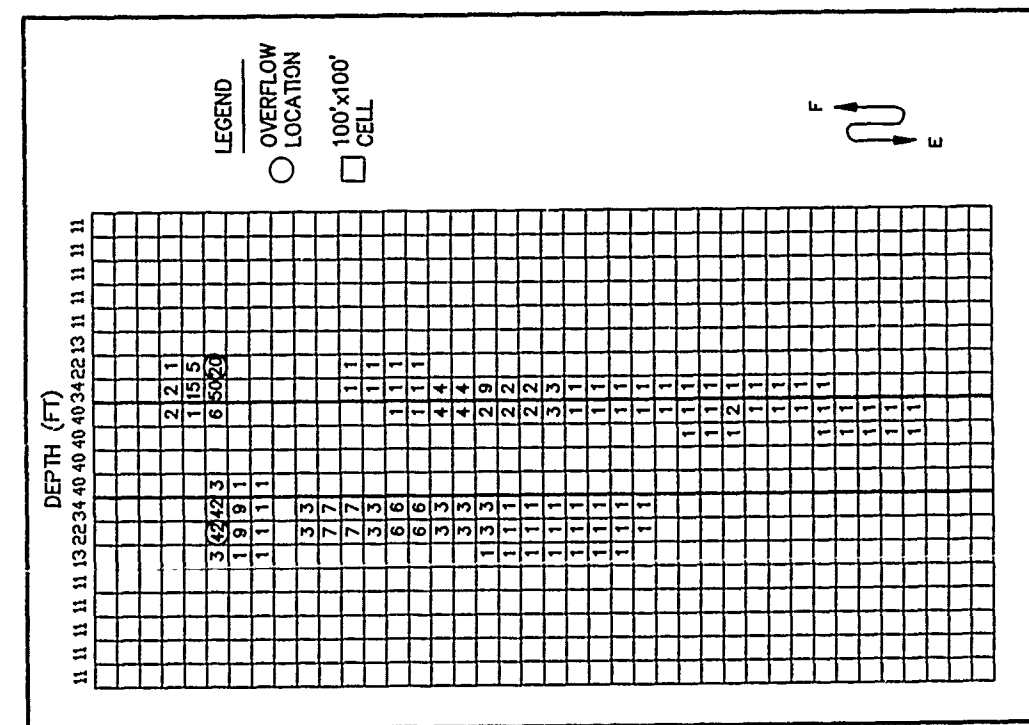


Figure 131. Computed depositional thickness (in centimeters) for overflow of new work material dredged in March 1990

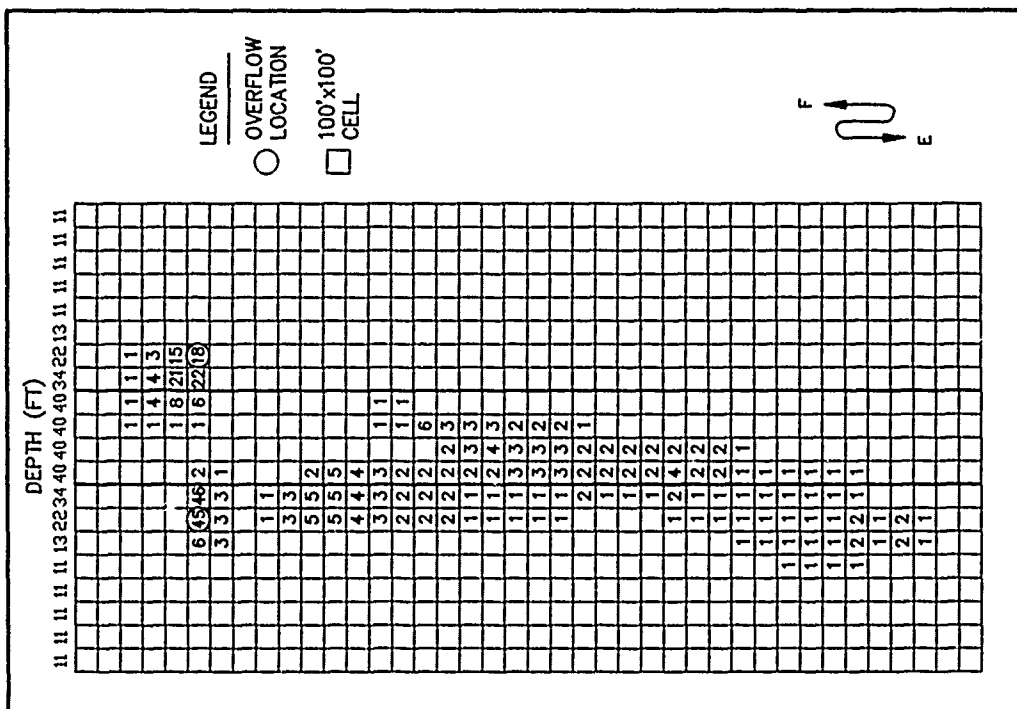


Figure 132. Computed depositional thickness (in centimeters) for overflow of new work material dredged in April 1990

PART VIII: SEDIMENT-PROFILING SURVEY*

As part of the overflow monitoring program, Science Applications International Corporation (SAIC) performed predisposal and postdisposal sediment-profile surveys at the two overflow test sites. The main objective of this aspect of the monitoring was to map the distribution of deposited sediments around the overflow sites. These data provide ground-truth information for the hydrodynamic numerical model predictions of the fate of overflow sediments. Sediment-profiling imagery also provides information on the physical, chemical, and biological conditions at each site and allows comparisons to be made of predisposal and postdisposal benthic characteristics.

Methodology

Because sediment-profiling imagery is unfamiliar to many resource managers, a brief description of the methodology for data acquisition, analysis techniques, and interpretive rationale is given. Field operations were conducted in Mobile Bay from the vessel SAMMY & ELAINE on November 2 and on December 2, 5, and 11, 1987. Ninety stations were occupied: 10 stations for each of three baseline surveys (this includes an initial November effort which was aborted due to a scheduling problem with the dredging contract, and lower and upper bay sites), and 30 stations for the postdisposal surveys at each site. For each survey, sampling grids were established to ensure effective coverage of potentially affected areas. Two replicate sediment-profile images were obtained at each station.

Navigation

Navigational control of the survey vessel during this project was provided by the SAIC Integrated Navigation System (INS). This system consisted of a Northstar 800 LORAN-C receiver interfaced to a Compaq Portable II Model II microcomputer. While providing positional control of the survey vessel through steering commands (i.e. range, bearing to target) and a visual plot of the ship's position in relation to the station location relayed to the helmsman through a video display, the system also recorded the ship's position both on paper and magnetic disk at each station sampled. This allowed return to predisposal stations during postdisposal surveys.

* Written by Gene Revelas, Science Applications International, Inc.

LORAN-C was chosen as the positioning system in this project, because it is a totally self-contained, passive system, requires no shoreside personnel to tend transponders, and is thus more cost-effective. The drawback to using LORAN-C is that the system is inherently less accurate in geodetic positioning than other systems. The LORAN-C lines of position that are drawn on most nautical charts are theoretical in nature and are typically calculated by computer. They are corrected for commonly known sources of error, such as overland transmission paths and secondary phase corrections; this results in a positioning system with an accuracy on the order of ± 100 m. While navigating offshore, errors of this magnitude may be acceptable. However, when sampling close inshore at stations located less than 100 to 500 m apart, it is highly desirable to obtain positioning with greater accuracy. Therefore, a calibration procedure was utilized during this project which resulted in a much more accurate LORAN-C receiver at a location whose position was known with a high degree of certainty. With the resulting calibration factors applied to the incoming LORAN-C coordinates, the ship's geodetic position was calculated to an accuracy of ± 50 m in Mobile Bay.

The theoretical LORAN-C coordinates for the FR-6 (Fowl River 6) US Geodetic Survey benchmark were calculated using the SAIC INS software. The geodetic position of this mark was obtained from the WES field representative. The theoretical coordinates were compared to the actual coordinates observed on the LORAN-C receiver when placed at the FR-6 benchmark located adjacent to the Fowl River Marina, and calibration factors for central Mobile Bay were calculated. Because LORAN-C time delays vary temporally, this calibration procedure was performed both on 2 November and 2 December (immediately prior to each survey operation). It is interesting to note that the LORAN-C calibration factors did vary between November and December. On November 2, the Whiskey slave cal-factor was -0.17 μsec and the Yankee slave factor was -0.85 μsec . On December 2, the Whiskey and Yankee cal-factors were -0.27 and -0.93 μsec , respectively.

Sediment-profile images

Sediment-profile images were taken using a Benthos Model 3731 Sediment-Profile Camera (Benthos Inc., North Falmouth, MA; Figure 134). The camera consists of a wedge-shaped prism with a Plexiglas face plate; light is provided by an internal strobe. The back of the prism has a mirror mounted at a 45-deg angle to reflect the profile of the sediment-water interface up to the camera, which is mounted horizontally on the top of the prism. The prism

is filled with distilled water, and because the object to be photographed is directly against the face plate, turbidity of the ambient seawater is never a limiting factor. The camera prism is mounted on an assembly that can be moved up and down by producing tension or slack on the winch wire. As the camera is lowered, tension on the winch wire keeps the prism in the up position. The support frame hits the bottom first, leaving the area to be photographed directly under the prism undisturbed. Once the camera's frame touches the bottom, slack on the winch wire allows the prism to vertically cut the seafloor. The rate of fall of the optical prism into the bottom is controlled by an adjustable "passive" hydraulic piston. This allows the optical prism to enter the bottom at approximately 6 cm/sec. This slow bottom fall rate ensures that the descending prism does not impact the bottom at a high rate and therefore minimizes disturbance of the sediment-water interface. The bottom edge of the optical prism (shaped like an inverted periscope) consists of a blade that cuts a vertical profile of the bottom. The prism is driven several centimeters into the seafloor by the weight of the assembly. The camera trigger is tripped on impact with the bottom, activating a 13-sec time delay on the shutter release; this gives the prism a chance to obtain maximum penetration before a photo is taken. As the camera is raised to a height of about 10 ft from the bottom, a wiper blade automatically cleans off any sediment adhering to the prism faceplate; the film is automatically advanced by a motor drive, the strobes are recharged, and the camera can be lowered for another replicate image.

When the camera is brought to the surface, prism penetration is estimated from a penetration indicator that measures the distance the prism falls relative to the camera base. If penetration is inadequate, two weight packs, each capable of holding 125 lb of lead (in 25-lb increments), can be loaded to give the assembly increased penetration (e.g., for work in sandy or high-shear strength, compacted sediments). If penetration appears too great, adjustable stops, which control the distance the prism can descend, can be lowered, and "mud" doors can be attached to each side of the frame to increase the bearing surface of the entire unit. For this project, no weights were required to obtain adequate penetration, and the adjustable stops were placed at 12 in.

Data analysis

Sediment-profile measurements of all physical parameters and some biological parameters are measured directly from either black-and-white or color film negatives using a video digitizer and computer image analysis

system. For this project, black-and-white film (Panatomic-X) was used for several stations during each predisposal survey to allow same-day processing and "quick-look" assessment of environmental gradients. For postdisposal surveys, color film (Kodachrome-64) was used to maximize detection of potentially extremely thin layers of overflow dredged material.

Negatives or slides are used for analysis instead of positive prints in order to avoid changes in image density that can accompany the printing of a positive image. The image analysis system can discriminate up to 256 different gray scales, so subtle features can accurately be digitized and measured. Proprietary SAIC software allows the measurement and storage of data on 21 different variables for each sediment-profile image obtained (Figure 135). Before all measurements from each image are stored on disk, a summary display is made on the screen so the operator can verify if the values stored in memory for each variable are within expected range; if anomalous values are detected, software options allow remeasurement before storage on disk. All computer data disks are backed up by redundant copies at the end of each analytical day. All data stored on disks are printed out on data sheets for editing by the principal investigator and as a hard-copy backup of the data stored on disk; a separate data sheet is generated for each image (Figure 135). All data sheets are edited and verified by a senior-level scientist before being approved for final data synthesis, statistical analyses, and interpretation. Automatic disk storage of all parameters measured allows data from any variables of interest to be compiled, sorted, displayed graphically, contoured, or compared statistically.

Sediment type determination

The sediment grain-size major mode and range are visually estimated from the photographs by overlaying a grain-size comparator that is at the same scale. This comparator was prepared by photographing a series of Udden-Wentworth size classes (equal to or less than coarse silt up to granule and larger sizes) through the sediment-profile camera. Seven grain-size classes are on this comparator: 4 phi, 4 to 3 phi, 3 to 2 phi, 2 to 1 phi, 1 to 0 phi, 0 to 1 phi, and <-1 phi. The lower limit of optical resolution of the photographic system is about 62 μ , allowing recognition of grain sizes equal to or greater than coarse silt. The accuracy of this method has been documented by comparing image-derived estimates with grain-size statistics determined from laboratory sieve analyses.

Prism penetration depth

The sediment-profile camera prism penetration depth is determined by measuring both the largest and smallest linear distance between the sediment-water interface and the bottom of the film frame. The image analysis software automatically averages these maximum and minimum values to determine the average penetration depth.

Surface boundary roughness

Surface boundary roughness is determined by measuring the vertical distance (parallel to the film border) between the highest and lowest points of the sediment-water interface. In addition, the origin of this small-scale topographic relief is indicated when it is evident (physical or biogenic). In sandy sediments, boundary roughness can be a measure of sand wave height. On silt-clay bottoms, boundary roughness values often reflect biogenic features such as fecal mounds or surface burrows.

Mud clasts

When fine-grained, cohesive sediments are disturbed, either by physical bottom scour or faunal activity (e.g. decapod foraging), intact clumps of sediment are often scattered about the seafloor. These mud clasts can be seen at the sediment-water interface in sediment-profile images. During analysis, the number of clasts is counted, the diameter of a typical clast is measured, and the oxidation state is assessed. Depending on their place of origin and the depth of disturbance of the sediment column, mud clasts can be reduced or oxidized (the oxidation state is apparent from their reflectance value; see redox potential discontinuity (RPD) section below). Also, once at the sediment-water interface, these sediment clumps are subject to bottom-water oxygen levels and bottom currents. Based on laboratory microcosm observations of reduced sediments placed within an aerobic environment, oxidation of reduced surface layers to depths of 1 to 2 mm by diffusion alone is quite rapid, occurring within 6 to 12 hr (Germano 1983). Consequently, the detection of reduced mud clasts in an obviously aerobic setting suggests a recent origin. The size and shape of mud clasts, e.g., angular versus rounded, is also considered. Mud clasts may be moved about and broken by bottom currents and/or animals (macrofauna or meiofauna) (Germano 1983). Over time, large angular clasts become small and rounded. Overall, the abundance, distribution, oxidation state, and appearance of mud clasts are used to make inferences about the recent pattern of seafloor disturbance in an area.

Apparent redox
potential discontinuity depth

Aerobic near-surface marine sediments have a higher reflectance value relative to underlying hypoxic or anoxic sediments. This is readily apparent in sediment-profile images and is due to the fact that oxidized surface sediment contains particles coated with ferric hydroxide (an olive color when associated with particles), while the sulphidic sediments below this oxygenated layer are grey to black. The boundary between the colored ferric hydroxide surface sediment and underlying grey to black sediment is called the apparent redox potential discontinuity.

The depth of the apparent RPD in the sediment column is an important time-integrator of dissolved oxygen conditions within sediment pore waters. In the absence of bioturbating organisms, this high-reflectance layer (in muds) will typically be 1 to 3 mm thick (Rhoads 1974). This depth is related to the rate of supply of molecular oxygen (by Fickian diffusion) into the bottom, and the consumption of that oxygen by the sediment and associated microflora. In sediments that have very high sediment oxygen demand (SOD), the sediment may lack a high-reflectance layer even when the overlying water column is aerobic.

In the presence of bioturbating macrofauna, the thickness of the high reflectance layer may be several centimeters thick. The relationship between the thickness of this high-reflectance layer and the presence or absence of free molecular oxygen (poise) in the associated pore waters must be determined with caution. The boundary (or horizon) that separates the positive Eh region of the sediment column from the underlying negative Eh region is called the redox potential discontinuity. The exact location of this $Eh = 0$ potential can be accurately determined only with microelectrodes; hence, the relationship between the change in optical reflectance, as imaged with the sediment-profile camera, and the actual RPD can only be determined by making the appropriate in situ Eh measurements. For this reason, the optical reflectance boundary, as imaged, is described as the "apparent" RPD, and it is mapped as a mean value. In most cases, the depth of the actual $Eh = 0$ horizon will be slightly shallower than the depth of the optical reflectance boundary. This is because bioturbation organisms can mix ferric hydroxide-coated particles downward into the bottom below the $Eh = 0$ horizon. As a result, the apparent mean RPD depth can be used as an estimate of the depth of pore water exchange, usually through pore water irrigation (bioturbation).

The depression of the apparent RPD within the sediment is relatively slow in organic-rich muds (on the order of 200 to 300 μ per day); therefore, this parameter has a long time constant (Germano and Rhoads 1984). The rebound in the apparent RPD is also slow (Germano 1983). Significant (i.e., measurable) changes in the apparent RPD depth using the sediment-profiling optical technique can be detected over periods of 1 or 2 months. This parameter is best used to document changes (or gradients) that develop over a seasonal or yearly cycle related to water temperature effects on bioturbation rates, seasonal hypoxia, SOD, and infaunal recruitment.

Another important characteristic of the apparent RPD is the contrast in reflectance values at this boundary. This contrast is related to the interactions among the degree of organic-loading and bioturbational activity in the sediment, and the levels of bottom water dissolved oxygen in an area. High inputs of labile organic material increase SOD, and subsequently, sulphate reduction rates (and the abundance of sulphide end products). This results in more highly reduced (lower reflectance) sediments at depth and higher RPD contrasts.

Infaunal successional stage

The mapping of successional stages, as employed in this project, is based on the theory that organism-sediment interactions follow a predictable sequence after a major seafloor perturbation. This theory states that primary succession results in the predictable appearance of macrobenthic invertebrates belonging to specific functional types following a benthic disturbance. These invertebrates interact with sediment in specific ways. Because functional types are the biological units of interest, a sequential appearance of particular invertebrate species or genus is not required to describe the successional process. This theory is formally developed in Rhoads and Germano (1982) and Rhoads and Boyer (1982).

The term disturbance is used here to define natural processes, such as seafloor erosion, changes in seafloor chemistry, foraging disturbances that cause major reorganization of the resident benthos, or anthropogenic impacts, such as power plants, pollution impacts from industrial discharge, etc. An important aspect of using this successional approach to interpret benthic monitoring results is relating organism-sediment relationships to the dynamical aspects of end-member seres. This involves deducing dynamics from structure, a technique pioneered by Johnson (1972) for marine soft-bottom habitats. The application of an inverse methods approach to benthic

monitoring requires the in situ measurements of salient structural features of the organism-sediment relationships measured through sediment-profiling technology.

Pioneering assemblages (Stage I assemblages) usually consist of dense aggregations of near-surface living, tube-dwelling polychaetes; alternately, the opportunistic mactrid bivalve *Mulinia* may colonize initially in dense aggregations after a disturbance (Santos and Simon 1980b, Rhoads and Germano 1982). These functional types are usually associated with a shallow redox boundary; bioturbation depths are shallow, particularly in the earliest stages of colonization. In the absence of further disturbance, these early successional assemblages are eventually replaced by infaunal deposit feeders; the start of this "infaunalization" process is designated arbitrarily as a Stage II sere. Typical Stage II species are shallow-dwelling bivalves or, as is common in Long Island sound, tubicolous amphipods. Amphipods appear to participate in the Tampa Bay successional sequence in a similar way. In studies of hypoxia-induced benthic defaunation events in Tampa Bay, ampeliscid amphipods appeared as the second temporal dominant in two of the four recolonization cycles (Santos and Simon 1980a, 1980b).

Stage III taxa, in turn, represent high-order successional stages typically found in low-disturbance regimes. These invertebrates are infaunal, and many feed at depth in a head-down orientation. The localized feeding activity results in distinctive excavations called feeding voids. Diagnostic features of these feeding structures include a generally semicircular shape with a flat bottom and arched roof, and a distinct granulometric change in the sediment particles overlying the floor of the structure. This relatively coarse-grained material represents particles rejected by the head-down deposit-feeder. These deep-dwelling infaunal taxa preferentially ingest the finer sediment particles. Other subsurface structures, e.g., burrows or methane gas bubbles, do not exhibit these characteristics. The bioturbational activities of these deposit-feeders are responsible for aerating the sediment and causing the redox horizon to be located several centimeters below the sediment-water interface. In the retrograde transition of Stage III to Stage I, it is sometimes possible to recognize the presence of relict (i.e., collapsed and inactive) feeding voids. These end-member stages (Stages I and III) are easily recognized in sediment-profile images by the presence of dense assemblages of near-surface polychaetes and/or the presence of subsurface feeding voids; both types of assemblages may be present in the same image.

Additional biological parameters

Several additional biological parameters are measured from the negatives using the computer image analysis system. These include the density (number/linear centimeter) of polychaete and/or amphipod tubes at the interface; the minimum and maximum depth of fecal pellet layers; and the minimum and maximum depth of feeding voids. Also, dominant faunal type (i.e., epifauna or infauna) and apparent species richness are estimated.

Organism-sediment index

A multiparameter Organism-Sediment Index (OSI) has been constructed to characterize habitat quality. Habitat quality is defined relative to two end-member standards. The lowest value is given to those bottoms that have low or no dissolved oxygen in the overlying bottom water, no apparent macrofaunal life, and methane gas present in the sediment (see Rhoads and Germano 1982, 1986 for criteria for these conditions). The OSI for such a condition is -10. At the other end of the scale, an aerobic bottom with a deeply depressed RPD, evidence of a mature macrofaunal assemblage, and no apparent methane gas bubbles at depth will have an OSI value of +11. The OSI is arrived at by summing the subset indices for mean RPD depth, successional stage, and chemical parameters. This index is an excellent parameter for mapping disturbance gradients in an area and documenting ecosystem recovery after disturbance (Germano and Rhoads 1984; Revelas, Germano, and Rhoads 1987).

Results of Sediment-Profiling Surveys

The lower bay site was centered on Beacon 44. The predisposal sediment-profile survey was conducted on December 2, 1987, the overflow tests on December 3 and 4, and the postdisposal survey on December 5. The upper bay site was centered on a point 300 m south of Beacon 66. The predisposal sediment-profile survey took place on December 5, 1987, overflow tests occurred on December 4 to 9, and the postdisposal survey was performed on December 11.

Lower bay predisposal survey

General. The following narrative provides an overview of the physical and biological conditions that existed at the lower bay site (as inferred from the sediment-profile images) during the predisposal survey. Specific image measurements are presented only when they provide insight into potentially

important benthic features or processes. A data sheet including all measured parameters for each image analyzed is illustrated by Figure 135.

The sampling grid for the predisposal survey at the lower bay site consisted of 10 stations randomly placed on both sides of the channel in the vicinity of Beacon 44 (Figure 136). The coordinates for each station occupied are presented in Table 41.

Benthic characteristics. All stations consist predominantly of silt-clay sediments (major mode ≥ 4 phi units). Subordinate fractions of very fine and fine sand (4-3 and 3-2 phi) are also evident at most stations, especially those located immediately adjacent to the channel, i.e., FR-1, 14, and 18. A single station, 3, appears to consist largely of clay (Figure 136). This is evidenced by the extremely fine-grained and textureless appearance of the sediments. Figure 136 also shows the distribution of bottom features indicative of seafloor kinetic processes. Excluding Station 11, mud clasts, varying widely in size, shape, and apparent oxidation state, are observed at all stations. These clasts indicate that the seafloor has been recently disturbed. The cause of this disturbance is most likely a combination of natural (e.g., wind waves, biological foraging) and anthropogenic forces (e.g., trawling). Figure 137 shows the frequency distribution of boundary roughness values. Small-scale relief ranges from 0.3 to 3.0 cm, reflecting both biogenic and physical disturbance factors. In terms of the top few centimeters of the sediment-water interface, the lower bay site represents a relatively unstable environment; that is, sediment transport is fairly common.

The distribution of apparent RPD depths is given in Figure 138, and the RPD frequency distribution is shown in Figure 139. The contours in Figure 138 delimit the area exhibiting RPD depths greater than 2.0 cm. This region of relatively deep apparent RPD runs parallel to the channel, extending approximately 200 m east and west. Beyond this swath, RPD depths are shallow. Station 3, approximately 600 m east of the channel, exhibits the shallowest RPD (0.62 cm); this extremely shallow oxidized layer may indicate the recent erosion of surface sediments. The observed pattern in RPD depths likely reflects the large-scale pattern of water movement and gradients of organic enrichment in Mobile Bay. Apparently, water exchange (between the Bay and Gulf of Mexico) is most efficient within and immediately adjacent to the main navigation channel. This flushing replenishes water column oxygen levels and allows relatively well-developed RPD depths to be established. In peripheral regions away from the channel, water column oxygen levels are apparently not

readily replenished, resulting in shallow RPD depths. In addition, increased levels of organic loading (resulting in higher sediment oxygen demand), due to peripheral point and/or nonpoint sources of organic inputs (e.g., sewage outfalls, terrestrial runoff) as well as primary production, may exist in the shallow, lateral portions of the bay.

The distribution of infaunal successional stages is shown in Figure 138. Evidence of Stage III taxa (head-down deposit feeders) is observed in at least one replicate from all stations except station 12A. These high-order successional infauna appear to be more patchy in their distribution away from the channel. For example, fringe stations (FR-1, 14, and 18) show relatively large voids in both replicate images, while most of the outlying stations (e.g., 3, 5, 15) exhibit Stage III taxa only in one of two replicates. Very small, surface-dwelling tubicolous polychaetes (Stage I taxa) are also present in most images. Although never abundant, these forms are most prevalent at stations 3 and 11, where they occur in densities of 1 to 2 per linear centimeters (as measured across the sediment-water interface). A number of images have been assigned a transitional successional status, Stage I going to Stage II. These images, while lacking unequivocal evidence of deep-dwelling infauna, exhibit some evidence of biogenic mixing. This evidence usually consists of indistinct subsurface pockets filled with relatively coarse-grained sediments or traces of burrow-like structures. The Stage I going to Stage II designation indicates that some "infaunalization" is occurring at the site, but head-down deposit feeding taxa are not fully established.

The mapped distribution of OSI values is shown in Figure 140. The OSI summarizes both sedimentological and biological information to provide an index of the degree of benthic disturbance or "stress" in an area. The indices convey information about relative benthic conditions when they are viewed in spatial or temporal context to adjacent stations. Based on our experience in mapping the OSI in coastal areas throughout North America and Europe, we have found that values less than 7 are generally found at stations that have experienced recent physical disturbance or are chemically stressed (e.g., organically loaded, contaminated by petrochemicals). Figure 140 shows that the region adjacent to the channel represents a less disturbed benthic region than the outlying areas. Again, this appears to reflect enhanced water exchange and/or decreased organic enrichment near the channel.

Lower bay postdisposal survey

General. The sampling grid for the postdisposal survey at the lower bay site consisted of 30 stations concentrated around the overflow point on the eastern edge of the channel (Figure 141). This grid was based on observations of the overflow survey team, which indicated that plume dispersal away from the scow was minimal (0 to 200 m) and largely confined within the channel (trending north to south). The coordinates for each postdisposal station are given in Table 41.

Distribution of overflow deposits. The distribution and thickness of overflow dredged material are shown in Figure 142. Overflow layers were relatively distinct at nine stations, all located within 150 m of the overflow point (station CTR). Two types of layers were apparent in the images: dark sediment bands located immediately below the sediment-water interface and thin surface floccular layers. Overflow layers ranged from 0.40 to 1.82 cm in thickness, with the thickest layer measured at station 100N. A group of eight stations surrounding the region of distinct layers exhibited equivocal evidence of some surface deposition. For example, in some cases, these "deposits" consisted of discontinuous layers of very small mud clasts. These equivocal depositional layers extend as far as stations 500N, 500S, and FR-1. Overall, it is clear that limited and small-scale deposition of overflow material occurred immediately adjacent to the lower bay test site. For purposes of hydrodynamic modeling, only the overflow deposits within the solid contour in Figure 142 should be considered well-defined.

Benthic characteristics. As observed in the predisposal survey, the area surveyed consisted predominantly of silt-clay sediments (major mode ≥ 4 phi units at all stations). Widespread small-scale disturbance of the sediment-water interface is evidenced by the presence of mud clasts at 26 of the 30 stations. Stations immediately adjacent to the areas of dredging and overflow do not appear markedly disturbed compared with outlying areas or their predisposal condition.

The postdisposal distribution of apparent RPD depths is given in Figure 143, and the RPD frequency distribution is included in Figure 139. Overall, there is no significant difference in the predisposal and postdisposal RPD values (Kruskal-Wallis test; $p = 0.6090$). In general, relatively deep apparent RPD values are still found adjacent to the channel, while outlying areas show thinner oxidized surface layers. Several stations immediately adjacent to both the eastern and western flanks of the channel

show shallower RPD values than those observed during the predisposal survey. This apparent discrepancy may represent real impacts of the dredging and monitoring activity in the area. That is, increased boat activity, overflow operations, and bottom sampling may be enhancing bottom disturbance and the erosion of oxidized surface layers. The passage of shrimp trawls over the bottom during bay shrimping activities may also have contributed to these observations. In addition, the pattern may represent natural small-scale patchiness in benthic conditions. Sediment-profile stations occupied in both surveys (e.g., 14 and FR-1) are likely several meters apart (0 to 50 m based on the accuracy of LORAN-C navigation). Depending on the exact infaunal community composition at each locale, the measured RPD depth may vary on a very small spatial scale.

The postdisposal distribution of infaunal successional stages is shown in Figure 144. Evidence of Stage III taxa (head-down deposit feeders) is again widespread. Except for stations CTR, 50N, and 50E, all stations within 200 m of the channel show Stage III seres in both replicates. Further east and west of the channel, Stage III taxa are apparently more patchy in distribution. The distribution of Stage III taxa is also patchy at the three stations (CTR, 50N, and 50E) immediately adjacent to the site of the overflow operation. This may simply reflect real small-scale patchiness in the distribution of these head-down feeding taxa. Alternately, the overflow operation may have resulted in a temporary modification in the feeding rates of these organisms. It seems very unlikely, however, that the relatively small amount of overflow material deposited at these sites would result in any long-term change in the composition of the benthic assemblages.

The postdisposal distribution of the Organism-Sediment Index (Figure 145) shows that, overall, the pattern observed in the predisposal survey remains, with the region adjacent to the channel representing the least "disturbed" benthic region. An exception to this pattern is the area in the vicinity of the overflow point. This small region (100-m circle) appears to have been affected by the operation. Again, however, given the small scale of the disposal operation, it seems unlikely that the apparent disturbance will persist.

Upper bay predisposal survey

General. The sampling grid for the upper bay predisposal survey consisted of 10 stations centered on the location of the overflow barge (approximately 500 m south of Beacon 66). Based on the results of the lower

bay study, most stations were located close to the disposal point (Figure 146). The coordinates for each station occupied are given in Table 41.

Benthic characteristics. As in the lower bay, all stations consisted predominantly of silt-clay sediments (major mode ≥ 4 phi units). Subordinate fractions of very fine and fine sand (4-3 and 3-2 phi) are also evident in some images; however, these coarse-grained fractions are less prevalent than at the lower site. Mud clasts are present at the sediment-water interface at all stations except station 2-200SE (Figure 146). Again, this indicates that surface sediments are subject to frequent small-scale disturbance. The frequency distribution of boundary roughness values further supports this inference, showing that a wide range of relief exists at the site (Figure 147). This small-scale topography reflects both physical and biogenic processes.

The predisposal distribution of apparent RPD depths at the upper bay site is given in Figure 148, and the RPD frequency distribution is presented in Figure 149. The RPD values are generally shallower at the upper bay site than the lower site (compare Figure 149 with Figure 139). This may reflect baywide north-south gradients in water exchange and organic enrichment. The contours in Figure 148 delimit the area exhibiting relatively high RPD depths (i.e. greater than 1.5 cm). All these areas occur immediately adjacent to the channel. Although the pattern is not as distinct as in the lower bay, this seems to illustrate the influence of the channel on large-scale circulation in the bay.

Infaunal successional stages are also included in Figure 148. Evidence of Stage III taxa is patchy (one of two replicates) at 6 of the 10 stations and at all stations not immediately adjacent to the channel. Low densities ($<1/\text{cm}$) of very small, surface-dwelling tubicolous polychaetes are present at six stations. Small surface-dwelling worms are most abundant at Beacon 66 (2/lin cm).

As in the lower bay, the upper bay predisposal distribution of Organism-Sediment Index values indicates that the least disturbed regions, in terms of apparent RPD depths and successional status, occur close to the channel (Figure 150). Overall, the upper bay exhibits lower OSI values than the lower bay. Again, this appears to reflect regional (baywide) patterns of water exchange and organic enrichment.

Upper bay postdisposal survey .

The postdisposal sampling grid at the upper bay site was similar to the lower bay grid and consisted of 30 stations concentrated around the overflow point (Figure 151). As in the lower bay, the overflow survey team indicated that plume dispersal away from the scow was minimal (0 to 200 m) and largely confined within the channel (trending north-south). The coordinates for each postdisposal station are given in Table 41.

Distribution of overflow deposits. The distribution and thickness of overflow dredged material at the upper site are shown in Figure 151. Overflow layers were less distinct than at the lower site. This may be due to an unavoidable 24-hr hiatus between the cessation of overflow operations (which occurred ahead of the planned schedule) and the postdisposal survey, although wind conditions during this period were not severe. Distinct layers were evident only at stations CTR and 100N, while equivocal surface deposits were observed at eight other locations. Given the natural occurrence of surface sediment transport, it is unclear if these latter deposits represent overflow layers or naturally occurring resuspended sediments (or fecal layers). The thickest distinct overflow layer (1.04 cm) was observed at station 100N. Despite the somewhat more extensive overflow operations conducted at the upper site relative to the lower site, markedly less extensive overflow deposits are apparent. The reason for this is not known. It may reflect a real discrepancy in the patterns of sediment dispersal and deposition associated with each operation or site-specific differences in water current velocities. Alternatively, the extra day between overflow tests and the postdisposal monitoring which occurred at the upper site may have allowed the deposit to disperse or become less readily detectable in the images. At both sites, however, it is clear that only limited and small-scale deposition of overflow material occurred during these tests.

Benthic characteristics. There was no marked change in the physical characteristics (e.g., grain-size, boundary roughness) of the upper bay site between the predisposal and postdisposal surveys. Two stations intentionally located 50 and 100 m north of Beacon 66 (the dredging site) do not appear disturbed relative to other areas. This suggests that bottom disturbance caused by the hydraulic dredge was largely restricted to the immediate channel environment.

The postdisposal distribution of apparent RPD depths is given in Figure 153. The contours delimit areas exhibiting RPD depths greater than

1.5 cm. Again, the deeper RPD depths are generally restricted to regions close to the channel. Overall, there is no significant difference in the RPD values between the predisposal and postdisposal surveys (Kruskal-Wallis test; $p = 0.1019$).

The postdisposal distribution of infaunal successional stages is shown in Figure 154. Evidence of Stage III taxa (head-down deposit feeders) is again widespread, especially near the channel. There is no evidence of change in the macrofaunal assemblages due to the overflow tests.

The postdisposal distribution of the Organism-Sediment Index (Figure 155) shows that the most highly disturbed stations are those 500 m or more away from the channel. These lower values clearly reflect preexisting conditions not associated with the overflow tests. The lack of change in RPD values and infaunal successional status between the predisposal and postdisposal surveys parallels the observance of no change in OSI values in the vicinity of the disposal point.

November survey - lower bay test site

General. On November 2, 1987, 20 stations were occupied in the vicinity of Beacon 44, the lower bay overflow test site. This survey was intended to be a predisposal survey, but scheduling problems delayed the entire project. Nonetheless, images from 10 of these stations were analyzed to serve as a temporal reference and as additional baseline information for the lower bay test site. The sampling grid for the November survey was similar to the lower bay predisposal survey and consisted of stations randomly placed around Beacon 44 (Figure 156). The coordinates for each station occupied are given in Table 41.

Benthic characteristics. All stations occupied in the November survey consisted predominantly of silt-clay sediments (major mode ≥ 4 phi units), with subordinate fractions of very fine and fine sand (4-3 and 3-2 phi). Mud clasts were present at the sediment-water interface at all stations, indicating widespread near-surface disturbance. Small-scale surface relief (boundary roughness) values were similar to those observed in both December surveys (Kruskal-Wallis test; $p = 0.4078$; Figure 157). Overall, there were no marked changes in the apparent bottom kinetic regimes at this site between November and December.

The November distribution of apparent RPD depths at the lower bay site is given in Figure 158, and the RPD frequency distribution is included in Figure 159. As with the boundary roughness values, RPD depths, taken

together, do not significantly vary among the three lower bay surveys (Kruskal-Wallis test; $p = 0.2910$). In terms of the spatial distribution of RPD values, as observed in December, apparent oxidized layers deepen toward the channel. Again, this pattern seems to illustrate the influence of the channel on large-scale water exchange in the bay, and possibly east-west organic enrichment gradients.

The distribution of infaunal successional stages observed in November is included in Figure 158. Evidence of Stage III taxa is seen at all stations. There is no obvious spatial pattern in the overall distribution of infaunal seres. Small, surface-dwelling tubicolous polychaetes are most abundant (2/lin cm) at station 13. The distribution of these surface-dwelling forms is similar to that observed in December.

The November distribution of Organism-Sediment Index values reveals a less distinct pattern than that observed 1 month later (Figure 159). Relatively high OSI values (≥ 7) are observed adjacent to the channel. However, two outlying stations (3 and 10) also show high OSI values. This more even distribution of values appears to reflect a greater abundance of Stage III seres in the area away from the channel than observed in December. It is unknown whether this change represents a real decrease in the activity (or abundance) of head-down feeders between November and December or is simply related to the inherent patchiness of these taxa and is an "artifact" of the small numbers of replicate images obtained at each station.

Summary and Conclusions

The sediment-profile data presented here indicated that limited and small-scale deposition occurred in the vicinity of the barges during overflow tests at two sites in Mobile Bay. These sedimentation data are summarized, by station, in Table 42. Overall, deposition appeared to be restricted to the immediate vicinity of the barges (within 100 to 200 m), and all observed layers were thin (less than 2 cm thick). Depositional layers were more widespread and had a greater apparent impact on benthic conditions at the lower site than the upper site.

Physical measurements (e.g., mud clasts, boundary roughness) indicate that both sites were characterized by apparently natural, widespread surface disturbance. Given the water depths at each site (3 to 5 m) and the survey

season, this result is not unexpected. There was no obvious difference between the kinetic regimes of the near-channel stations and outlying areas.

Chemical and biological parameters (e.g., RPD depths, infaunal successional status) indicate a gradient in conditions from the channel fringe outward (both east and west). The near-channel environment (at both sites) exhibits deeper apparent RPD values and higher abundances of Stage III infauna than outlying areas. This pattern is likely related to enhanced water circulation in and adjacent to the channel and/or enhanced organic enrichment (higher sediment oxygen demand) toward the margins of the bay. A north-south gradient in benthic conditions is also evident. Overall, apparent RPD values are deeper, and animal-sediment interactions are more fully developed at the lower site than the upper site. Again, this appears to represent large-scale (baywide) patterns in water circulation and exchange with the Gulf of Mexico and/or regional gradients in levels of organic enrichment.

References

- Germano, J. D. 1983. Infaunal succession in Long Island Sound: Animal-sediment interactions and the effects of predation. Ph.D. dissertation, Yale University, New Haven, CT.
- Germano, J. D., and Rhoads, D. C. 1984. REMOTS sediment profiling at the Field Verification Program (FVP) Disposal Site. Dredging '84: Proceedings of the Conference, American Society of Civil Engineers, November 14-16, Clearwater, FL, pp 536-544.
- Johnson, R. G. 1972. Conceptual models of benthic marine communities. Models of Paleobiology. Schopf, ed. Freeman, Cooper, and Co., San Francisco, CA, pp 145-159.
- Revelas, E. C., Germano, J. D., and Rhoads, D. C. 1987. REMOTS: Reconnaissance of benthic environments. Coastal Zone '87: Proceedings of the Conference, Waterways Division, American Society of Civil Engineers, May 26-29, Seattle, WA, pp 2069-2083.
- Rhoads, D. C. 1974. Organism-sediment relations on the muddy seafloor. Oceanography and Marine Biology Annual Review 12:263-300.
- Rhoads, D. C., and Boyer, L. F. 1982. The effects of marine benthos on physical properties of sediments. Pages 3-52 in Animal-Sediment Relations: The Biogenic Alteration of Sediments. P. L. McCall and M. S. Tevesz, eds. Plenum Press, New York.
- Rhoads, D. C., and Germano, J. D. 1982. Characterization of benthic processes using sediment profile imaging: An efficient method of remote ecological monitoring of the seafloor (REMOTS System). Marine Ecology Progress Series 8:115-128.
- _____. 1986. Interpreting long-term changes in benthic community structure: A new protocol. Hydrobiologia 142:291-308.

Santos, S. L., and Simon, J. L. 1980a. Marine soft-bottom community establishment following annual defaunation: Larval or adult recruitment? Marine Ecology Progress Series 2:235-241.

_____. 1980b. Response of soft-bottom benthos to annual catastrophic disturbance in a south Florida estuary. Marine Ecology Progress Series 3:347-355.

Table 41
Lower Bay Site, Survey Coordinates

<u>Station</u>	<u>Latitude</u>	<u>Longitude</u>
<u>Predisposal Survey</u>		
FR-1	30 24.558N	088 01.119W
1	30 24.725N	088 00.671W
11	30 24.136N	088 01.485W
12A	30 24.990N	088 01.330W
3	30 24.385N	088 00.460W
5	30 24.124N	088 00.644W
7A	30 24.943N	088 00.705W
14	30 24.435N	088 01.140W
15	30 35.659N	088 01.334W
18	30 24.659N	088 00.801W
<u>Postdisposal Survey</u>		
CTR	30 24.513N	088 00.889W
1000N	30 25.091N	088 00.806W
500N	30 24.794N	088 00.841W
200N	30 24.643N	088 00.879W
100N	30 24.594N	088 00.876W
50N	30 24.575N	088 00.885W
50S	30 24.449N	088 00.894W
100S	30 24.422N	088 00.915W
200S	30 24.332N	088 00.930W
500S	30 24.226N	088 00.922W
1000S	30 23.995N	088 00.966W
500SE	30 24.400N	088 00.774W
200SE	30 24.439N	088 00.812W
100SE	30 24.465N	088 00.848W
50SE	30 24.505N	088 00.858W
50E	30 24.531N	088 00.836W
100E	30 24.551N	088 00.791W
200E	30 24.530N	088 00.735W
500E	30 24.519N	088 00.599W
REF1	30 24.023N	088 00.209W
REF2	30 24.504N	088 00.037W
500NE	30 24.702N	088 00.654W
200NE	30 24.601N	088 00.784W
100NE	30 24.562N	088 00.823W
50NE	30 24.555N	088 00.863W
14	30 24.429N	088 01.101W
400SW	30 24.335N	088 01.101W
FR-1	30 24.611N	088 01.109W
REF3	30 24.045N	088 02.025W
REF4	30 24.665N	088 01.753W
<u>November Survey</u>		
FR-1	30 24.558N	088 01.119W
9	30 23.727N	088 01.346W
10	30 24.052N	088 02.044W
11	30 24.136N	088 01.485W
3	30 24.385N	088 00.460W
5	30 24.124N	088 00.644W
14	30 24.435N	088 01.140W
13	30 24.656N	088 01.755W
17	30 23.837N	088 00.799W
18	30 24.659N	088 00.801W

Table 42
Location and Thickness of Overflow Depositional
Layers Detected in REMOTS Images

<u>Station</u>	<u>Thickness of Layer, cm</u>
<u>Lower Bay Site</u>	
CTR	0.77
50N	0.91
100N	1.82
50NE	1.42
50E	0.59
50SE	0.40
100SE	0.63
50S	0.57
100S	0.57
<u>Upper Bay Site</u>	
CTR	0.58
100N	1.04

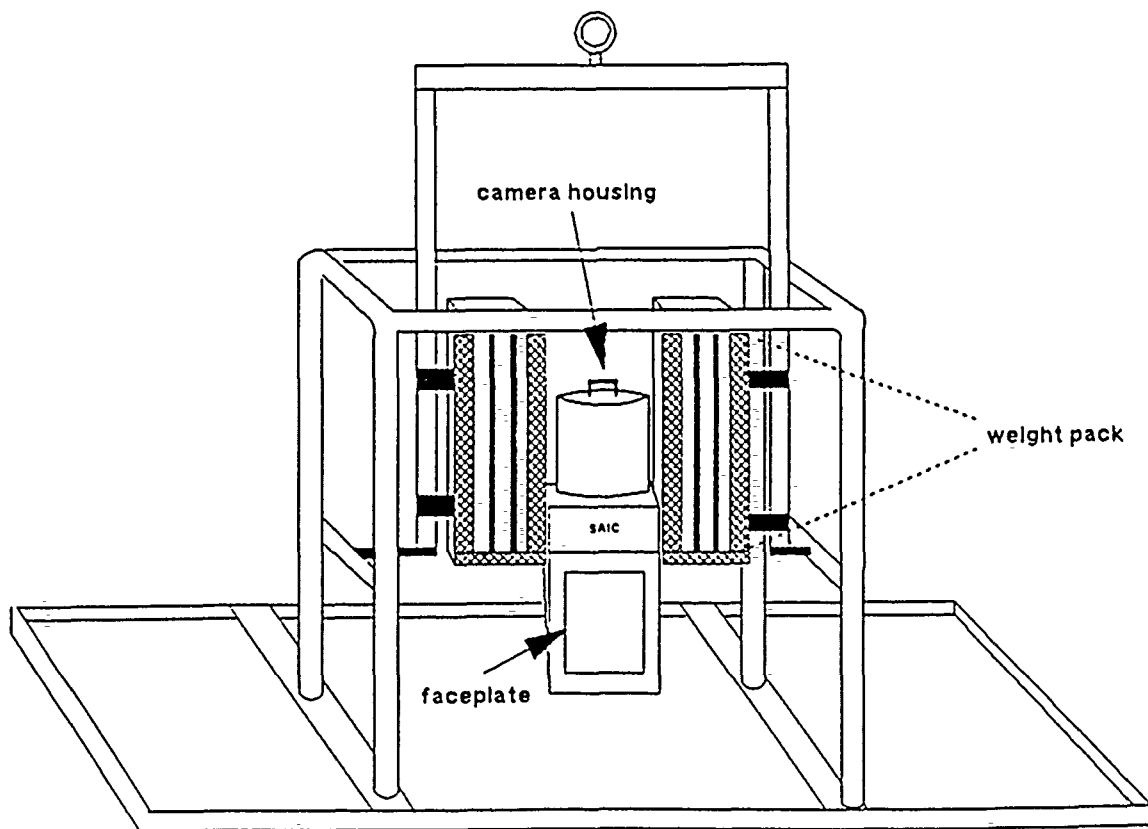


Figure 134. REMOTS sediment-profile camera

REMOTS DATA SHEET
Science Applications

PROJECT: MOBILE LOWER BY POST-DISPOSAL STATION: 506/B
FIELD DATE: 12/5/67 FRAME #: 16
Measurements By: GCR Time of Photo: 10:22

Data Record #: 14

***** PHYSICAL - CHEMICAL PARAMETERS *****

1. Grain Size:
Major Mode: $\geq 4 \phi$ Range: $\geq 4-3 \phi$
2. Total Prism Penetration Depth:
Minimum: 11.76 cm. Maximum: 14.19 cm. Average: 12.98 cm.
3. Surface Boundary Roughness: 2.28 cm. ----- Physical
4. Mud Clasts
of Clasts: 0
Average Diameter: 0 cm. Status: NA
5. Mean Redox Depth: 2.76 cm.
6. Redox Rebound (former distance from sed. surface): Not Present
7. Methane Gas Pockets: Not Present
Number: 0 Area: 0 sq. cm.
Min. Range: 0 cm. Max. Range: 0 cm. Average Depth: 0 cm.
8. Low Dissolved Oxygen in Overlying Water: No
9. Dredged Material thickness (cm.): Not Present
10. Additional Measurement: .83 cm. Label: FLOC
11. Comment: DK SURF FLOC

***** BIOLOGICAL PARAMETERS *****

12. Epifauna: None Visible
13. Tube Density (#/linear cm.): 0
14. Tube Type: NA
15. Fecal Pellet layer:
Min. Thickness: 0 cm. Max. Thickness: 0 cm. Average: 0 cm.
16. Microbial Aggregations Present?: No
17. Feeding Voies -- Average Depth: 10.2 cm.
Number: 1 Minimum Depth: 9.6 cm. Maximum Depth: 10.8 cm.
18. Faunal Dominants: Infauna
19. Apparent Species Richness: Medium
20. Successional Stage: STAGE 3
21. Organism-Sediment Index: ?

Figure 135. REMOTS data sheet

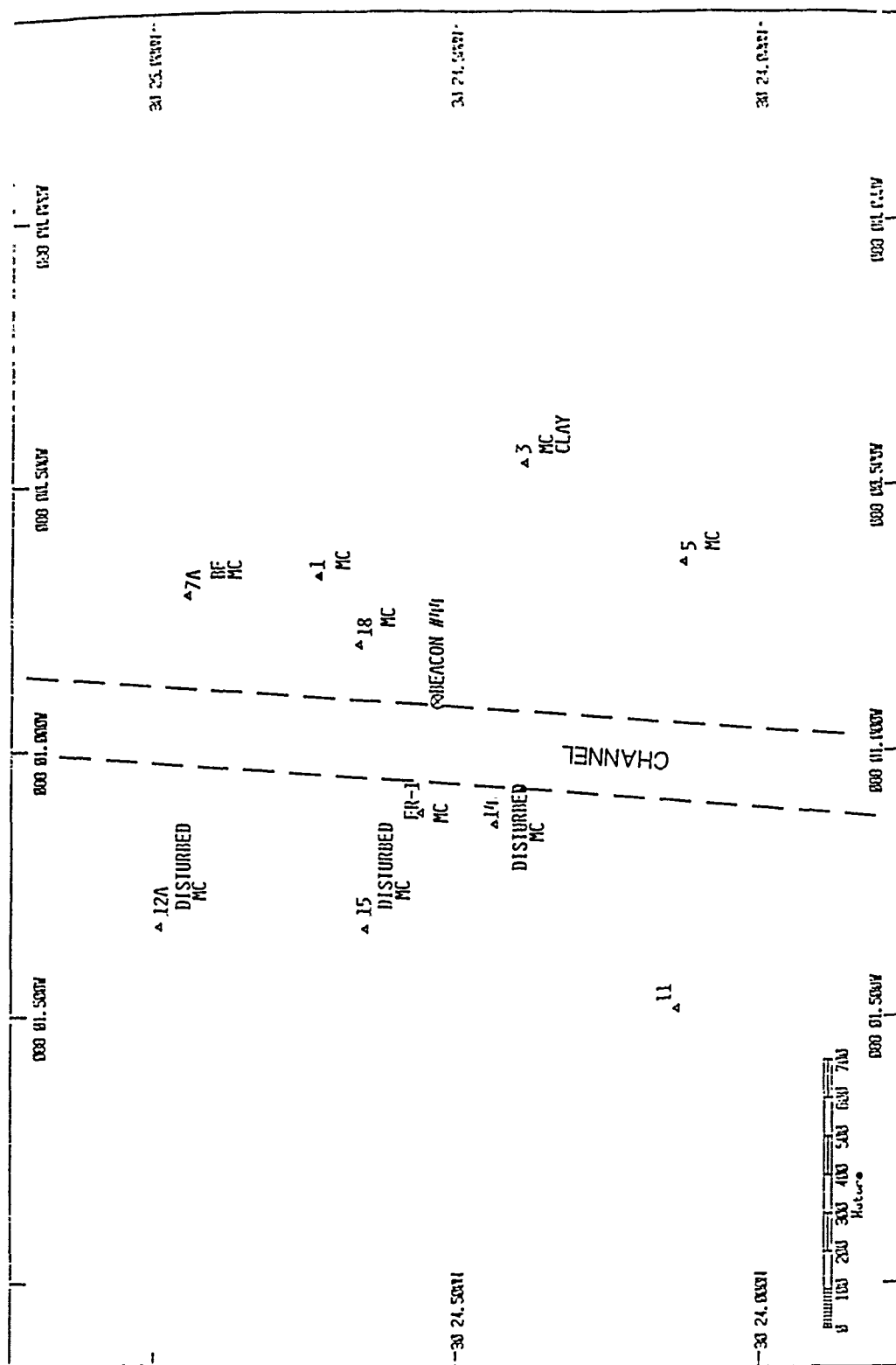
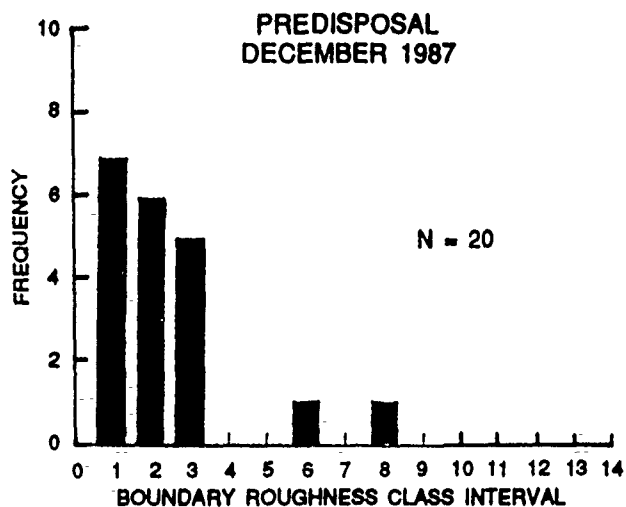


Figure 136. Distribution of lower site predisposal stations. Markedly disturbed sites are indicated, as well as the distribution of mud clasts (MC) and bed forms (BF)



KEY

CLASS INTERVAL	RANGE OF BOUNDARY ROUGHNESS, CM
1	0.0 - 0.6
2	0.6 - 1.0
3	1.0 - 1.4
4	1.4 - 1.8
5	1.8 - 2.2
6	2.2 - 2.6
7	2.6 - 3.0
8	3.0 - 3.4
9	3.4 - 3.8
10	3.8 - 4.2
11	4.2 - 4.6
12	4.6 - 5.0

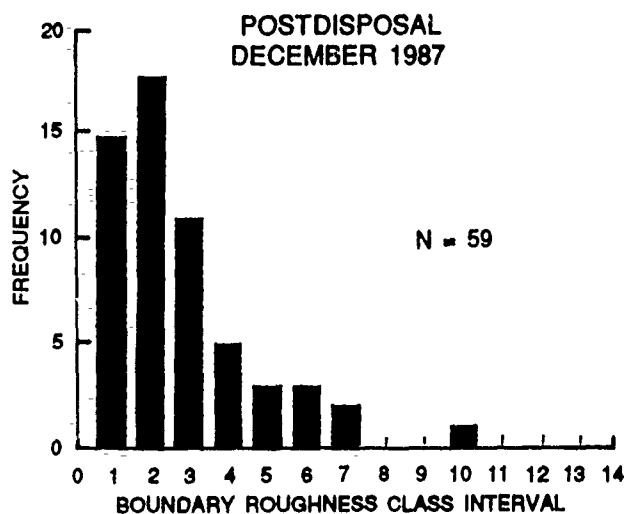


Figure 137. Frequency distributions of small-scale boundary roughness values for the lower bay predisposal and postdisposal surveys

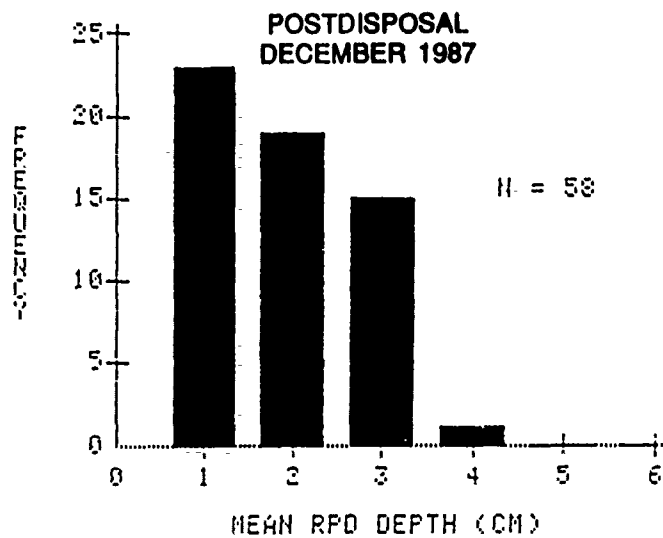
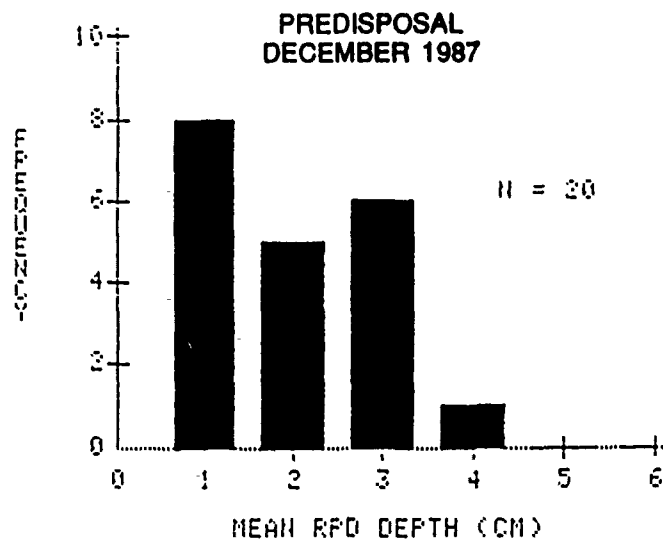


Figure 139. Frequency distributions of apparent RPD depths for predisposal and postdisposal surveys at the lower site

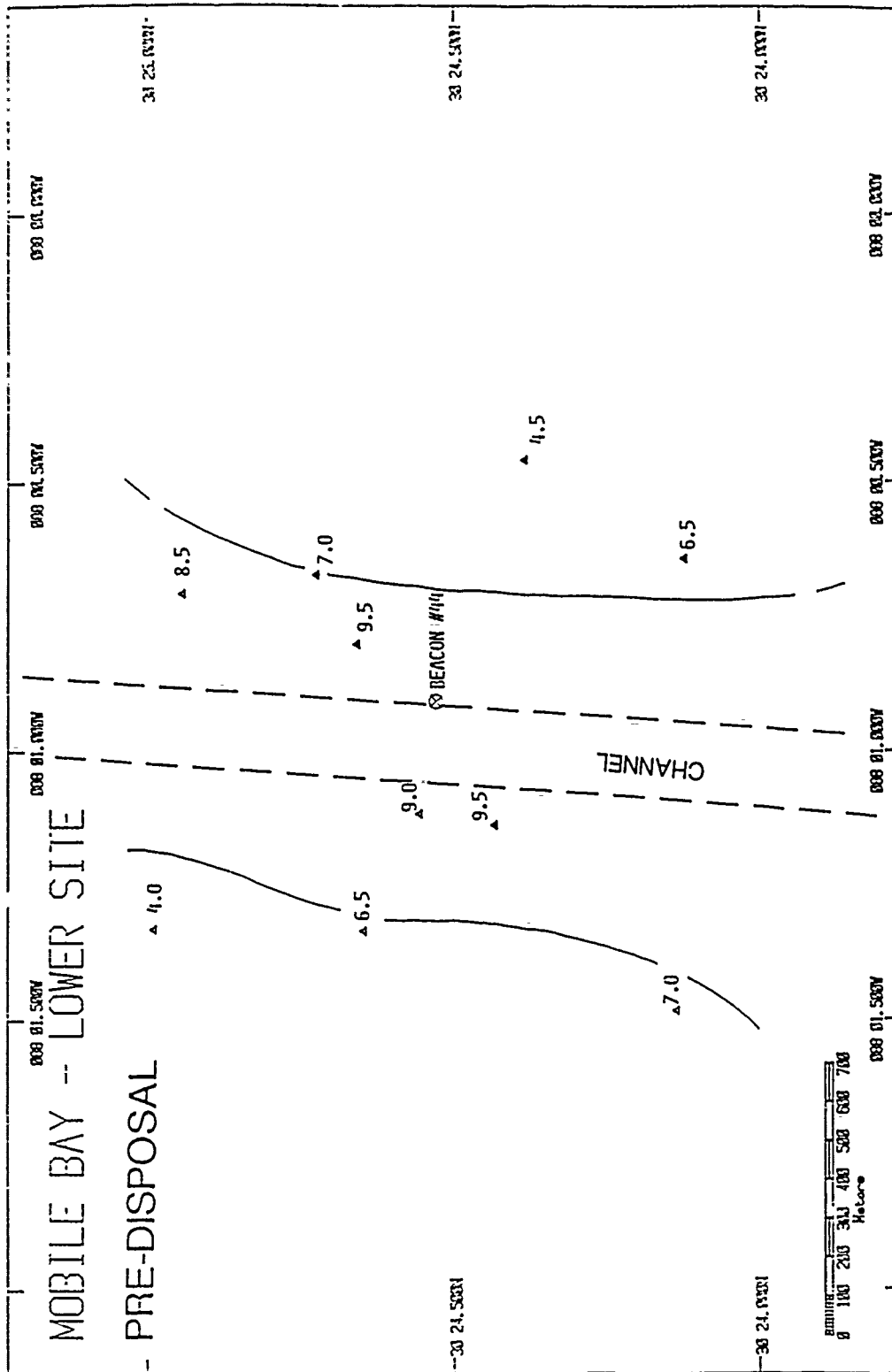


Figure 140. Predisposal distribution of Organism-Sediment Index values at the lower site. (OSI value represents the average of the replicates. Contours delimit areas with OSIs less than 7.0)

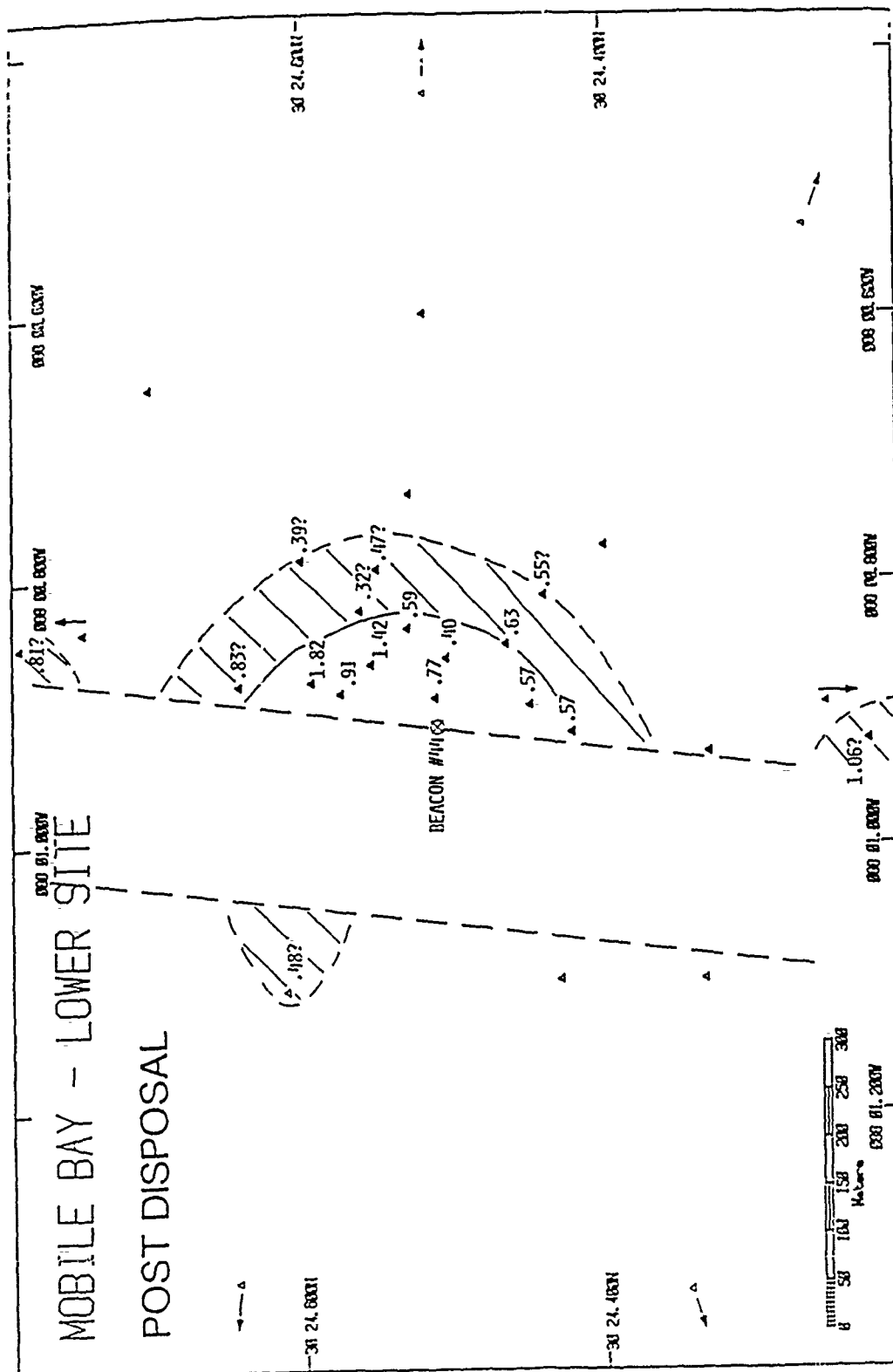


Figure 142. Distribution and thickness (centimeters) of overflow depositional layers at the lower site. (Solid line encloses distinct layers. Hatched area represents a region of "possible" overflow sedimentation. Arrows indicate stations located beyond margins of chart)

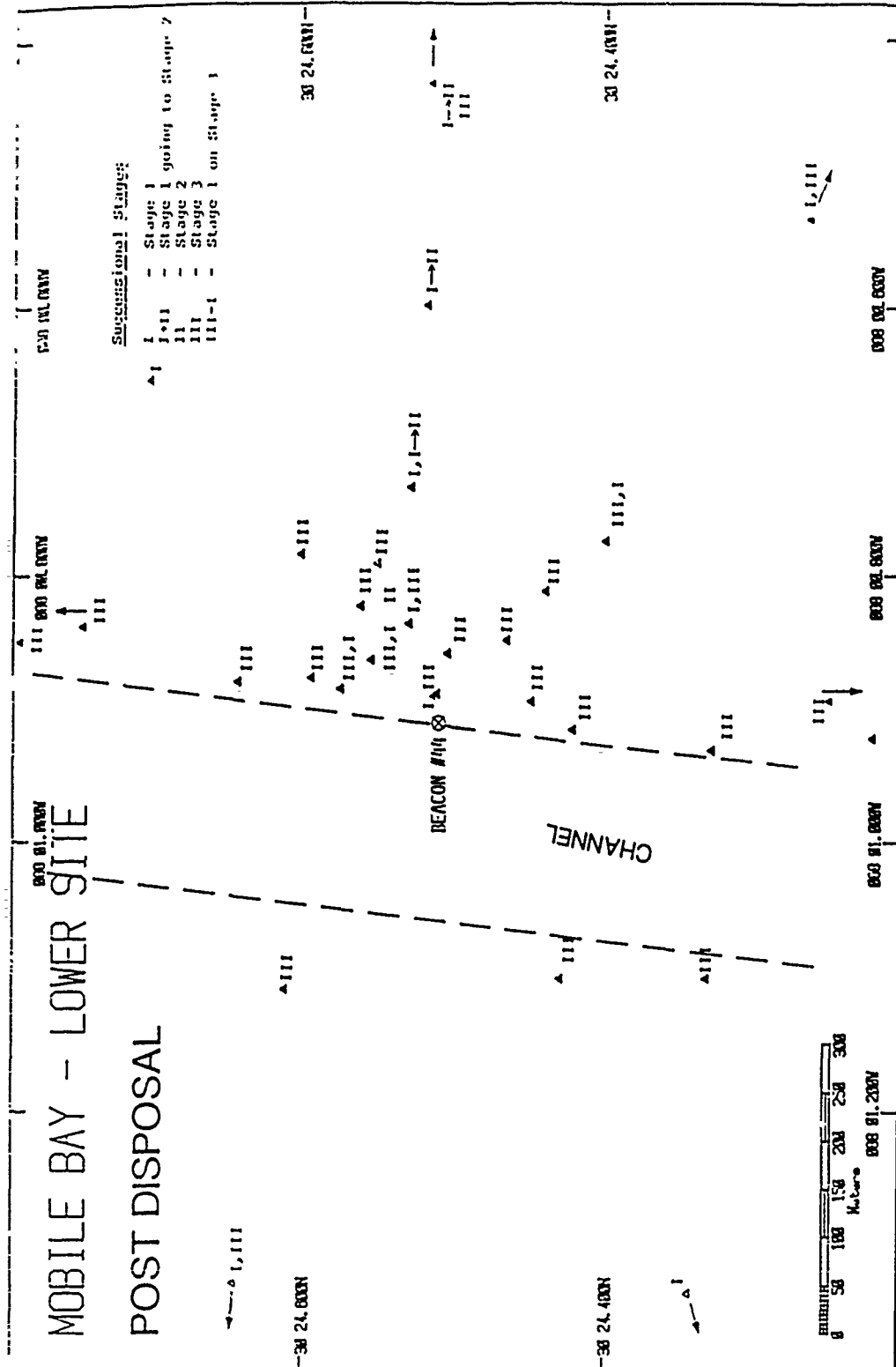


Figure 144. Postdisposal distribution of infaunal successional stages at the lower site (arrows indicate stations located beyond margins of chart)

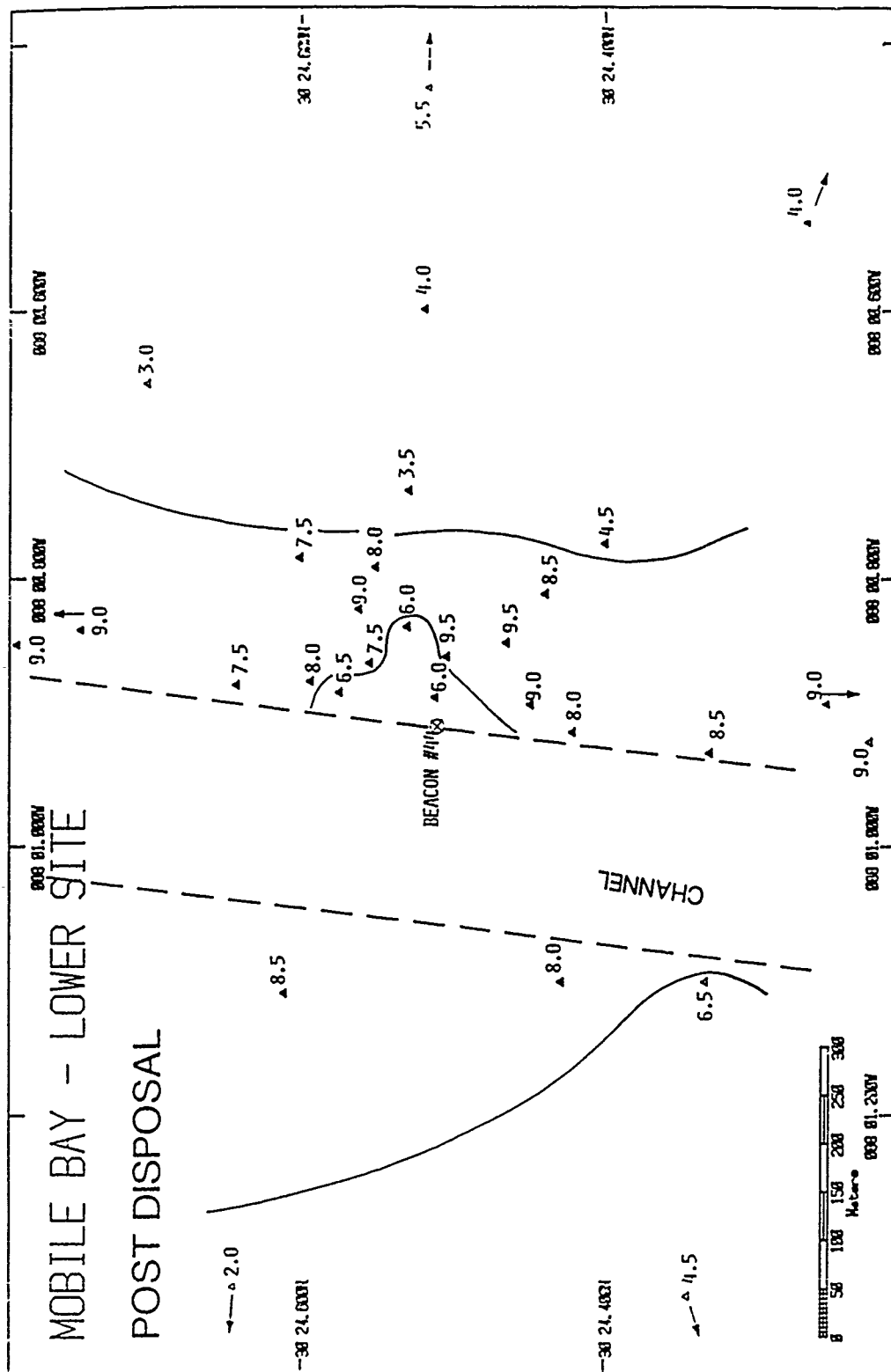


Figure 145. Postdisposal distribution of Organism-Sediment Index values, averaged by station, at the lower site. (Contours delimit areas with OSI values less than 7.0; arrows indicate stations located beyond margins of chart)

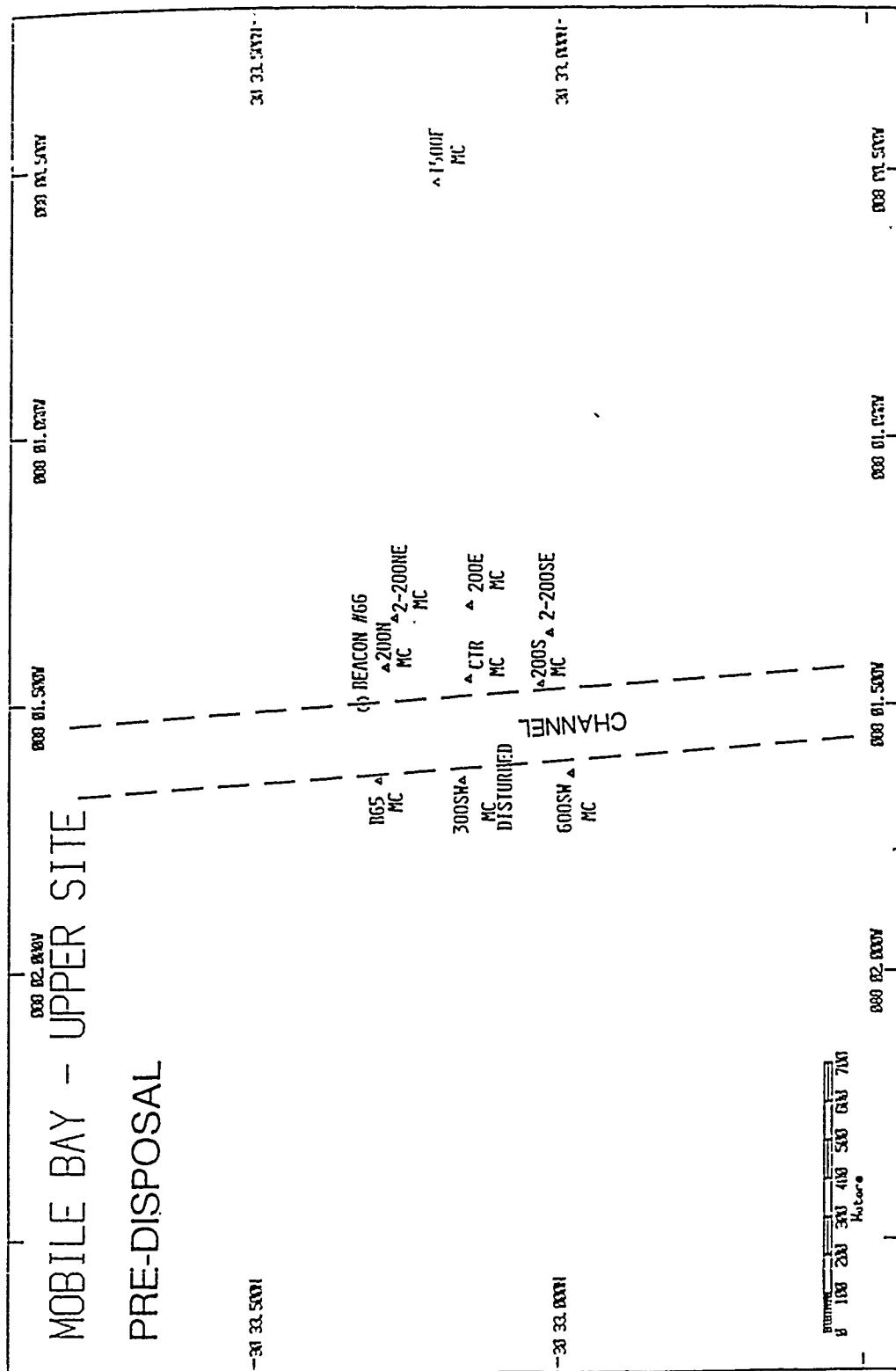
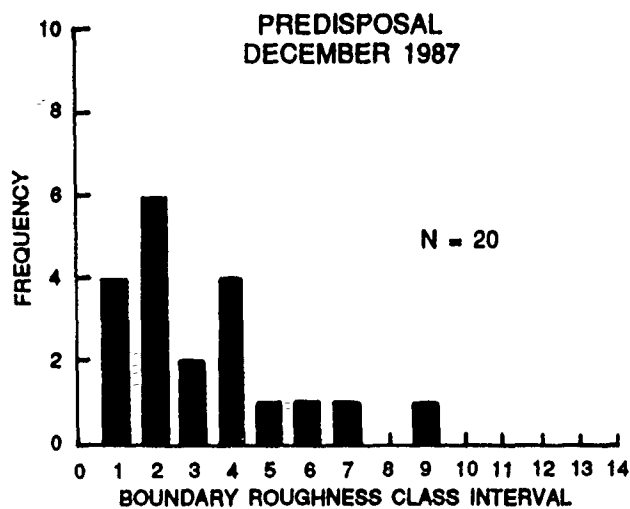


Figure 146. Distribution and designations of predisposal stations at the upper site. Markedly disturbed sites, as well as the distribution of mud clasts (MC), are indicated



KEY

CLASS INTERVAL	RANGE OF BOUNDARY ROUGHNESS, CM
1	0.0 - 0.6
2	0.6 - 1.0
3	1.0 - 1.4
4	1.4 - 1.8
5	1.8 - 2.2
6	2.2 - 2.6
7	2.6 - 3.0
8	3.0 - 3.4
9	3.4 - 3.8
10	3.8 - 4.2
11	4.2 - 4.6
12	4.6 - 5.0

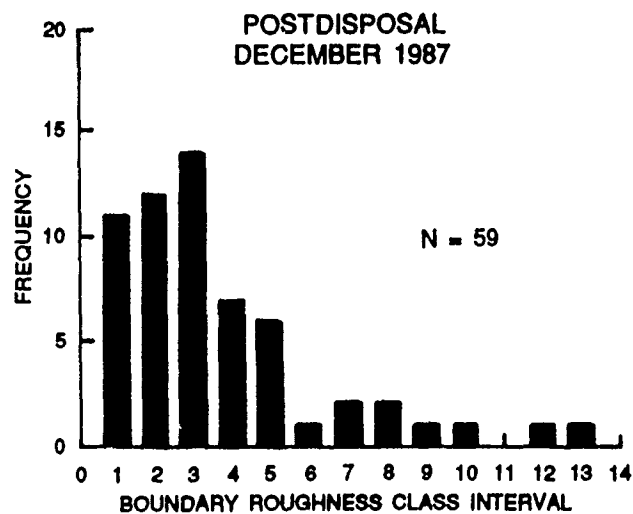


Figure 147. Predisposal and postdisposal frequency distributions of boundary roughness values at the upper site

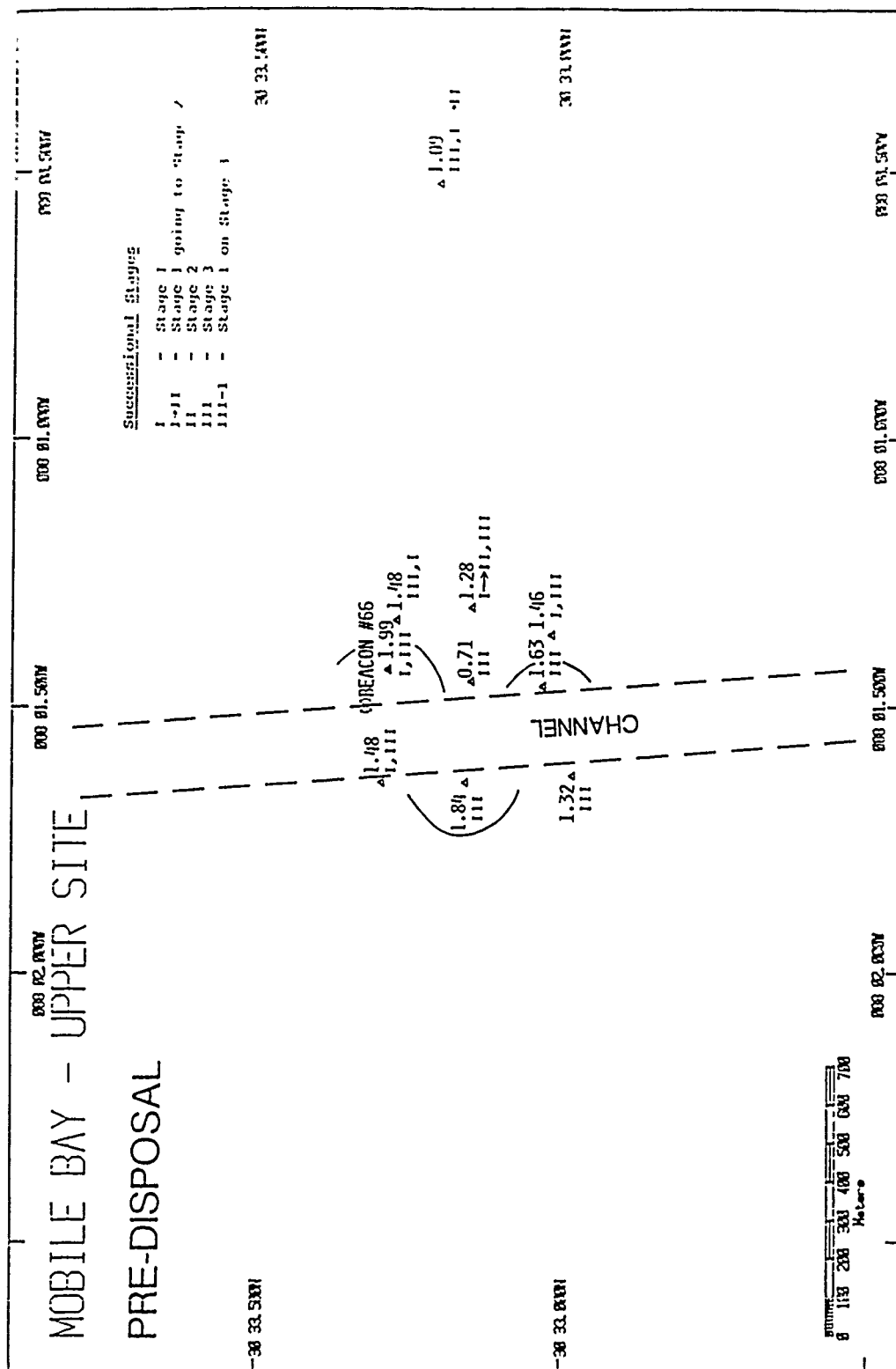


Figure 148. Predisposal of Mobile Bay - Upper Site showing RPD depths (centimeters) and infaunal successional stages at the Mobile Bay site. (Contours enclose areas with RPD depths greater than 1.5 cm)

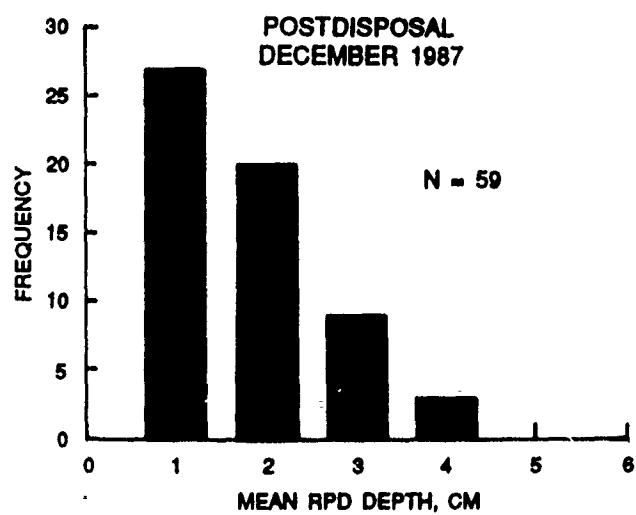
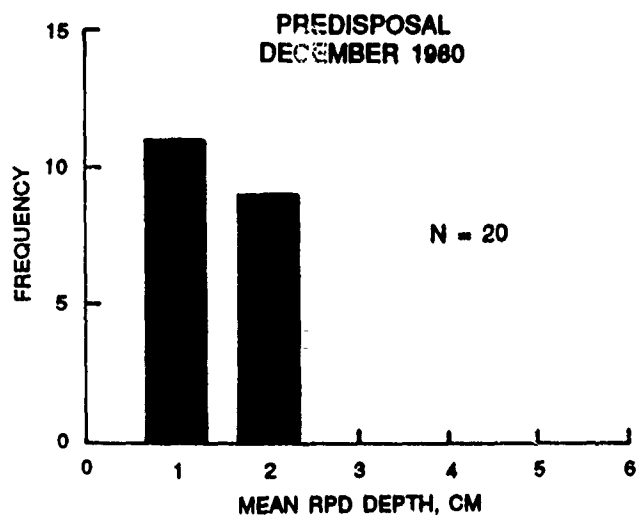
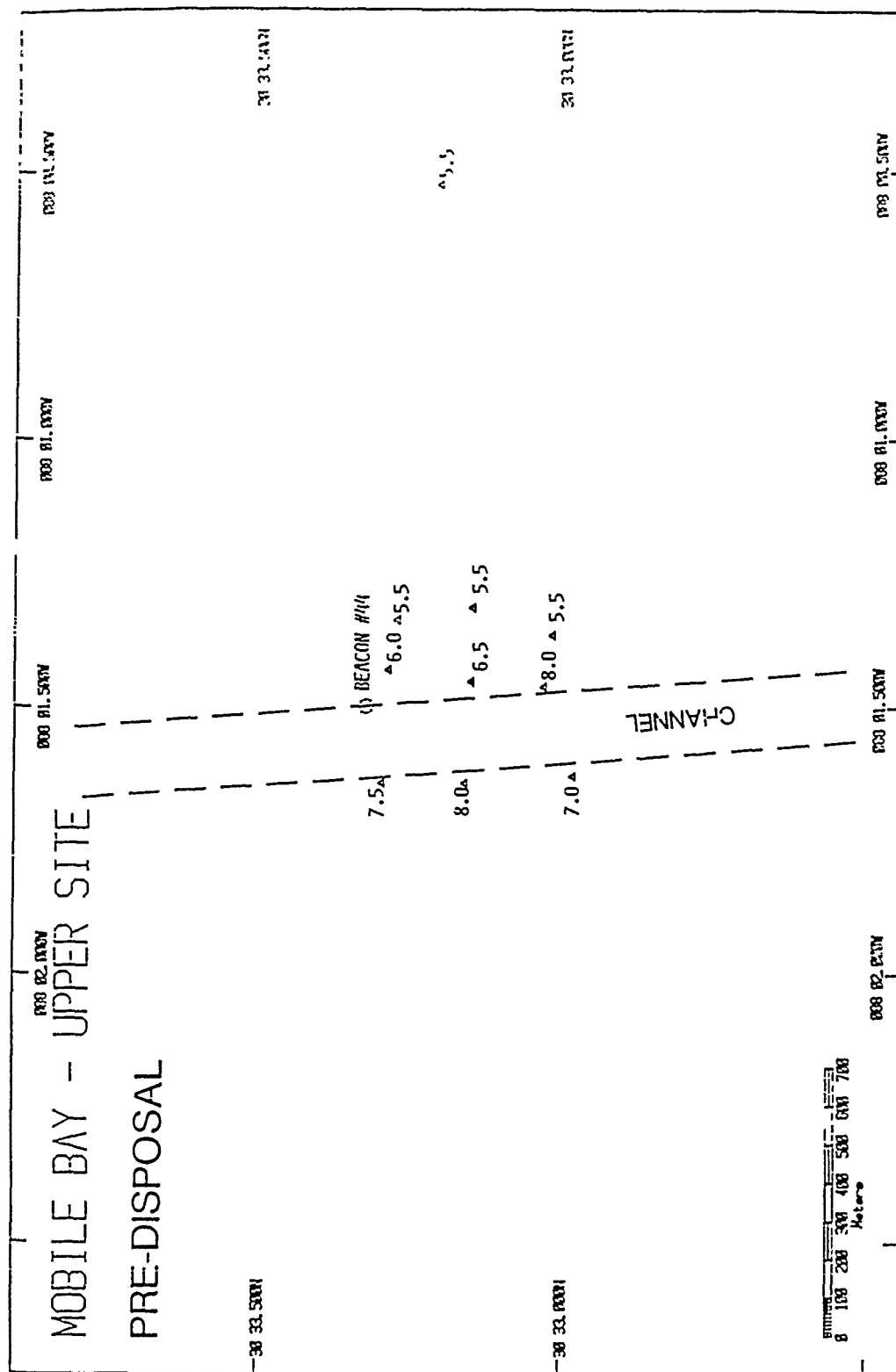


Figure 149. Predisposal and postdisposal frequency distributions of RPD values at the upper site



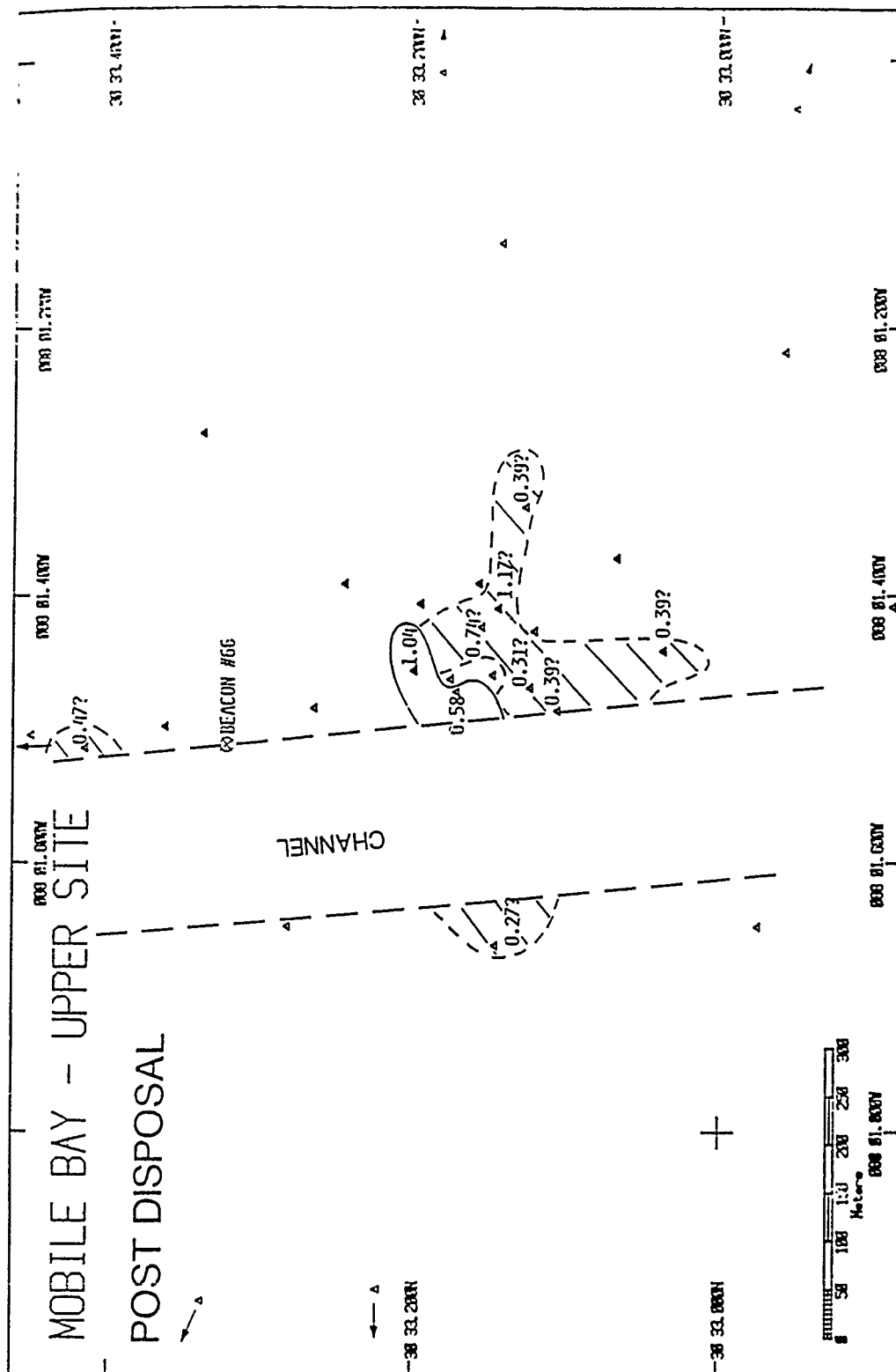


Figure 152. Distribution and thickness (centimeters) of overflow depositional layers. (Solid line encloses distinct layers. Hatched areas represent regions of "possible" overflow sedimentation. Arrows indicate stations located beyond margins of chart)

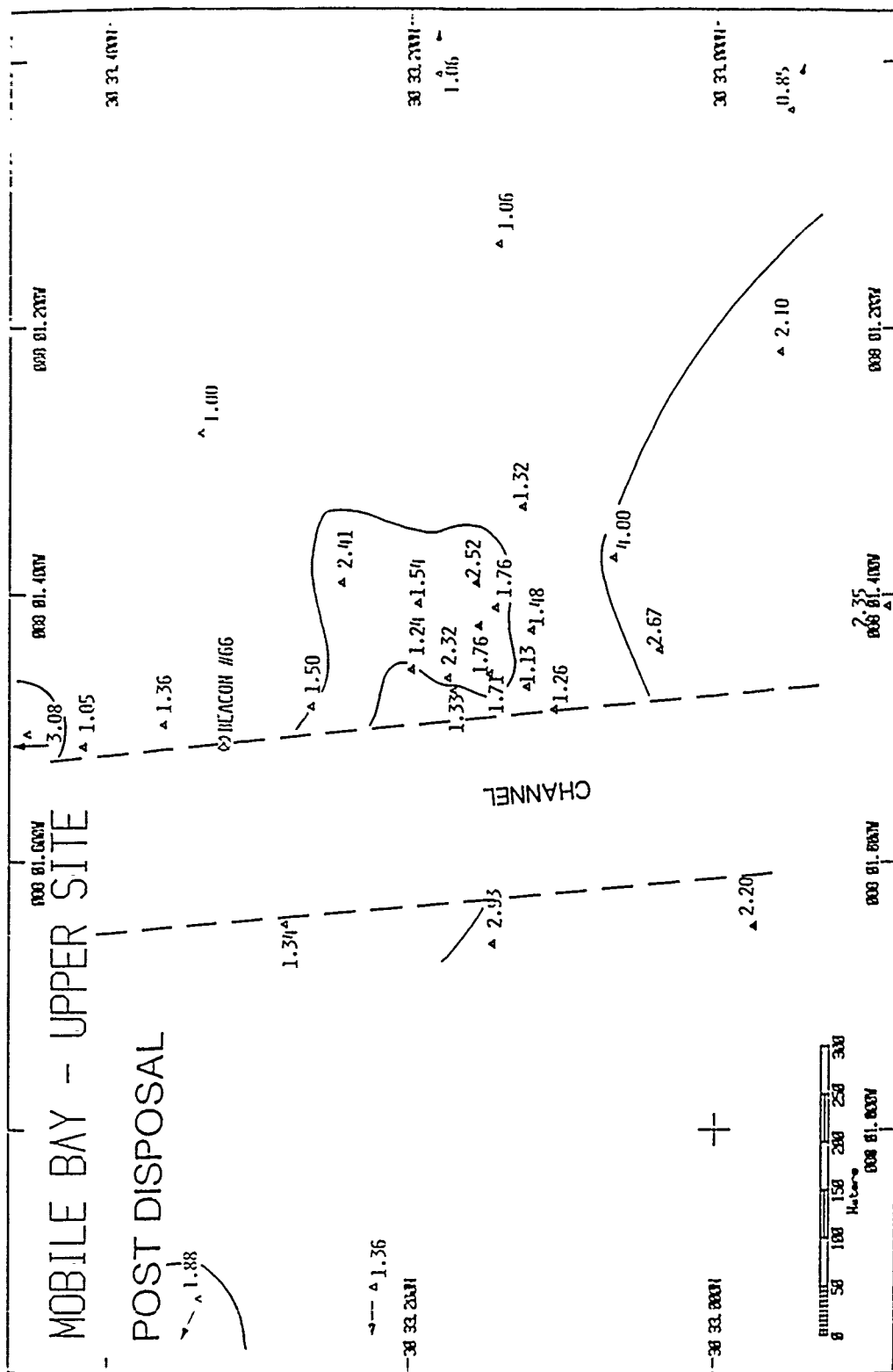
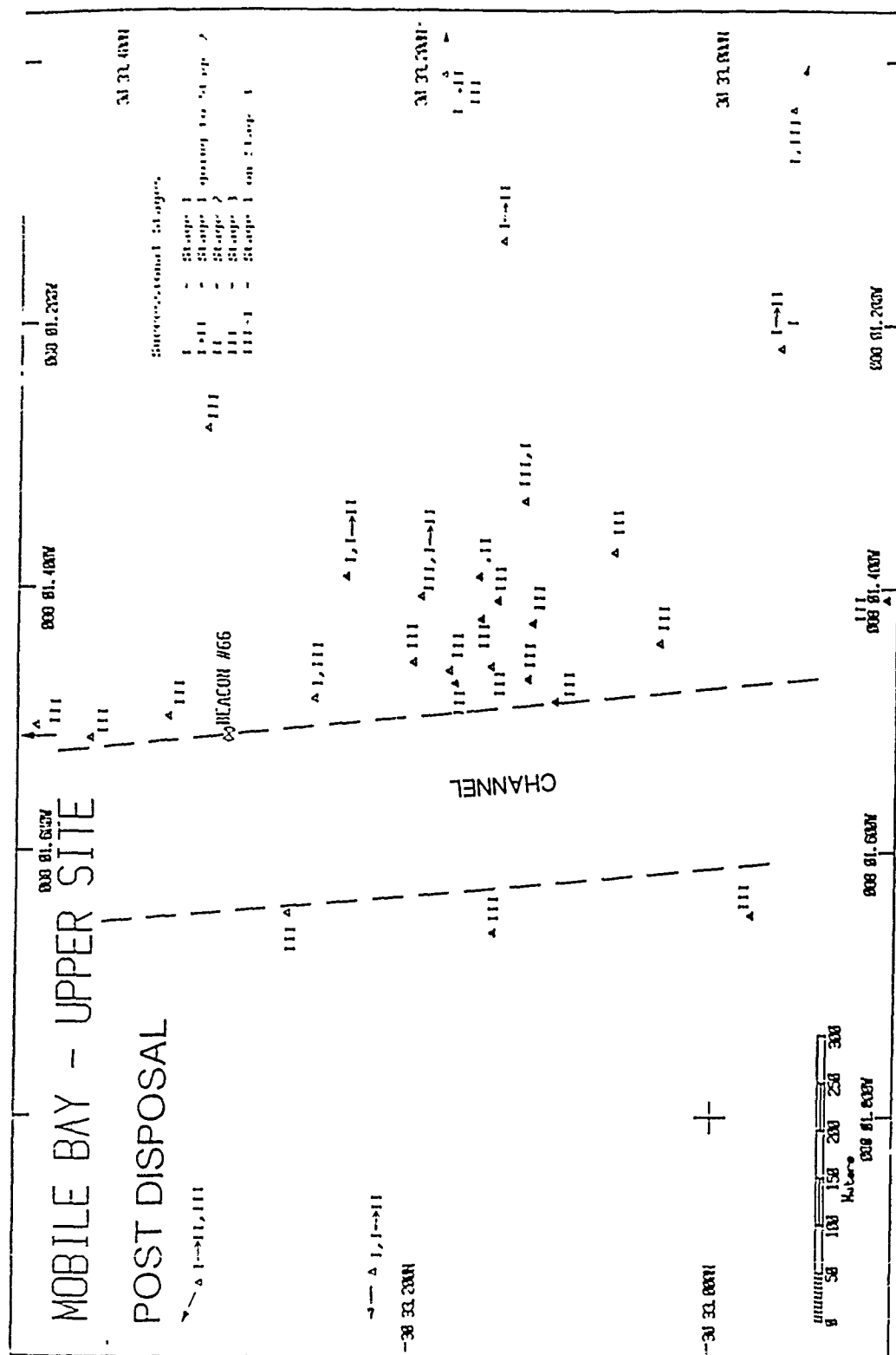


Figure 153. Postdisposal distribution of apparent RPD depths (centimeters) at the upper site. (Contours delimit areas with RPD depths greater than 1.5 cm; arrows indicate stations located beyond margins of chart)



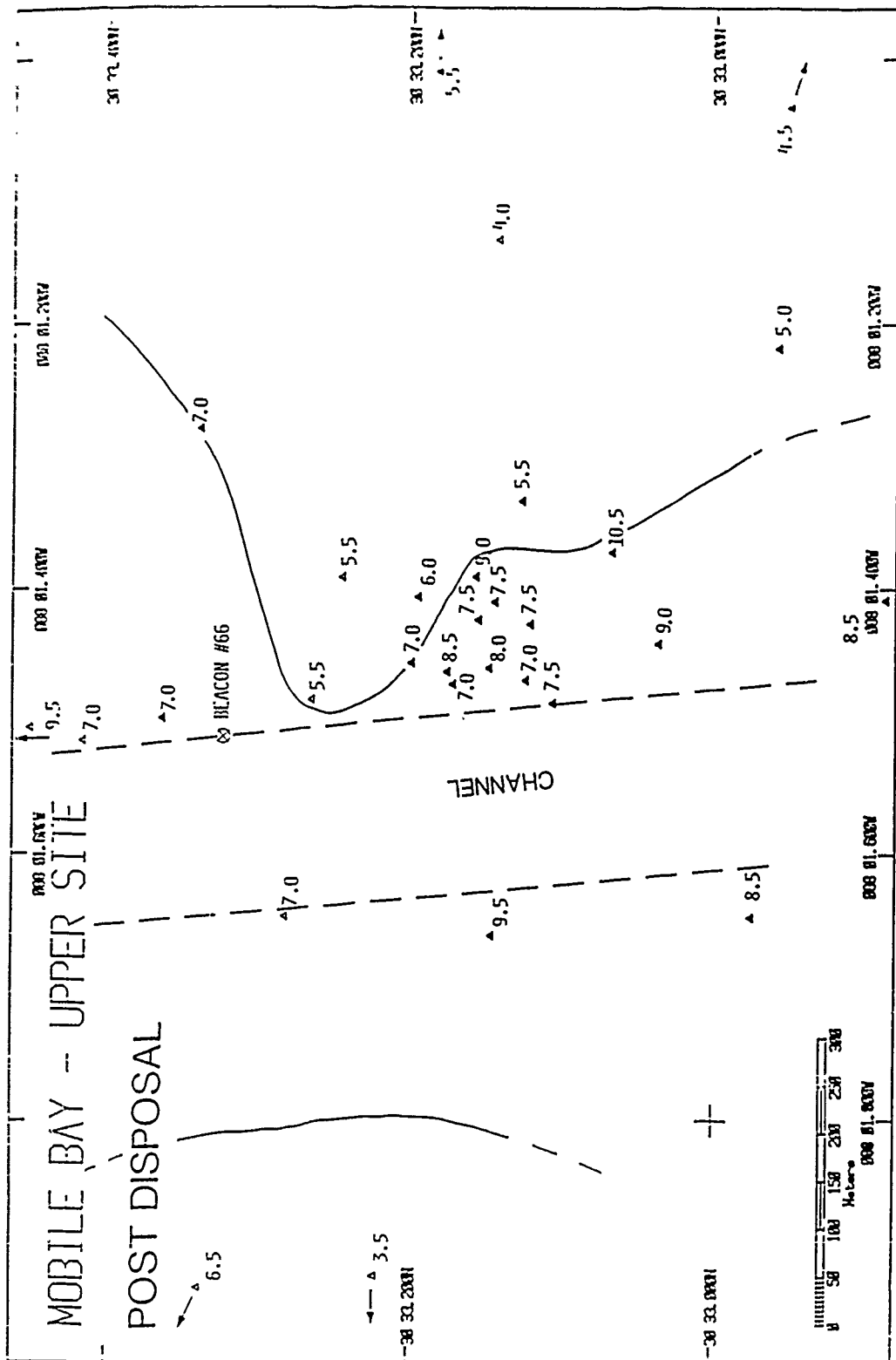


Figure 155. Postdisposal distribution of Organism-Sediment Index values, averaged by station, at the upper site. (Contours delimit areas with OSI values less than 7.0; arrows indicate stations located beyond margins of chart)

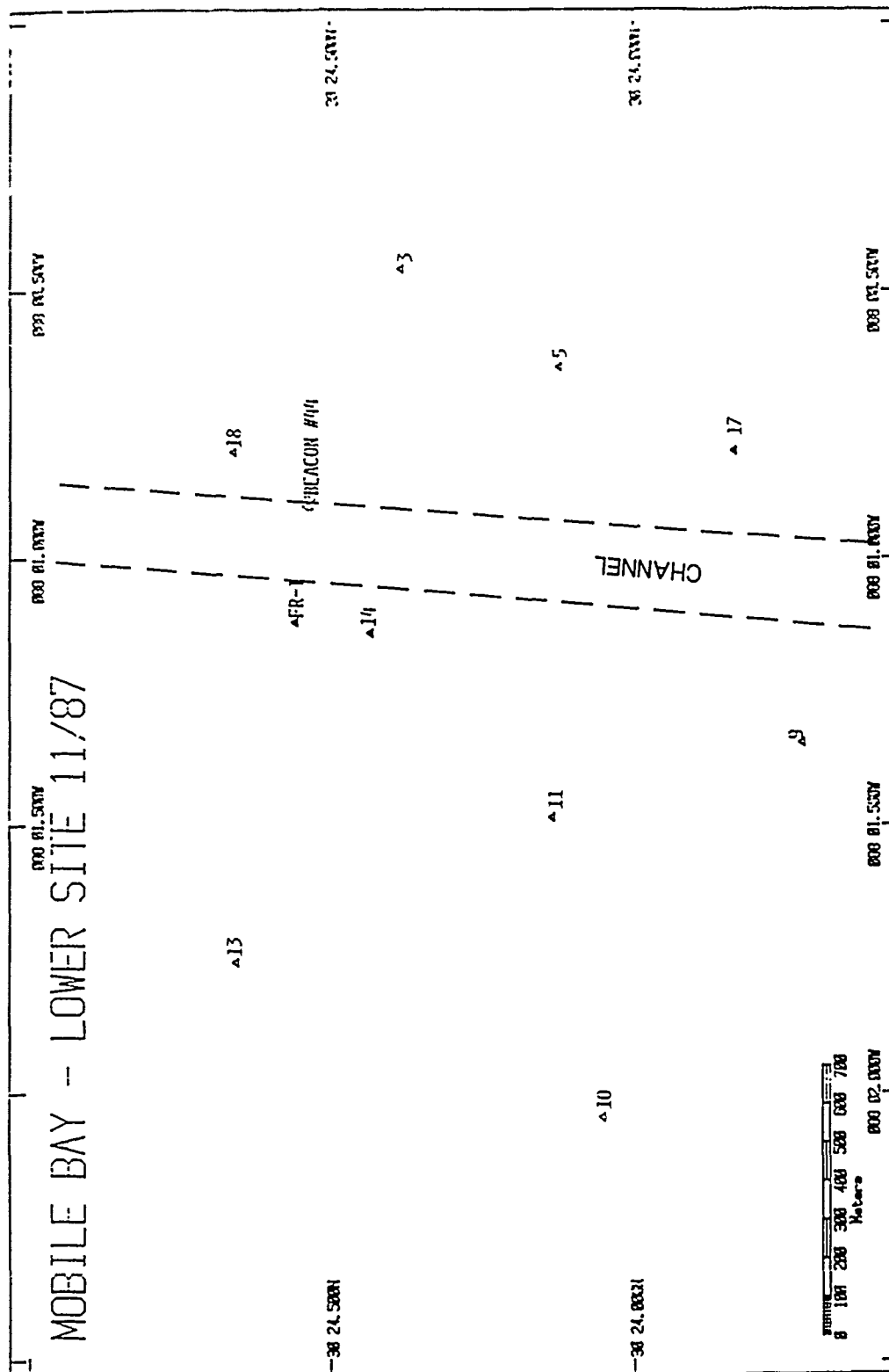
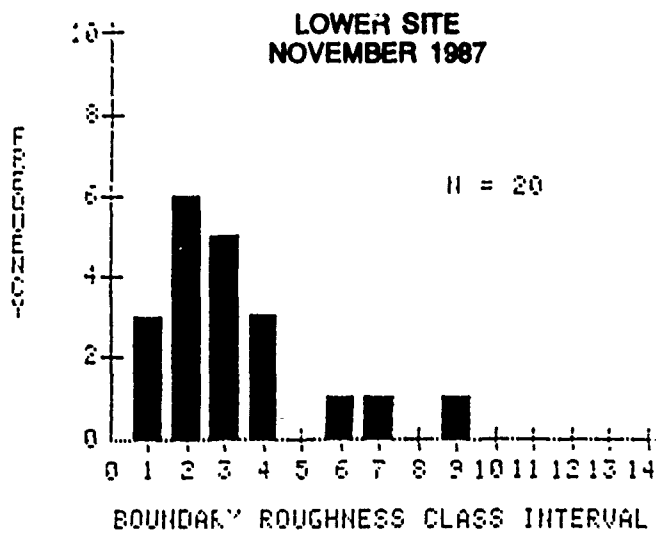


Figure 156. Locations and designations of REMOTS stations occupied during November survey of the lower site



KEY

<u>CLASS INTERVAL</u>	<u>RANGE OF BOUNDARY ROUGHNESS, CM</u>
1	0.0 - 0.6
2	0.6 - 1.0
3	1.0 - 1.4
4	1.4 - 1.8
5	1.8 - 2.2
6	2.2 - 2.6
7	2.6 - 3.0
8	3.0 - 3.4
9	3.4 - 3.8
10	3.8 - 4.2
11	4.2 - 4.6
12	4.6 - 5.0

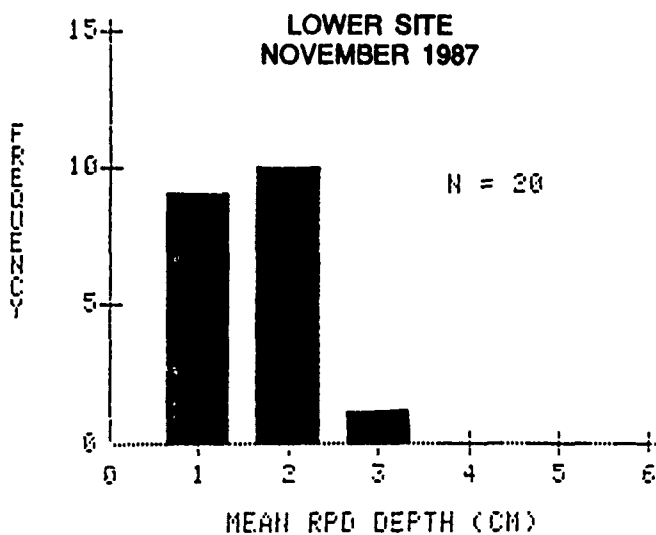


Figure 157. Frequency distributions of boundary roughness values and apparent RPD depths at the lower bay site in November

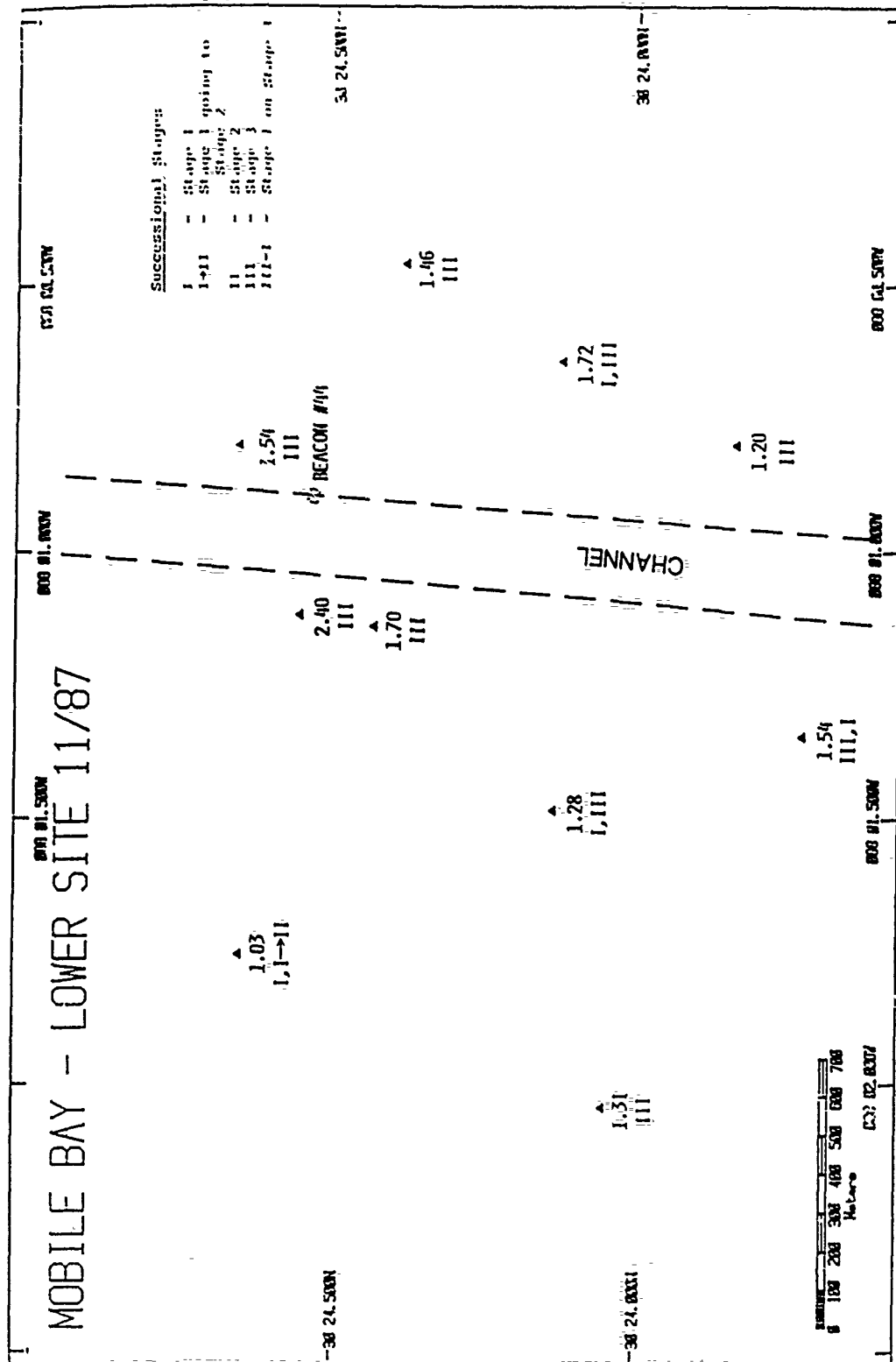


Figure 158. Distribution of apparent RPD depths (centimeters) and infaunal successional stages at the lower site in November

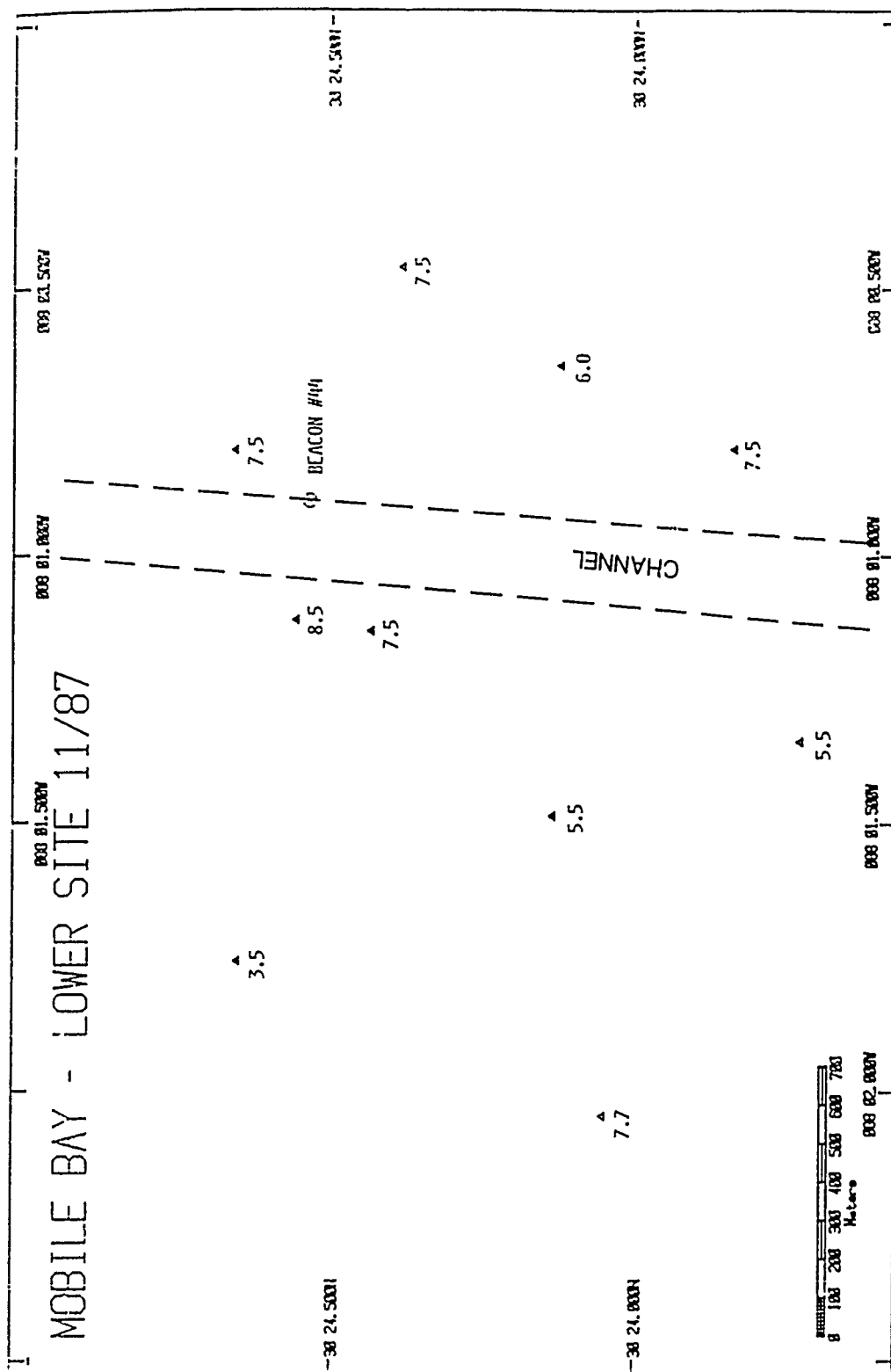


Figure 159. Distribution of Organism-Sediment Index values, averaged by station, at the lower site in November

PART IX: ENVIRONMENTAL ASSESSMENT OF BARGE OVERFLOW
IN MOBILE BAY, ALABAMA

The term impact as used in the environmental realm connotes detectable changes in physical, chemical, or biological components of an ecosystem. In its simplest form, an impact refers to a biological response to some physical or chemical alteration to preexisting conditions as the result of human activities or natural events. In this case, the activity is a particular mode of dredging and disposal of dredged materials. The preceding sections have described the physical water column and benthic alterations attributable to hydraulic dredging and barge overflow events at two sites in Mobile Bay. This section will treat biological responses to these alterations.

A hypothetical overflow event from a typical hopper barge loading process will resemble a point source discharge of sediment into Mobile Bay. In evaluating the types of environmental impacts that would most likely occur with such a discharge, emphasis should be placed on those resources at highest risk of exposure to induced physical and water quality alterations. The most probable impacts fall into two categories: (a) impacts associated with elevated concentrations of suspended sediments and (b) impacts associated with increased rates of sedimentation. Water column impacts would necessarily be short-term, as governed by the duration of overflows at the point along the main ship channel being dredged, and by the duration of settlement of sediment particles out of suspension. Exposure of planktonic or nektonic organisms to overflow suspended sediment fields would be limited by passive dispersal of plankton by tidal and wind-generated water currents, and by active avoidance responses, if any, by mobile nekton. Estuarine macrobenthic organisms, however, are highly site tenacious and generally incapable of rapid dispersal as adults. Consequently, benthic assemblages represent a sensitive component of the bay's ecosystem response to dredging and disposal operations, including overflow events. In view of their sedentary behavior, high abundance, relative ease of quantitative sampling, and recognized importance in trophic dynamics, benthos have logically become the focus of estuarine monitoring programs (Armstrong 1987). In the following discussion, the state of knowledge of soft-bottom benthic assemblages in Mobile Bay will be summarized.

* Written by Douglas Clarke and Jurij Homziak, Environmental Laboratory, WES; and Michael Dardeau, Dauphin Island Sea Lab.

This will provide a basis for appraising the potential impacts of overflow on local benthic communities.

Characterization of Mobile Bay Benthic Communities

Vittor (1979) summarized the published and unpublished studies conducted during the 1970s, noting that of 10 studies, only 2 examined seasonal trends. Figure 160 depicts the locations of these studies in the Mobile Bay system and includes additional studies performed since the publication of Vittor's review. Most of the studies examined benthos within rather confined areas of the bay. As shown in Figure 160, reaches of the lower and west-central portions of the bay have received most attention. Thus, there are definite spatial as well as temporal limitations to existing knowledge of the bay's benthic communities. Results of several studies have been made available in the form of a student project, a master's thesis, and several contract final reports (Crozier 1979; Gulf Universities Research Consortium 1979; Johnson 1980; TechCon, Inc. 1980; Marine Environmental Sciences Consortium 1983; Ranasinghe 1983). In addition, two recent Corps-sponsored projects examined benthic communities at sites within Mobile Bay (US Army Engineer District, Mobile 1982, 1987). The only seasonal study to examine infauna along the entire north-south axis of the bay, however, was conducted in 1980-81 under the auspices of the Alabama Coastal Area Board (CAB). The results of this survey have never been published, although several syntheses have been made available (Blancher 1982, Hopkins 1987). This section will draw on these syntheses as well as the original data base in order to provide an overview of benthic infaunal populations along the central north-south axis of Mobile Bay where overflow impacts would be most likely to occur.

Six stations among the CAB data set can be used to represent a range of hydrographic conditions present in Mobile Bay and adjacent estuarine waters (Figure 161). At each CAB station, sampling was allocated among five sites: a central site (A) surrounded by four sites (B-E) equidistant from each other on the perimeter of a circle with a 105-m radius (see inset, Figure 161). The CAB data therefore allow a detailed analysis of spatial patchiness of benthos along the north-south axis of the bay. Each site was sampled at approximately monthly intervals between April 1980 and April 1981. Six 0.1-sq m Petersen grab samples were taken at each site for a total of 30 replicates per station. Sediment grain size and total organic carbon analysis samples were obtained

for each of the four peripheral sites. Temperature, conductivity, and dissolved oxygen were measured 0.5 m above the bottom at site A. Station depths ranged from 2.5 to 6.0 m.

The middle bay CAB stations (5-7), which correspond to the central portion of the bay as delimited by the lower and upper overflow test sites, are roughly equivalent in depth, sediment composition, and total organic carbon (Table 43). These sediment grain sizes correlate well with Isphording and Lamb's (1980) characterization of the Mobile Bay bottom sediment distribution pattern (see Part II; Figure 3). Station 4, in Bon Secour Bay, has a comparatively higher organic content and a greater percentage of particles in the clay size category.

As is typical of a river-dominated estuary, mean annual salinities increase from the upper bay to the lower bay at all levels of the water column. Species richness likewise increases from north to south. Mean annual number of individuals (i.e. density), however, is generally higher at the stations most influenced by river discharge, including Station 4.

All three middle bay stations (5-7) have comparable total numbers of species and are numerically dominated by the capitellid polychaete *Mediomastus ambiseta*. The polychaetes *Leitoscoloplos robustus* and *Pseudeurythoe ambigua* are codominants at Station 5. Mean density of all taxa is lowest at Station 5, but species richness here is the highest of the middle bay stations, with 15 species present at abundances greater than 1 percent. Of these, the gastropods *Haminoea succinea* and *Utriculastra canaliculata* and the shrimp *Ogyrides alphaerostris* do not attain this degree of relative importance at any other station.

CAB Station 6, which was dominated by *Mulinia lateralis* (bivalve), as well as *Mediomastus ambiseta*, had relatively few species more abundant than 1 percent of total abundance. Each of these seven species is also present at Station 4, although not necessarily in comparable numbers. *Mediomastus ambiseta*, *Mulinia lateralis*, and *Mulinia pontchartrainensis* dominated CAB Station 7. This station is transitional, containing several species (such as the polychaetes *Paraprionospio pinnata* and *Sigambra bassi*) that are not abundant farther up the estuary and others (such as the bivalve *M. pontchartrainensis* and the polychaete *Capitella capitata*), which are abundant only in the upper reaches.

To summarize, *Mediomastus ambiseta* and *Mulinia lateralis* are numerical dominants throughout most of the bay. Several species (*Leitoscoloplos*

robustus, *Pseudeurythoe ambigua*, *Cossura soyeri*, and *Paraprionospio pinnata*) contribute primarily to communities in the polyhaline to mesohaline reaches of the bay. The relative contribution of other species is greatest in the mesohaline portion (e.g., *Sigambra bassi*) or in the mesohaline to oligohaline range (e.g., *Macoma mitchelli*, *Capitella capitata*, *Mulinia pontchartrainensis*, *Neanthes succinea*, *Rangia cuneata*, and *Texadina sphinctostoma*). Seasonal distribution patterns of the total infaunal community are driven largely by polychaete population dynamics. Exceptions occurred, as exemplified by spring samples at CAB Stations 6, 7, and 8 where recruitment of juvenile molluscs resulted in significant increases in their abundance. Seasonal patterns in benthic assemblage composition are consistent with the hydrographic regime and are similar at each station. A high-flow, warmwater infaunal assemblage from April to July is especially apparent at Stations 4-7. Other seasonal groups evident at most stations include a late summer group (August and September), a fall group (October and November) when water temperatures are decreasing, and a winter group (December through March).

Densities of infaunal species in middle Mobile Bay fall within the range of those reported from mud bottoms of other southeastern estuaries. Also, many of the dominant species are common in other southeastern estuaries. Although several of these species (*Mediomastus ambiseta*, *Streblospio benedicti*, *Mulinia lateralis*, and *M. pontchartrainensis*) have been characterized as indicators of organic enrichment (Wass 1967), they are ubiquitous in southeastern estuaries because of their ability to withstand chronic physical disturbance and conditions stressful to other organisms (Simon and Dauer 1977, Flint and Younk 1983). *Mediomastus* is a burrowing deposit feeder that feeds near the sediment surface (Fauchald and Jumars 1979). These spionid polychaetes occupy shallow, fragile tubes and, like *Mulinia*, feed at the sediment-water interface, utilizing particles both from the sediment surface and in suspension. Although sedentary, their trophic role as surface feeders restricts their influence on subsurface sediments. Consequently, their effects on sediment oxygenation and nutrient regeneration via bioturbation are negligible (Dauer, Maybury, and Ewing 1981; Flint and Kalke 1986a,b). These species represent r-selected taxa, which have short life cycles and high reproductive rates, allowing them to rapidly colonize disturbed habitat (Dauer and Simon 1976, Simon and Dauer 1977) and to persist in spite of constantly changing conditions (Flint and Younk 1983, Dauer 1984). In addition, these opportunistic species, by virtue of their high abundances and ready

availability, serve as important forage for higher order consumers (Virnstein 1977).

Other species, however, such as *Leitoscoloplos robustus* and *Cossura soyeri*, are subsurface deposit feeders. *Leitoscoloplos* feed in a head-down position, ingesting particles as deep as 13 cm in the sediment column and egesting them upon the sediment surface (Myers 1977; Rice, Bianchi, and Roper 1986). Deposit feeders that utilize relatively deep sediment vertically mix particles in the top several centimeters of sediment, with profound effects on the, redox potential discontinuity (RPD) (see Part VIII), microbial distributions, and benthic nutrient regeneration (Aller 1978, 1982; Aller and Yingst 1985; Flint and Kalke 1986a). Maldanid polychaetes, another group of subsurface deposit feeders, were present at all stations but only in very low numbers. "Conveyor belt" deposit feeders are often characteristic members of a late successional stage, a stage that is not well represented in Mobile Bay. Rhoads and Germano (1986) have suggested that the metabolism of labile detritus by these species prevents its accumulation. The dense tube mats of surface feeders, on the other hand, may trap and store high biochemical oxygen demand organic matter, contributing to hypoxic events.

A third group of species are middle level carnivores. *Glycinde solitaria*, *Parandalia americana*, *Sigambra* spp., and *Lumbrineris verrilli* are predatory burrowing polychaetes, while *Pseudeurythoe ambigua*, *Haminoea succinea*, and *Utriculostris canaliculata* scavenge and hunt on the surface of the sediment. These species are especially prominent at CAB Stations 4 and 5 and are much less important at stations to the north and south. Predatory infauna add a level of trophic complexity to infaunal communities (Commuto and Ambrose 1985).

One caveat to interpretation of the CAB data set should be noted. Sampling occurred in what might be considered an atypical year during which the system was recovering from effects of a coastal hurricane and higher than average freshwater input (Schroeder and Wiseman 1986). Storm-induced resuspension of sediments may have influenced substrate conditions such that benthic communities sampled may have been temporarily dominated by opportunistic species (Boesch, Diaz, and Virnstein 1976; Johnson 1980). Some populations may have been dramatically reduced within the estuary (Modlin and Dardeau 1987) in a fashion similar to that reported by Boesch, Diaz, and Virnstein (1976). Flint (1983) and Armstrong (1987), however, reported that 4 months after record freshwater input to Corpus Christi Bay, total abundance

and biomass of benthic infaunal communities increased dramatically, presumably as a result of nutrient and detrital inputs associated with the freshet. In spite of these recognized limitations of the CAB data base, it does represent the most complete picture of benthic communities in Mobile Bay, and serves as a benchmark for comparative investigations.

Environmental Concerns Associated with Disposal

Suspended sediment effects

Several broad areas of concern for environmental impacts associated with any form of open-water dredging and disposal focus upon potential effects of suspended and deposited sediments. Relevant reports characterizing physical aspects of suspended sediment fields (Bohlen and Tramontano 1977; Yagi, Koiwa, and Miyazaki 1977; Barnard 1978; Bohlen, Cundy, and Tramontano 1979; Lunz, Clarke, and Fredette 1984; Tavalaro 1984; LaSalle et al., in preparation; Palermo, Homziak, and Teeter 1990) provide a basis for comparison to the magnitude of alterations observed in the present study. Concentrations of suspended sediments measured during the overflow events are reported in a preceding section (see Part VI). Model simulations of suspended sediment fields for each set of overflow test conditions are also provided (see Part VII). The results of these efforts indicate that although absolute concentrations can reach significant levels (up to 2,400 mg/ℓ), such concentrations would be limited to the immediate vicinity of the overflow entry point into the water column, and would decay to much lower concentrations in a relatively short period of time. Generally, suspended sediment concentrations greater than 100 mg/ℓ above ambient were confined to an area within 200 to 300 ft of the barge over the shallow flats and within 500 ft of the barge in the upper half of the water column in the channel. Field observations indicated that almost all of the overflow material reentered the channel below the barge without significant entrainment into the water column or transport across the adjacent shallow flats.

An examination of the current state of knowledge of natural phenomena and anthropogenic activities that cause sediment resuspension can add insight into the magnitude of physical alterations induced by overflow events. Postma (1967) has described the mechanisms leading to resuspension. Winds associated with storms may commonly raise suspended sediment levels in estuaries and embayments to 1,000 to 1,500 mg/ℓ (Oviatt et al. 1981, Sosnowski 1984,

Gabrielson and Lukatelich 1985, Stumpf 1988). The shallow nature of the Mobile Bay estuary suggests that this range of ambient suspended sediments occurs on a frequent basis, perhaps with a seasonal timing coincident with the passage of weather frontal systems. Seasonal and storm pulses in river discharge and runoff are known to elevate suspended sediment levels by 100 to 150 mg/l, and peak concentrations of 600 mg/l above ambient have been reported in other southeastern estuaries (Bigg 1970, Bohlen 1975, Stumpf 1988). Normal tidal fluctuations and dynamic circulation processes within estuaries can raise suspended sediment concentrations by at least 50 mg/l (Oviatt and Nixon 1975), and extremes of over 1,000 mg/l have been reported during spring tides (Vale and Sundby 1987). Commercial and/or recreational shrimp trawling has been documented to elevate suspended sediment concentrations to 5,000 mg/l at the trawl and 100 to 500 mg/l above ambient 100 m astern of the trawl (May 1973; Markay and Putman 1976; Schubel, Carter, and Wise 1979). The effects of deep-draft vessel and barge traffic (due to resuspension from bow pressure waves and propeller wash) in estuaries have not been accurately measured, but almost certainly contribute to resuspension of sediments in heavily used waterways (McCauley, Parr, and Hancock 1977). In freshwater habitats, ship passage may generate suspended sediment fields in the 200- to 1,000-mg/l concentration range (Holland 1986; Aldridge, Payne, and Miller 1987). These studies imply that the Mobile Bay system is subject to frequent resuspension events that are analogous to overflow events in many ways. Resuspension due to dredging has been likened to storm resuspension in terms of absolute concentrations (Bohlen 1975). Storm resuspension occurs over a much greater spatial scale, but may be shorter on a temporal scale. This example can be applied to overflow events as exemplified by Palermo, Homziak, and Teeter (1990) and the present study.

Resource agencies are particularly concerned about the potential detrimental effects of suspended sediments on the eggs and larvae of marine and estuarine fishes and shellfishes. These life history stages of fishes are known to be sensitive to stress (Rosenthal and Alderdice 1976), and the survival or mortality of the egg and larval stages primarily determines the year class strength of many fish species. However, because the causal factors by which suspended sediments affect eggs and larvae are complex and poorly understood, it is difficult to draw definitive conclusions from the available literature. Field derivations of mortalities attributable to single factors such as suspended sediments are currently impossible to achieve with accuracy.

Therefore, most information on suspended sediment effects is gleaned from laboratory studies and extrapolated to field situations. This approach has inherent limitations in that the dose-duration relationship is critical to interpretation, and many studies have used suspended sediment concentrations that do not reflect concentrations characteristic of actual perturbations. Extensive reviews of the pertinent literature are provided by Priest (1981) and Schubel, Williams, and Wise (1977). Other reports (Schubel and Wang 1973; Auld and Schubel 1978; Morgan, Rasin, and Noe 1983) offer information on tolerances of mid-Atlantic estuarine species that indirectly support the generally high tolerance of species adapted to naturally turbid systems. Table 44 (from Lunz, Clarke, and Fredette 1984) lists the results of a number of pertinent studies. Except for suspended sediment concentrations measured in the immediate vicinity of the overflow, the suspended sediment plumes would not represent a significant risk to fishes at the project site. For example, Schubel, Williams, and Wise (1977) concluded that the semibouyant eggs of striped bass (*Morone saxatilis*) could tolerate suspended sediment concentrations of up to 1,000 mg/l for extended periods. Similarly, Kiorboe et al. (1981) reported that embryonic development and hatching of herring (*Clupea harengus*) were not impaired by either long-term moderate concentrations (up to 300 mg/l) or short-term high concentrations (up to 500 mg/l) of suspended sediment.

Shipp (1987) has summarized the locations of spawning sites and the distributions of egg and larval stages of fishes utilizing the Mobile Bay estuary. In general, the spawning sites and egg stages of most species are confined to the high-salinity areas of lower Mobile Bay and adjacent coastal waters. Larval stages show a somewhat more dispersed distribution. There is some evidence that larval stages are more sensitive to elevated concentrations of suspended sediments than are eggs of the small species (Auld and Schubel 1978). Boehlert (1984) observed that adhesion of sediment particles to the epidermis may exert a smothering effect, although adhesion was noted only at concentrations above 1,000 mg/l. Boehlert also observed that larvae exposed to concentrations at or above 4,000 mg/l for 24 hr experienced severe gill abrasion. Larvae did not show significant mortality even at experimental concentrations up to 8,000 mg/l, although the possibility of sublethal effects remained. These concentrations and durations are well above those that would be created by the overflow operations. Priest (1981) concluded that suspended sediment concentrations sufficient to induce a 50-percent mortality in

laboratory experiments of fish larvae were far in excess of levels characteristic of dredging operations. This statement would also apply to the overflow operations examined in the present study.

If consideration is given to the technical evidence for tolerances of egg and larval stages of fishes, and to reasonable expectations of durations of exposure (assuming passive transport of these stages through the project area), an estimate of risk to these resources can be obtained. A conservative estimate of a concentration at which no adverse impact would occur would be 500 mg/l (LaSalle et al., in preparation). In fact, a strong case can be made that if concentrations were below 1,000 m/l at a distance of 500 m downstream of the operating dredge and overflow, there would be no significant risk to fish eggs or larvae.

A widely scattered body of literature treats the effects of suspended sediments on juvenile and adult stages of fishes. Wallen (1951) exposed juveniles and adults of a number of freshwater species to a wide range of silt-clay suspensions. Highest concentrations were well above those typical of dredging operations. Wallen (1951) found lethal concentrations to be equal to or greater than 16,500 mg/l following exposure durations from 3.5 to 17 days for all 16 species tested. Behavioral signs of stress for most species were not apparent at suspended sediment concentrations under 20,000 mg/l. Sherk, O'Connor, and Neumann (1975), working with juvenile Atlantic menhaden (*Brevoortia tyrannus*), determined that a lethal concentration producing 10-percent mortality (LC_{10} value) of 1,540 mg/l was obtained after a 24-hr exposure to Fuller's earth (a combination of clay and siliceous material). Using in situ bioassays, Jeane and Pine (1975) studied the effects of elevated turbidities at dredging sites on juvenile chinook salmon. No significant mortality was observed among juveniles exposed to fine sediment suspensions. Peddicord and McFarland (1978) reported that rainbow trout, a fish adapted to highly oxygenated and clear waters, showed no significant mortality after 22 days at concentrations at or below 2,000 mg/l, and 95-percent survival occurred at concentrations approaching 4,300 mg/l. Other studies have exposed caged specimens to in situ levels of suspended and deposited sediments at actual dredging sites (Ingle 1952, Ritchie 1970) with little or no indication of detrimental effects. Ritchie (1970) found no evidence of gill pathology in specimens of 11 estuarine fish species prior to and after exposure to dredging conditions. Sherk, O'Connor, and Neumann

(1975), however, noted disrupted gill tissue and increased mucus production in white perch exposed to sublethal suspended sediment concentrations (650 mg/l).

A great deal of evidence supports the fact that juvenile and adult estuarine fishes are moderately to extremely tolerant of elevated suspended sediment levels. Fishes are highly mobile organisms capable of avoidance of intolerable turbidity fields. The spatial extent of turbidity plumes associated with barge overflows under the Mobile Bay test conditions was sufficiently small that physical effects on juvenile and adult fishes would be extremely unlikely.

The reduction of dissolved oxygen (DO) to levels below 2 to 4 ppm has been a concern voiced in relation to resources in the vicinity of an operating dredge. Dissolved oxygen reduction, however, has been demonstrated to be a short-term phenomenon (on the order of minutes to an hour dependent on the duration of resuspension) and of minimal magnitude for most concentrations of suspended sediment created. This effect would be minimized by the hydrodynamics of the channel-influenced flows at the project sites.

The presence of the dredging equipment or the suspended sediment plume itself has been suggested to have an effect on the distribution and movement of fishes, particularly anadromous species. There is little evidence, however, to support this contention. Most accounts of fish movements in relation to dredges are anecdotal, and these seem to point out an attraction response (Ingle 1952). Harper (1973) sampled fishes in a disposal plume and in reference areas of ambient "clear" waters. He found that where abundances of individuals differed between turbid and ambient water trawl catches, the average number of individuals in the turbid plume was much higher. This may be an artifact of differential effectiveness of the trawl in clear versus turbid waters. However, additional studies show the same general preference of estuarine fishes for turbid waters. Recently, Cyrus and Blaber (1987a,b) suggested that juveniles of fishes inhabiting estuaries either prefer or are indifferent to turbid waters. This lack of demonstrated avoidance of turbidity plumes, coupled with the absence of major stocks of anadromous fishes in Mobile Bay, suggests that overflow operations would not pose a threat to movements of juvenile or adult fishes. Because the barge overflow operation would involve intermittent periods of no overflow during filling and cycling of the barges, the probability of this type of impact would be further reduced.

Most shellfishes inhabiting turbid estuaries have been shown to be tolerant of suspended sediment concentrations significantly higher (several thousand milligrams per liter) than those encountered beyond the immediate point of overflow in this study. A review of the published literature (summarized in Table 44, after Lunz, Clarke, and Fredette 1984) reveals that most reported detrimental effects on shellfish were for suspended sediment concentrations several times higher than those created by dredging operations, and for exposure durations of 5 to 21 days (Stern and Stickle 1978; Priest 1981; LaSalle et al., in preparation).

Although there are no productive oyster reefs in the vicinity of the Mobile Bay ship channel, the status of knowledge regarding suspended sediment effects on oysters is adequate to obtain a perspective of potential overflow impacts. Reduced respiratory pumping rates observed by Loosanoff and Tommers (1948) for oysters held at suspended sediment concentrations between 100 and 4,000 mg/l represent a compensatory mechanism by these bivalves to effectively limit their exposure to adverse conditions over the short term. Exposure for extended periods had no adverse effect on adult oysters. Davis and Hidu (1969) reported substantial incidences (22 percent) of abnormal development in American oyster eggs exposed to relatively low suspended sediment concentrations, but did not report the exposure durations. In contrast, developing oyster larvae showed enhanced growth rates at suspended sediment concentrations up to 500 mg/l (Davis 1960, Davis and Hidu 1969). Higher concentrations were required to hinder growth or cause increased mortality.

Carriker (1986) provides an extensive review of the literature dealing with suspended sediment effects on oyster larvae. In general, concentrations below 180 mg/l for embryos and below 500 mg/l for veligers can be beneficial, whereas higher concentrations appear to become increasingly harmful. Suspended sediment apparently has little effect on feeding or movement of larvae through the water column.

Reduction of DO concentrations to less than 1 to 2 ppm may affect demersal eggs, larvae, or adults of shellfishes in the vicinity of the hypoxic water mass. However, it is likely that mixing in the dynamic flows in and near the ship channel would prevent such drastic DO reduction to occur under the overflow conditions tested. Morrison (1971) reported that the eggs of the hard clam (*Mercenaria*) were tolerant of oxygen concentrations as low as 0.5 ppm, with mortality noted only at 0.2 ppm. Dissolved oxygen requirements of oysters (see review by Sellers and Stanley 1984) are not likely to be

threatened by conditions in the near field, and particularly not in the far field, of an overflow operation in Mobile Bay. A review by Bishop, Gosselink, and Slone (1980) suggests that shrimp would also be unaffected by DO levels at an overflow site. Mobile, nonsessile juvenile and adult shellfishes should be able to avoid patches of low DO. Sessile forms such as oysters can isolate themselves from unfavorable conditions for extended periods. It would therefore appear that suspended sediment plumes associated with overflow operations would not pose a significant threat of direct effects on shellfish resources.

As in the case of fishes, it has been hypothesized that suspended sediment plumes may interfere in the movements of shrimps and crabs. Although there has been little study of the effects of suspended sediments on blue crabs (*Callinectes* spp.), Van Engel (1982) has noted that soft-shell crab landings tend to decrease in the aftermath of storms that increased suspended sediment levels. However, this tendency also correlates with decreased salinity, increased concentrations of pollutants, and other confounding factors. The distribution of blue crabs in turbid estuaries and their behavioral association with the substrate, including burying behavior, would indicate that these crabs are highly tolerant of suspended sediment concentrations.

Harper (1973) reported that the average number of macrobenthic invertebrates in the turbid waters of a sediment disposal operation was much greater than in waters of ambient turbidities. Where differences in abundance did occur, the blue crab, brown shrimp (*Penaeus aztecus*), and grass shrimp (*Palaemonetes pugio*) were more abundant in turbid rather than ambient waters. White shrimp (*Penaeus setiferus*) did not differ in abundance between ambient and turbid water samples. Harper (1973) used optical rather than gravimetric measures of turbidity. Consequently, direct comparisons between absolute concentrations of suspended sediments for turbid versus ambient waters in his study cannot be made. The pattern of nonavoidance of the area of the dredging operation, however, is readily apparent.

Other observations and experimental evidence support the preference of brown shrimp for turbid waters. Viosca (1958) and May (1973) reported that brown shrimp were attracted to the turbid water surrounding operating dredges. Brown shrimp are also generally found on bottoms of easily suspended fine silts and clays, and actively selected such fine substrates in laboratory studies (see review in Larsen, Van Den Avyle, and Bozeman 1986). Both brown

and white shrimp are closely associated with waters characterized by high levels of suspended sediments (Kutkuhn 1966). Studies have demonstrated that inshore catches of shrimp along the gulf coast are positively correlated with estuarine turbidity (Linder and Bailey 1969). Both brown and white shrimp have been known to increase their activity and to more effectively avoid predation in turbid water (Minello, Zimmerman, and Martinez 1986). Both species also appear to prefer low-light, turbid water conditions (see reviews by Muncy 1984 and Larsen, Van Den Avyle, and Bozeman 1986). In fact, shrimp trawling often generates suspended sediments in the same general concentrations as many dredging operations (Markay and Putnam 1976; Schubel, Carter, and Wise 1979) with no apparent detrimental suspended sediment effects on the target shrimp populations. In Mobile Bay, shrimping activities often focus on the ship channel itself. The occurrence of high densities of shrimp in this generally turbid habitat, which is regularly disturbed by deep-draft ship traffic, tends to support a conclusion of negligible impact on the movements of shrimps and crabs.

There is evidence that levels of suspended materials created by dredging do not exceed those created by wind-wave resuspension, conditions for which many estuarine organisms are well adapted (May 1973; McCauley, Parr, and Hancock 1977). A summary of "typical" Mobile Bay wind conditions and actual wind conditions during the period of the overflow tests will assist in placing natural and dredging-induced resuspension into perspective. Schroeder and Wiseman (1985) analyzed 10 years of wind speed and direction data collected at Dauphin Island, Alabama, at the southern extent of Mobile Bay. Table 45 is a summary of these data. Given the assumption that sustained winds of between 10 and 15 knots can initiate resuspension in the shallow Mobile Bay system, the data indicate that wind speeds equal to or greater than 10 knots occurred during 26.37 percent of the observations, and wind speeds equal to or greater than 15 knots occurred during 6.75 percent of the observations. Although the temporal factor needed to define "sustained" winds and the effects of shifting directions are not readily apparent in these data, it is clear that wind-wave resuspension is a frequent and important phenomenon in Mobile Bay. Organisms inhabiting the bay must cope with these events periodically. At least one common infaunal species, *Streblospio benedicti*, will leave its tube, swim through the water, resettle to the substrate after turbulence has subsided, and build a new tube (Foster 1971). Many other infaunal organisms that occupy

surficial sediment layers are similarly adapted to recurrent disturbances of the bottom during their life histories.

Wind data for the period of the overflow tests (November 30-December 11) are presented in Figures 162-167. These data were collected on an hourly basis at the Dauphin Island Sea Lab at the eastern end of Dauphin Island, Alabama. Because the point of data collection lies at the southern terminus of Mobile Bay, velocity and direction data are probably more accurate reflections of conditions at the lower bay test site than at the upper bay test site. These data are useful, however, in describing the general weather conditions prior to and during individual overflow tests and should be considered in interpretation of sediment-profiling imagery results and predictions of sedimentation.

Wind velocities during the overall test period ranged from 0 to 25 knots. Overflow Test 1 was preceded by a 24-hr period of slack winds, which began to increase as the test was initiated (Figures 162-163). Winds were out of the southwest at less than 10 knots at the conclusion of the test. Overflow Tests 2 and 3 occurred during a period of 8- to 13-knot winds coming from the west and northwest (Figure 164a). Overflow Tests 4 and 5 took place during 6- to 14-knot winds out of the east (Figure 165a). The highest wind speeds to occur during the study coincided with Overflow Test 6. Westerly winds increased to above 20 knots during this test (Figure 165b). Relatively high wind speeds of 10 to 18 knots in a westerly direction continued through Overflow Test 7 (Figure 166a). Overflow Test 8 was conducted during a relatively calm period of variable winds generally less than 5 knots out of the north (Figure 166b).

As is evident in the aerial photographs taken during several of the overflow tests (see Photos C1-C12, Appendix C), background turbidities over the shallow areas adjacent to the main ship channel were high as a result of wind-wave resuspension of bay bottom sediments. This contributed to plume-tracking difficulties during several tests (see Part VI). Wave heights were sufficiently high on several occasions to preclude the safe operation of small boats, and these efforts were aborted for Tests 3 through 6.

Deposited sediment effects

Specific topics of concern have been expressed by resource agencies in relation to the potential effects of estuarine open-water disposal of dredged material particularly for benthic communities. One type of potential impact involves burial and suffocation of benthos when thick layers of dredged

material (especially fluid muds) are present at a site for extended periods of time. The magnitude of the impact to the benthic community will depend on numerous factors. For example, impacts are more severe when the sediment characteristics of the dredged material overburden are very dissimilar to those of the preexisting substrate. The actual thickness of the overburden is important, because many benthic taxa can vertically migrate through layers of approximately 6 cm (Maurer 1967; Maurer et al. 1978, 1986). Thus, the scale of the impact is related to the thickness, persistence, and areal extent of the dredged material overburden. Estimates of these parameters are provided for the barge overflow scenarios and are discussed in more detail below.

There appears to be no utilization by fishes of the upper side slopes of the channel along the project reach as spawning habitat. Consequently, there is little risk of smothering demersal eggs with overflow deposits.

A second category of concern, i.e., long-term changes in benthic community structure, involves a temporal aspect (Allen and Hardy 1980). Long-term changes in diversity or biomass are more likely to occur when disposed sediments do not match the characteristics of the preexisting bottom. This would generally not be the case for barge overflow, however, as the discharge occurs within a relatively short distance from the source of sediments being dredged. Subtle differences may occur when the deposited sediments, generally fines, are placed on hydrodynamically energetic bottoms adjacent to the channel that have been winnowed to consist of somewhat coarser sediments. Over time, however, the same hydrodynamic forces would tend to winnow the newly deposited sediments as well. The fact that the discharge takes place in the channel proper would enhance this process.

Uptake of contaminants (e.g., organic pollutants and heavy metals) is another category of concern. This type of concern would be significant if contaminants were indeed present in quantities exceeding accepted criteria for open-water disposal. In the case of the Mobile Bay main navigation channel, however, contaminants have not been determined to be present in significant concentrations. This concern would be even less notable for net work deepening dredged materials because these materials would likely contain even fewer contaminants.

A fourth type of concern has particular relevance to the consequences of historical dredging projects in Mobile Bay. The concern has been expressed that the accumulation of dredged materials disposed in designated areas parallel to both sides of the upper channel altered the flushing

characteristics of shallow soft-bottom habitats beyond the lateral extent of the disposal areas. Greater dispersive forces, however, exist in the larger expanses of the mid to lower reaches of the bay. With regard to this specific concern, barge overflow would appear to be a relatively safe option in that almost all of the disposed material falls back into the channel rather than on the adjacent shallow flats. This "advantage" of overflow is as much an incidental operational factor as a planned consideration. The draft of a fully loaded hopper barge is approximately 20 ft. Therefore, in the Mobile Bay system, the point of overflow will always occur over the channel proper (Figure 168). The hydraulics of tidal currents within a deep channel adjacent to relatively shallow flats enhances the probability that overflow material will be entrained into the channel and prevented from immediate or substantial dispersion into the shallow flat habitats.

Juveniles of shellfishes that assume sessile (e.g., oyster spat) or burrowing (e.g., clams) modes of existence may be particularly susceptible to increase sedimentation rates in the vicinity of dredging operations. An additional concern involves the possible inhibition of settling by oyster larvae on hard surfaces covered by silt. Galtsoff (1964) suggested that as little as 1 to 2 mm of silt may be sufficient to prevent settling by oyster larvae on shell clutch. As pointed out by Carriker (1986), however, the fact that larvae can attach to surfaces fouled by mucoid films, microbes, and detritus supports the concept that oyster larvae are indeed capable of dealing with relatively unclean surfaces. In this study, sedimentation layers detectable by sediment-profiling imagery (approximately 2 to 3 mm) were confined to within 100 m of the test sites (see Part VIII).

Van Dolah, Calder, and Knott (1984) found that effects of open-water disposal of fine-grained sediment on infaunal communities were minimized when strong tidal currents were present.

To ascertain the magnitude of potential sedimentation impacts due to barge overflow in Mobile Bay, calculations were made, based on the numerical model predictions of sediment deposition, of the cumulative amounts of sediment deposited along a moving 2,000-ft section of channel as a dredging-barge overflow operation progressed northward. Calculations essentially superimposed consecutive overflow deposits within appropriate 100 × 100-ft cells. The number of overflow events at a given point along the channel was taken to be a function of the rate of advance of the dredge, assuming that the available length of pipeline allowed a 900- to 1,000-ft total advance before

the barge-loading location was moved. Hypothetical overflow operations were conducted on both the west and the east sides of the channel. Model outputs for both flood and ebb tide conditions were also incorporated based on the average barge-filling and overflow cycle for either maintenance or new work scenarios. Figures 169-205 depict the patterns of sediment deposition for each set of maintenance and new work conditions (monthly scenarios for a typical operation; see Part VII). Because impacts to shallow flat habitats are of primary concern, all deposition in cells lying above the 20-ft depth contour are shown. All sediment deposition below the 20-ft depth contour represents material reentering the channel. Even along the 20-ft contour, the prevailing slope is declined toward the channel, such that any material newly settled on the bottom would tend to move toward the channel. All material settling out above the 20-ft contour was assumed to be available for transport to the adjacent shallow flats.

Under all conditions examined, sediment deposition was confined to within 550 ft of the channel's 20-ft contour. In 72 of 74 scenarios modeled (including maintenance and new work operations on either side of the channel), deposition was limited to within 200 ft of the channel. These results agree with the "ground truth" information on sediment deposition obtained by sediment-profiling imagery (see Part VIII). The estimates of sediment accumulation in cells within 200 ft of the channel do indicate significant amounts of deposition. The extreme value calculated was 247 cm of deposition for a cell in a November new work operation scenario. In terms of maximum deposition, there appears to be a greater probability of more significant deposits as a result of new work rather than maintenance overflows. As shown in Table 46, the average maximum deposition in any cell for the 10 maintenance runs was 39.3 cm of deposited sediment, whereas a mean of 52.9 cm was calculated for the 27 new work runs.

Biological response of the benthos to overflow

Impacts to benthic communities due to overflows conducted in a manner consistent with the test conditions would be expected to be minimal. The amount of bottom habitat receiving sufficient overburden material would be restricted to the vicinity of the upper side slope of the channel. Because of the hydrodynamics of this habitat (i.e., strong tidal flushing due to proximity to the channel), deposited material would likely be dispersed in a relatively short time. Almost all of the deposited material would ultimately

reenter the channel. Therefore, at any given point along the channel, acute impacts would be restricted to a small spatial extent, and recovery would be enhanced by the fairly rapid removal of any overburden accumulation. The rate of advance of the dredging operation northward would ensure that the temporal duration of impacts to the benthos along the channel would be minimal. Insufficient amounts of overflow material would be transported to adjacent shallow flats habitat to cause a detectable response. Sedimentation rates in these habitats would be well within the normal range for tidal, diurnal, and seasonal fluctuations to which the benthic communities are preadapted.

Reference to the CAB data set for Mobile Bay benthic communities may elucidate the scope of potential impacts to benthos. As shown in Figure 206, a few species generally dominate the numerical abundances of the benthic communities in the upper, middle, and lower reaches of the estuary. Four dominant species include the bivalve molluscs *Mulinia pontchartrainensis* and *M. lateralis* and the polychaetes *Mediomastus ambiseta* and *Leitoscoloplos robustus*. Recovery rates of any benthic assemblage disturbed by overflow materials would be dependent on availability of recruits of these and other species. Recovery would be enhanced by species having protracted periods of reproduction and recruitment. Species having narrow windows of recruitment would be most susceptible to major impacts, and contribute to prolonged recovery periods. Figures 207-210 depict the seasonal abundances of the four dominant infaunal species. *Mediomastus* flourishes during the spring and early summer, when river discharge and runoff are high, particularly in the middle portion of the estuary. In contrast, *Leitoscoloplos* is essentially absent from the low-salinity stations, but abundant in the fall, winter, and spring at the middle and lower bay stations. The *Mulinia* species occur predominantly in the upper reaches of the estuary. *M. pontchartrainensis* was restricted to the upper bay, whereas *M. lateralis* sporadically occurred in lower bay samples. The recruitment periods of each species appears sufficiently long that reoccupation of disturbed habitats would be likely in relatively short periods of time.

A general pattern of rapid recovery of Mobile Bay benthos from thin-layer disposal of dredged materials along the entrance channel to East Fowl River, Alabama, was documented in a recent study (USAED, Mobile 1987). A similar response pattern would be expected in bay habitats subjected to sedimentation pulses due to overflow operations. Acute impacts would be limited to relatively small patches of bottom along the upper slopes of the

channel and adjacent shallow flats. Additional bottom habitat area would receive sediments mimicking the thin-layer disposal project. Recovery, representing a combination of newly recruited individuals of opportunistic species and preexisting benthos able to vertically migrate up through thin overburdens of dredged material, would be a fairly rapid process.

References

- Aldridge, D. W., Payne, B. S., and Miller, A. C. 1987. The effects of intermittent exposure to suspended solids and turbulence on three species of freshwater mussels. *Environmental Pollution* 45:17-28.
- Allen, K. O., and Hardy, J. W. 1980. Impacts of navigational dredging on fish and wildlife: A literature review. FWS/OBS-80/07. US Fish and Wildlife Service, Biological Services Program.
- Aller, R. C. 1978. Experimental studies of changes produced by deposit feeders on pore water, sediment and overlying water chemistry. *American Journal of Science* 278:1185-1234.
- _____. 1982. The effects of macrobenthos on chemical properties of marine sediments and overlying waters. Pages 53-102 in *Animal-Sediment Relations: The Biogenic Alteration of Sediments*. P. L. McCall and M. J. Tevesz, eds. Plenum Press, New York.
- Aller, R. C., and Yingst, J. Y. 1985. Effects of the marine deposit-feeders *Heteromastus filiformis* (polychaeta), *Macoma balthica* (bivalvia) on averaged sedimentary solute transport, reaction rates, and microbial distributions. *Journal of Marine Research* 43:615-645.
- Armstrong, N. E. 1987. The ecology of open-bay bottoms of Texas: A community profile. Biological Report 85(7.12). US Fish and Wildlife Service.
- Auld, A. H., and Schubel, J. R. 1978. Effects of suspended sediment on fish eggs and larvae; a laboratory assessment. *Estuarine and Coastal Marine Science* 6:153-164.
- Barnard, W. D. 1978. Prediction and control of dredged material dispersion around dredging and open-water pipeline disposal operations. Technical Report DS-78-13. US Army Engineer Waterways Experiment Station, Vicksburg, MS.
- Biggs, R. B. 1970. Project A. Geology and hydrography. Pages 7-15 in *Gross physical and biological effects of overboard spoil disposal in upper Chesapeake Bay*. Special Report No. 3. Natural Resources Institute, University of Maryland, College Park, MD.
- Bishop, J. M., Gosselink, J. G., and Slone, J. H. 1980. Oxygen consumption and haemolymph osmolality of brown shrimp (*Penaeus aztecus*). *Fishery Bulletin* 78:741-757.
- Blancher, E. C. 1982. Establishing a biological benchmark for Mobile Bay: Rationale, methods and progress. Final Report to the Alabama Coastal Area Board.

- Boehlert, G. W. 1984. Abrasive effects of Mount Saint Helens ash upon epidermis of yolk sac larvae of Pacific herring. *Marine Environmental Research* 12:113-126.
- Boesch, D. F., Diaz, R. J., and Virnstein, R. W. 1976. Effects of tropical storm Agnes on soft-bottom macrobenthic communities of the James and York estuaries and the lower Chesapeake Bay. *Chesapeake Science* 17:246-259.
- Bohlen, W. F. 1975. An investigation of suspended material concentration in eastern Long Island Sound. *Journal of Geophysical Research* 80:5089-5100.
- Bohlen, W. F., and Tramontano, J. M. 1977. An investigation of the impact of dredging operations on suspended sediment material transport in the lower Thames River estuary. National Oceanic and Atmospheric Administration, Middle Atlantic Fisheries Center, Highlands, NJ.
- Bohlen, W. F., Cundy, D. F., and Tramontano, J. M. 1979. Suspended material distributions in the wake of estuarine channel dredging operations. *Estuarine and Coastal Marine Science* 9:699-711.
- Carriker, M. R. 1986. Influence of suspended particles on biology of oyster larvae in estuaries. *American Malacological Bulletin, Special Edition* No. 3(1986):41-49.
- Commuto, J. A., and Ambrose, W. G., Jr. 1985. Predatory infauna and trophic complexity in soft-bottom communities. Pages 323-333 in *Proceedings of the 19th European Marine Biology Symposium*. Cambridge University Press, Cambridge.
- Crozier, G. G. 1979. Baseline data collection, experimental monitoring program, Theodore ship channel and barge channel extension, Mobile Bay, Alabama. Final Report. US Army Engineer District, Mobile. 2 vols (unpublished).
- Cyrus, D. P., and Blaber, S. J. M. 1987a. The influence of turbidity on juvenile marine fishes in estuaries; Part I. Field studies at Lake St. Lucia on the southeastern coast of Africa. *Journal of Experimental Marine Biology and Ecology* 109:53-70.
- _____. 1987b. The influence of turbidity on juvenile marine fishes in estuaries; Part II. Laboratory studies, comparisons with field data and conclusions. *Journal of Experimental Marine Biology and Ecology* 109:71-91.
- Dauer, D. M. 1984. High resilience to disturbance of an estuarine polychaete community. *Bulletin of Marine Science* 34(1):170-174.
- Dauer, D. M., and Simon, J. L. 1976. Repopulation of the polychaete fauna of an intertidal habitat following defaunation: Species equilibrium. *Oecologia (Berlin)* 22:99-117.
- Dauer, H. C., Maybury, C. A., and Ewing, M. R. 1981. Feeding behavior and general ecology of several spionid polychaetes from the Chesapeake Bay. *Journal of Experimental Marine Biology and Ecology* 54:21-38.
- Davis, H. C. 1960. Effects of turbidity-producing materials in sea water on eggs and larvae of the clam *Venus (Mercenaria) mercenaria*. *Biological Bulletin* 118:48-54.

- Davis, H. C., and Hidu, H. 1969. Effects of turbidity-producing substances in sea water on eggs and larvae of three genera of bivalve mollusks. *Veliger* 11:316-323.
- Fauchald, K., and Jumars, P. A. 1979. The diet of worms: A study of polychaete feeding guilds. *Oceanography and Marine Biology Annual Review* 17:193-284.
- Flint, R. W. 1983 (Aug). Freshwater inflow and estuarine dynamics as characterized by benthic processes. Pages 3-20 in R. J. Varnell, ed. *Water Quality and Wetlands Management, Conference Proceedings*. New Orleans, LA.
- Flint, R. W., and Kalke, R. D. 1986a. Biological enhancement of estuarine benthic community structure. *Marine Ecology Progress Series* 31:23-33.
- _____. 1986b. Niche characterization of dominant estuarine benthic species. *Estuarine, Coastal and Shelf Science* 22:657-674.
- Flint, R. W., and Younk, J. A. 1983. Estuarine Benthos: Long-term community structure variations, Corpus Christi Bay, Texas. *Estuaries* 6(2):126-141.
- Foster, N. M. 1971. Spionidae (Polychaeta) of the Gulf of Mexico and the Caribbean Sea. *Studies on the Fauna of Curacao and Other Caribbean Islands* 36(129):1-183.
- Gabrielson, J. O., and Lukatelich, R. J. 1985. Wind-related resuspension of sediments in the Peel-Harvey estuarine system. *Estuarine, Coastal and Shelf Science* 20:135-145.
- Galtsoff, P. S. 1964. The American oyster *Crassostrea virginica* Gmelin. *Fishery Bulletin* 64:1-480.
- Gulf Universities Research Consortium. 1979. A final report on the Alabama coastal zone ecology and water quality data information sources and existing benthic data evaluation. Report No. 170.
- Harper, D. E. 1973. Effects of siltation and turbidity on the benthos and nekton; Appendix D5, Environmental impact assessment of shell dredging in San Antonio Bay, Texas; Volume V, pp 114-123. Texas A&M Research Foundation, College Station, TX.
- Holland, L. E. 1986. Effects of barge traffic on distribution and survival of ichthyoplankton and small fishes in the upper Mississippi River. *Transactions of the American Fisheries Society* 115:162-165.
- Hopkins, T. S. 1987. Seasonality and structure of soft bottom benthic assemblages in Mobile Bay - East Mississippi Sound. Dauphin Island Sea Lab Technical Report 87-002. Dauphin Island, AL.
- Ingle, R. M. 1952. Studies on the effect of dredging operations upon fish and shellfish. Technical Series, No. 5. State of Florida Board of Conservation, Tallahassee, FL.
- Isphording, W. C., and Lamb, G. M. 1980. The sediments of Mobile Bay: A report for the Alabama Coastal Area Board. Dauphin Island Sea Lab Technical Report 80-002. Dauphin Island, AL.
- Jeane, G. S., and Pine, R. E. 1975. Environmental effects of dredging and spoil disposal. *Journal of the Water Pollution Control Federation* 47:553-561.

- Johnson, P. G. 1980. Seasonal variations in benthic community structure in Mobile Bay, Alabama. M. S. thesis, University of Alabama, Birmingham.
- Kiorboe, T., Frantsen, E., Jensen, C., and Sorensen, G. 1981. Effects of suspended sediment on development and hatching of herring (*Clupea harengus* eggs). *Estuarine, Coastal and Shelf Science* 13:107-111.
- Kutkuhn, J. H. 1966. The role of estuaries in the development and perpetuation of commercial shrimp resources. Pages 16-36 in R. F. Smith, A. H. Swartz, and W. H. Massmann, eds. A symposium on estuarine fisheries. American Fisheries Society Special Publication No. 3.
- Lackey, J. B., Duncan, T. W., Fox, J. L., Markay, J. W., and Sullivan, J. H. 1973. A study of the effects of maintenance dredging in Mobile Bay, Alabama, on selected biological parameters. Contract Report to US Army Engineer District, Mobile, Mobile, AL.
- Larsen, S. C., Van Den Avyle, M. J., and Bozeman, E. L. 1986. Species profiles: Life histories and environmental requirements of coastal fishes and invertebrates (South Atlantic)--brown shrimp. US Fish and Wildlife Service Biological Report FWS/OBS-82/11. (Technical Report EL-82-4, US Army Engineer Waterways Experiment Station, Vicksburg, MS.)
- LaSalle, M. W., Homziak, J., Lunz, J. D., Clarke, D. G., and Fredette, T. J. A framework for assessing the need for seasonal restrictions on dredging and disposal operations. Technical report (in preparation). US Army Engineer Waterways Experiment Station, Vicksburg, MS.
- Linder, M. J., and Bailey, J. S. 1969. Distribution of brown shrimp (*Penaeus aztecus* Ives) as related to turbid water photographed from space. *Fishery Bulletin* 67:289-294.
- Loosanoff, V. L., and Tommers, F. D. 1948. Effects of suspended silt and other substances on rate of feeding of oysters. *Science* 107:69-70.
- Lunz, J. D., Clarke, D. G., and Fredette, T. J. 1984. Seasonal restrictions bucket dredging operations. Pages 371-383 in Proceedings of the Conference Dredging '84, November 14-16, 1984, Clearwater Beach, FL. American Society of Civil Engineers, New York, NY.
- Mackin, J. G. 1961. Canal dredging and silting in Louisiana bays. Publications of the Institute of Marine Science, University of Texas 7:262-314.
- Marine Environmental Sciences Consortium (MESC). 1983. Analysis of an environmental monitoring program, Theodore Ship Channel and barge channel extension, Mobile Bay, Alabama; Vols I and II. Dauphin Island Sea Lab Technical Report 83-003. Dauphin Island, AL.
- Markay, J. W., and Putnam, H. D. 1976. A study of the effects of maintenance dredging on selected ecological parameters in the Gulfport Ship Channel, Gulfport, MS. Pages 821-832 in Proceedings of the Specialty Conference on Dredging and Its Environmental Effects, January 26-28, 1976, Mobile, AL. American Society of Civil Engineers, New York, NY.
- Maurer, D. L. 1967. Burial experiments on marine pelecypods from Tamales Bay, California. *Veliger* 9:376-381.

- Maurer, D. L., Keck, R. T., Tinsman, J. C., Leathem, W. A., Wethe, C. A., Huntzinger, M., Lord, C., and Church, T. M. 1978. Vertical migration of benthos in simulated dredged material overburdens; Vol I: Marine benthos. Technical Report D-78-35. US Army Engineer Waterways Experiment Station, Vicksburg, MS.
- Maurer, D. L., Keck, R. T., Tinsman, J. C., Leathem, W. A., Wethe, C. A., Lord, C., and Church, T. M. 1986. Vertical migration and mortality of marine benthos in dredged material: A synthesis. *Internationale Revue Gesamten der Hydrobiologie* 71:49-63.
- May, E. B. 1973. Environmental effects of hydraulic dredging in estuaries. *Alabama Marine Research Bulletin* 9:1-85.
- McCauley, J. E., Parr, R. A., and Hancock, D. R. 1977. Benthic infauna and maintenance dredging: A case study. *Water Research* 11:233-242.
- Minello, T. J., Zimmerman, R. J., and Martinez, E. X. 1986. Fish predation of juvenile brown shrimp, *Penaeus aztecus* Ives: Effects of turbidity and substrates on predation rates. *Fishery Bulletin* 85:59-70.
- Modlin, R. F., and Dardeau, M. 1987. Seasonal and spatial distribution of cumaceans in the Mobile Bay estuarine system, Alabama. *Estuaries* 10(4):291-297.
- Morgan, R. P., Rasin, V. J., and Noe, L. A. 1983. Sediment effects on eggs and larvae of striped bass and white perch. *Transactions of the American Fisheries Society* 112:220-224.
- Morrison, G. 1971. Dissolved oxygen requirements for embryonic and larval development of the hard shell clam *Mercenaria mercenaria*. *Journal of the Fisheries Research Board of Canada* 28:379-381.
- Muncy, R. J. 1984. Species profiles: Life histories and environmental requirements of coastal fishes and invertebrates (South Atlantic)--white shrimp. US Fish and Wildlife Service Biological Report FWS/OBS-82/11.27. (Technical Report EL-82-4, US Army Engineer Waterways Experiment Station, Vicksburg, MS.)
- Myers, A. C. 1977. Sediment processing in a marine subtidal sandy bottom community; II. Biological consequences. *Journal of Marine Research* 35:633-647.
- Oviatt, C. A., and Nixon, S. W. 1975. Sediment resuspension and deposition in Narragansett Bay. *Estuarine and Coastal Marine Science* 3:201-217.
- Oviatt, C. A., Hunt, C. D., Vargo, G. A., and Kopchynski, K. W. 1981. Simulation of a storm event in marine microcosms. *Journal of Marine Research* 39:604-626.
- Palermo, M. R., Homziak, J., and Teeter, A. M. 1990. Evaluation of clamshell dredging and barge overflow, Military Ocean Terminal, Sunny Point, North Carolina. Technical Report D-90-6. US Army Engineer Waterways Experiment Station, Vicksburg, MS.
- Peddicord, R. K., and McFarland, V. A. 1978. Effects of suspended dredged material on aquatic animals. Technical Report D-78-29. US Army Engineer Waterways Experiment Station, Vicksburg, MS.

- Peddicord, R. K., McFarland, V. A., Belfiori, D. P., and Byrd, T. E. 1975. Effects of suspended solids on San Francisco Bay organisms, dredging disposal study; Appendix C - Physical impact. US Army Engineer District, San Francisco, San Francisco, CA.
- Postma, H. 1967. Sediment transport and sedimentation in the estuarine environment. Pages 155-179 in G. H. Lauff, ed. Estuaries, Publication No. 83. American Association for the Advancement of Science, Washington, DC.
- Priest, W. I. 1981. The effects of dredging impacts on water quality and estuarine organisms: A literature review. Pages 240-266 in Special Report in Applied Marine Science and Ocean Engineering, No. 274. Virginia Institute of Marine Science.
- Ranasinghe, J. A. 1983. A comparison of techniques to characterize benthic macrofaunal communities of middle Mobile Bay, Alabama. Plan II Report to the University of Alabama, Tuscaloosa, AL.
- Rhoads, D. C., and Germano, J. D. 1986. Interpreting long-term changes in benthic community structure: A new protocol. *Hydrobiologia* 142:291-308.
- Rice, D. L., Bianchi, T. S., and Roper, E. H. 1986. Experimental studies of sediment reworking and growth of *Scoloplos* spp. (Orbiniidae:Polychaeta). *Marine Ecology Progress Series* 30:9-19.
- Ritchie, D. E. 1970. Fish, Project F. Pages 50-59 in Gross physical and biological effects of overboard spoil disposal in upper Chesapeake Bay. Natural Resources Institute Special Report No. 3. University of Maryland, Solomons, MD.
- Rogers, B. A. 1969. Tolerance levels of four species of estuarine fishes to suspended mineral solids. M. S. thesis, University of Rhode Island, Kingston.
- Rosenthal, H., and Alderdice, D. F. 1976. Sublethal effects of environmental stressors, natural and pollutional, on marine fish eggs and larvae. *Journal of the Fisheries Research Board of Canada* 33:2047-2065.
- Saila, S. B., Polgar, T. T., and Rogers, B. A. 1968. Results of studies related to dredged sediment dumping in Rhode Island Sound. Proceedings of the Annual Northeastern Regional Anti-pollution Conference, 22-24 July 1968, pp 71-80.
- Schroeder, W. W., and Wiseman, W. J., Jr. 1985. An analysis of the winds (1974-1984) and sea level elevations (1973-1983) in coastal Alabama. Mississippi-Alabama Sea Grant Consortium Publ. No. MASGP-84-024.
- _____. 1986. Low-frequency shelf-estuarine exchange processes in Mobile Bay and other estuarine systems on the northern Gulf of Mexico. Pages 355-367 in D. A. Wolfe, ed. *Estuarine Variability*. Academic Press, New York.
- Schubel, J. R., Carter, H. H., and Wise, W. M. 1979. Shrimping as a source of suspended sediment in Corpus Christi Bay, Texas. *Estuaries* 2:201-203.

- Schubel, J. R., and Wang, J. C. S. 1973. The effects of suspended sediment on the hatching success of *Perca flavescens* (yellow perch), *Morone americana* (white perch), *Morone saxatilis* (striped bass), and *Alosa pseudoharengus* (alewife) eggs. Special Report No. 11. Chesapeake Bay Institute, Johns Hopkins University, Baltimore, MD.
- Schubel, J. R., Williams, A. D., and Wise, W. M. 1977. Suspended sediment in the Chesapeake and Delaware Canal. Special Report No. 11. Marine Science Research Center, State University of New York, Stony Brook.
- Sellers, M. A., and Stanley, J. G. 1984. Species profiles: Life histories and environmental requirements of coastal fishes and invertebrates (North Atlantic)--American oyster. US Fish and Wildlife Service Biological Report FWS/OBS-82/11.23. (Technical Engineer Waterways Experiment Station, Vicksburg, MS.)
- Sherk, J. A., O'Connor, J. M., and Neumann, D. A. 1975. Effects of suspended and deposited sediments on estuarine environments. Pages 541-558 in E. L. Cronin, ed. Estuarine Research, Vol II. Academic Press, New York.
- Shipp, R. L. 1987. Temporal distribution of finfish eggs and larvae around Mobile Bay. Pages 44-45 in T. Lowery, ed. Symposium on the Natural Resources of the Mobile Bay Estuary. Report 87-007. Mississippi-Alabama Sea Grant Consortium.
- Simon, J. L., and Dauer, D. M. 1977. Reestablishment of a benthic community following natural defaunation. Pages 139-154 in B. C. Coull, ed. Ecology of Marine Benthos. University of South Carolina Press, Columbia, SC.
- Sosnowski, R. A. 1984. Sediment resuspension due to dredging and storms: An analogous pair. Pages 609-617 in Proceedings of the Conference Dredging '84, November 14-16, 1984, Clearwater Beach, FL. American Society of Civil Engineers, New York, NY.
- Stern, E. M., and Stickle, W. B. 1978. Effects of turbidity and suspended material in aquatic environments. Technical Report D-78-21. US Army Engineer Waterways Experiment Station, Vicksburg, MS.
- Stumpf, R. P. 1988. Sediment transport in the Chesapeake Bay during floods: Analysis using satellite and surface observations. Journal of Coastal Research 4(1):1-15.
- Tavalaro, J. R. 1984. A sediment budget study of clamshell dredging and ocean disposal activities in the New York Bight. Environmental Geology and Water Sciences 6(3):133-140.
- Taylor, J. L. 1972. Some effects of oyster shell dredging on benthic invertebrates in Mobile Bay, Alabama. Contract Report to Alabama Attorney General Office, Montgomery, AL.
- Taylor, J. L. 1978. Evaluation of dredging and open water disposal on benthic environments: Gulf Intracoastal Waterway-Apalachicola Bay, Florida to Lake Borgne, Louisiana. Contract Report to US Army Engineer District, Mobile, Mobile, AL.
- TechCon, Inc. 1980. Environmental monitoring program of MOEPSI Well No. 1-76 (Mobile Bay State Lease 347 No. 1) in Mobile Bay, Alabama; Vol I: Environmental effects. Final Report to Mobil Oil Exploration and Producing Southeast, Inc., New Orleans, LA.

- US Army Engineer District (USAED), Mobile. 1982. Final report. Benthic macroinfaunal community characterization in Mississippi Sound and adjacent waters. Contract No. DACW01-80C427.
- _____. 1987. Final report: Monitoring environmental impacts associated with open-water thin-layer disposal of dredged material at Fowl River, AL. Contract No. DACW01, Mobile, AL.
- Vale, C., and Sundby, B. 1987. Suspended sediment fluctuations in the Tagus estuary on semi-diurnal and fortnightly time scales. *Estuarine, Coastal and Shelf Science* 25:495-508.
- Van Dolah, R. F., Calder, D. R., and Knott, D. M. 1984. Effects of dredging and open water disposal on benthic macroinvertebrates in a South Carolina estuary. *Estuaries* 7(1):28-37.
- Van Engel, W. A. 1982. Blue crab mortalities associated with pesticides, herbicides, temperature, salinity and dissolved oxygen. Pages 89-92 in H. M. Perry and W. A. Van Engel, eds. *Proceedings of the Blue Crab Colloquium, October 18-19, 1979, Biloxi, MS.* Gulf States Marine Fisheries Commission, Ocean Springs, MS.
- Viosca, P. 1958. Effect of dredging operations. Louisiana Wildlife and Fisheries Commission Biennial Report, 1956-1957.
- Virnstien, R. W. 1977. The importance of predation by crabs and fishes on benthic infauna in Chesapeake Bay. *Ecology* 58:1199-1217.
- Vittor, B. A. 1973. Preliminary report on the macrobenthos of lower Mobile Bay, Alabama. Contract Report to Coastal Ecosystem Management, Inc.
- _____. 1974. Effects of channel deepening on biota of a shallow Alabama estuary. *Journal of Marine Science, Alabama* 2(3):111-134.
- _____. 1978. Benthic macroinfaunal of Garrows Bend (Mobile Bay, Alabama). Contract Report to Alabama State Docks, Mobile, AL.
- _____. 1979. Benthos of the Mobile Bay estuary. Pages 143-149 in H. A. Loyacano and J. P. Smith, eds. *Symposium on the natural resources of the Mobile Bay Estuary. Report 87-007.* Mississippi-Alabama Sea Grant Consortium.
- Wallen, I. E. 1951. The direct effect of turbidity on fishes. *Bulletin of the Oklahoma Agricultural College, Biological Series* 2(48):1-27.
- Wass, M. L. 1967. Biological and physiological basis of indicator organisms and communities; II. Indicators of pollution. Pages 271-283 in T. A. Olsen and F. J. Burgess, eds. *Pollution and Marine Ecology.* John Wiley and Sons, New York.
- Wilson, W. B. 1950. The effects of sedimentation due to dredging operations on oysters in Copana Bay, Texas. M. S. thesis, Agricultural and Mechanical College of Texas.
- Yagi, T., Koiwa, T., and Miyazaki, S. 1977. Turbidity caused by dredging. Pages 1079-1109 in *Proceedings of WODCON VII: Dredging, Environmental Effects and Technology.* Texas A&M University, College Station, TX.

Table 43

Location and Sediment Characteristics of Alabama Coastal
Area Board (CAB) Benthic Stations

<u>CAB Station</u>	<u>Latitude/ Longitude</u>	<u>Depth, m</u>	<u>Sediment*</u>			<u>TOC (mg/kg)**</u>
			<u>Sand</u>	<u>Silt</u>	<u>Clay</u>	
2	30 14.3'N 88 01.1'W	6.0	41.7	17.7	40.2	13.8 \pm 4.7
4	30 18.3'N 87 55.9'N	2.5	3.3	15.5	81.2	20.0 \pm 2.3
5	30 21.0'N 87 59.7'W	3.5	7.9	22.5	69.4	14.9 \pm 1.4
6	30 26.4'N 87 59.1'W	3.8	4.8	24.1	71.8	16.2 \pm 1.8
7	30 32.5'N 87 59.1'W	3.5	9.4	31.6	58.8	16.9 \pm 6.5
8	30 36.8'N 87 59.0'N	3.5	10.9	43.5	45.8	17.0 \pm 5.2

* Percentage values.

** Total organic carbon values are annual means (\pm standard deviation).

Table 44

Results of Experimental Determinations of Effects of Suspended Sediments on Various Life History Stages of Fishes and Shellfishes (after Lunz, Clarke, and Fredette 1984)

Species	Stage	Suspended Sediment Concentration, mg/L	Exposure Duration	Type of Sediment	Degree of Effect	Reference
Yellow perch	Eggs	500	Not stated	Natural	No significant effect on hatching success; some delay in time to hatching noted in samples at ~100 mg/L (for all species)	Schubel and Wang (1973)
White perch						
Striped bass						
Alewife						
White perch		50-5,250		Natural (fine)	No significant effect on hatching success; definite delay in development at $\geq 1,500$ mg/L	Morgan, Rasin, and Noe (1983)
Striped bass		20-2,300		Natural (fine)	No significant effect on hatching success; definite delay in development at $\geq 1,300$ mg/L	
Atlantic herring		5-300	10 days	Natural	No significant effect on development or hatching success	Kiorboe et al. (1981)
Blueback herring		500	2 hr	Natural		
Alewife		50-5,000	Not stated	Natural (fine)	No significant effect on hatching success at all test concentrations	Auld and Schubel (1978)
American shad				(Same as above)		
Yellow perch				(Same as above)		
White perch				(Same as above)		
Striped bass	Larvae	1,626-5,380	24-48 hr		Significant effect on hatching success at 1,000 mg/L, but not at lower concentrations	
White perch		1,557-5,210	24-48 hr		(Same as above)	Morgan, Rasin, and Noe (1983)
Striped bass		50-1,000	4 days	Natural	15-42% mortality	
Yellow perch					20-57% mortality	
Striped bass					Survival significantly reduced at ≥ 500 mg/L	Auld and Schubel (1978)
Alewife		50-1,000	2-3 days	Natural	(Same as above)	
		50-1,000	4 days	Natural	Survival significantly reduced at ≥ 100 mg/L	
Spot	Adult	13,050	24 hr	Artificial	LC ₁₀	Sherk, O'Connor, and Neumann (1975)
Spot		68,750		Natural	LC ₁₀	
Striped killifish		23,770		Artificial	LC ₁₀	
Striped killifish		97,230		Natural	LC ₁₀	
Mummichog		24,470		Artificial	LC ₁₀	
Atlantic silverside		580		Artificial	LC ₁₀	
Bay anchovy		2,300		Artificial	LC ₁₀	
White perch		9,970		Natural	LC ₁₀	
White perch		3,050		Artificial	LC ₁₀	
Striped bass	Subadult	4,000	21 days	Natural	LC ₁₀	Peddicord and McFarland (1978)

(Continued)

(Sheet 1 of 3)

Table 44 (Continued)

Species	Stage	Suspended Sediment Concentration, mg/l	Exposure Duration	Type of Sediment	Degree of Effect	Reference
Cunner	Adult	133,000	12 hr	Natural (silt)	Median tolerance limit	Rogers (1969)
Cunner		100,000	24 hr		Median tolerance limit	
Cunner		72,000	48 hr		Median tolerance limit	
Mummichog		300,000	24 hr		No mortality	
Sheepshead minnow		300,000	24 hr		<30 percent mortality	
Cunner		100,000	24 hr		Median tolerance limit	Davis and Hidu (1969)
Stickleback		52,000	24 hr		Median tolerance limit	
American oyster	Eggs	188	Not stated	Natural (silt)	22 percent abnormal development	
		250		Natural (silt)	27 percent abnormal development	
		375		Natural (silt)	34 percent abnormal development	
		1,000		Artificial	No significant effect	Davis (1960)
		2,000		Artificial	No significant effect	
	Larvae	750	12 days	Natural (silt)	31 percent mortality	
Hard clam	Larvae	2,000	12 days	Artificial	20 percent mortality	
	Larvae	500	Not stated	Artificial	78 percent mortality	
	Eggs	750		Natural (silt)	8 percent abnormal development	Davis and Hidu (1969)
		1,000		Natural (silt)	21 percent abnormal development	
		1,500		Natural (silt)	35 percent abnormal development	
		125		Artificial	18 percent abnormal development	
		125		Artificial	25 percent abnormal development	
	Larvae	4,000		Artificial	31 percent abnormal development	Davis (1960)
	Larvae	1,300		Natural (silt)	No significant effect	
		500	12 days	Artificial	50 percent mortality	Peddicord et al. (1975)
Spot-tailed sand shrimp	Adult	50,000	200 hrs	Artificial	LC ₅₀	
Black-tailed sand shrimp	Subadult	21,500	21 days	Natural (contaminated)	20 percent mortality	Peddicord and McFarland (1978)
Dungeness crab	Adult	3,500	21 days	Natural (contaminated)	LC ₁₀	
Dungeness crab	Juvenile	2,000-20,000	25 days	Natural	No mortality at <4,300 mg/l; 38-percent mortality at 9,200 mg/l; abnormalities between 1,800 and 4,300 mg/l	Peddicord and McFarland (1978)
American lobster	Adult	50,000	Not stated	Artificial	No mortality	Saila, Polgar, Rogers (1968)
American oyster	Adult	4,000-32,000	Extended	Not stated	Detrimental	
American oyster	Adult	100-700	Not stated	Mud	No effect	
American oyster	Adult	100-4,000	Not stated	Silt	Reduced pumping	

(Continued)

(Sheet 2 of 3)

Table 44 (Continued)

Species	Stage	Suspended Sediment Concentra- tion, mg/l	Exposure Duration	Type of Sediment	Degree of Effect	Reference
Blue mussel	Subadult	100,000	5 days	Artificial	10 percent mortality	Peddicord et al. (1975)
Blue mussel	Adult	100,000	11 days	Artificial	10 percent mortality	
Blue mussel	Adult	96,000	200 hr	Artificial	LC ₅₀	

Figure 45

Summary of Wind Speed and Direction Data Measured on Dauphin Island,
Alabama, 1974-1984

Wind Speed knots	Direction Interval, degrees magnetic								
	N	NE	E	SE	S	SW	W	NW	
1	0.49	0.35	0.42	0.79	0.63	0.73	0.78	0.32	
2	0.88	0.64	0.93	1.43	1.29	1.19	1.55	0.69	
3	0.78	0.46	0.71	1.34	1.04	1.02	1.05	0.46	
4	1.27	0.79	1.18	1.91	2.05	1.39	1.36	0.70	
5	1.29	0.77	1.26	1.65	1.96	1.32	0.96	0.65	
6	1.45	0.90	1.47	1.64	1.91	1.19	0.80	0.64	
7	1.45	0.81	1.31	1.22	1.42	0.95	0.60	0.56	
8	1.47	0.95	1.35	1.18	1.16	0.65	0.44	0.52	
9	1.06	0.62	0.88	0.66	0.60	0.30	0.22	0.37	
10	1.56	0.84	1.13	0.69	0.55	0.27	0.26	0.46	
11	1.14	0.65	0.68	0.44	0.34	0.14	0.14	0.38	
12	1.33	0.68	0.75	0.40	0.30	0.10	0.12	0.40	
13	1.11	0.53	0.51	0.27	0.18	0.06	0.07	0.34	
14	1.13	0.52	0.36	0.16	0.12	0.03	0.09	0.39	
15	0.70	0.29	0.18	0.10	0.06	0.02	0.03	0.16	
16	0.87	0.28	0.19	0.09	0.03	0.01	0.03	0.22	
17	0.54	0.16	0.12	0.05	0.03	0.01	0.02	0.19	
18	0.41	0.10	0.06	0.03	0.02	0.01	0.03	0.15	
19	0.18	0.06	0.03	0.02	0.01	*	*	0.06	
20	0.25	0.05	0.04	0.02	0.02	*	0.01	0.09	
21	0.06	0.01	*	0.01	*	*	0.01	0.04	
22	0.01	0.02	0.01	0.01	0.01	*	0.01	0.04	
23	0.05	0.01	*	*	*	0.00	0.00	0.03	
24	0.04	0.01	*	0.01	0.01	0.00	*	0.02	
25	0.03	0.01	0.01	0.00	0.00	0.00	0.00	0.01	
26	0.02	*	*	*	0.00	*	0.00	0.01	
27	*	*	*	0.00	0.00	0.00	0.00	0.00	
28	0.01	*	*	*	*	0.00	0.00	*	
29	*	0.00	*	0.00	0.00	0.00	0.00	0.00	
30	*	0.00	*	0.00	0.00	0.00	0.00	0.00	
31	*	*	0.00	0.00	0.00	0.00	0.00	0.00	
32	*	0.00	0.00	0.00	0.00	0.00	0.00	0.00	
33	*	0.00	*	0.00	0.00	0.00	0.00	0.00	
35	*	0.00	0.00	0.00	0.00	0.00	0.00	0.00	
39	0.00	*	0.00	0.00	0.00	0.00	0.00	0.00	
Total									
>15	3.27	1.10	0.64	0.34	0.19	0.05	0.14	1.02	6.75
>10	9.54	4.32	4.07	2.30	1.68	0.65	0.82	2.99	26.37

Source: Schroeder and Wiseman (1985).

Note: Table values are percent frequencies of occurrence of a given wind speed for a direction interval.

* Percent occurrence less than 0.01.

Table 46

Maximum Sediment Deposits Within Any Cell for Each Monthly New
Work or Maintenance Material Overflow Simulation

<u>New Work</u>		<u>Maintenance</u>	
<u>Month</u>	<u>Deposit Thickness, cm</u>	<u>Month</u>	<u>Deposit Thickness, cm</u>
Nov (start)	68	Mar (start)	90
Apr	48	Apr	54
May	67	May	9
Jun	90	Jun	45
Jul	39	Jul	27
Aug	61	Oct	45
Sep	104	Nov	16
Oct	48	Dec	26
Nov	39	Jan	36
Dec	13	Feb (end)	45
Jan	13		
Feb	22	Mean = 39.3, n = 10	
Mar	16		
Apr	13		
May	26		
Jun	26		
Jul	26		
Aug	13		
Sep	91		
Oct	39		
Nov	247		
Dec	102		
Jan	44		
Feb	18		
Mar	39		
Apr	78		
May (end)	39		
Mean = 52.9, n = 27			

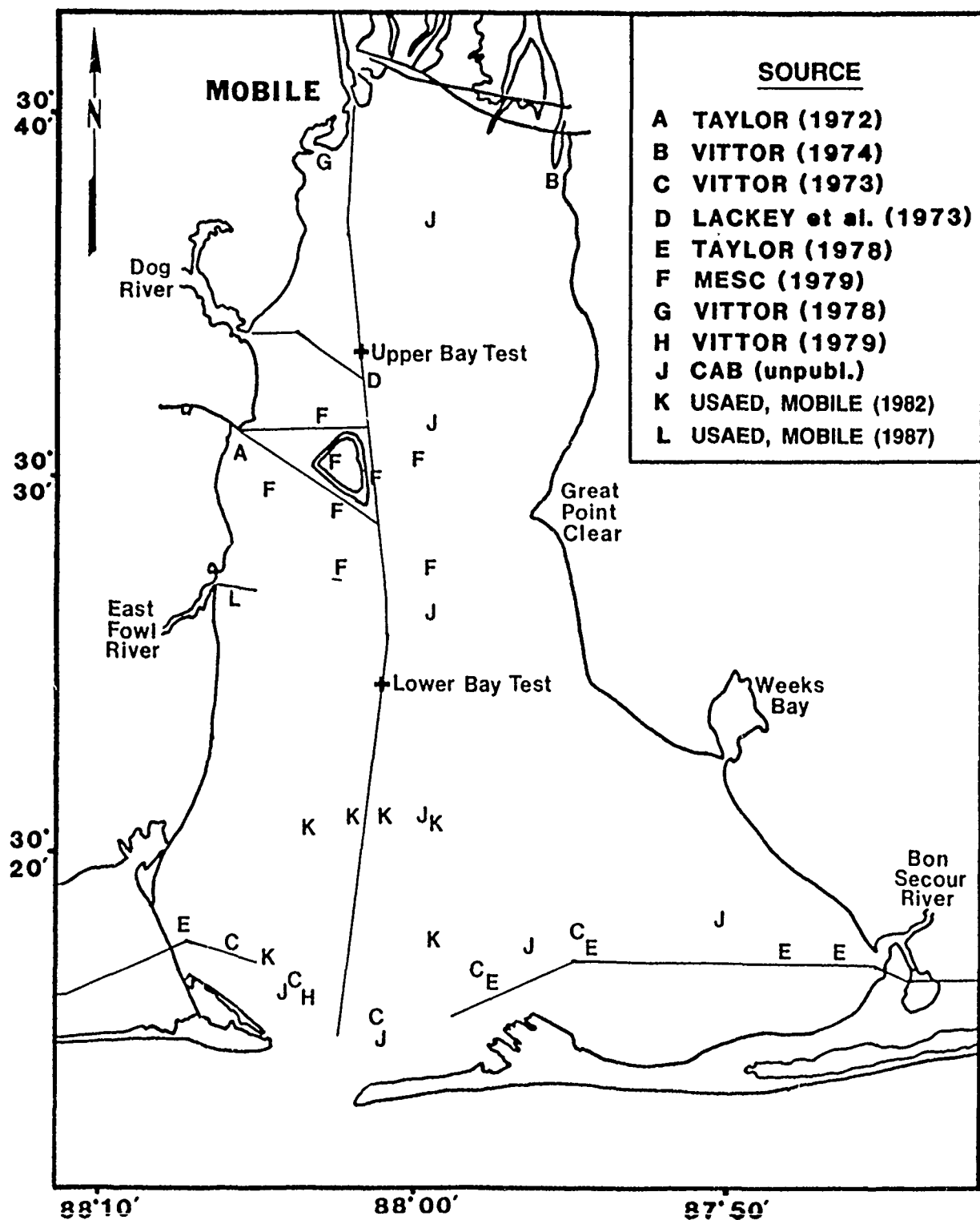


Figure 160. Locations of benthic infaunal community studies in Mobile Bay, Alabama

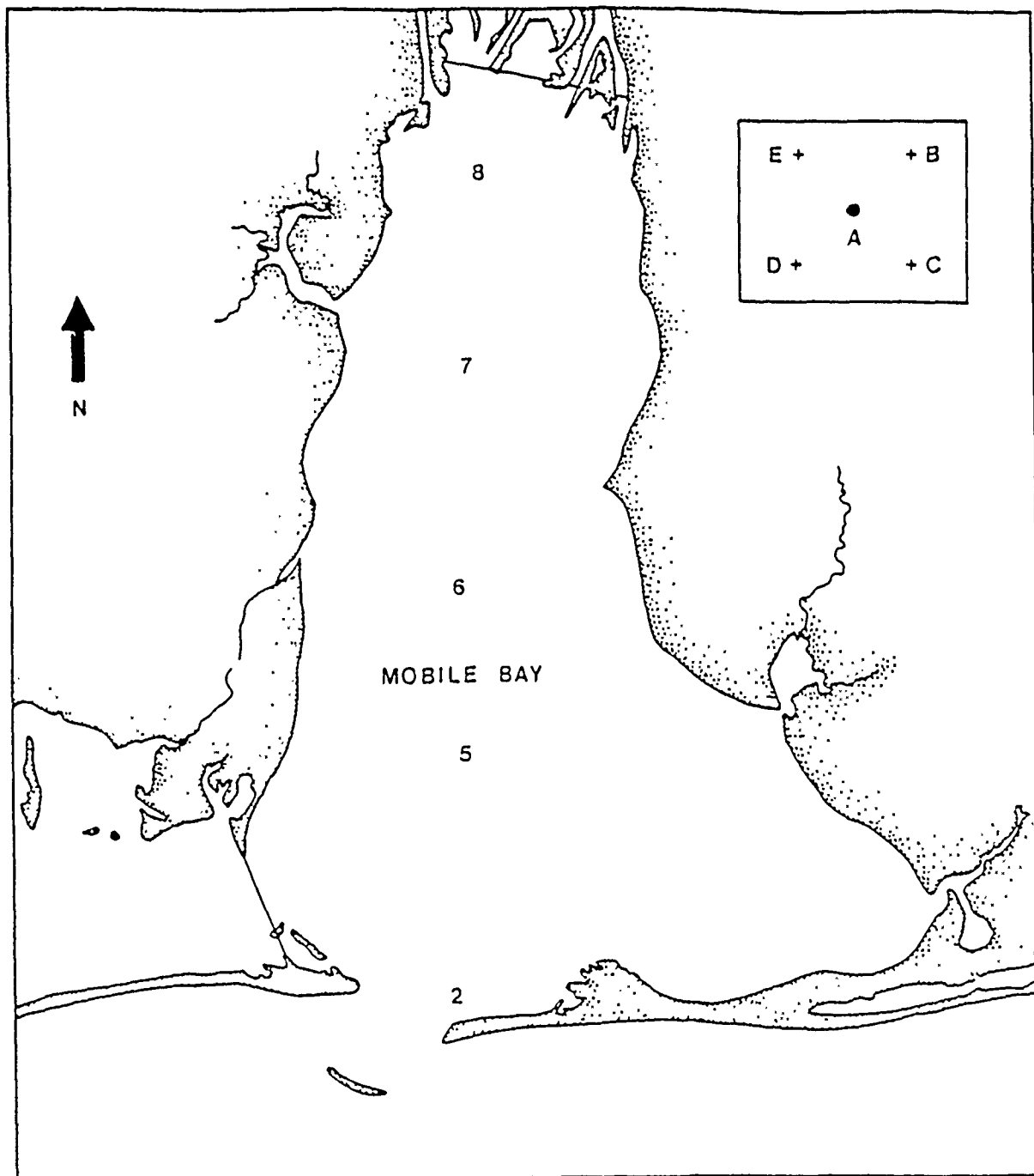


Figure 161. Alabama Coastal Area Board stations occupied during benthic macroinfaunal surveys of Mobile Bay, Alabama. Distribution of subsampling sites at each station displayed in the inset

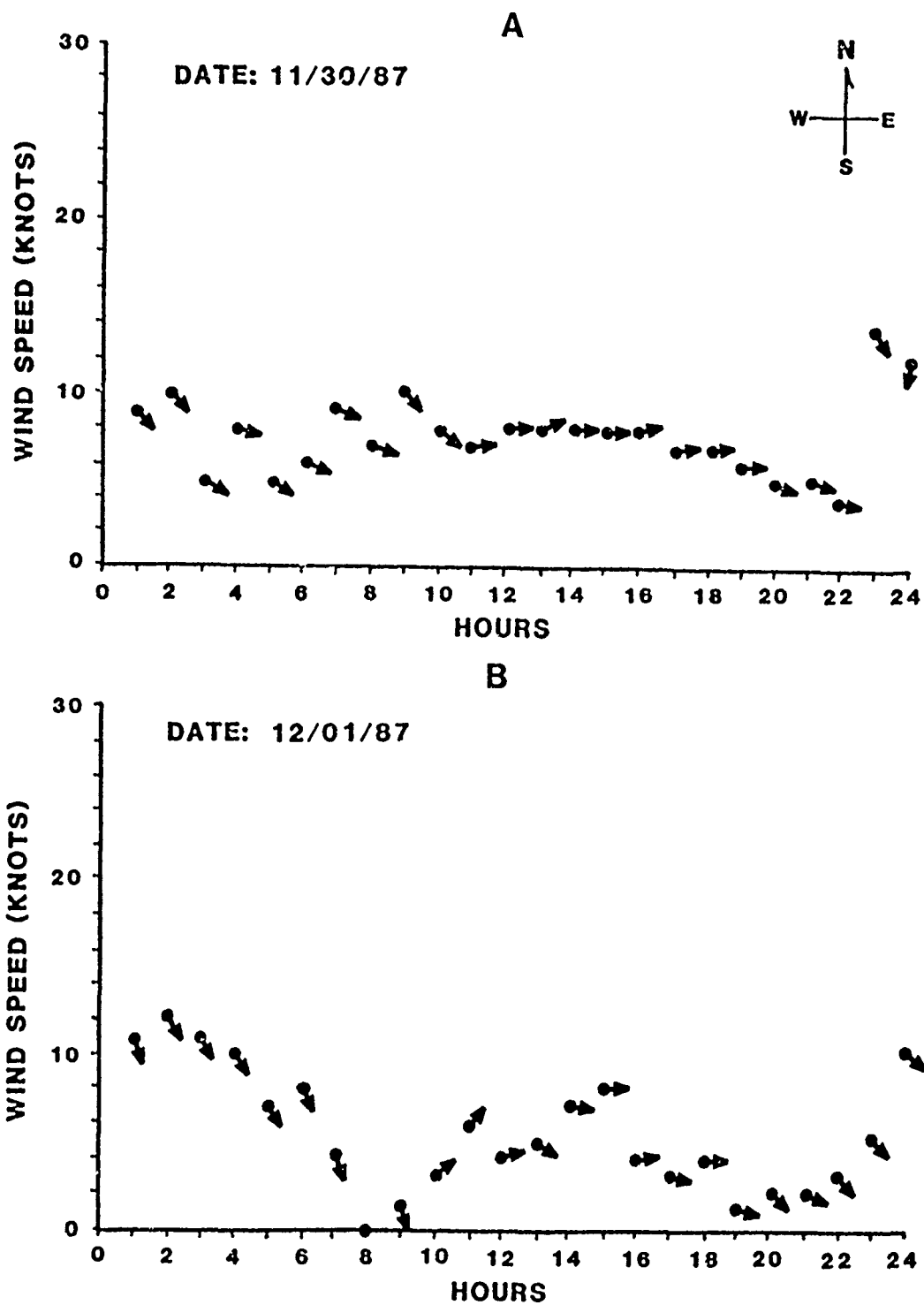


Figure 162. Hourly wind speed and direction at Dauphin Island, Alabama, on November 30 (A) and December 1 (B), 1987

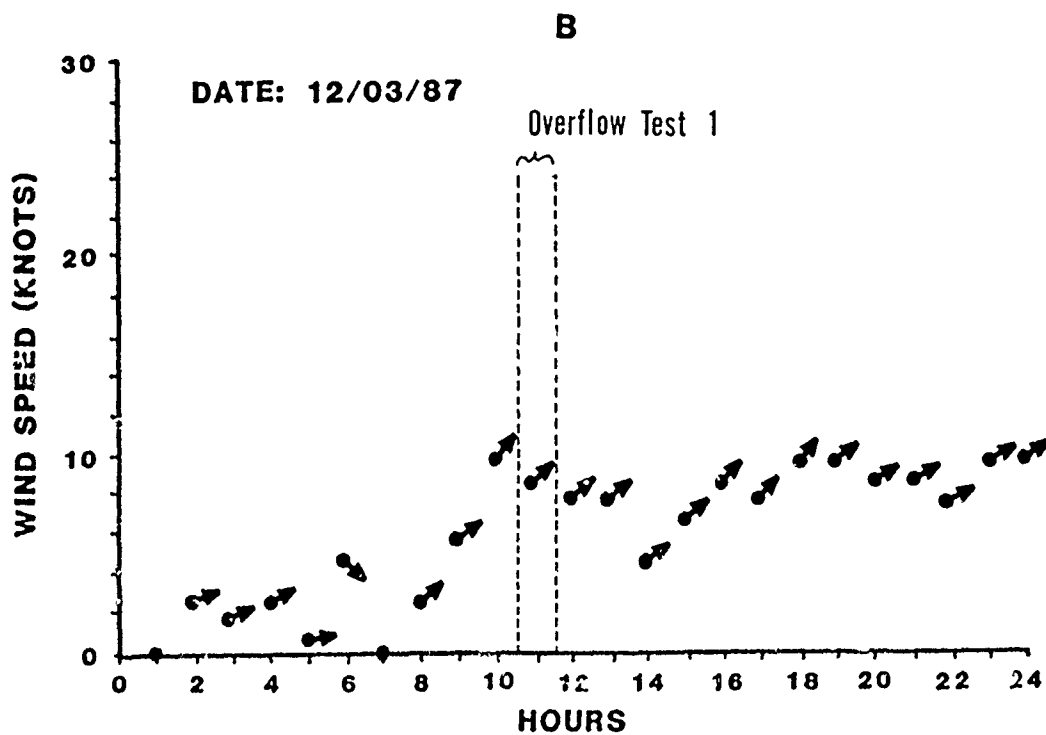
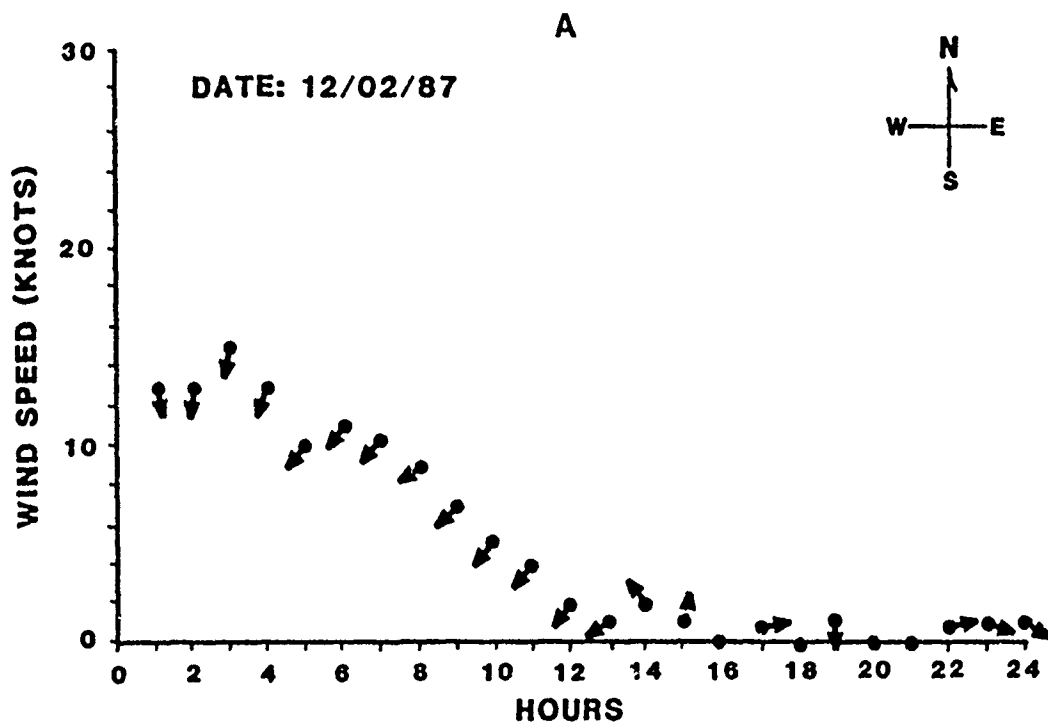


Figure 163. Hourly wind speed and direction at Dauphin Island, Alabama, on December 2 (A) and 3 (B), 1987

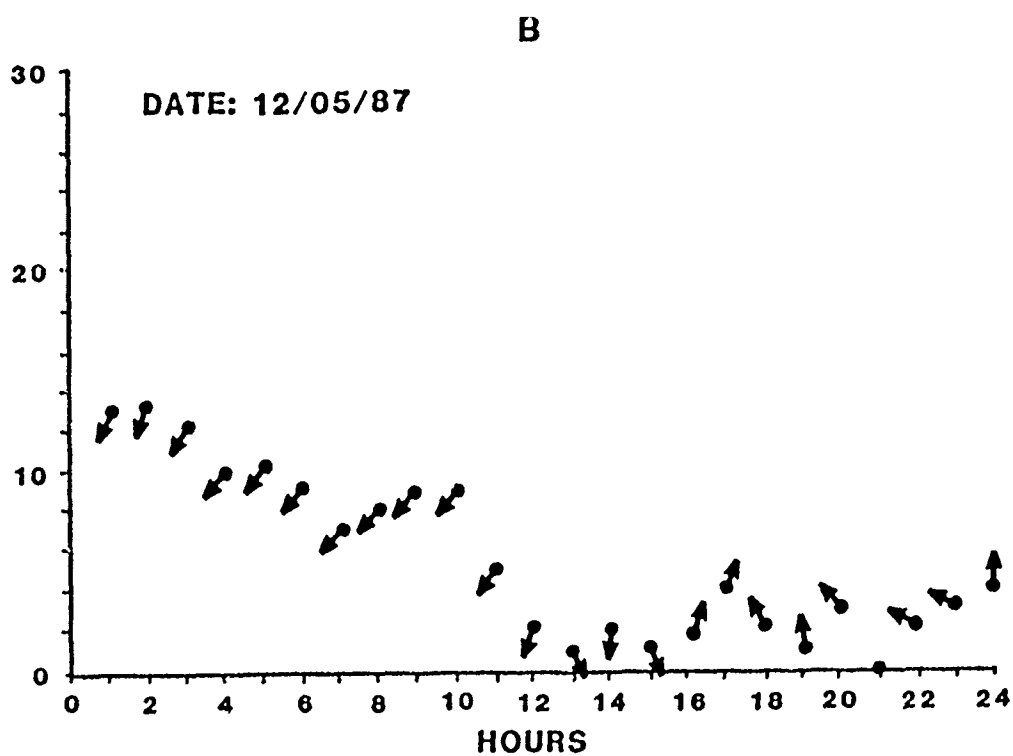
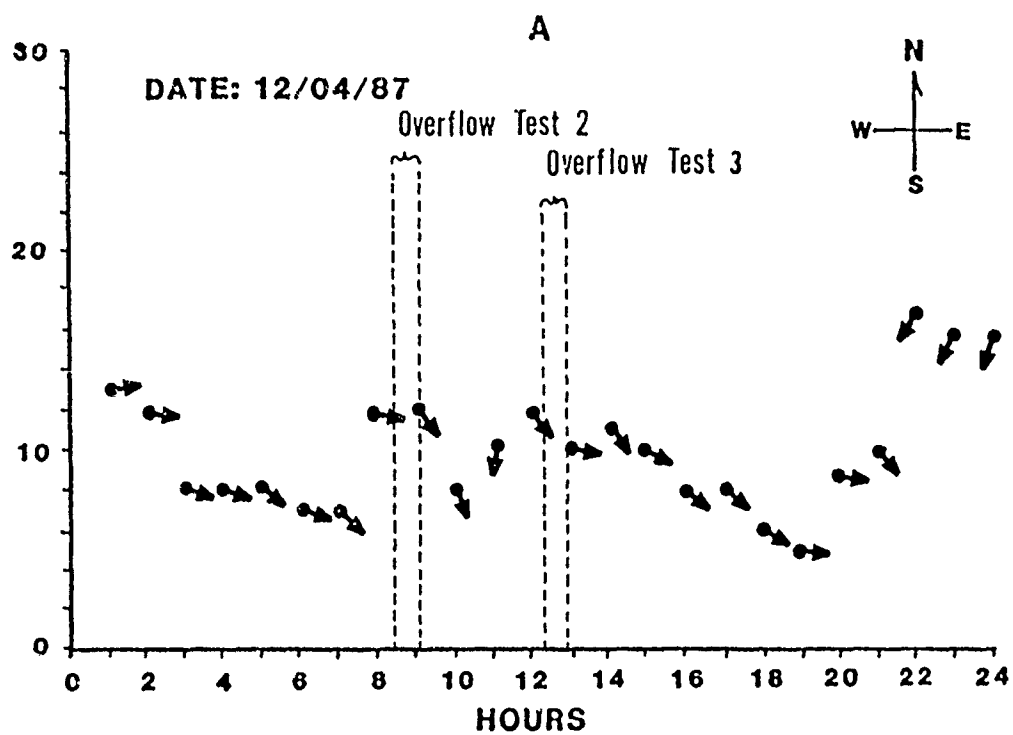


Figure 164. Hourly wind speed and direction at Dauphin Island, Alabama, on December 4 (A) and 5 (B), 1987

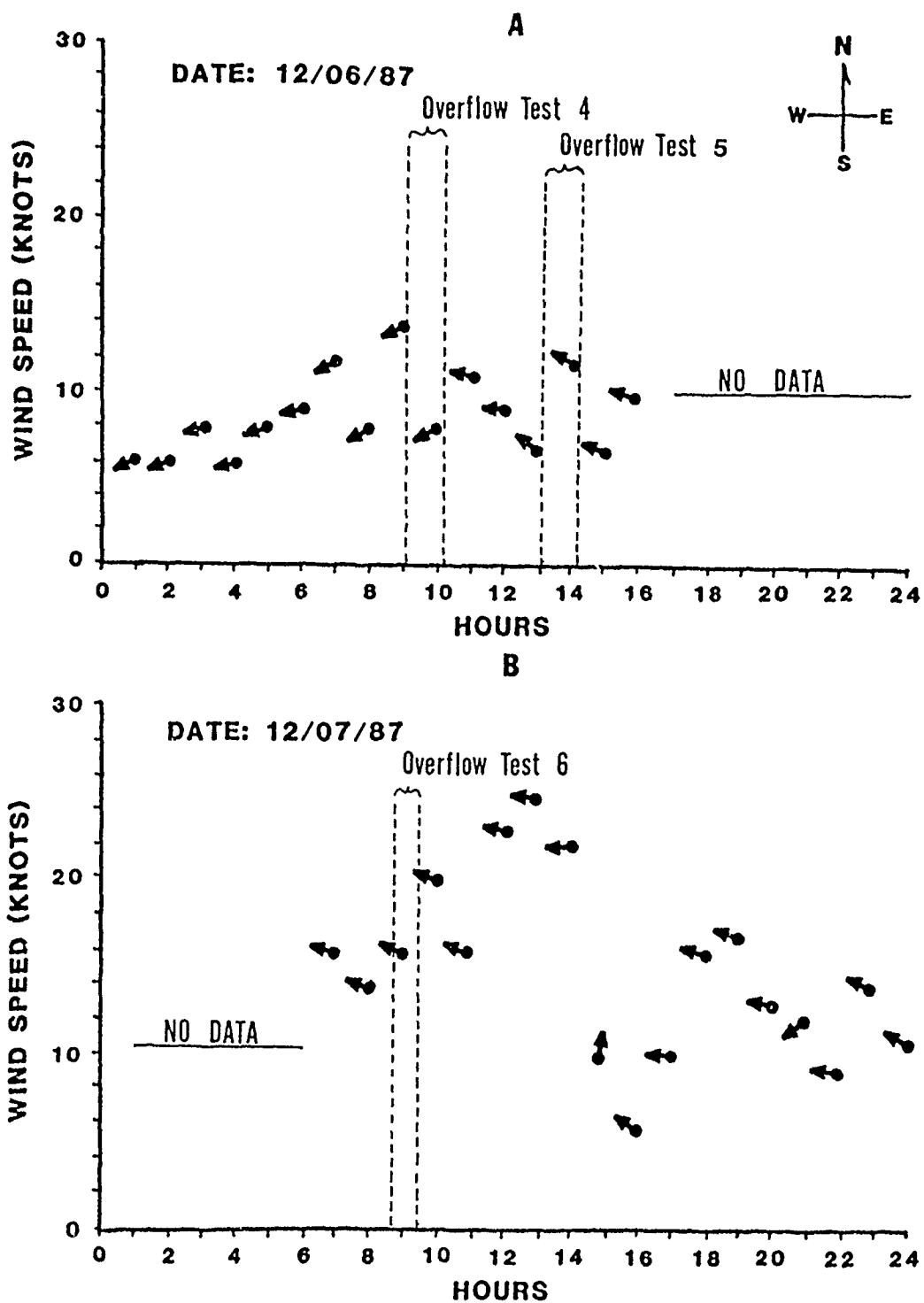


Figure 165. Hourly wind speed and direction at Dauphin Island, Alabama, on December 6 (A) and 7 (B), 1987

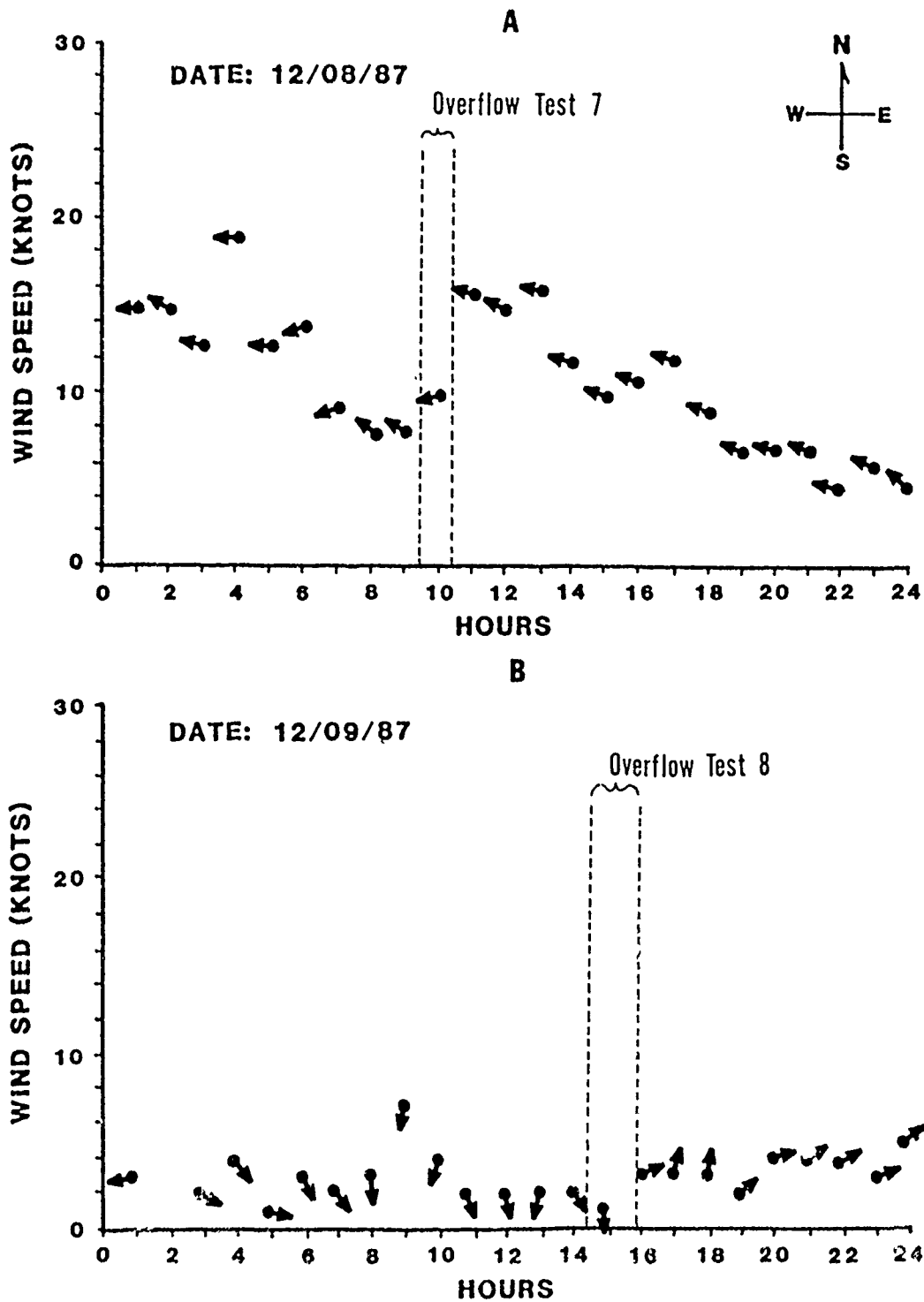


Figure 166. Hourly wind speed and direction at Dauphin Island, Alabama, on December 8 (A) and 9 (B), 1987

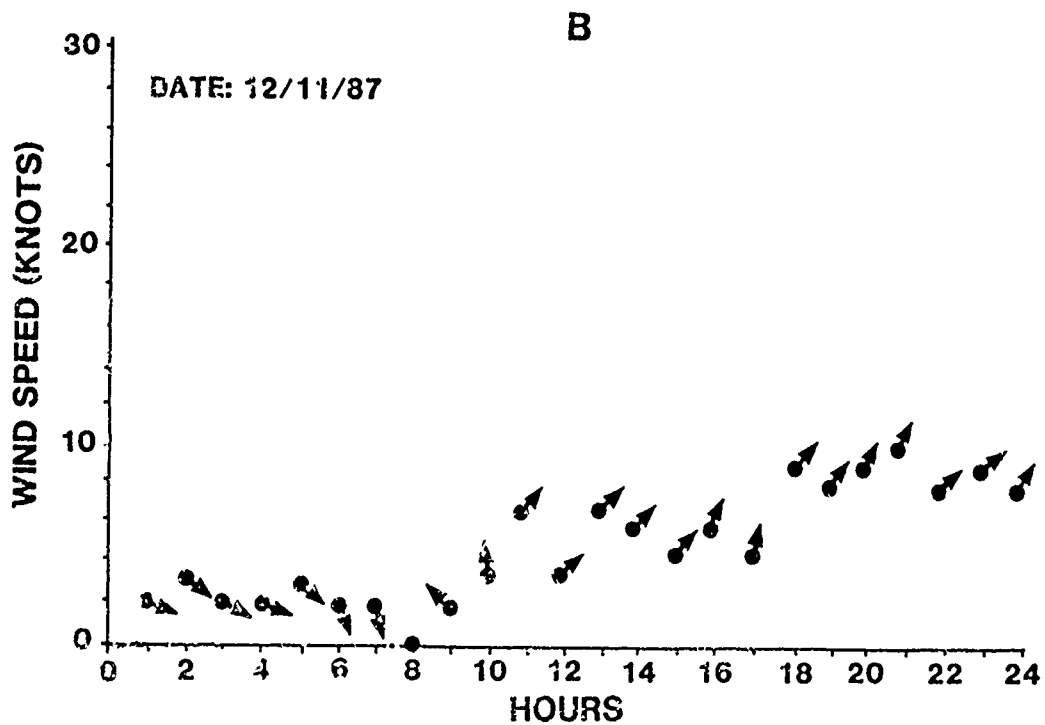
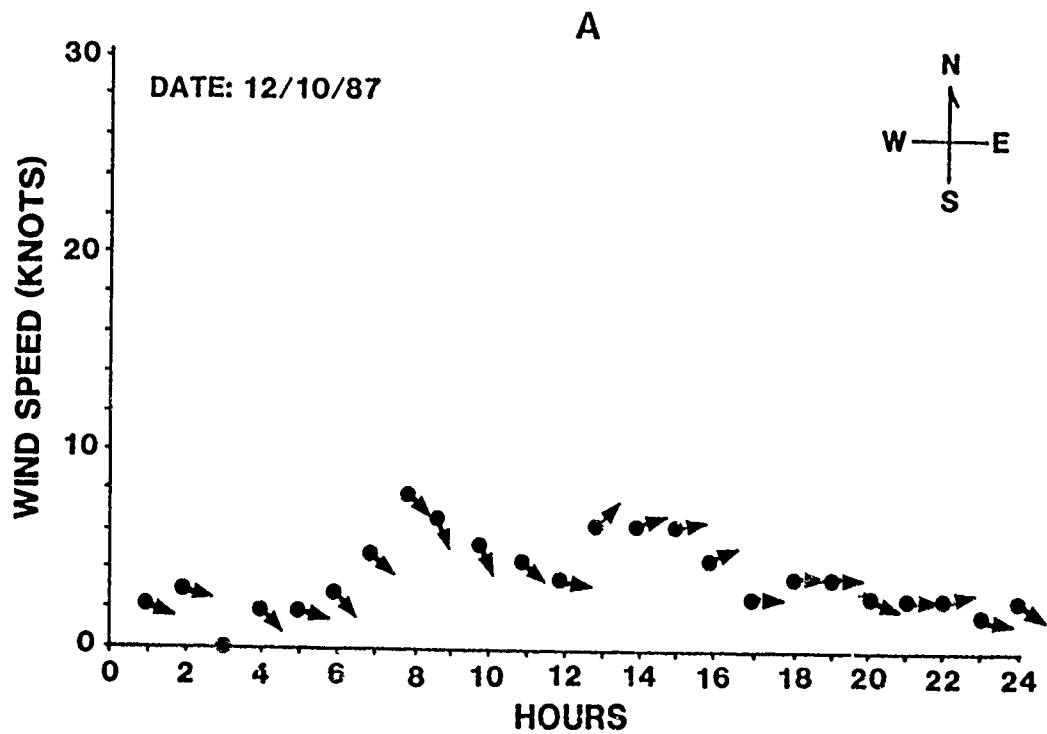


Figure 167. Hourly wind speed and direction at Dauphin Island, Alabama, on December 10 (A) and 11 (11), 1987

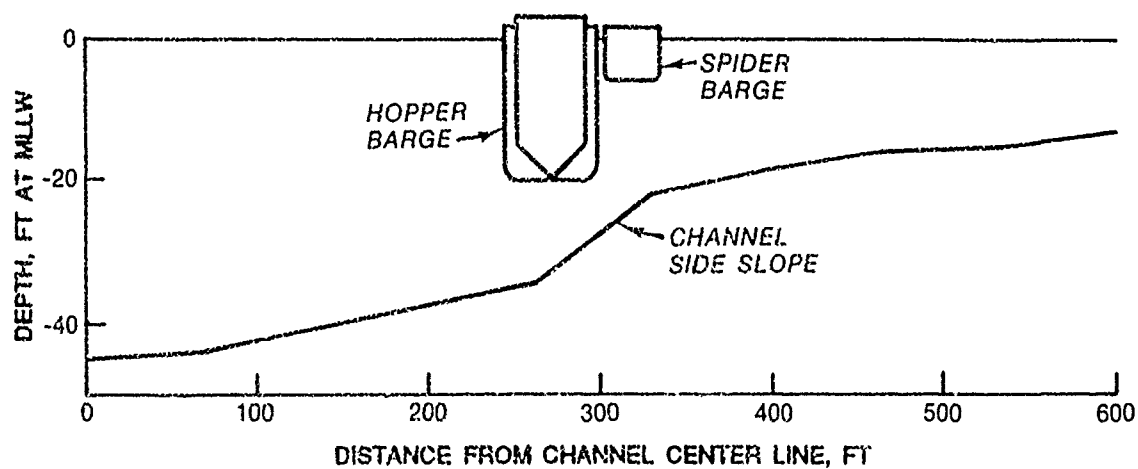


Figure 168. Mobile Bay ship channel cross section showing a typical depth profile and the relative position of hopper and spider barges as occurred during overflow tests

Point of Overflow
100 X 100 ft Cell

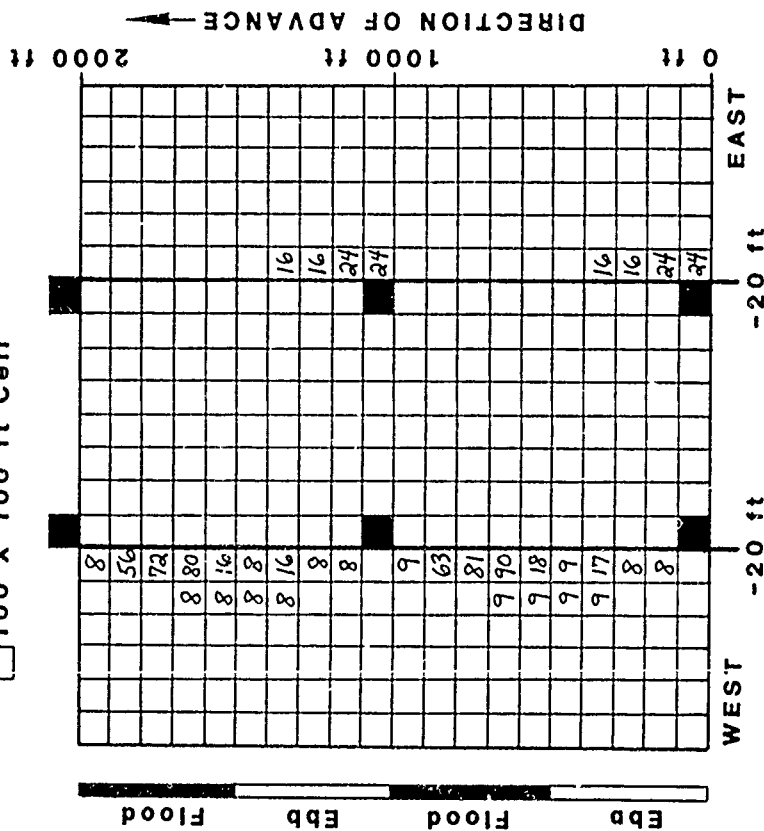


Figure 169. Sedimentation pattern (thickness, cm) for a hypothetical hopper barge overflow operation in Mobile Bay based on a model simulation for maintenance material during the month of March. Assumes a 60-ft advance of the dredge per barge load and a 90-min barge replacement cycle. Deposition in grid cells at a depth greater than 20 ft not shown

Point of Overflow
100 X 100 ft Cell

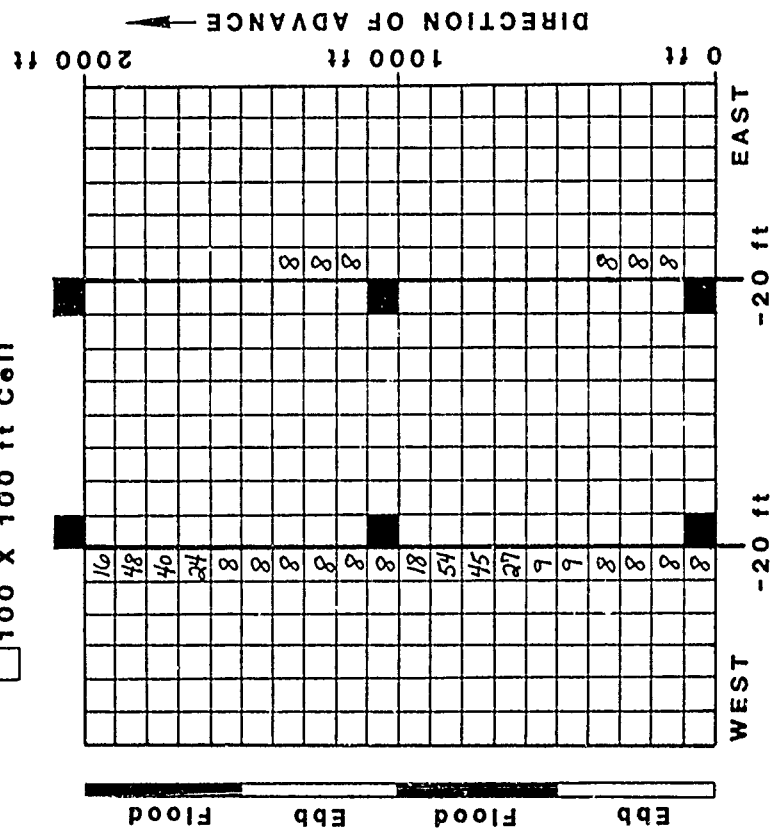
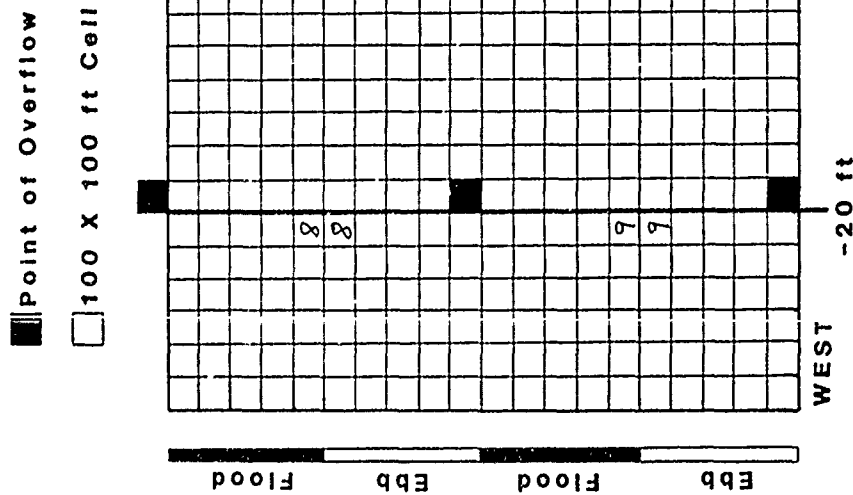




Figure 170. Sedimentation pattern (thickness, cm) for a hypothetical hopper barge overflow operation in Mobile Bay based on a model simulation for maintenance material during the month of April. Assumes a 60-ft advance of the dredge per barge load and a 90-min barge replacement cycle. Deposition in grid cells at a depth greater than 20 ft not shown



 Point of Overflow
 100 X 100 ft Cell

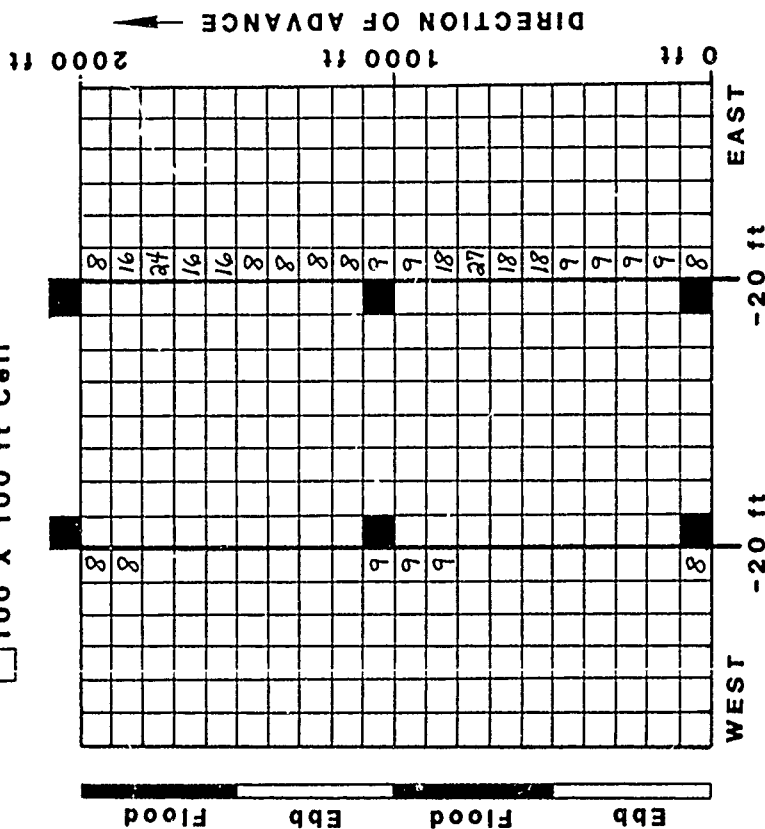




Figure 173. Sedimentation pattern (thickness, cm) for a hypothetical hopper barge overflow operation in Mobile Bay based on a model simulation for maintenance material during the month of July. Assumes a 60-ft advance of the dredge per barge load and a 90-min barge replacement cycle. Deposition in grid cells at a depth greater than 20 ft not shown

 Point of Overflow
 100 X 100 ft Cell

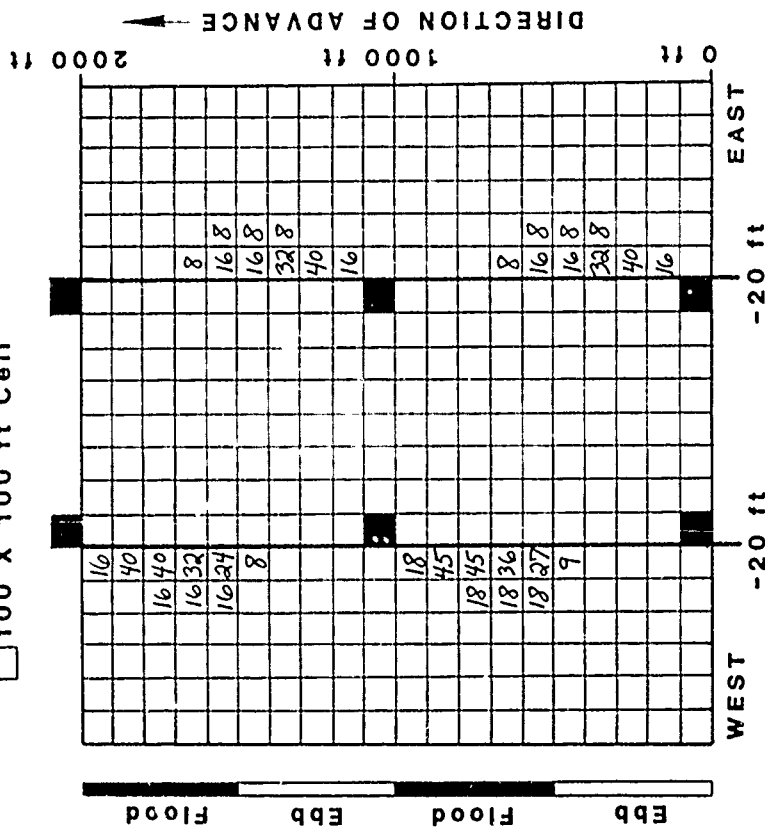


Figure 174. Sedimentation pattern (thickness, cm) for a hypothetical hopper barge overflow operation in Mobile Bay based on a model simulation for maintenance material during the month of October. Assumes a 60-ft advance of the dredge per barge load and a 90-min barge replacement cycle. Deposition in grid cells at a depth greater than 20 ft not shown

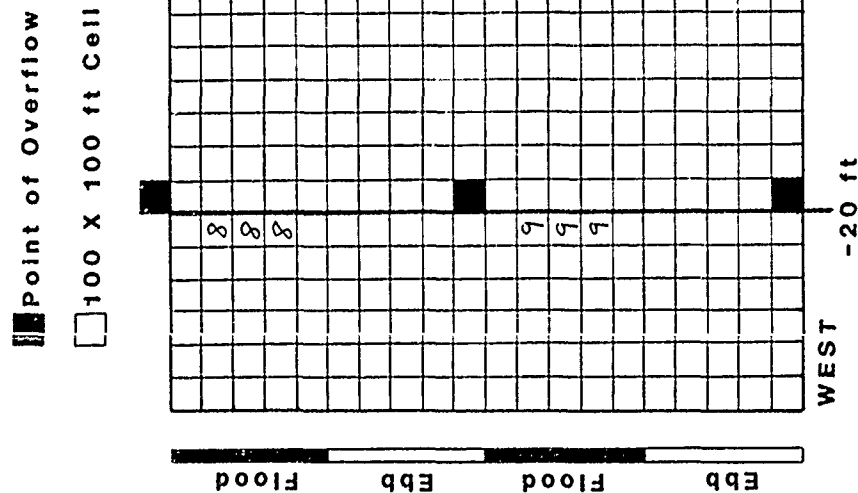


Figure 175. Sedimentation pattern (thickness, cm) for a hypothetical hopper barge overflow operation in Mobile Bay based on a model simulation for maintenance material during the month of November. Assumes a 60-ft advance of the dredge per barge load and a 90-min barge replacement cycle. Deposition in grid cells at a depth greater than 20 ft not shown

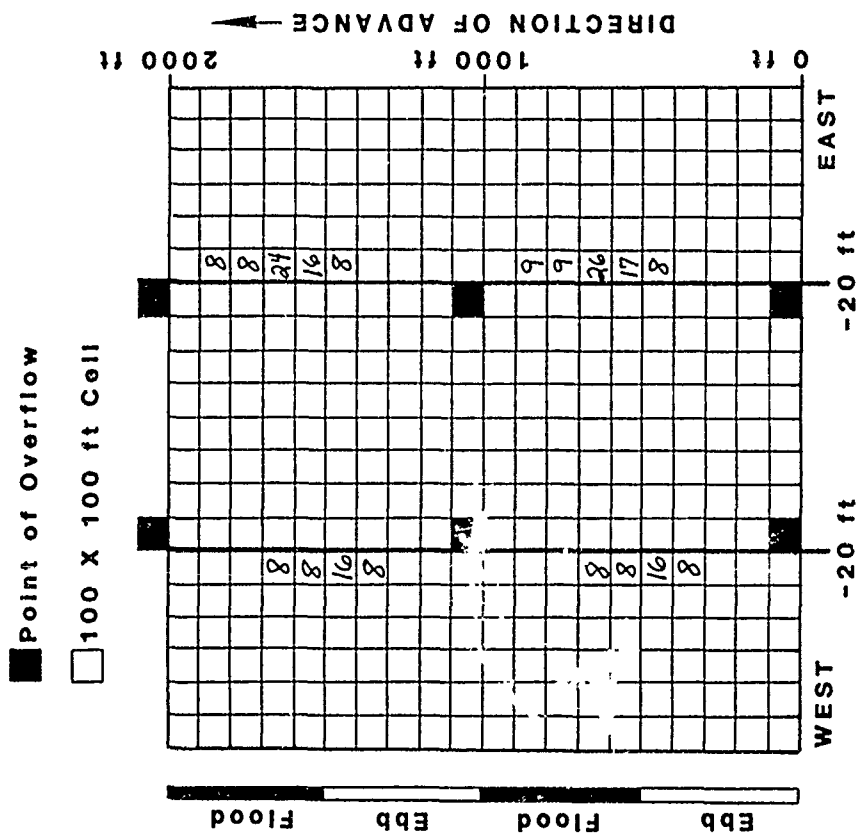


Figure 176. Sedimentation pattern (thickness, cm) for a hypothetical hopper barge overflow operation in Mobile Bay based on a model simulation for maintenance material during the month of December. Assumes a 60-ft advance of the dredge per barge load and a 90-min barge replacement cycle. Deposition in grid cells at a depth greater than 20 ft not shown

Point of Overflow

100 X 100 ft Cell

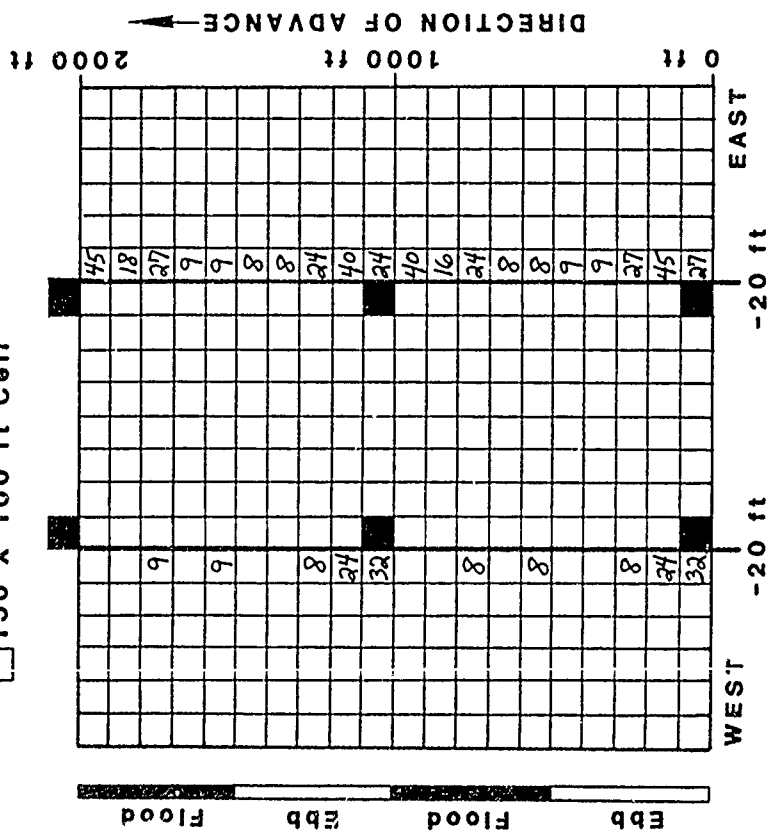


Figure 177. Sedimentation pattern (thickness, cm) for a hypothetical hopper barge overflow operation in Mobile Bay based on a model simulation for maintenance material during the month of January. Assumes a 60-ft advance of the dredge per barge load and a 90-min barge replacement cycle. Deposition in grid cells at a depth greater than 20 ft not shown

Point of Overflow

100 X 100 ft Cell

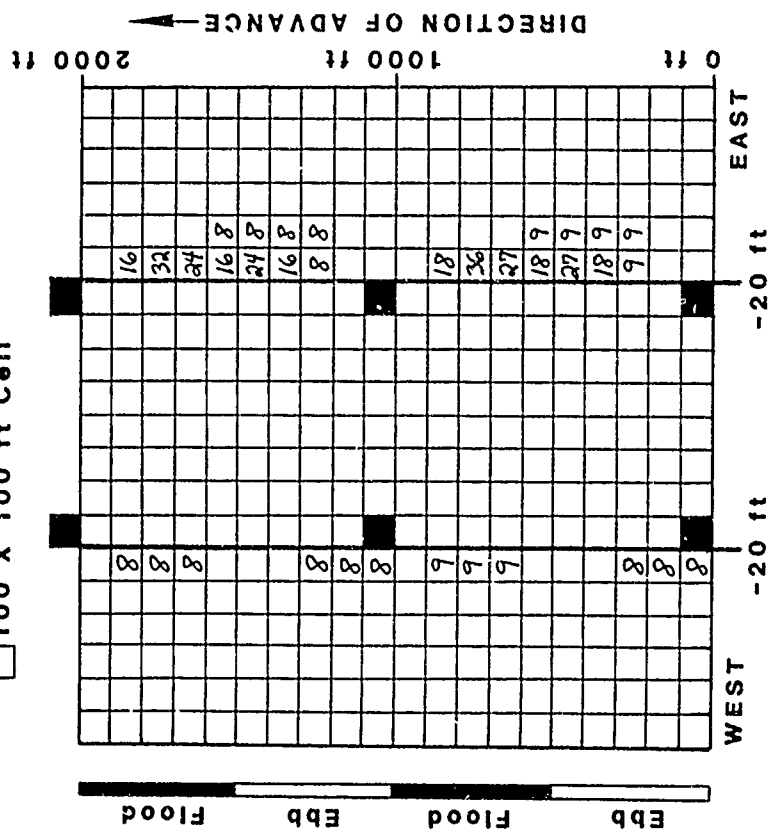


Figure 178. Sedimentation pattern (thickness, cm) for a hypothetical hopper barge overflow operation in Mobile Bay based on a model simulation for maintenance material during the month of February. Assumes a 60-ft advance of the dredge per barge load and a 90-min barge replacement cycle. Deposition in grid cells at a depth greater than 20 ft not shown

Point of Overflow

100 X 100 ft Cell

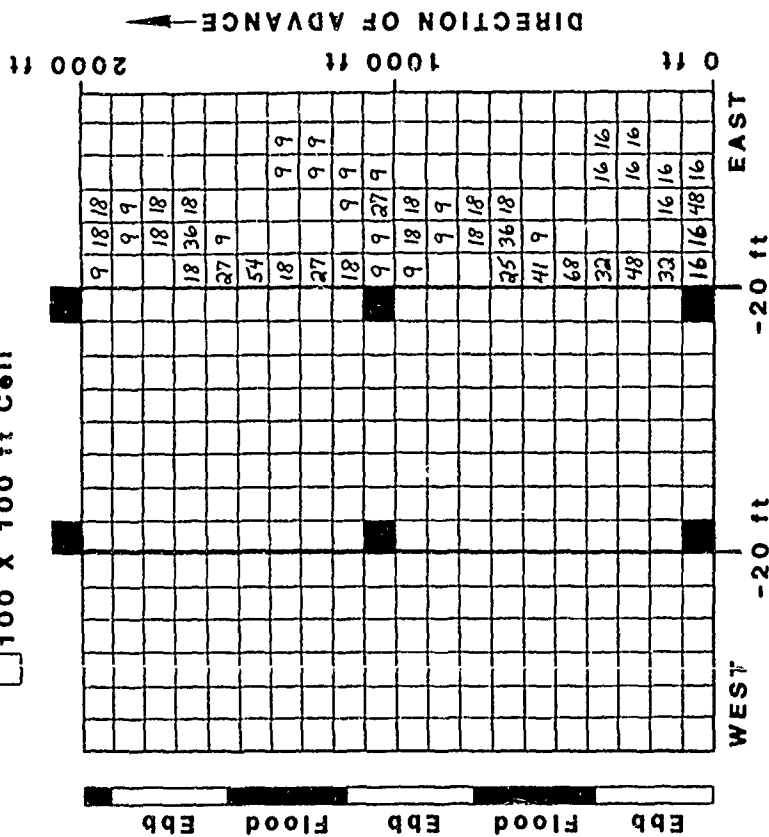


Figure 179. Sedimentation pattern (thickness, cm) for a hypothetical hopper barge overflow operation in Mobile Bay based on a model simulation for new work material during the month of November (first year of project). Assumes a 40-ft advance of the dredge per barge load and an 80-min barge replacement cycle. Deposition in grid cells at a depth greater than 20 ft not shown

Point of Overflow

100 X 100 ft Cell

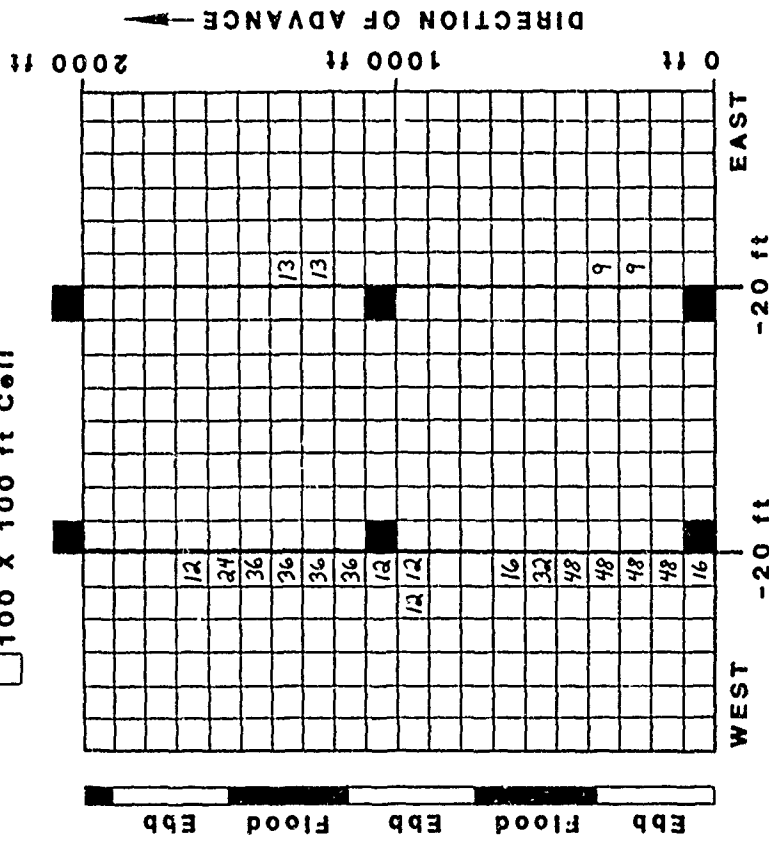


Figure 180. Sedimentation pattern (thickness, cm) for a hypothetical hopper barge overflow operation in Mobile Bay based on a model simulation for new work material during the month of April (first year of project). Assumes a 40-ft advance of the dredge per barge load and an 80-min barge replacement cycle. Deposition in grid cells at a depth greater than 20 ft not shown

Point of Overflow

100 X 100 ft Cell

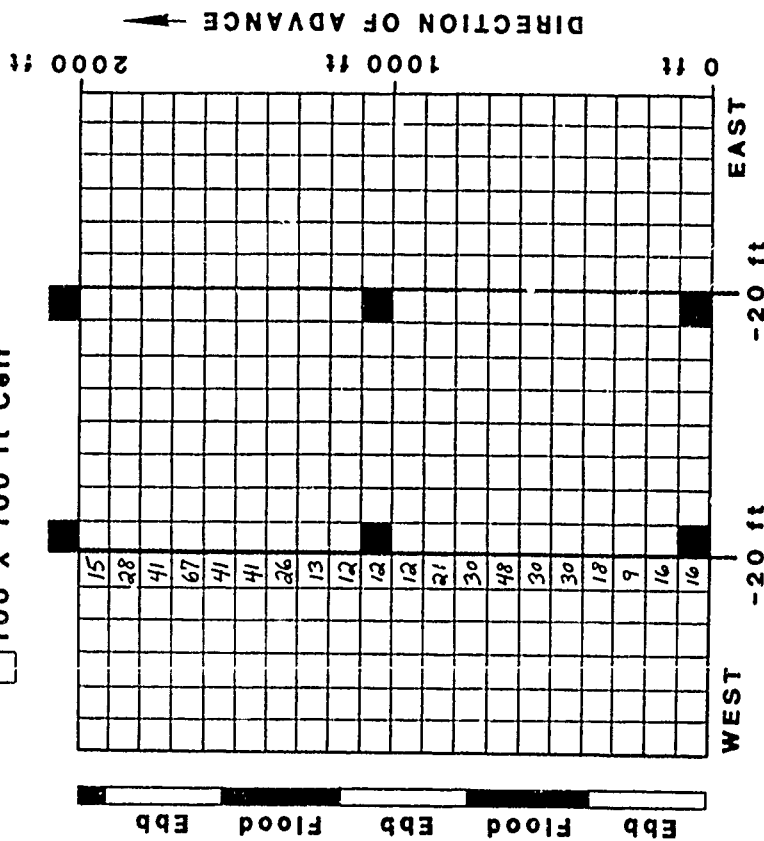


Figure 181. Sedimentation pattern (thickness, cm) for a hypothetical hopper barge overflow operation in Mobile Bay based on a model simulation for new work material during the month of May (first year of project). Assumes a 40-ft advance of the dredge per barge load and an 80-min barge replacement cycle. Deposition in grid cells at a depth greater than 20 ft not shown

Point of Overflow

100 X 100 ft Cell

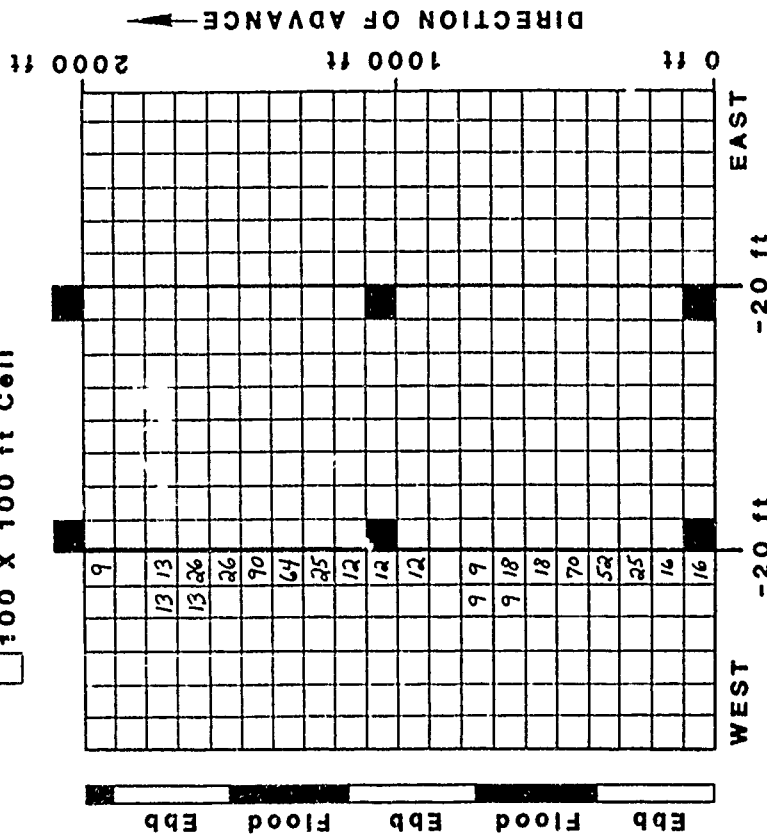


Figure 182. Sedimentation pattern (thickness, cm) for a hypothetical hopper barge overflow operation in Mobile Bay based on a model simulation for new work material during the month of June (first year of project). Assumes a 40-ft advance of the dredge per barge load and an 80-min barge replacement cycle. Deposition in grid cells at a depth greater than 20 ft not shown

Point of Overflow

100 X 100 ft Cell

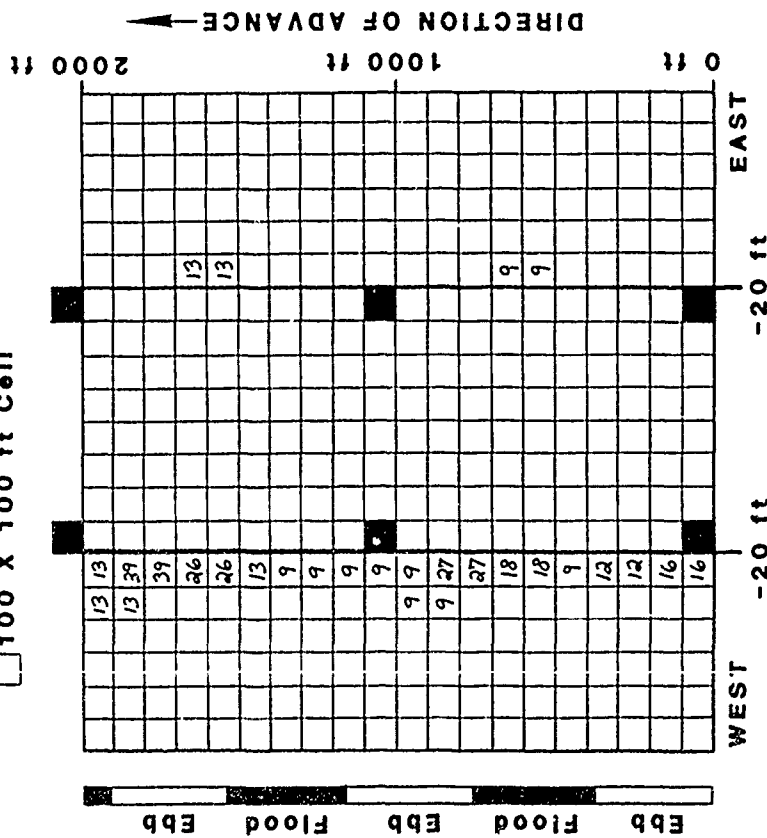


Figure 133. Sedimentation pattern (thickness, cm) for a hypothetical hopper barge overflow operation in Mobile Bay based on a model simulation for new work material during the month of July (first year of project). Assumes a 40-ft advance of the dredge per barge load and an 80-min barge replacement cycle. Deposition in grid cells at a depth greater than 20 ft not shown

Point of Overflow

100 X 100 ft Cell

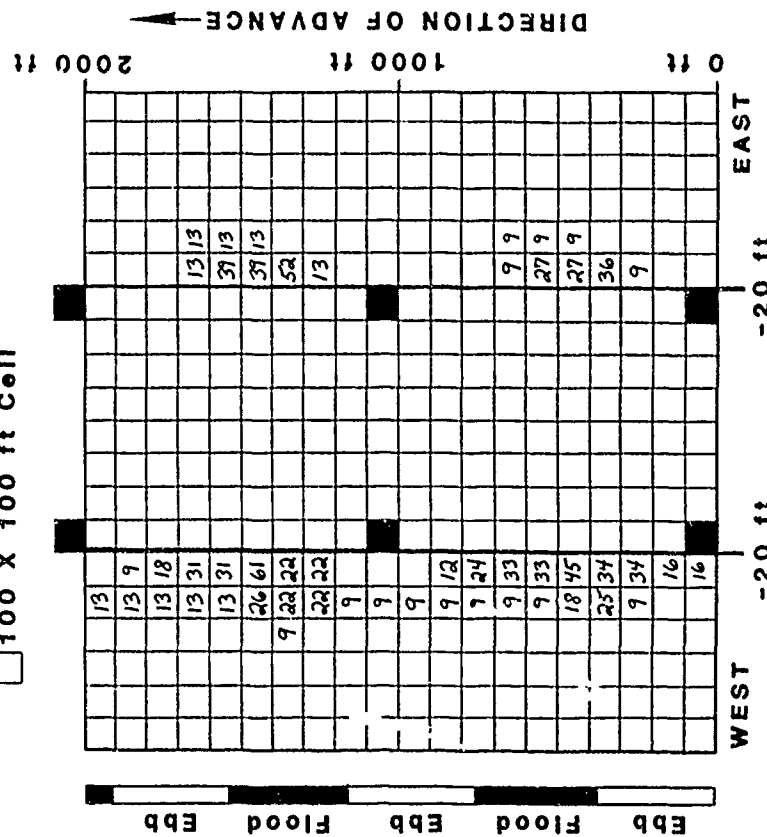


Figure 184. Sedimentation pattern (thickness, cm) for a hypothetical hopper barge overflow operation in Mobile Bay based on a model simulation for new work material during the month of August (first year of project). Assumes a 40-ft advance of the dredge per barge load and an 80-min barge replacement cycle. Deposition in grid cells at a depth greater than 20 ft not shown

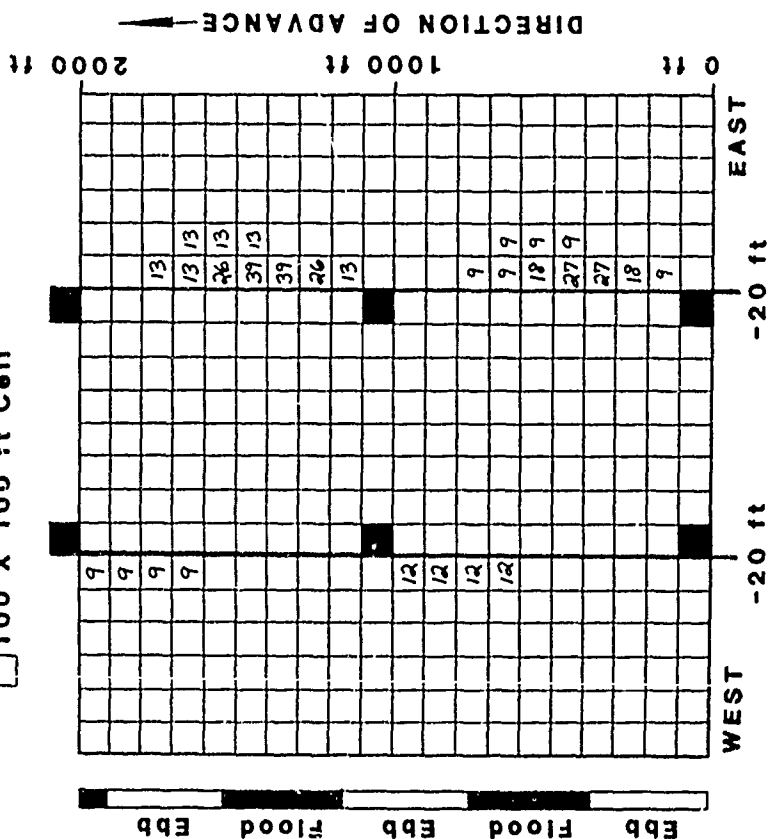


Figure 187. Sedimentation pattern (thickness, cm) for a hypothetical hopper barge overflow operation in Mobile Bay based on a model simulation for new work material during the month of November (second year of project). Assumes a 40-ft advance of the dredge per barge load and an 80-min barge replacement cycle. Deposition in grid cells at a depth greater than 20 ft not shown

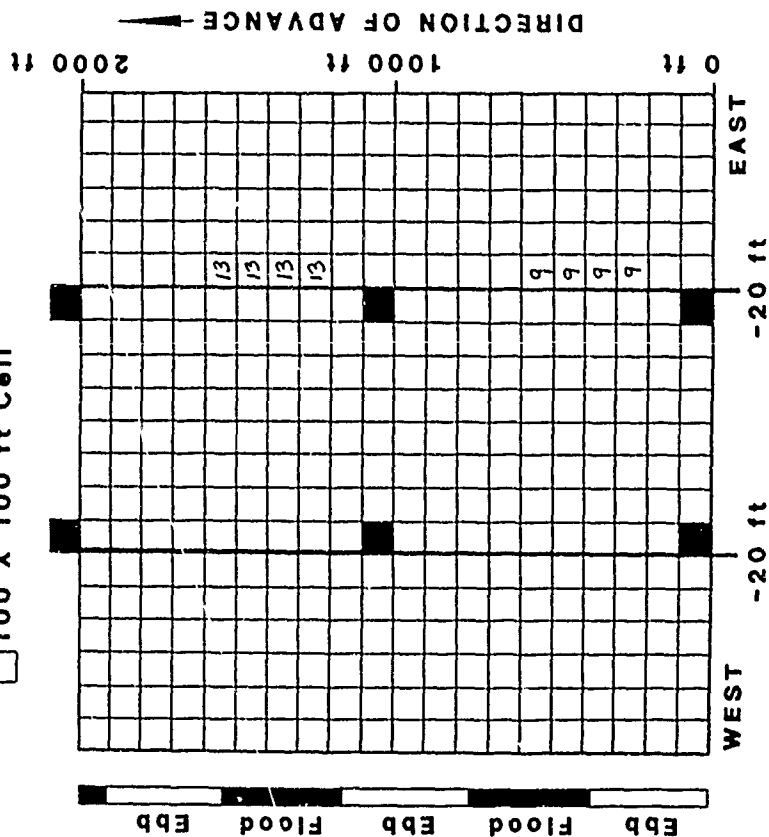


Figure 188. Sedimentation pattern (thickness, cm) for a hypothetical hopper barge overflow operation in Mobile Bay based on a model simulation for new work material during the month of December (second year of project). Assumes a 40-ft advance of the dredge per barge load and an 80-min barge replacement cycle. Deposition in grid cells at a depth greater than 20 ft not shown

Point of Overflow

100 X 100 ft Cell

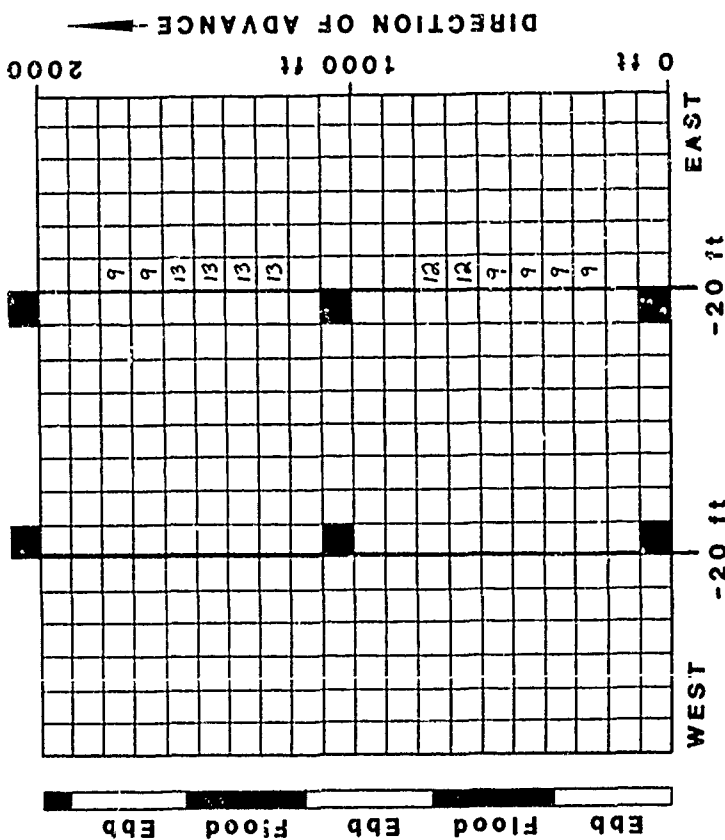


Figure 189. Sedimentation pattern (thickness, cm) for a hypothetical hopper barge overflow operation in Mobile Bay based on a model simulation for new work material during the month of January (second year of project). Assumes a 40-ft advance of the dredge per barge load and an 80-min barge replacement cycle. Deposition in grid cells at a depth greater than 20 ft not shown

Point of Overflow

100 X 100 ft Cell

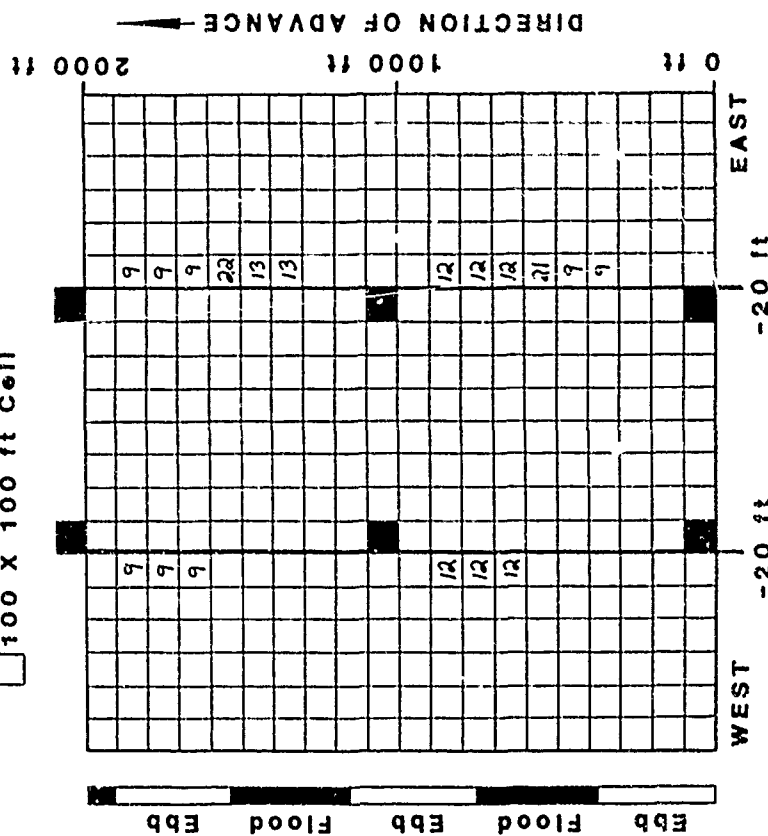


Figure 190. Sedimentation pattern (thickness, cm) for a hypothetical hopper barge overflow operation in Mobile Bay based on a model simulation for new work material during the month of February (second year of project). Assumes a 40-ft advance of the dredge per barge load and an 80-min barge replacement cycle. Deposition in grid cells at a depth greater than 20 ft not shown

Point of Overflow
100 X 100 ft Cell

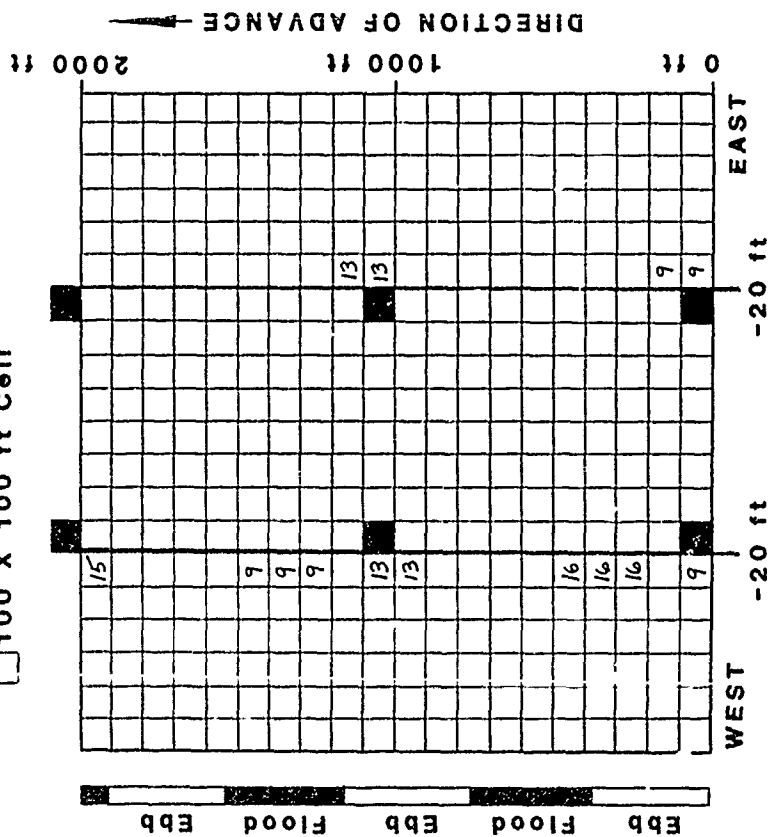


Figure 191. Sedimentation pattern (thickness, cm) for a hypothetical hopper barge overflow operation in Mobile Bay based on a model simulation for new work material during the month of March (second year of project). Assumes a 40-ft advance of the dredge per barge load and an 80-min barge replacement cycle. Deposition in grid cells at a depth greater than 20 ft not shown

Point of Overflow
100 X 100 ft Cell

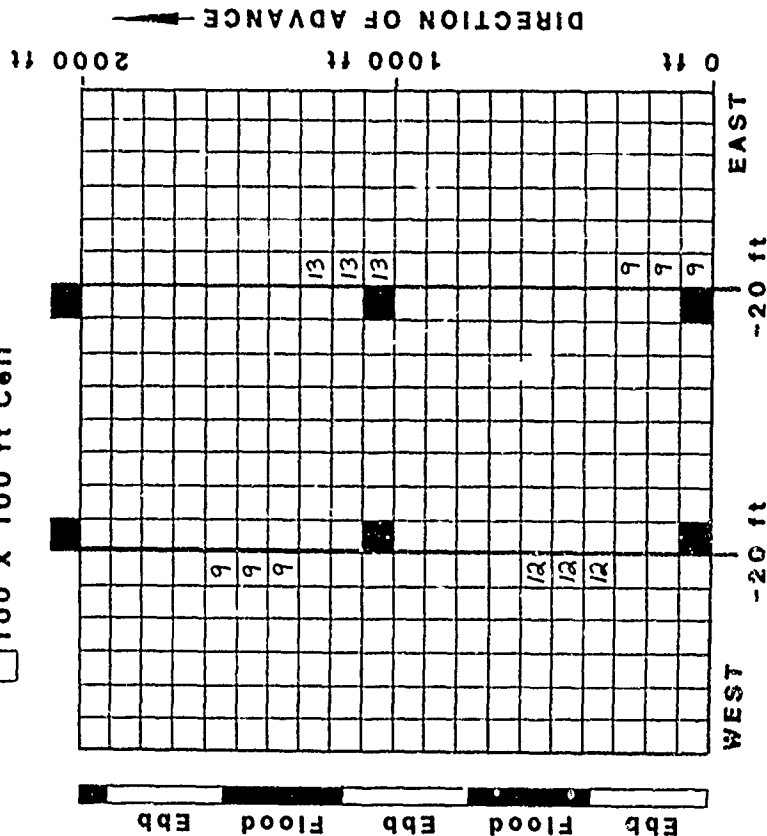




Figure 192. Sedimentation pattern (thickness, cm) for a hypothetical hopper barge overflow operation in Mobile Bay based on a model simulation for new work material during the month of April (second year of project). Assumes a 40-ft advance of the dredge per barge load and an 80-min barge replacement cycle. Deposition in grid cells at a depth greater than 20 ft not shown

 Point of Overflow
 100 X 100 ft Cell

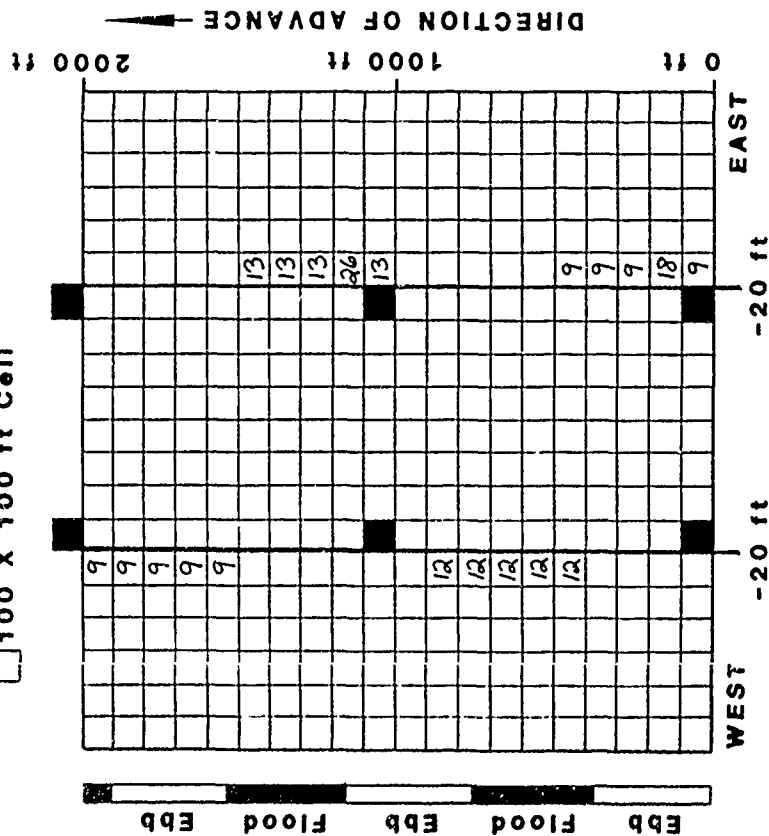


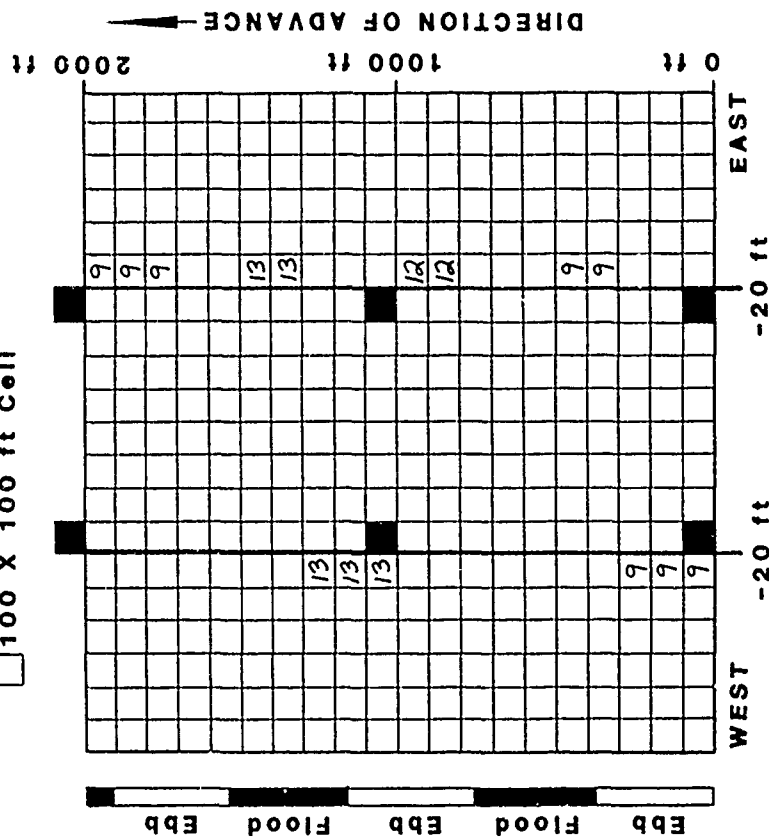




Figure 195. Sedimentation pattern (thickness, cm) for a hypothetical hopper barge overflow operation in Mobile Bay based on a model simulation for new work material during the month of July (second year of project). Assumes a 40-ft advance of the dredge per barge load and an 80-min barge replacement cycle. Deposition in grid cells at a depth greater than 20 ft not shown

 Point of Overflow
 100 X 100 ft Cell



 Point of Overflow
 100 X 100 ft Cell

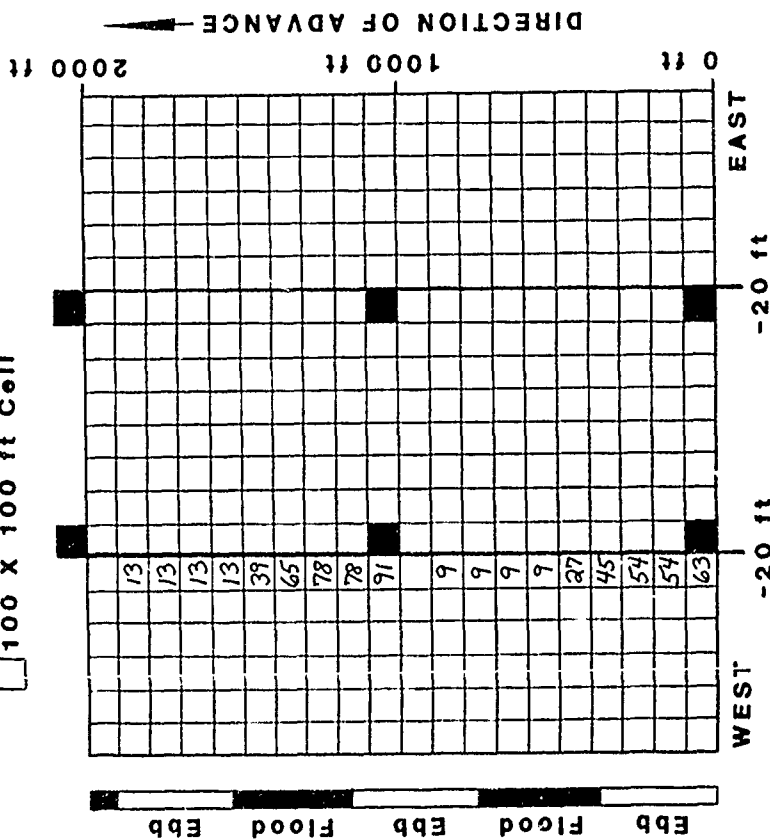




Figure 197. Sedimentation pattern (thickness, cm) for a hypothetical hopper barge overflow operation in Mobile Bay based on a model simulation for new work material during the month of September (second year of project). Assumes a 40-ft advance of the dredge per barge load and an 80-min barge replacement cycle. Deposition in grid cells at a depth greater than 20 ft not shown

 Point of Overflow
 100 X 100 ft Cell

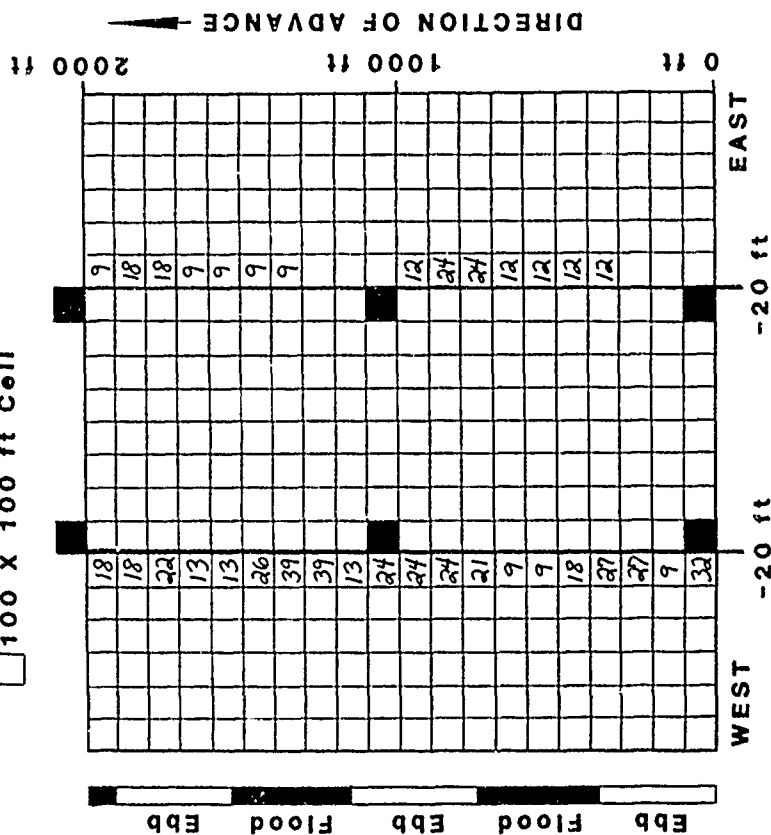


Figure 198. Sedimentation pattern (thickness, cm) for a hypothetical hopper barge overflow operation in Mobile Bay based on a model simulation for new work material during the month of October (second year of project). Assumes a 40-ft advance of the dredge per barge load and an 80-min barge replacement cycle. Deposition in grid cells at a depth greater than 20 ft not shown

Point of Overflow

100 X 100 ft Cell

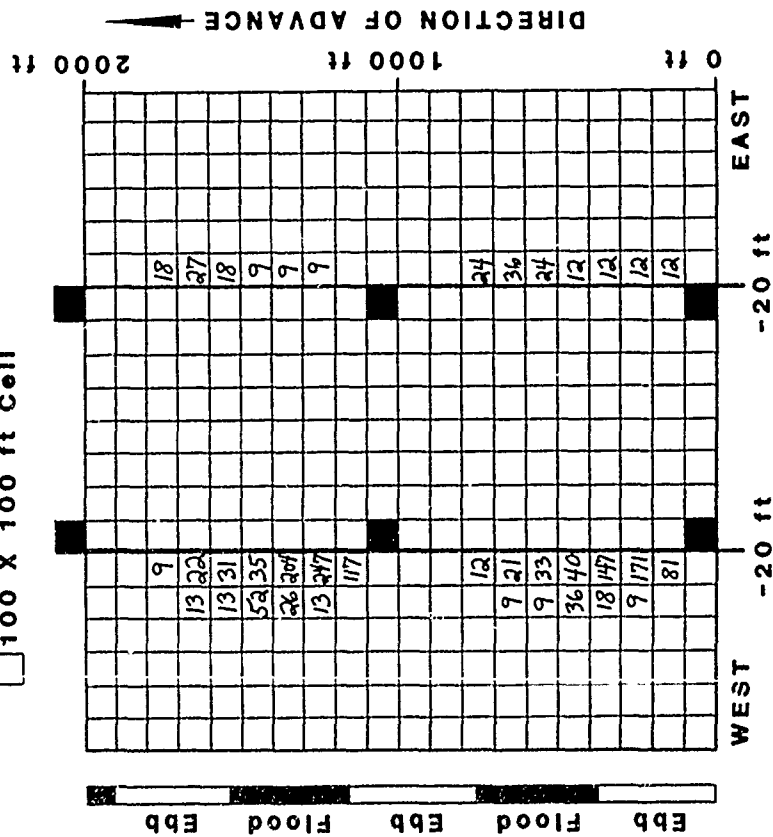


Figure 199. Sedimentation pattern (thickness, cm) for a hypothetical hopper barge overflow operation in Mobile Bay based on a model simulation for new work material during the month of November (third year of project). Assumes a 40-ft advance of the dredge per barge load and an 80-min barge replacement cycle. Deposition in grid cells at a depth greater than 20 ft not shown

Point of Overflow

100 X 100 ft Cell

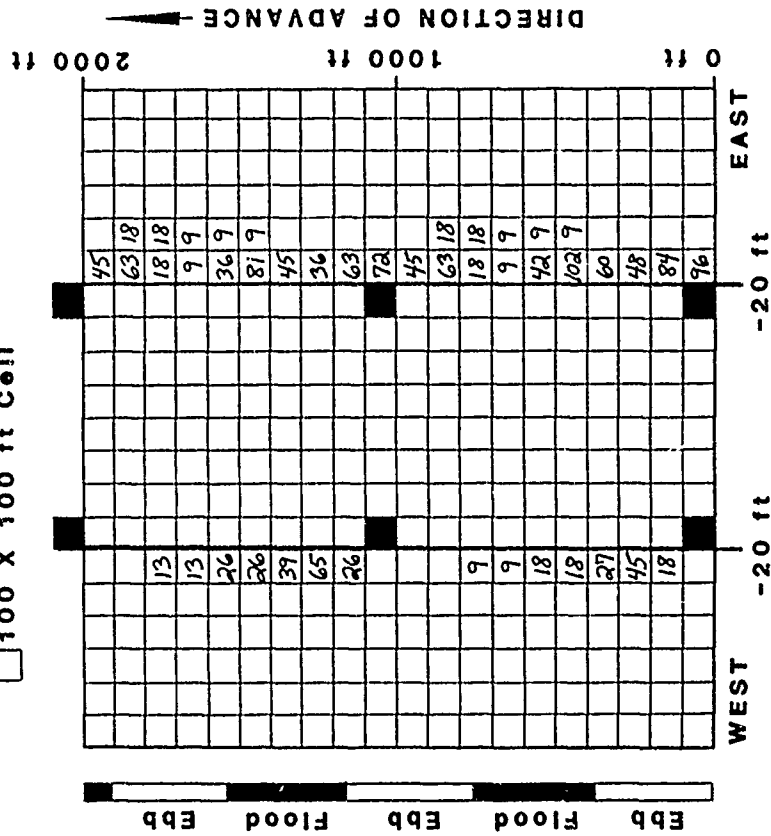


Figure 200. Sedimentation pattern (thickness, cm) for a hypothetical hopper barge overflow operation in Mobile Bay based on a model simulation for new work material during the month of December (third year of project). Assumes a 40-ft advance of the dredge per barge load and an 80-min barge replacement cycle. Deposition in grid cells at a depth greater than 20 ft not shown

Point of Overflow

100 X 100 ft Cell

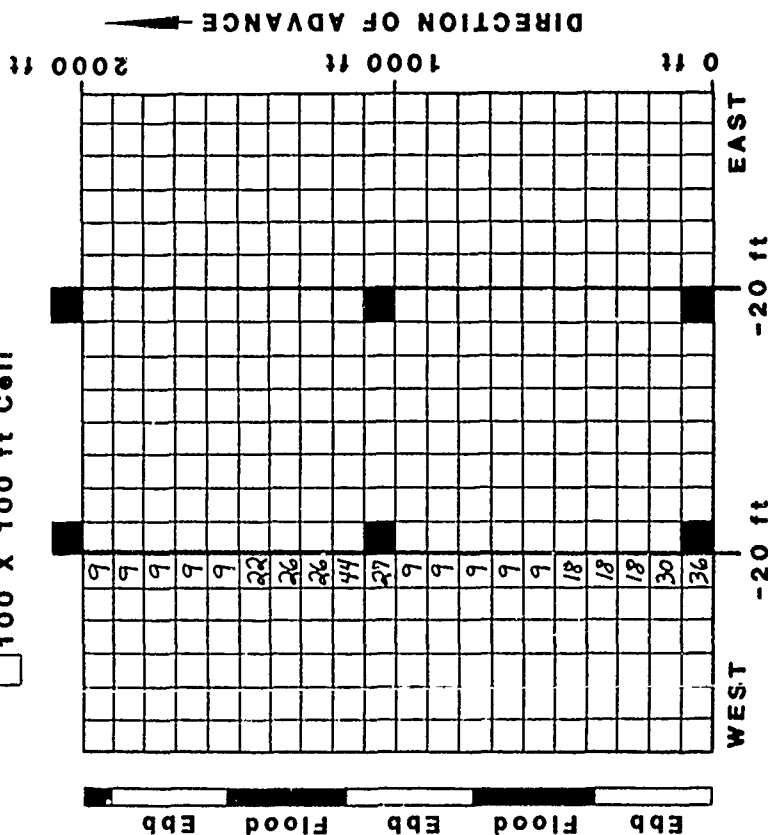


Figure 201. Sedimentation pattern (thickness, cm) for a hypothetical hopper barge overflow operation in Mobile Bay based on a model simulation for new work material during the month of January (third year of project). Assumes a 40-ft advance of the dredge per barge load and an 80-min barge replacement cycle. Deposition in grid cells at a depth greater than 20 ft not shown

Point of Overflow

100 X 100 ft Cell

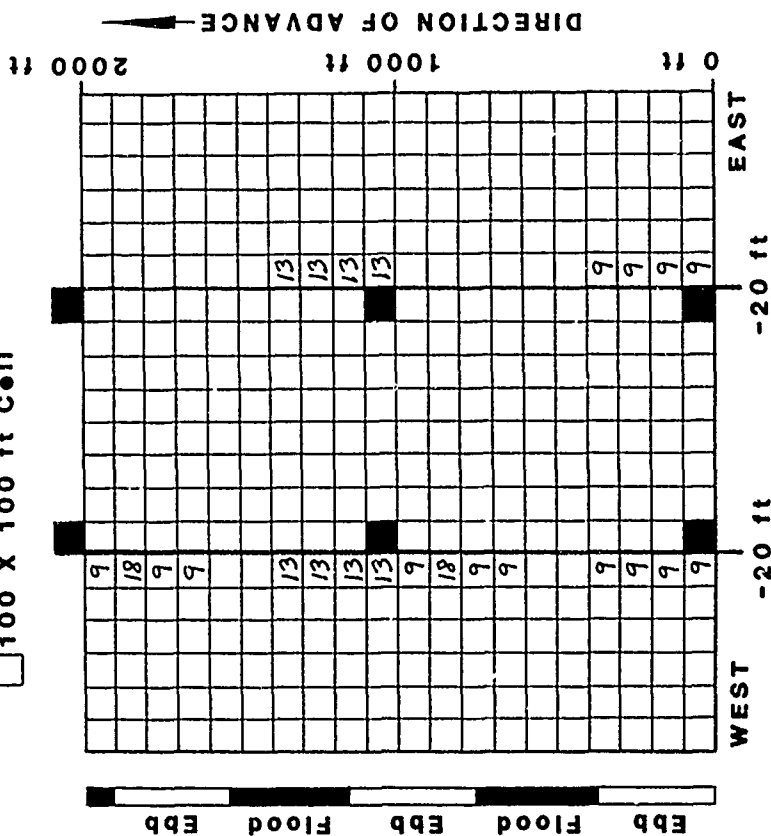


Figure 202. Sedimentation pattern (thickness, cm) for a hypothetical hopper barge overflow operation in Mobile Bay based on a model simulation for new work material during the month of February (third year of project). Assumes a 40-ft advance of the dredge per barge load and an 80-min barge replacement cycle. Deposition in grid cells at a depth greater than 20 ft not shown

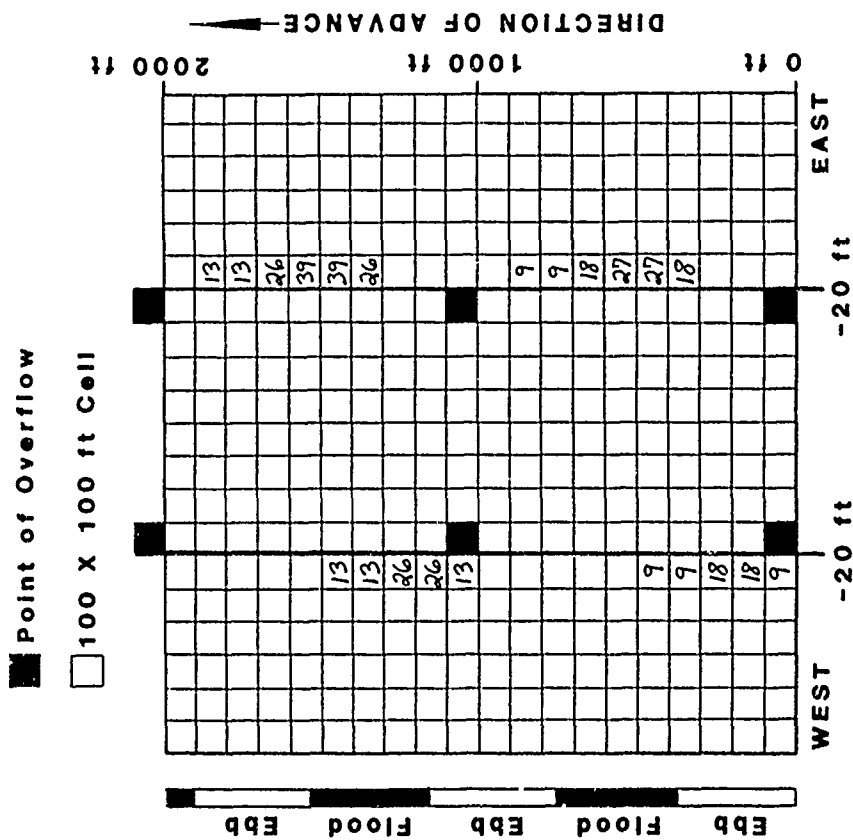


Figure 205. Sedimentation pattern (thickness, cm) for a hypothetical hopper barge overflow operation in Mobile Bay based on a model simulation for new work material during the month of May (third year of project). Assumes a 40-ft advance of the dredge per barge load and an 80-min barge replacement cycle. Deposition in grid cells at a depth greater than 20 ft not shown

SPECIES	STATION					LIFE MODE	FEED- ING GUILD
	2	5	6	7	8		
(M) <i>Mulinia lateralis</i>	■	□	■	■	□	S/B	SF/DF
(P) <i>Mediomastus ambiseta</i>	□	■	■	■	■	S/B	DF
(P) <i>Paraprionospio pinnata</i>	□	□	□	□		S/T	SF/DF
(P) <i>Leitoscoloplos robustus</i>	□	□	□			D/B	DF
(P) <i>Pseudeurythoe ambigua</i>	□	□				S	C/SC
(P) <i>Cossura soyeri</i>	□					D/B	DF
(P) <i>Lumbrineris verrilli</i>	□					S/B	DF/C
(P) <i>Magelona sp. A.</i>	□					S/B	DF
(P) <i>Glycinde solitaria</i>		□				B	C
(P) <i>Sigambra tentaculata</i>		□				B	C
(M) <i>Haminoea succinea</i>		□				S	C/H
(M) <i>Tornatina canaliculata</i>		□				B	C
(S) <i>Ogyrides alphaerostris</i>		□				S/B	DF/SF
(P) <i>Hobsonia florida</i>		□			□	S/T	DF
(P) <i>Sigambra bassi</i>		□	□	□		B	C
(M) <i>Macoma mitchelli</i>			□	□	□	S	SF/DF
(P) <i>Parandalia americana</i>		□			□	D/B	C
(P) <i>Sireblospio benedicti</i>		□		□	□	S/T	SF/DF
(M) <i>Mulinia pontchartrainensis</i>				□	■	S/B	SF/DF
(P) <i>Capitella capitata</i>				□	□	S/B	DF
(P) <i>Neanthes succinea</i>					□	S/B	DF/SC
(M) <i>Rangia cuneata</i>					□	B	SF
(M) <i>Texadina sphinctostoma</i>					□	S	DF

% OF TOTAL ABUNDANCE		
□	□	■
1 - 10	11 - 20	> 20

Figure 206. Distribution among stations, life mode (D = deep-dwelling, S = surface, B = burrower, T = tube builder), and feeding guild (C = carnivore, H = herbivore, SF = suspension feeder, DF = deposit feeder, SC = scavenger) of dominant benthos in Mobile Bay, Alabama

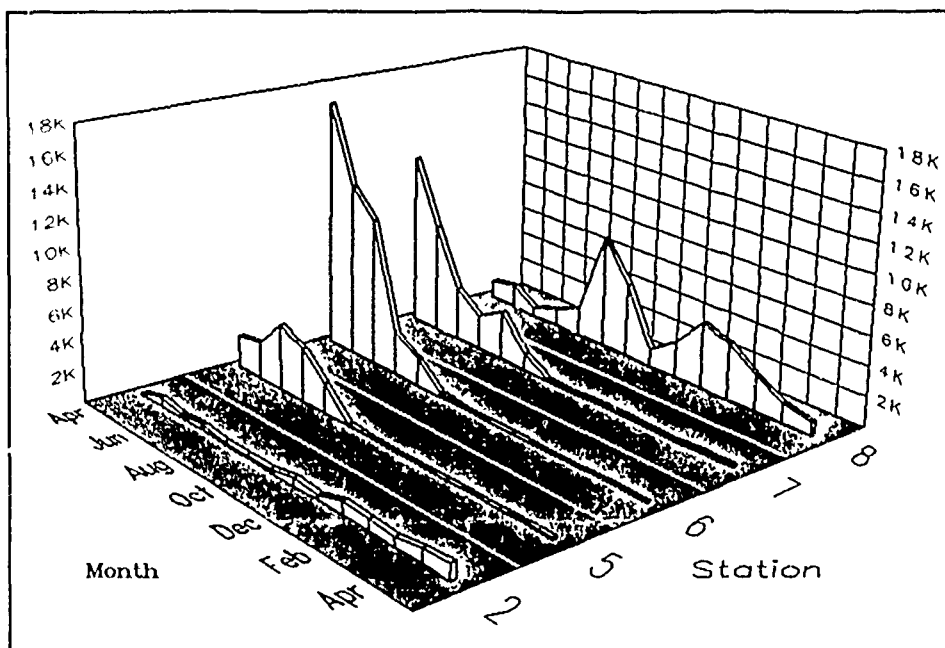


Figure 207. Distribution and seasonal abundance of the polychaete *Mediomastus ambiseta* in Mobile Bay

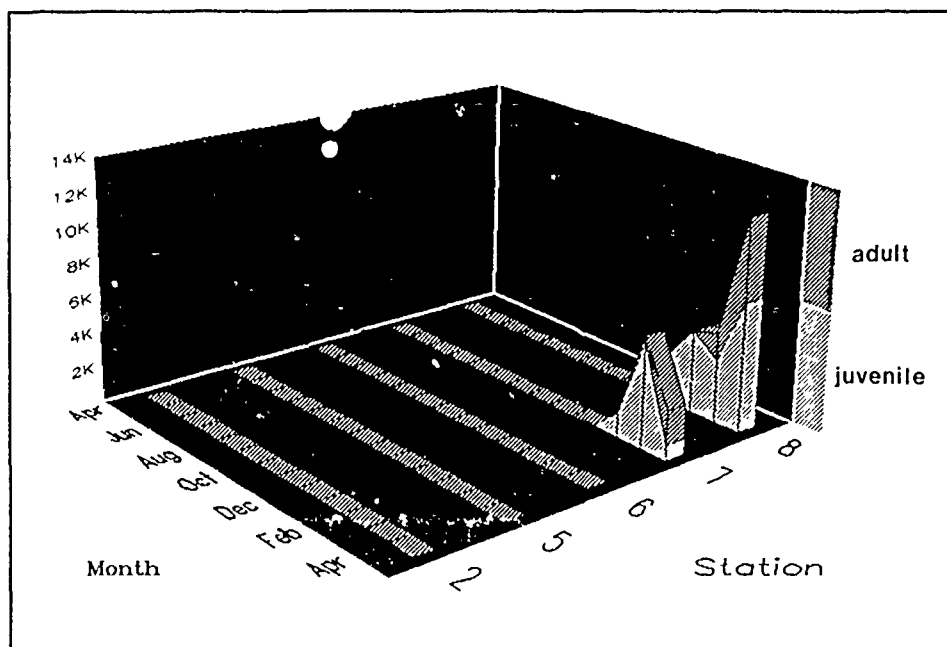


Figure 208. Distribution and seasonal abundance of the bivalve mollusc *Mulinia pontchartrainensis* in Mobile Bay

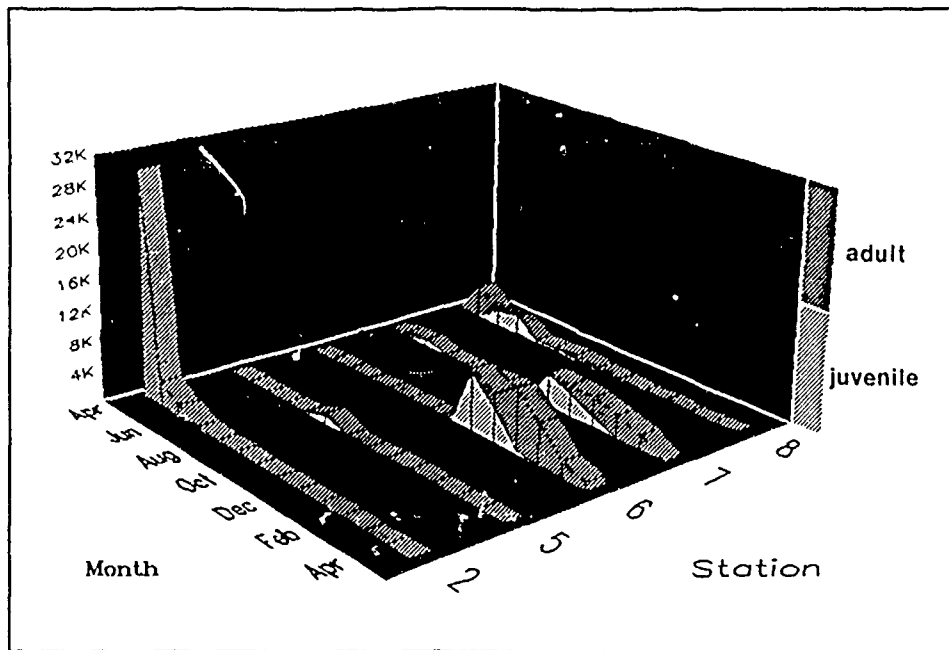


Figure 209. Distribution and seasonal abundance of the bivalve mollusc *Mulinia lateralis* in Mobile Bay

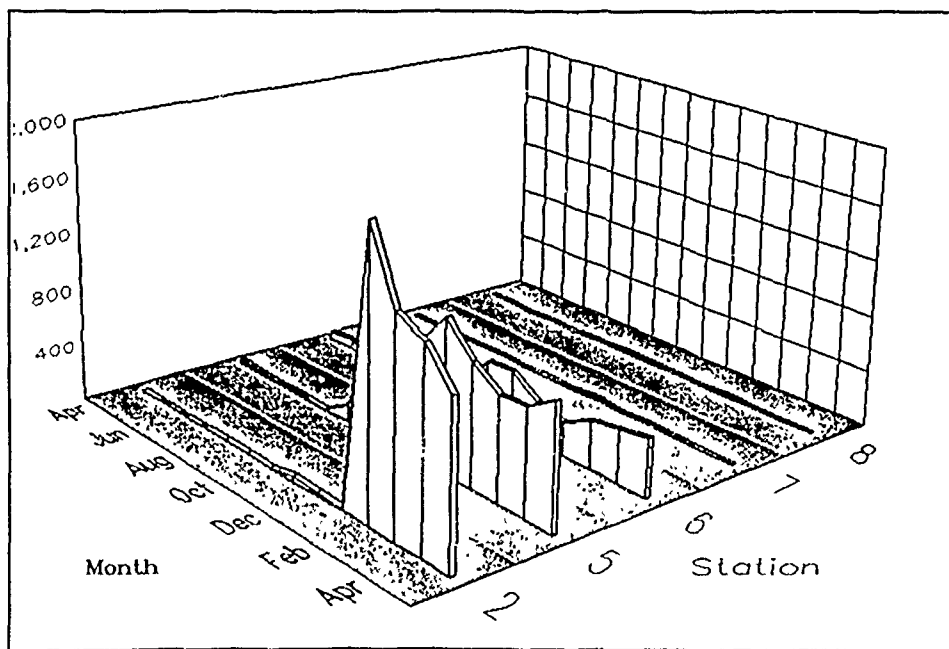


Figure 210. Distribution and seasonal abundance of the polychaete *Leitoscoloplos robustus* in Mobile Bay

APPENDIX A: HOPPER BARGE OPERATIONS DATA

Table A1
Dump Scow Draft Readings for Test 1*

<u>Time</u> <u>CST</u>	<u>Time</u> <u>After Start, min</u>	<u>Change</u> <u>in Draft, ft</u>
1036	1	0.05
1038	3	0.55
1040	5	1.05
1042	7	1.47
1044	9	2.01
1046	11	2.56
1048	13	3.07
1050	15	3.58
1052	17	4.09
1054	19	4.58
1056	21	5.10
1058	23	5.58
1100	25	6.06
1102	27	6.53
1104	29	6.98
1106	31	7.39
1108	33	7.75
1110	35	8.13
1112	37	8.48
1114	39	8.79
1116	41	9.09
1118	43	9.30
**1120	45	9.49
1122	47	9.57
1124	49	9.59
1126	51	9.61
1128	53	9.63
1130	55	9.66
1132	57	9.68
1134	59	9.68
**1136	61	9.69
1138	63	9.56

* For a discussion of these tests, see Part IV of the main text.

** Note: The barge began filling at 1035 CST. Overflow began at 1119. Filling stopped at 1135, and overflow ended at 1137.

Table A2
Dump Scow Draft Readings for Test 2

<u>Time</u> <u>CST</u>	<u>Time</u> <u>After Start, min</u>	<u>Change</u> <u>in Draft, ft</u>
0828	1	0.17
0830	3	0.82
0832	5	1.50
0834	7	2.23
0836	9	3.02
0838	11	3.74
0840	13	4.50
0842	15	5.25
0844	17	5.98
0846	19	6.71
0848	21	7.42
0850	23	8.13
0852	25	8.82
0854	27	9.52
0856	29	10.19
*0858	31	10.37
0900	33	10.41
0902	35	10.44
0904	37	10.42
0906	39	10.44
*0908	41	10.31
0910	43	10.28
0912	45	10.27
0914	47	10.27

* Note: The barge began filling at 0827 CST. Overflow began at 0857. Filling stopped at 0907, and overflow ended at 0913.

Table A3

Dump Scow Draft Readings for Test 3

<u>Time</u> <u>CST</u>	<u>Time</u> <u>After Start, min</u>	<u>Change</u> <u>in Draft, ft</u>
1222	3	1.0
1225	6	1.7
1230	11	3.4
1235	16	5.5
1240	21	7.1
1245	26	9.1
*1248	29	10.1
1250	31	10.5
1252	33	10.6
1254	35	11.0
1256	37	10.9
1258	39	10.9
*1300	41	10.9

* Note: The barge began filling at 1219 CST. Overflow occurred at 1248. The filling stopped at 1300 and overflow ended at 1305. These values were obtained manually from the deck of the barge due to failure of the electronic water-level recording equipment.

Table A4
Dump Scow Draft Readings for Test 4

<u>Time</u> <u>CST</u>	<u>Time</u> <u>After Start, min</u>	<u>Change</u> <u>in Draft, ft</u>
0908	1	0.06
0910	3	0.49
0912	5	1.11
0914	7	1.75
0916	9	2.27
0918	11	2.81
0920	13	3.43
0922	15	4.08
0924	17	4.67
0926	19	5.27
0928	21	5.86
0930	23	6.45
0932	25	6.99
0934	27	7.50
0936	29	8.02
0938	31	8.59
0940	33	9.09
*0942	35	9.55
0944	37	9.94
0946	39	10.06
0948	41	10.05
0950	43	10.10
0952	45	10.12
0954	47	10.11
0956	49	10.13
0958	51	10.16
1000	53	10.16
1002	55	10.15
1004	57	10.17
1006	59	10.20
1008	61	10.19
1010	63	10.18
1012	65	10.22
*1014	67	10.23
1016	69	10.13
1018	71	10.05
1020	73	10.01
1022	75	10.00

* Note. The barge began filling at 0907 CST. Overflow occurred at 0943. The filling stopped at 1015, and overflow ended at 1021.

Table A5
Dump Scow Draft Readings for Test 5

<u>Time</u> <u>CST</u>	<u>Time</u> <u>After Start, min</u>	<u>Change</u> <u>in Draft, ft</u>
1311	1	0.03
1313	3	0.20
1315	5	0.81
1317	7	1.53
1319	9	2.18
1321	11	2.79
1323	13	3.38
1325	15	4.03
1327	17	4.66
1329	19	5.26
1331	21	5.82
1333	23	6.38
1335	25	6.99
1337	27	7.56
1339	29	8.03
1341	31	8.60
1343	33	9.17
1345	35	9.74
*1347	37	10.25
1349	39	10.43
1351	41	10.44
1353	43	10.47
1355	45	10.44
1357	47	10.48
1359	49	10.49
1401	51	10.52
1403	53	10.48
1405	55	10.52
1407	57	10.52
1409	59	10.52
1411	61	10.49
1413	63	10.53
1415	65	10.51
*1417	67	10.51
1419	69	10.34
1421	71	10.32
1423	73	10.30

* Note: The barge began filling at 1310. Overflow occurred at 1346. Filling stopped at 1416, and overflow ended at 1422.

Table A6
Dump Scow Draft Readings for Test 6

<u>Time</u> <u>CST</u>	<u>Time</u> <u>After Start, min</u>	<u>Change</u> <u>in Draft, ft</u>
0847	1	0.03
0849	3	0.63
0851	5	1.38
0853	7	2.15
0855	9	2.95
0857	11	3.68
0859	13	4.40
0901	15	5.09
0903	17	5.84
0905	19	6.59
0907	21	7.28
0909	23	7.95
0911	25	8.67
0913	27	9.34
*0915	29	10.23
0917	31	10.64
0919	33	10.82
0921	35	10.83
0923	37	10.83
0925	39	10.87
0927	41	10.91
0929	43	10.88
0931	45	10.92
0933	47	10.99
0935	49	11.00
0937	51	10.99
*0939	53	11.00
0941	55	10.95
0943	57	10.72

* Note: The barge began filling at 0846 CST. Overflow occurred at 0915. Filling stopped at 0940, and overflow ended at 0942.

Table A7
Dump Scow Draft Readings for Test 7*

<u>Time</u> <u>CST</u>	<u>Time</u> <u>After Start, min</u>	<u>Change</u> <u>in Draft, ft</u>
0931	1	2.91
0933	3	3.84
0935	5	4.85
0937	7	5.69
0939	9	6.49
0941	11	7.24
0943	13	7.98
0945	15	8.63
0947	17	9.25
0949	19	9.94
0951	21	10.54
0953	23	11.13
0955	25	11.79
**0957	27	12.35
0959	29	12.78
1001	31	12.85
1003	33	12.91
1005	35	12.93
1007	37	12.90
1009	39	12.98
1011	41	12.96
1013	43	12.95
1015	45	13.03
1017	47	12.98
1019	49	12.98
1021	51	13.01
1023	53	13.01
**1025	55	13.01
1027	57	12.87
1029	59	12.81

* Only the bow readings were available from this test. Also, no 0.0 value for the empty barge was obtained, so these readings are the actual pressure readings from the sensor.

** The barge began filling at 0930 CST. Overflow began at 0957. The filling stopped at 1025, and overflow ended at 1028.

Table A8
Dump Scow Draft Readings for Test 8

<u>Time CST</u>	<u>Time After Start, min</u>	<u>Change in Draft, ft</u>
1430	2	0.68
1432	4	1.60
1434	6	2.45
1436	8	3.28
1438	10	4.15
1440	12	5.00
1442	14	5.77
1444	16	6.55
1446	18	7.34
1448	20	8.16
1450	22	8.93
1452	24	9.62
1454	26	10.16
1456	28	10.48
1458	30	10.66
*1500	32	10.75
1502	34	10.83
1504	36	10.90
1506	38	10.93
1508	40	10.90
1510	42	10.92
1512	44	11.02
1514	46	11.07
1516	48	11.05
1518	50	11.04
1520	52	11.12
1522	54	11.13
1524	56	11.12
1526	58	11.14
1528	60	11.21
1530	62	11.25
1532	64	11.23
1534	66	11.26
1536	68	11.27
1538	70	11.35
1540	72	11.32
1542	74	11.34
1544	76	11.39
1546	78	11.41
1548	80	11.42
1550	82	11.44
*1552	84	11.57
1554	86	11.46
1556	88	11.32
1558	90	11.30

* Note: Dredging began 1428 CST. Overflow occurred at 1459. Filling stopped at 1552, and overflow stopped at 1558.

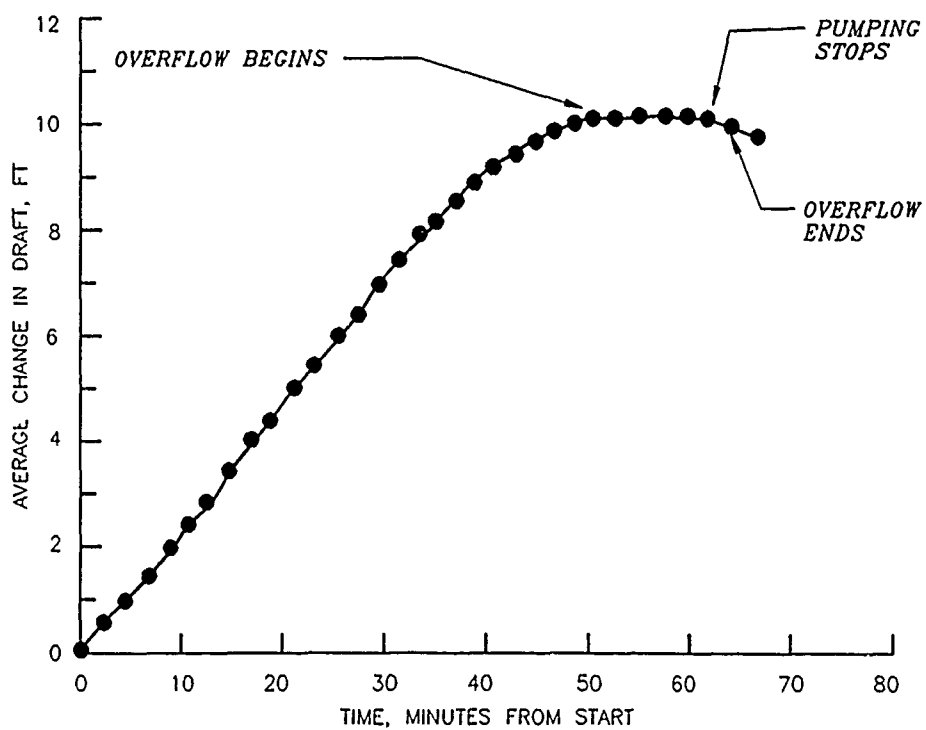


Figure A1. Change in barge draft during loading - Test 1
(lower site, maintenance material)

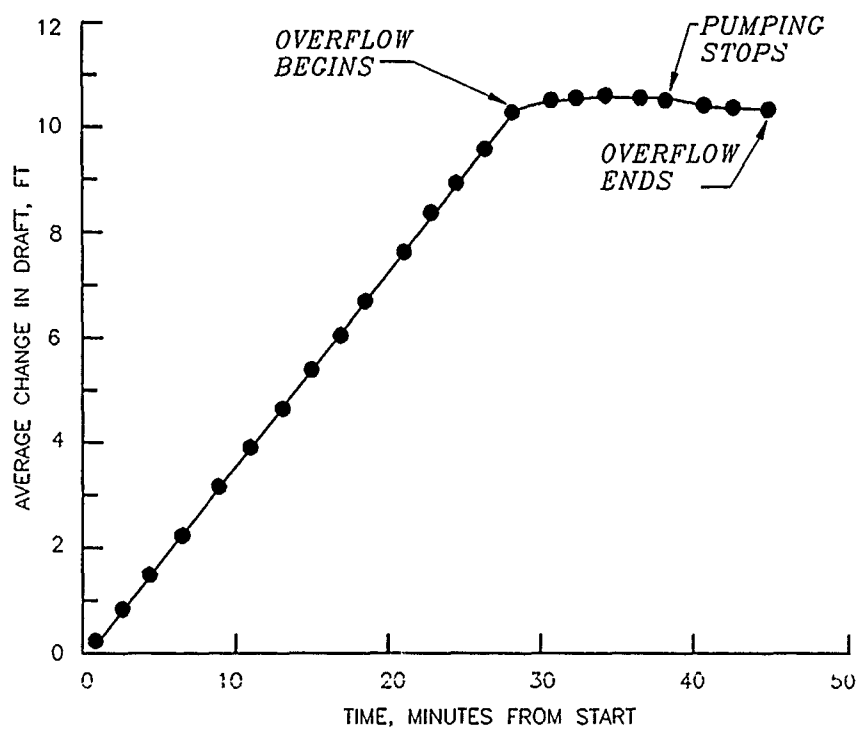


Figure A2. Change in barge draft during loading - Test 2
(lower site, new work material)

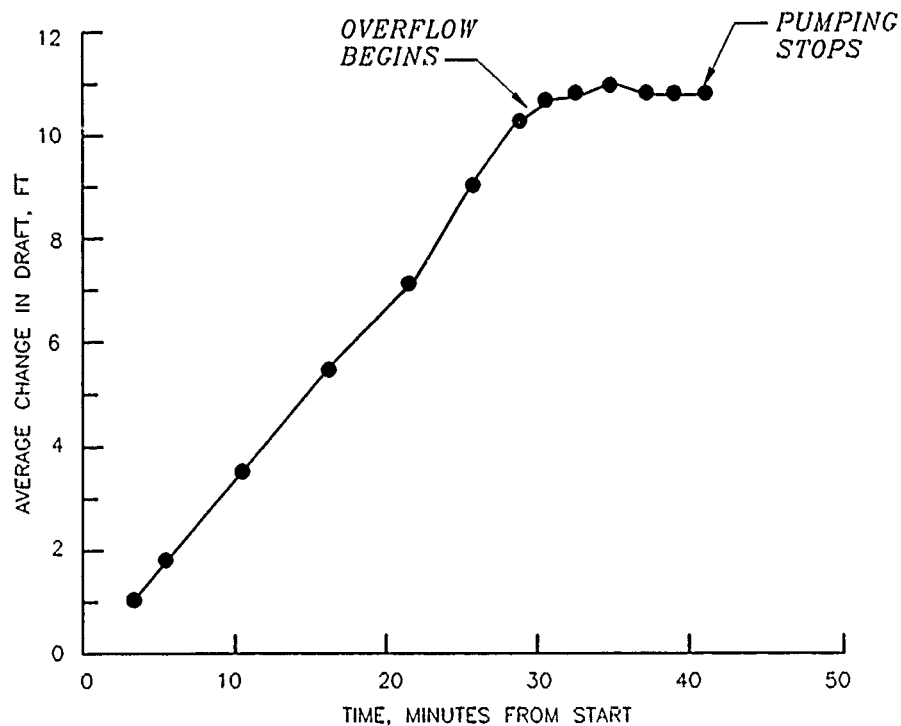


Figure A3. Change in barge draft during loading - Test 3
(lower site, new work material)

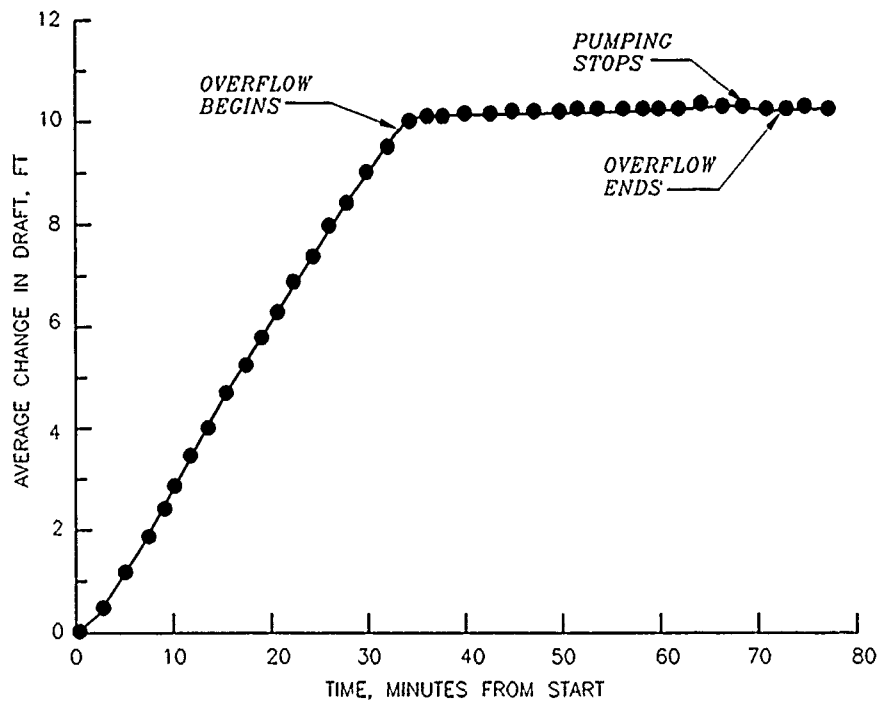


Figure A4. Change in barge draft during loading - Test 4
(upper site, maintenance material)

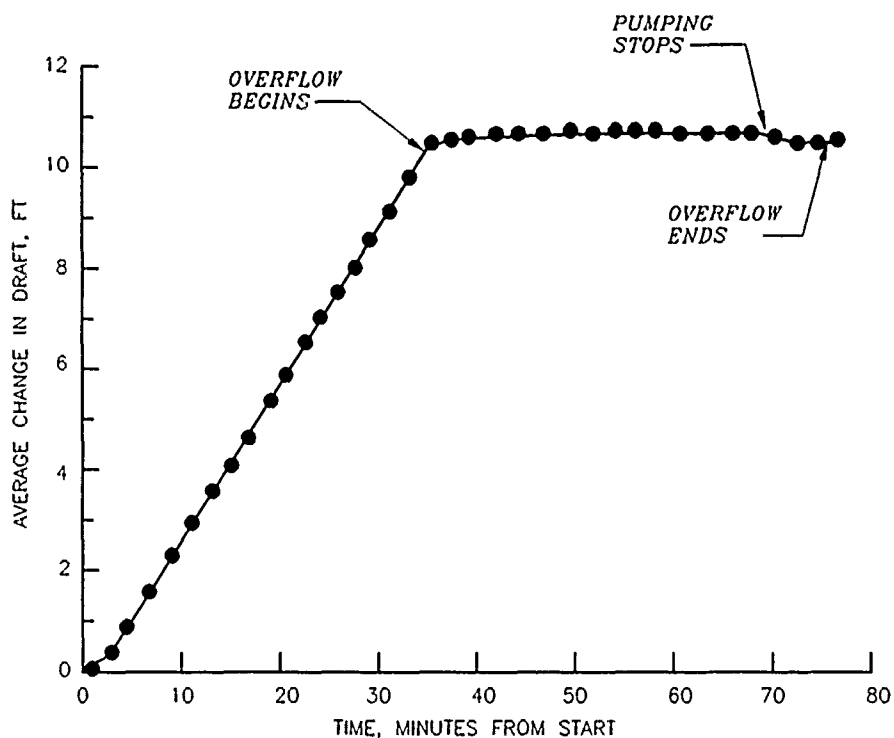


Figure A5. Change in barge draft during loading - Test 5 (upper site, maintenance material)

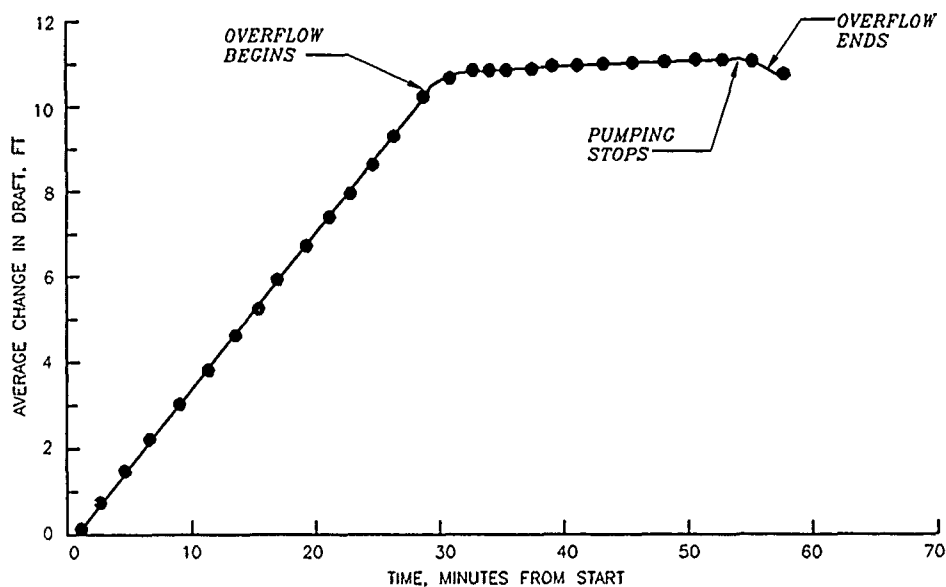


Figure A6. Change in barge draft during loading - Test 6 (upper site, new work material)

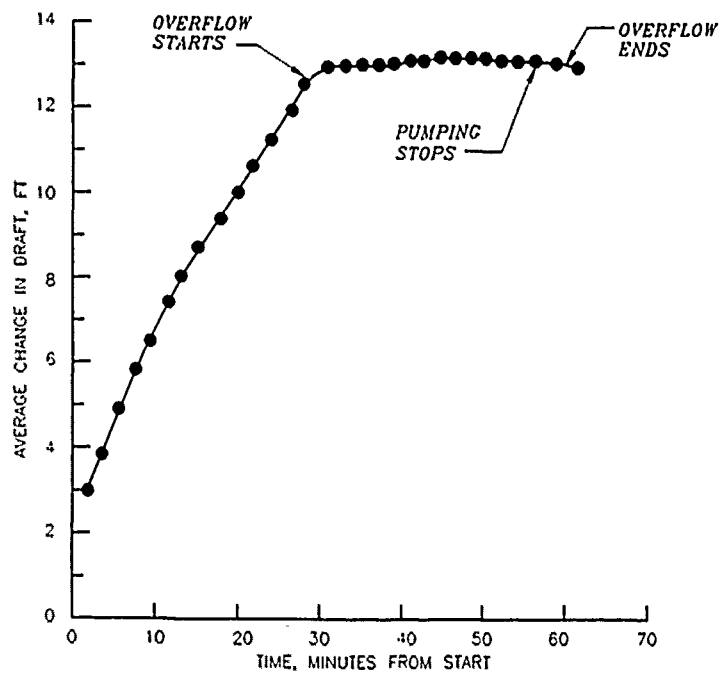


Figure A7. Change in barge draft during loading - Test 7 (upper site, new work material)

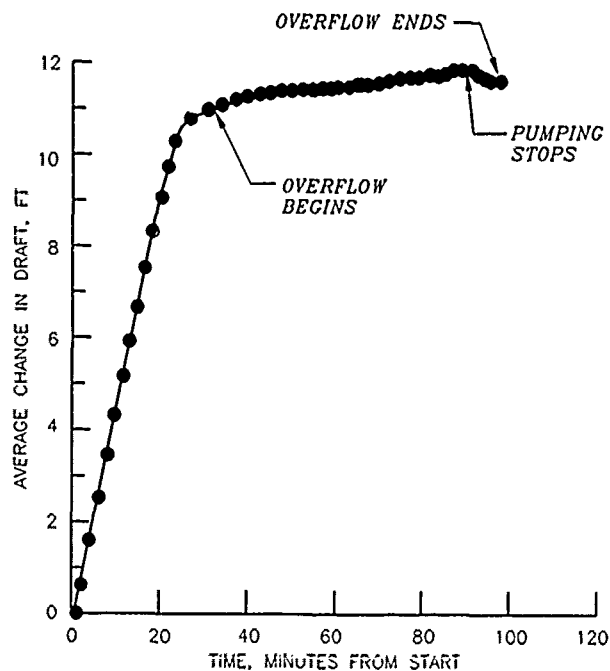


Figure A8. Change in barge draft during loading - Test 8 (upper site, new work material)

APPENDIX B: REPRESENTATIVE MONTHLY BOUNDARY CONDITIONS

Mean monthly high and low tides (NGVD) at Dauphin Island and at Cedar Point and their phase relationship were tabulated from available literature (Schroeder and Wiseman 1985).^{*} These values are shown in Table B1. The mean high tide and low tide values are used to construct a simple cosine curve diurnal tide, illustrated in Figure B1. These tides are applied at the Gulf of Mexico computational boundary and the Mississippi Sound computational boundary with the proper phase relationship between them.

Mean monthly freshwater inflow rates to Mobile Bay were determined, and the distribution of the flow was estimated from data published by the US Geological Survey (Psinakis 1987) and the US Army Engineer District, Mobile (1985). These data and results are presented in Tables B2 and B3.

Results from physical model tests conducted at the Waterways Experiment Station (Lawing, Boland, and Bobb 1975) provided an indication of how the freshwater inflow rate to Mobile Bay varies over the tidal cycle. For a significant portion of the tidal cycle, the riverflows are negative, i.e., the flow is from Mobile Bay up into the river systems. The ratio of hourly flow rate to average flow rate was estimated (see Table B4). The times are referenced to high tide at Main Pass. The estimated flow rate ratios were considered to be the same for all months of the year. When the time-varying flow is averaged over the complete tidal cycle, the average freshwater flow rate is obtained.

The actual river flow rate distribution applied to the model for each monthly application is shown in Figures B1-B12. Time is referenced to high tide at Main Pass.

The dominant monthly wind conditions were determined from meteorological data (Schroeder and Wiseman 1985) and are presented in Table B5. These dominant monthly wind conditions were considered constant during the numerical model simulation for each month.

^{*} See References for Part VII of the main text.

Table B1
Mean Monthly High and Low Tides (NGVD)
at Dauphin Island and at Cedar Point

<u>Month</u>	<u>Dauphin Island</u>		<u>Cedar Point</u>		<u>Phase*</u> <u>hr</u>
	<u>High Tide</u> <u>ft</u>	<u>Low Tide</u> <u>ft</u>	<u>High Tide</u> <u>ft</u>	<u>Low Tide</u> <u>ft</u>	
January	1.0	-0.74	0.75	-0.77	0.33 lag
February	1.16	-0.60	0.60	-0.68	0.60 lag
March	1.40	-0.34	0.84	-0.17	0.15 lead
April	1.37	-0.20	1.20	-0.15	0.17 lag
May	1.35	-0.07	1.22	-0.01	0.50 lag
June	1.37	-0.20	1.07	-0.15	0.27 lag
July	1.50	-0.26	1.22	-0.10	0.67 lag
August	1.44	-0.00	1.26	0.19	0.20 lag
September	1.42	0.18	1.39	0.39	0.00
October	1.25	0.10	1.17	0.05	0.50 lag
November	1.0	-0.15	1.30	-0.07	0.55 lag
December	0.98	-0.55	0.95	-0.65	1.0 lag

* Phase of Cedar Point tide relative to Dauphin Island tide.

Table B2
Division of Freshwater Inflow to Mobile Bay

<u>Month</u>	<u>Mean Monthly Flow Rate, cfs</u>	<u>Percent of Total Flow Rate</u>			
		<u>Mobile River</u>	<u>Tensaw River</u>	<u>Apalachee River</u>	<u>Blakeley River</u>
January	106,000	28	33	15	24
February	109,000	28	33	15	24
March	152,000	29	32	15	24
April	168,000	29	32	15	24
May	86,000	27	33	15	25
June	39,000	27	33	15	25
July	24,000	26	33	15	26
August	22,000	26	33	15	26
September	20,000	26	33	15	26
October	32,000	26	33	15	25
November	41,000	27	33	15	25
December	80,000	27	33	15	25

Table B3
Average Freshwater Inflow to Mobile Bay

<u>Month</u>	<u>Total Flow, cfs</u>	<u>Distribution of Flow, cfs</u>		
		<u>Mobile River</u>	<u>Tensaw River</u>	<u>Apalachee and Blakeley Rivers</u>
January	106,000	29,680	34,980	41,340
February	109,000	30,520	35,970	42,510
March	152,000	44,080	48,640	59,280
April	168,000	48,720	53,760	65,520
May	86,000	23,220	28,380	34,400
June	39,000	10,530	12,870	15,600
July	24,000	6,240	7,920	9,840
August	22,000	5,720	7,260	9,020
September	20,000	5,200	6,600	8,200
October	32,000	8,320	10,560	13,120
November	41,000	11,070	13,530	16,400
December	80,000	21,690	26,400	32,000

Table B4
Ratio of Hourly Flow Rate to Average
Flow Rate into Mobile Bay

<u>Time, hr*</u>	<u>Under 100,000 cfs</u> <u>Total Flow</u>	<u>Over 100,000 cfs</u> <u>Total Flow</u>
0	-0.528	-0.11
1	-0.878	-0.14
2	-1.24	-0.18
3	-1.58	-0.21
4	-1.24	-0.18
5	-1.06	-0.14
6	-0.79	-0.11
7	-0.53	-0.07
8	-0.26	-0.04
9	0.0	0.0
10	0.80	0.60
11	1.60	1.19
12	2.40	1.78
13	3.20	
2.37 14	3.98	2.95
15	4.80	3.56
16	4.80	3.56
17	3.98	2.95
18	3.20	2.37
19	2.40	1.78
20	1.60	1.19
21	0.80	0.59
22	0.0	0.0
23	-0.24	-0.04
24	-0.53	-0.07

* Times are referenced to high tide at Main Pass.

Table B5
Dominant Monthly Wind Conditions

<u>Month</u>	<u>Magnitude</u> <u>knots</u>	<u>Direction</u>
January	11	N
February	10	N
March	7	SE
April	7	SE
May	7	SE
June	6	S
July	6	S
August	7	E
September	9	N
October	9	N
November	10	N
December	11	N

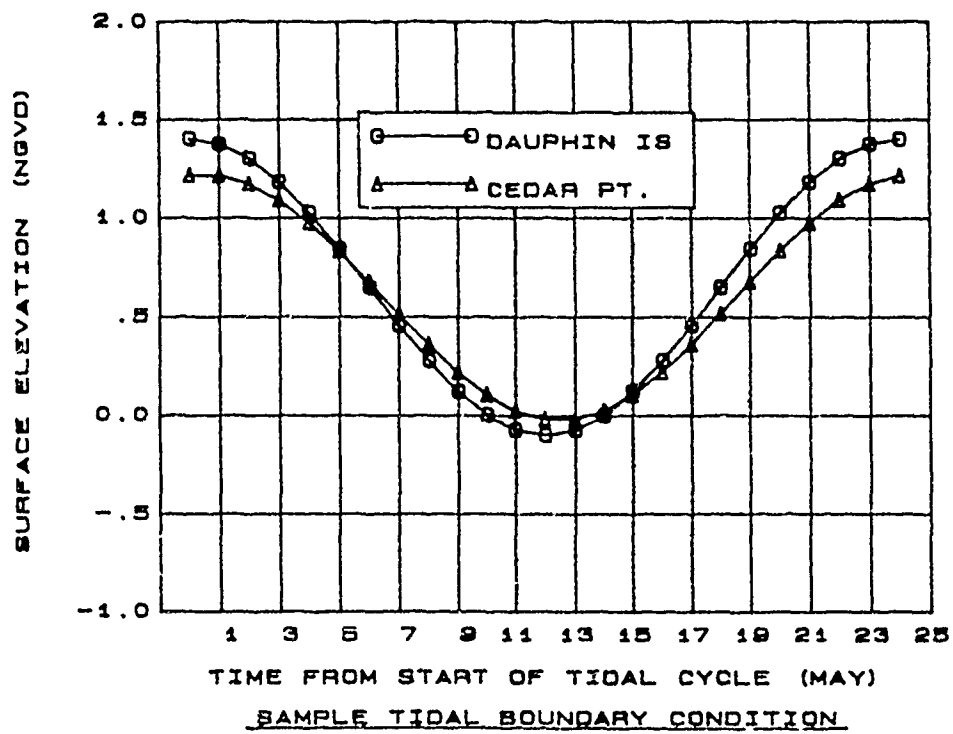


Figure B1. Sample diurnal tide boundary conditions

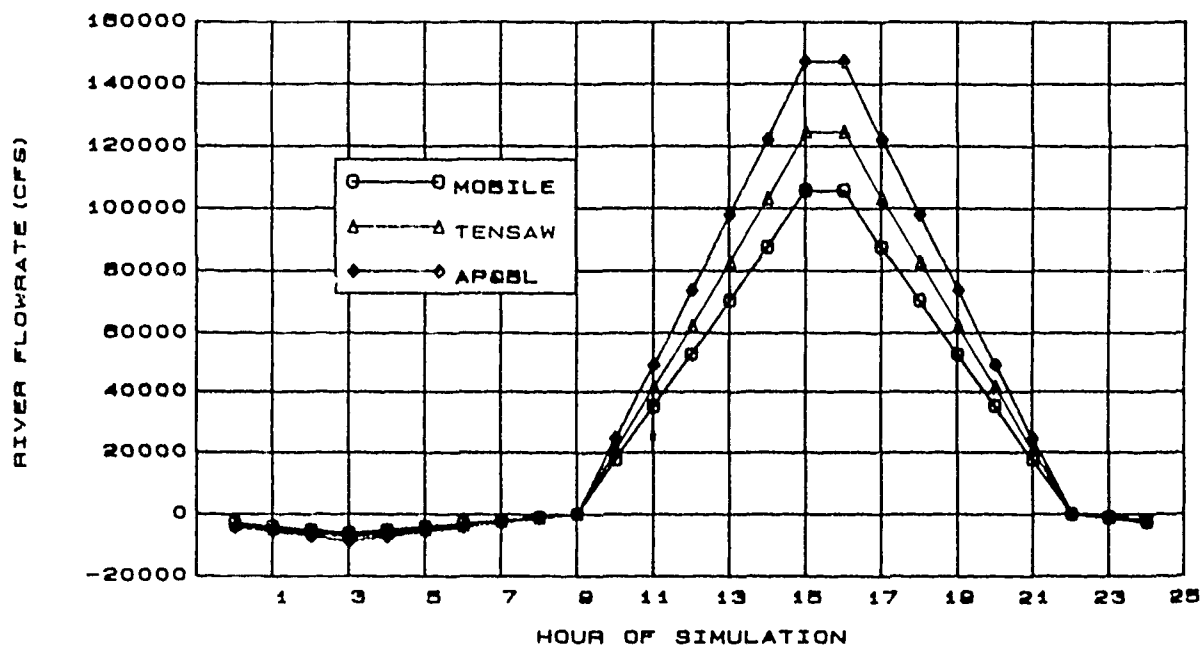


Figure B2. Variation of river flow rate with time for January

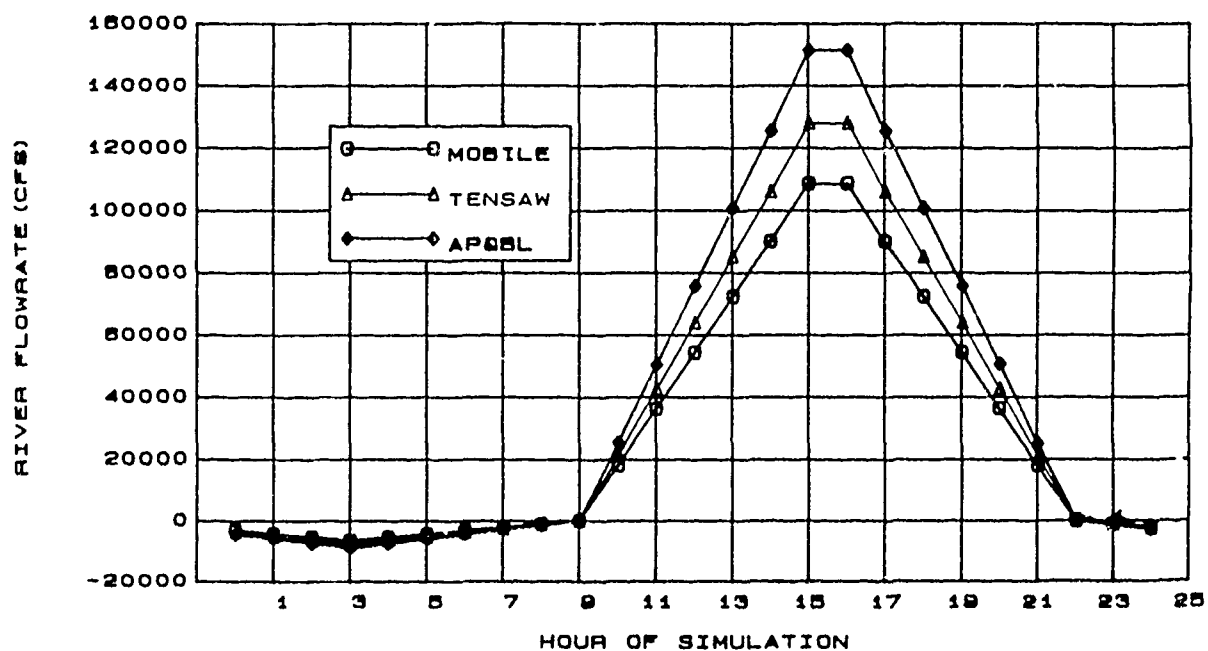


Figure B3. Variation of river flow rate with time for February

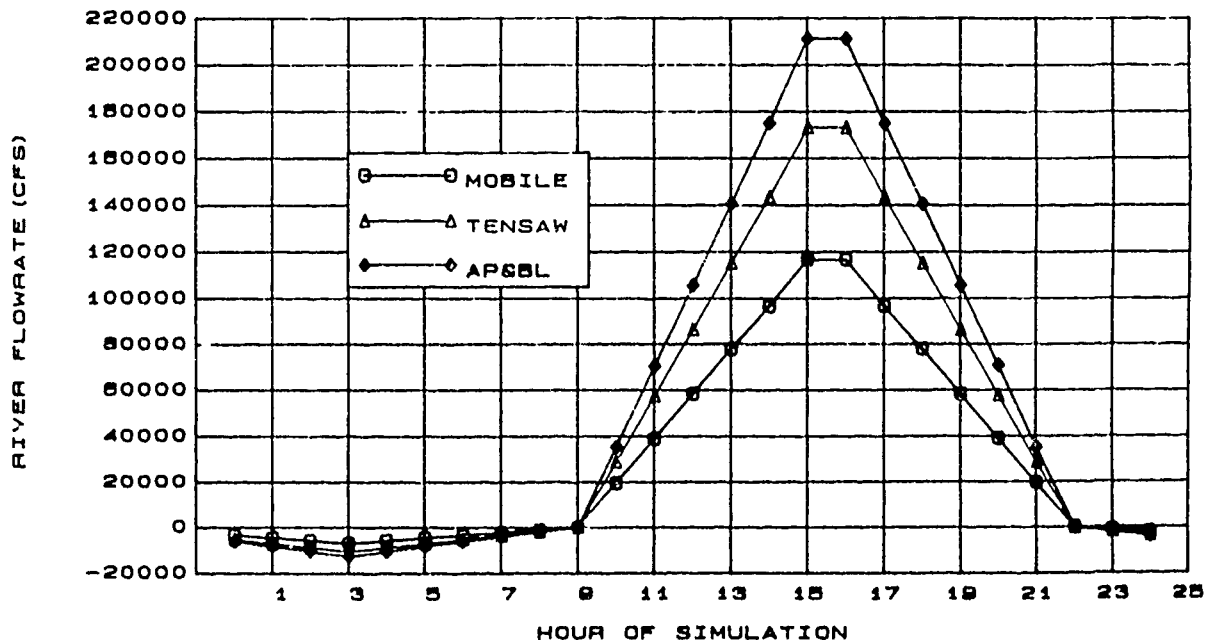


Figure B4. Variation of river flow rate with time for March

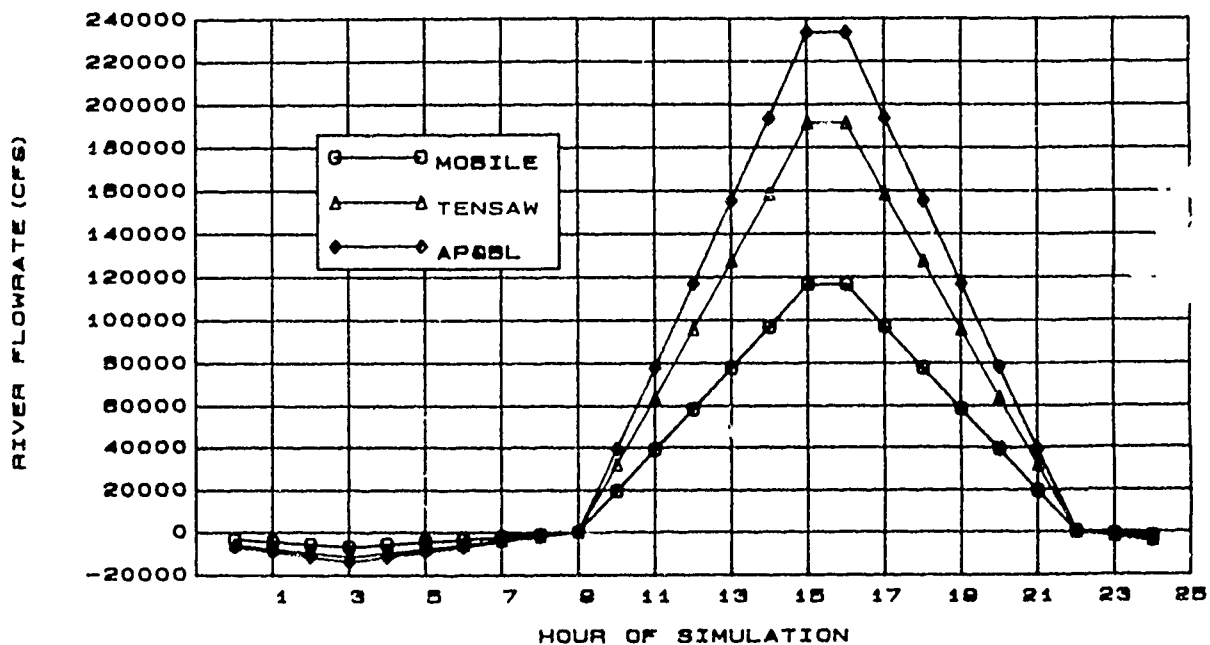


Figure B5. Variation of river flow rate with time for April

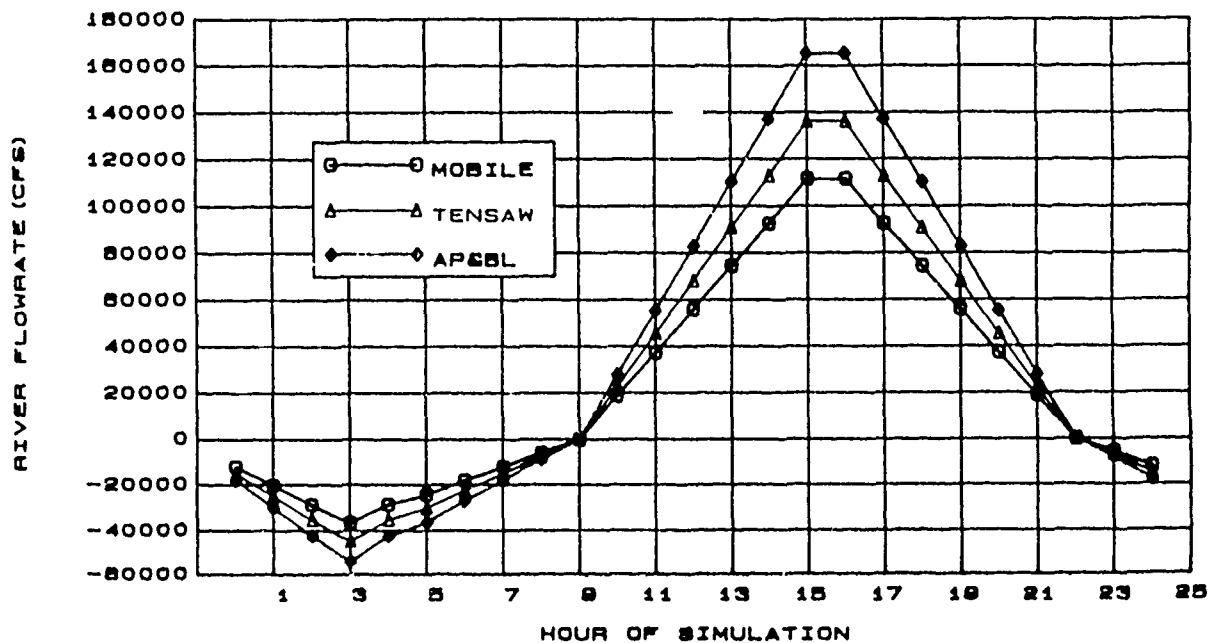


Figure B6. Variation of river flow rate with time for May

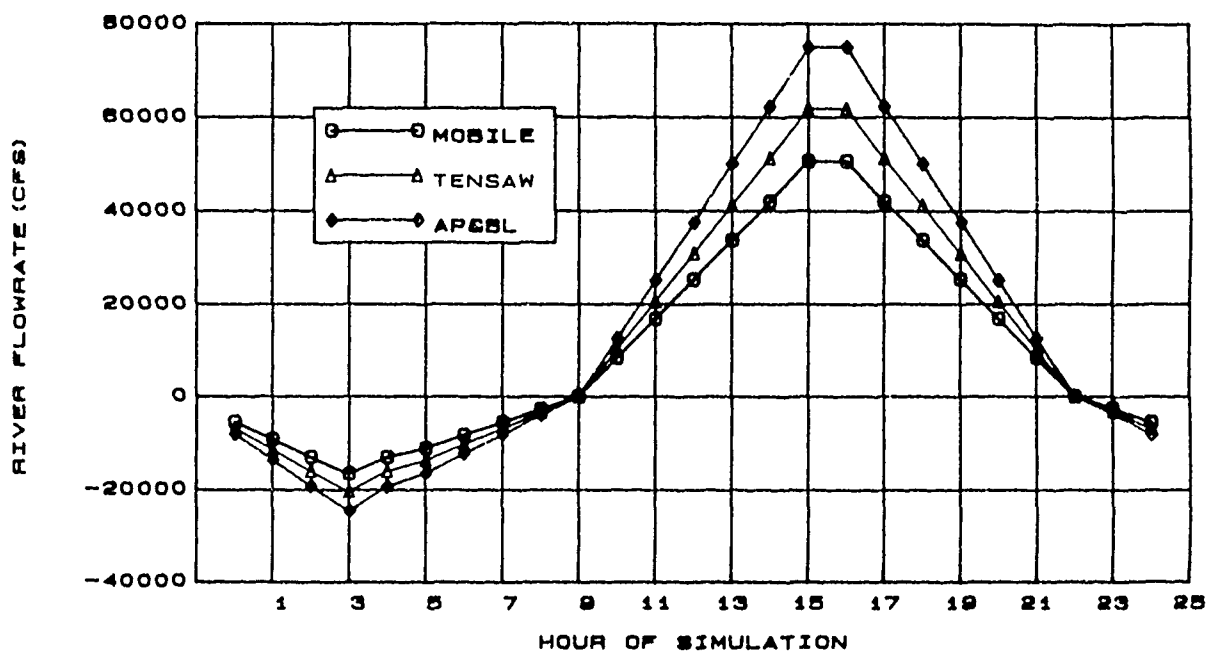


Figure B7. Variation of river flow rate with time for June

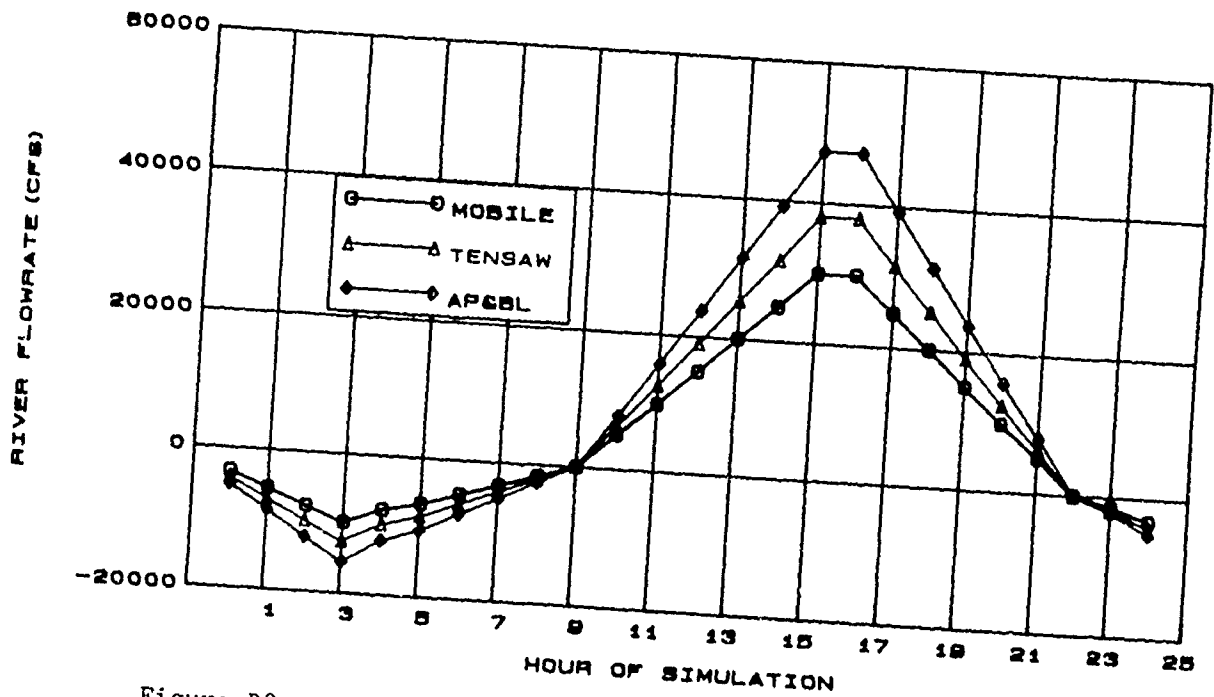


Figure B8. Variation of river flow rate with time for July

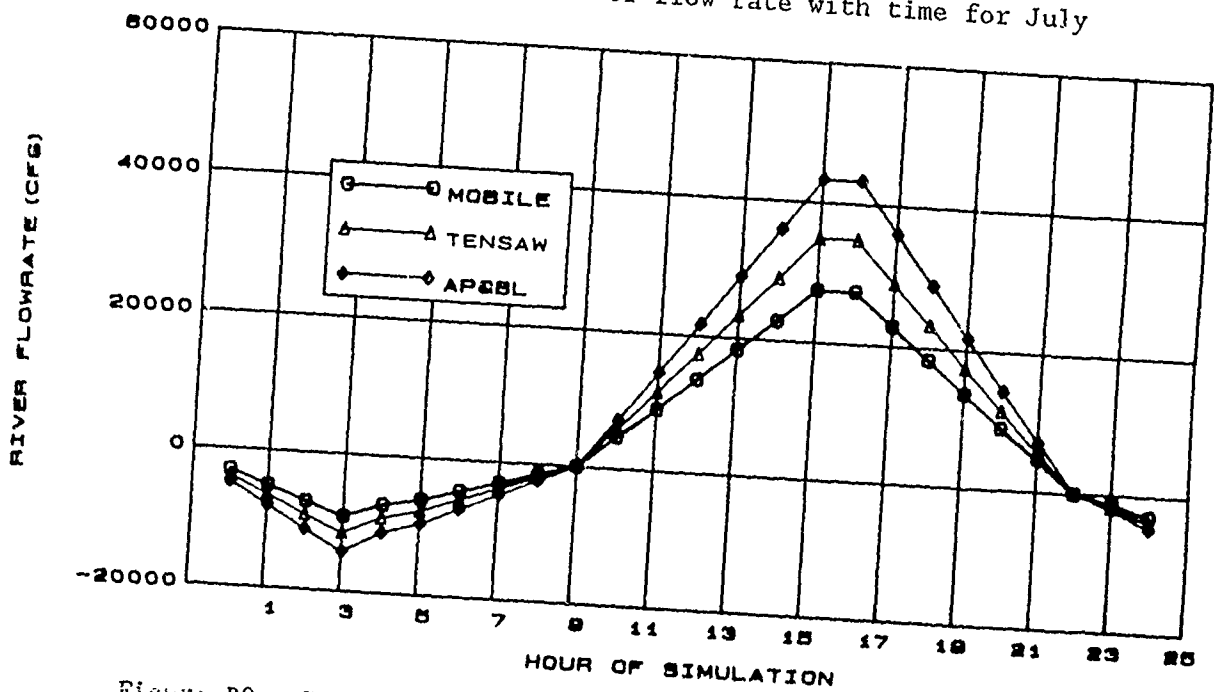


Figure B9. Variation of river flow rate with time for August

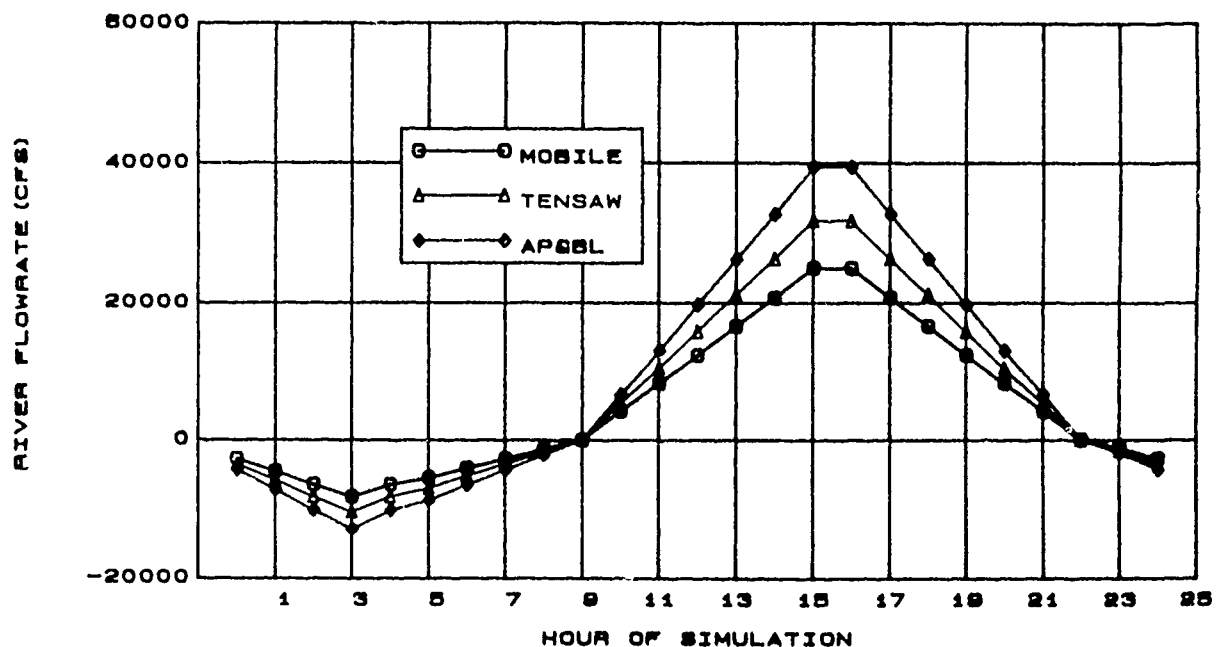


Figure B10. Variation of river flow rate with time for September

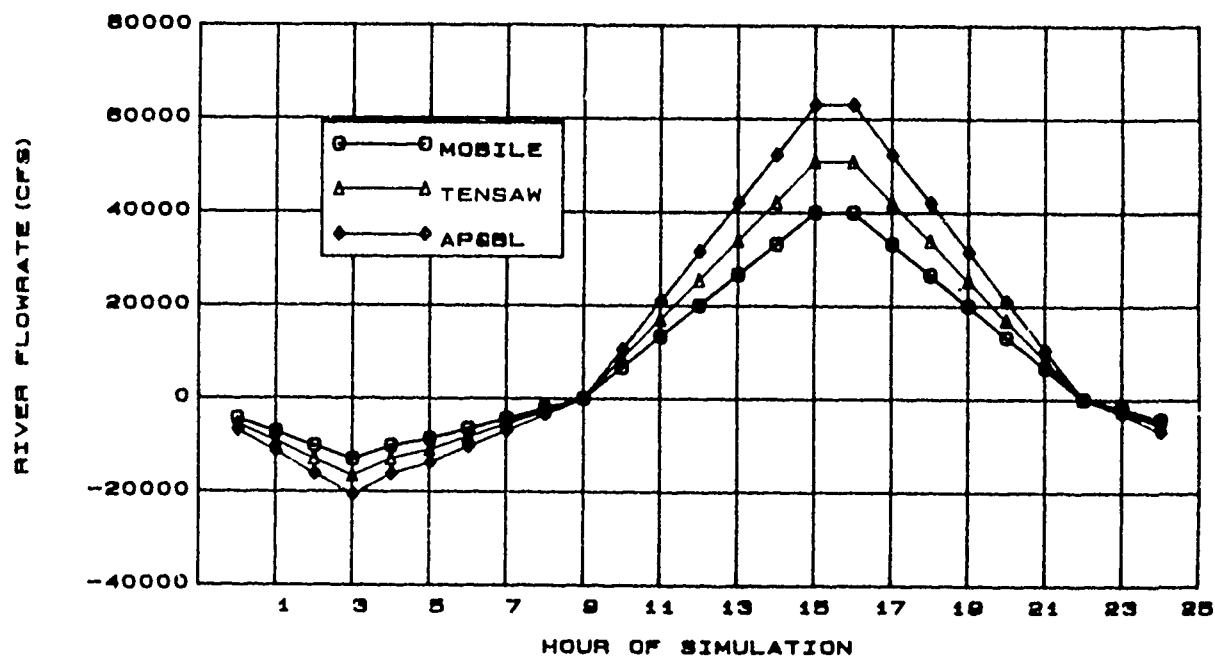


Figure B11 Variation of river flow rate with time for October

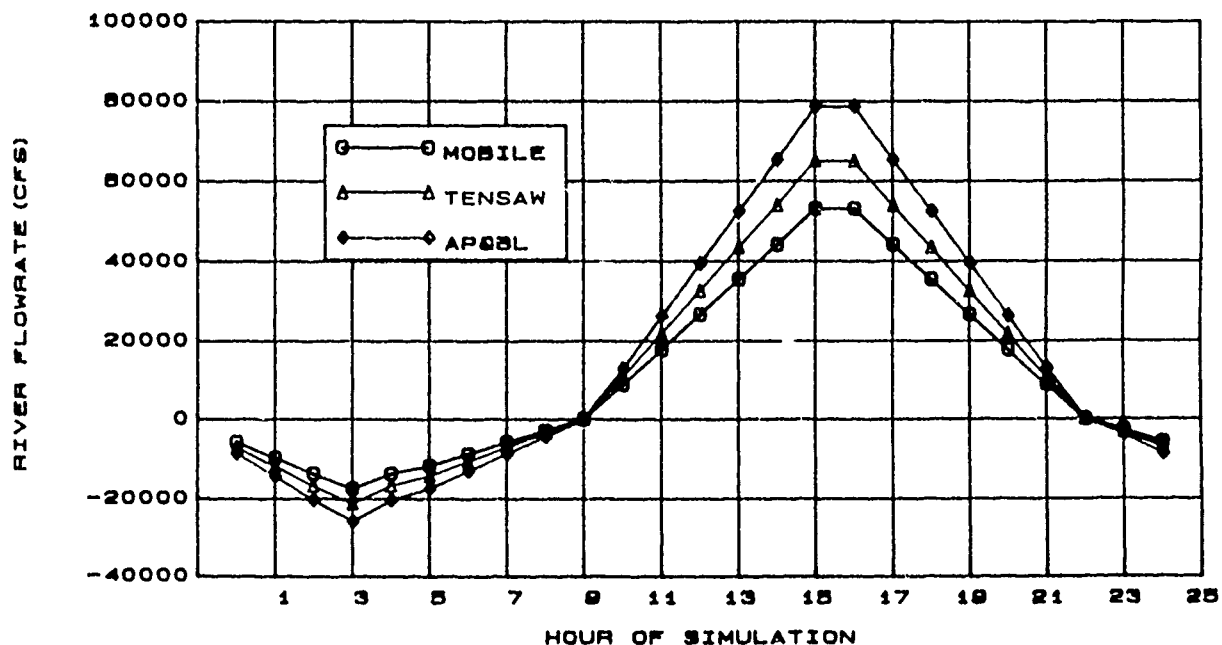


Figure B12. Variation of river flow rate with time for November

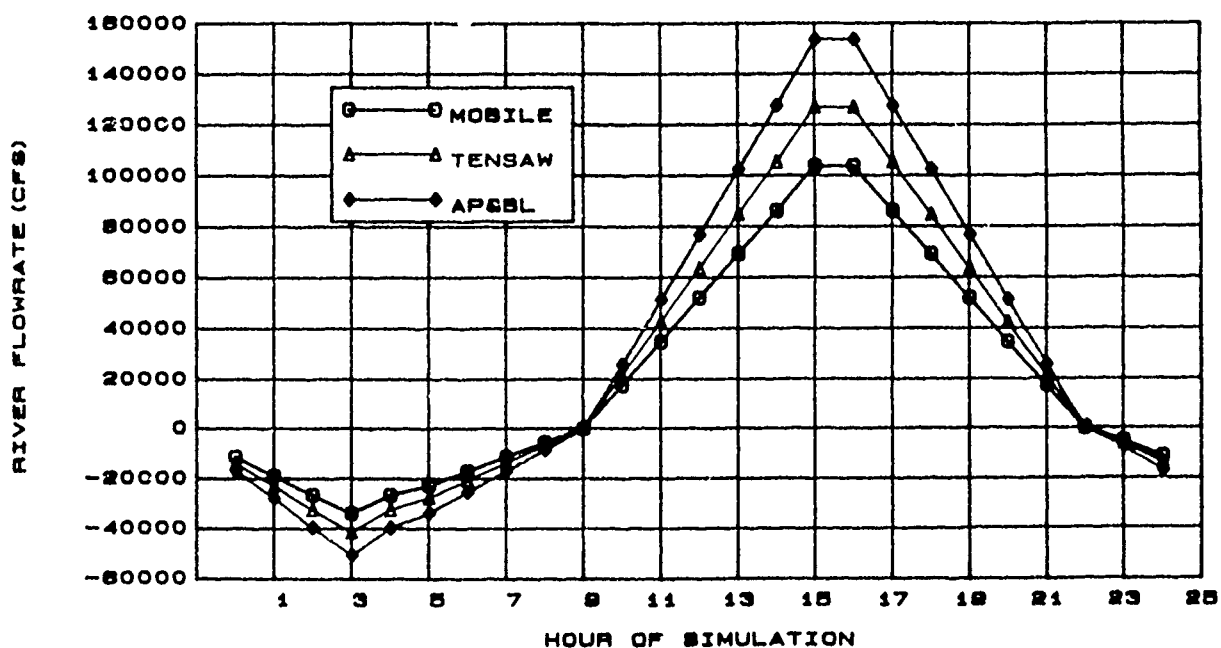


Figure B13. Variation of river flow rate with time for December

APPENDIX C: OVERFLOW TEST OPERATIONS

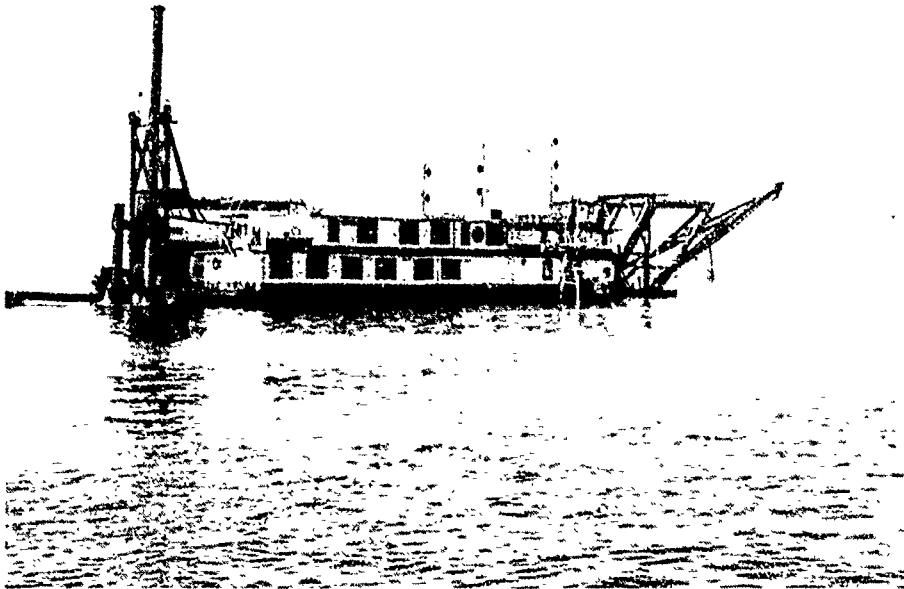


Figure C1. Hydraulic dredge *George D. Williams*

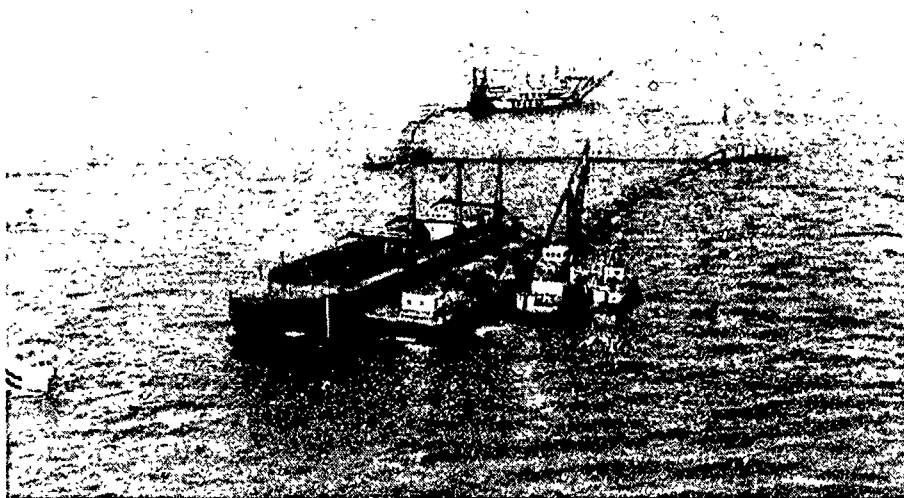


Figure C2. Operational configuration of the Mobile Bay overflow tests. Hydraulic dredge in the background with pipeline in "zig-zag" formation leading to the hopper barge, spider barge, and tenders (left to right) in foreground

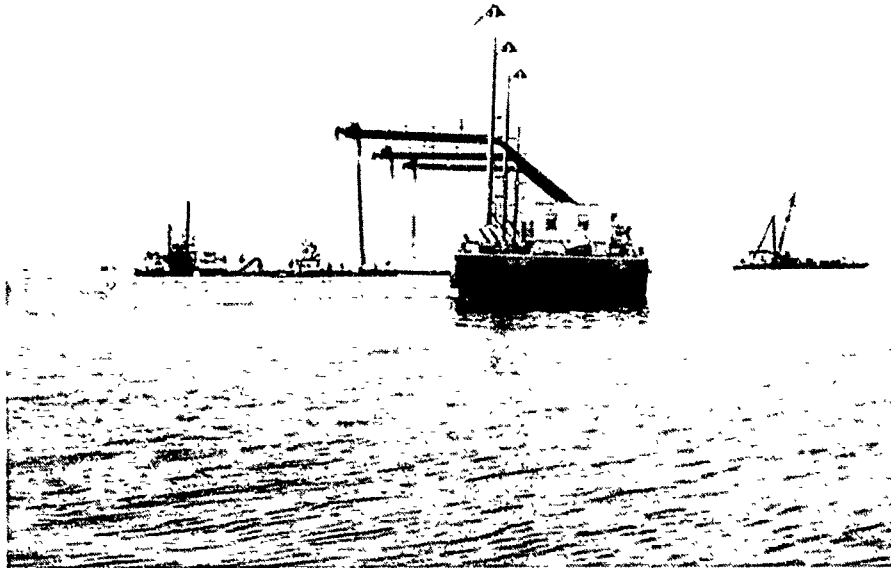


Figure C3. Spider barge ready to receive hopper barge. Note the manifold system to spread the loading along the axis of the hopper barge. Three of the six flexible downcomers have been sucked into the manifold by backpressure at the conclusion of the previous overflow test. The downcomers reextended when the dredge renewed pumping

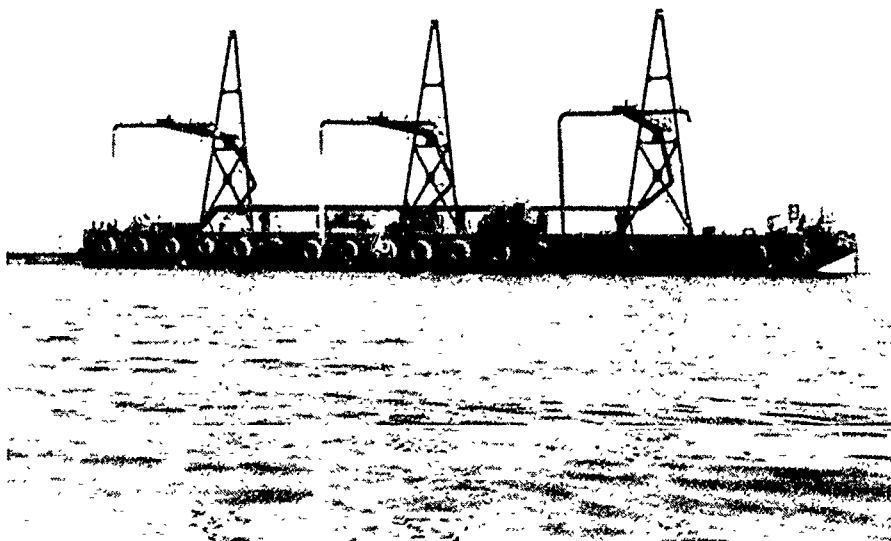


Figure C4. Lateral view of spider barge

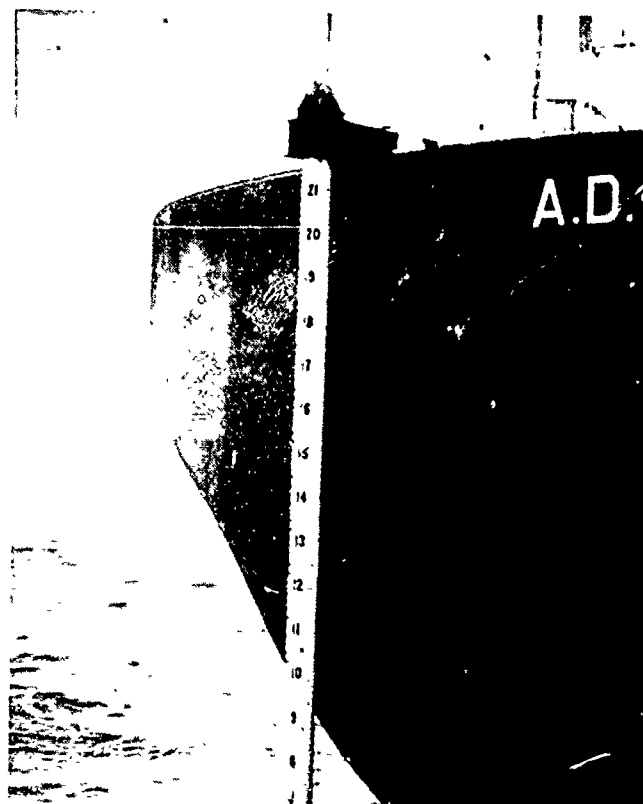


Figure C5. Stilling well at the bow of the hopper barge used to house a draft monitoring staff gage



Figure C6. Spider barge manifold and flexible downcomer system

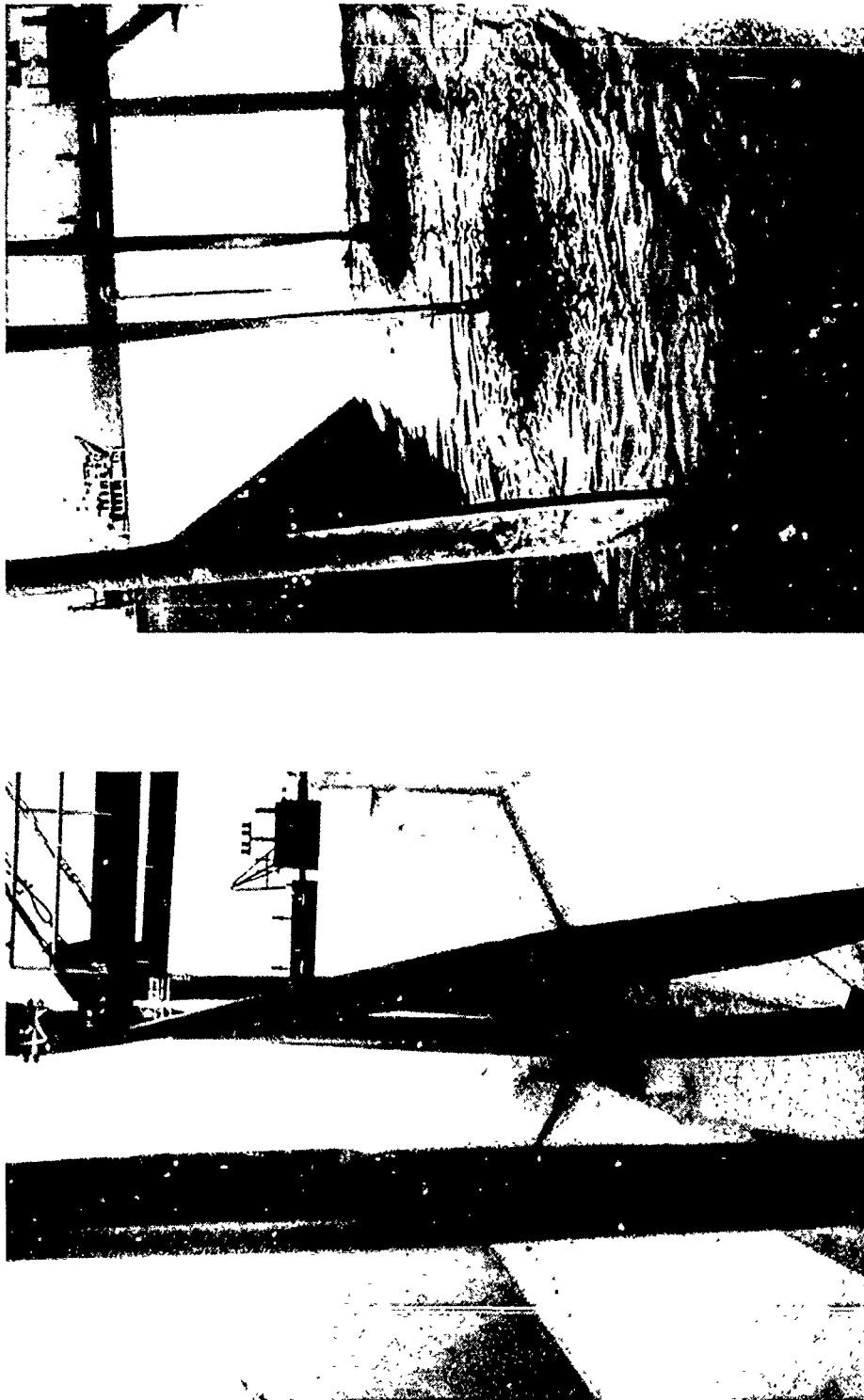


Figure C7. Empty hopper barge prior to (left photo) and during (right) filling process

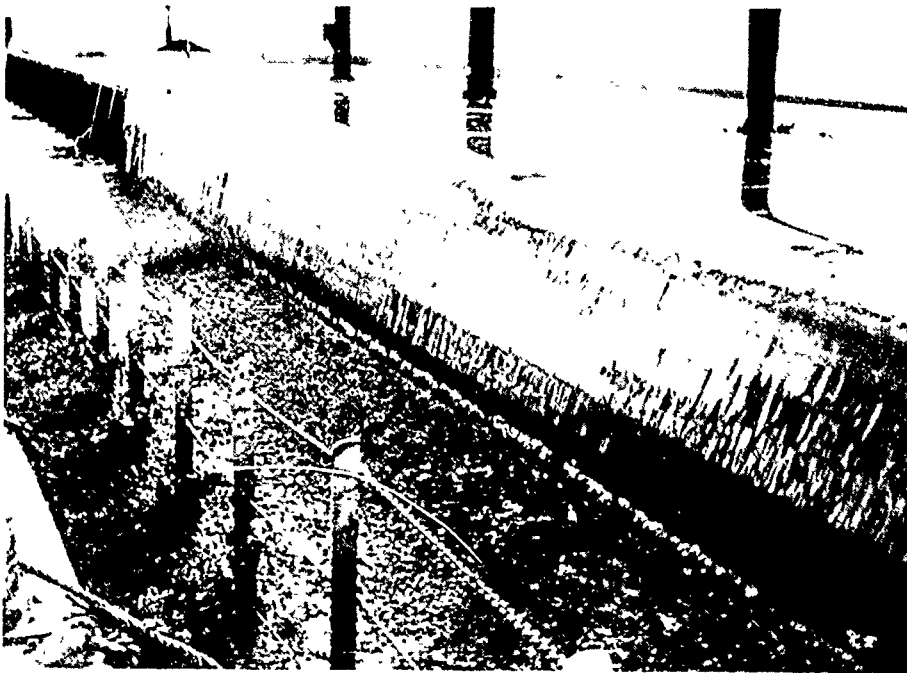


Figure C8. Overflow material cascading over the hopper barge coaming

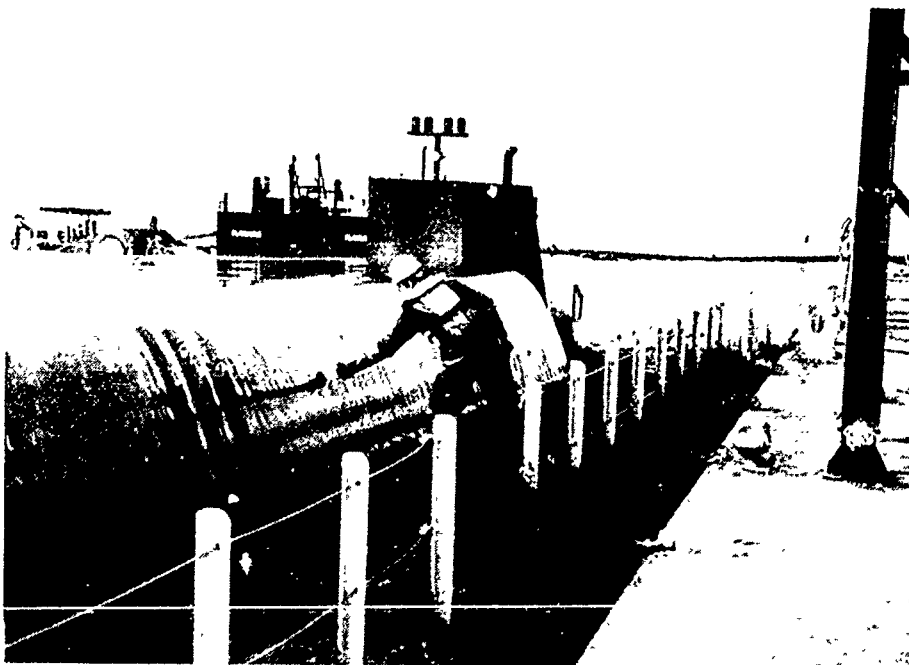


Figure C9. Sampling the overflow for sediment analysis

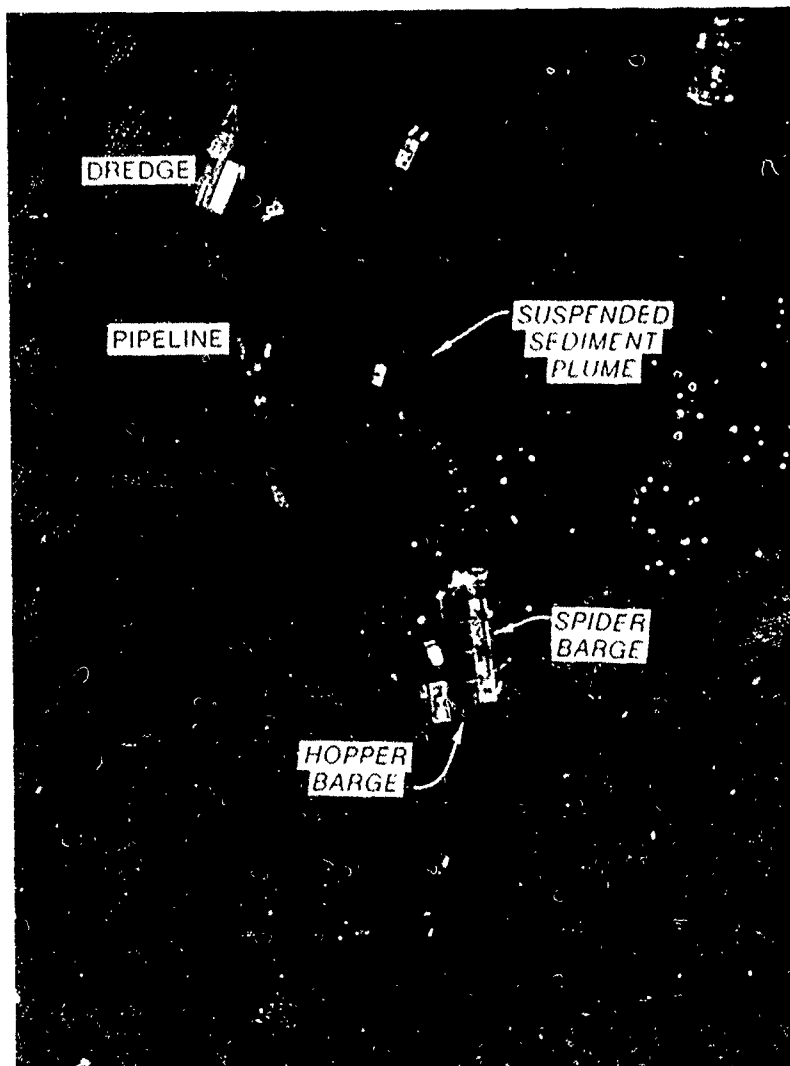


Photo C1. Overflow Test 1, lower bay maintenance material, December 3, 1967 (altitude 2,000 ft, wind NE 10 knots, flooding tide)

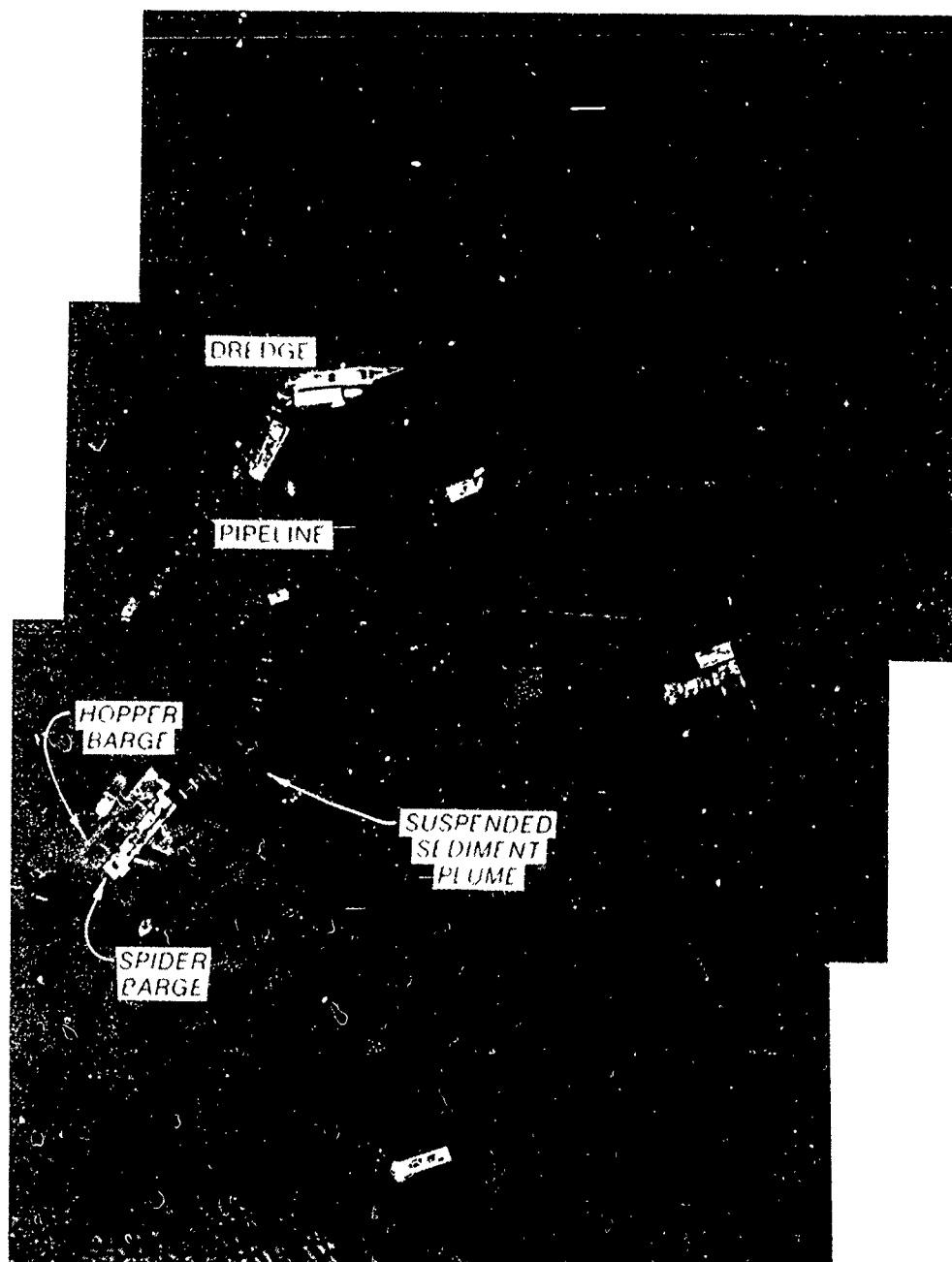


Photo C2. Overflow Test 1, lower bay maintenance material, December 3, 1987 (altitude 2,000 ft, wind NE 10 knots, flooding tide)

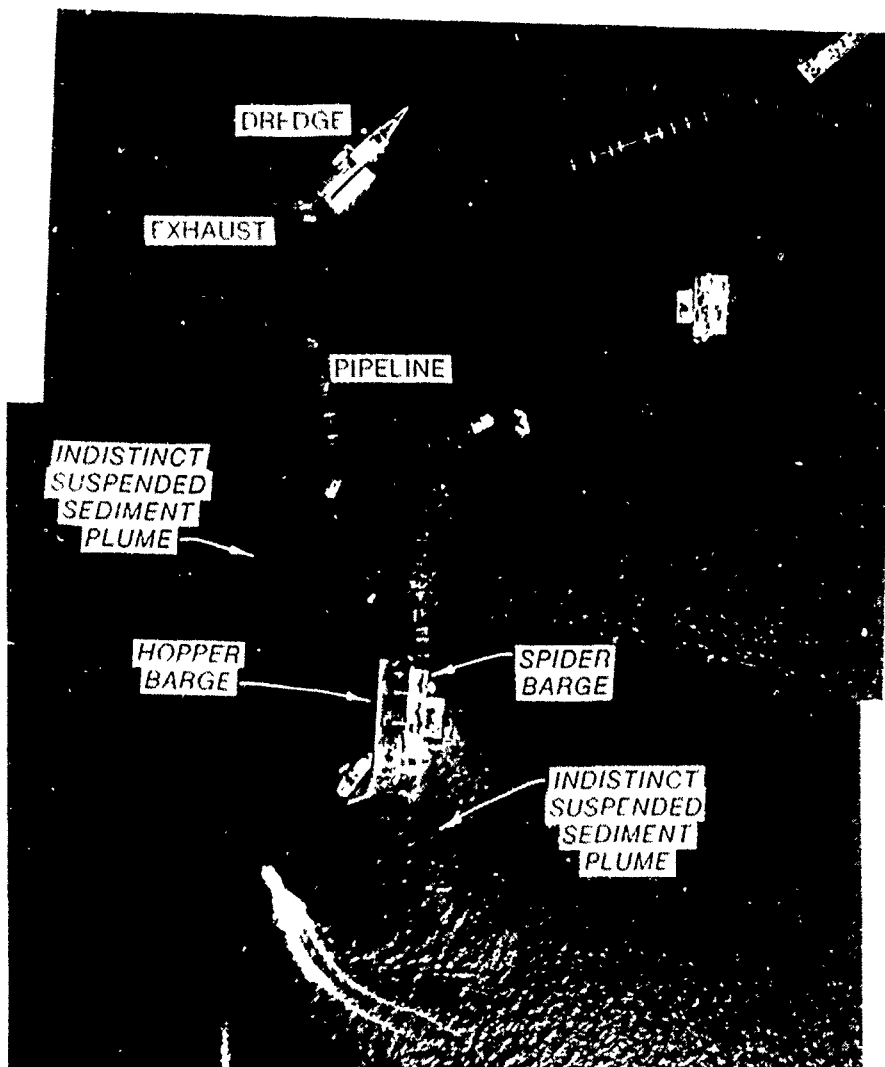


Photo C3. Overflow Test 4, upper bay maintenance material, December 6, 1987 (altitude 1,500 ft, wind SW 7-14 knots, ebbing tide)

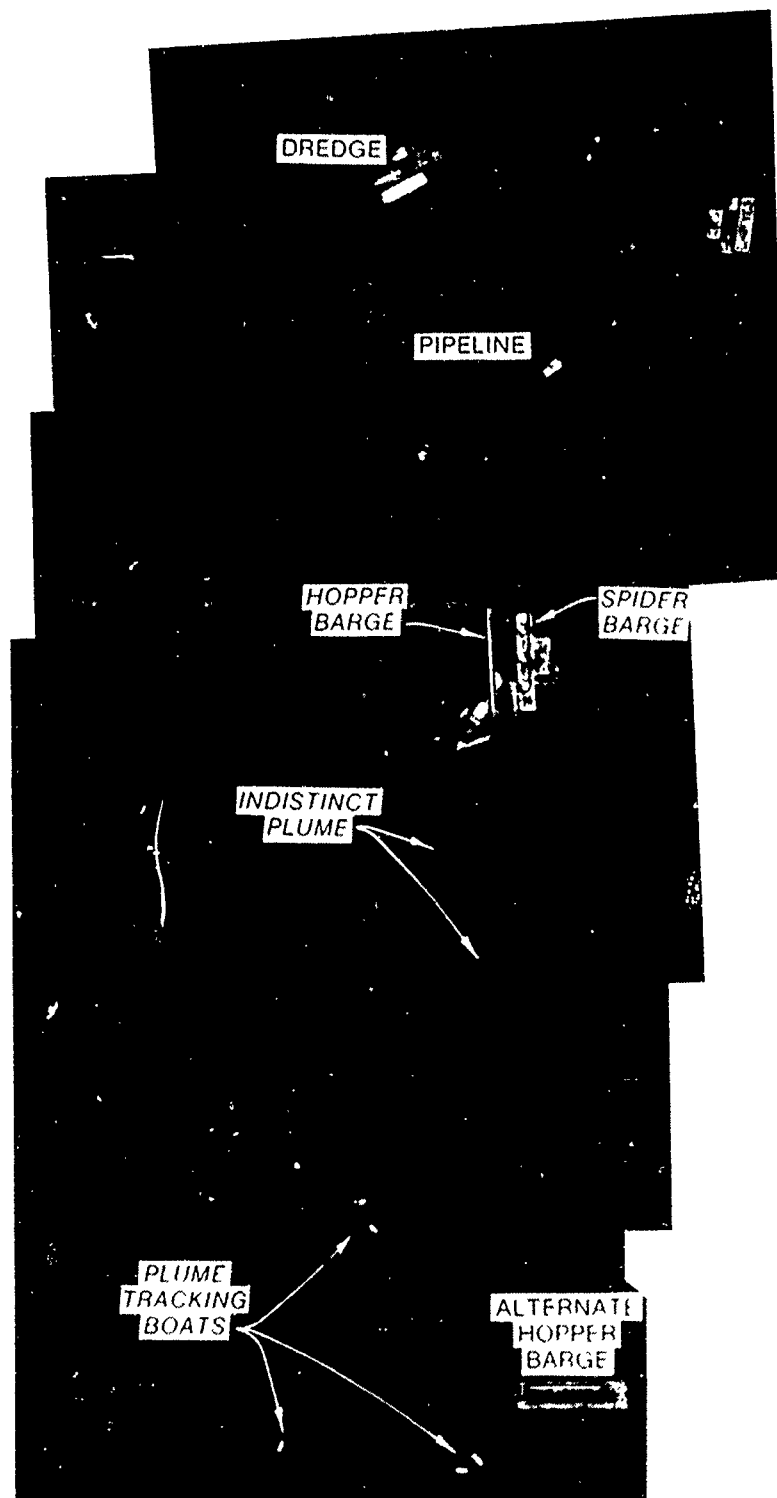


Photo C4. Overflow Test 4, upper bay maintenance material, December 6, 1987 (altitude 1,500 ft, wind SW 7-14 knots, ebbing tide)

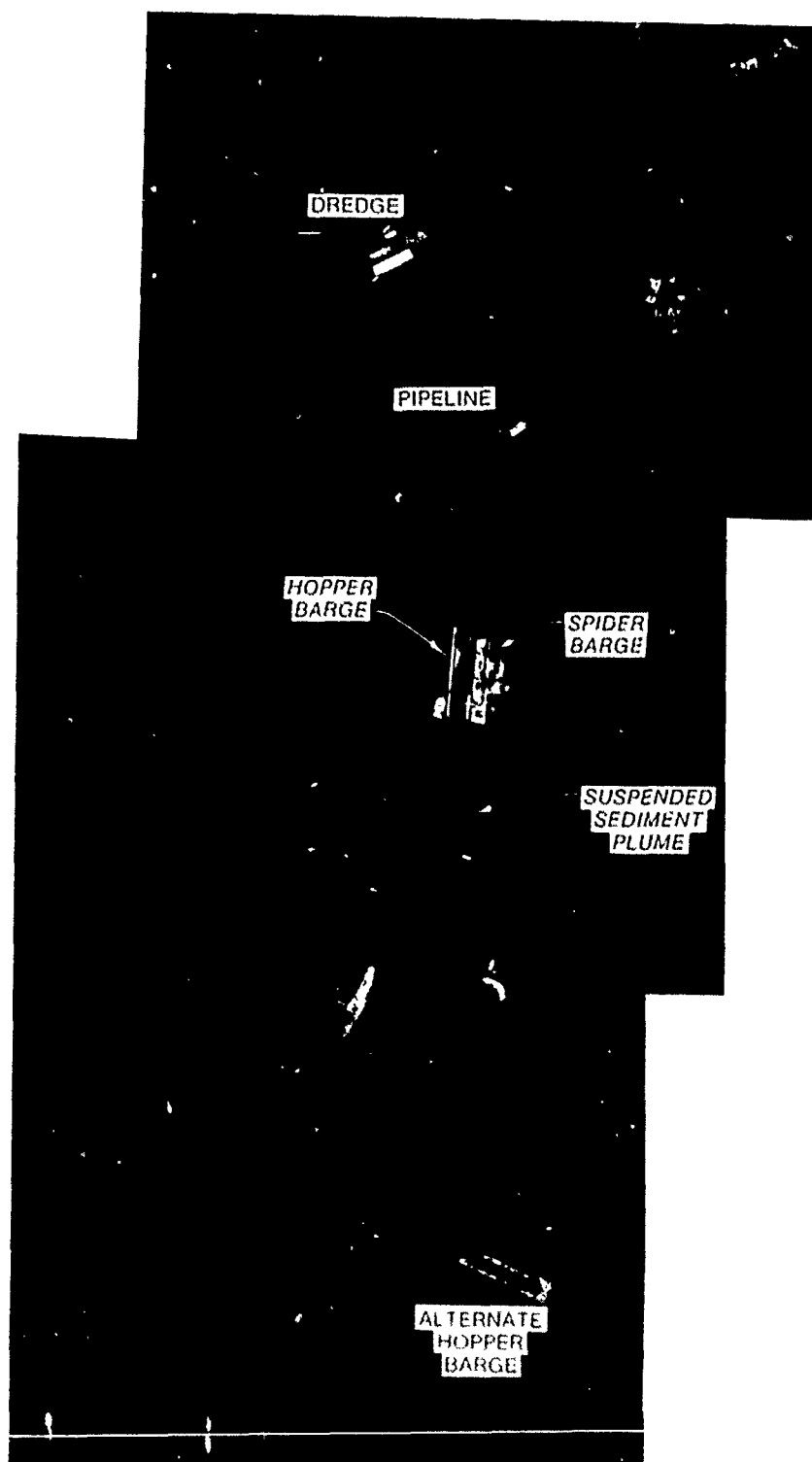


Photo C5. Overflow Test 4, upper bay maintenance material, December 6, 1987 (altitude 1,500 ft, wind SW 7-14 knots, ebbing tide)

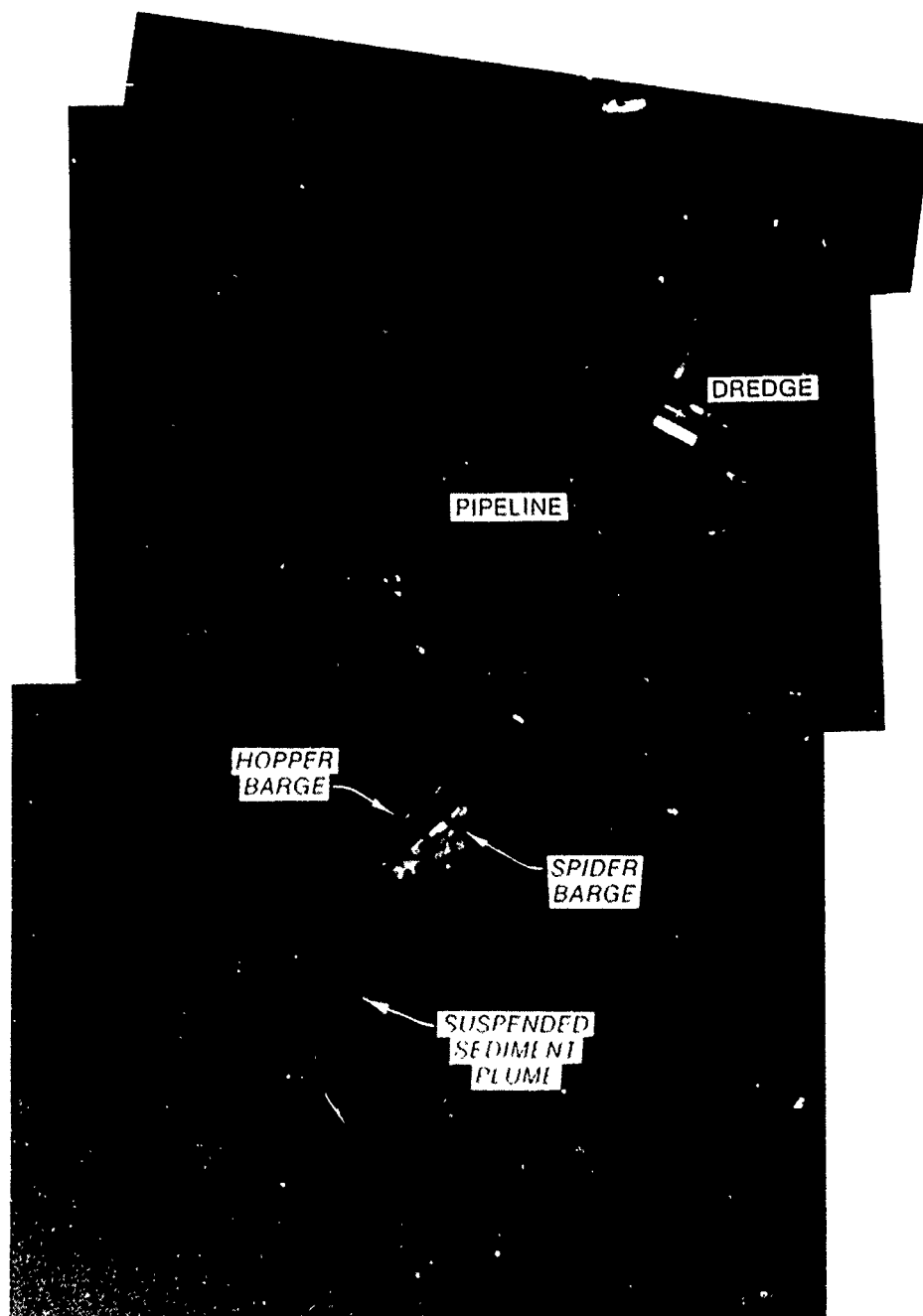


Photo C6. Overflow Test 5, upper bay maintenance material, December 6, 1987 (altitude 1,500 ft, wind NE 6-12 knots, flooding tide (surface slack))

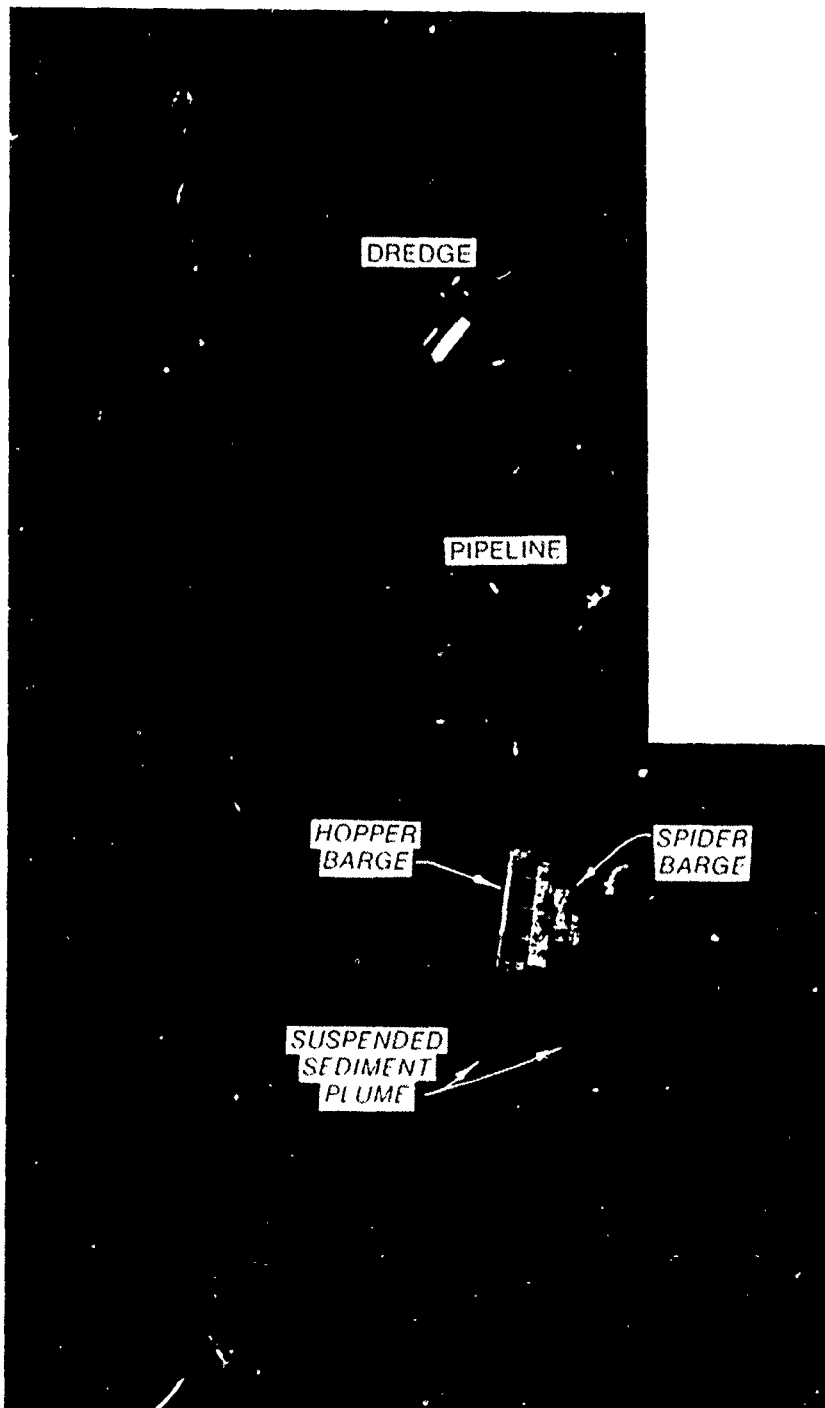


Photo C7. Overflow Test 5, upper bay maintenance material, December 6, 1987 (altitude 1,500 ft, wind NE 6-12 knots, flooding tide (surface ebb))

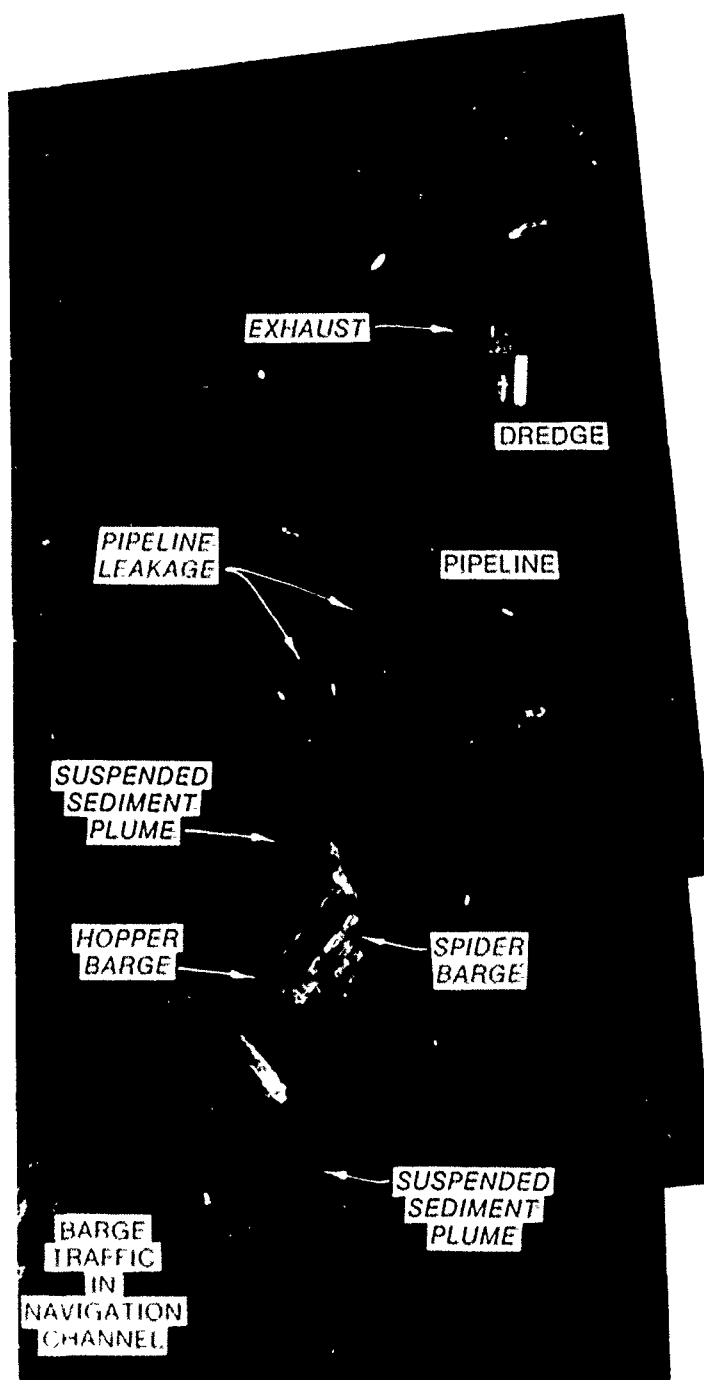


Photo C8. Overflow Test 5, upper bay maintenance material, December 6, 1987 (altitude 1,500 ft, wind NE 6-12 knots, flooding tide (surface slack))

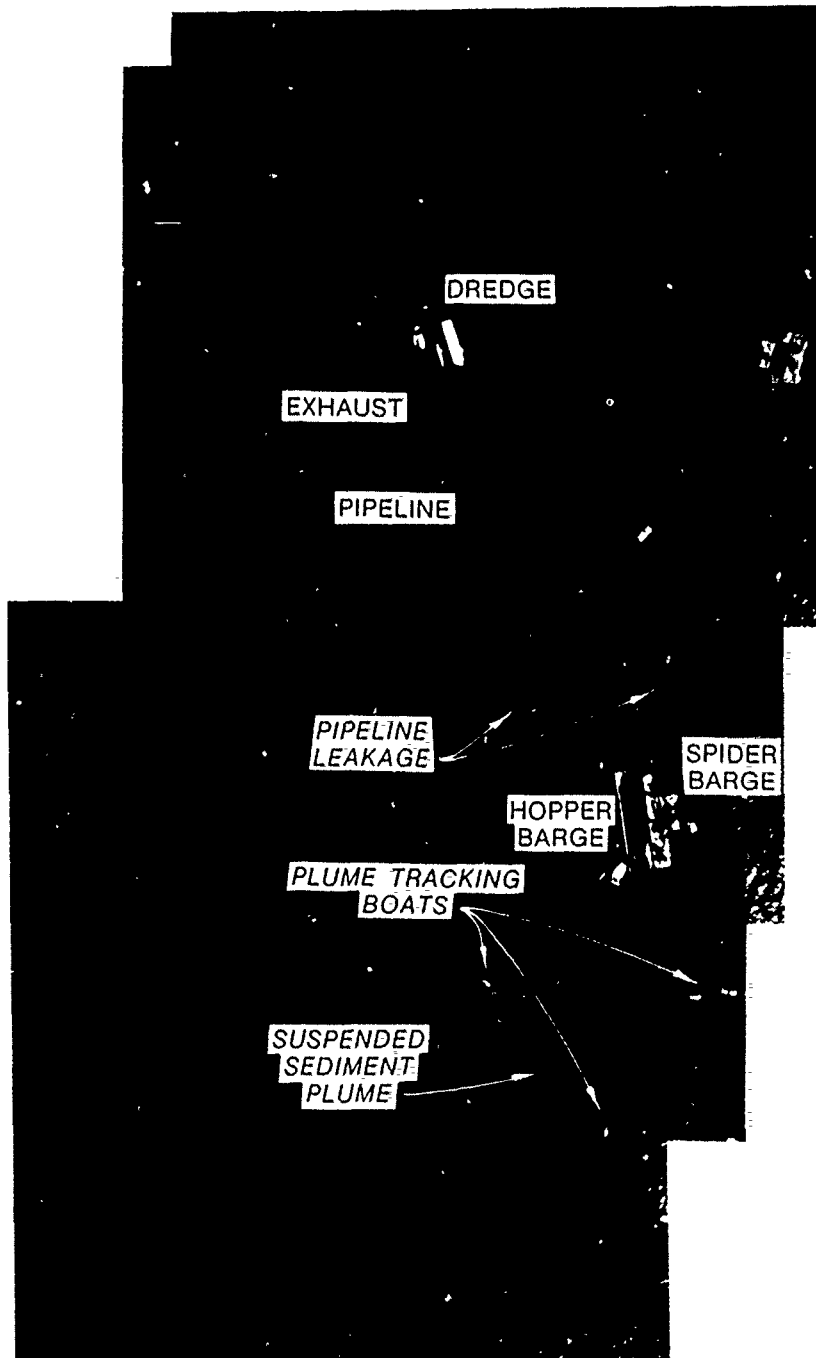


Photo C9. Overflow Test 5, upper bay maintenance material, December 6, 1987 (altitude 1,500 ft, wind SW 7-14 knots, ebbing tide)

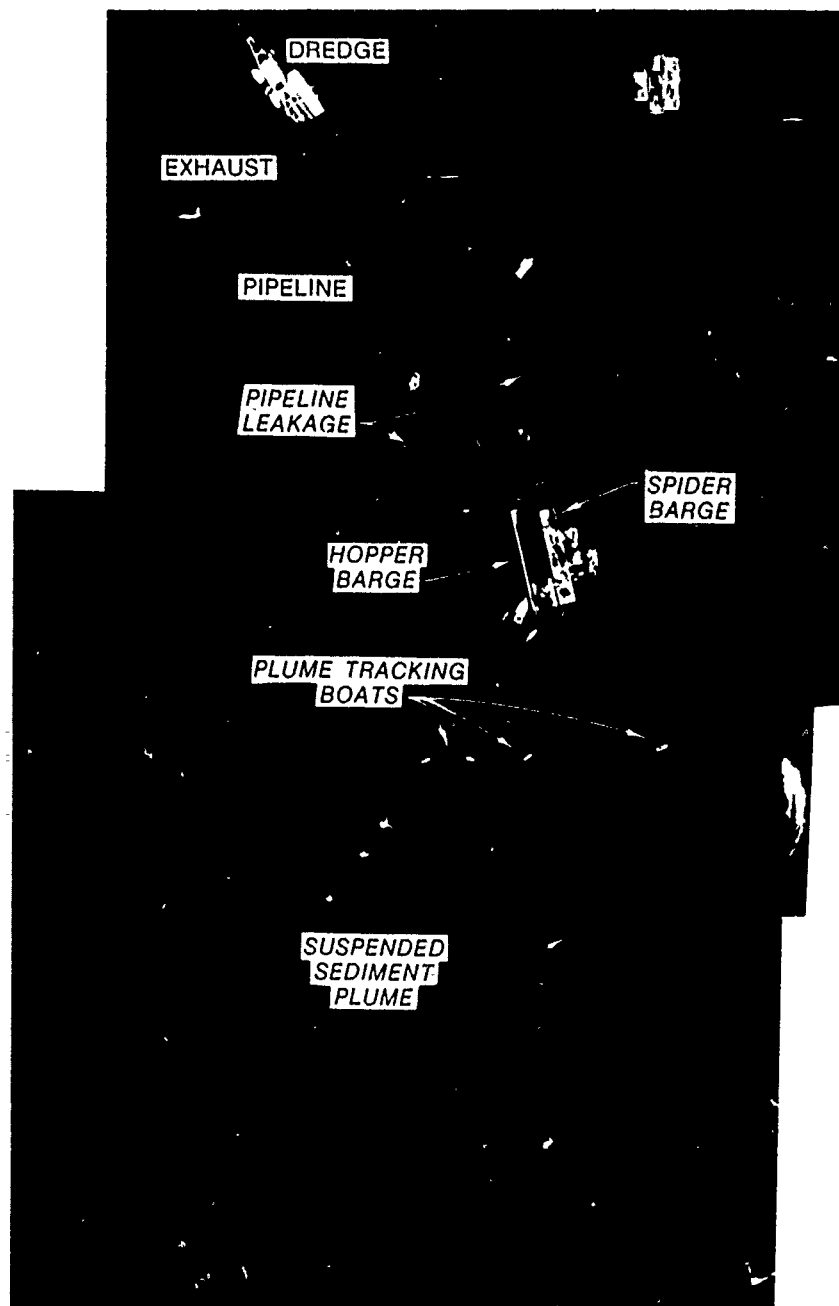


Photo C10. Overflow Test 6, upper bay maintenance material, December 6, 1987 (altitude 1,500 ft, wind SW 7-14 knots, ebbing tide)